



## Durham E-Theses

---

### *Secondary flows and losses in gas turbines.*

Graves, C.P.

#### How to cite:

---

Graves, C.P. (1985) *Secondary flows and losses in gas turbines.*, Durham theses, Durham University.  
Available at Durham E-Theses Online: <http://etheses.dur.ac.uk/1238/>

#### Use policy

---

The full-text may be used and/or reproduced, and given to third parties in any format or medium, without prior permission or charge, for personal research or study, educational, or not-for-profit purposes provided that:

- a full bibliographic reference is made to the original source
- a [link](#) is made to the metadata record in Durham E-Theses
- the full-text is not changed in any way

The full-text must not be sold in any format or medium without the formal permission of the copyright holders.

Please consult the [full Durham E-Theses policy](#) for further details.

**SECONDARY FLOWS AND LOSSES IN  
GAS TURBINES**

**Volume II of II**

**CHRISTOPHER PAUL GRAVES**

**Department of Engineering  
University of Durham**

**A thesis submitted for the degree of Doctor of Philosophy  
of the University of Durham**

**March 1985**

**The copyright of this thesis rests with the author.  
No quotation from it should be published without  
his prior written consent and information derived  
from it should be acknowledged.**



**16. MAY 1986**

**BEST COPY**

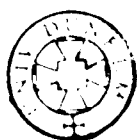
**AVAILABLE**

Variable print quality

## LIST OF FIGURES

### Volume Two

- 3.1 Low Speed Wind Tunnel Working Section and Cascade Arrangement
  - 3.2 Position of Blade Surface Pressure Tappings at Midspan
  - 3.3 Positions of the Experimental Traversing Slots
  - 3.4 Cascade Sign Convention
  - 3.5 Cascade Endwall Boundary Layer Disturber
  - 3.6 Data Acquisition System
  - 3.7 Pressure Probe Arrangement
  - 3.8 Hot Wire Probe Stem Arrangement
  - 3.9 Probe Traversing Gear
  - 3.10 Data Acquisition System for Pressure Probe Traversing
  - 3.11 Data Acquisition System for Hot Wire Probe Traversing
  - 3.12 Pressure Probe Calibration Mounting
  - 3.13 Hot Wire Probe Calibration Jet
  - 3.14 Hot Wire Probe Calibration Jet Traverse Data
  - 3.15 A Typical Hot Wire Anemometer Calibration
  - 3.16 Conditional Sampling of Pressure Probe Data
  - 3.17 Conditional Sampling Method
  - 3.18 Five-Hole Probe Data Analysis
  - 3.19 Five-Hole Probe  $\phi$  and  $\psi$  at  $\alpha=0$
  - 3.20 Five-Hole Probe Data Analysis: An Analysis Cell
  - 3.21 A Contour Plotting Cell
  - 3.22 Thick Line Plotting Algorithm
  - 3.23 A Vector Scaling Cell
- Slot 1 Data (Figures 4.1 - 4.7)
- 4.1 Experimental Data Points
  - 4.2 Total Pressure Loss Coefficient Contours



- 4.3 Streamwise Spanwise Angle Contours
- 4.4 Yaw Angle Contours
- 4.5 Vector Plot of Secondary Velocities
- 4.6 Static Pressure Coefficient Contours
- 4.7 Total Velocity Magnitude Contours
- 4.8 Section Through An Idealized Passage Vortex

Slot 2 Data (Figures 4.9 – 4.15)

- 4.9 Experimental Data Points
- 4.10 Total Pressure Loss Coefficient Contours
- 4.11 Total Velocity Magnitude Contours
- 4.12 Vector Plot of Secondary Velocities
- 4.13 Spanwise Angle Contours
- 4.14 Yaw Angle Contours
- 4.15 Static Pressure Coefficient Contours

Slot 3 Data (Figures 4.16 – 4.22)

- 4.16 Experimental Data Points
- 4.17 Total Pressure Loss Coefficient Contours
- 4.18 Total Velocity Magnitude Contours
- 4.19 Vector Plot of Secondary Velocities
- 4.20 Spanwise Angle Contours
- 4.21 Yaw Angle Contours
- 4.22 Static Pressure Coefficient Contours

Slot 4 Data (Figures 4.23 – 4.29)

- 4.23 Experimental Data Points
- 4.24 Total Pressure Loss Coefficient Contours
- 4.25 Total Velocity Magnitude Contours
- 4.26 Vector Plot of Secondary Velocities

- 4.27 Spanwise Angle Contours
- 4.28 Yaw Angle Contours
- 4.29 Static Pressure Coefficient Contours

Slot 5 Data (Figures 4.30 – 4.36)

- 4.30 Experimental Data Points
- 4.31 Total Pressure Loss Coefficient Contours
- 4.32 Total Velocity Magnitude Contours
- 4.33 Vector Plot of Secondary Velocities
- 4.34 Spanwise Angle Contours
- 4.35 Yaw Angle Contours
- 4.36 Static Pressure Coefficient Contours

Slot 6 Data (Figures 4.37 – 4.43)

- 4.37 Experimental Data Points
- 4.38 Total Pressure Loss Coefficient Contours
- 4.39 Total Velocity Magnitude Contours
- 4.40 Vector Plot of Secondary Velocities
- 4.41 Spanwise Angle Contours
- 4.42 Yaw Angle Contours
- 4.43 Static Pressure Coefficient Contours

Slot 7 Data (Figures 4.44 – 4.50)

- 4.44 Experimental Data Points
- 4.45 Total Pressure Loss Coefficient Contours
- 4.46 Total Velocity Magnitude Contours
- 4.47 Vector Plot of Secondary Velocities
- 4.48 Spanwise Angle Contours
- 4.49 Yaw Angle Contours
- 4.50 Static Pressure Coefficient Contours

4.51 Blade Passage Loss Core Development and Loci  
of Passage Vortex Centre and Loss Core Peak

Slot 8 Data (Figures 4.52 – 4.58)

4.52 Experimental Data Points  
4.53 Total Pressure Loss Coefficient Contours  
4.54 Total Velocity Magnitude Contours  
4.55 Vector Plot of Secondary Velocities  
4.56 Spanwise Angle Contours  
4.57 Yaw Angle Contours  
4.58 Static Pressure Coefficient Contours

Slot 9 Data (Figures 4.59 – 4.65)

4.59 Experimental Data Points  
4.60 Total Pressure Loss Coefficient Contours  
4.61 Total Velocity Magnitude Contours  
4.62 Vector Plot of Secondary Velocities  
4.63 Spanwise Angle Contours  
4.64 Yaw Angle Contours  
4.65 Static Pressure Coefficient Contours

Slot 10 Data (Figures 4.66 – 4.73)

4.66 Experimental Data Points  
4.67 Total Pressure Loss Coefficient Contours  
4.68 Midspan Tangential Traverse Results  
4.69 Total Velocity Magnitude Contours  
4.70 Vector Plot of Secondary Velocities  
4.71 Spanwise Angle Contours  
4.72 Yaw Angle Contours  
4.73 Static Pressure Coefficient Contours

- 4.74 Loss Core Development Downstream of the Blade Passage
- 4.75 Loci of Passage Vortex Centre and Loss Core Peak
- 4.76 Pitchwise Mass Meaned Data Upstream of the Cascade
- 4.77 Pitchwise Mass Meaned Overturning Angle Within the Blade Passage
- 4.78 Pitchwise Mass Meaned Total Pressure Loss Coefficient Within the Blade Passage
- 4.79 Pitchwise Mass Meaned Overturning Angle Downstream of the Cascade
- 4.80 Pitchwise Mass Meaned Total Pressure Loss Coefficient Downstream of the Cascade
- 4.81 Development of Area Mass Averaged Total Pressure Loss Coefficient
- 4.82 Development of Secondary Losses
- 4.83 Normalized Cascade Mass Flow Rate

#### Plots on Constant Span Surfaces

- 4.84 Plot on Plane 20.1 mm from Perspex Endwall (Five-Hole Probe Data) Experimental Data Points

#### Total Pressure Loss Coefficient Contours (Figures 4.85 – 4.95)

- 4.85 Plot on Plane 1.0 mm from Perspex Endwall (Three-Hole Probe Data)
- 4.86 Plot on Plane 5.0 mm from Perspex Endwall (Five-Hole Probe Data)
- 4.87 Plot on Plane 5.0 mm from Perspex Endwall (Three-Hole Probe Data)
- 4.88 Plot on Plane 20.1 mm from Perspex Endwall (Five-Hole Probe Data)
- 4.89 Plot on Plane 20.1 mm from Perspex Endwall (Three-Hole Probe Data)
- 4.90 Plot on Plane 40.0 mm from Perspex Endwall (Five-Hole Probe Data)
- 4.91 Plot on Plane 60.0 mm from Perspex Endwall (Five-Hole Probe Data)



- 4.92 Plot on Plane 80.0 mm from Perspex Endwall  
(Five-Hole Probe Data)
- 4.93 Plot on Plane 100.1 mm from Perspex Endwall  
(Five-Hole Probe Data)
- 4.94 Plot on Plane 140.1 mm from Perspex Endwall  
(Five-Hole Probe Data)
- 4.95 Plot on Plane 220.1 mm from Perspex Endwall  
(Five-Hole Probe Data)

Total Velocity Magnitude Contours (Figures 4.96 - 4.100)

- 4.96 Plot on Plane 1.0 mm from Perspex Endwall  
(Three-Hole Probe Data)
- 4.97 Plot on Plane 20.1 mm from Perspex Endwall  
(Five-Hole Probe Data)
- 4.98 Plot on Plane 20.1 mm from Perspex Endwall  
(Three-Hole Probe Data)
- 4.99 Plot on Plane 50.1 mm from Perspex Endwall  
(Five-Hole Probe Data)
- 4.100 Plot on Plane 220.1 mm from Perspex Endwall  
(Five-Hole Probe Data)
- 4.101 Two Dimensional Velocity Distribution  
Predicted Values

Vector Plots of Axial and Tangential Velocities (Figures 4.102-4.112)

- 4.102 Plot on Plane 1.0 mm from Perspex Endwall  
(Three-Hole Probe Data)
- 4.103 Plot on Plane 2.0 mm from Perspex Endwall  
(Three-Hole Probe Data)
- 4.104 Plot on Plane 3.0 mm from Perspex Endwall  
(Three-Hole Probe Data)
- 4.105 Plot on Plane 4.0 mm from Perspex Endwall  
(Three-Hole Probe Data)
- 4.106 Plot on Plane 5.0 mm from Perspex Endwall  
(Three-Hole Probe Data)
- 4.107 Plot on Plane 7.4 mm from Perspex Endwall  
(Three-Hole Probe Data)

- 4.108 Plot on Plane 15.0 mm from Perspex Endwall  
(Five-Hole Probe Data)
- 4.109 Plot on Plane 40.0 mm from Perspex Endwall  
(Five-Hole Probe Data)
- 4.110 Plot on Plane 60.0 mm from Perspex Endwall  
(Five-Hole Probe Data)
- 4.111 Plot on Plane 100.1 mm from Perspex Endwall  
(Five-Hole Probe Data)
- 4.112 Plot on Plane 220.1 mm from Perspex Endwall  
(Five-Hole Probe Data)
- 4.113 Plot on Plane 20.1 mm from Perspex Endwall  
(Five-Hole Probe Data) Spanwise Angle Contours
- 4.114 Plot on Plane 20.1 mm from Perspex Endwall  
(Five-Hole Probe Data) Yaw Angle Contours
- 4.115 Plot on Plane 220.1 mm from Perspex Endwall  
(Five-Hole Probe Data) Spanwise Angle Contours
- 4.116 Plot on Plane 220.1 mm from Perspex Endwall  
(Five-Hole Probe Data) Yaw Angle Contours

Static Pressure Coefficient Contours (Figures 4.117 - 4.122)

- 4.117 Plot on Plane 1.0 mm from Perspex Endwall  
(Three-Hole Probe Data)
- 4.118 Plot on Plane 20.1 mm from Perspex Endwall  
(Five-Hole Probe Data)
- 4.119 Plot on Plane 20.1 mm from Perspex Endwall  
(Three-Hole Probe Data)
- 4.120 Plot on Plane 30.0 mm from Perspex Endwall  
(Five-Hole Probe Data)
- 4.121 Plot on Plane 60.0 mm from Perspex Endwall  
(Five-Hole Probe Data)
- 4.122 Plot on Plane 220.1 mm from Perspex Endwall  
(Five-Hole Probe Data)
- 4.123 Two Dimensional Static Pressure Coefficient Distribution  
Predicted Values

Plots on Pseudo Stream Surfaces

Averaged Tangential Experimental Points (Figures 4.124 - 4.125)

- 4.124 93.3% of Blade Pitch Less Thickness from Suction Surface

4.125 6.7% of Blade Pitch Less Thickness from Suction Surface

Experimental Data Points (Figures 4.126 – 4.127)

4.126 93.3% of Blade Pitch Less Thickness from Suction Surface

4.127 6.7% of Blade Pitch Less Thickness from Suction Surface

Total Pressure Loss Coefficient Contours (Figures 4.128 – 4.139)

4.128 93.3% of Blade Pitch Less Thickness from Suction Surface

4.129 85.4% of Blade Pitch Less Thickness from Suction Surface

4.130 77.5% of Blade Pitch Less Thickness from Suction Surface

4.131 69.7% of Blade Pitch Less Thickness from Suction Surface

4.132 61.8% of Blade Pitch Less Thickness from Suction Surface

4.133 53.9% of Blade Pitch Less Thickness from Suction Surface

4.134 46.1% of Blade Pitch Less Thickness from Suction Surface

4.135 38.2% of Blade Pitch Less Thickness from Suction Surface

4.136 30.3% of Blade Pitch Less Thickness from Suction Surface

4.137 22.5% of Blade Pitch Less Thickness from Suction Surface

4.138 14.6% of Blade Pitch Less Thickness from Suction Surface

4.139 6.7% of Blade Pitch Less Thickness from Suction Surface

4.140 Spanwise Migration of the Loss Core

Total Velocity Magnitude Contours (Figures 4.141 – 4.142)

4.141 93.3% of Blade Pitch Less Thickness from Suction Surface

4.142 6.7% of Blade Pitch Less Thickness from Suction Surface

Vector Plots of Axial and Spanwise Velocities (Figures 4.143 – 4.154)

4.143 93.3% of Blade Pitch Less Thickness from Suction Surface

4.144 ~~85.4~~ 85.4% of Blade Pitch Less Thickness from Suction Surface

4.145 77.5% of Blade Pitch Less Thickness from Suction Surface

4.146 69.7% of Blade Pitch Less Thickness from Suction Surface

4.147 61.8% of Blade Pitch Less Thickness from Suction Surface

- 4.148 53.9% of Blade Pitch Less Thickness from Suction Surface
- 4.149 46.1% of Blade Pitch Less Thickness from Suction Surface
- 4.150 38.2% of Blade Pitch Less Thickness from Suction Surface
- 4.151 30.3% of Blade Pitch Less Thickness from Suction Surface
- 4.152 22.5% of Blade Pitch Less Thickness from Suction Surface
- 4.153 14.6% of Blade Pitch Less Thickness from Suction Surface
- 4.154 6.7% of Blade Pitch Less Thickness from Suction Surface
- 4.155 6.7% of Blade Pitch Less Thickness from Blade  
Suction Surface Yaw Angle Contours
- 4.156 Zero Cross Flow Angle Contours Close to the Blade  
Suction Surface

Static Pressure Coefficient Contours (Figures 4.157 to 4.161)

- 4.157 93.3% of Blade Pitch Less Thickness from Suction Surface
- 4.158 53.9% of Blade Pitch Less Thickness from Suction Surface
- 4.159 38.2% of Blade Pitch Less Thickness from Suction Surface
- 4.160 22.5% of Blade Pitch Less Thickness from Suction Surface
- 4.161 6.7% of Blade Pitch Less Thickness from Suction Surface
- 4.162 Blade Surface Static Pressure Coefficient Distribution  
(Showing Data from Adjacent Passages)
- 4.163 Blade Surface Static Pressure Coefficient Distribution  
Natural Boundary Layer Data
- 4.164 Plot on Blade Pressure Surface  
Location of Blade Surface Static Pressure Tappings
- 4.165 Plot on Blade Suction Surface  
Location of Blade Surface Static Pressure Tappings
- 4.166 Plot on Blade Pressure Surface Natural Boundary Layer Data  
Static Pressure Coefficient Contours
- 4.167 Plot on Blade Suction Surface Natural Boundary Layer Data  
Static Pressure Coefficient Contours

Slot 1 – Mean Flow Hot Wire Probe Data (Figures 5.1 – 5.4)

- 5.1 Hot Wire Experimental Data Points
- 5.2 Total Velocity Magnitude Contours
- 5.3 Yaw Angle Contours
- 5.4 Pitchwise Mass Meaned Hot Wire Probe Data
- 5.5 Slot 1 – Streamwise Spanwise Angle Contours  
(As New Wire Sensitivities)
- 5.6 Slot 1 – Streamwise Spanwise Angle Contours  
(Run End Wire Sensitivities)

Slot 1 – Fluctuating Flow Hot Wire Probe Data  
(Figures 5.7 – 5.14)

- 5.7 Normalized Turbulent Kinetic Energy Contours
- 5.8 Turbulence Intensity Contours for  $u'$
- 5.9 Turbulence Intensity Contours for  $v'$
- 5.10 Turbulence Intensity Contours for  $w'$
- 5.11 Slot1 – Pitchwise Mass Meaned Relative  
Turbulence Intensities  
(As New Wire Sensitivities)
- 5.12 Slot 1 – Pitchwise Mass Meaned Relative  
Turbulence Intensities  
(Run End Wire Sensitivities)
- 5.13 Normalized Shear Stress Contours (From  $uv$  Correlation)
- 5.14 Normalized Shear Stress Contours (From  $uw$  Correlation)

Slot 8 Mean Flow Hot Wire Probe Data (Figures 5.15 – 5.19)

- 5.15 Hot Wire Experimental Data Points
- 5.16 Total Velocity Magnitude Contours
- 5.17 Yaw Angle Contours
- 5.18 Pitchwise Mass Meaned Hot Wire Probe Data
- 5.19 Spanwise Angle Contours

Slot 8 Fluctuating Flow Hot Wire Probe Data  
(Figures 5.20 – 5.26)

- 5.20 Normalized Turbulent Kinetic Energy Contours
- 5.21 Turbulence Intensity Contours for  $u'$
- 5.22 Turbulence Intensity Contours for  $v'$
- 5.23 Turbulence Intensity Contours for  $w'$
- 5.24 Pitchwise Mass Meaned Relative Turbulence Intensities
- 5.25 Pitchwise Mass Meaned Relative Turbulent Kinetic Energy and Total Pressure Loss Coefficient
- 5.26 Normalized Shear Stress Contours (From  $uv$  Correlation)
- 5.27 Normalized Shear Stress Contours (From  $uw$  Correlation)

Slot 1 Data (Figures 6.1 – 6.7)

- 6.1 Experimental Data Points Thickened Inlet Boundary Layer
- 6.2 Total Pressure Loss Coefficient Contours Thickened Inlet Boundary Layer
- 6.3 Total Pressure Loss Coefficient Contours Thinned Inlet Boundary layer
- 6.4 Streamwise Spanwise Angle Contours Thickened Inlet Boundary Layer
- 6.5 Streamwise Spanwise Angle Contours Thinned Inlet Boundary Layer
- 6.6 Total Velocity Magnitude Contours Thickened Inlet Boundary Layer
- 6.7 Total Velocity Magnitude Contours Thinned Inlet Boundary Layer

Slot 8 Data – (Figures 6.8 – 6.14)

- 6.8 Total Pressure Loss Coefficient Contours Thickened Inlet Boundary Layer
- 6.9 Total Pressure Loss Coefficient Contours Thinned Inlet Boundary Layer
- 6.10 Comparison of the Three Inlet Boundary Layer Loss Cores

- 6.11 Vector Plot of Secondary Velocities  
Thickened Inlet Boundary Layer
- 6.12 Vector Plot of Secondary Velocities  
Thinned Inlet Boundary Layer
- 6.13 Static Pressure Coefficient Contours  
Thickened Inlet Boundary Layer
- 6.14 Static Pressure Coefficient Contours  
Thinned Inlet Boundary Layer

Slot 10 Data (Figures 6.15 – 6.22)

- 6.15 Experimental Data Points  
Thickened Inlet Boundary Layer
- 6.16 Total Pressure Loss Coefficient Contours  
Thickened Inlet Boundary Layer
- 6.17 Total Pressure Loss Coefficient Contours  
Thinned Inlet Boundary Layer
- 6.18 Comparison of the Three Inlet Boundary Layer Loss Cores
- 6.19 Vector Plot of Secondary Velocities  
Thickened Inlet Boundary Layer
- 6.20 Vector Plot of Secondary Velocities  
Thinned Inlet Boundary Layer
- 6.21 Static Pressure Coefficient Contours  
Thickened Inlet Boundary Layer
- 6.22 Static Pressure Coefficient Contours  
Thinned Inlet Boundary Layer
- 6.23 Pitchwise Mass Meaned Yaw Angle Upstream of  
the Cascade
- 6.24 Pitchwise Mass Meaned Total Pressure Loss  
Coefficient Upstream of the Cascade
- 6.25 Slot 8 Pitchwise Mass Meaned Yaw Angle
- 6.26 Slot 10 Pitchwise Mass Meaned Yaw Angle
- 6.27 Slot8 Pitchwise Mass Meaned Total Pressure  
Loss Coefficient
- 6.28 Slot 10 Pitchwise Mass Meaned Total Pressure  
Loss Coefficient

- 6.29 Blade Surface Static Pressure Coefficient  
Distribution Thickened Boundary Layer Data
- 6.30 Blade Surface Static Pressure Coefficient  
Distribution Thinned Boundary Layer Data
- 6.31 Plot on Blade Pressure Surface Thickened Boundary  
Layer Data Static Pressure Coefficient Contours
- 6.32 Plot on Blade Pressure Surface Thinned Boundary  
Layer Data Static Pressure Coefficient Contours
- 6.33 Plot on Blade Suction Surface Thickened Boundary  
Layer Data Static Pressure Coefficient Contours
- 6.34 Plot on Blade Suction Surface Thinned Boundary  
Layer Data Static Pressure Coefficient Contours
- 7.1 The Triangular Loss Core
- 7.2 Durham Cascade  
Exit Angle Prediction Natural Inlet Boundary layer
- 7.3 Durham Cascade  
Secondary Loss Prediction Natural Inlet Boundary Layer
- 7.4 Durham Cascade  
Exit Angle Prediction Thickened Inlet Boundary Layer
- 7.5 Durham Cascade  
Secondary Loss Prediction Thickened Inlet Boundary Layer
- 7.6 Durham Cascade  
Exit Angle Prediction Thinned Inlet Boundary Layer
- 7.7 Durham Cascade  
Secondary Loss Prediction Thinned Inlet Boundary Layer
- 7.8 Carrick's Cascade  
Secondary Loss Prediction Zero Inlet Skew Low Reynolds Number
- 7.9 Carrick's Cascade  
Secondary Loss Prediction High Inlet Skew Low Reynolds Number
- 7.10 Sjolander's Cascade Secondary Loss Prediction
- 7.11 Test Turbine Nozzle Guide Vane Exit Angle Prediction
- 7.12 Test Turbine Nozzle Guide Vane Secondary Loss Prediction
- 7.13 Test Turbine Rotor Exit Angle Prediction
- 7.14 Test Turbine Rotor Secondary Loss Prediction



AIII.1 Hot Wire Probe Velocity Components

AIII.2 Hot Wire Probe Cascade Velocity Components

# LOW SPEED WIND TUNNEL WORKING SECTION AND CASCADE ARRANGEMENT

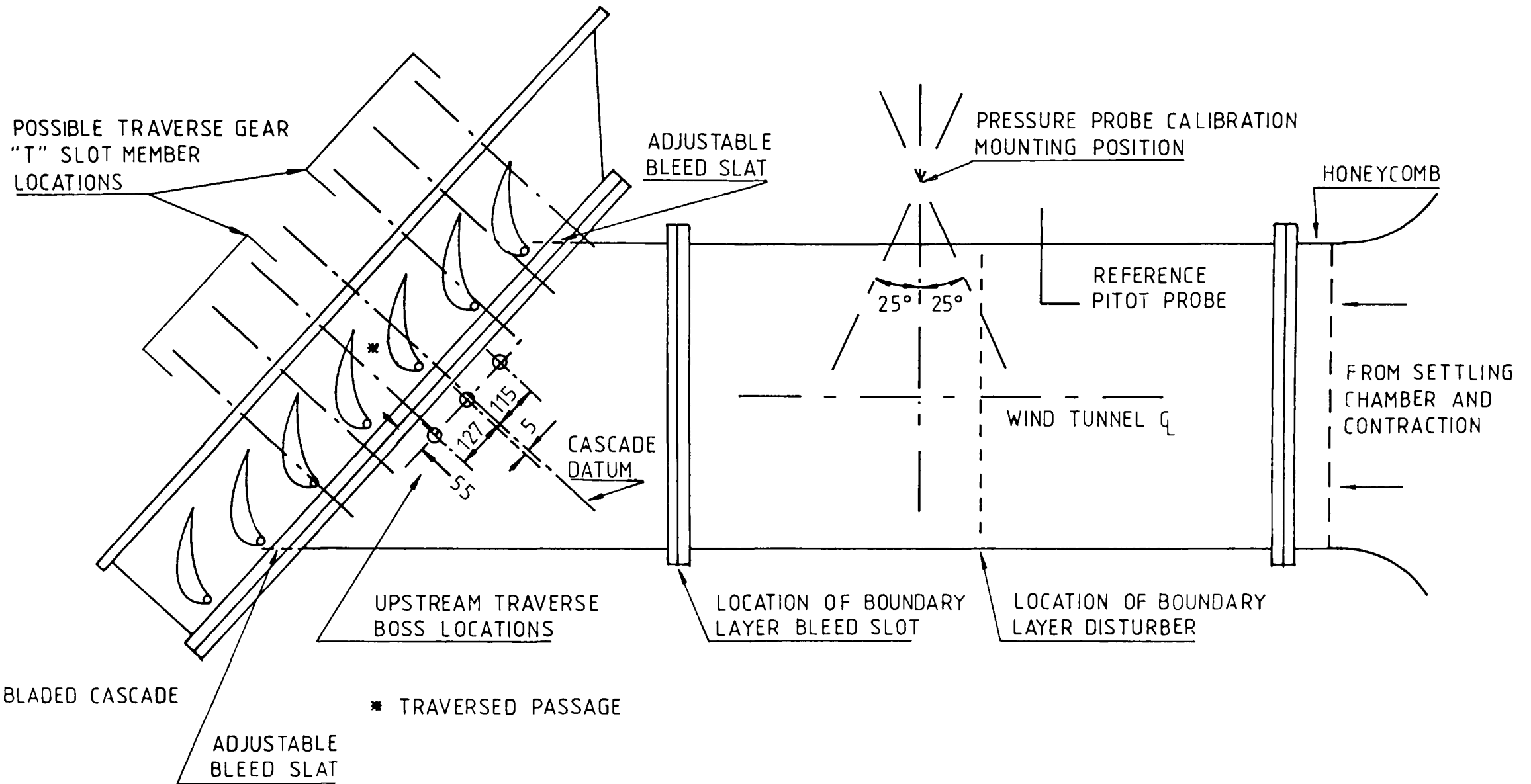


FIGURE 3.1

# POSITION OF BLADE SURFACE PRESSURE TAPPINGS AT MIDSPAN

X-AXIS TANGENTIAL CO-ORDINATE FROM TRAILING EDGE DATUM (MM)

Y-AXIS AXIAL CO-ORDINATE FROM TRAILING EDGE DATUM (MM)

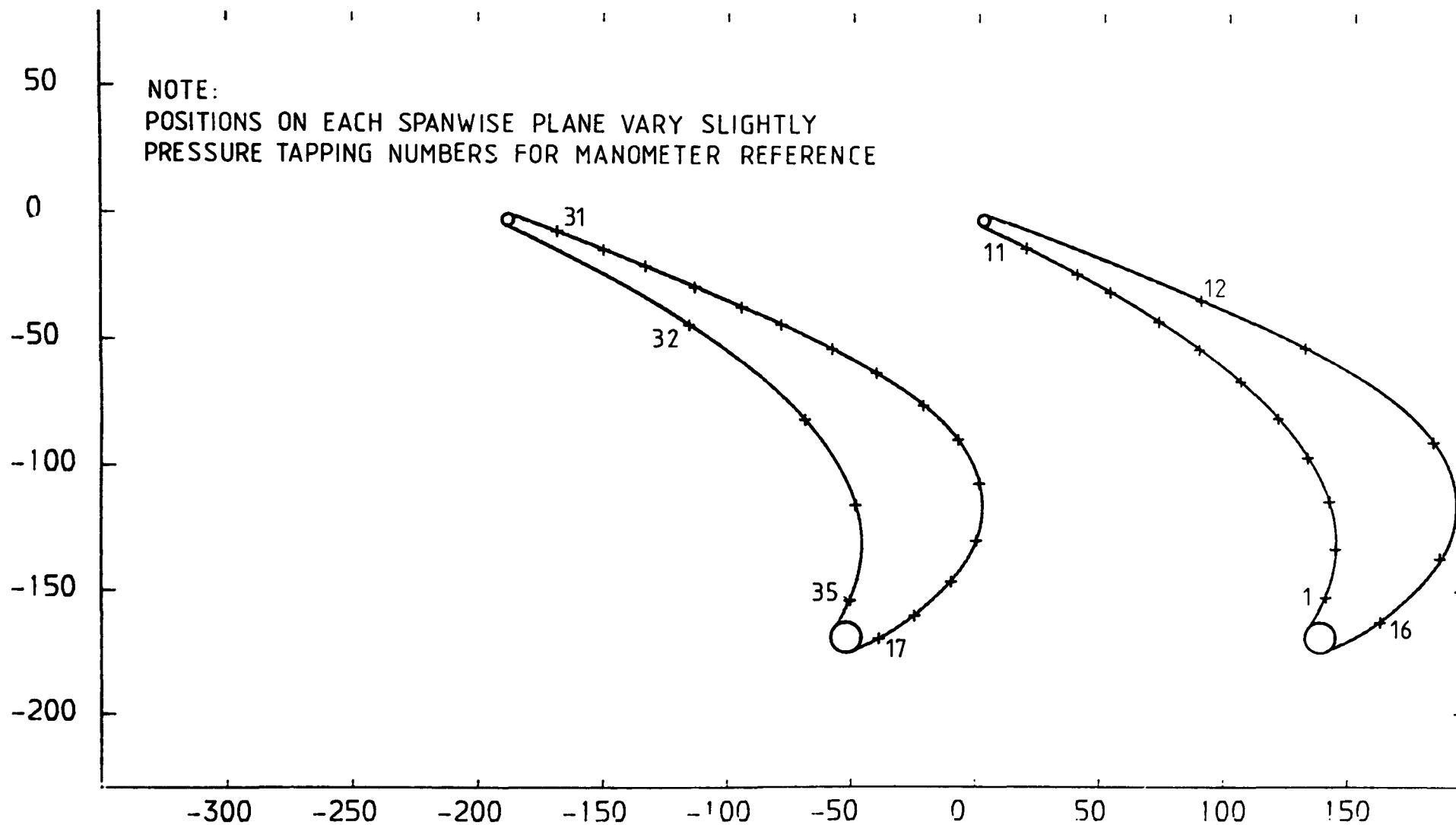


FIGURE 3.2

POSITIONS OF THE EXPERIMENTAL TRAVERSING SLOTS

X-AXIS TANGENTIAL CO-ORDINATE FROM TRAILING EDGE DATUM (MM)

Y-AXIS AXIAL CO-ORDINATE FROM TRAILING EDGE DATUM (MM)

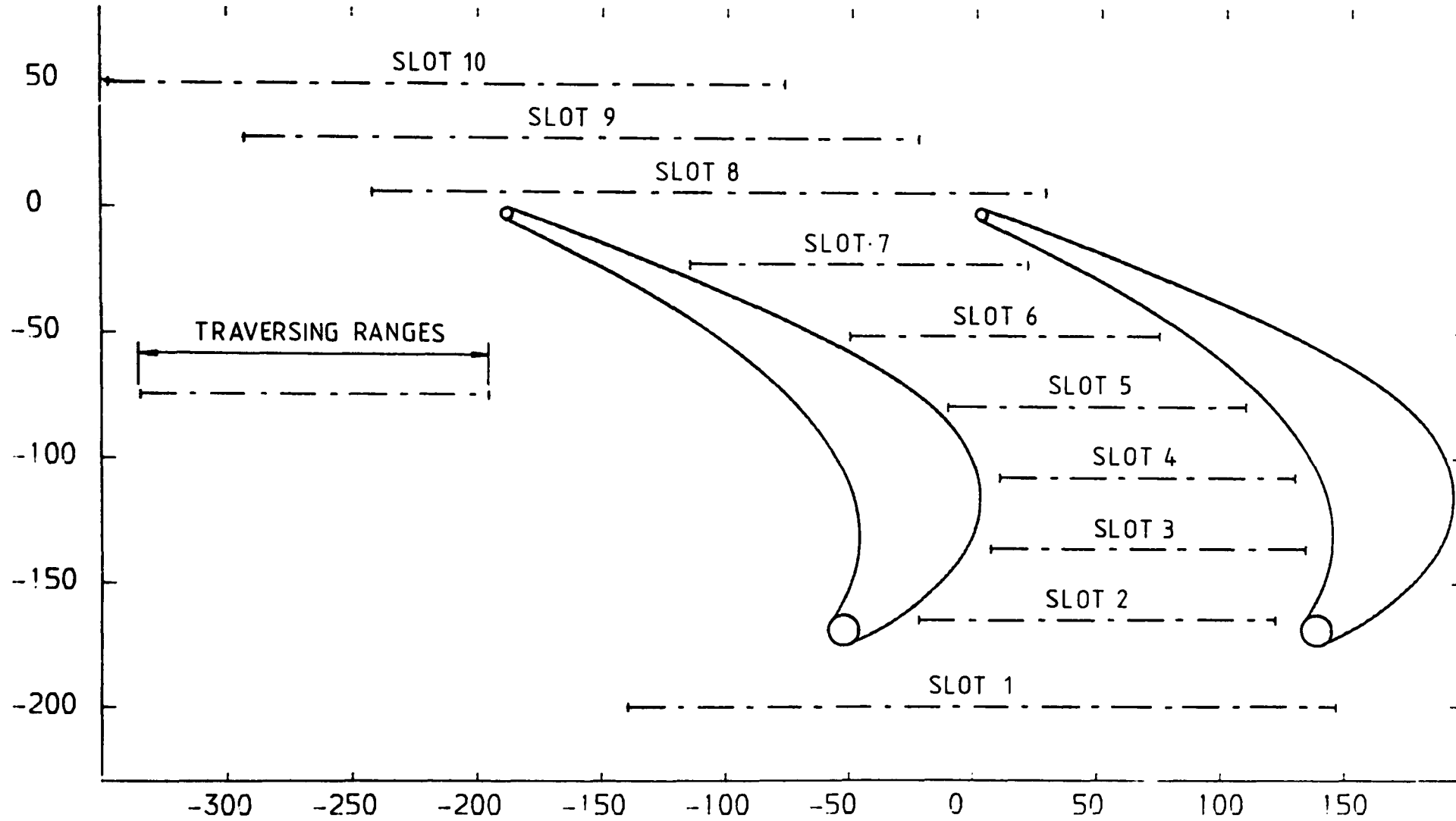


FIGURE 3.3

CASCADE SIGN CONVENTION

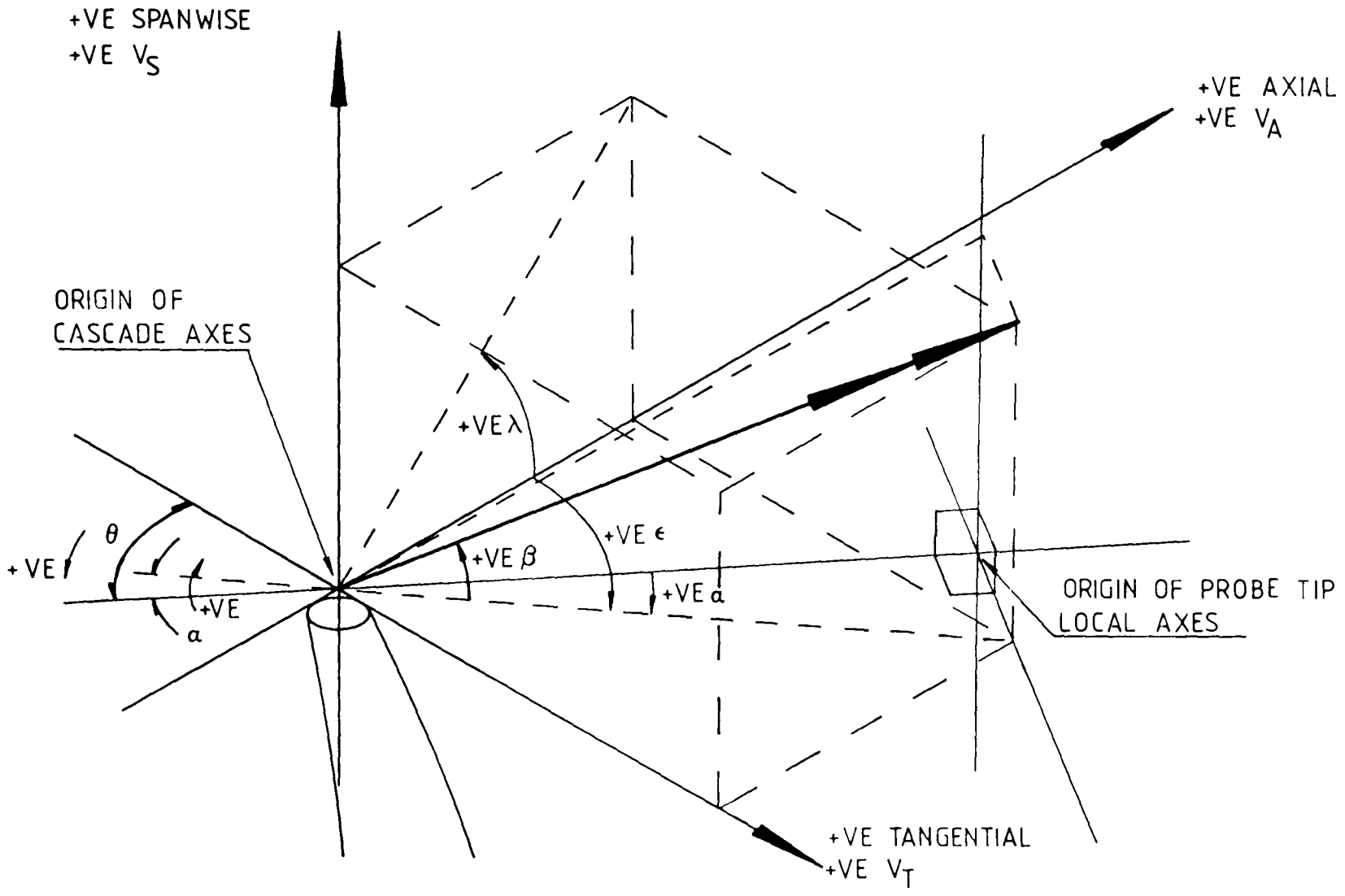


FIG 3.4

CASCADE ENDWALL BOUNDARY LAYER DISTURBER

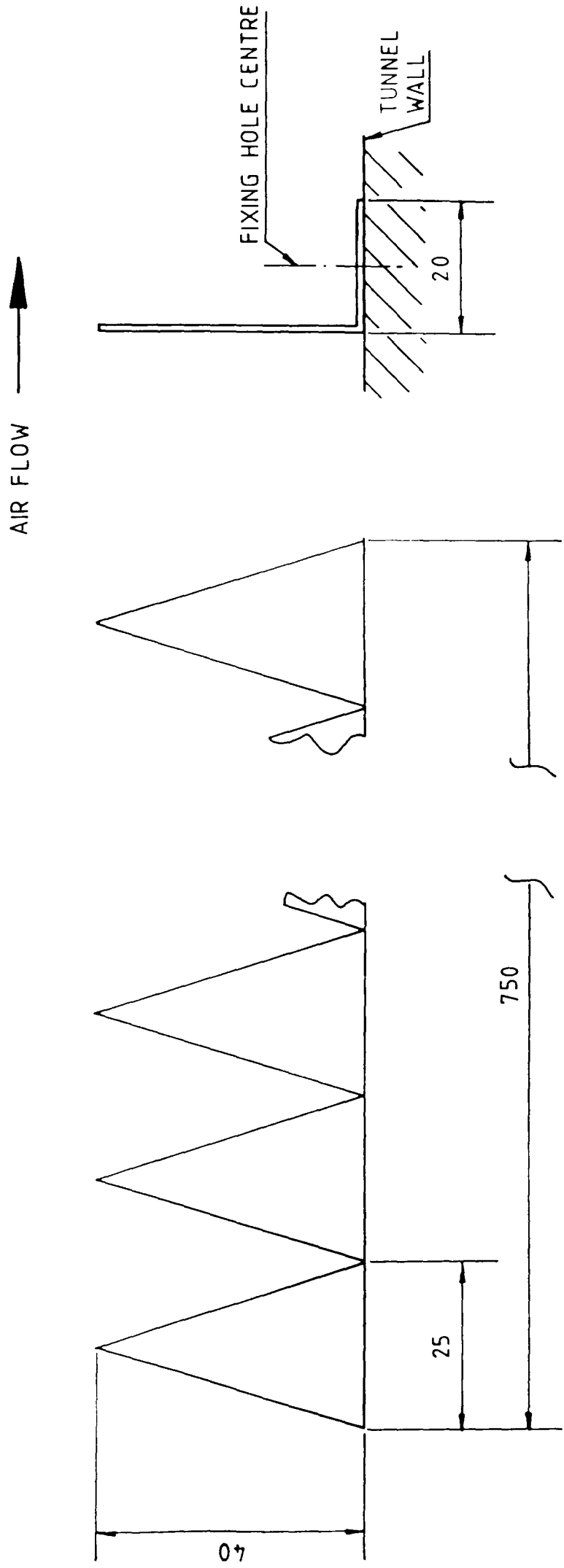


FIGURE 3.5

# DATA ACQUISITION UNIT

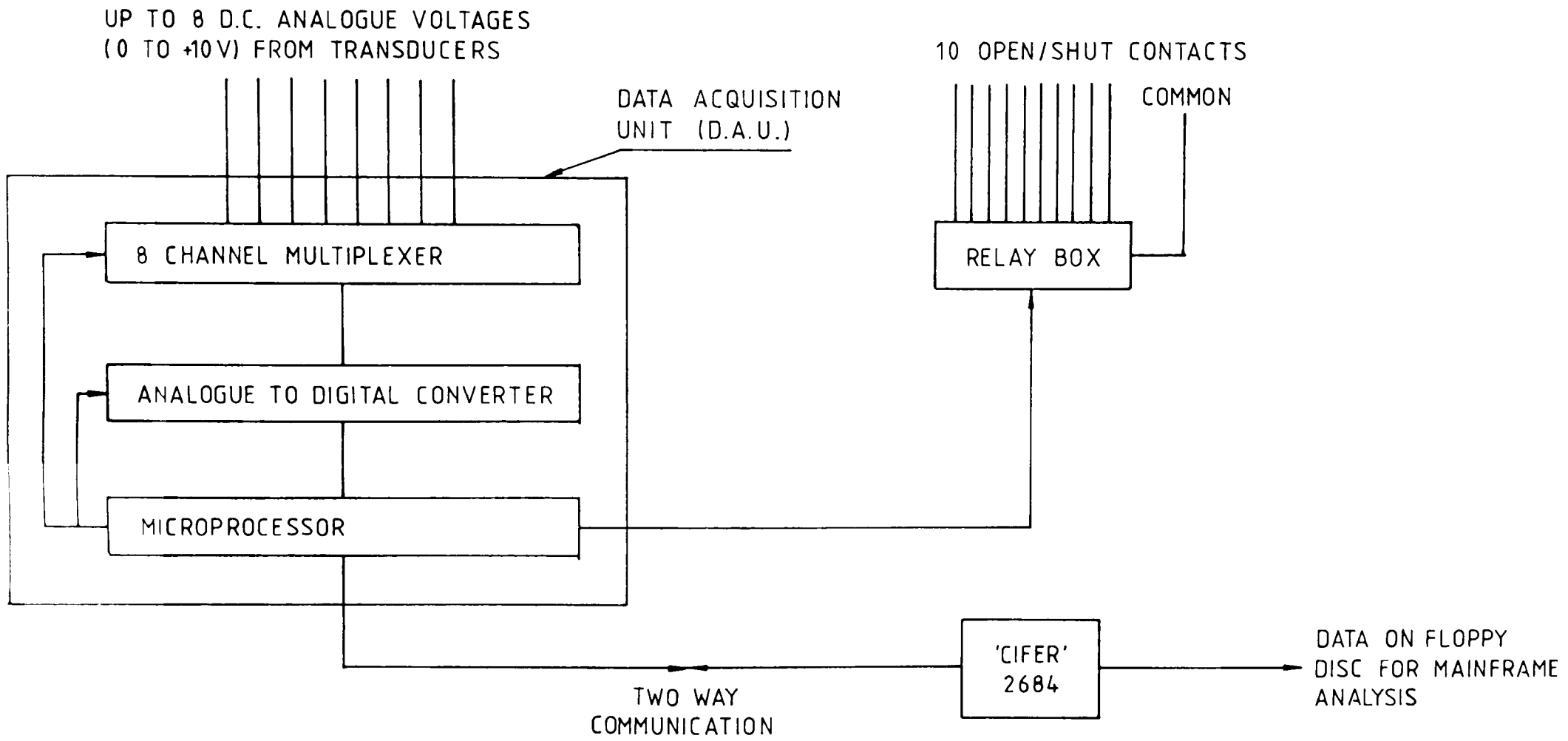


FIGURE 3.6

# PRESSURE PROBE ARRANGEMENT

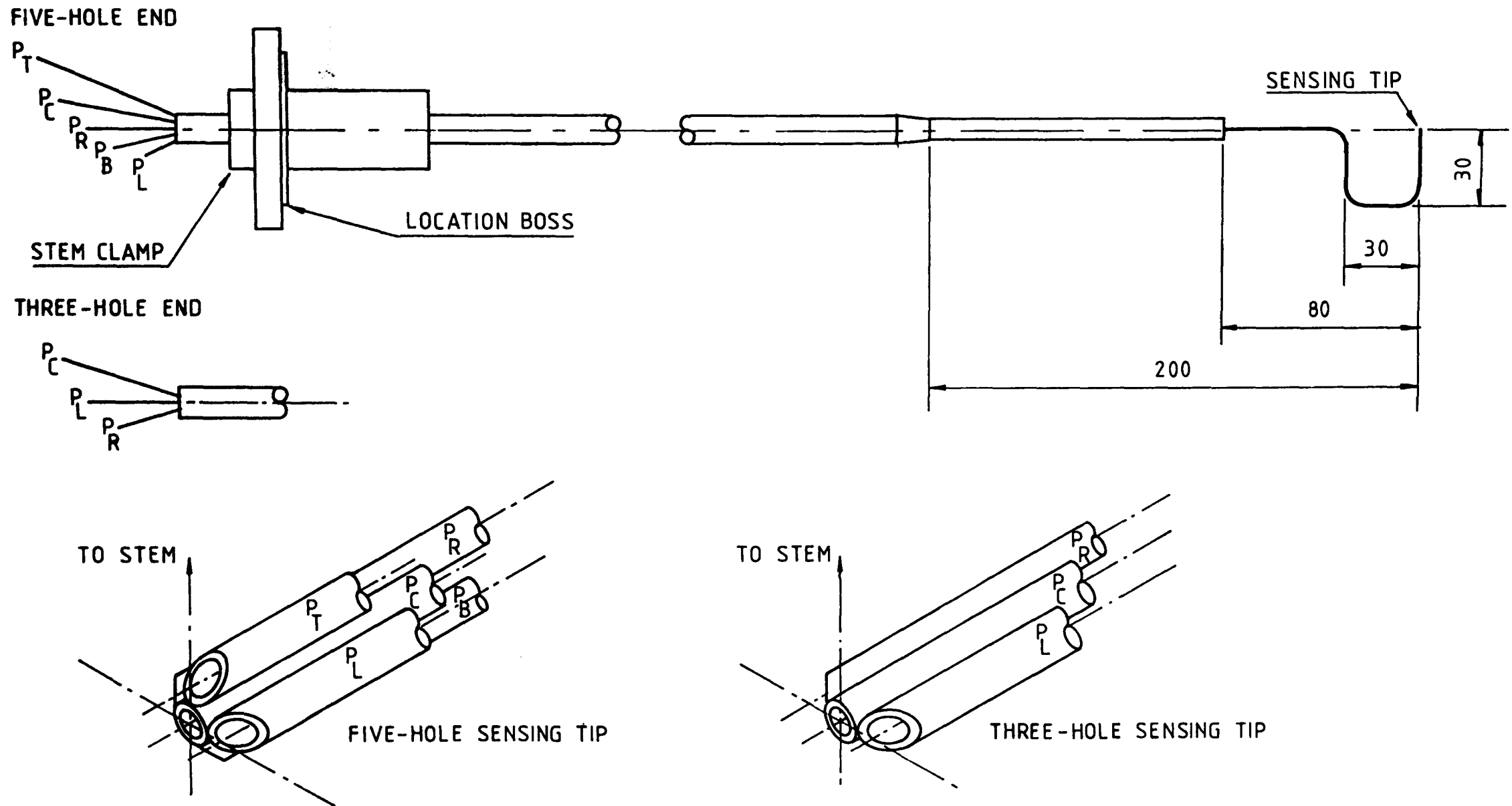
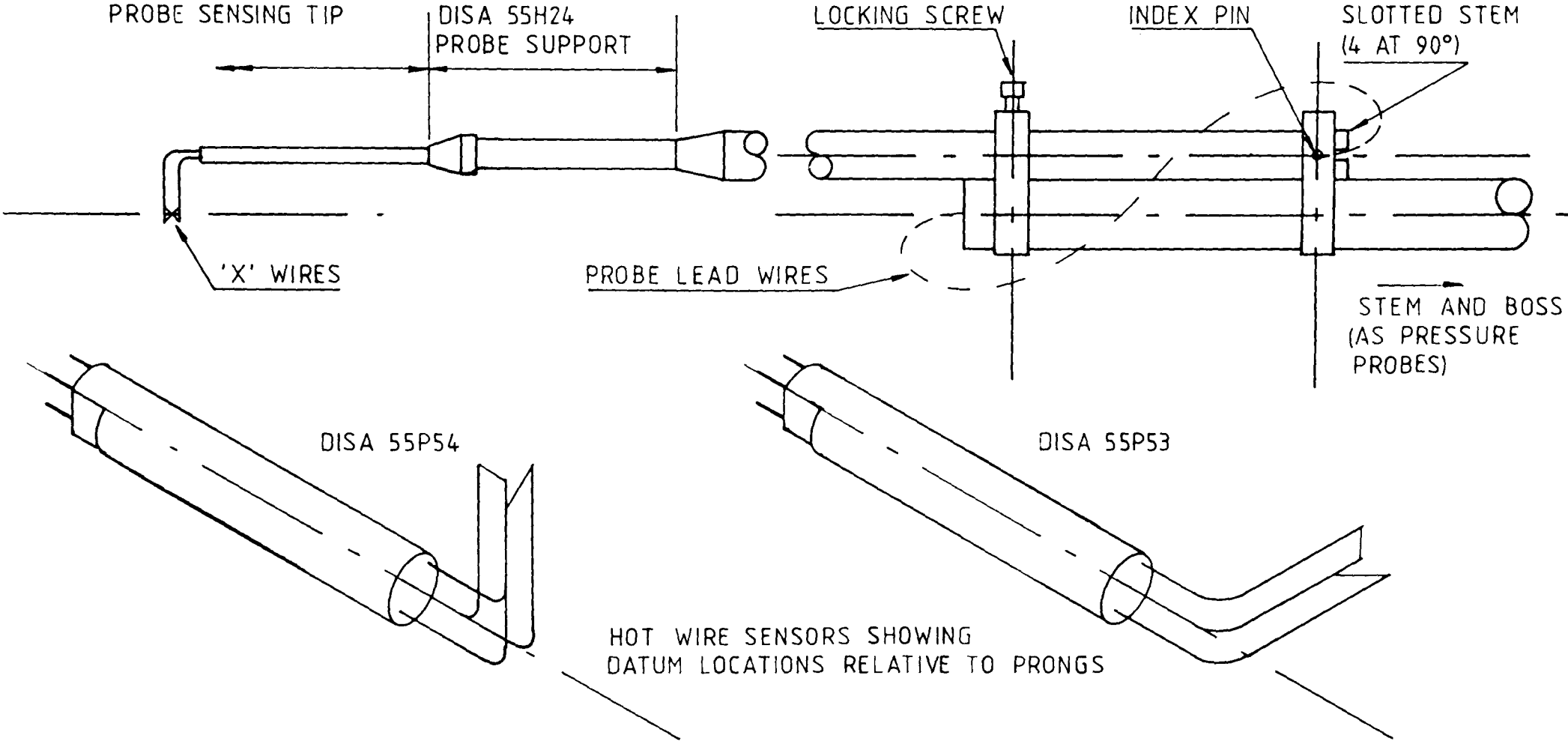


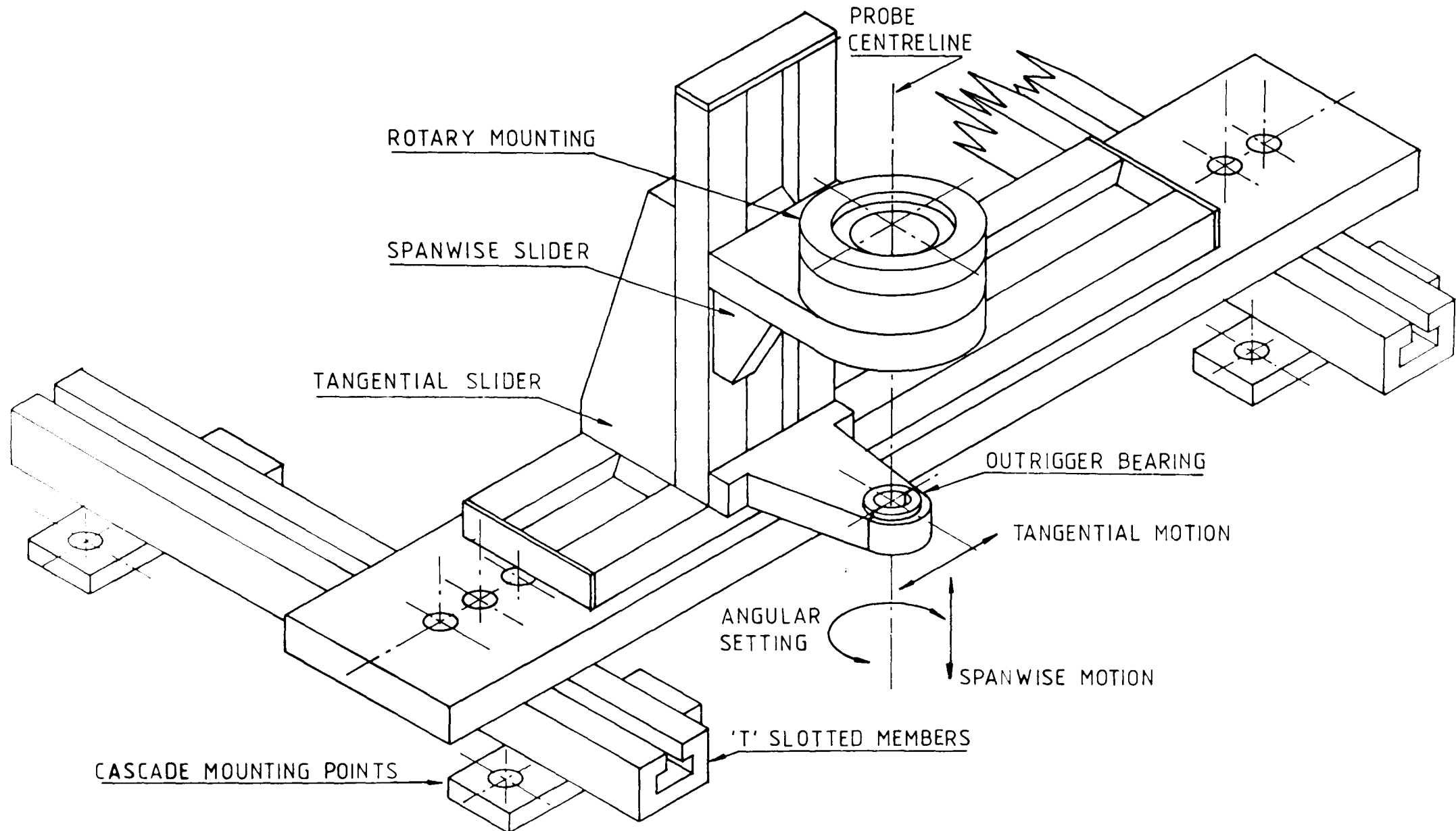
FIGURE 3.7



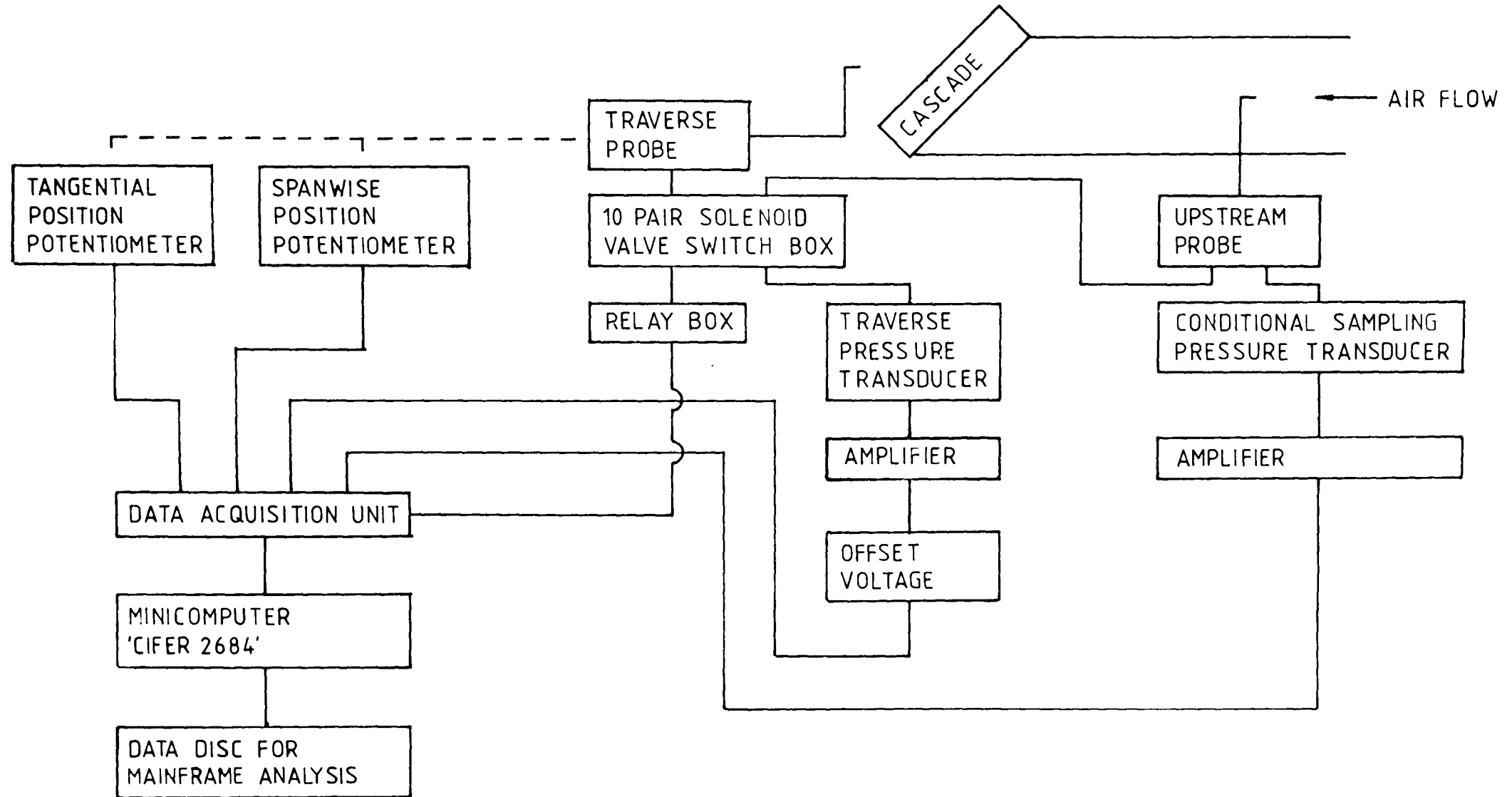
# HOT WIRE PROBE STEM ARRANGEMENT



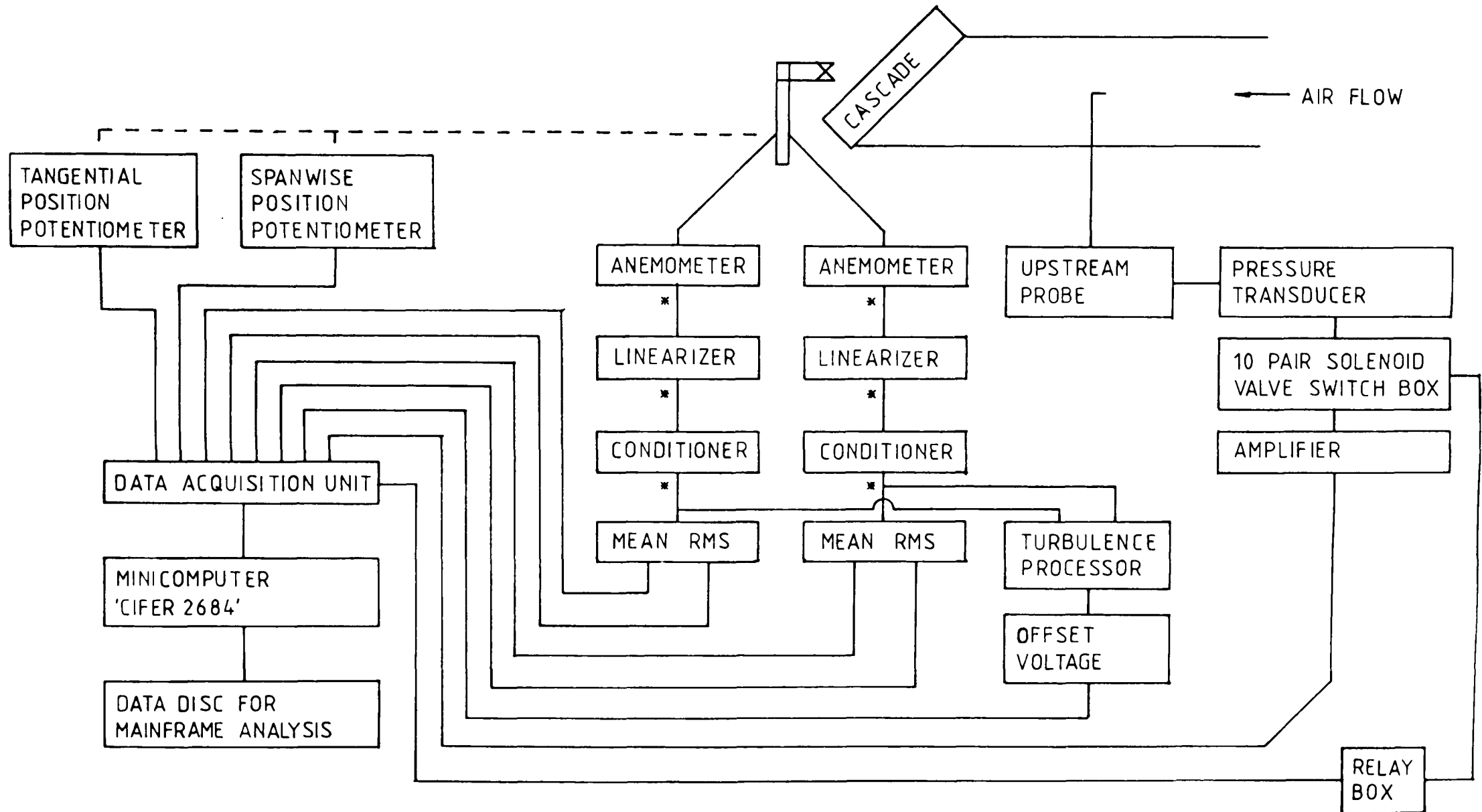
# PROBE TRAVERSING GEAR



# DATA ACQUISITION SYSTEM FOR PRESSURE PROBE TRAVERSING



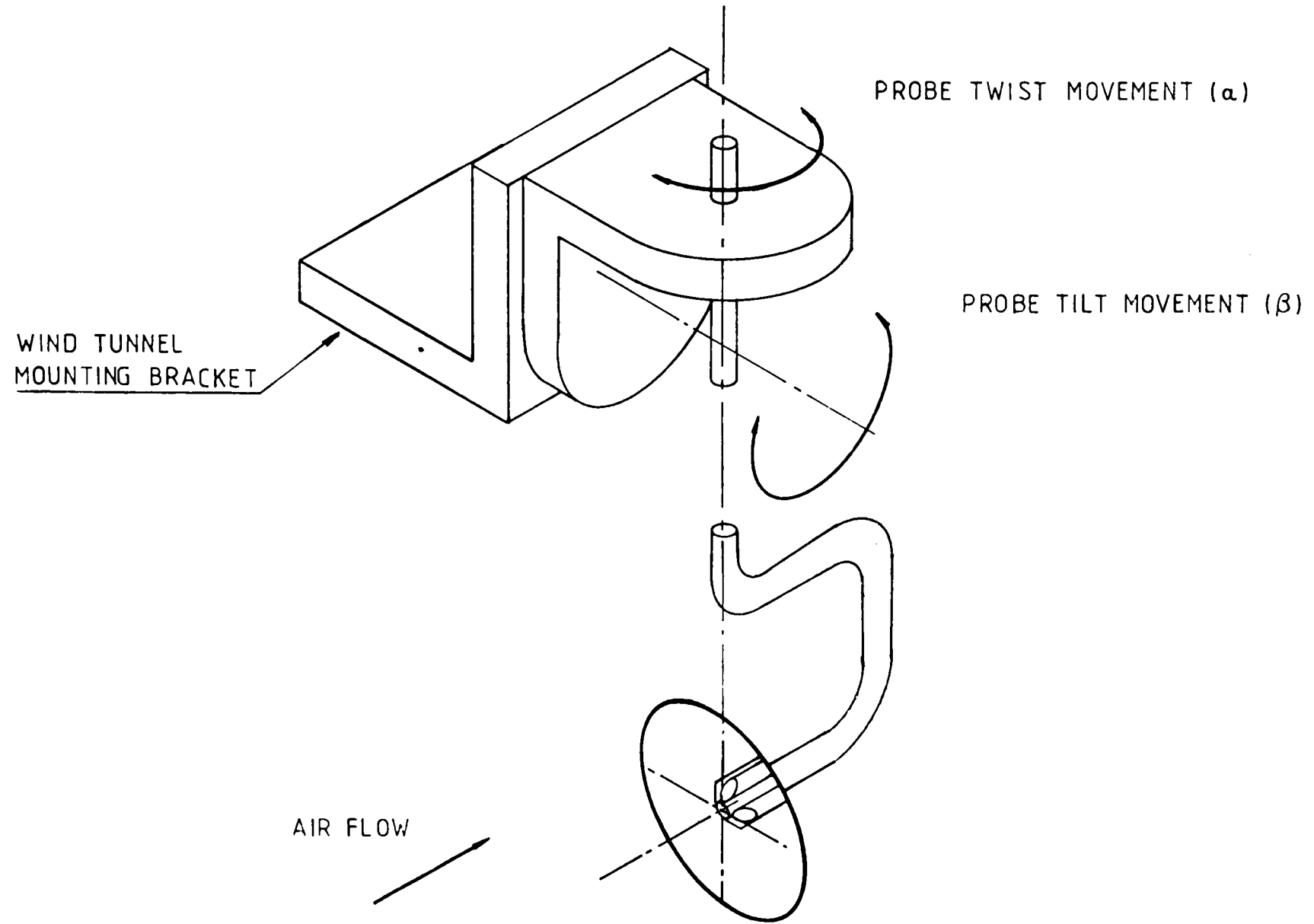
# DATA ACQUISITION SYSTEM FOR HOT WIRE PROBE TRAVERSING



▪ OSCILLOSCOPE CONNECTION POINT FOR SIGNAL VALIDATION

FIGURE 2.11

# PRESSURE PROBE CALIBRATION MOUNTING



# HOT WIRE PROBE CALIBRATION JET

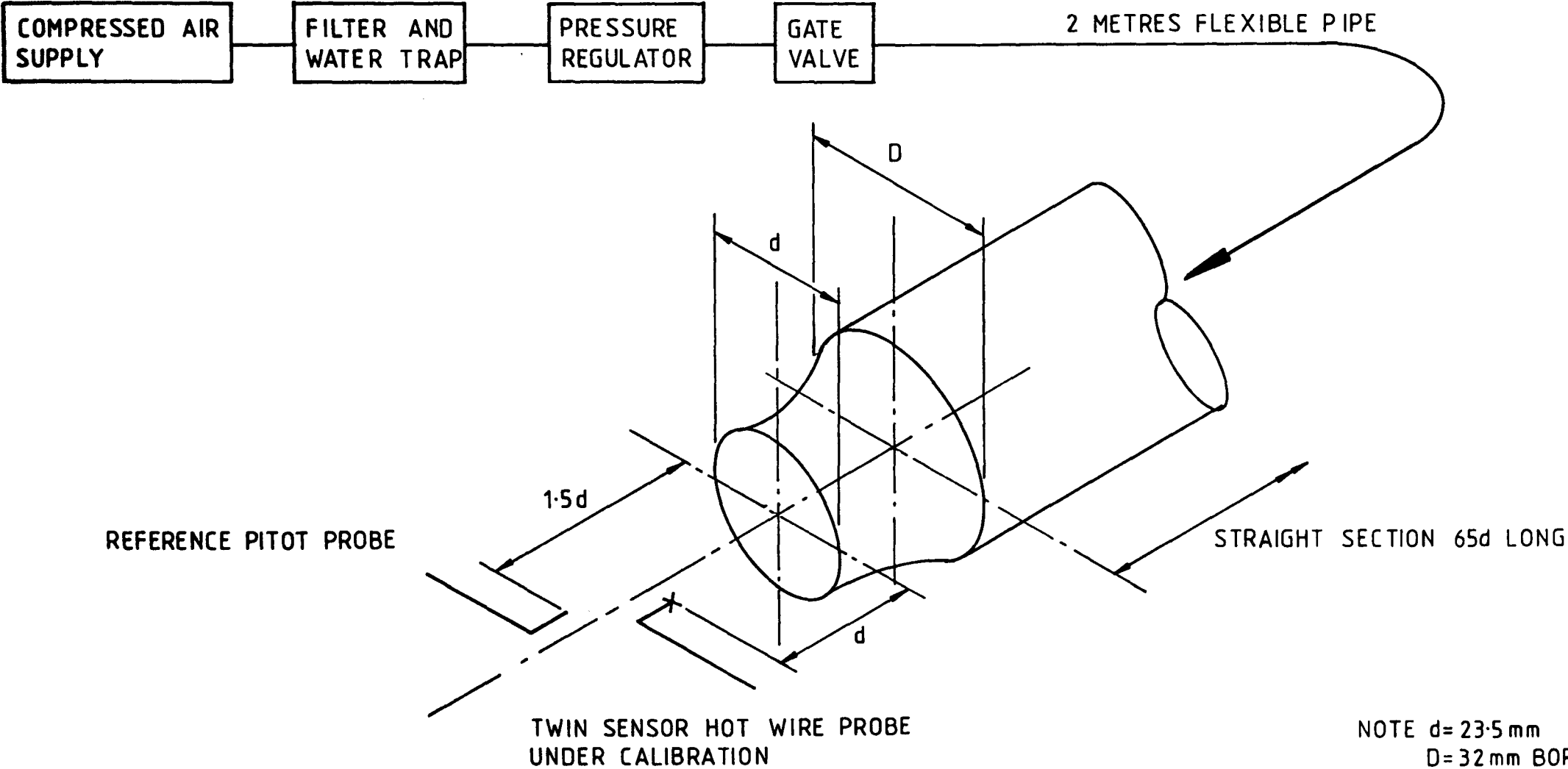


FIGURE 3.43

# HOT WIRE PROBE CALIBRATION JET TRAVERSE DATA

X-AXIS RADIAL TRAVERSE POSITION NORMALIZED USING NOZZLE RADIUS

Y-AXIS LOCAL JET VELOCITY NORMALIZED USING CENTRAL VELOCITY

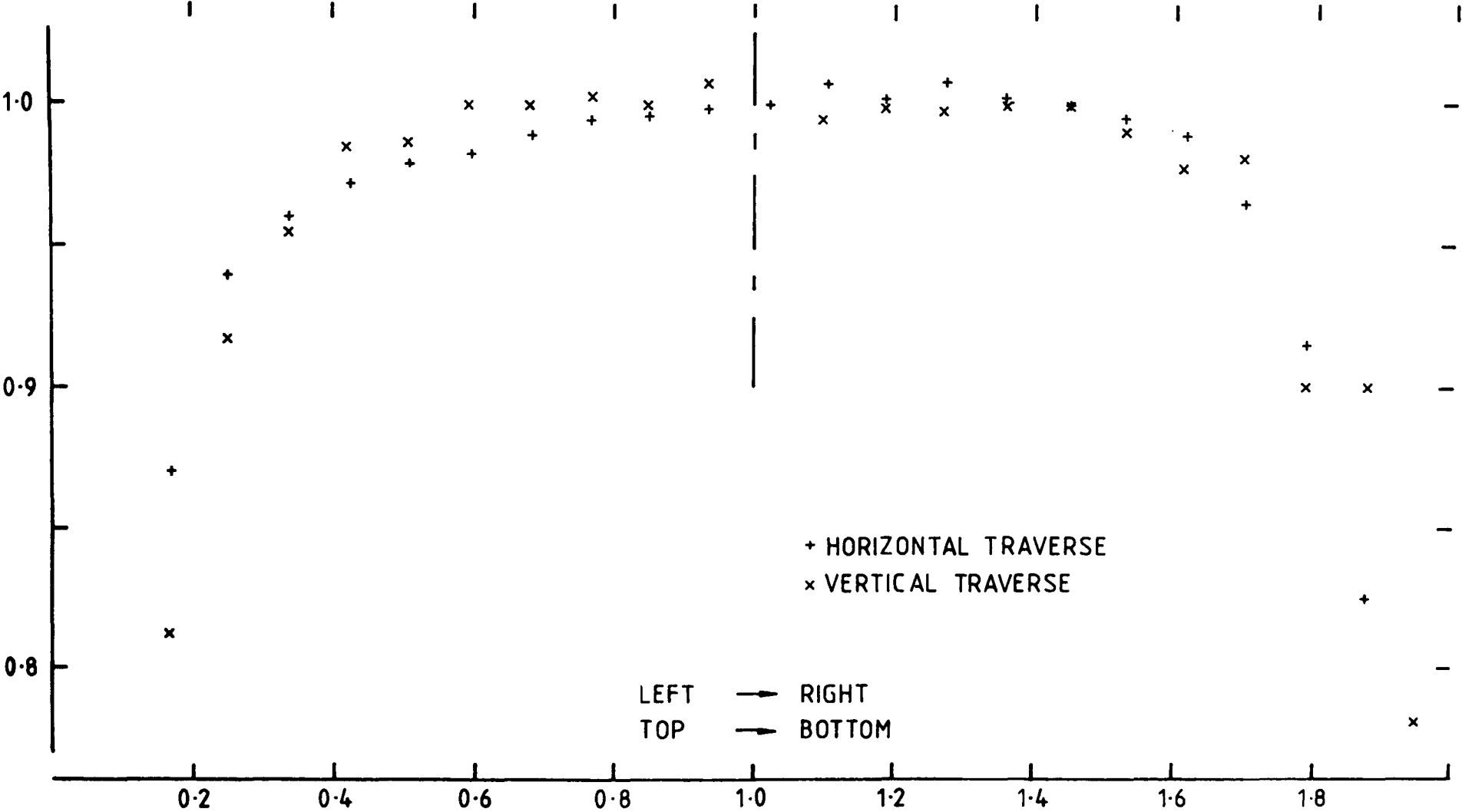


FIGURE 3.14

# A TYPICAL HOT WIRE ANEMOMETER CALIBRATION

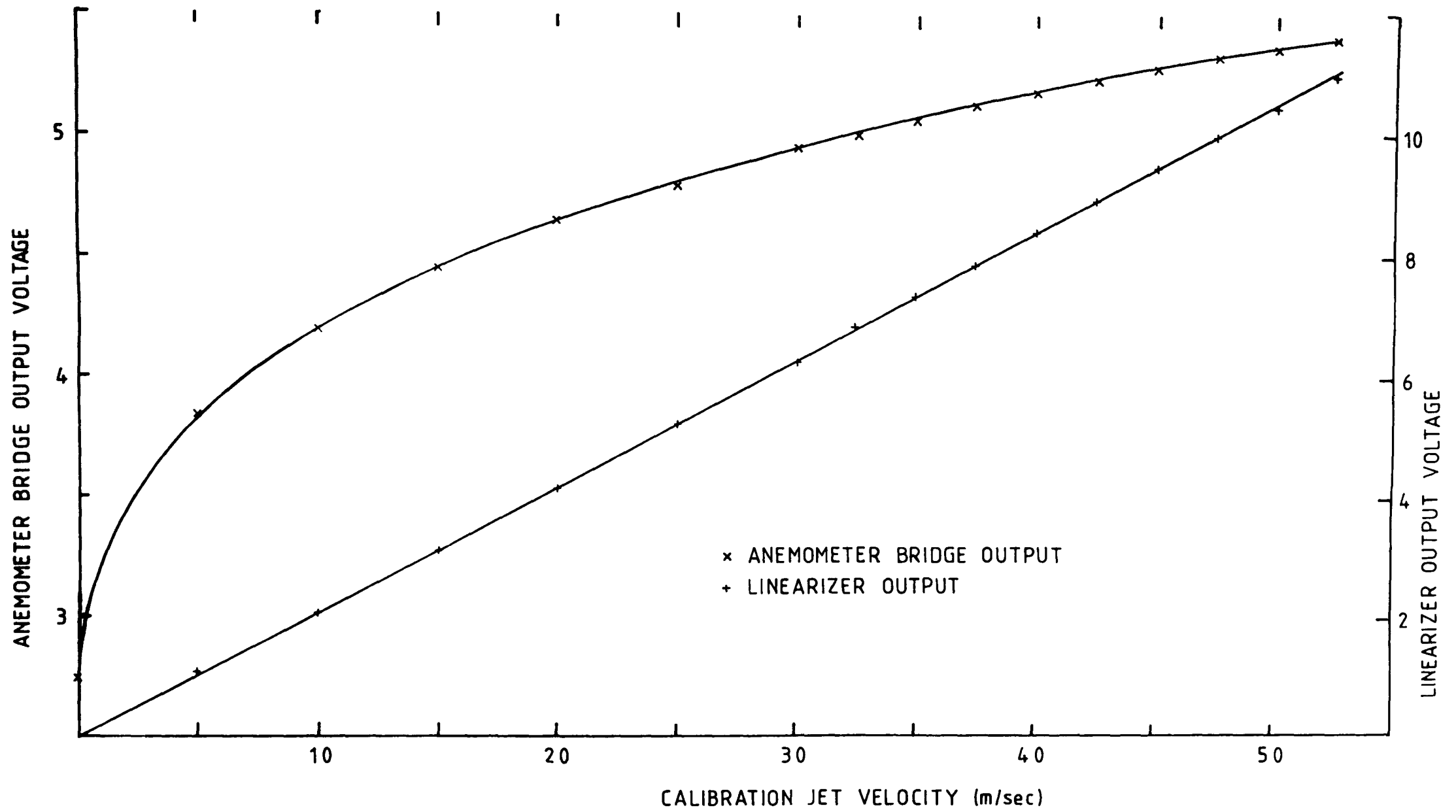


FIGURE 3.15



# CONDITIONAL SAMPLING OF PRESSURE PROBE DATA

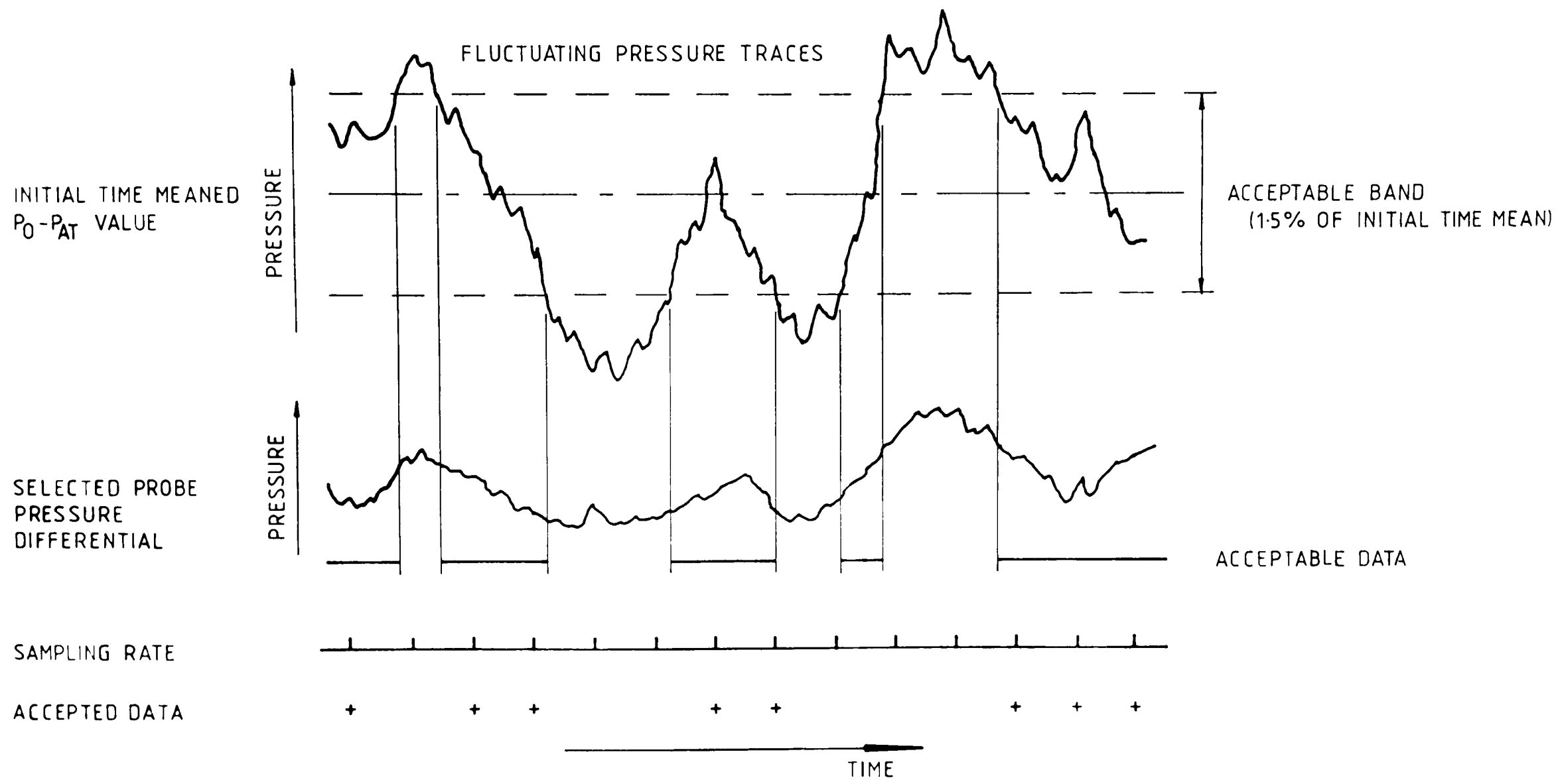
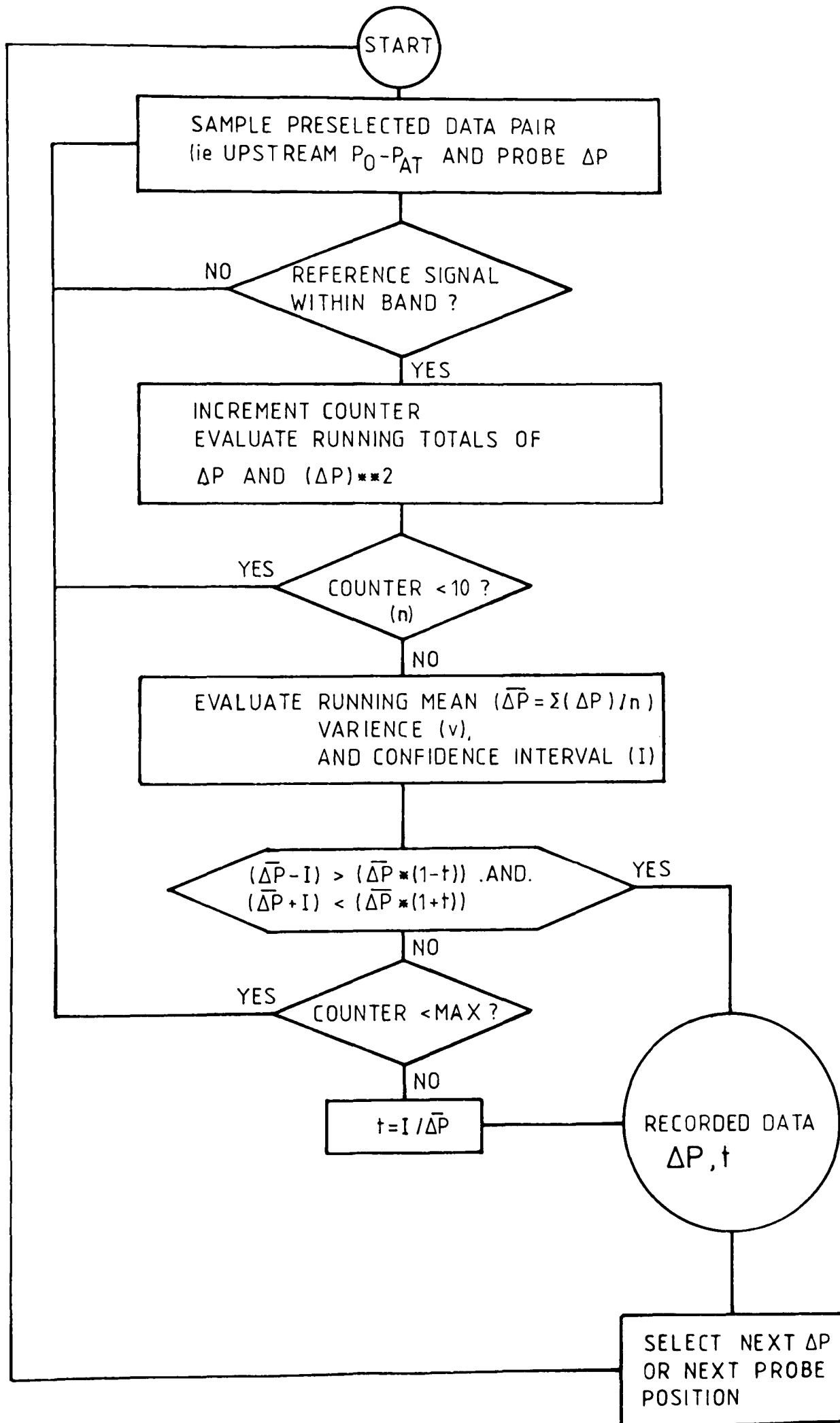


FIGURE 3.16

# CONDITIONAL SAMPLING METHOD



NOTE : AT START TOLERANCE (t) = ±1%

FIGURE 3.17

# FIVE-HOLE PROBE DATA ANALYSIS

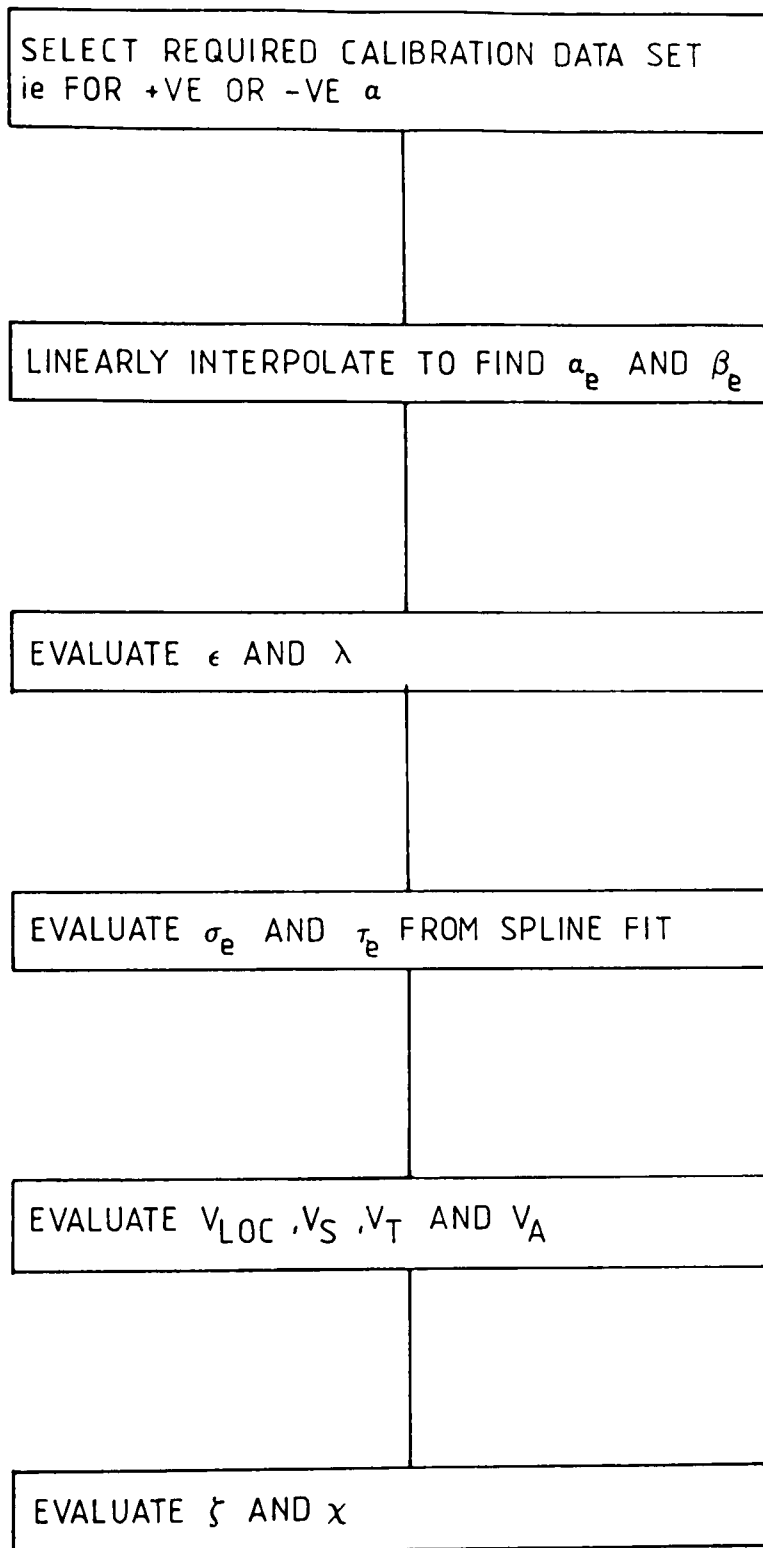


FIGURE 3.18

FIVE-HOLE PROBE  $\phi$  AND  $\psi$  AT  $\alpha=0^\circ$

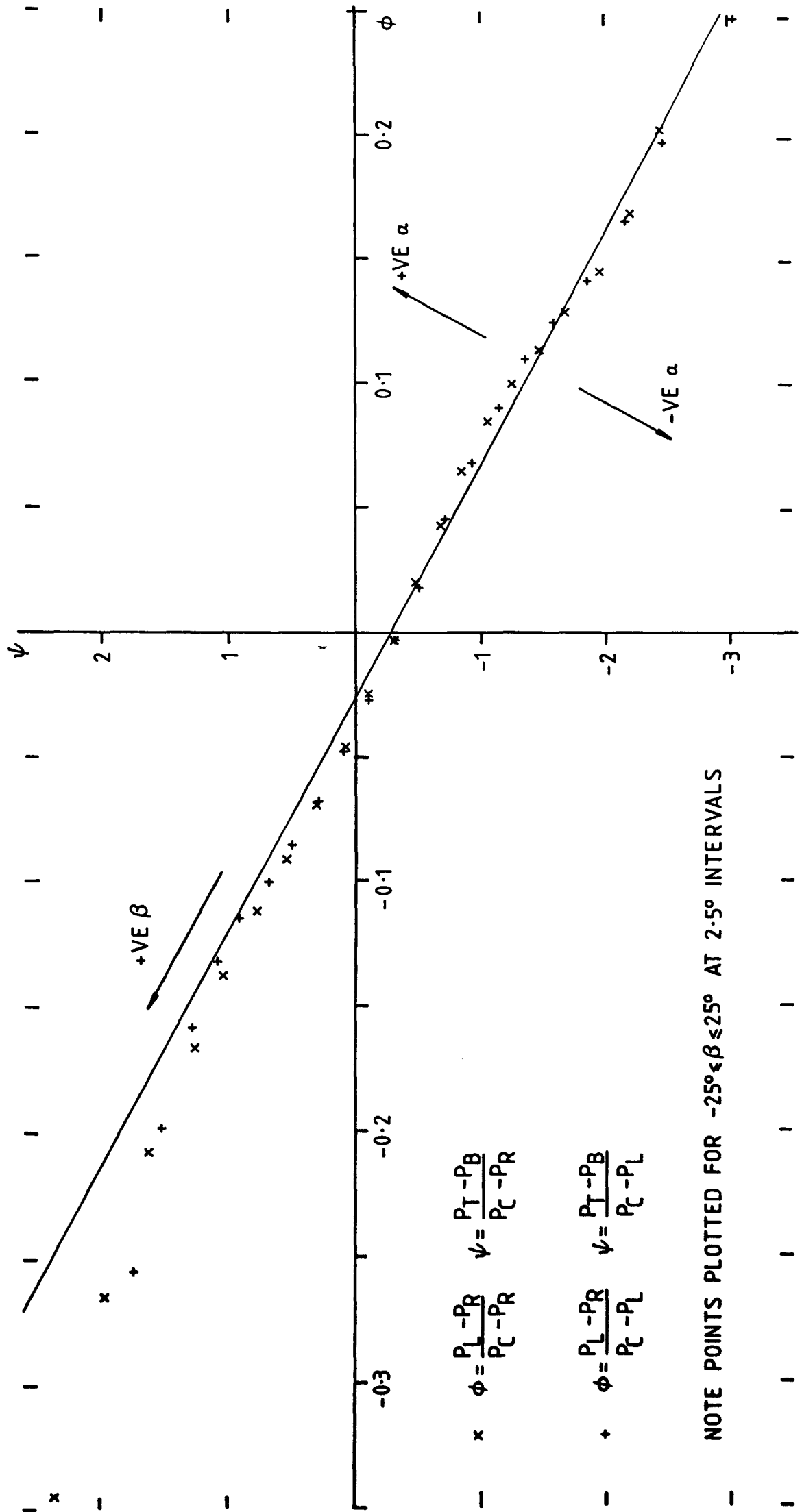
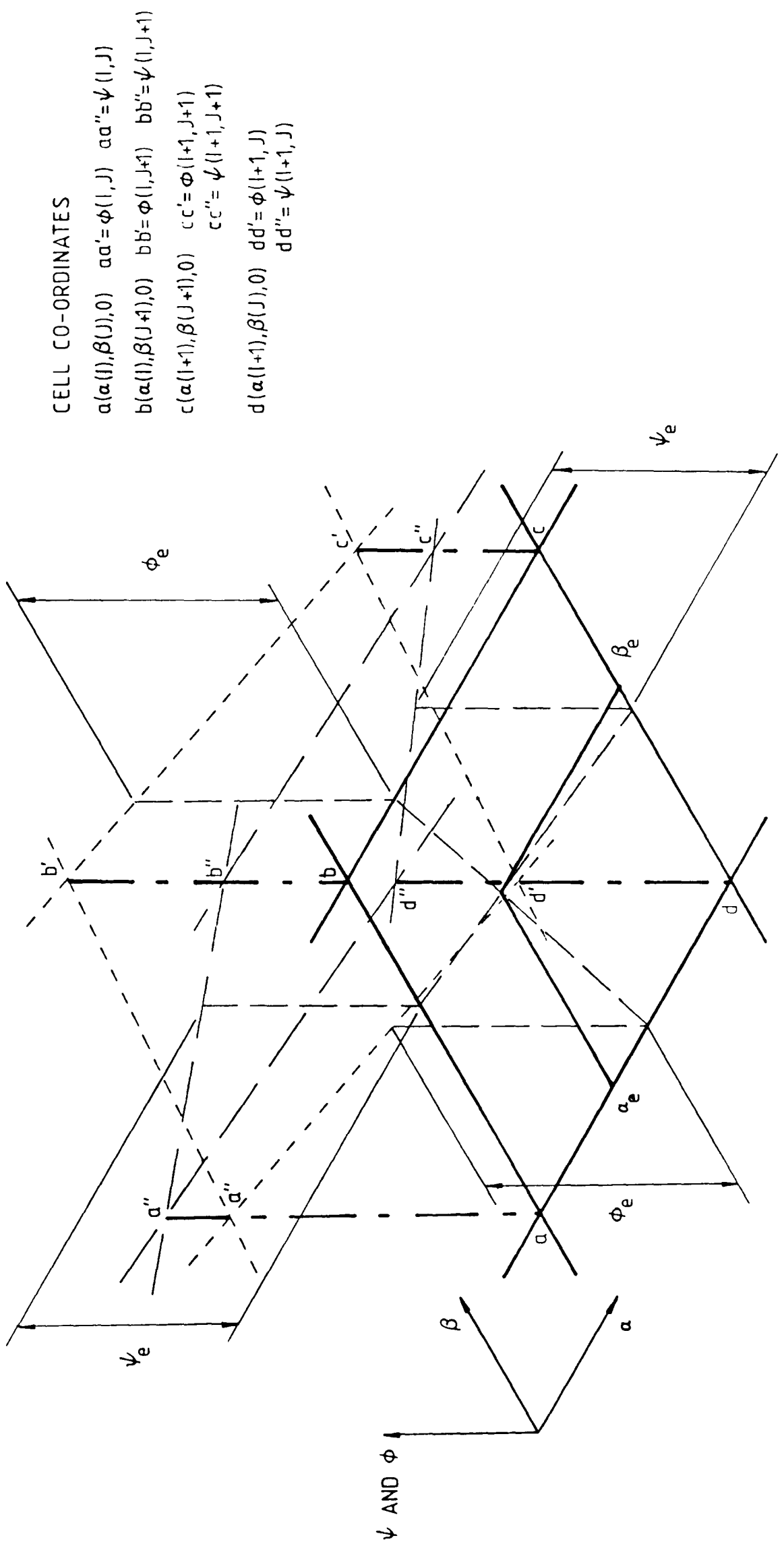


FIGURE 3.19

# FIVE-HOLE PROBE DATA ANALYSIS : AN ANALYSIS CELL



**CELL CO-ORDINATES**

- $a(\alpha(l), \beta(j), 0)$      $a a' = \phi(l, j)$      $a a'' = \psi(l, j)$
- $b(\alpha(l), \beta(j+1), 0)$      $b b' = \phi(l, j+1)$      $b b'' = \psi(l, j+1)$
- $c(\alpha(l+1), \beta(j+1), 0)$      $c c' = \phi(l+1, j+1)$
- $c c'' = \psi(l+1, j+1)$
- $d(\alpha(l+1), \beta(j), 0)$      $d d' = \phi(l+1, j)$
- $d d'' = \psi(l+1, j)$

FIGURE 3.20

# A CONTOUR PLOTTING CELL

## CELL CO-ORDINATES

$a(X(I-1), Y(I-1, J), Z(I-1, J))$

$b(X(I-1), Y(I-1, J+1), Z(I-1, J+1))$

$c(X(I), Y(I, J+1), Z(I, J+1))$

$d(X(I), Y(I, J), Z(I, J))$

$e(0.5 \times (X(I-1) + X(I)), 0.25 \times (Y(I-1, J) + Y(I-1, J+1) + Y(I, J+1) + Y(I, J)), 0.25 \times (Z(I-1, J) + Z(I-1, J+1) + Z(I, J+1) + Z(I, J)))$

## NOTE:

POINTS  $a, b, c, d, e$  ARE ON 'Z' DATA SURFACE

POINTS  $a', b', c', d', e'$  ARE ON PLOT PLANE

(ie  $Z=0$ )

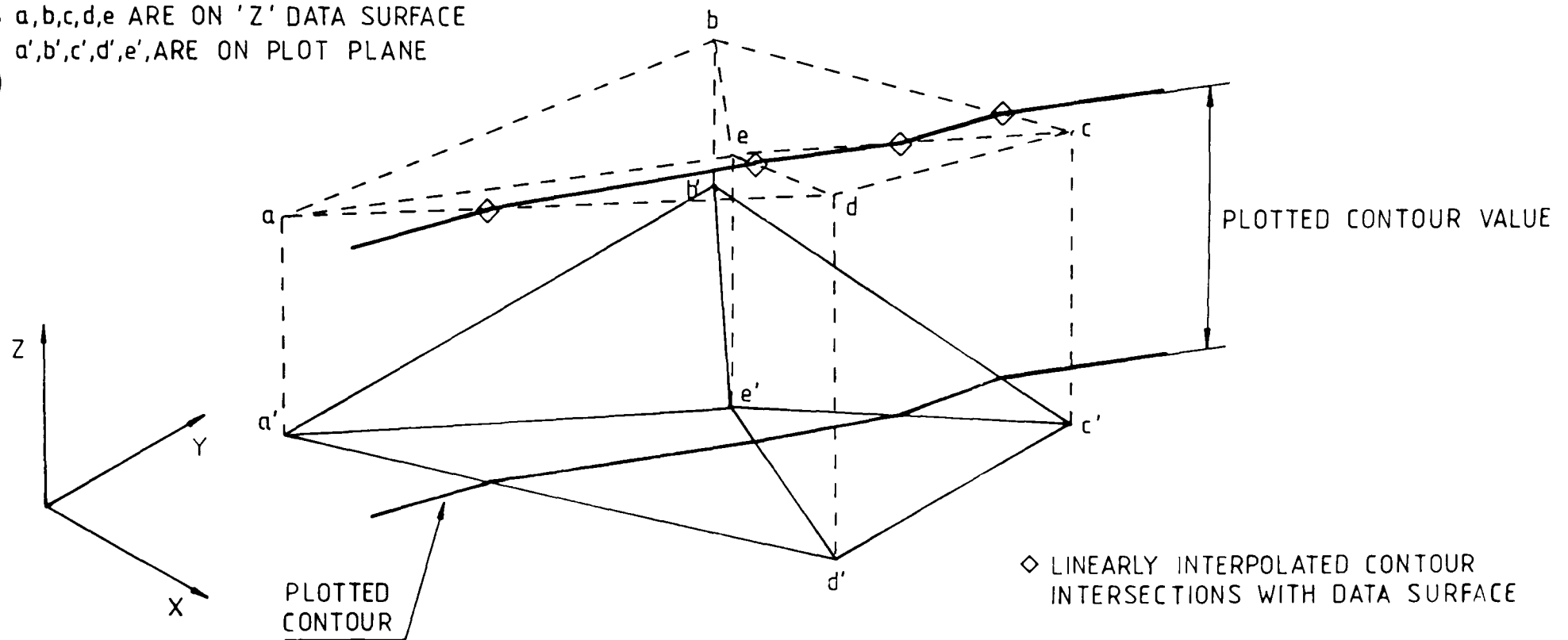


FIGURE 3.21

# THICK LINE PLOTTING ALGORITHM

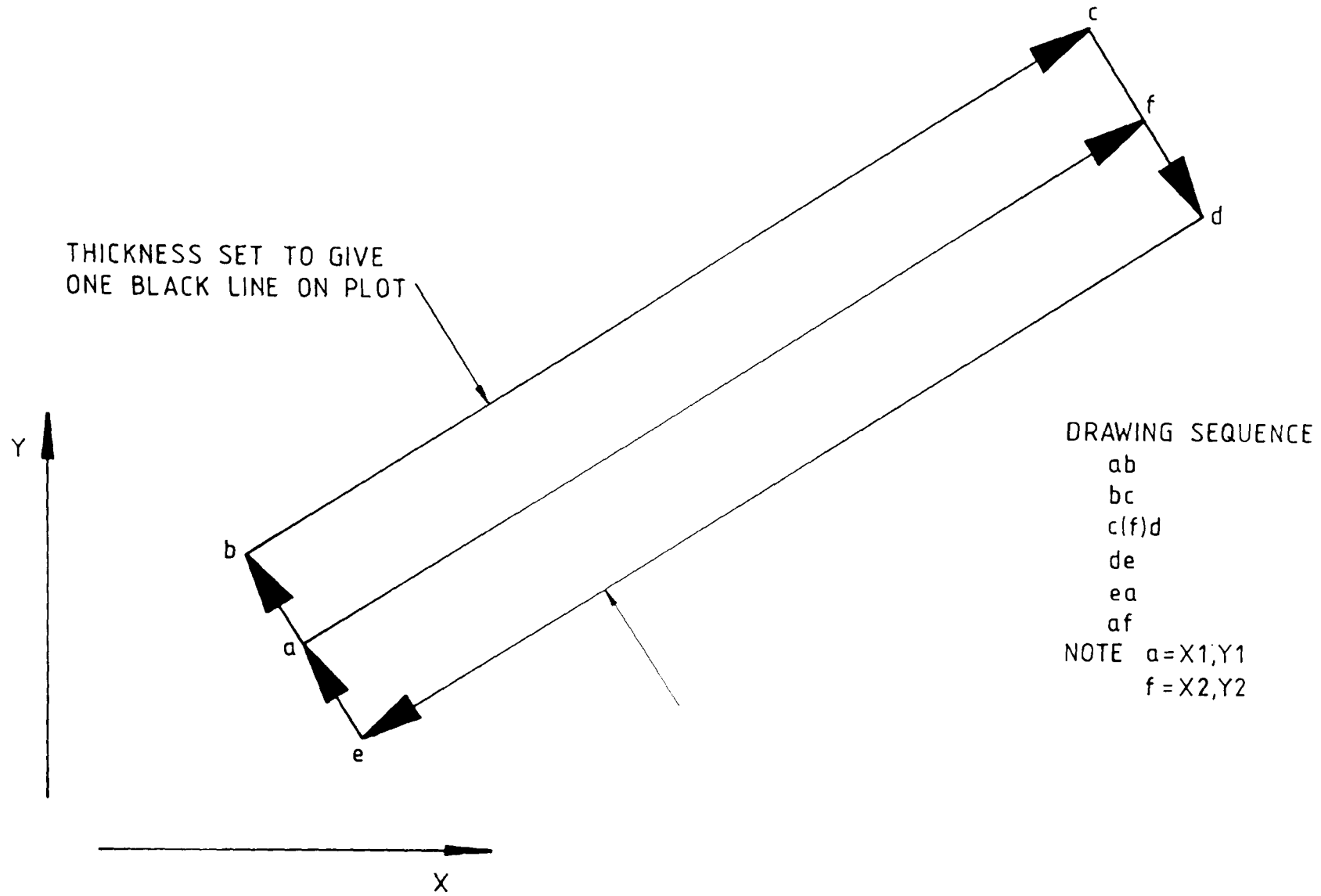


FIGURE 3.22

# A VECTOR SCALING CELL

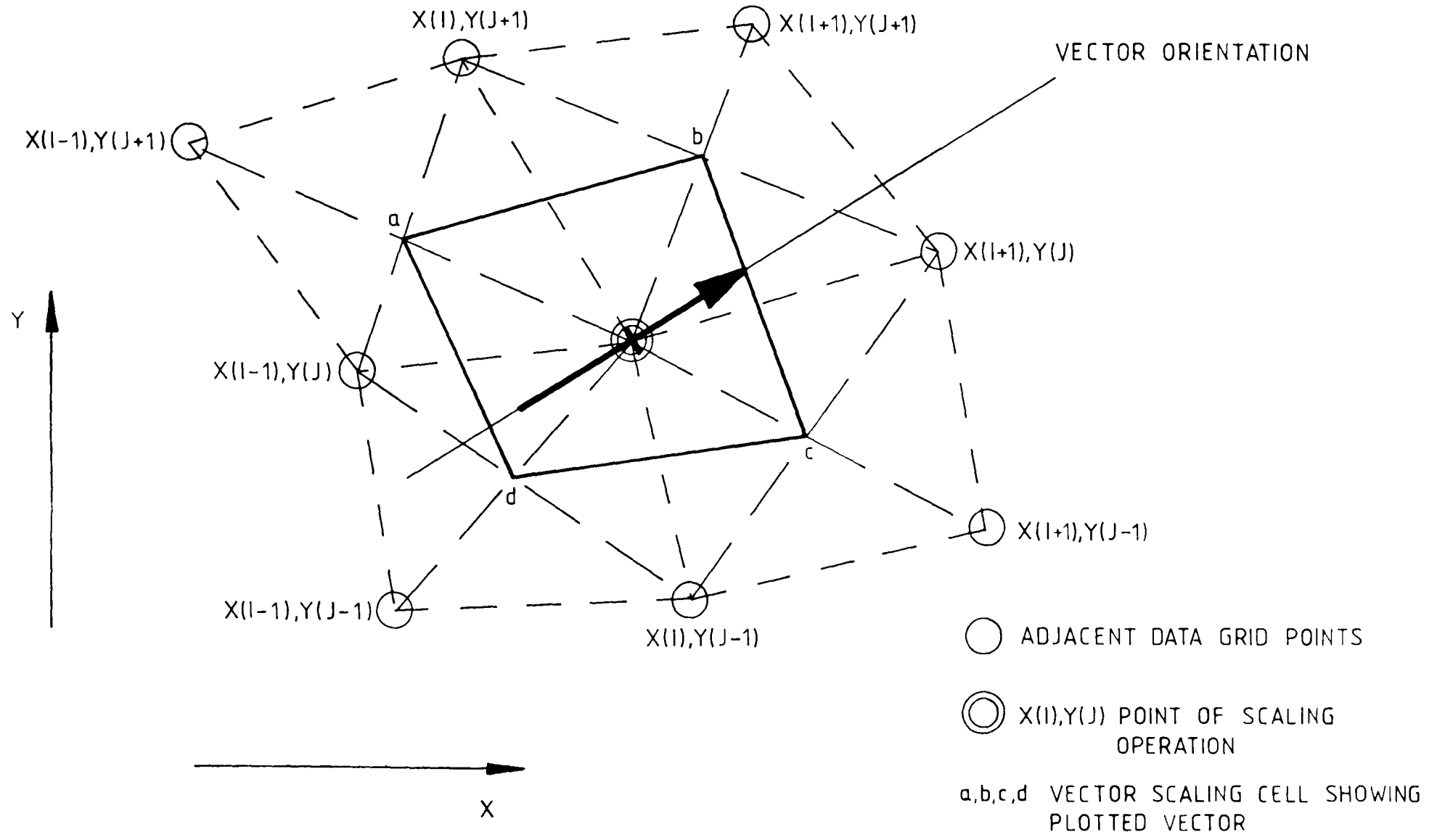


FIGURE 3.13



SLOT 1 EXPERIMENTAL DATA POINTS

NATURAL INLET BOUNDARY LAYER

X-AXIS TANGENTIAL CO-ORDINATE FROM TRAILING EDGE DATUM (MM)

Y-AXIS SPANWISE CO-ORDINATE FROM PERSPEX ENDWALL (MM)

+ PROBE DATA X MANUALLY INTERPOLATED DATA \* EXTRAPOLATED DATA

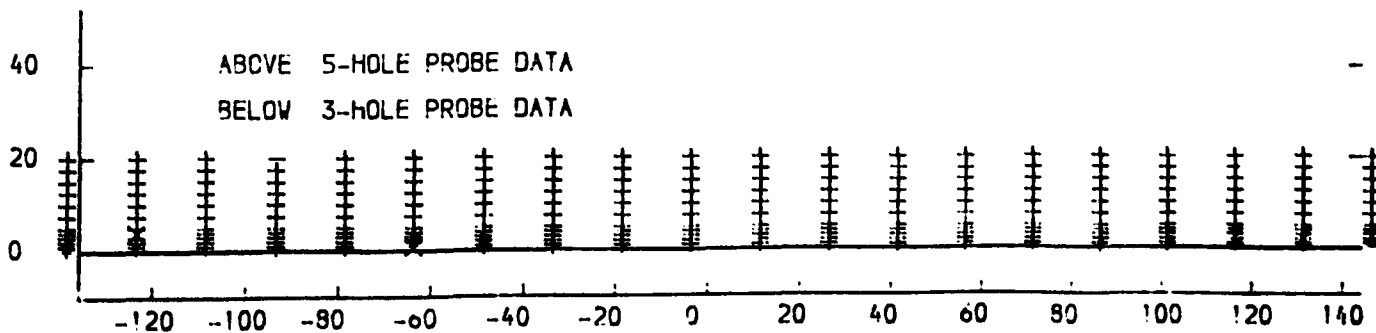
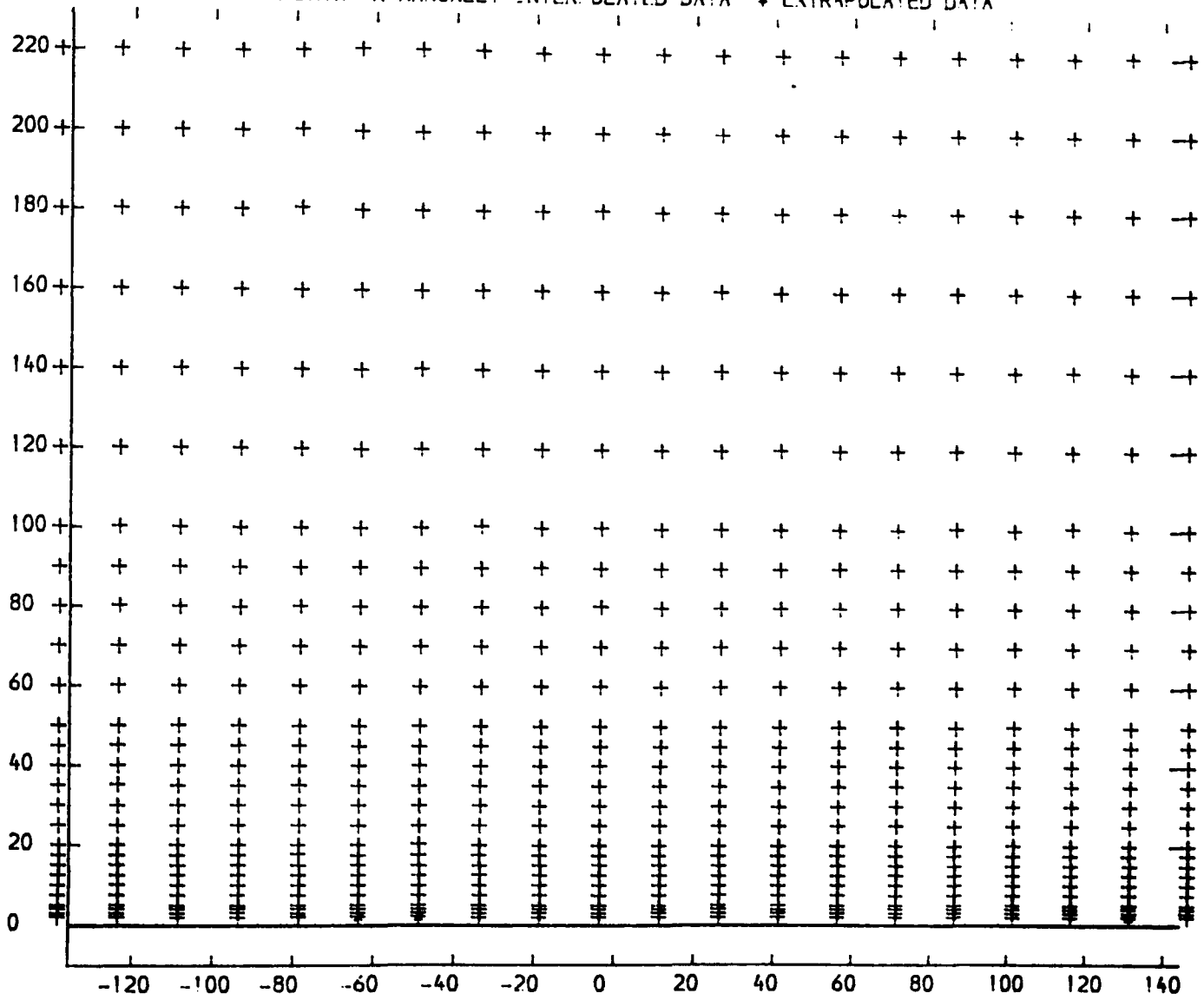


FIGURE 4.1

SLOT 1 TOTAL PRESSURE LOSS COEFFICIENT (  $(P_0! - P_{0LOCAL}) / (P_0! - P_1)$  ) CONTOURS  
 NATURAL INLET BOUNDARY LAYER  
 X-AXIS TANGENTIAL CO-ORDINATE FROM TRAILING EDGE DATUM (MM)  
 Y-A/IS SPANWISE CO-ORDINATE FROM PERSPEX ENDWALL (MM)

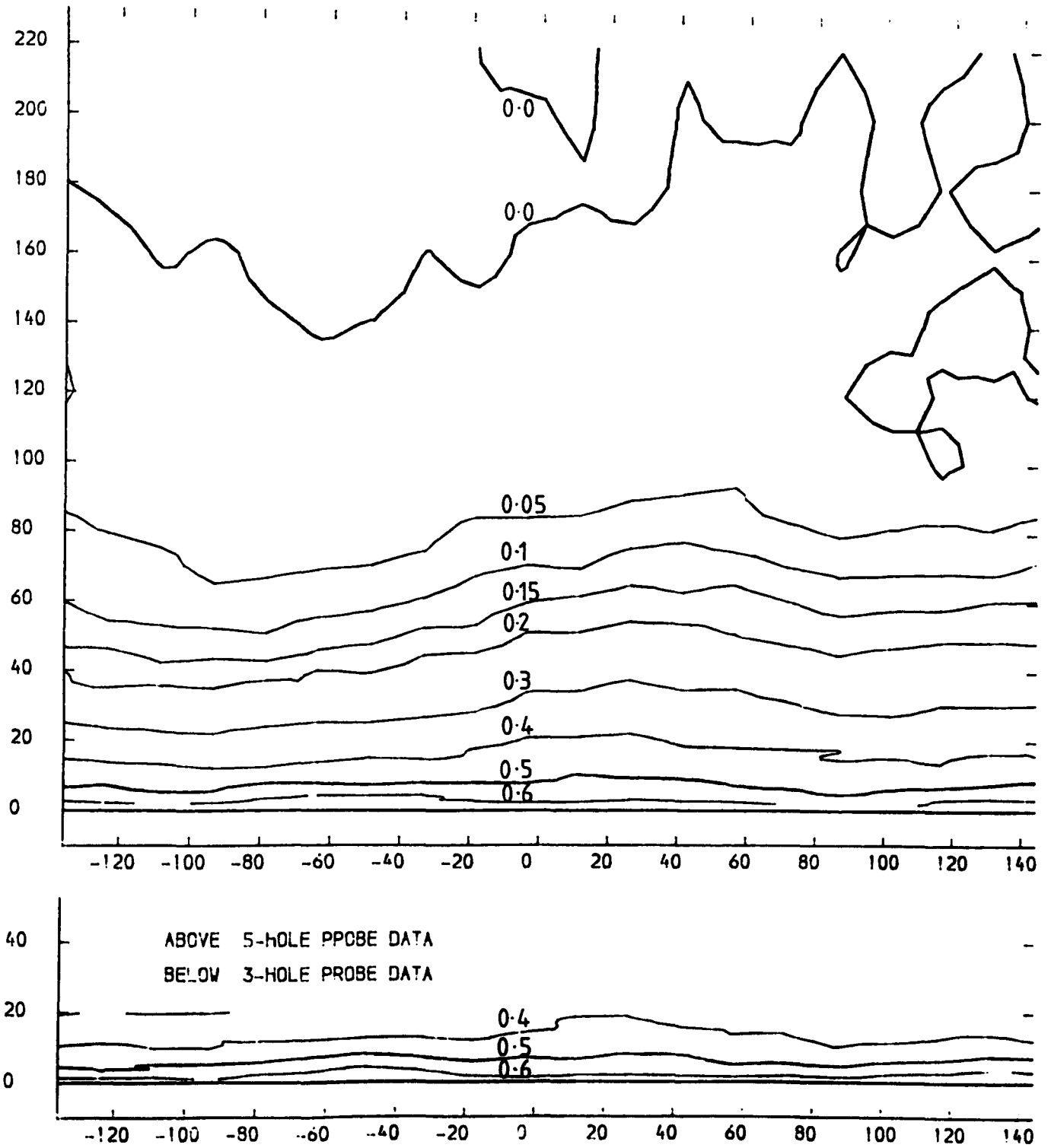
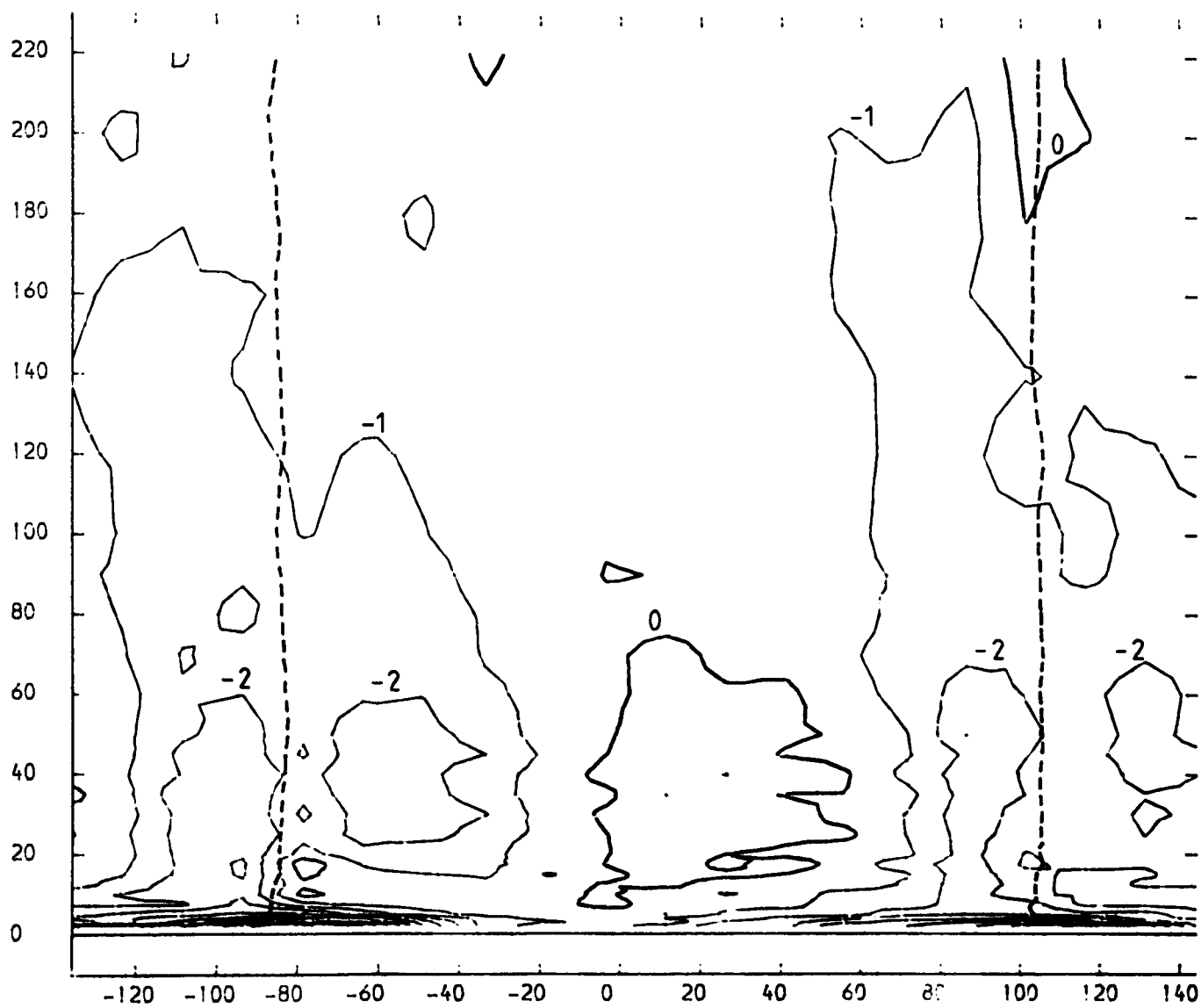


FIGURE 4.2

SLOT 1 STREAMWISE SPANWISE ANGLE CONTOURS (CONTOUR UNITS DEGREES)  
NATURAL INLET BOUNDARY LAYER  
X-AXIS TANGENTIAL CO-ORDINATE FROM TRAILING EDGE DATUM (MM)  
Y-AXIS SPANWISE CO-ORDINATE FROM PERSPEX ENDWALL (MM)



----- 44° YAW ANGLE CONTOUR

FIGURE 4.3

SLOT 1 YAW ANGLE CONTOURS (CONTOUR UNITS DEGREES)

NATURAL INLET BOUNDARY LAYER

X-AXIS TANGENTIAL CO-ORDINATE FROM TRAILING EDGE DATUM (MM)

Y-AXIS SPANWISE CO-ORDINATE FROM PERSPEX ENDWALL (MM)

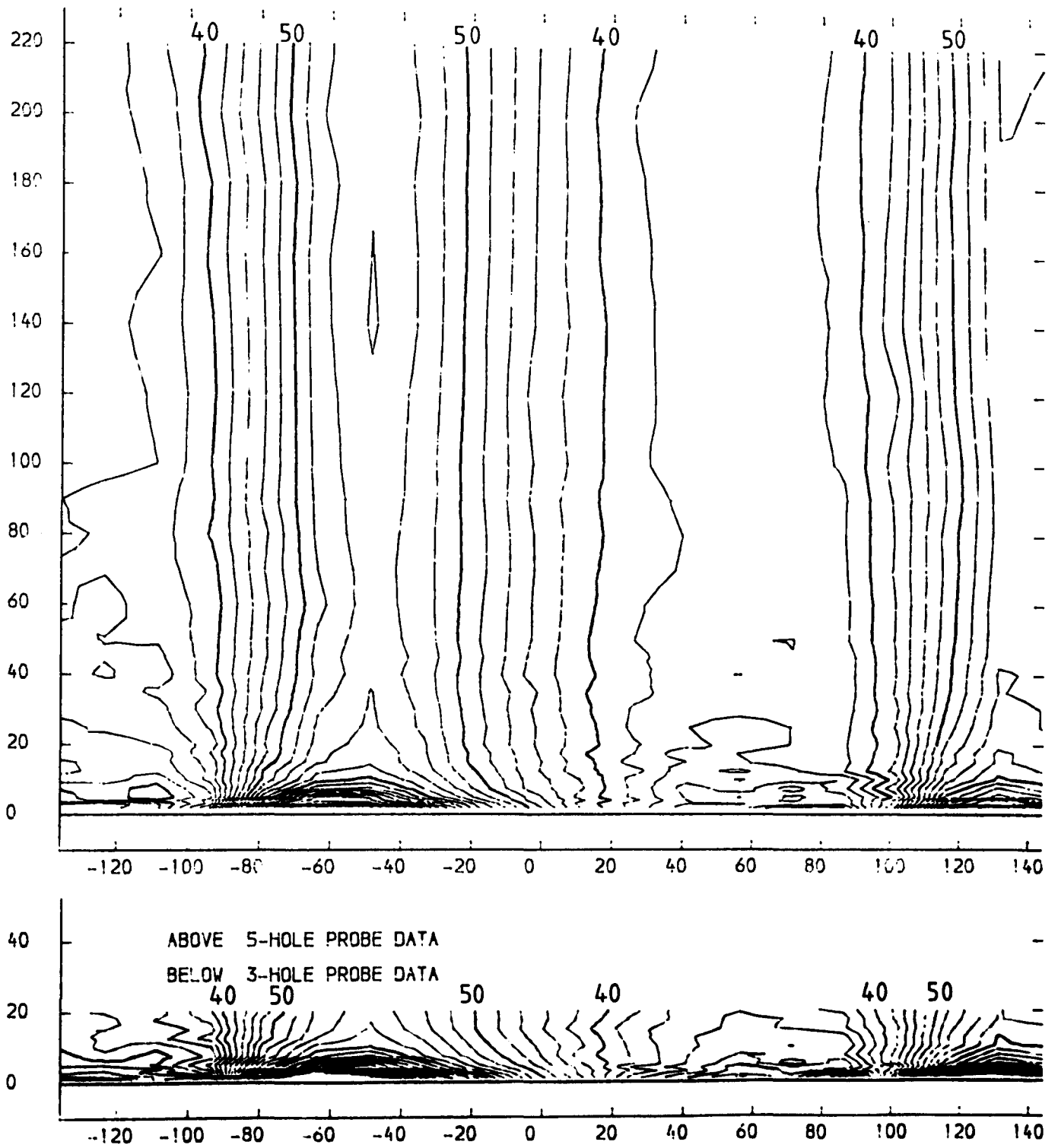


FIGURE 4.4

SLOT 1 VECTOR PLOT OF SECONDARY VELOCITIES  $(V_T(\text{SEC}) = V_T(\text{LOC}) - V_T(\text{M.S.}) + V_A(\text{LOC}) / V_A(\text{M.S.}))$   
NATURAL INLET BOUNDARY LAYER  
X-AXIS TANGENTIAL CO-ORDINATE FROM TRAILING EDGE DATUM (MM)  
Y-AXIS SPANWISE CO-ORDINATE FROM PERSPEX ENDWALL (MM)  
VECTOR SCALE 20 METRES/SEC

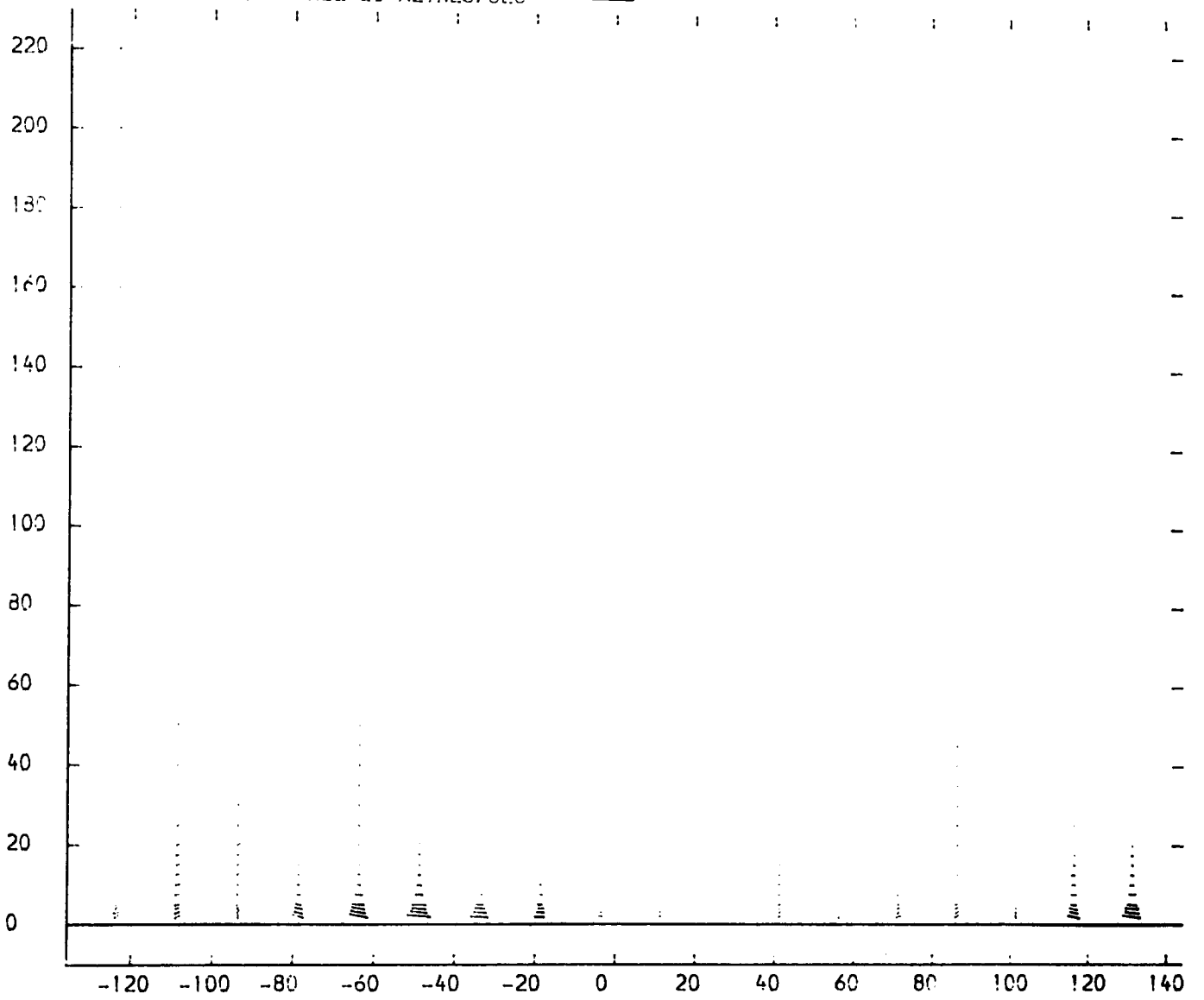


FIGURE 4.5

SLOT 1 STATIC PRESSURE COEFFICIENT  $(P1 - PLOCAL) / (P01 - P1)$  CONTOURS  
 NATURAL INLET BOUNDARY LAYER  
 X-AXIS TANGENTIAL CO-ORDINATE FROM TRAILING EDGE DATUM (MM)  
 Y-AXIS SPANWISE CO-ORDINATE FROM PERSPEX ENDWALL (MM)

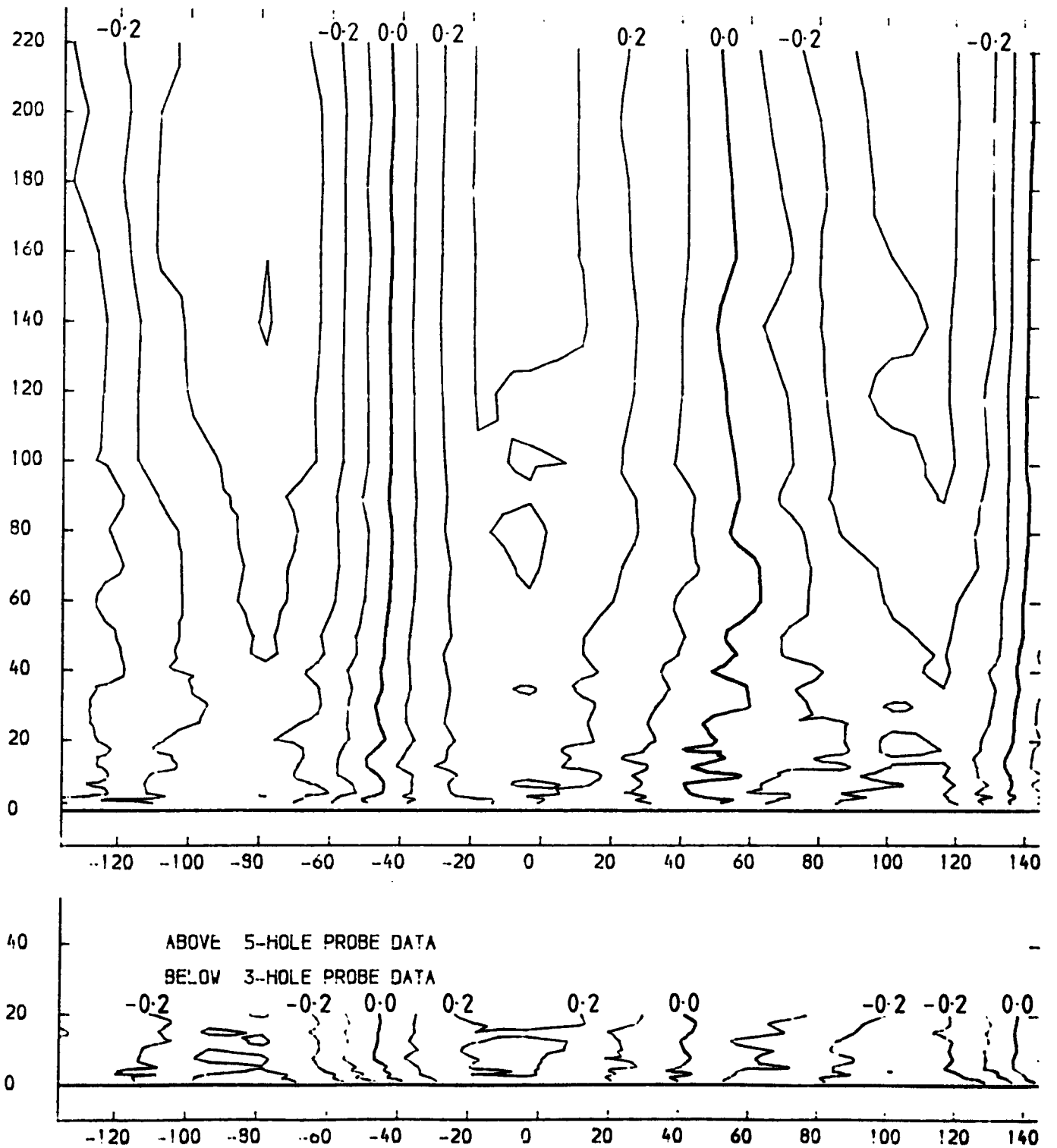


FIGURE 4.6

SLOT 1 TOTAL VELOCITY MAGNITUDE CONTOURS (CONTOUR UNITS METRES/SEC)  
 NATURAL INLET BOUNDARY LAYER  
 X-AXIS TANGENTIAL CO-ORDINATE FROM TRAILING EDGE DATUM (MM)  
 Y-AXIS SPANWISE CO-ORDINATE FROM PERSPEX ENDWALL (MM)

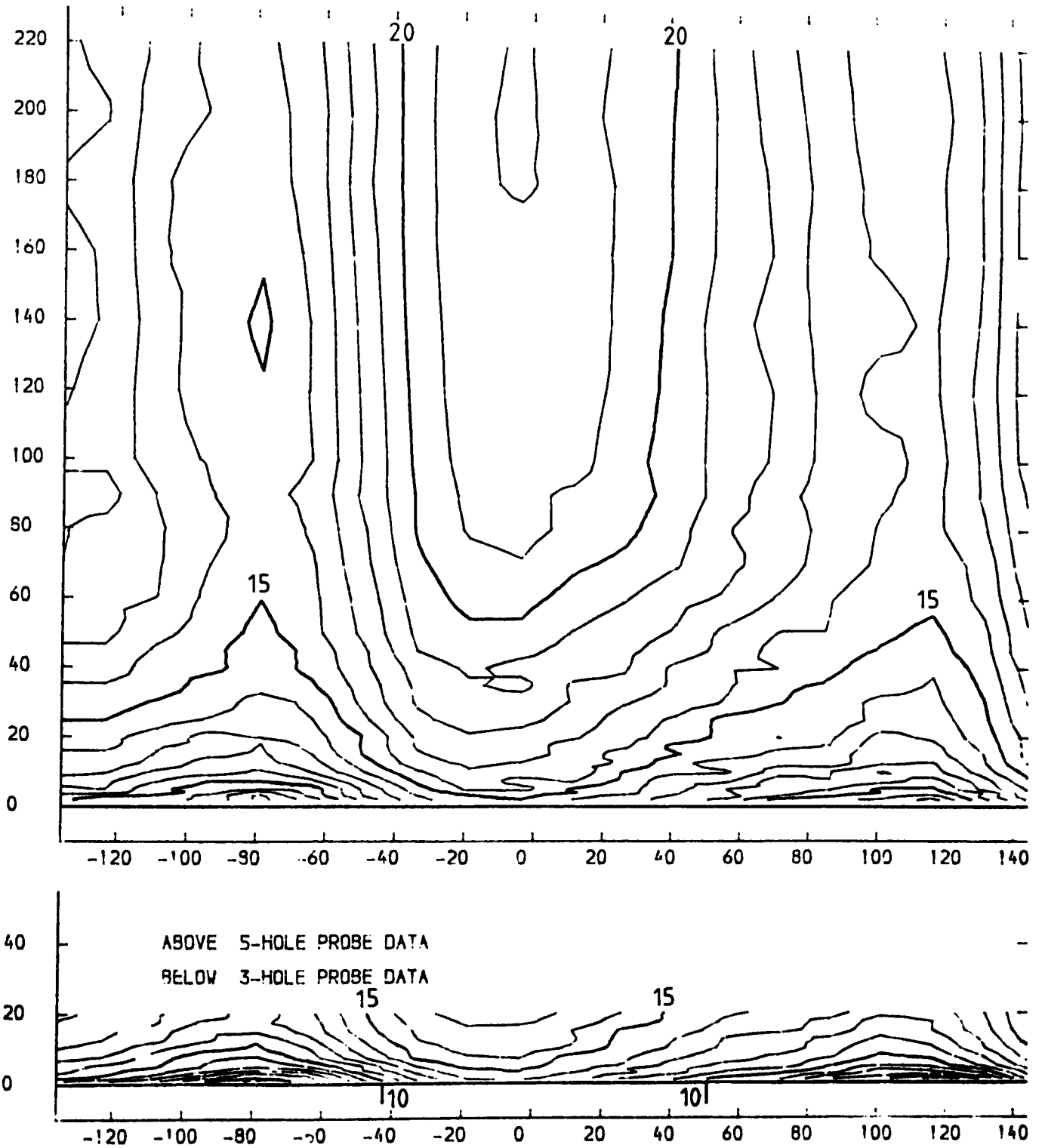
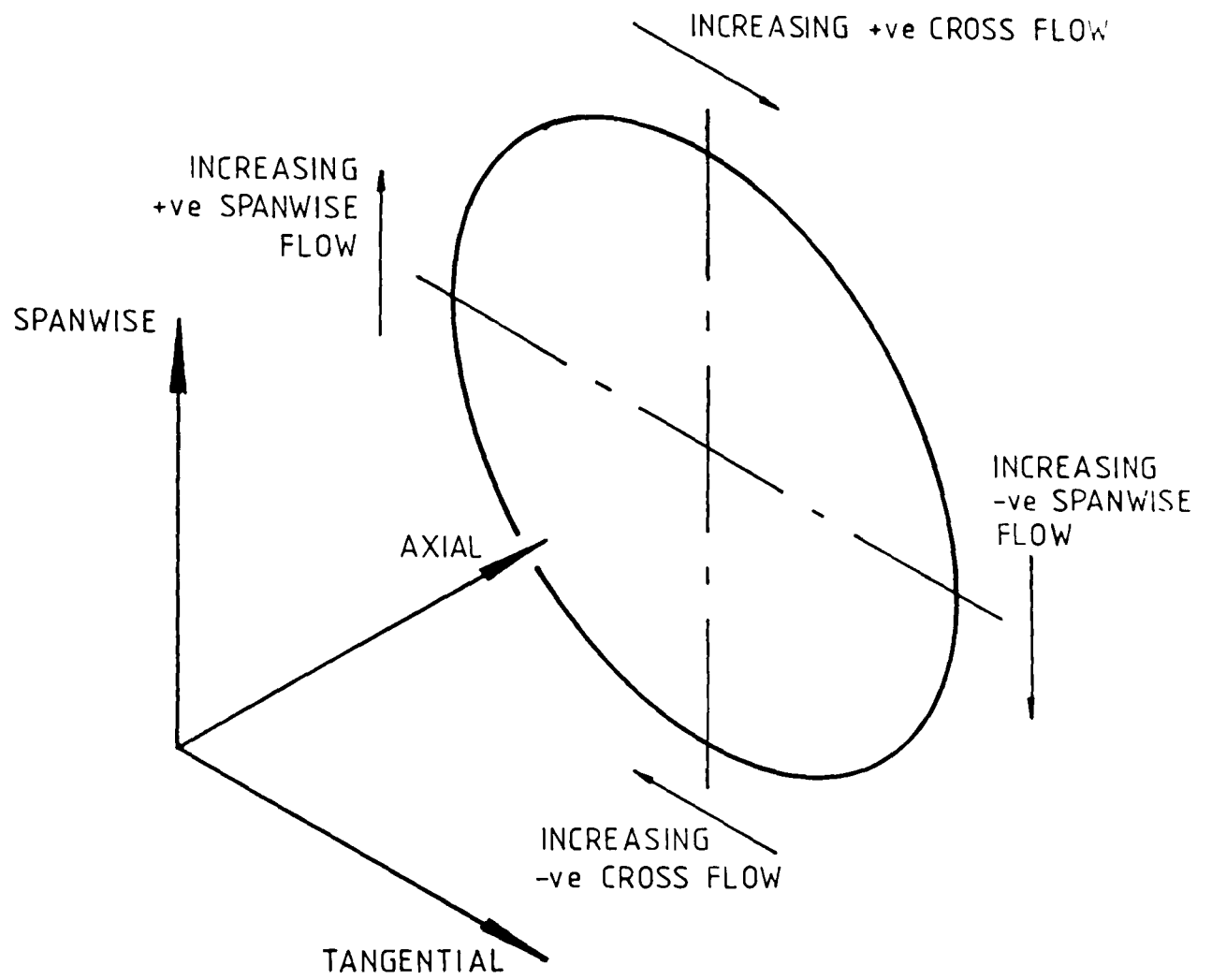


FIGURE 4.7

# SECTION THROUGH AN IDEALIZED PASSAGE VORTEX

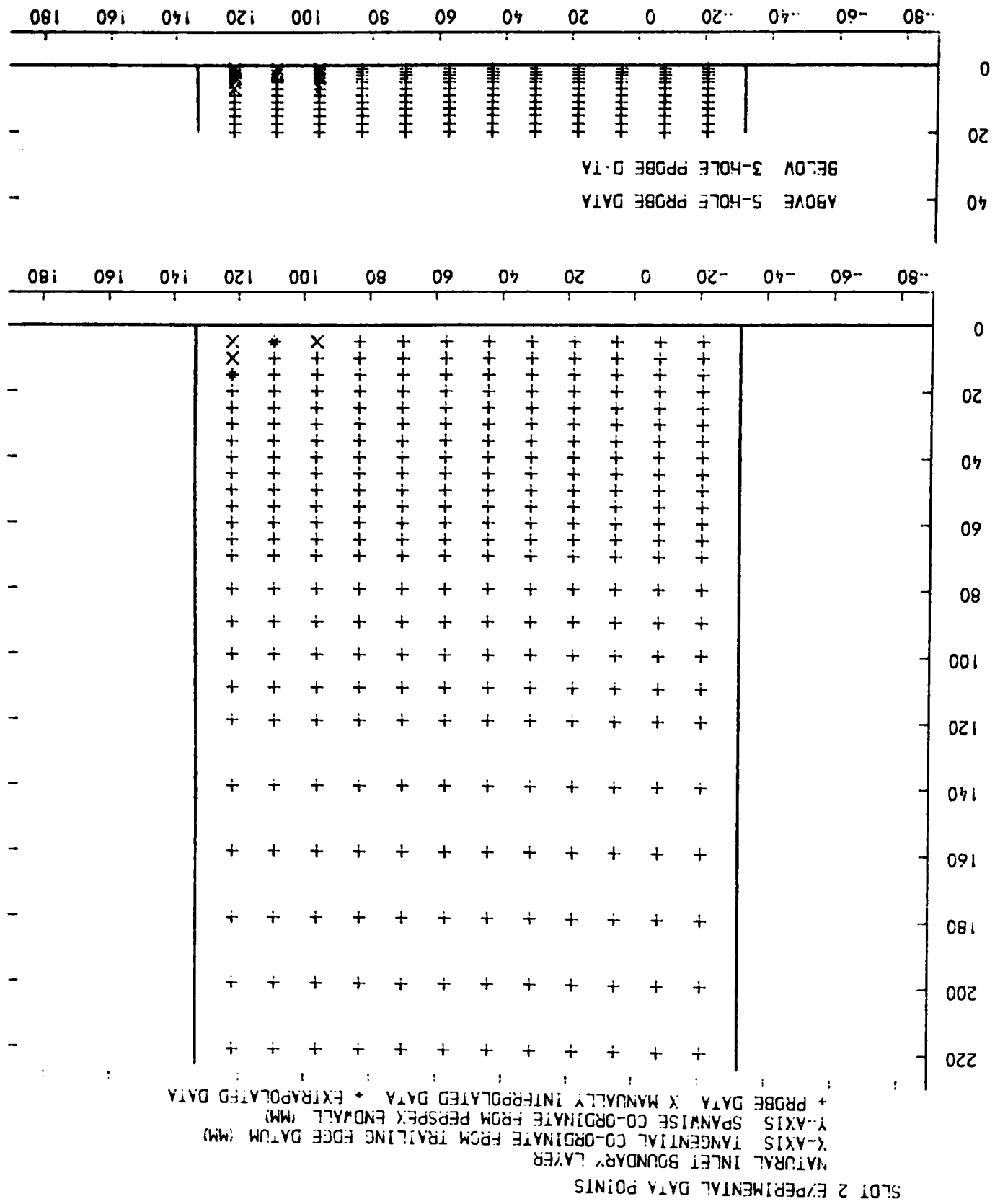


$$\begin{aligned} \text{CROSS FLOW ANGLE} &= \epsilon(\text{LOCAL}) - \epsilon(\text{MIDSPAN}) \\ &= -\text{ve OVERTURNING ANGLE} \end{aligned}$$

FIGURE 4.8



FIGURE 4.9



SLOT 2 TOTAL PRESSURE LOSS COEFFICIENT  $(P_{01} - P_{0LOCAL}) / (P_{01} - P_{11})$  CONTOURS  
 NATURAL INLET BOUNDARY LAYER  
 X-AXIS TANGENTIAL CO-ORDINATE FROM TRAILING EDGE DATUM (MM)  
 Y-AXIS SPANWISE CO-ORDINATE FROM PERSPEX ENDWALL (MM)

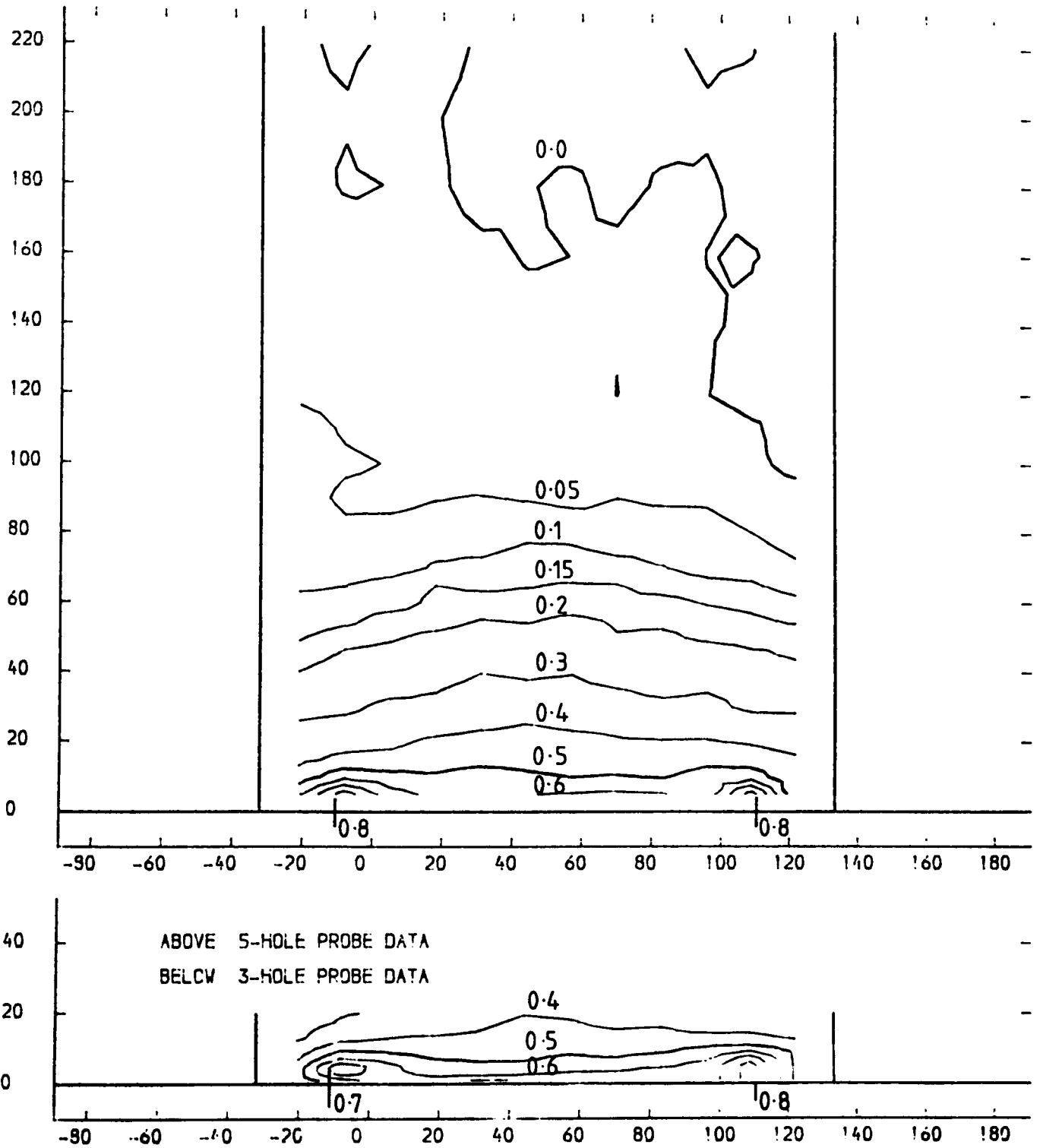


FIGURE 4.10

SLOT 2 TOTAL VELOCITY MAGNITUDE CONTOURS (CONTOUR UNITS METRES/SEC)  
 NATURAL INLET BOUNDARY LAYER  
 X-AXIS TANGENTIAL CO-ORDINATE FROM TRAILING EDGE DATUM (MM)  
 Y-AXIS SPANWISE CO-ORDINATE FROM PERSPEX ENDWALL (MM)

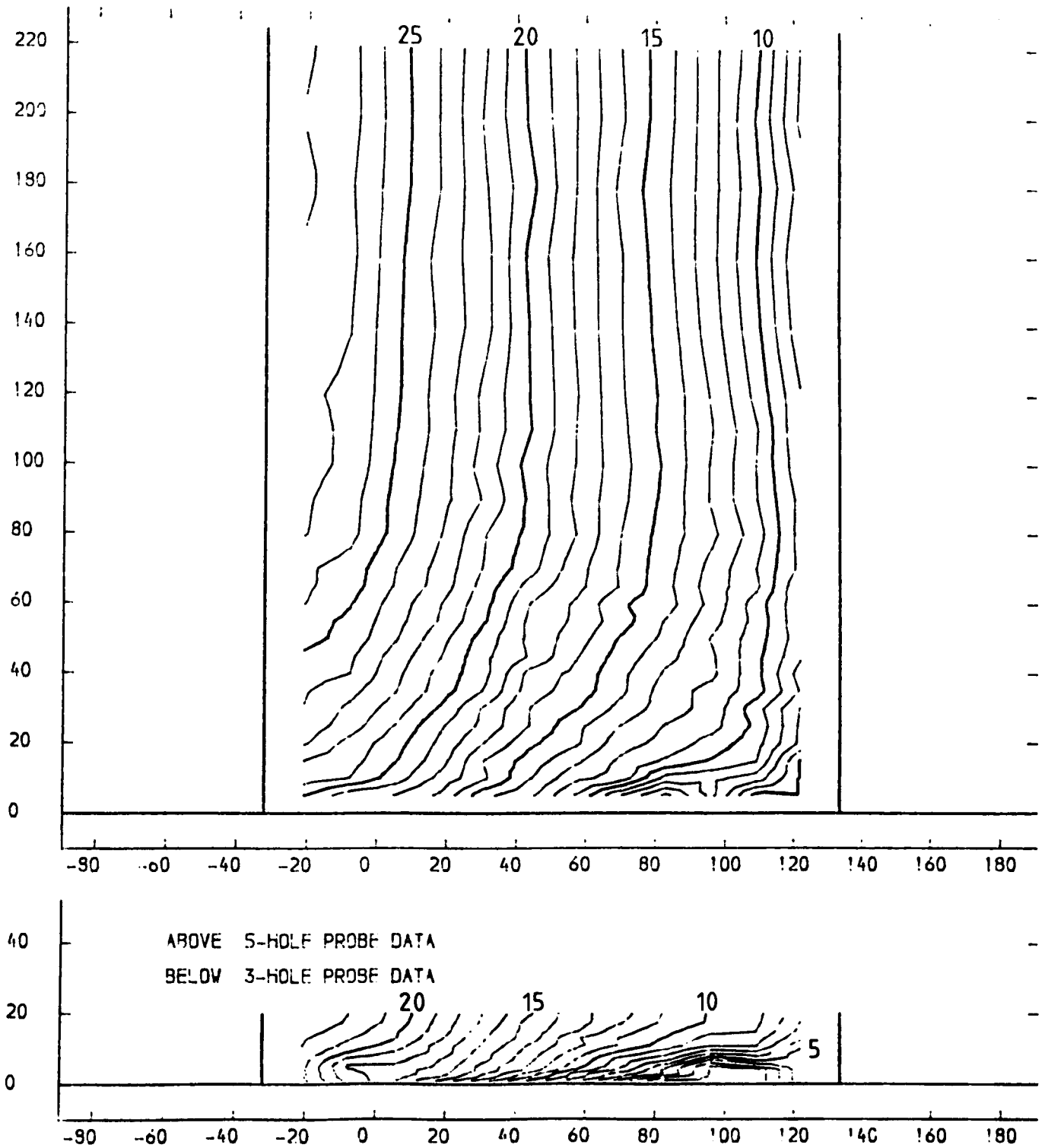
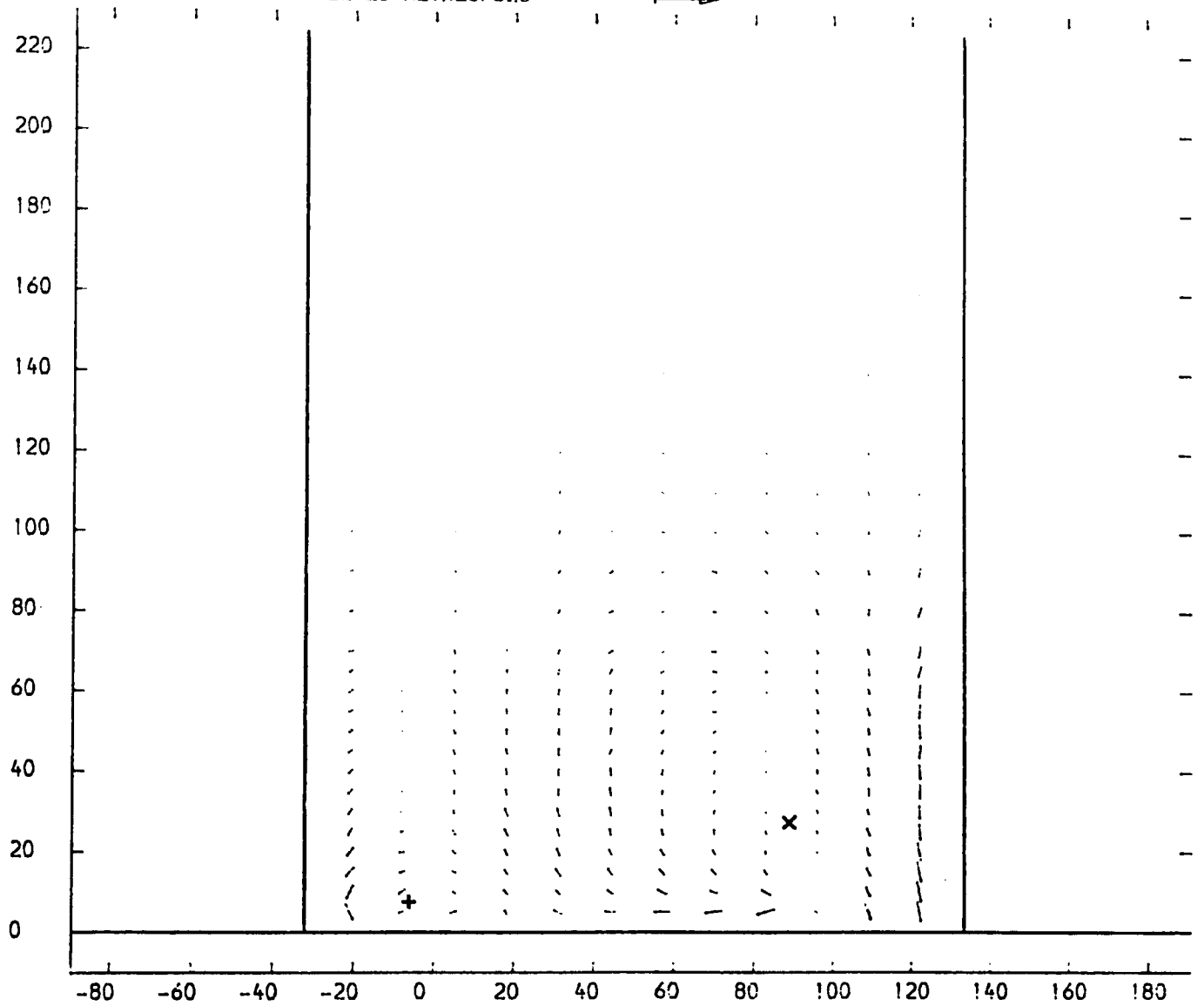


FIGURE 4.11

SLOT 2 VECTOR PLOT OF SECONDARY VELOCITIES  $(V_T(\text{SEC}) = V_T(\text{LOC}) - V_T(\text{M.S.}) + V_A(\text{LOC}) / V_A(\text{M.S.}))$   
 NATURAL INLET BOUNDARY LAYER  
 X-AXIS TANGENTIAL CO-ORDINATE FROM TRAILING EDGE DATUM (MM)  
 Y-AXIS SPANWISE CO-ORDINATE FROM PERSPEX ENDWALL (MM)  
 VECTOR SCALE 20 METRES/SEC



× PASSAGE VORTEX CENTRE  
 + SUCTION SIDE LEG VORTEX CENTRE

FIGURE 4.12

SLOT 2 SPANWISE ANGLE (PITCH ANGLE) CONTOURS (CONTOUR UNITS DEGREES)  
NATURAL INLET BOUNDARY LAYER  
X-AXIS TANGENTIAL CO-ORDINATE FROM TRAILING EDGE DATUM (MM)  
Y-AXIS SPANWISE CO-ORDINATE FROM PERSPEX ENDWALL (MM)

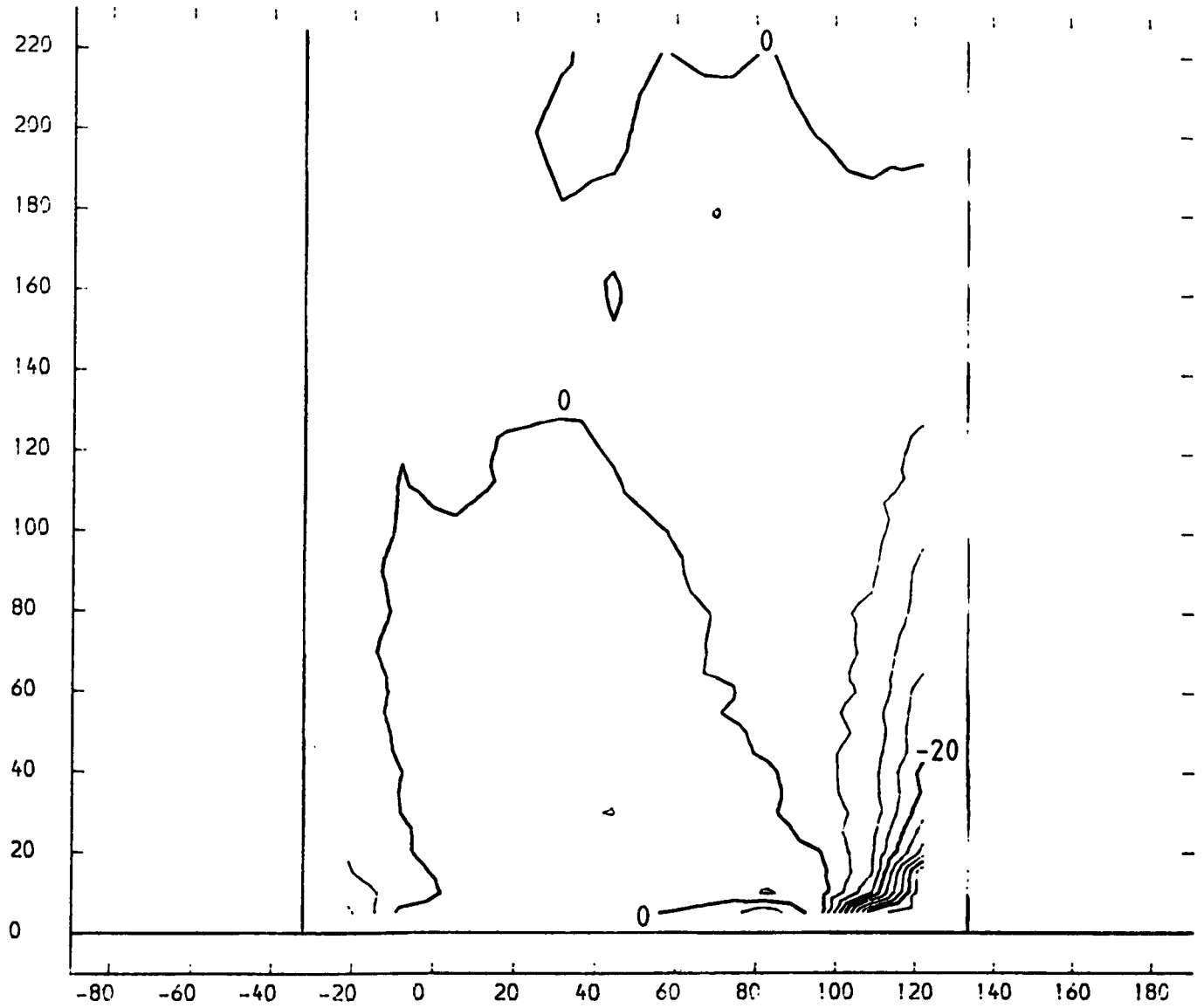


FIGURE 4.13

SLOT 2 YAW ANGLE CONTOURS (CONTOUR UNITS DEGREES)  
 NATURAL INLET BOUNDARY LAYER  
 X-AXIS TANGENTIAL CO-ORDINATE FROM TRAILING EDGE DATUM (MM)  
 Y-AXIS SPANWISE CO-ORDINATE FROM PERSPEX ENDWALL (MM)

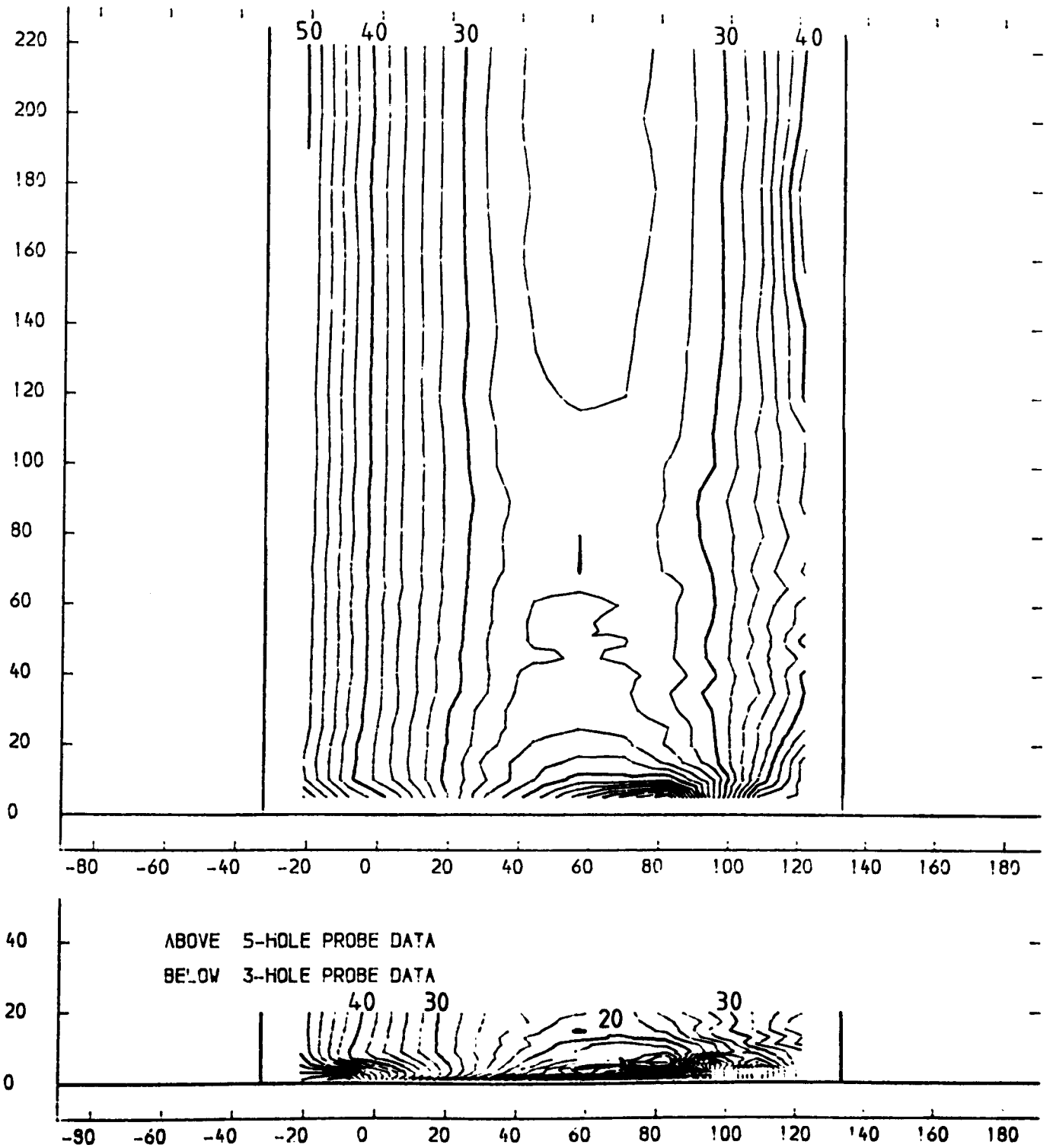


FIGURE 4.14

SLOT 2 STATIC PRESSURE COEFFICIENT  $(P1 - PLOCAL) / (P01 - P1)$  CONTOURS  
 NATURAL INLET BOUNDARY LAYER  
 X-AXIS TANGENTIAL CO-ORDINATE FROM TRAILING EDGE DATUM (MM)  
 Y-AXIS SPANWISE CO-ORDINATE FROM PERSPEX ENDWALL (MM)

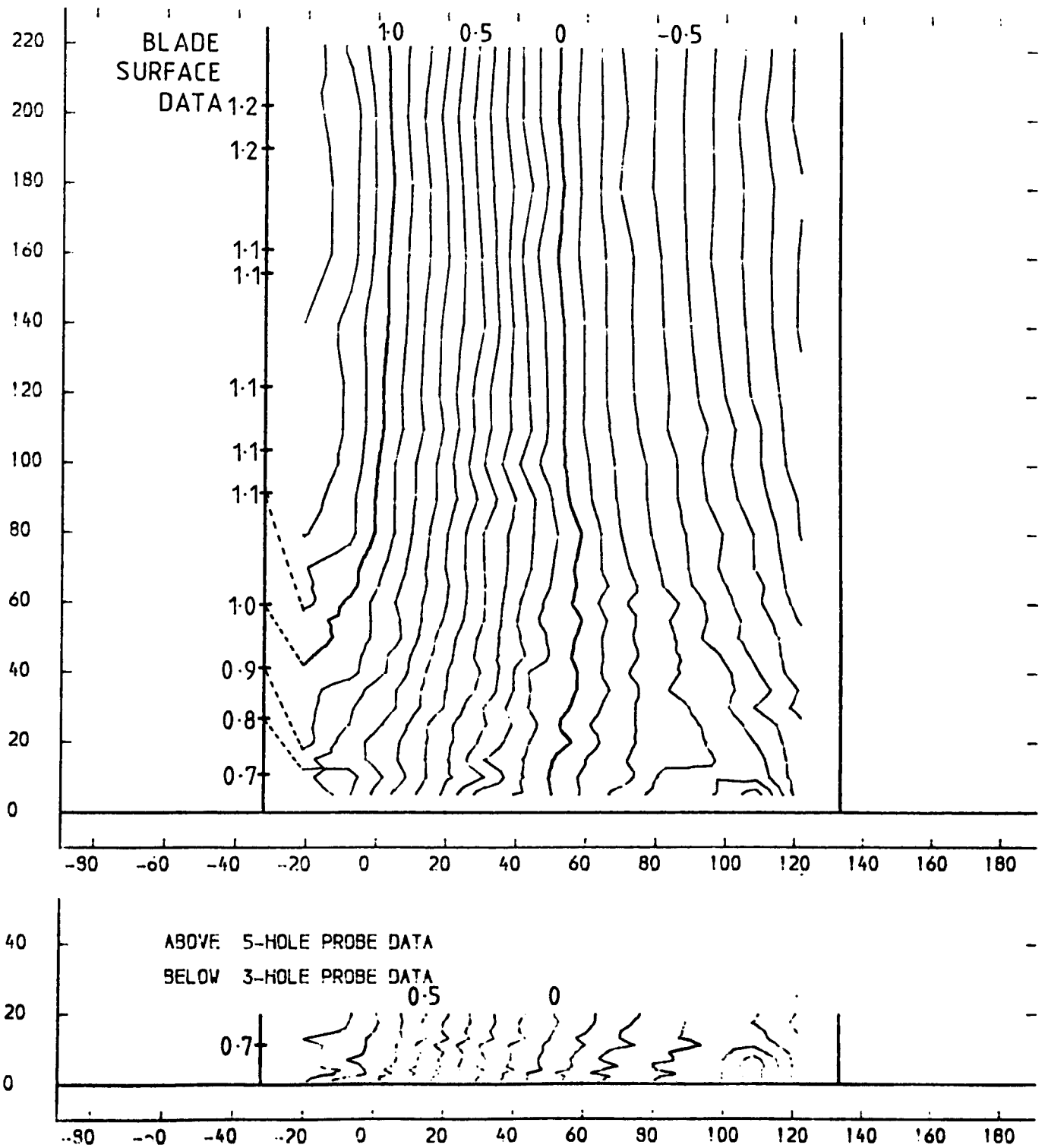


FIGURE 4.15

SLOT 3 EXPERIMENTAL DATA POINTS

NATURAL INLET BOUNDARY LAYER

X-AXIS TANGENTIAL CO-ORDINATE FROM TRAILING EDGE DATUM (MM)

Y-AXIS SPANWISE CO-ORDINATE FROM PERSPEX ENDWALL (MM)

+ PROBE DATA X MANUALLY INTERPOLATED DATA \* EXTRAPOLATED DATA

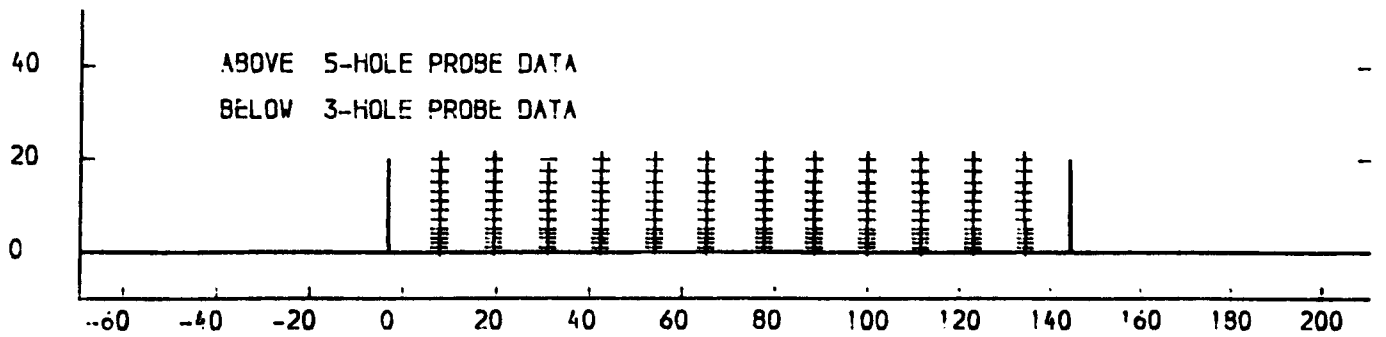
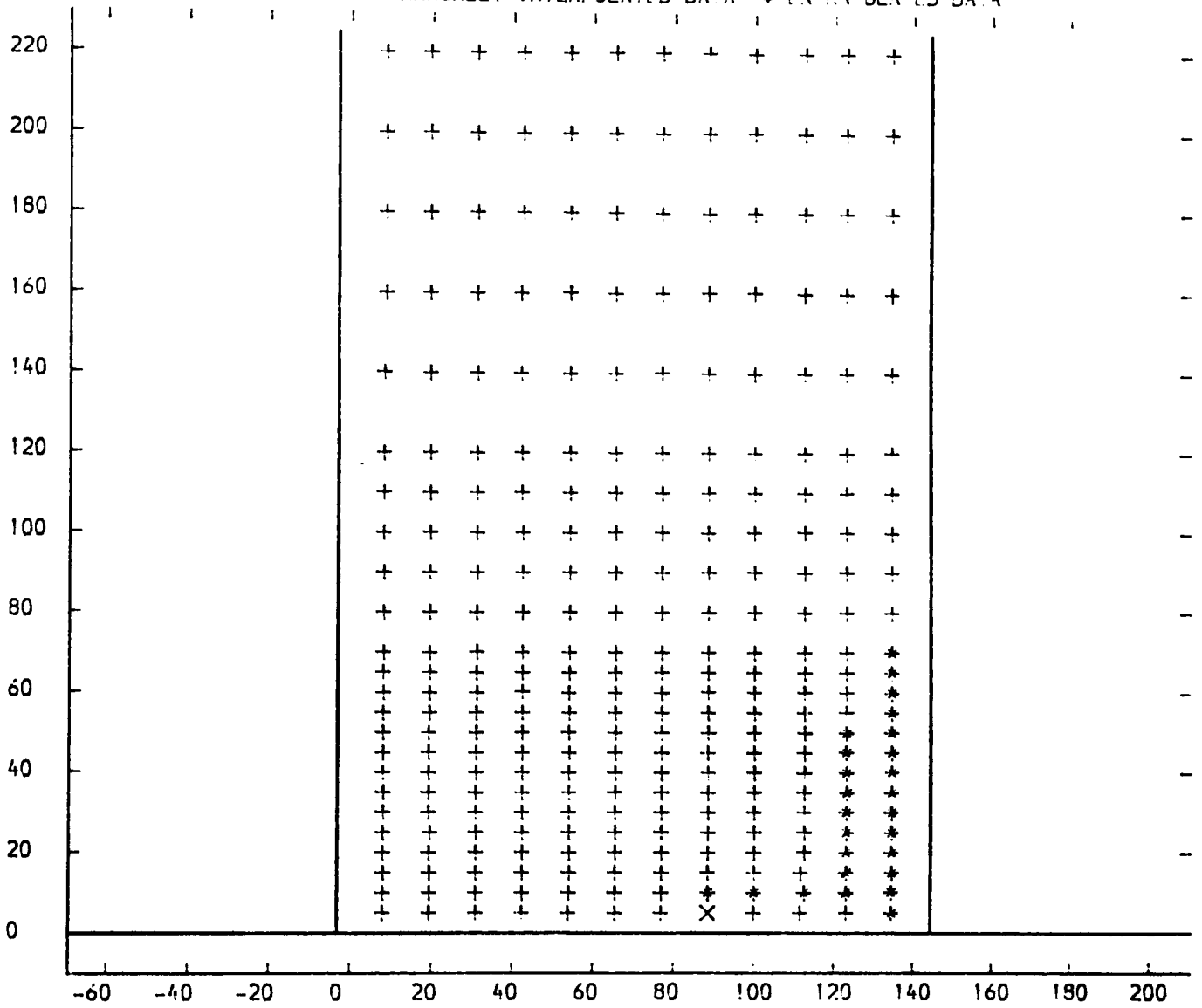


FIGURE 4.16



SLOT 3 TOTAL PRESSURE LOSS COEFFICIENT  $(P_{01} - P_{0LOCAL}) / (P_{01} - P_{11})$  CONTOURS  
 NATURAL INLET BOUNDARY LAYER  
 X-AXIS TANGENTIAL CO-ORDINATE FROM TRAILING EDGE DATUM (MM)  
 Y-AXIS SPANWISE CO-ORDINATE FROM PERSPEX ENDWALL (MM)

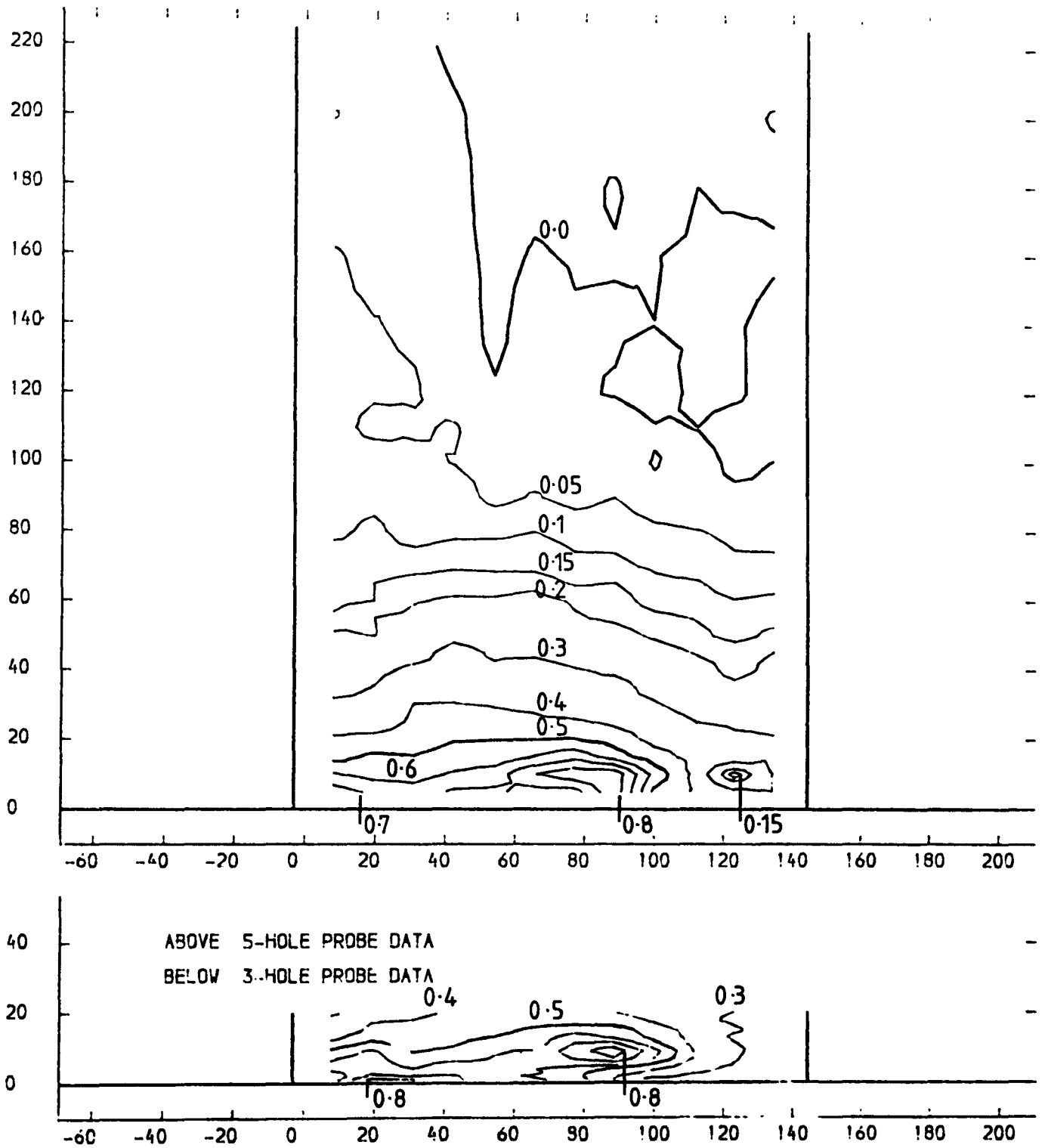


FIGURE 4.17

SLOT 3 TOTAL VELOCITY MAGNITUDE CONTOURS (CONTOUR UNITS METRES/SEC)  
 NATURAL INLET BOUNDARY LAYER  
 X-AXIS TANGENTIAL CO-ORDINATE FROM TRAILING EDGE DATUM (MM)  
 Y-AXIS SPANWISE CO-ORDINATE FROM PERSPEK ENDWALL (MM)

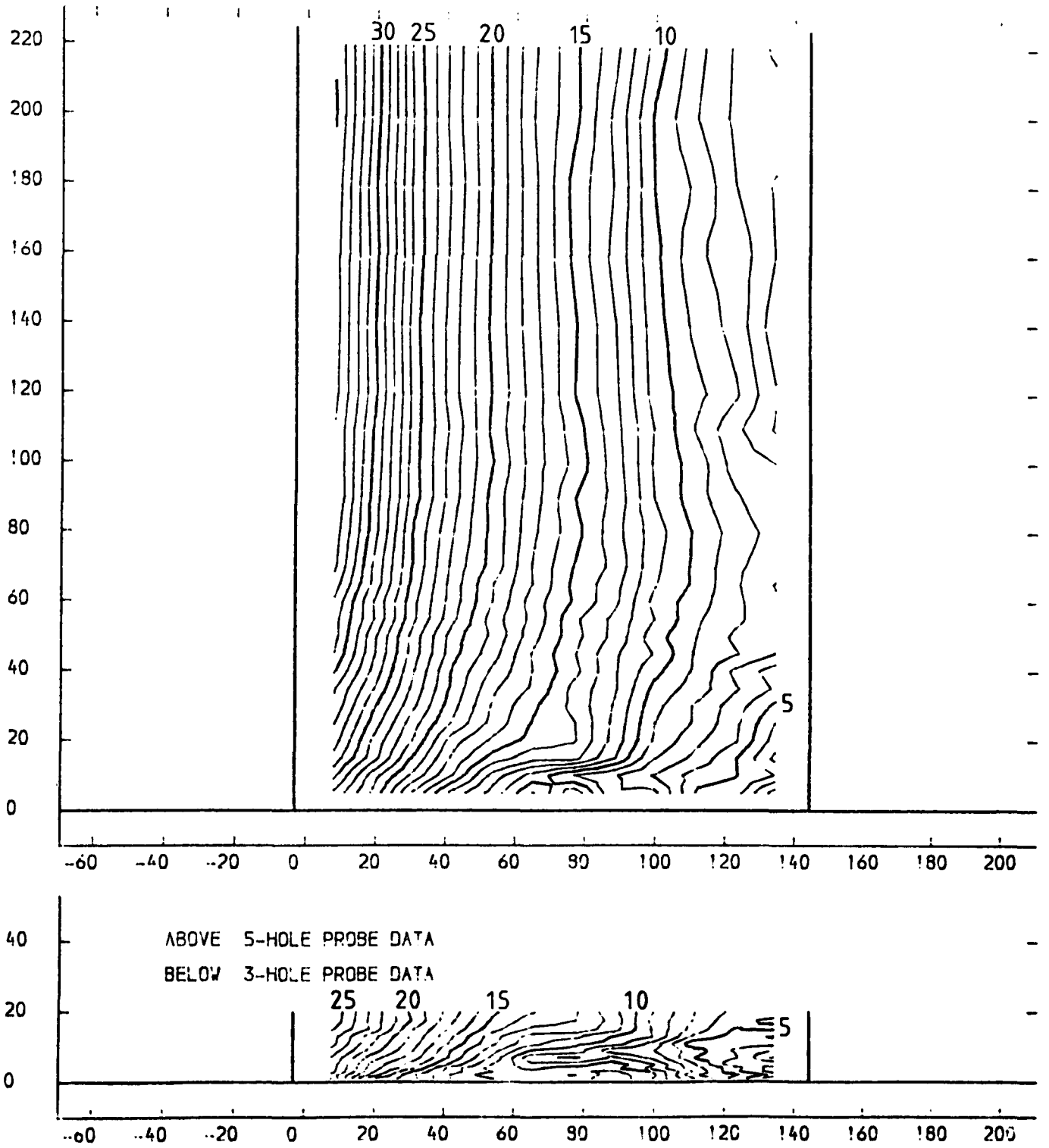
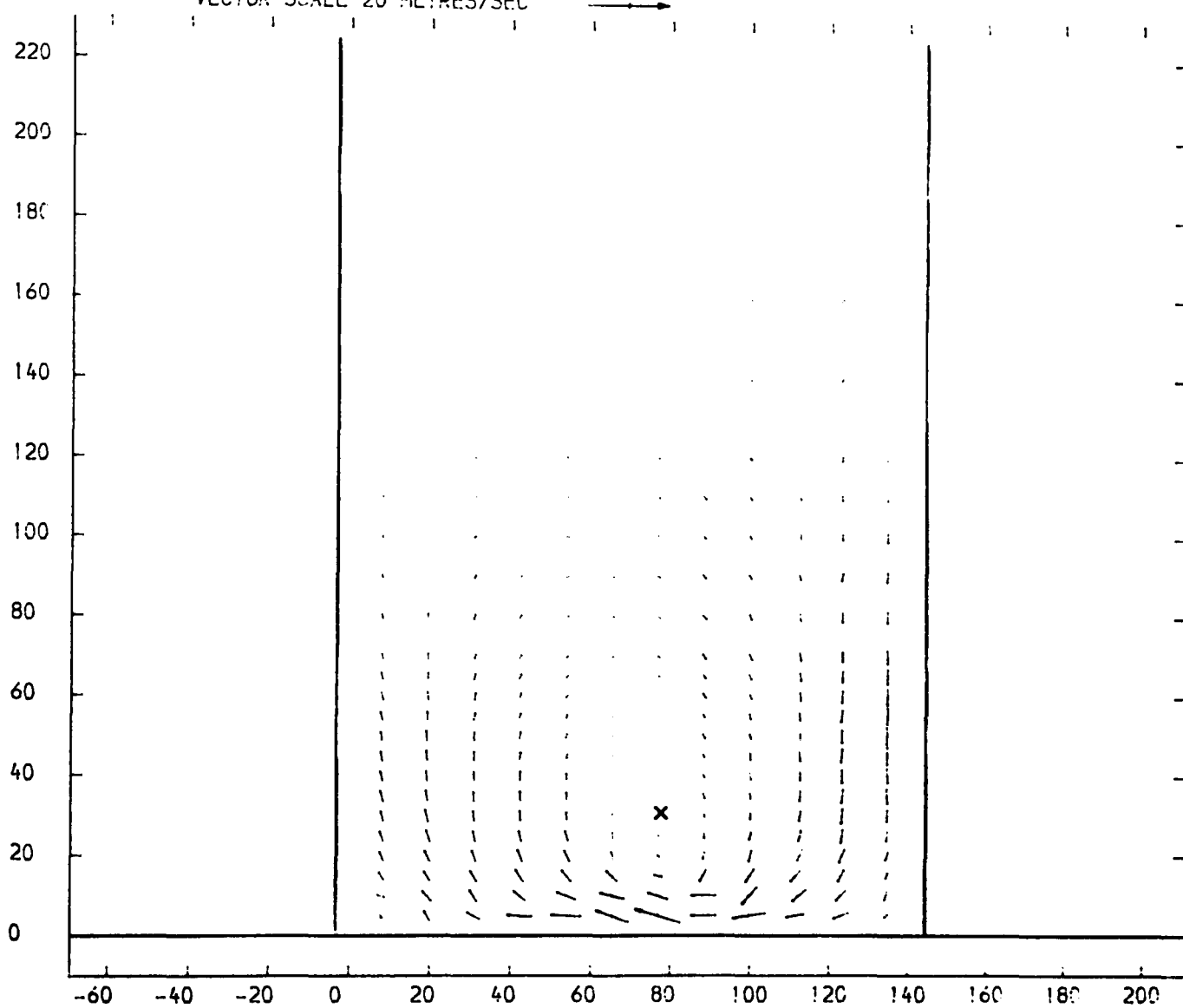


FIGURE 4.18

SLOT 3 VECTOR PLOT OF SECONDARY VELOCITIES  $(V_T(\text{SEC}) = V_T(\text{LOC}) - V_T(\text{M.S.}) + V_A(\text{LOC}) / V_A(\text{M.S.}))$   
 NATURAL INLET BOUNDARY LAYER  
 X-AXIS TANGENTIAL CO-ORDINATE FROM TRAILING EDGE DATUM (MM)  
 Y-AXIS SPANWISE CO-ORDINATE FROM PERSPEX ENDWALL (MM)  
 VECTOR SCALE 20 METRES/SEC



x PASSAGE VORTEX CENTRE

FIGURE 4.19

SLOT 3 SPANWISE ANGLE (PITCH ANGLE) CONTOURS (CONTOUR UNITS DEGREES)  
NATURAL INLET BOUNDARY LAYER  
X-AXIS TANGENTIAL CO-ORDINATE FROM TRAILING EDGE DATUM (MM)  
Y-AXIS SPANWISE CO-ORDINATE FROM PERSPEX ENDWALL (MM)

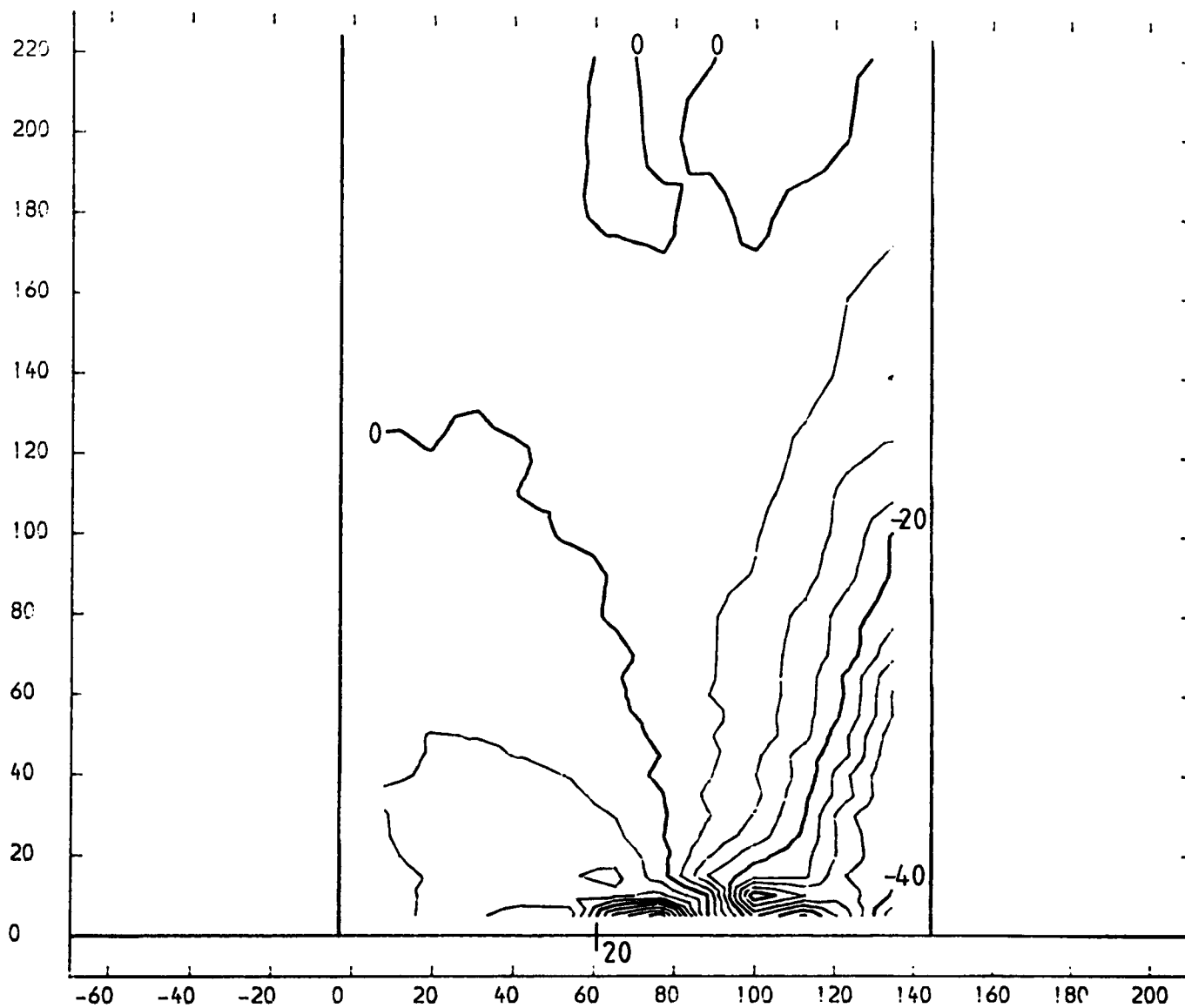


FIGURE 4.20

SLOT 3 YAW ANGLE CONTOURS (CONTOUR UNITS DEGREES)  
 NATURAL INLET BOUNDARY LAYER  
 X-AXIS TANGENTIAL CO-ORDINATE FROM TRAILING EDGE DATUM (MM)  
 Y-AXIS SPANWISE CO-ORDINATE FROM PERSPEX ENDWALL (MM)

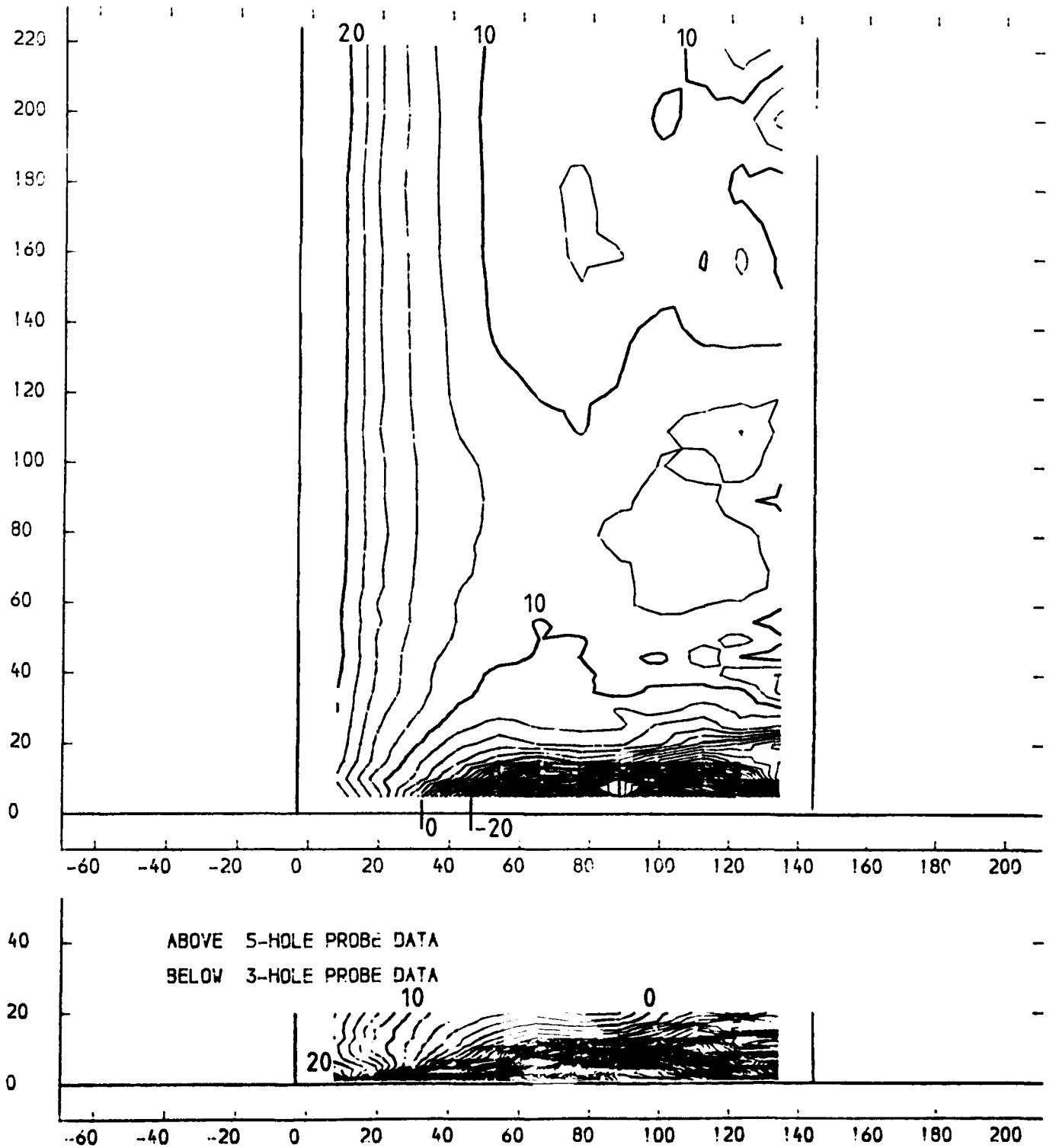


FIGURE 4.21

SLOT 3 STATIC PRESSURE COEFFICIENT  $(P1 - PLOCAL) / (P01 - P1)$  CONTOURS  
 NATURAL INLET BOUNDARY LAYER  
 X-AXIS TANGENTIAL CO-ORDINATE FROM TRAILING EDGE DATUM (MM)  
 Y-AXIS SPANWISE CO-ORDINATE FROM PERSPEX ENDWALL (MM)

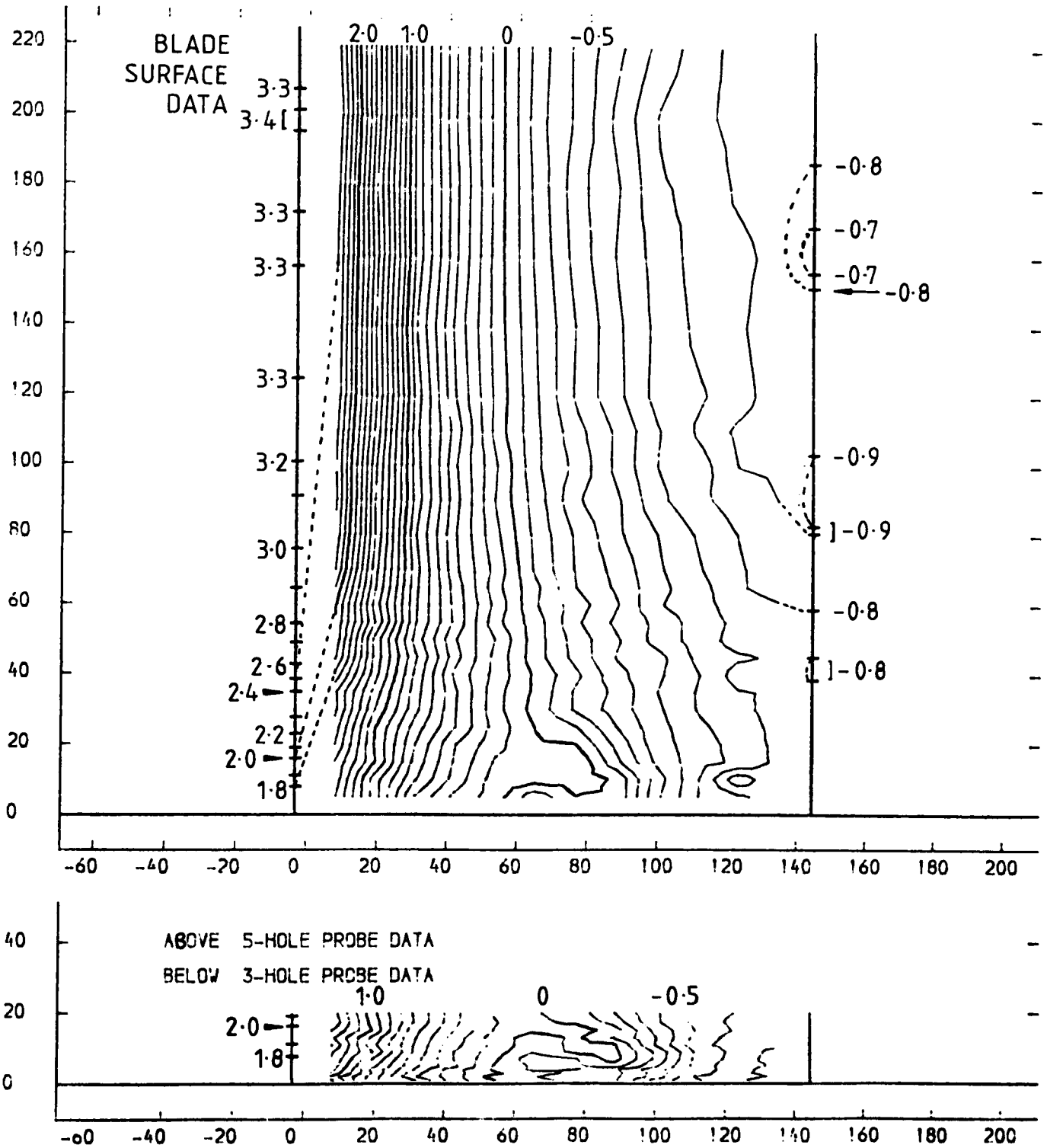


FIGURE 4.22

SLOT 4 EXPERIMENTAL DATA POINTS

NATURAL INLET BOUNDARY LAYER

X-AXIS TANGENTIAL CO-ORDINATE FROM TRAILING EDGE DATUM (MM)

Y-AXIS SPANWISE CO-ORDINATE FROM PERSPEX ENDWALL (MM)

+ PROBE DATA X MANUALLY INTERPOLATED DATA \* EXTRAPOLATED DATA

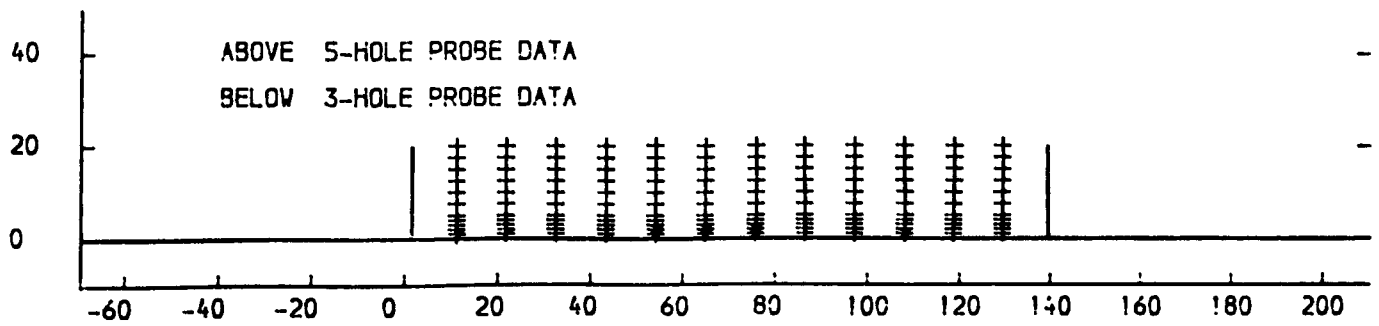
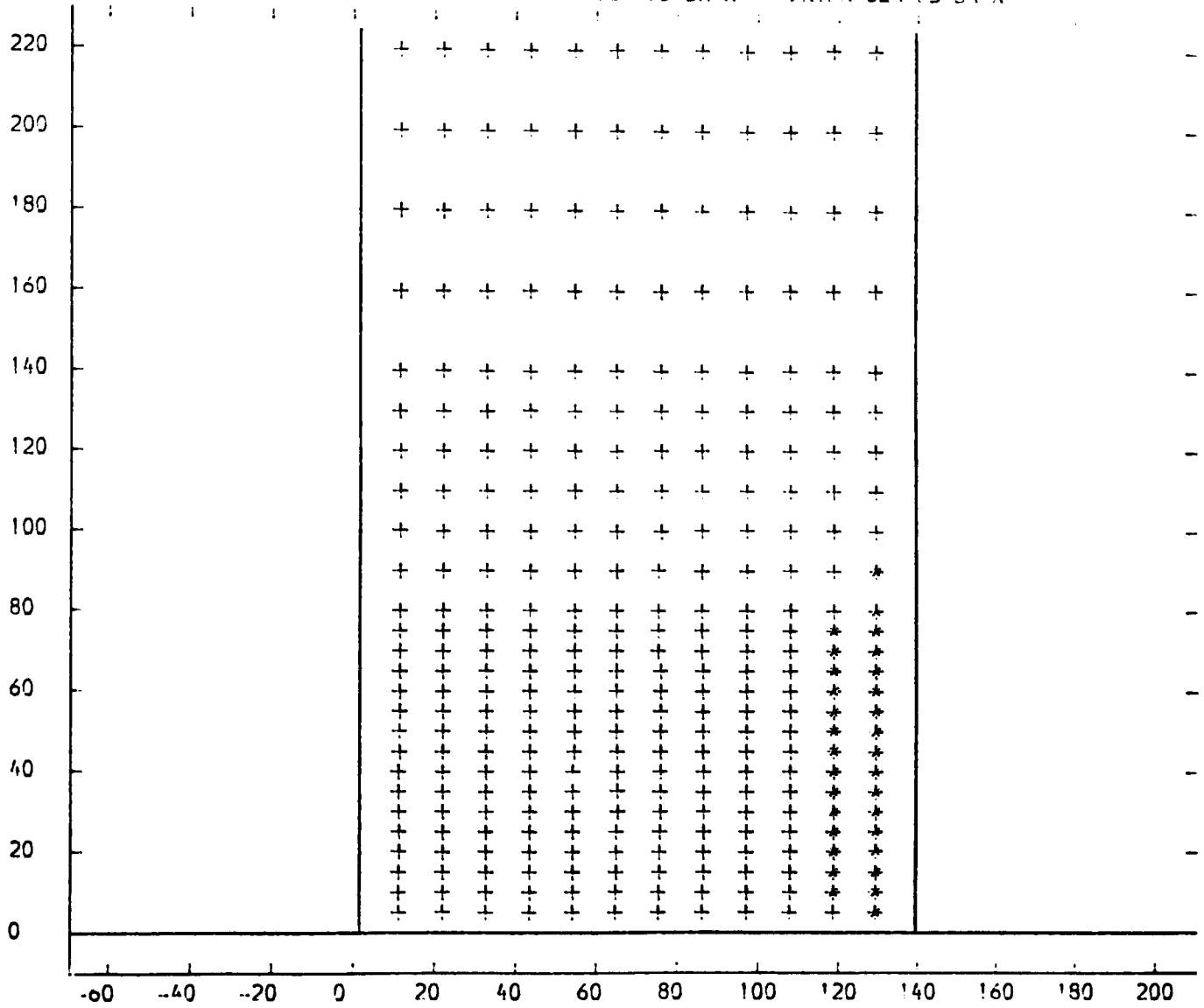


FIGURE 4.23

SLOT 4 TOTAL PRESSURE LOSS COEFFICIENT (  $(P_{01}-P_{01CCAL}) / (P_{01}-P_{11})$  ) CONTOURS  
 NATURAL INLET BOUNDARY LAYER  
 X-AXIS TANGENTIAL CO-ORDINATE FROM TRAILING EDGE DATUM (MM)  
 Y-AXIS SPANWISE CO-ORDINATE FROM PERSPEX ENDWALL (MM)

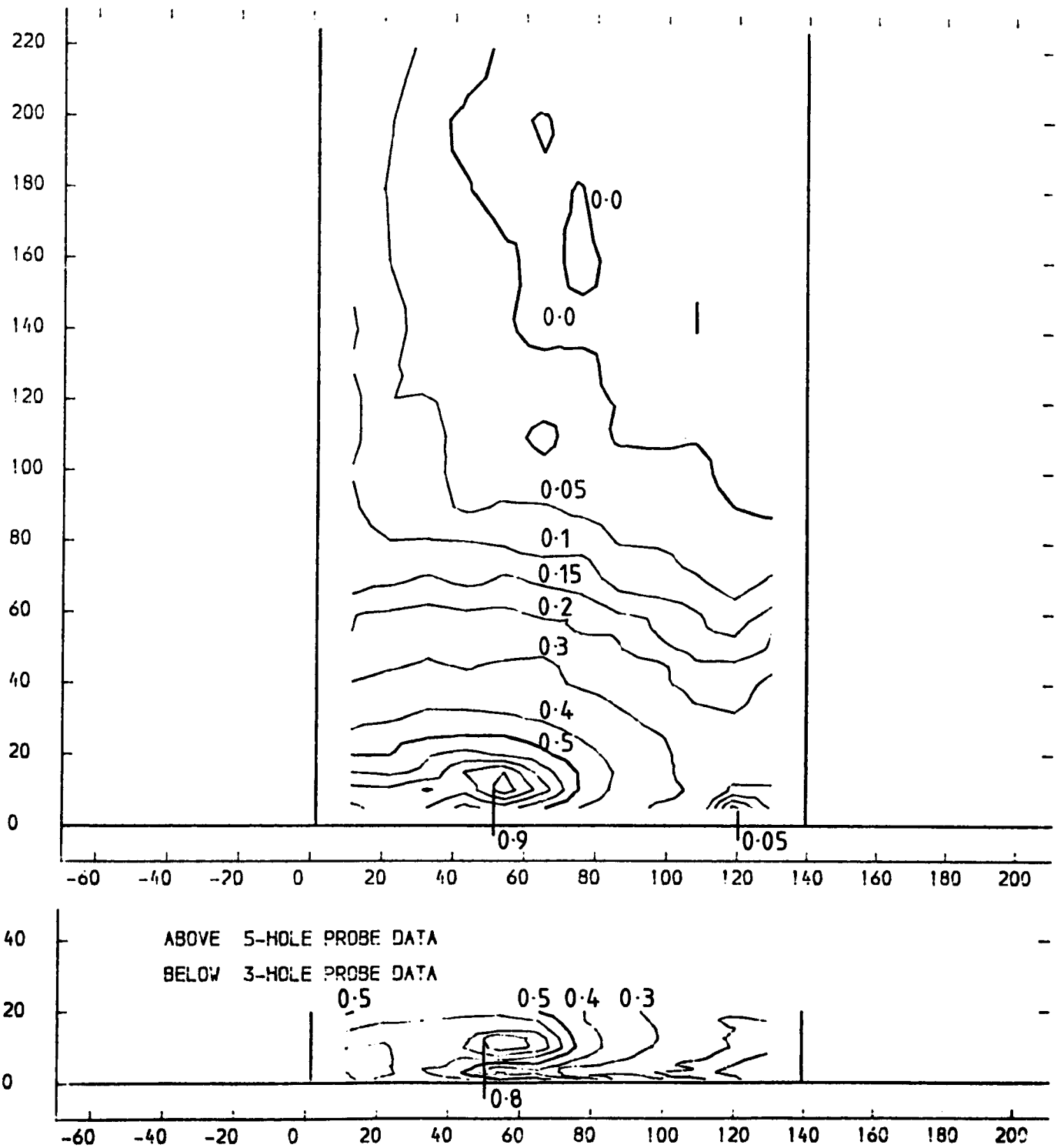


FIGURE 4.24



SLOT 4 TOTAL VELOCITY MAGNITUDE CONTOURS (CONTOUR UNITS METRES, SEC)  
 NATURAL INLET BOUNDARY LAYER  
 X-AXIS TANGENTIAL CO-ORDINATE FROM TRAILING EDGE DATUM (MM)  
 Y-AXIS SPANWISE CO-ORDINATE FROM PERSPEX ENDWALL (MM)

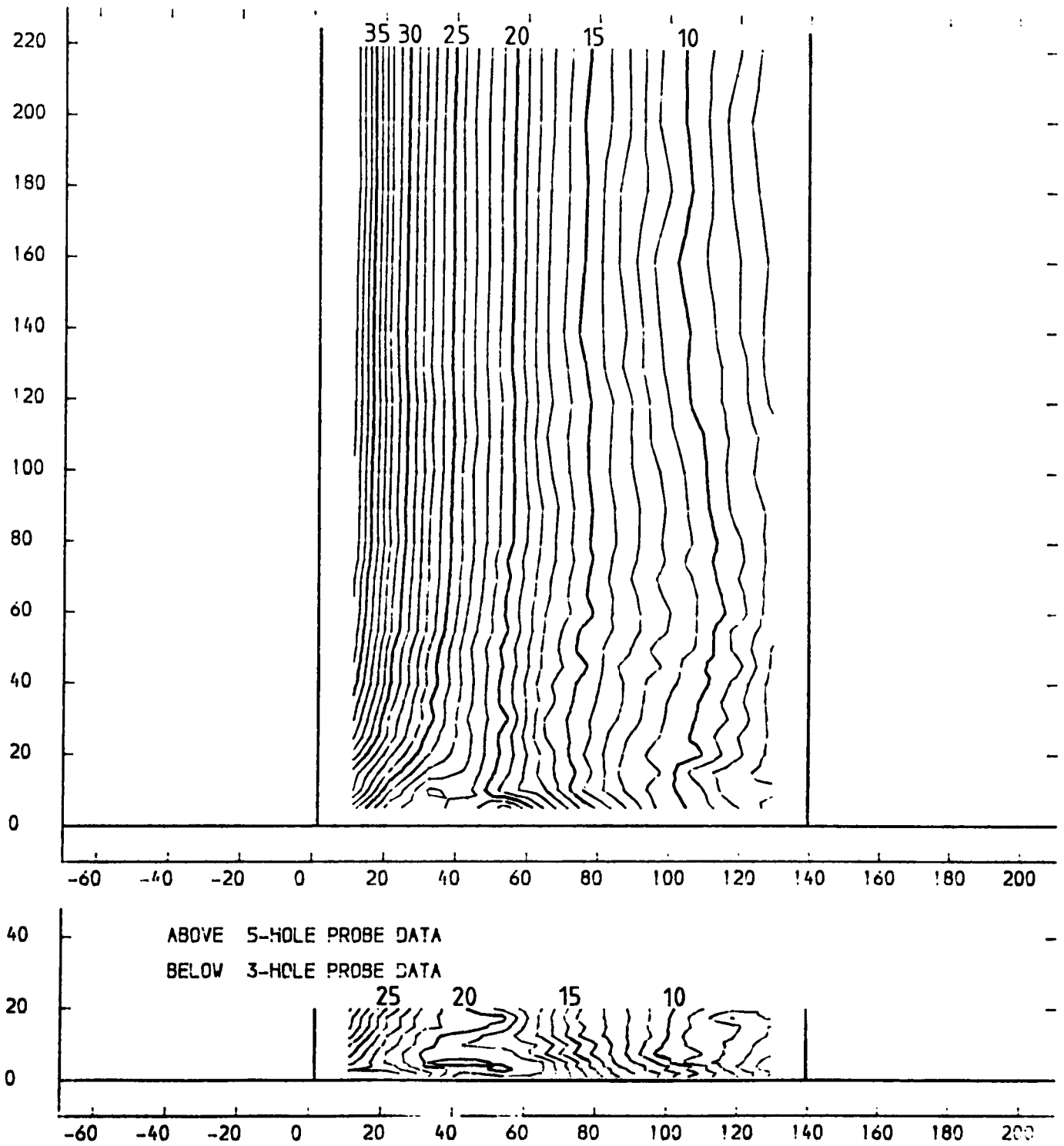
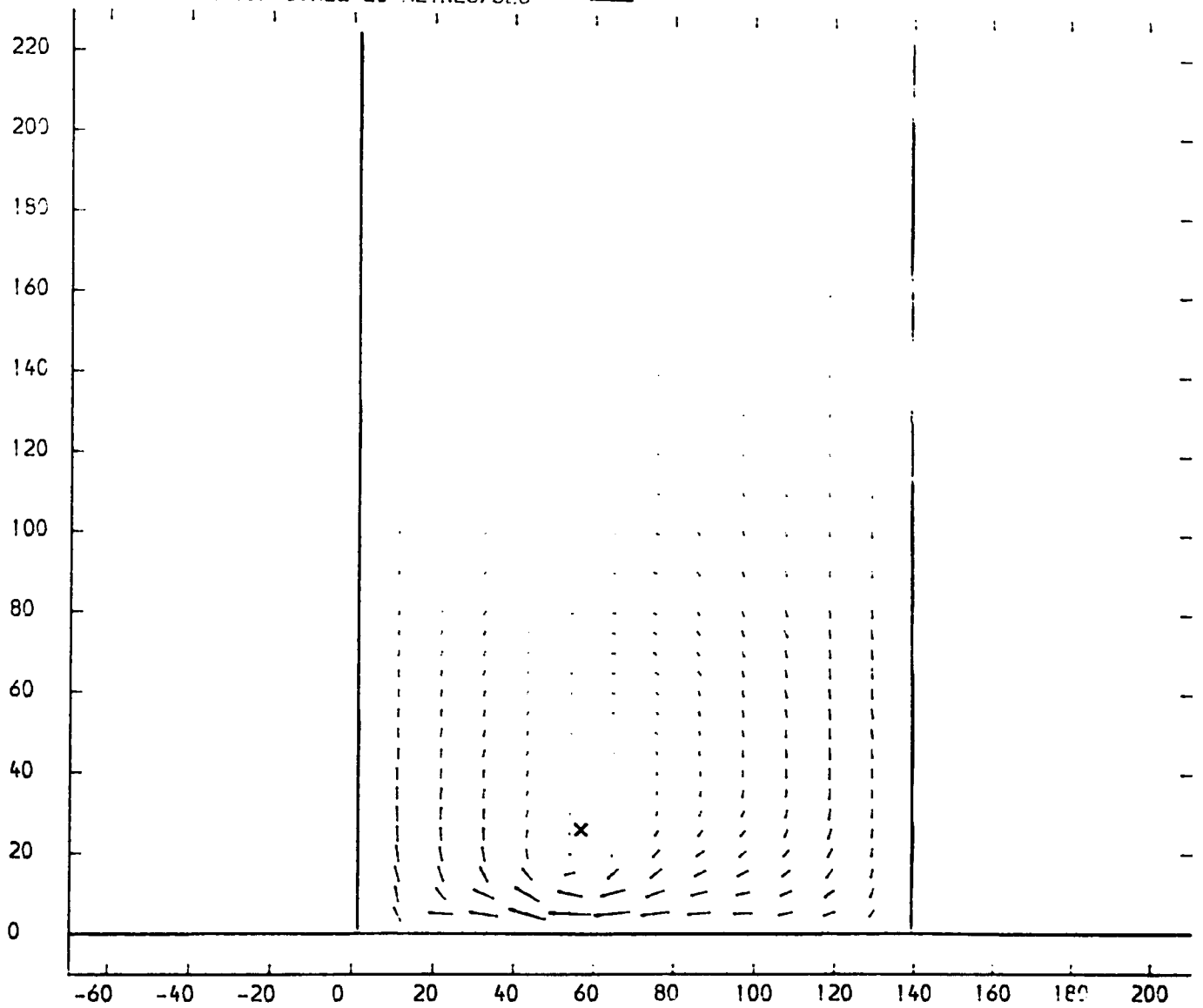


FIGURE 4.25

SLOT 4 VECTOR PLOT OF SECONDARY VELOCITIES  $(V_T(\text{SEC}) = V_T(\text{LOC}) - V_T(\text{M.S.}) + V_A(\text{LOC}) / V_A(\text{M.S.}))$   
 NATURAL INLET BOUNDARY LAYER  
 X-AXIS TANGENTIAL CO-ORDINATE FROM TRAILING EDGE DATUM (MM)  
 Y-AXIS SPANWISE CO-ORDINATE FROM PERSPEX ENDWALL (MM)  
 VECTOR SCALE 20 METRES/SEC



x PASSAGE VORTEX CENTRE

FIGURE 4.26

SLOT 4 SPANWISE ANGLE (PITCH ANGLE) CONTOURS (CONTOUR UNITS DEGREES)  
NATURAL INLET BOUNDARY LAYER  
X-AXIS TANGENTIAL CO-ORDINATE FROM TRAILING EDGE DATUM (MM)  
Y-AXIS SPANWISE CO-ORDINATE FROM PERSPEX ENDWALL (MM)

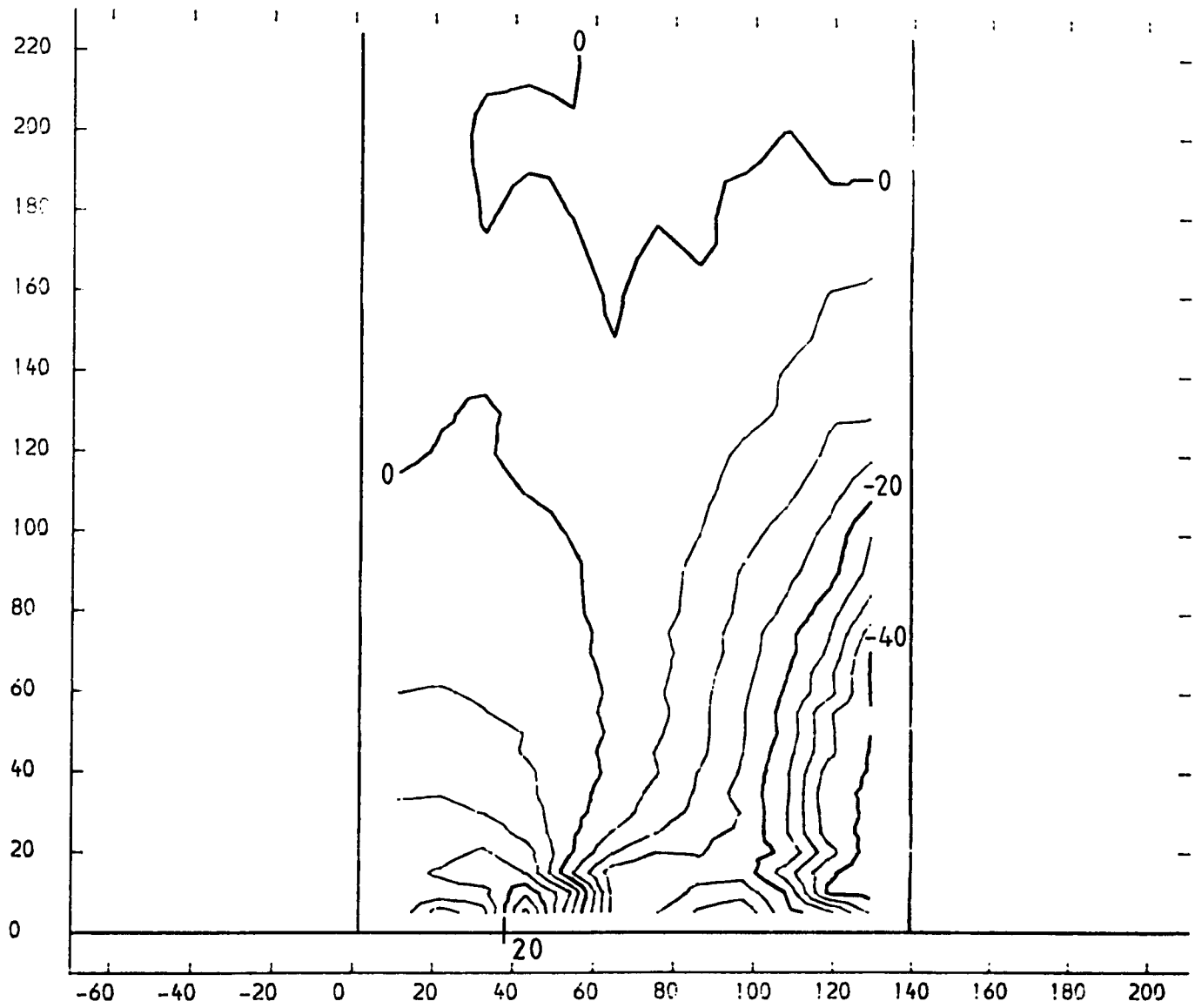


FIGURE 4.27

SLOT 4 YAW ANGLE CONTOURS (CONTOUR UNITS DEGREES)  
 NATURAL INLET BOUNDARY LAYER  
 X-AXIS TANGENTIAL CO-ORDINATE FROM TRAILING EDGE DATUM (MM)  
 Y-AXIS SPANWISE CO-ORDINATE FROM PERSPEX ENDWALL (MM)

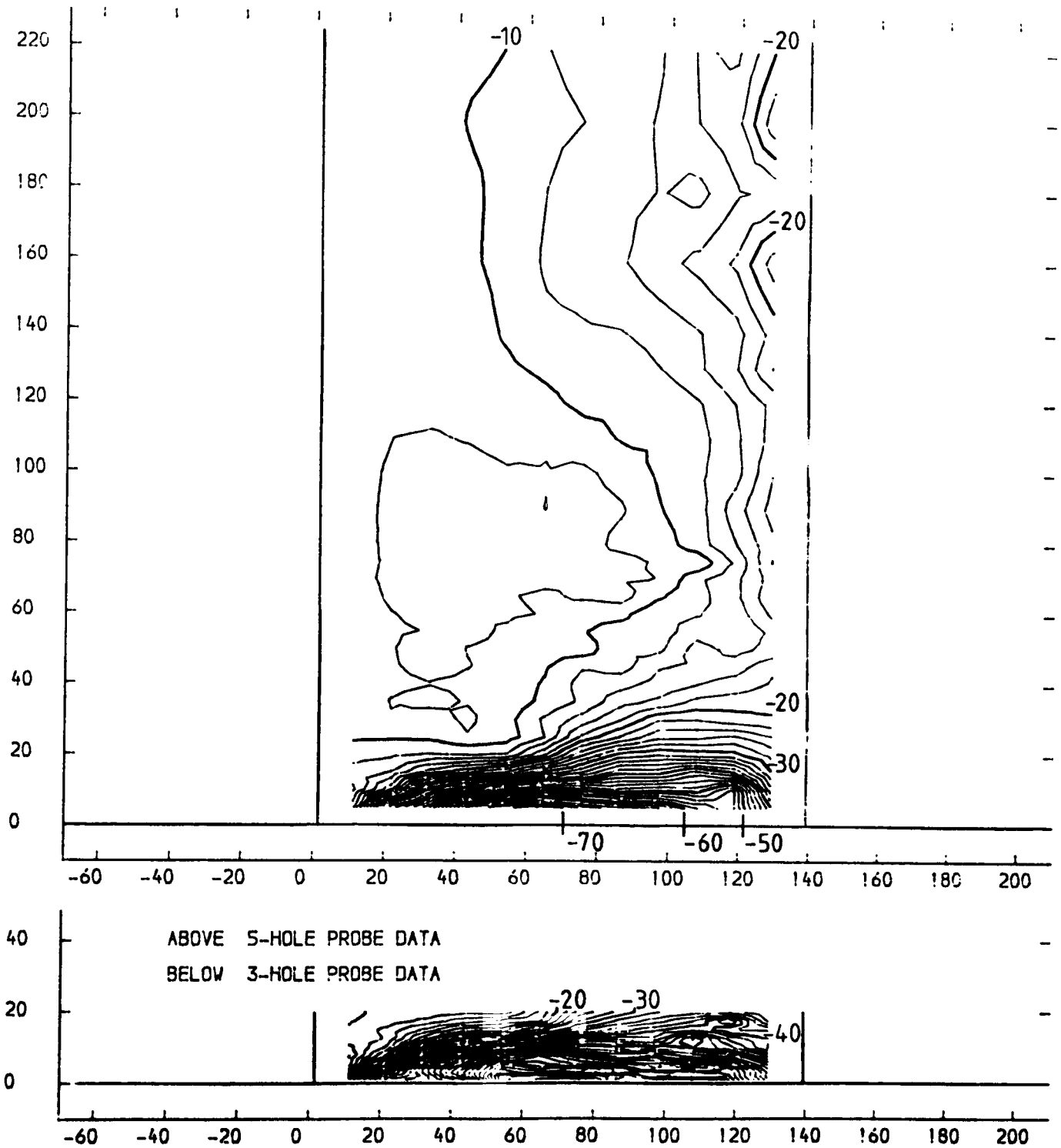


FIGURE 4.28

SLOT 4 STATIC PRESSURE COEFFICIENT  $(P1-LOCAL)/(P01-P1)$  CONTOURS

NATURAL INLET BOUNDARY LAYER

X-AXIS TANGENTIAL CO-ORDINATE FROM TRAILING EDGE DATUM (MM)

Y-AXIS SPANWISE CO-ORDINATE FROM PERSPEX ENDWALL (MM)

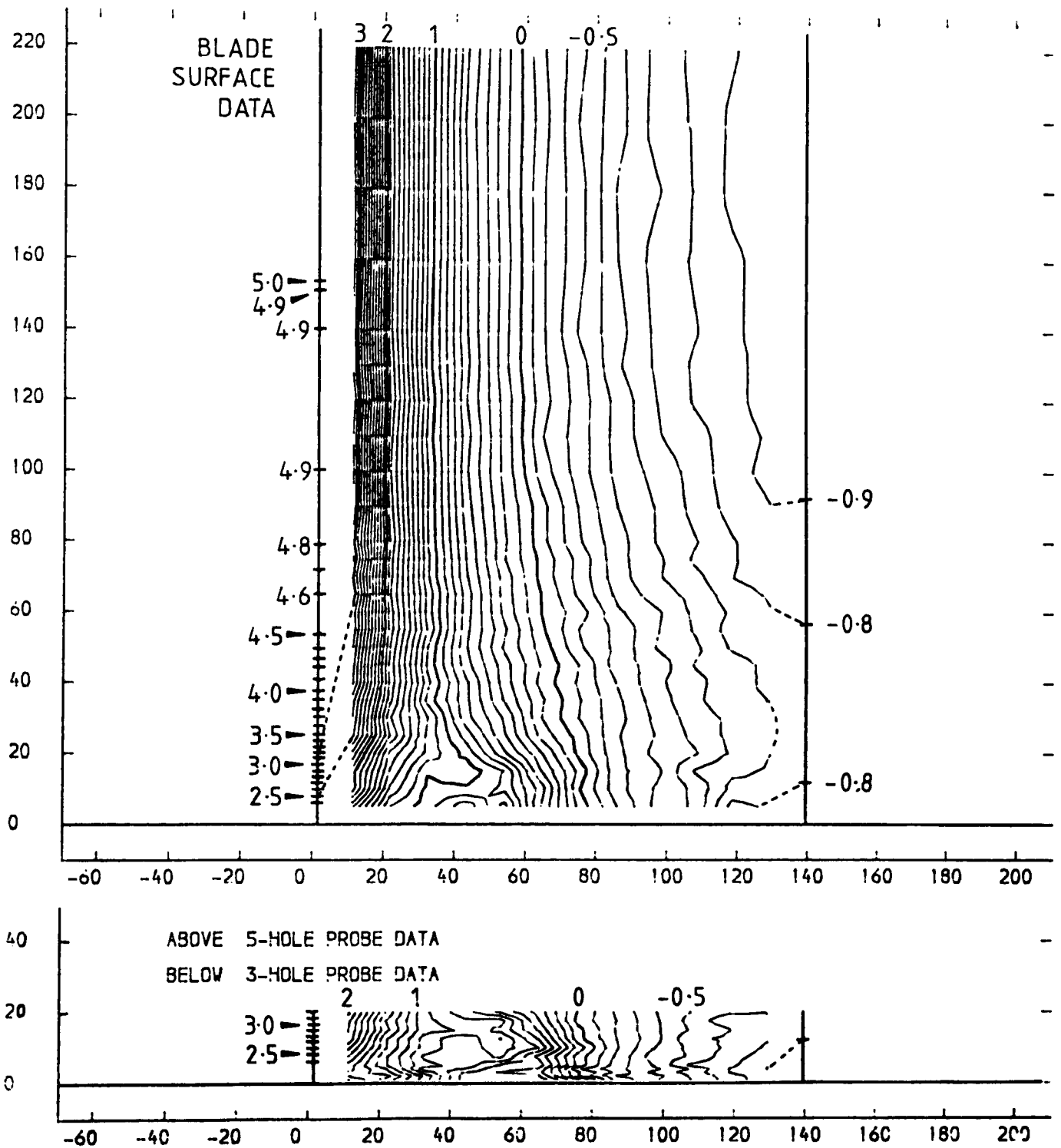


FIGURE 4.29

SLOT 5 EXPERIMENTAL DATA POINTS

NATURAL INLET BOUNDARY LAYER

X-AXIS TANGENTIAL CO-ORDINATE FROM TRAILING EDGE DATUM (MM)

Y-AXIS SPANWISE CO-ORDINATE FROM PERSPEX ENDWALL (MM)

+ PROBE DATA X MANUALLY INTERPOLATED DATA \* EXTRAPOLATED DATA

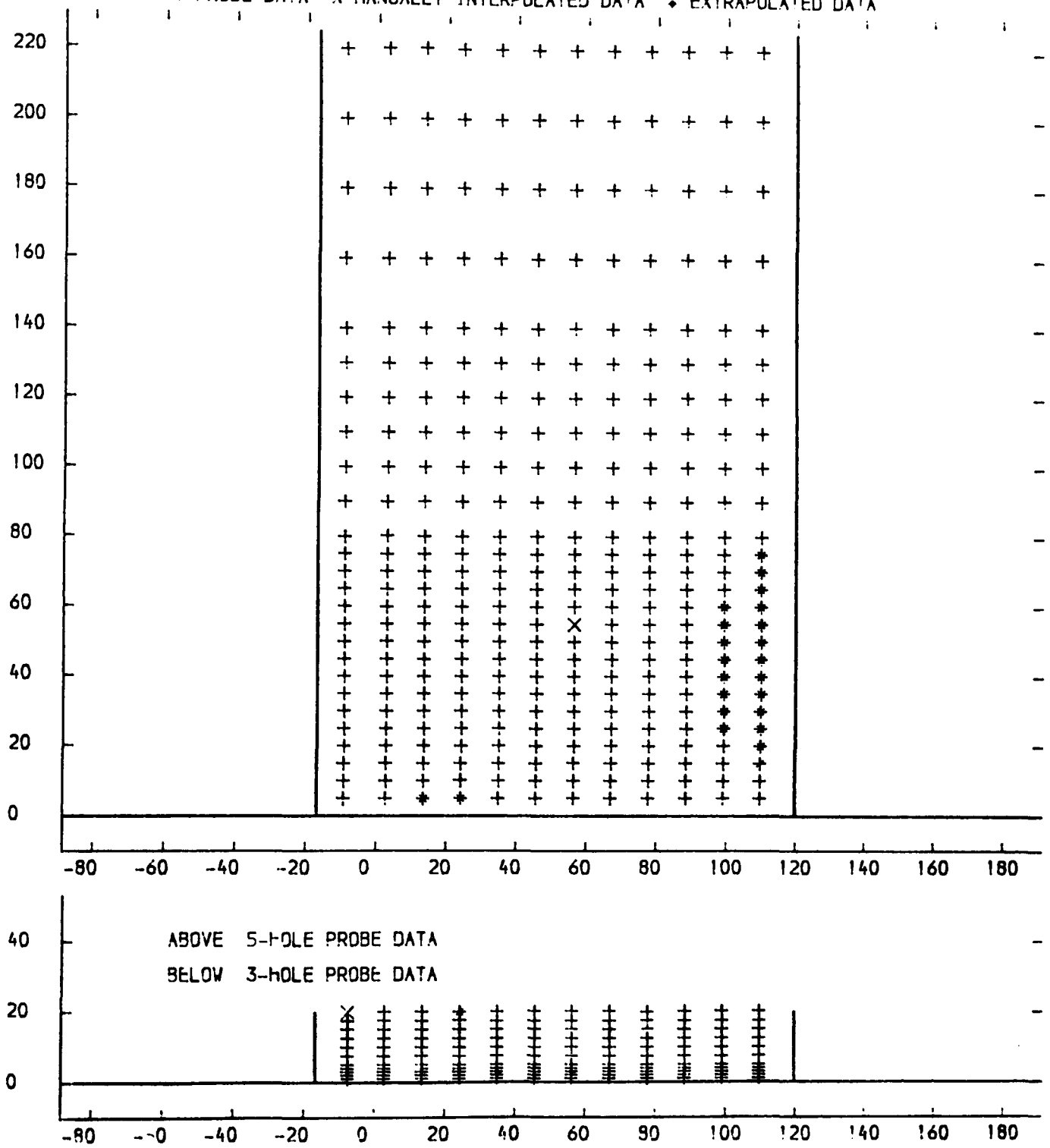


FIGURE 4.30

SLOT 5 TOTAL PRESSURE LOSS COEFFICIENT (  $(P_{01}-P_{0LOCAL}) / (P_{01}-P_1)$  ) CONTOURS  
 NATURAL INLET BOUNDARY LAYER  
 X-AXIS TANGENTIAL CO-ORDINATE FROM TRAILING EDGE DATUM (MM)  
 Y-AXIS SPANWISE CO-ORDINATE FROM PERSPEX ENDWALL (MM)

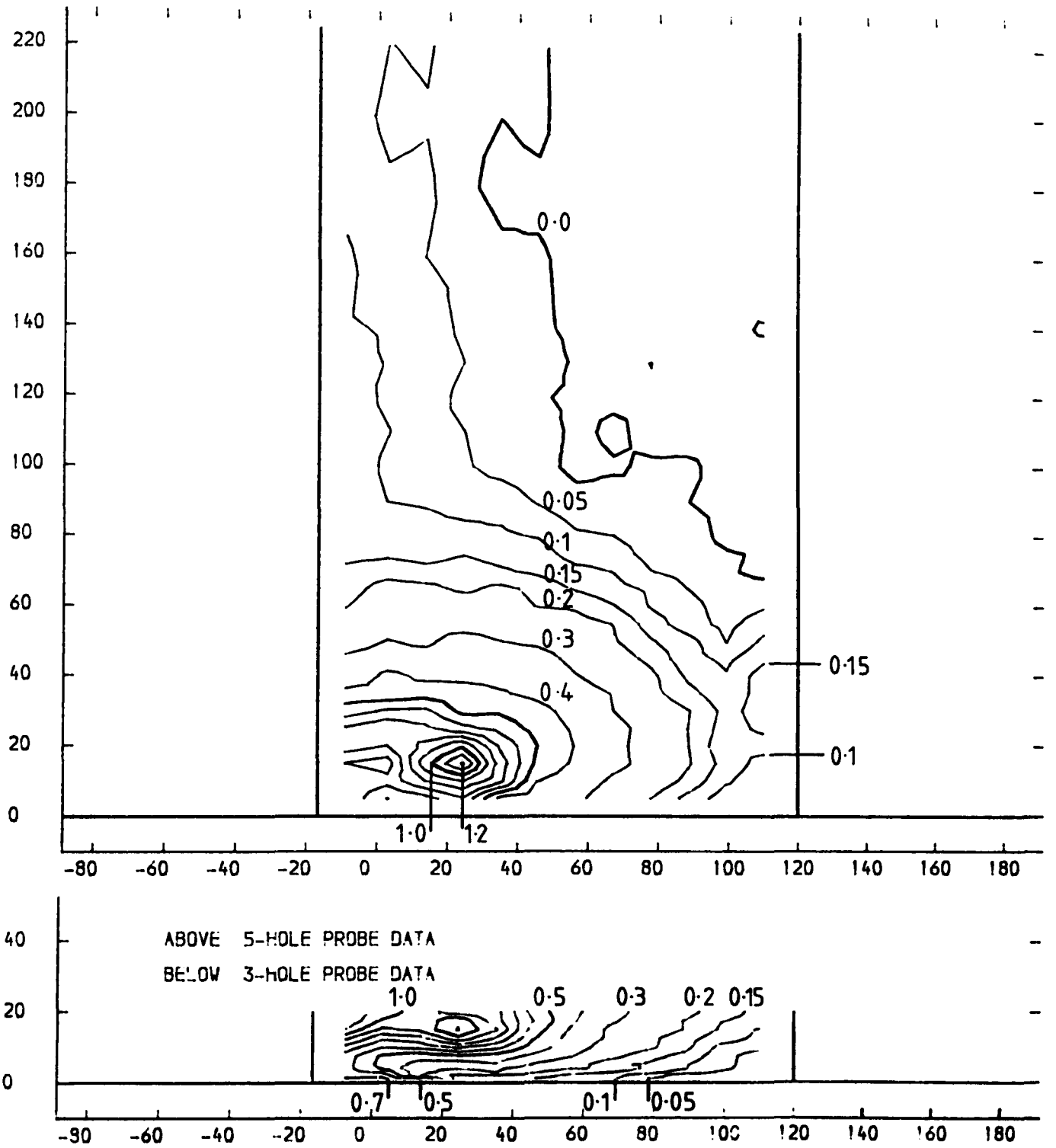


FIGURE 4.31

SLOT 5 TOTAL VELOCITY MAGNITUDE CONTOURS (CONTOUR UNITS METRES/SEC)  
 NATURAL INLET BOUNDARY LAYER  
 X-AXIS TANGENTIAL CO-ORDINATE FROM TRAILING EDGE DATUM (MM)  
 Y-AXIS SPANWISE CO-ORDINATE FROM PERSPEX ENDWALL (MM)

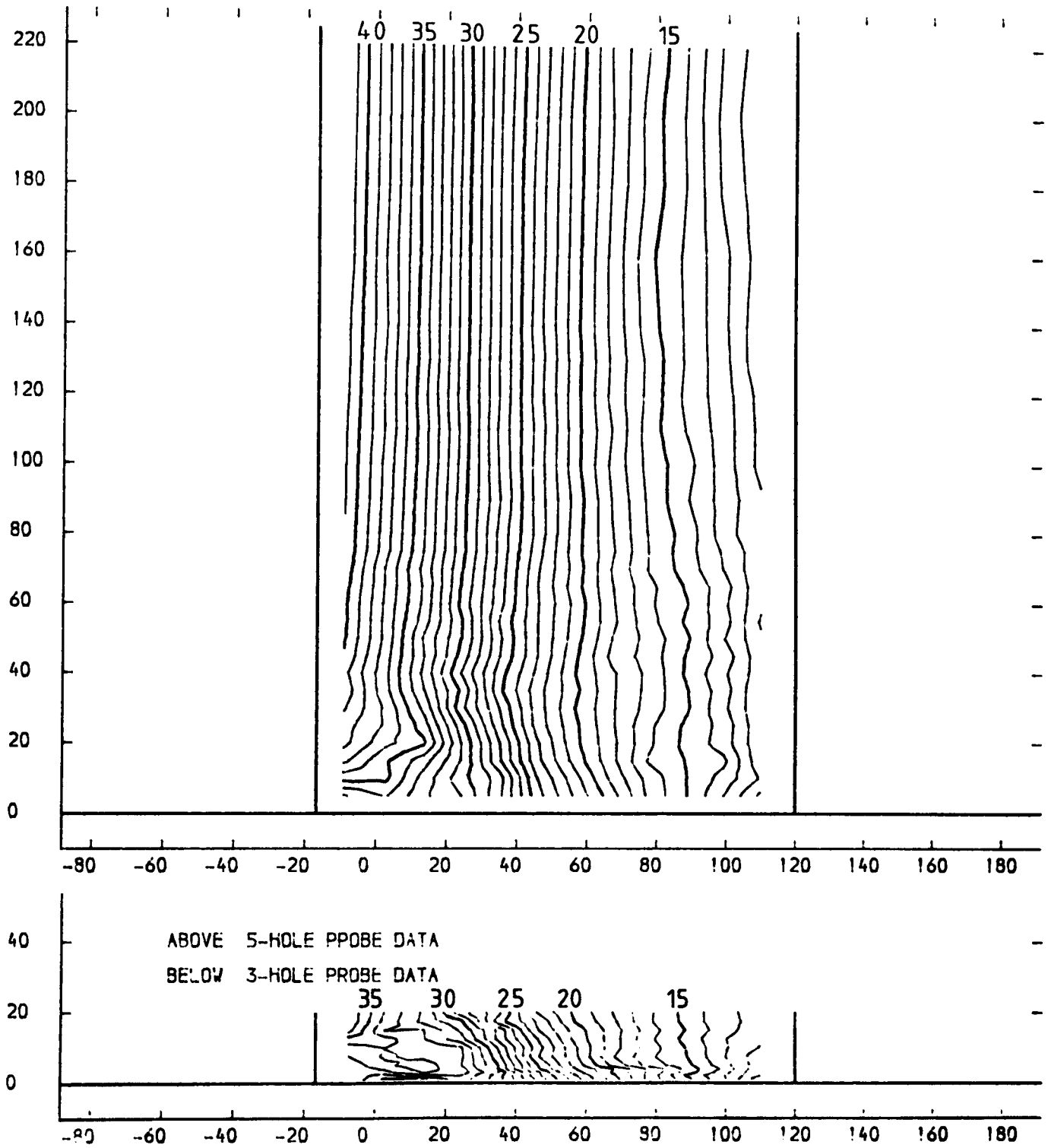
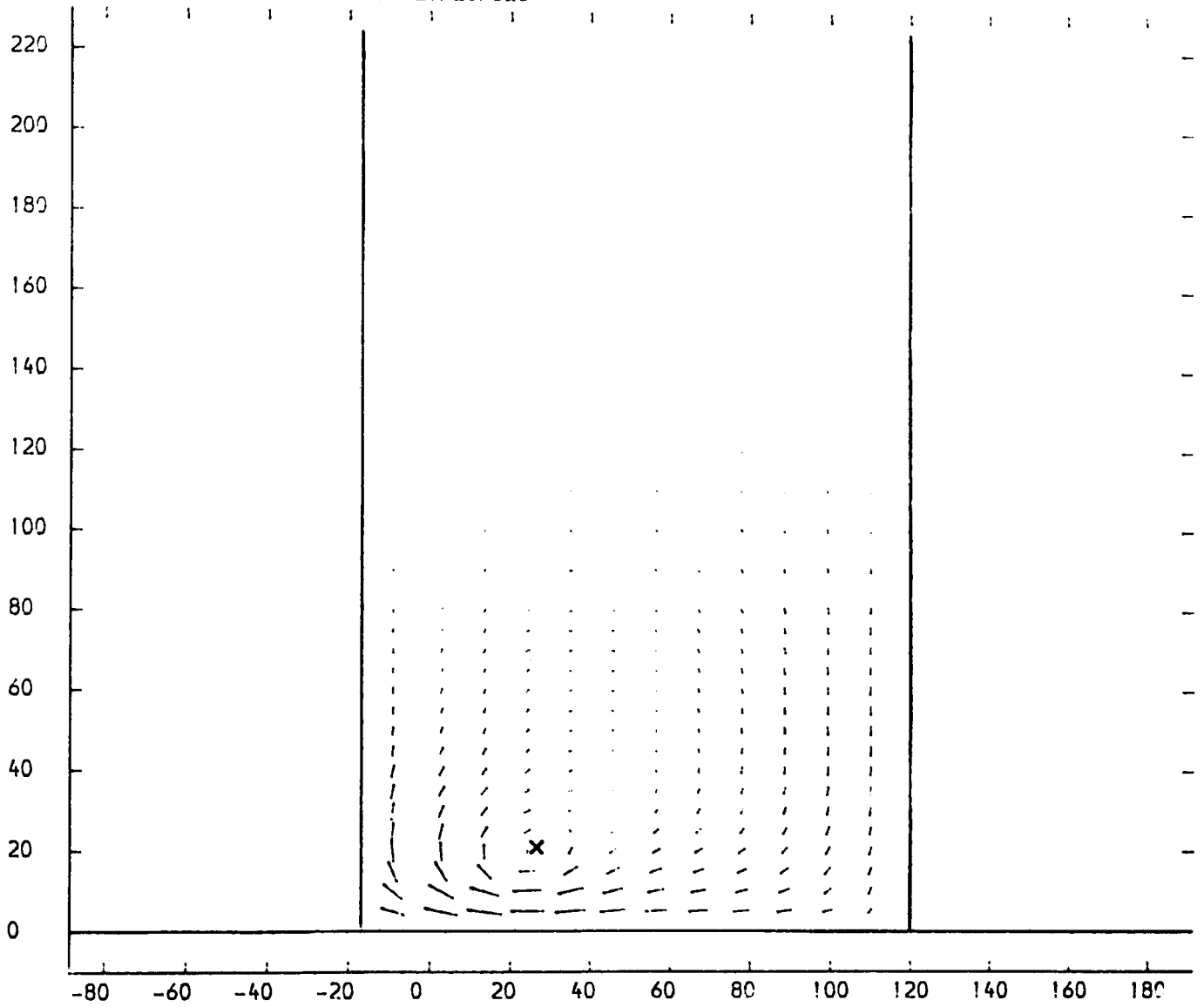


FIGURE 4.32



SLOT 5 VECTOR PLOT OF SECONDARY VELOCITIES  $(V_T(\text{SEC}) = V_T(\text{LOC}) - V_T(\text{M.S.}) + V_A(\text{LOC}) / V_A(\text{M.S.}))$   
 NATURAL INLET BOUNDARY LAYER  
 X-AXIS TANGENTIAL CO-ORDINATE FROM TRAILING EDGE DATUM (MM)  
 Y-AXIS SPANWISE CO-ORDINATE FROM PERSPEX ENDWALL (MM)  
 VECTOR SCALE 20 METRES/SEC



× PASSAGE VORTEX CENTRE

FIGURE 4.33

SLOT 5 SPANWISE ANGLE (PITCH ANGLE) CONTOURS (CONTOUR UNITS DEGREES)  
NATURAL INLET BOUNDARY LAYER  
X-AXIS TANGENTIAL CO-ORDINATE FROM TRAILING EDGE DATUM (MM)  
Y-AXIS SPANWISE CO-ORDINATE FROM PERSPEX ENDWALL (MM)

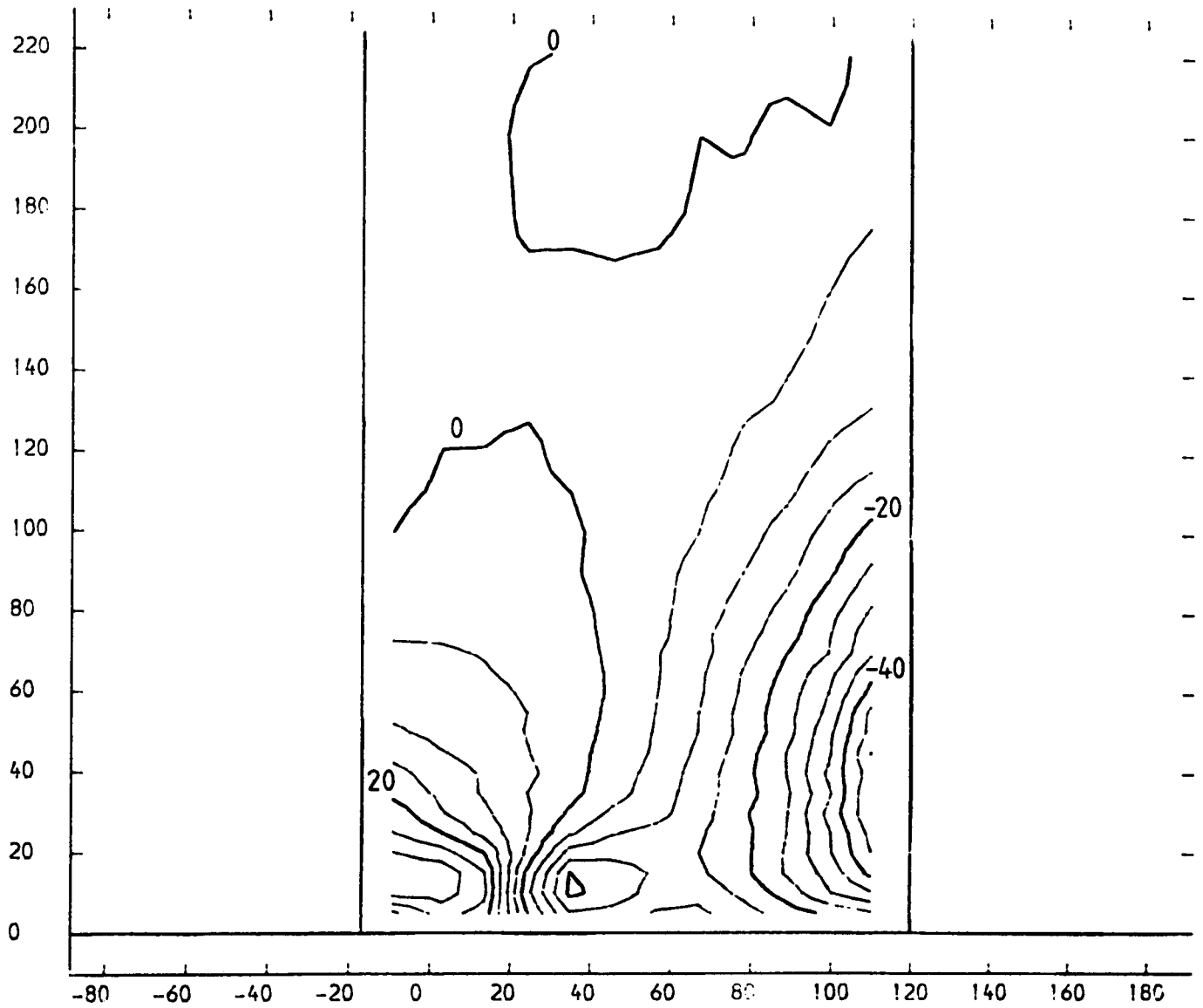


FIGURE 4.34

SLOT 5 YAW ANGLE CONTOURS (CONTOUR UNITS DEGREES)  
 NATURAL INLET BOUNDARY LAYER  
 X-AXIS TANGENTIAL CO-ORDINATE FROM TRAILING EDGE DATUM (MM)  
 Y-AXIS SPANWISE CO-ORDINATE FROM PERSPEX ENDWALL (MM)

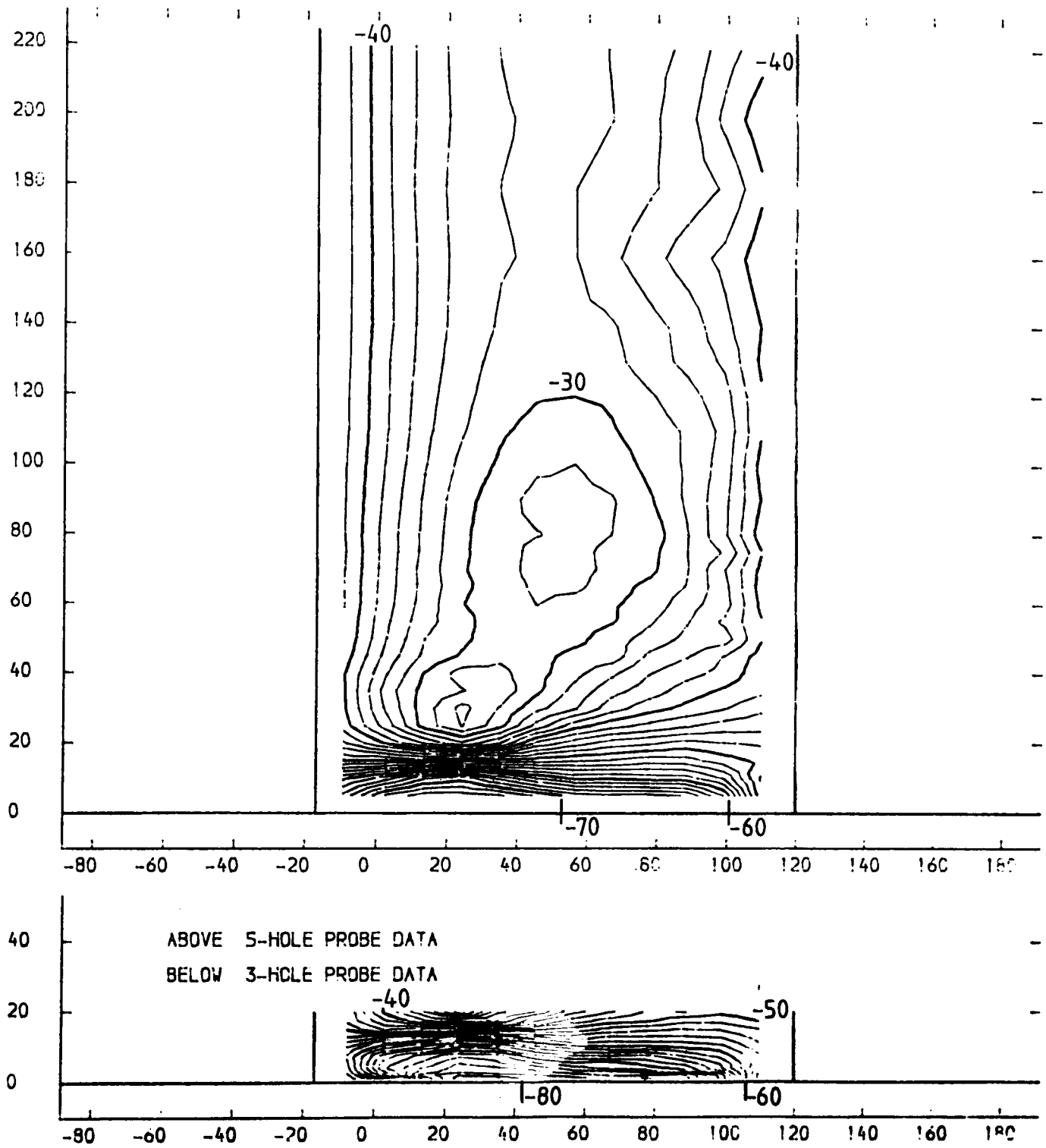


FIGURE 4.35

SLOT 5 STATIC PRESSURE COEFFICIENT (  $(P1-PLOCAL)/(P01-P1)$  ) CONTOURS  
 NATURAL INLET BOUNDARY LAYER  
 X-AXIS TANGENTIAL CO-ORDINATE FROM TRAILING EDGE DATUM (MM)  
 Y-AXIS SPANWISE CO-ORDINATE FROM PERSPEX ENDWALL (MM)

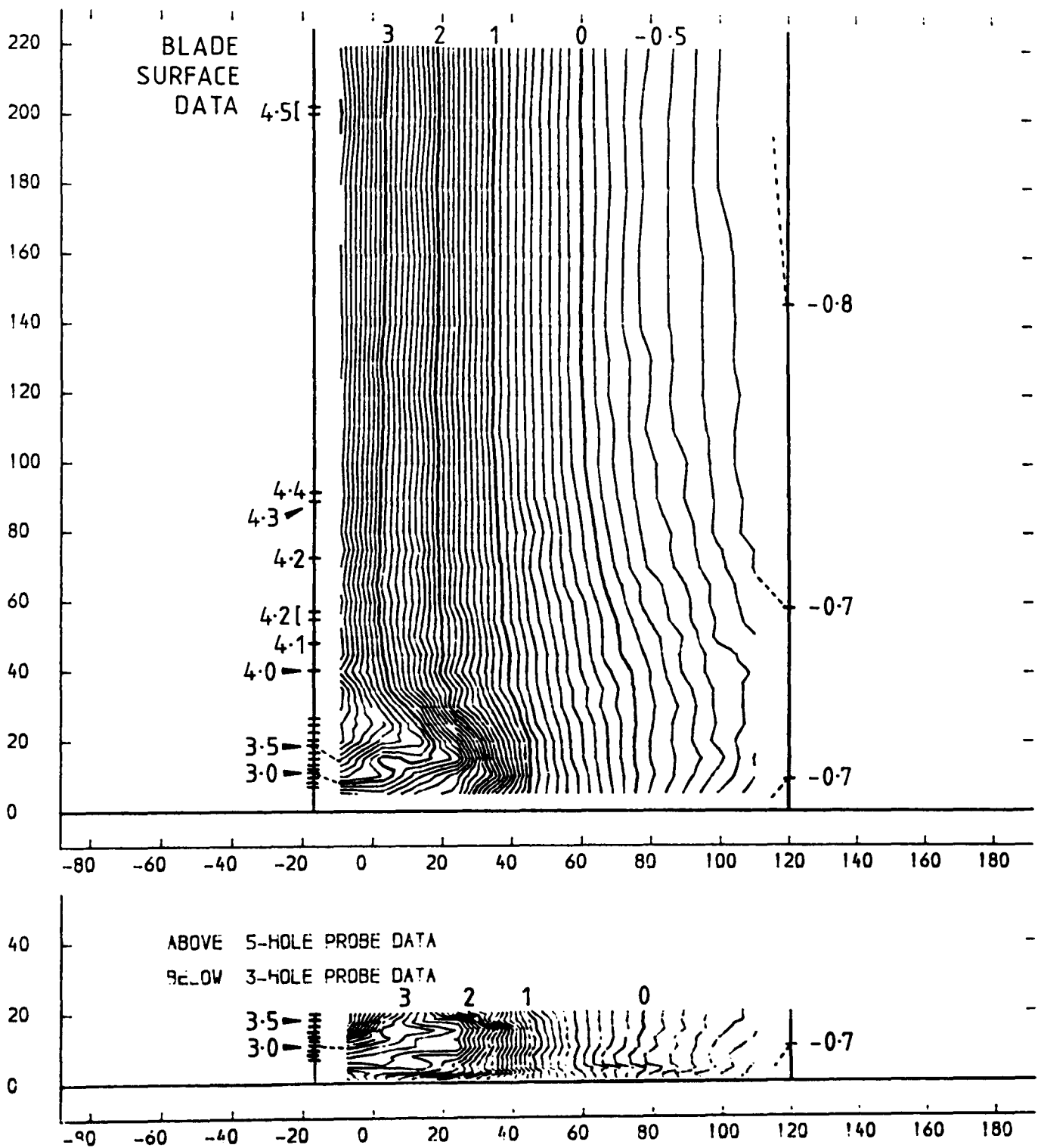


FIGURE 4.36

SLOT 6 EXPERIMENTAL DATA POINTS

NATURAL INLET BOUNDARY LAYER

X-AXIS TANGENTIAL CO-ORDINATE FROM TRAILING EDGE DATUM (MM)

Y-AXIS SPANWISE CO-ORDINATE FROM PERSPEX ENDWALL (MM)

+ PROBE DATA X MANUALLY INTERPOLATED DATA \* EXTRAPOLATED DATA

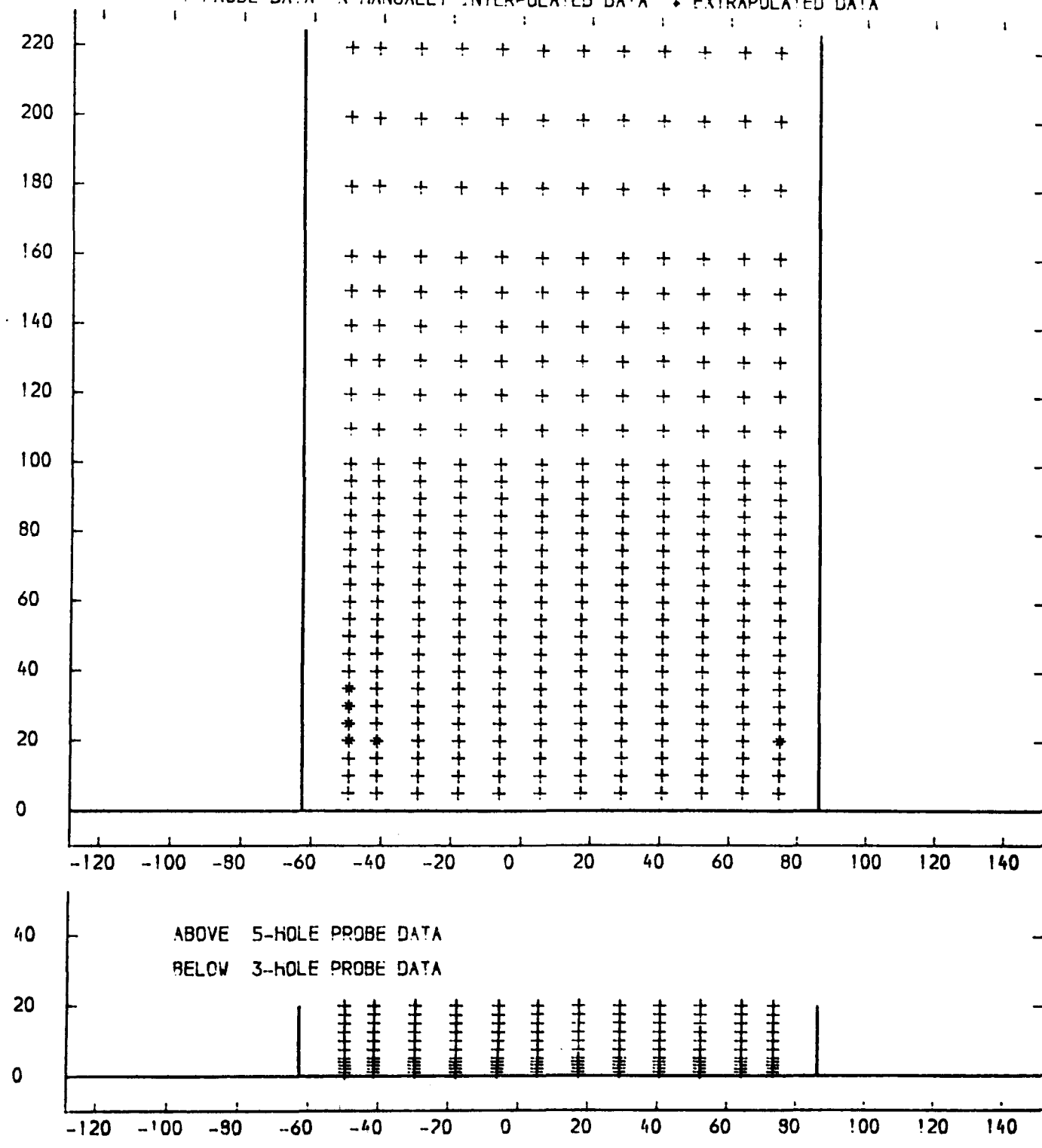


FIGURE 4.37

SLOT 6 TOTAL PRESSURE LOSS COEFFICIENT (  $(P_{01}-P_{0LOCAL}) / (P_{01}-P_{11})$  ) CONTOURS  
 NATURAL INLET BOUNDARY LAYER  
 X-AXIS TANGENTIAL O-ORDINATE FROM TRAILING EDGE DATUM (MM)  
 Y-AXIS SPANWISE CO-ORDINATE FROM PERSPEX ENDWALL (MM)

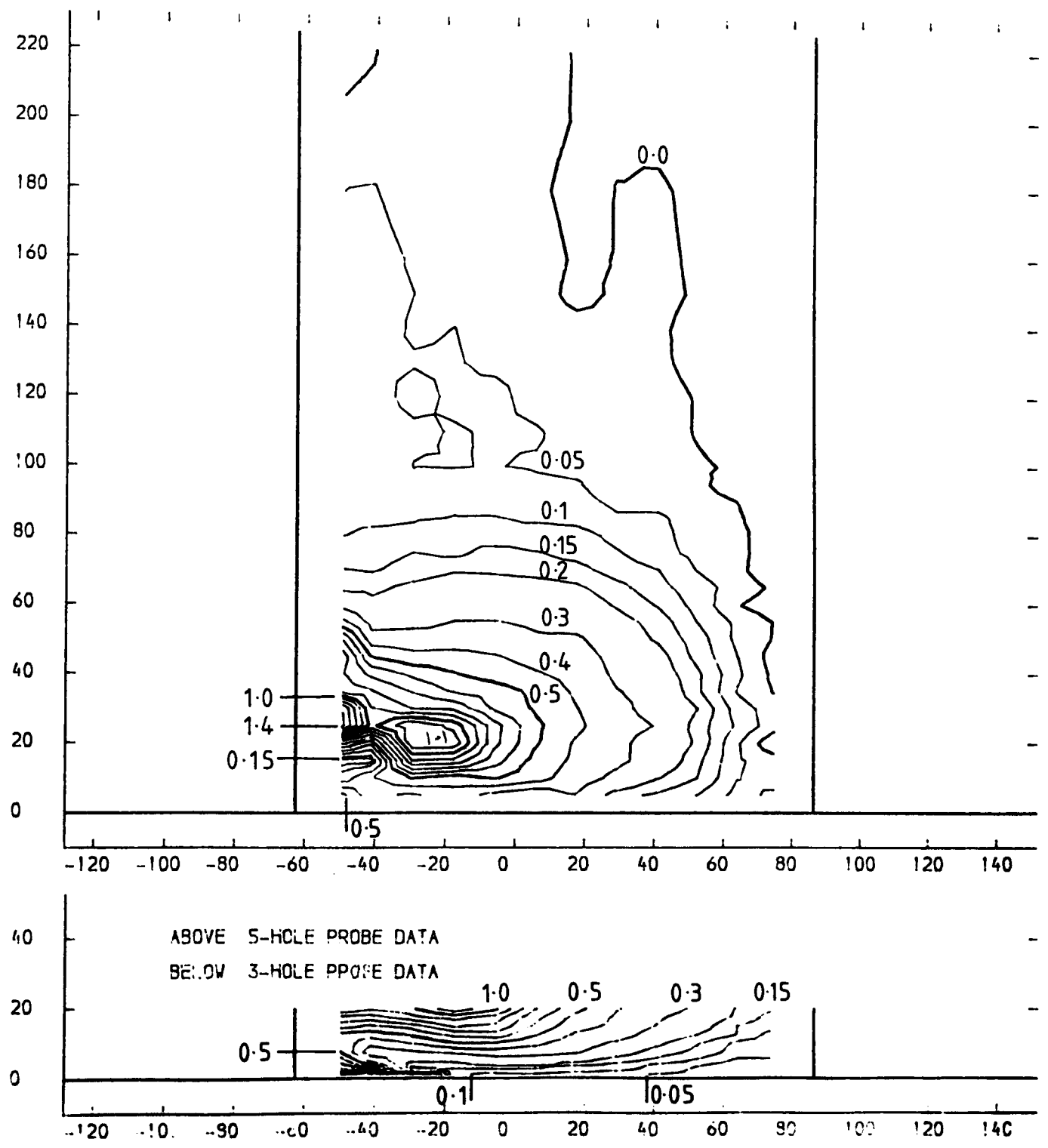


FIGURE 4.38

SLOT 6 TOTAL VELOCITY MAGNITUDE CONTOURS (CONTOUR UNITS METRES/SEC)  
 NATURAL INLET BOUNDARY LAYER  
 X-AXIS TANGENTIAL CO-ORDINATE FROM TRAILING EDGE DATUM (MM)  
 Y-AXIS SPANWISE CO-ORDINATE FROM PERSPEX ENDWALL (MM)

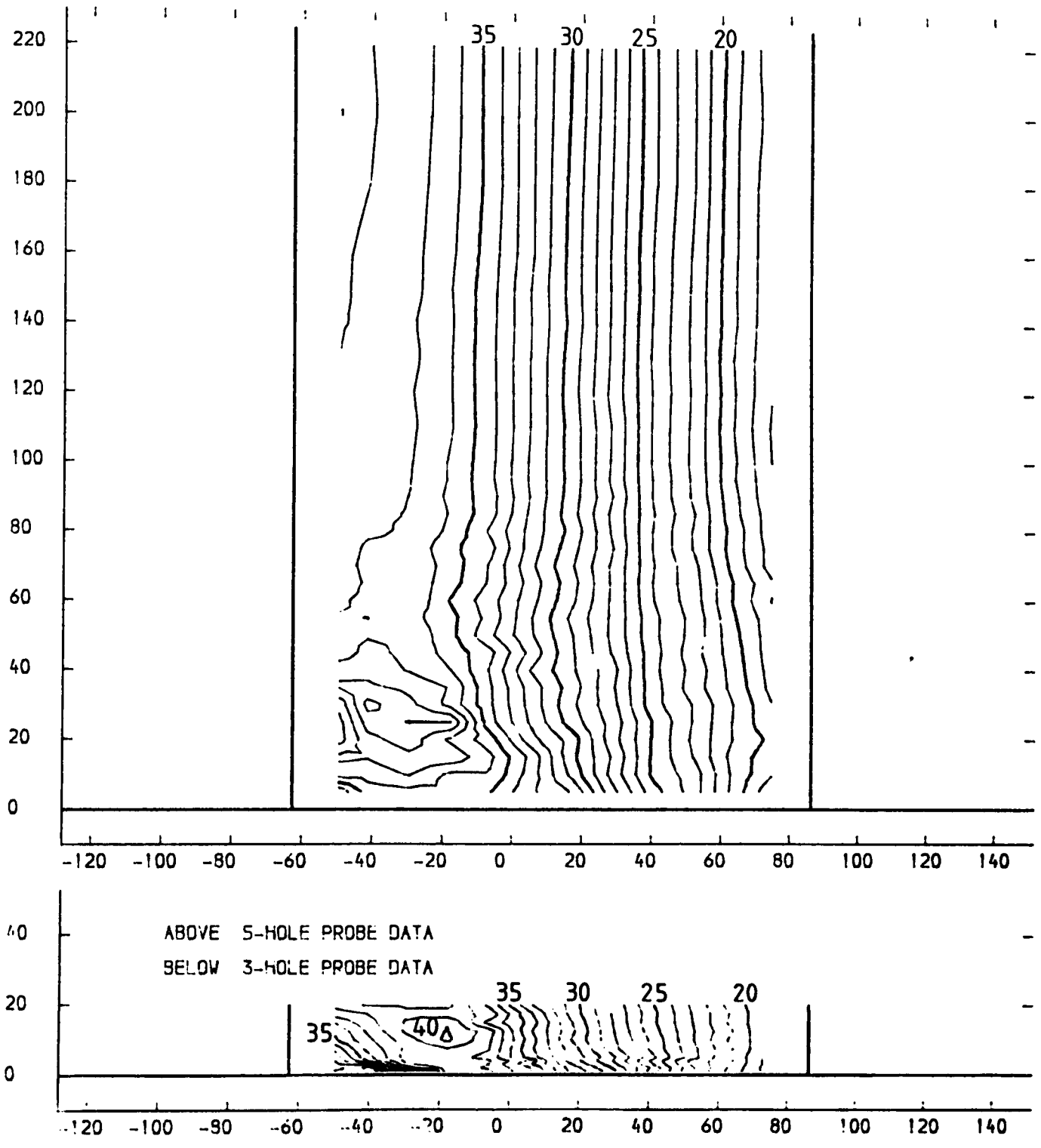
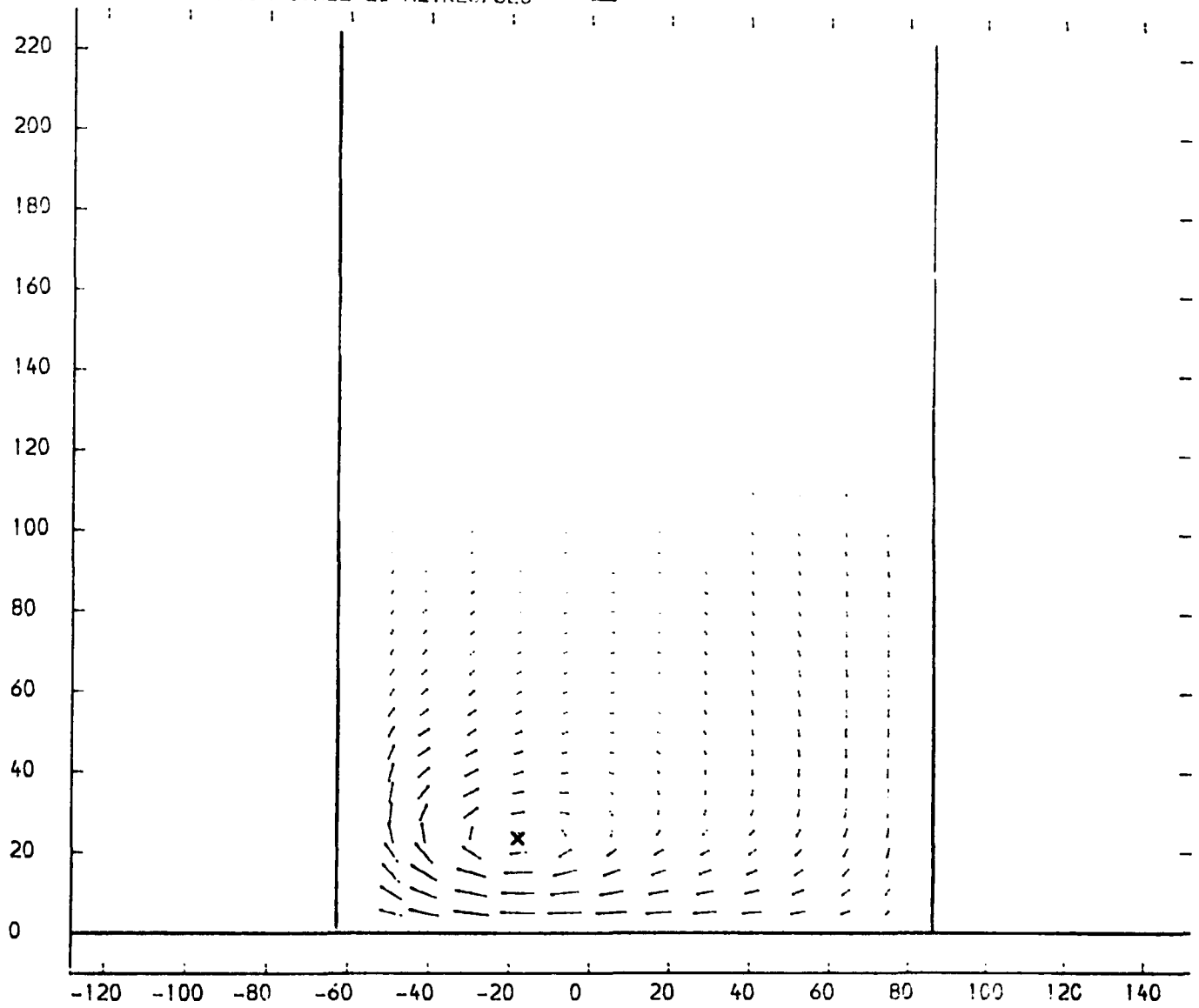


FIGURE 4.39

SLOT 6 VECTOR PLOT OF SECONDARY VELOCITIES  $(V_T(\text{SEC}) = V_T(\text{LOC}) - V_T(\text{M.S.}) + V_A(\text{LOC}) / V_A(\text{M.S.}))$   
 NATURAL INLET BOUNDARY LAYER  
 X-AXIS TANGENTIAL CO-ORDINATE FROM TRAILING EDGE DATUM (MM)  
 Y-AXIS SPANWISE CO-ORDINATE FROM PERSPEX ENDWALL (MM)  
 VECTOR SCALE 20 METRES/SEC



x PASSAGE VORTEX CENTRE

FIGURE 4.40



SLOT 6 SPANWISE ANGLE (PITCH ANGLE) CONTOURS (CONTOUR UNITS DEGREES)  
NATURAL INLET BOUNDARY LAYER  
X-AXIS TANGENTIAL CO-ORDINATE FROM TRAILING EDGE DATUM (MM)  
Y-AXIS SPANWISE CO-ORDINATE FROM PERSPEX ENDWALL (MM)

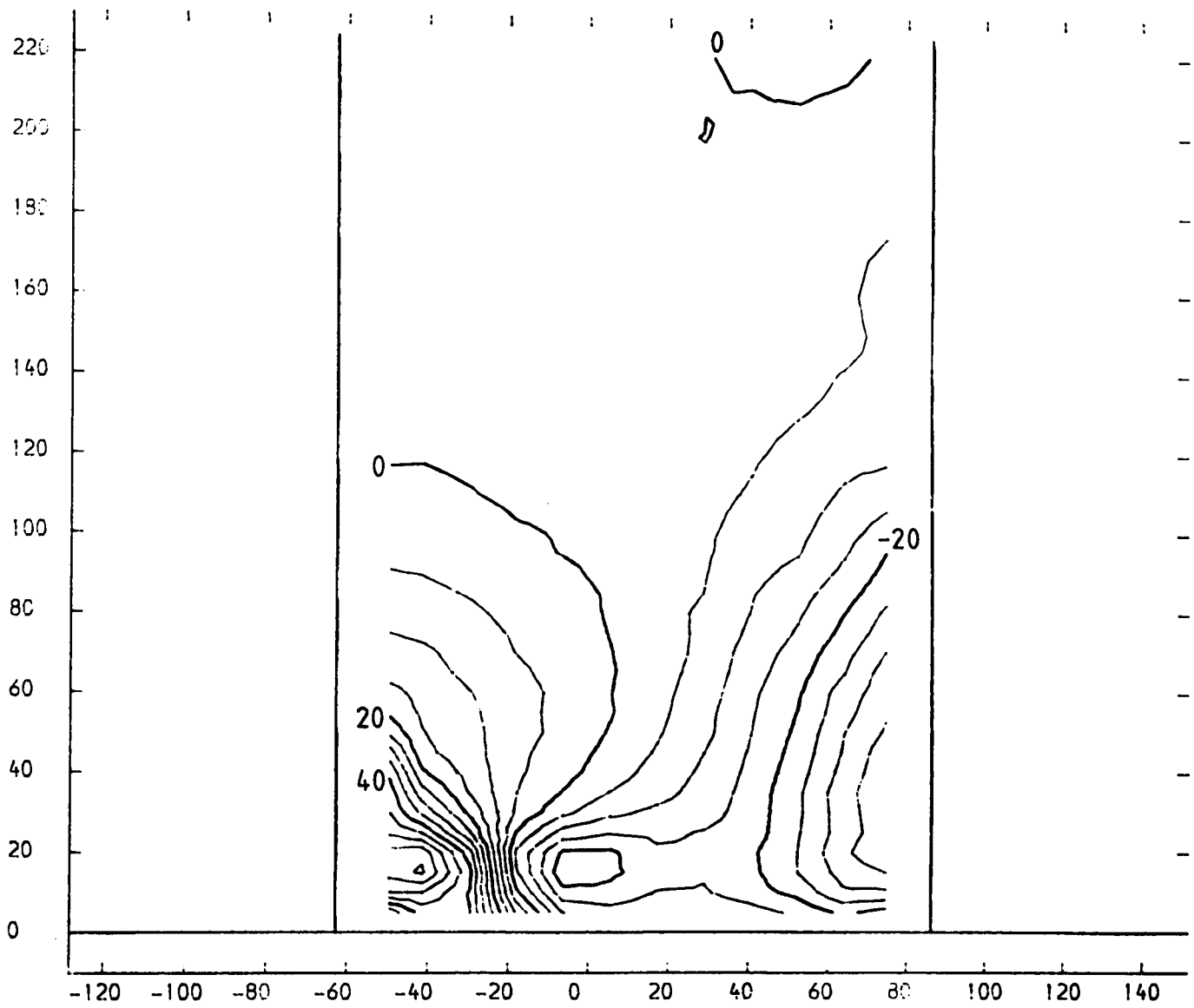


FIGURE 4.41

SLOT 6 YAW ANGLE CONTOURS (CONTOUR UNITS DEGREES)  
 NATURAL INLET BOUNDARY LAYER  
 X-AXIS TANGENTIAL CO-ORDINATE FROM TRAILING EDGE DATUM (MM)  
 Y-AXIS SPANWISE CO-ORDINATE FROM PERSPEX ENDWALL (MM)

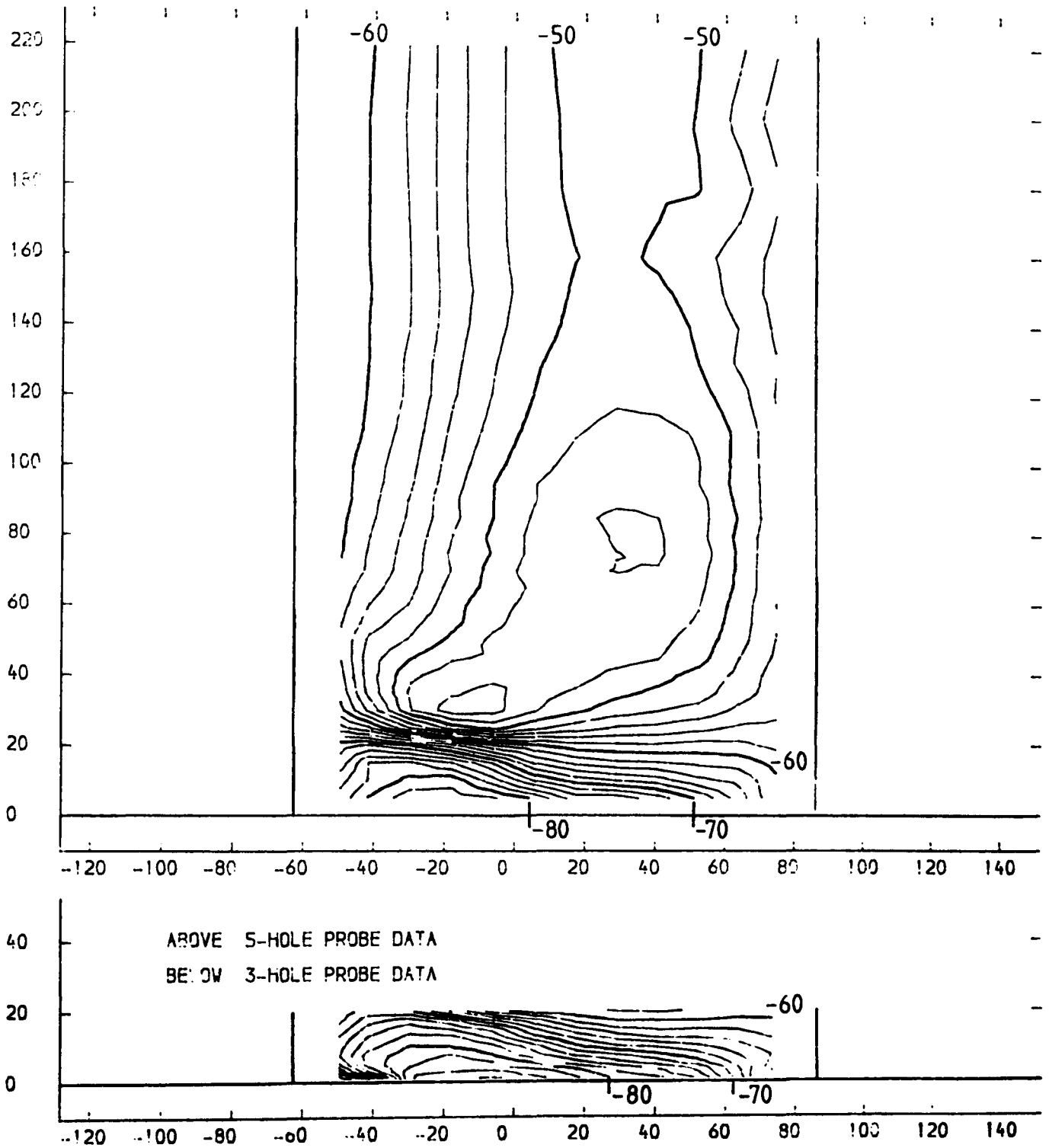


FIGURE 4.42

SLOT 6 STATIC PRESSURE COEFFICIENT (  $(P!-PLOCAL) / (P0!-P!)$  ) CONTOURS  
 NATURAL INLET BOUNDARY LAYER  
 X-AXIS TANGENTIAL CO-ORDINATE FROM TRAILING EDGE DATUM (MM)  
 Y-AXIS SPANWISE CO-ORDINATE FROM PERSPEX ENDWALL (MM)

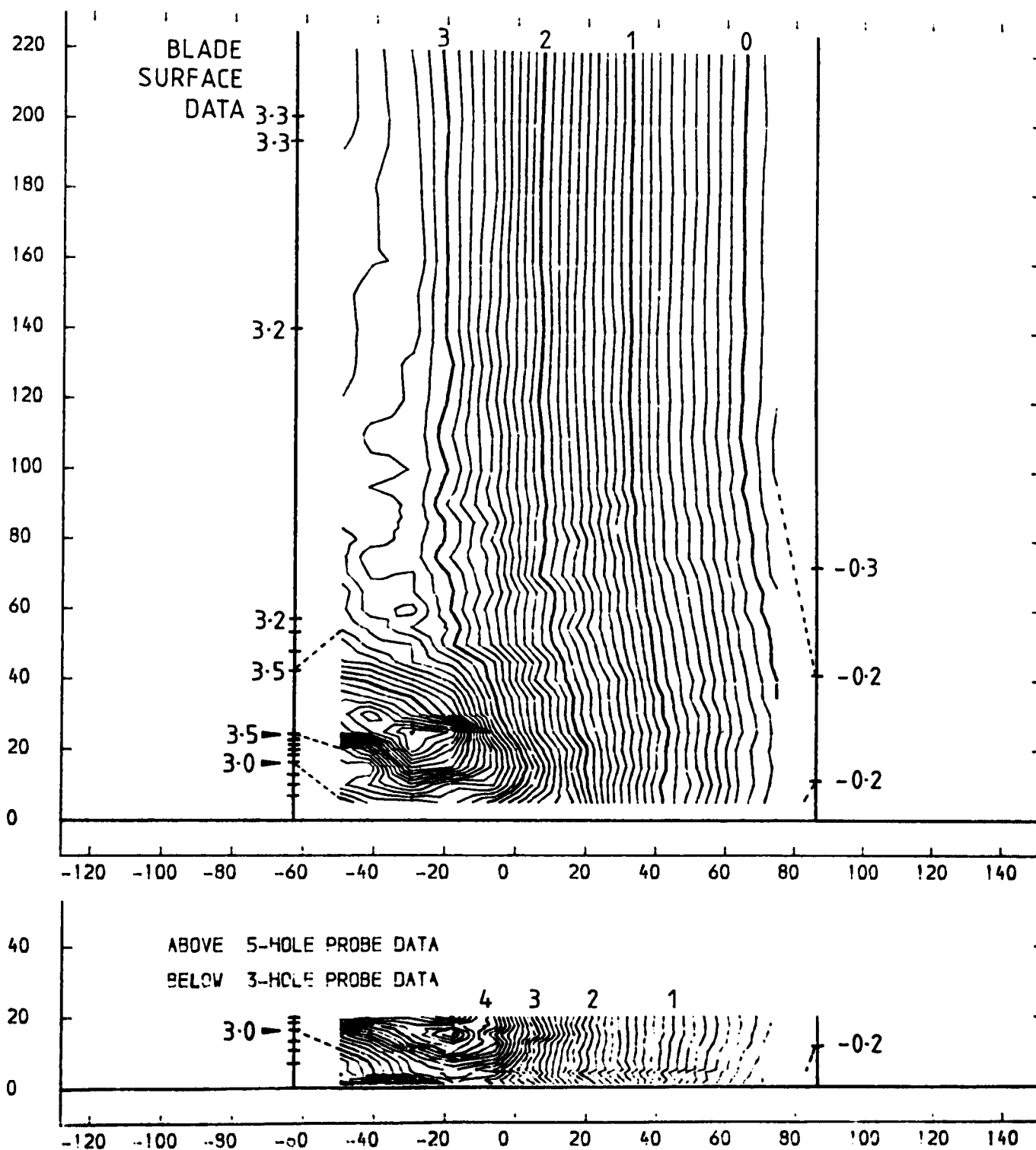


FIGURE 4.43

SLOT 7 EXPERIMENTAL DATA POINTS

NATURAL INLET BOUNDARY LAYER

X-AXIS TANGENTIAL CO-ORDINATE FROM TRAILING EDGE DATUM (MM)

Y-AXIS SPANWISE CO-ORDINATE FROM PERSPEX ENDWALL (MM)

+ PROBE DATA x MANUALLY INTERPOLATED DATA \* EXTRAPOLATED DATA

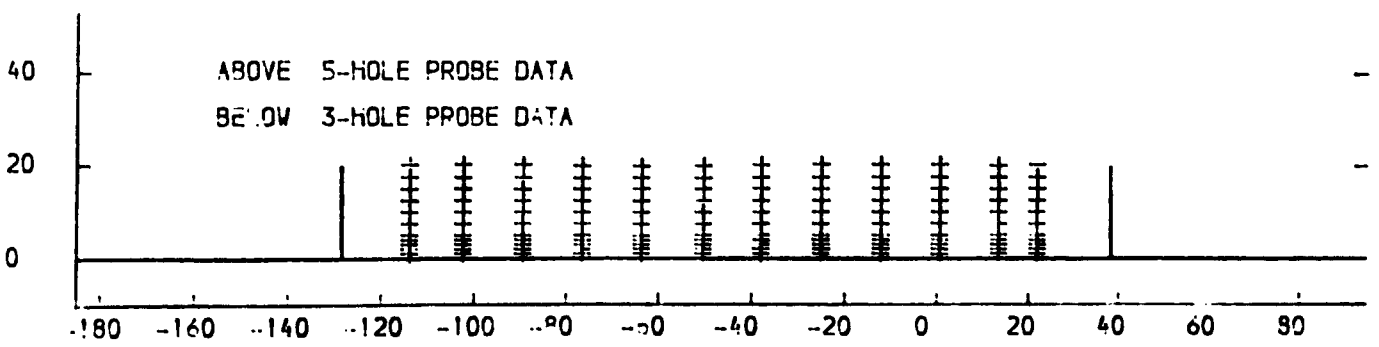
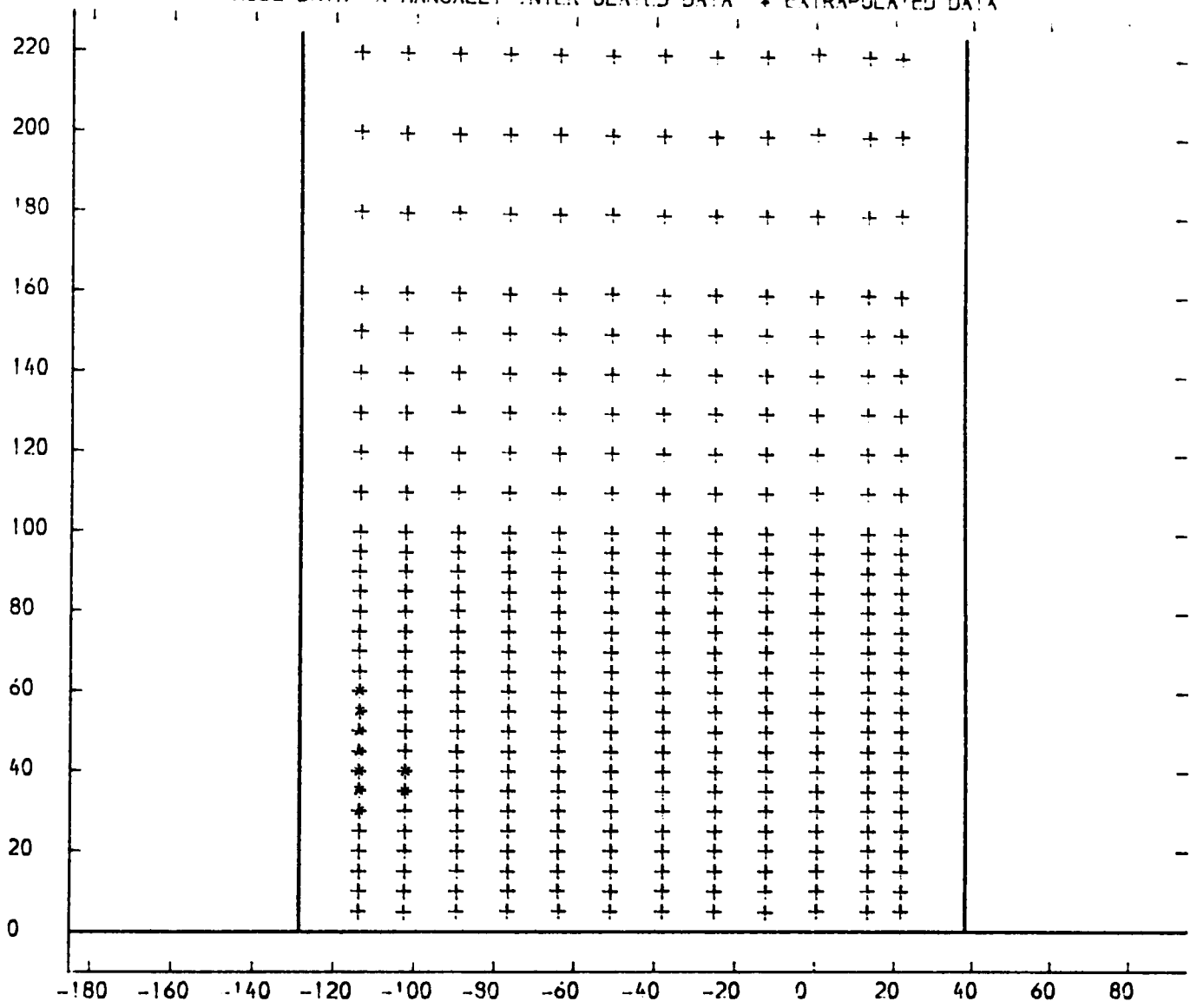


FIGURE 4.44

SLOT 7 TOTAL PRESSURE LOSS COEFFICIENT  $\frac{(P_{01} - P_{0LOCAL})}{(P_{01} - P_{1})}$  CONTOURS  
 NATURAL INLET BOUNDARY LAYER  
 X-AXIS TANGENTIAL CO-ORDINATE FROM TRAILING EDGE DATUM (MM)  
 Y-AXIS SPANWISE CO-ORDINATE FROM PERSPEX ENDWALL (MM)

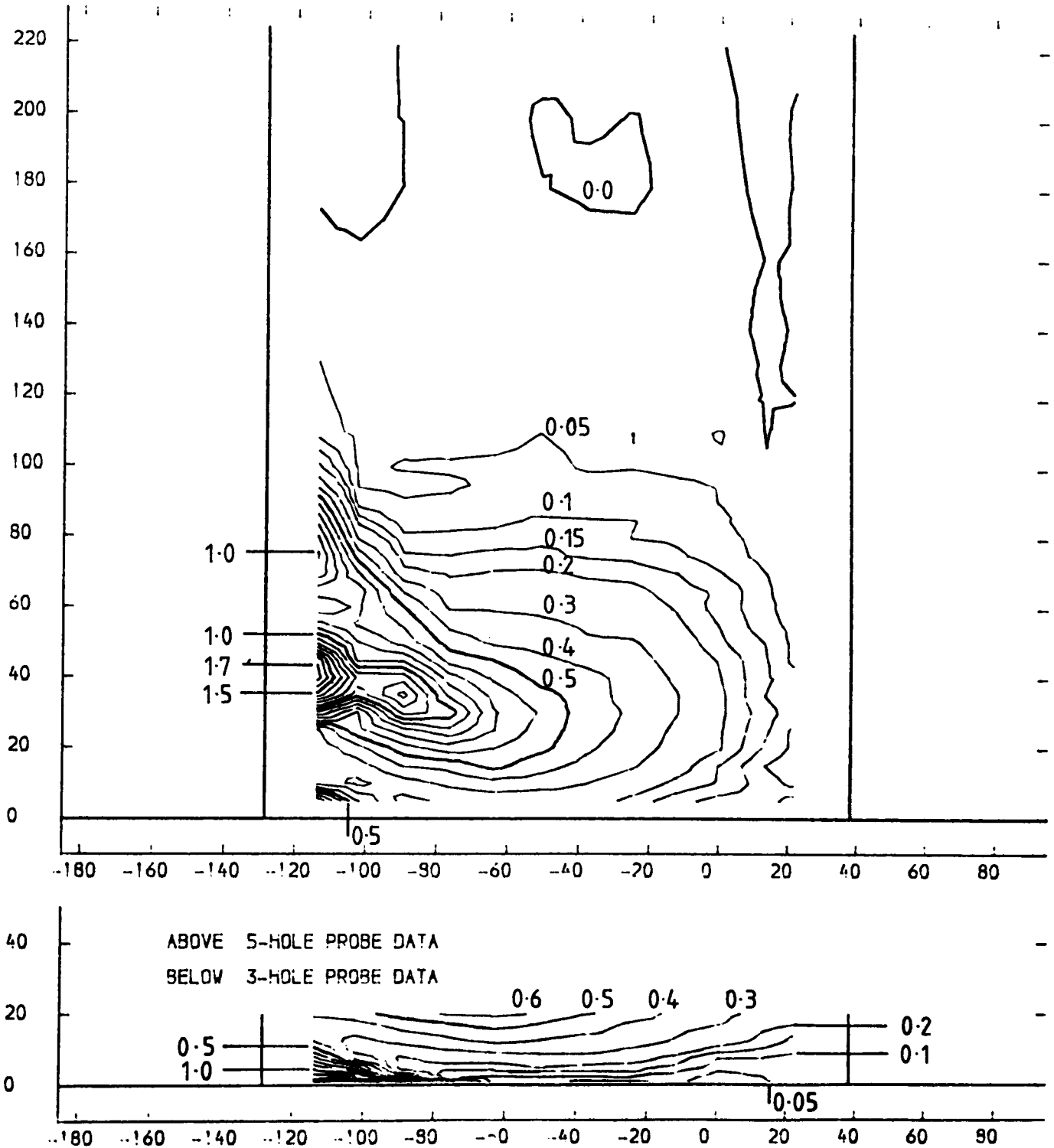


FIGURE 4.45

SLOT 7 TOTAL VELOCITY MAGNITUDE CONTOURS (CONTOUR UNITS METRES/SEC)  
 NATURAL INLET BOUNDARY LAYER  
 X-AXIS TANGENTIAL CO-ORDINATE FROM TRAILING EDGE DATUM (MM)  
 Y-AXIS SPANWISE CO-ORDINATE FROM PERSPECT ENDWALL (MM)

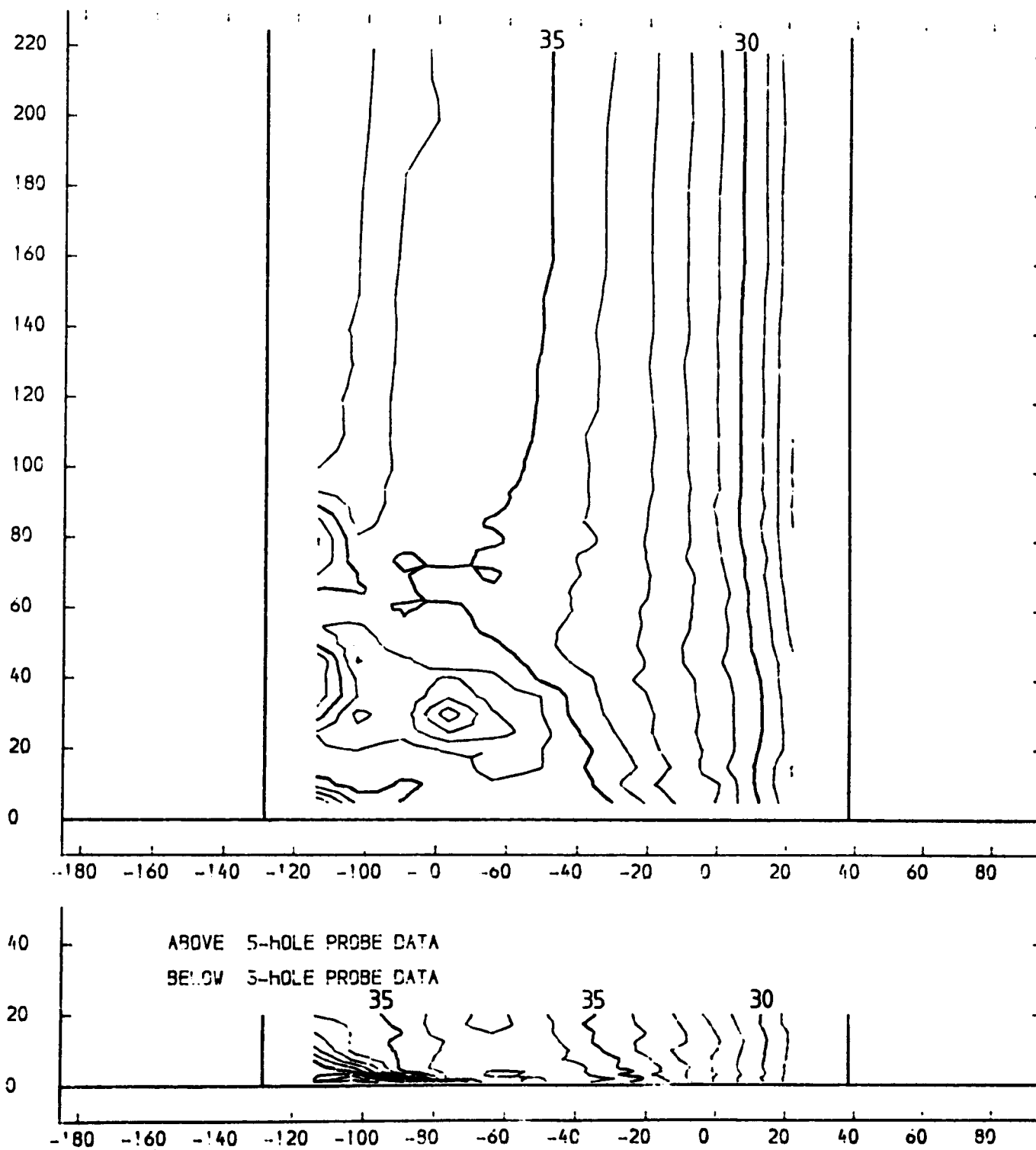


FIGURE 4.46

SLOT 7 VECTOR PLOT OF SECONDARY VELOCITIES (VT (SEC) = VT (LOC) / VT (M. S.) + VA (LOC) / VA (M. S.))  
 NATURAL INLET BOUNDARY LAYER  
 X-AXIS TANGENTIAL CO-ORDINATE FROM TRAILING EDGE DATUM (MM)  
 Y-AXIS SPANWISE CO-ORDINATE FROM PERSPEX ENDWALL (MM)  
 VECTOR SCALE 20 METRES/SEC

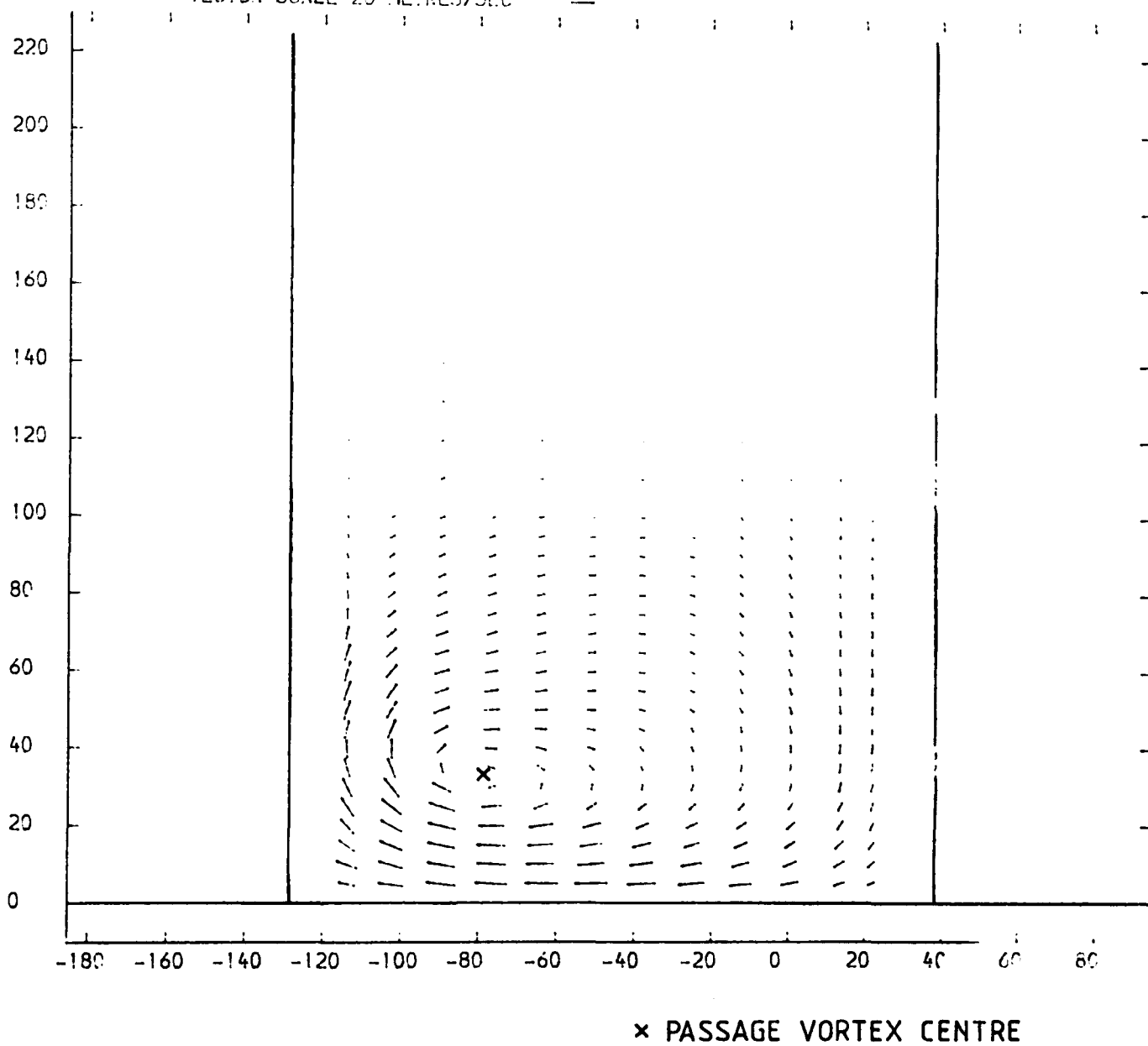


FIGURE 4.47

SLOT 7 SPANWISE ANGLE (PITCH ANGLE) CONTOURS (CONTOUR UNITS DEGREES)  
NATURAL INLET BOUNDARY LAYER  
X-AXIS TANGENTIAL CO-ORDINATE FROM TRAILING EDGE DATUM (MM)  
Y-AXIS SPANWISE CO-ORDINATE FROM PERSPEX ENDWALL (MM)

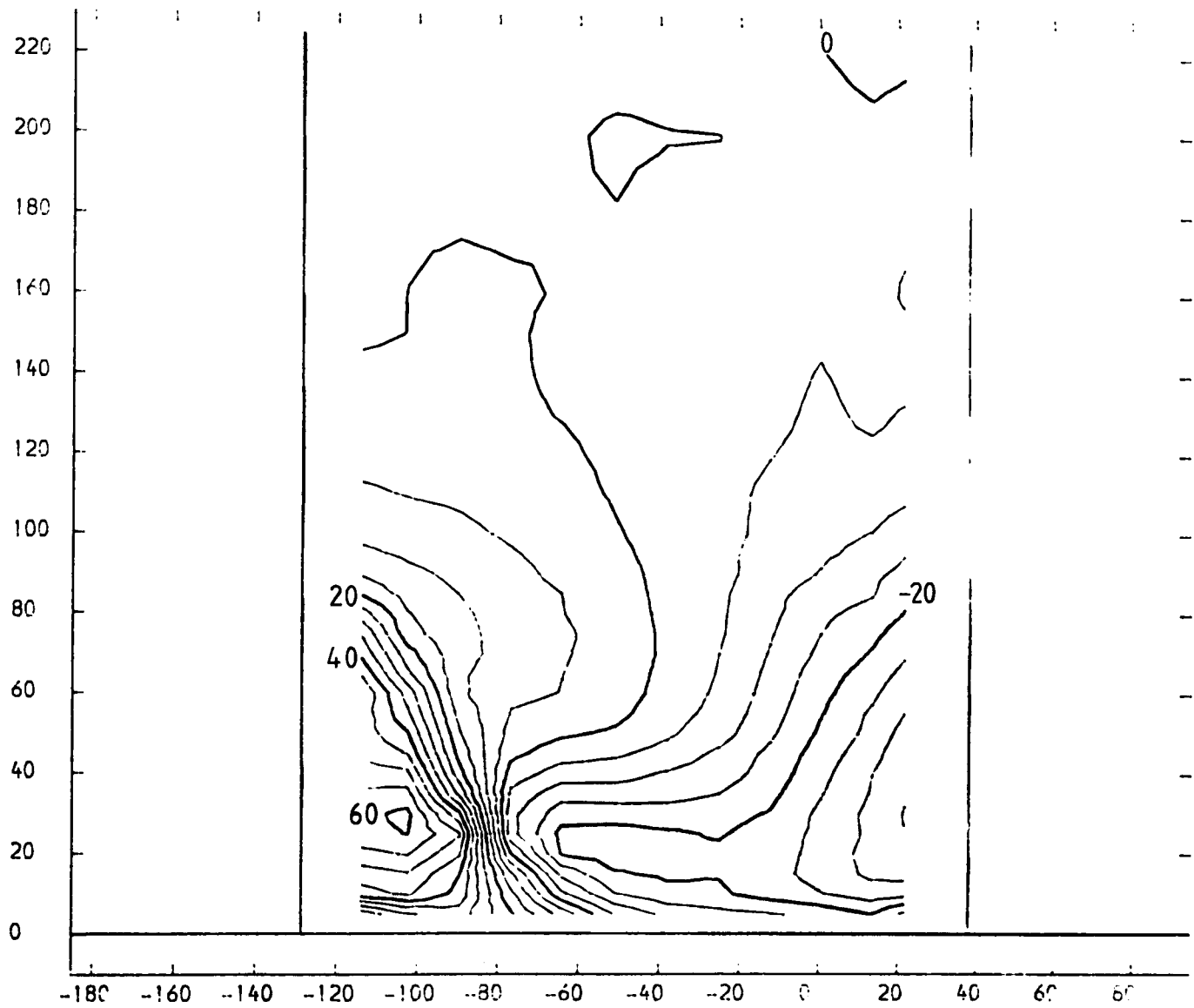


FIGURE 4.48



SLOT 7 YAW ANGLE CONTOURS (CONTOUR UNITS DEGREES)  
 NATURAL INLET BOUNDARY LAYER  
 X-AXIS TANGENTIAL CO-ORDINATE FROM TRAILING EDGE DATUM (MM)  
 Y-AXIS SPANWISE CO-ORDINATE FROM PERSPEX ENDWALL (MM)

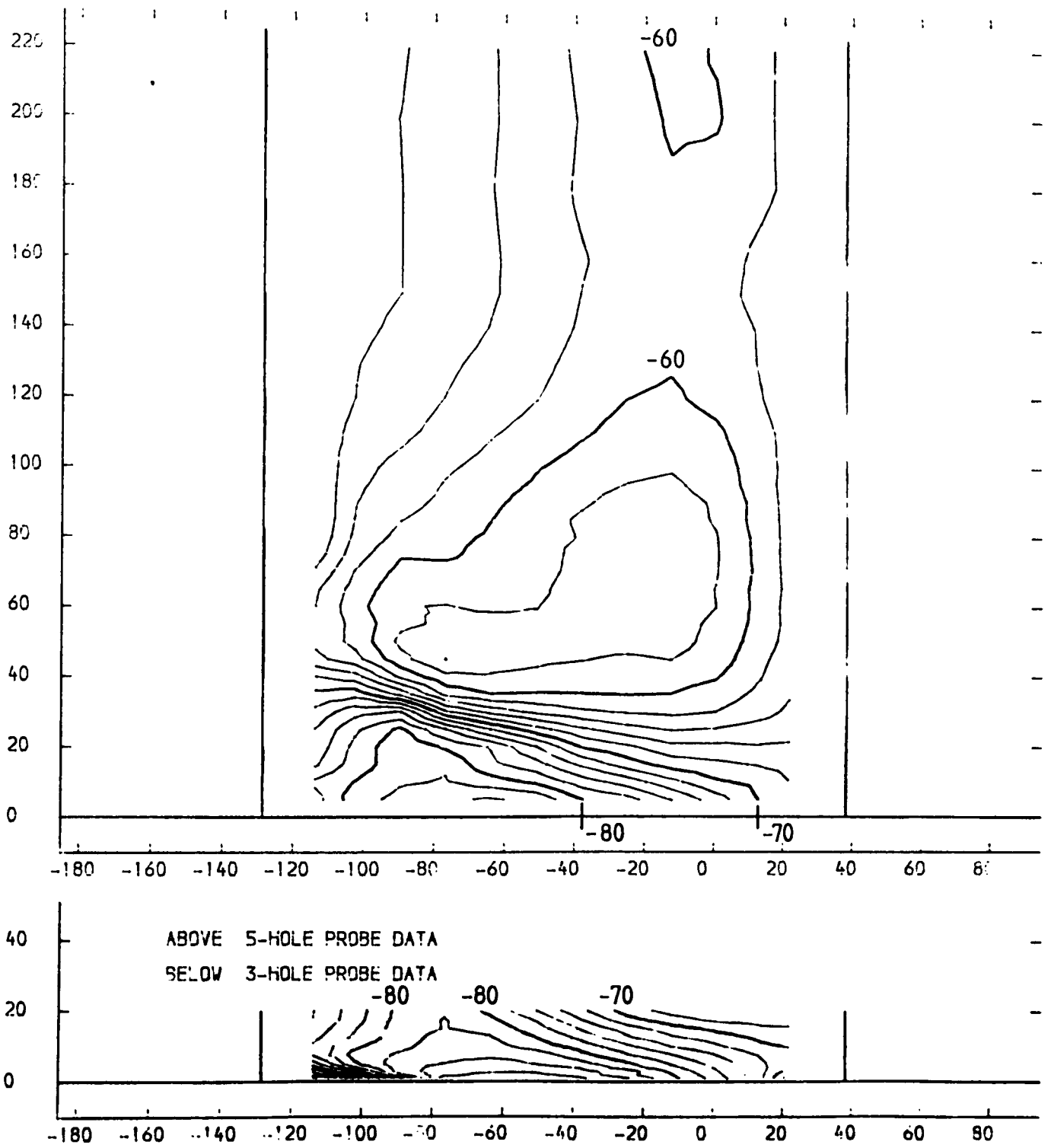


FIGURE 4.49

SLOT 7 STATIC PRESSURE COEFFICIENT  $(P1-PLLOCAL)/(P01-P1)$  CONTOURS  
 NATURAL INLET BOUNDARY LAYER  
 X-AXIS TANGENTIAL CO-ORDINATE FROM TRAILING EDGE DATUM (MM)  
 Y-AXIS SPANWISE CO-ORDINATE FROM PERSPEX ENDWALL (MM)

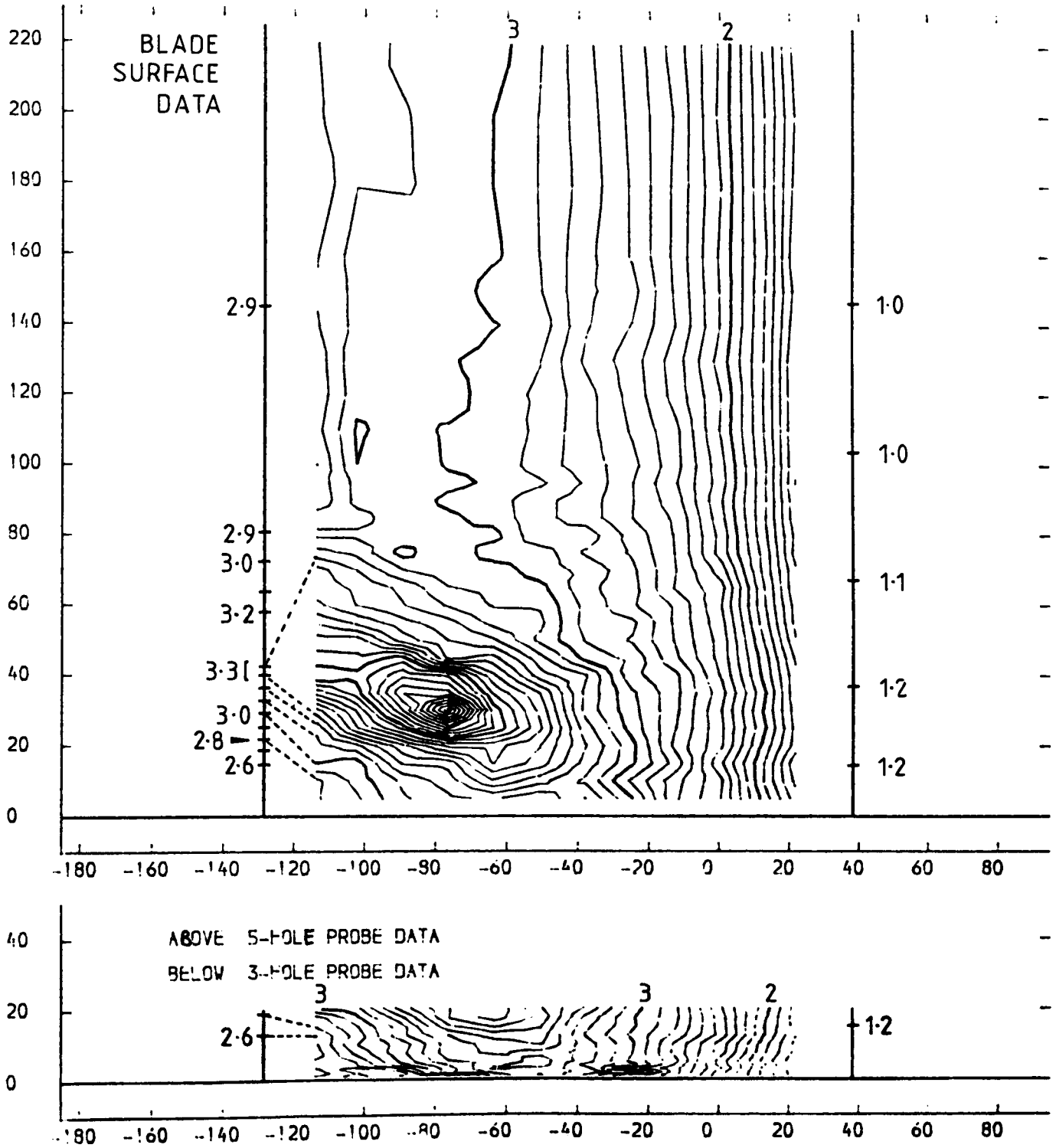
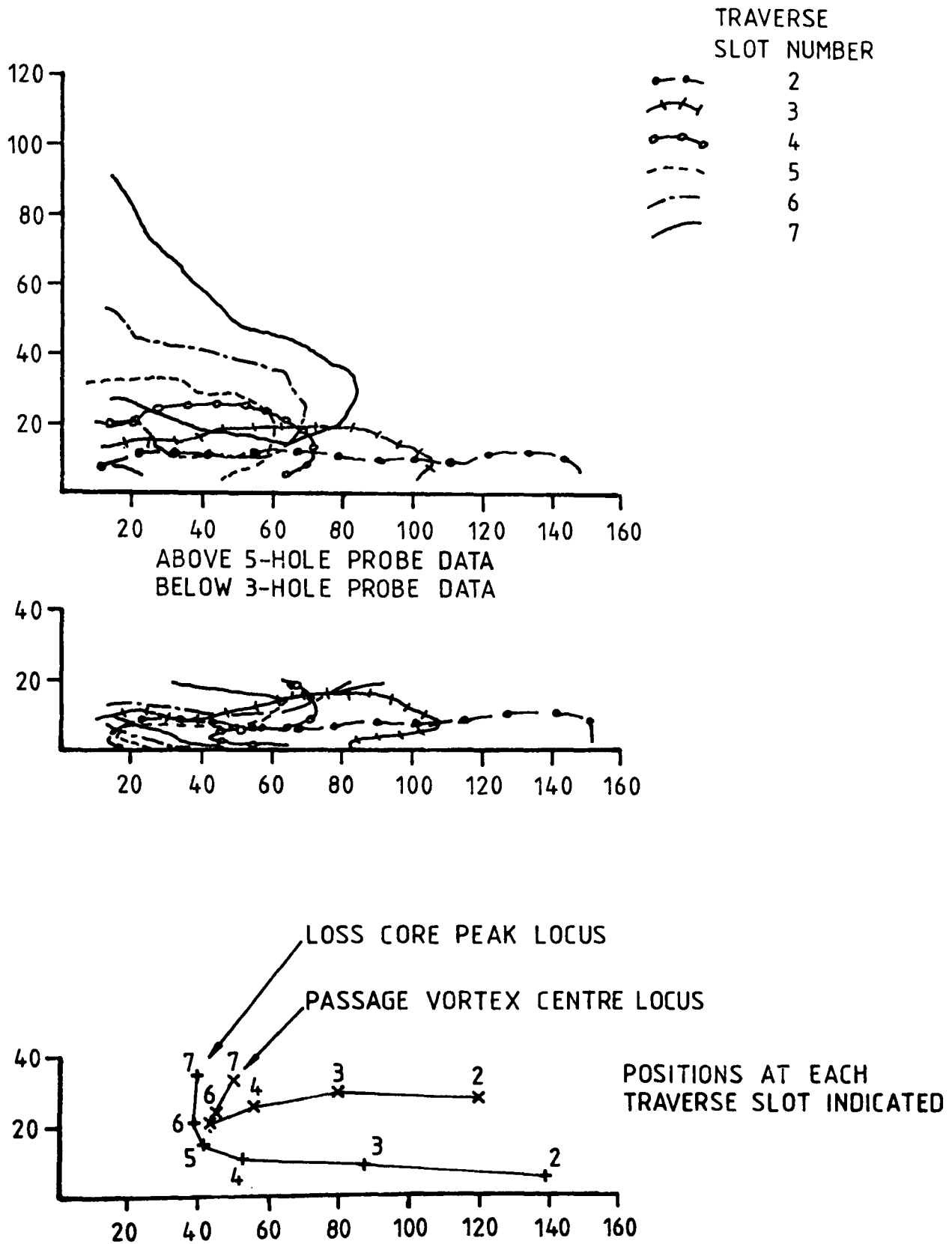


FIGURE 4.50

# BLADE PASSAGE LOSS CORE DEVELOPMENT AND LOCI OF PASSAGE VORTEX CENTRE AND LOSS CORE PEAK

X-AXIS TANGENTIAL CO-ORDINATE FROM BLADE SUCTION SURFACE (MM)  
 Y-AXIS SPANWISE CO-ORDINATE FROM PERSPEX ENDWALL (MM)



PASSAGE VORTEX CENTRE SITUATED AT INTERSECTION OF ZERO SPANWISE AND ZERO CROSS FLOW ANGLE CONTOURS ON EACH PROBE TRAVERSE PLANE

FIGURE 4.51

SLOT 8 EXPERIMENTAL DATA POINTS

NATURAL INLET BOUNDARY LAYER

X-AXIS TANGENTIAL CO-ORDINATE FROM TRAILING EDGE DATUM (MM)

Y-AXIS SPANWISE CO-ORDINATE FROM PERSPEX ENDWALL (MM)

+ PROBE DATA X MANUALLY INTERPOLATED DATA \* EXTRAPOLATED DATA

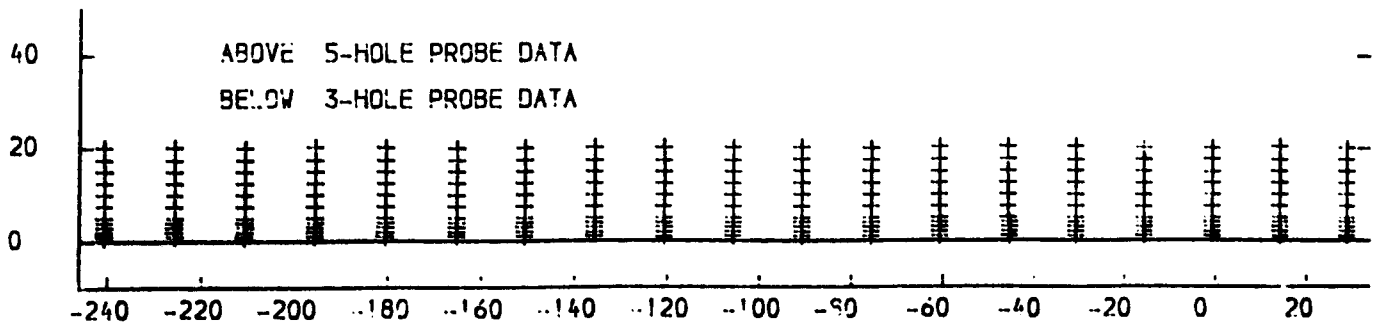
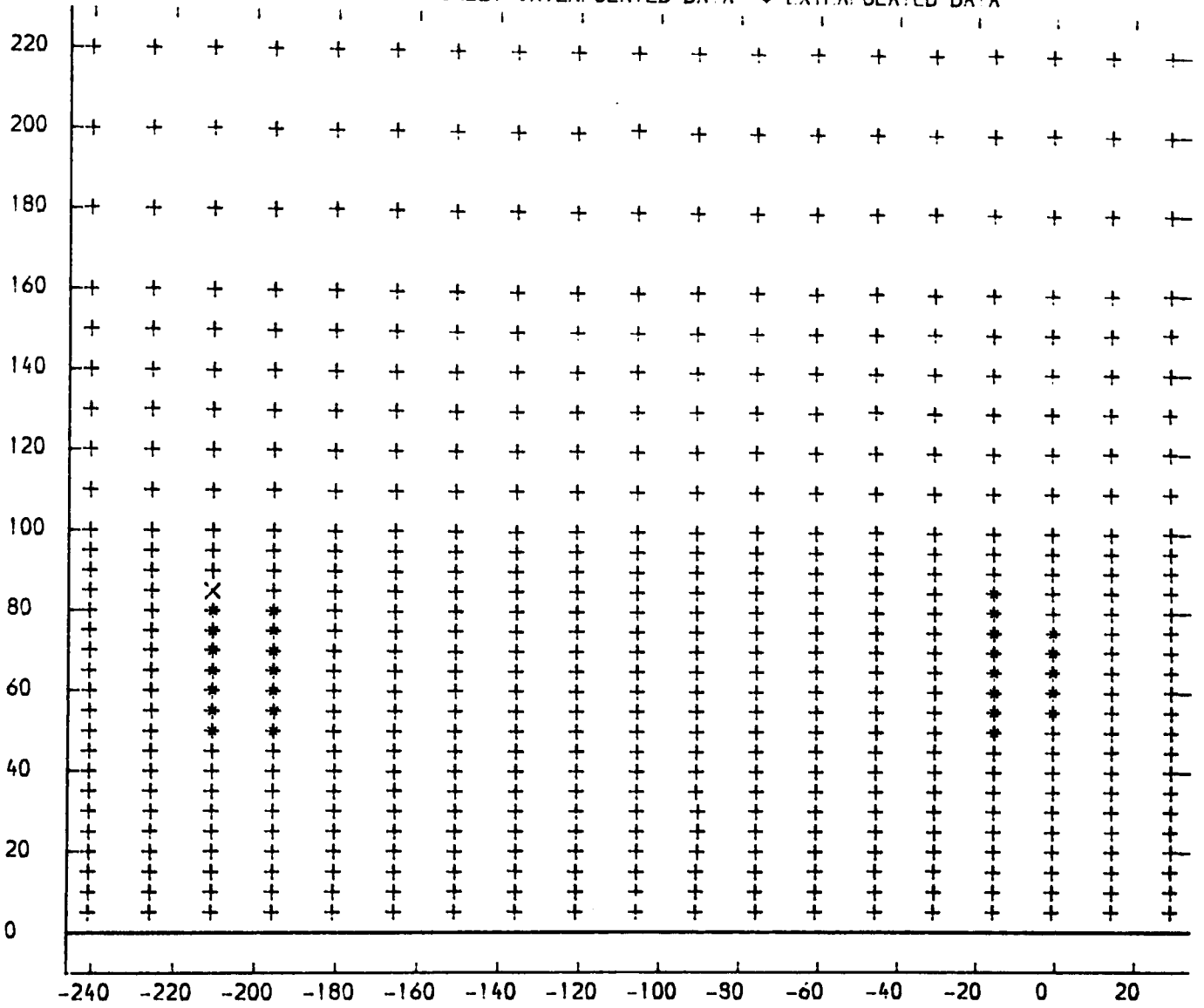


FIGURE 4.52

SLOT 8 TOTAL PRESSURE LOSS COEFFICIENT  $(P_{01} - P_{0LOCAL}) / (P_{01} - P_{01})$  CONTOURS  
 NATURAL INLET BOUNDARY LAYER  
 Y-AXIS TANGENTIAL CO-ORDINATE FROM TRAILING EDGE DATUM (MM)  
 X-AXIS SPANWISE CO-ORDINATE FROM PERSPEX ENDWALL (MM)

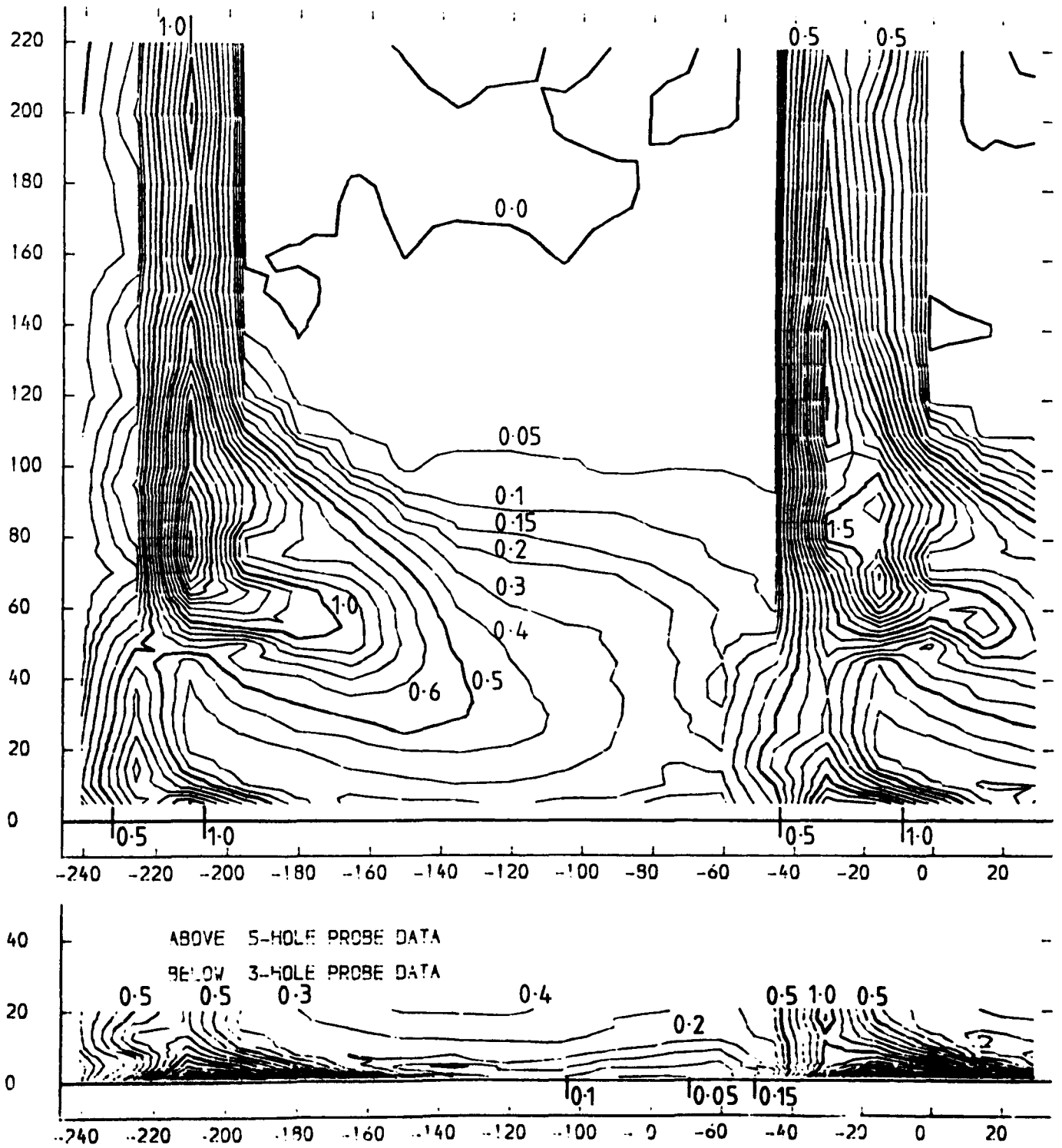


FIGURE 4.53

SLOT 8 TOTAL VELOCITY MAGNITUDE CONTOURS (CONTOUR UNITS METRES/SEC)  
 NATURAL INLET BOUNDARY LAYER  
 X-AXIS TANGENTIAL CO-ORDINATE FROM TRAILING EDGE DATUM (MM)  
 Y-AXIS SPANWISE CO-ORDINATE FROM PERSPEX ENDWALL (MM)

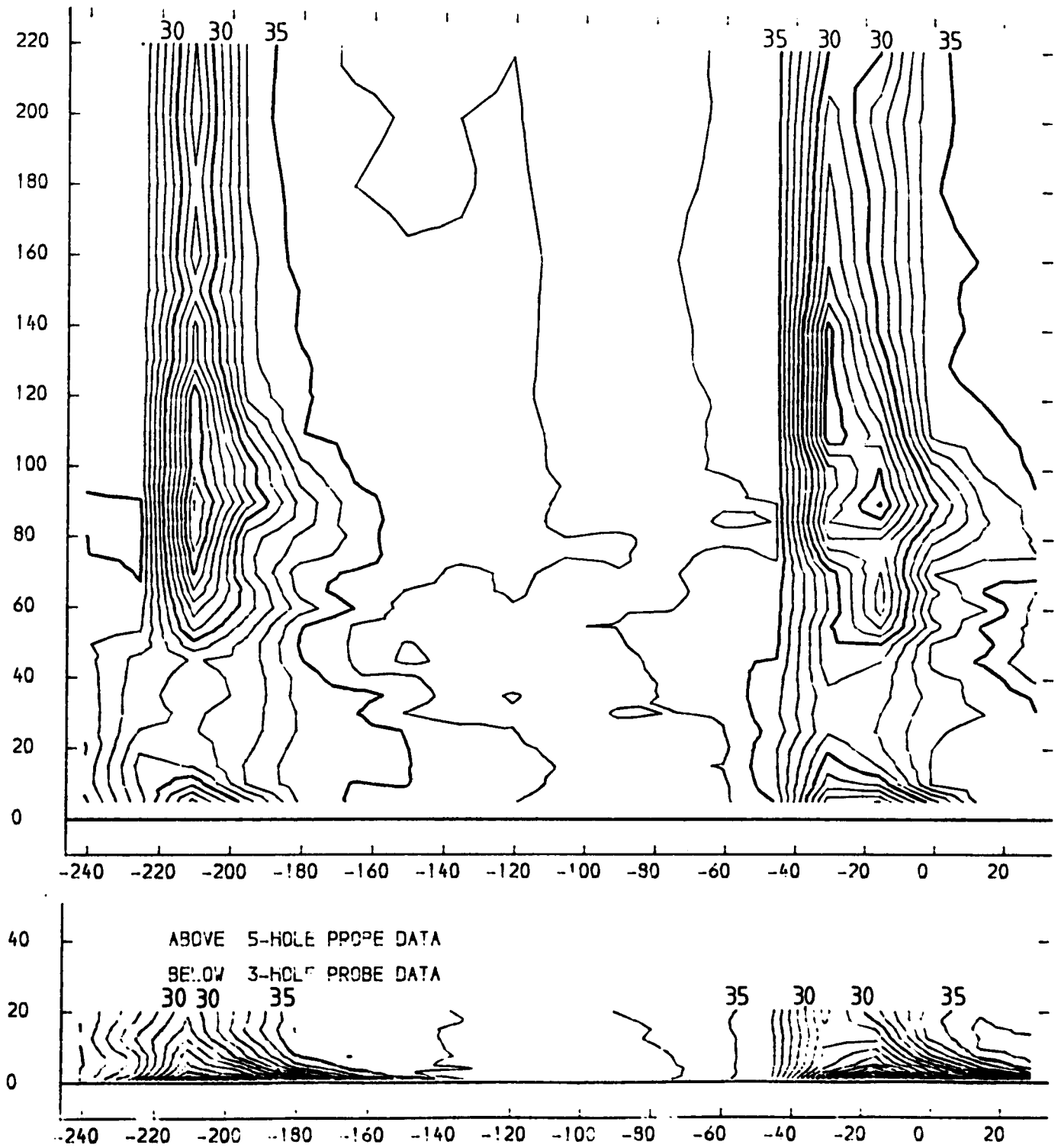
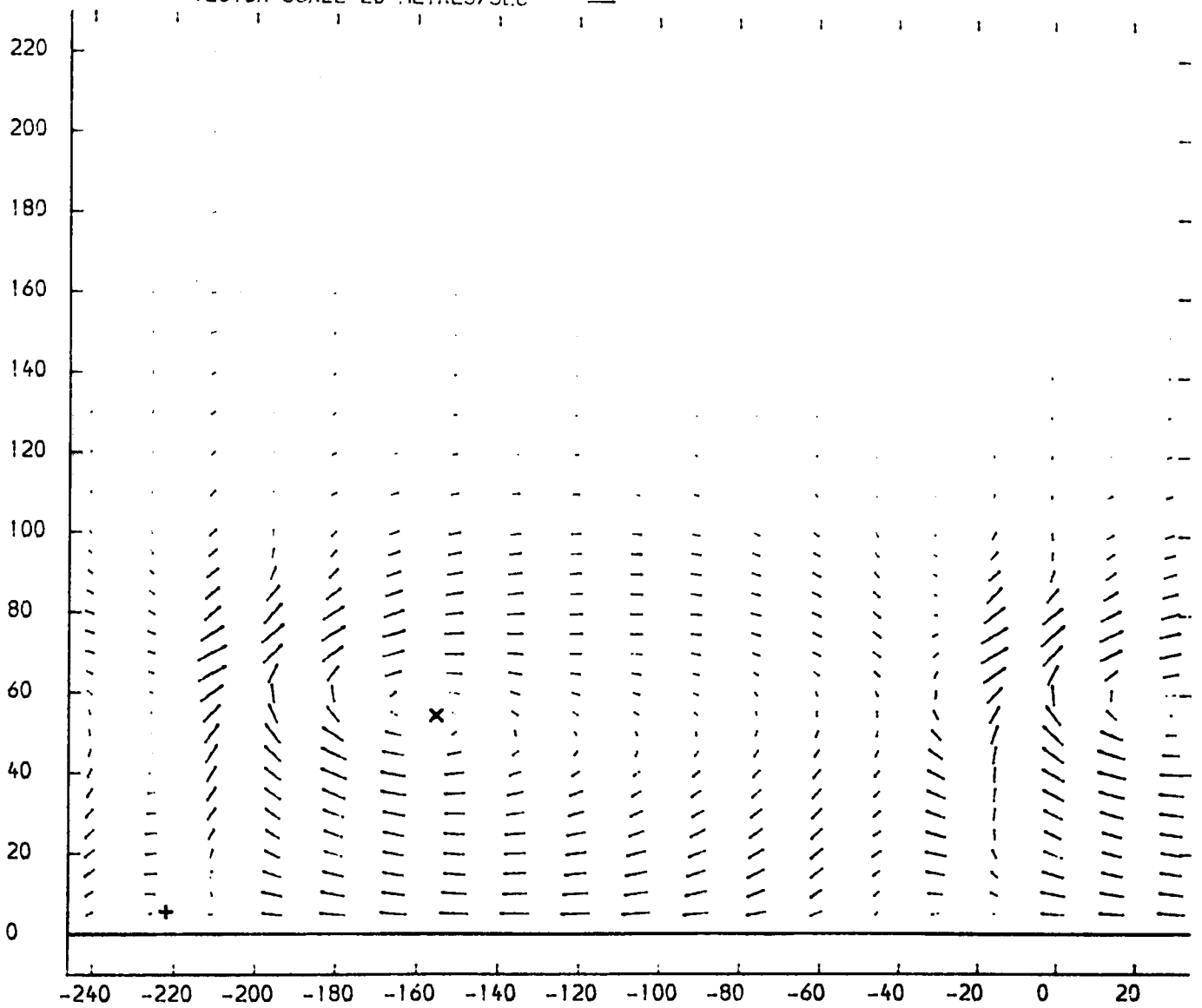


FIGURE 4.54

SLOT 8 VECTOR PLOT OF SECONDARY VELOCITIES  $(V_T(\text{SEC}) = V_T(\text{LOC}) - V_T(\text{M.S.}) + V_A(\text{LOC}) / V_A(\text{M.S.}))$   
 NATURAL INLET BOUNDARY LAYER  
 X-AXIS TANGENTIAL CO-ORDINATE FROM TRAILING EDGE DATUM (MM)  
 Y-AXIS SPANWISE CO-ORDINATE FROM PERSPEX ENDWALL (MM)  
 VECTOR SCALE 20 METRES/SEC



x PASSAGE VORTEX CENTRE  
 + COUNTER VORTEX CENTRE

FIGURE 4.55

SLOT 8 SPANWISE ANGLE (PITCH ANGLE) CONTOURS (CONTOUR UNITS DEGREES)  
NATURAL INLET BOUNDARY LAYER  
X-AXIS TANGENTIAL CO-ORDINATE FROM TRAILING EDGE DATUM (MM)  
Y-AXIS SPANWISE CO-ORDINATE FROM PERSPEX ENDWALL (MM)

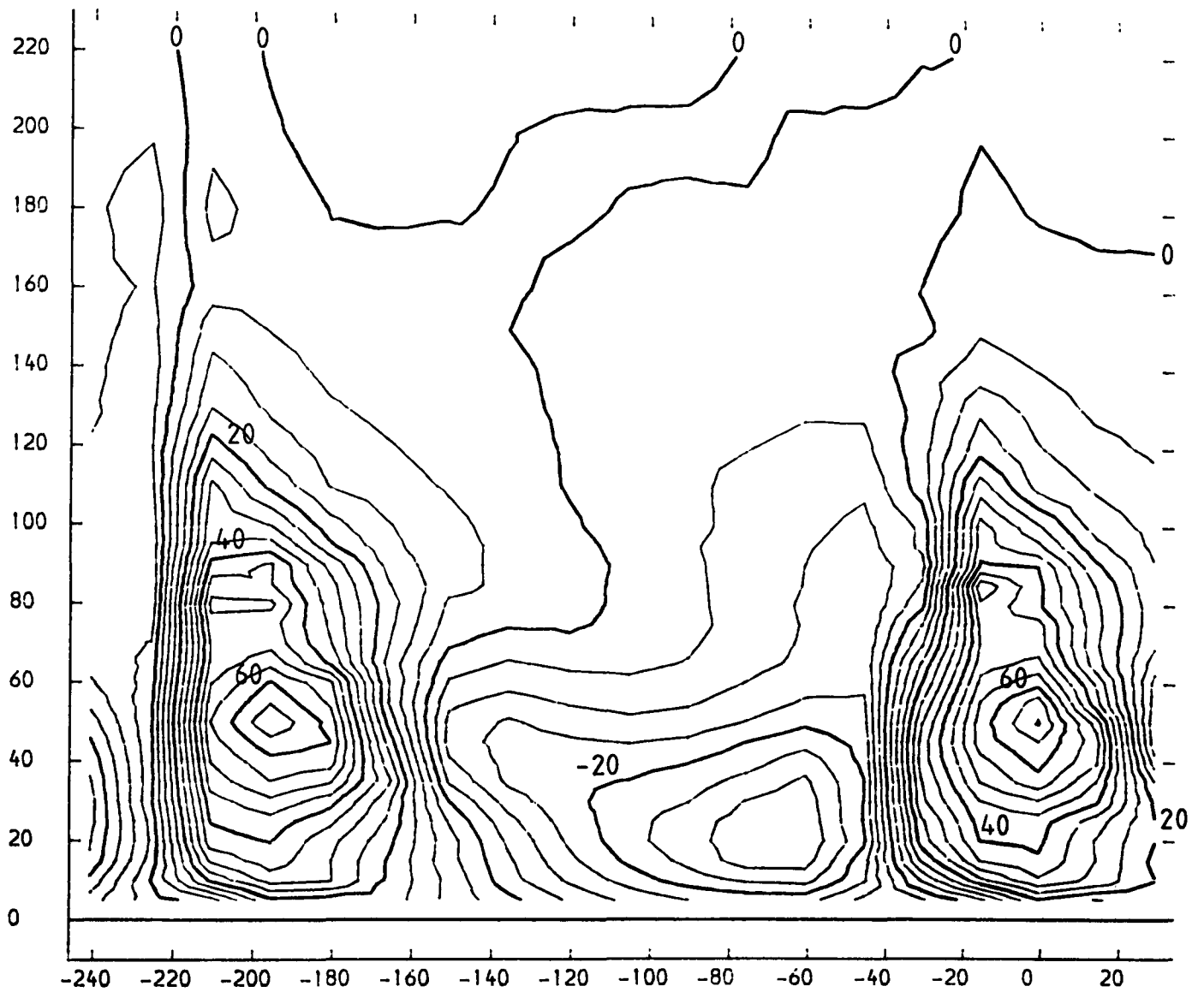


FIGURE 4.56



SLOT 8 YAW ANGLE CONTOURS (CONTOUR UNITS DEGREES)  
 NATURAL INLET BOUNDARY LAYER  
 X-AXIS TANGENTIAL CO-ORDINATE FROM TRAILING EDGE DATUM (MM)  
 Y-AXIS SPANWISE CO-ORDINATE FROM PERSPEX ENDWALL (MM)

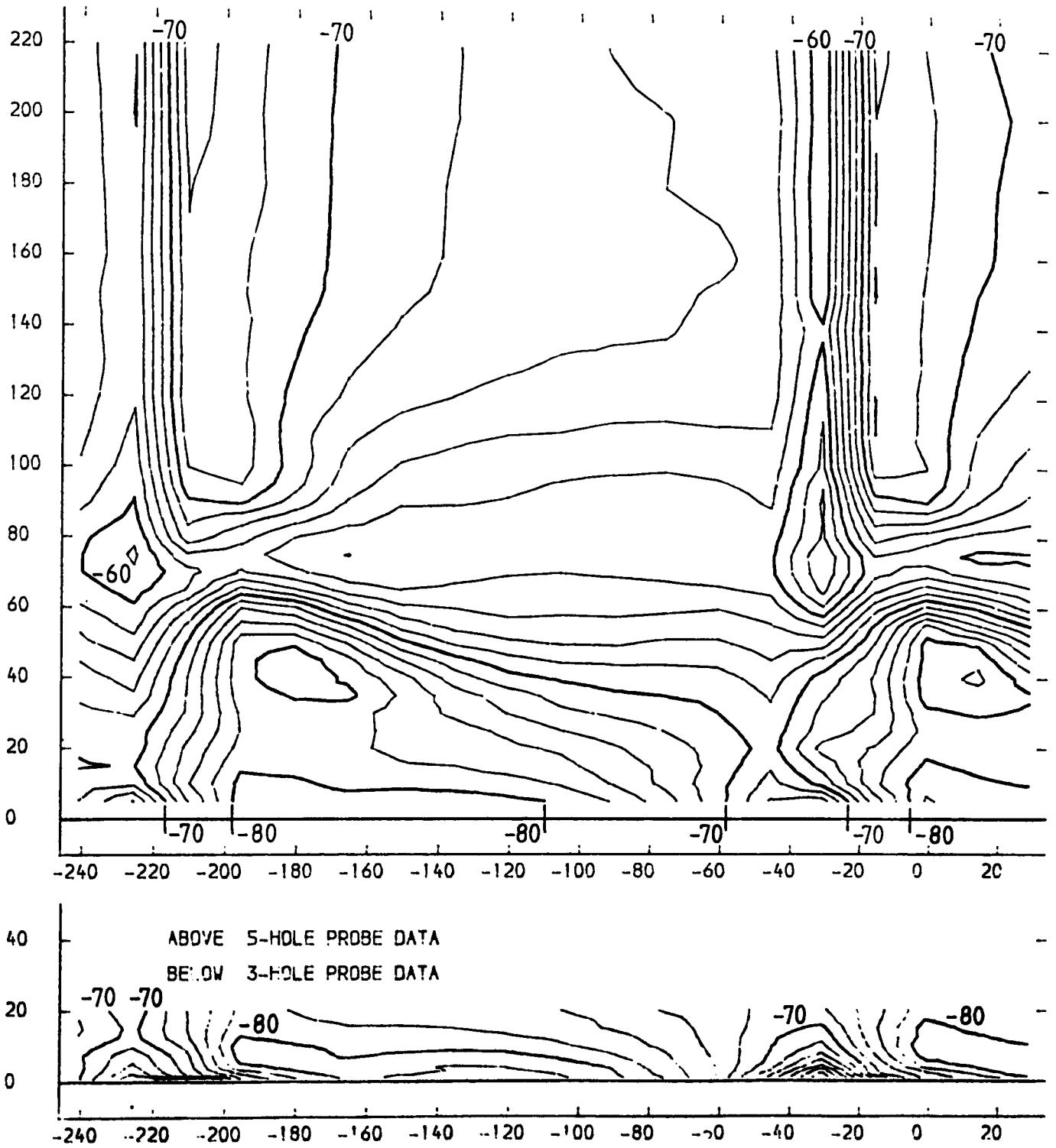


FIGURE 4.57

SLOT 8 STATIC PRESSURE COEFFICIENT (  $(P1 - PLOCAL) / (P01 - P1)$  ) CONTOURS  
 NATURAL INLET BOUNDARY LAYER  
 X-AXIS TANGENTIAL CO-ORDINATE FROM TRAILING EDGE DATUM (MM)  
 Y-AXIS SPANWISE CO-ORDINATE FROM PERSPEX ENDWALL (MM)

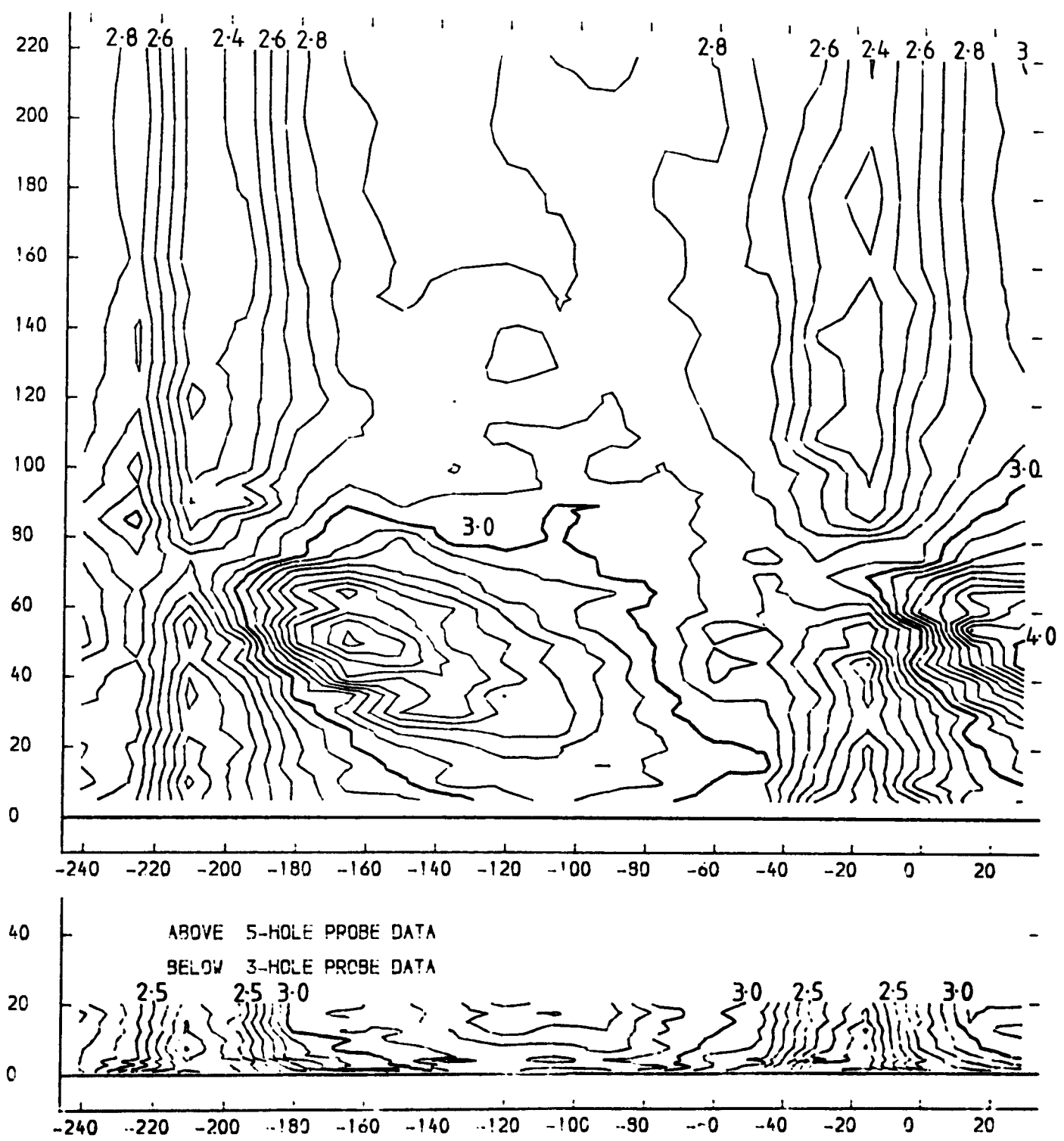


FIGURE 4.58

SLOT 9 EXPERIMENTAL DATA POINTS

NATURAL INLET BOUNDARY LAYER

X-AXIS TANGENTIAL CO ORDINATE FROM TRAILING EDGE DATUM (MM)

Y-AXIS SPANWISE CO-ORDINATE FROM PERSPEX ENDWALL (MM)

+ PROBE DATA X MANUALLY INTERPOLATED DATA \* EXTRAPOLATED DATA

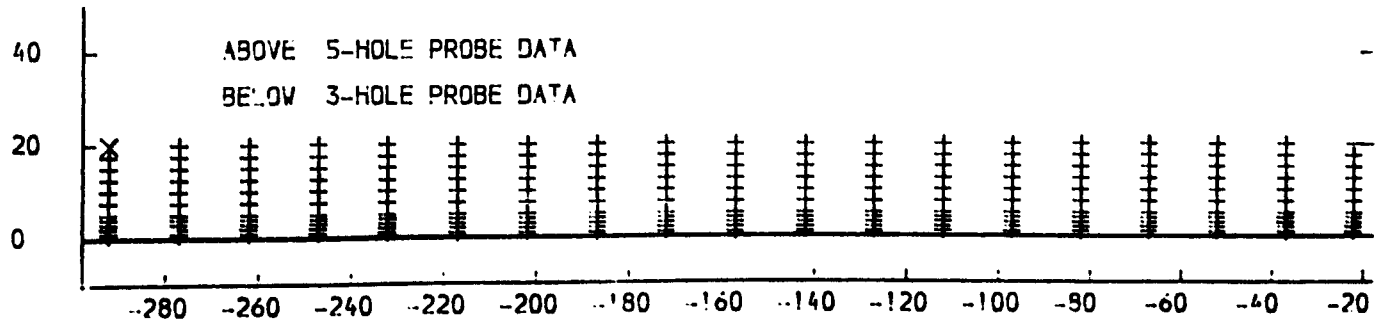
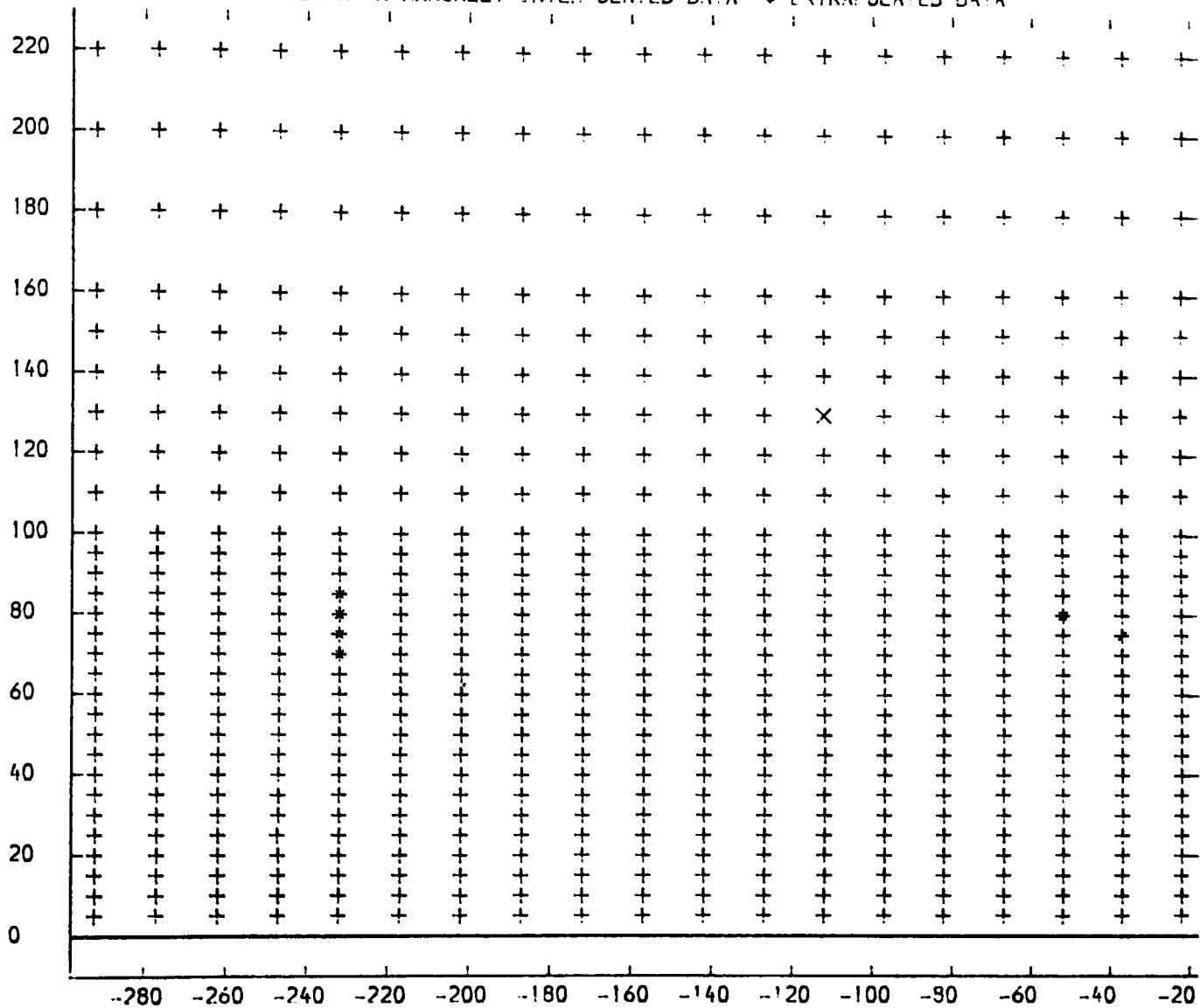


FIGURE 4.59

SLOT 9 TOTAL PRESSURE LOSS COEFFICIENT (  $(P_{01} - P_{0LOCAL}) / (P_{01} - P_1)$  ) CONTOURS  
 NATURAL INLET BOUNDARY LAYER  
 X-AXIS TANGENTIAL O-ORDINATE FROM TRAILING EDGE DATUM (MM)  
 Y-AXIS SPANWISE CO-ORDINATE FROM PERSPEX ENDWALL (MM)

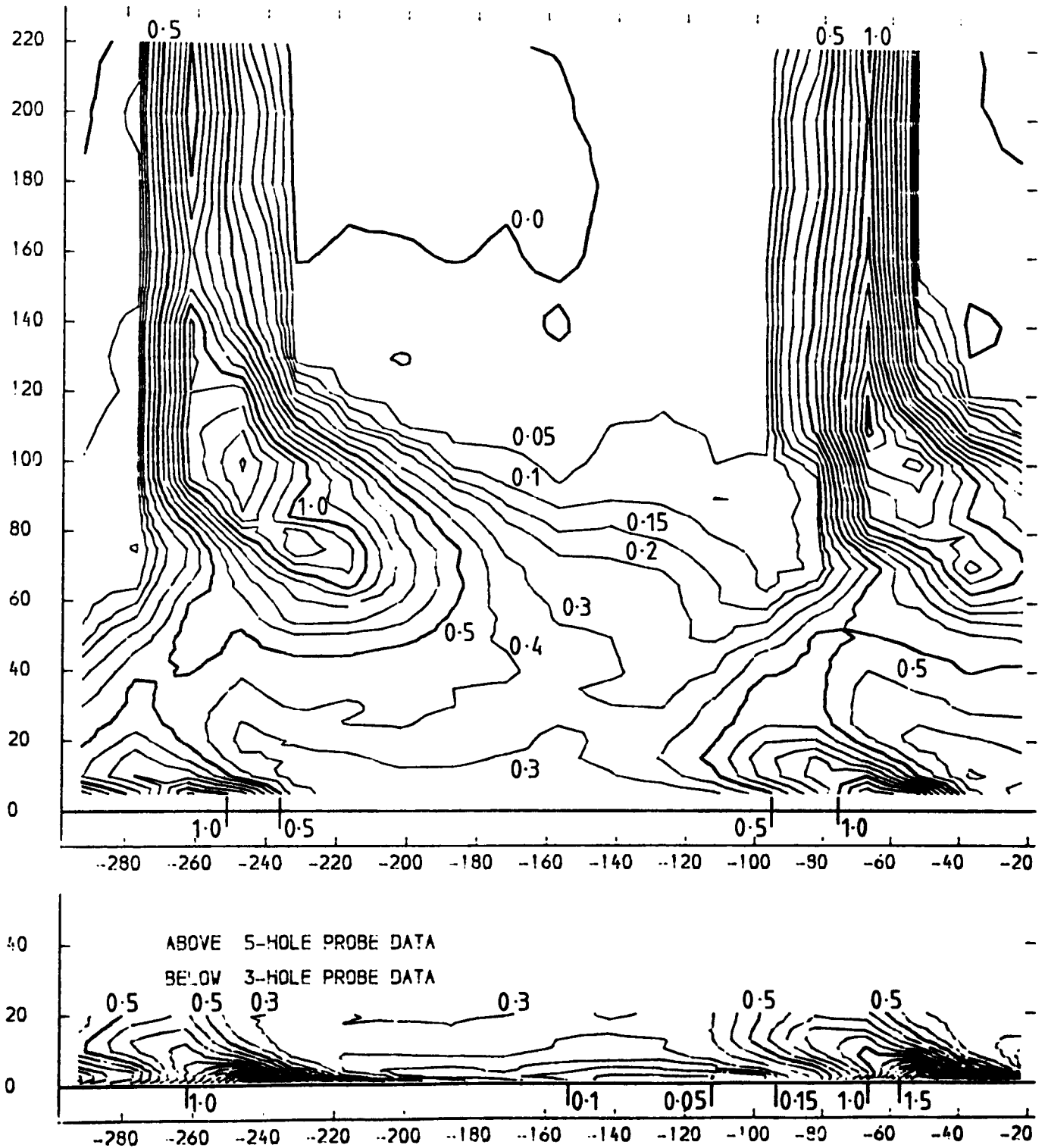


FIGURE 4.60

SLOT 9 TOTAL VELOCITY MAGNITUDE CONTOURS (CONTOUR UNITS METRES/SEC)  
 NATURAL INLET BOUNDARY LAYER  
 X-AXIS TANGENTIAL CO-ORDINATE FROM TRAILING EDGE DATUM (MM)  
 Y-AXIS SPANWISE CO-ORDINATE FROM PERSPEX ENDWALL (MM)

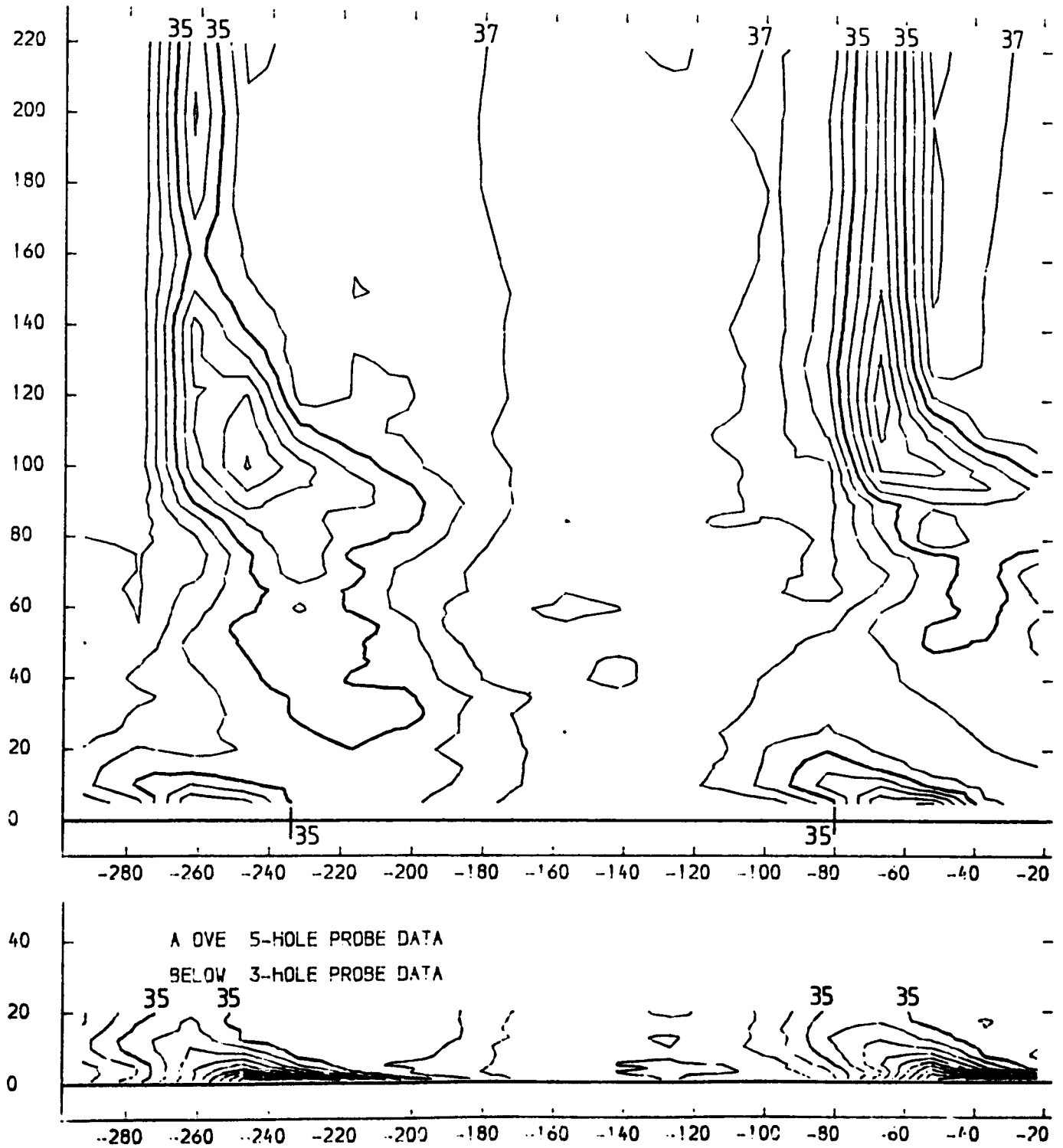
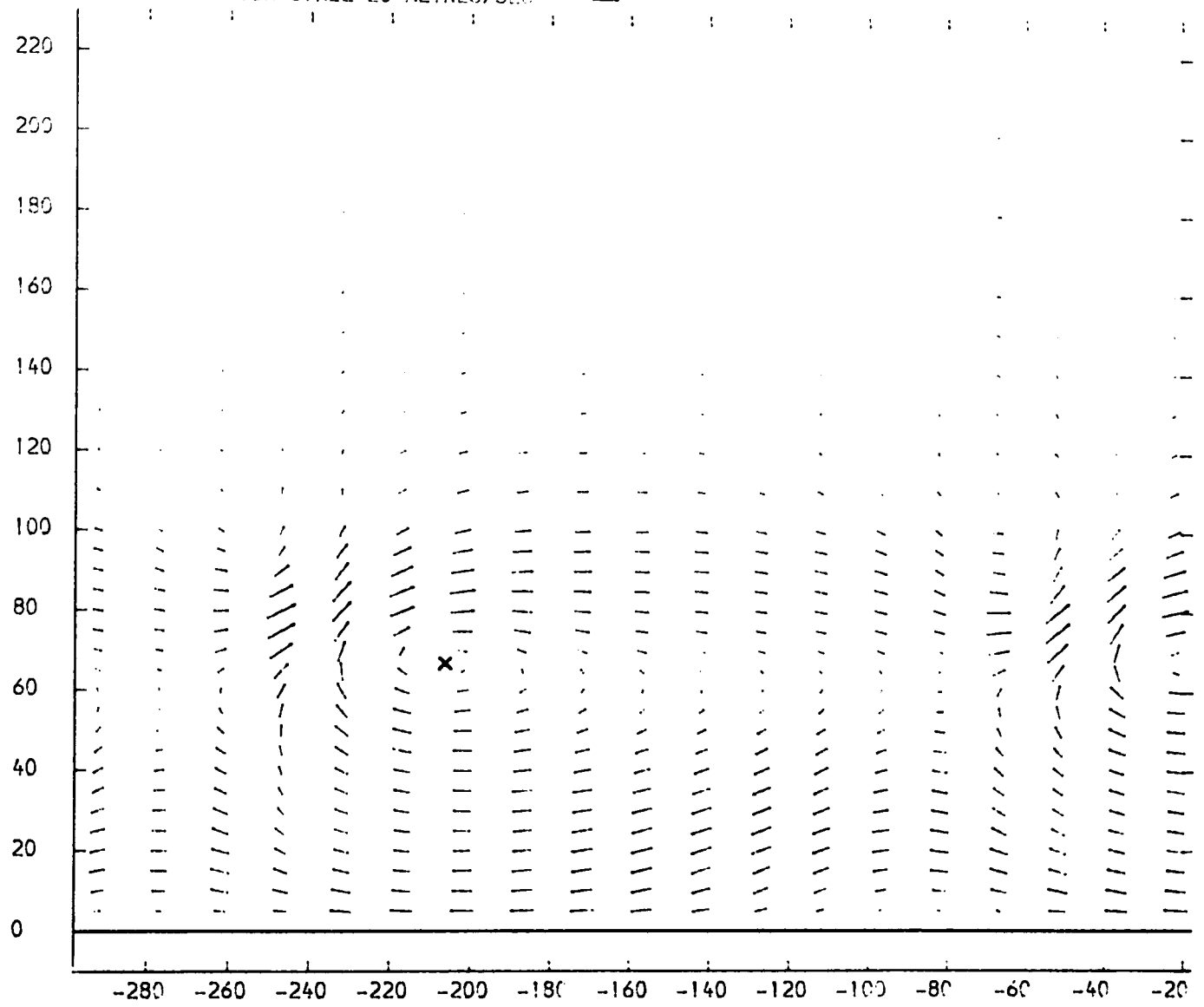


FIGURE 4.61

SLOT 2 VECTOR PLOT OF SECONDARY VELOCITIES  $(V_T(\text{SEC}) = V_T(\text{LOC}) - V_T(\text{M.S.}) + V_A(\text{LOC}) / V_A(\text{M.S.}))$   
 NATURAL INLET BOUNDARY LAYER  
 X-AXIS TANGENTIAL CO-ORDINATE FROM TRAILING EDGE DATUM (MM)  
 Y-AXIS SPANWISE CO-ORDINATE FROM PERSPEX ENDWALL (MM)  
 VECTOR SCALE 20 METRES/SEC



x PASSAGE VORTEX CENTRE

FIGURE 4.62

SLOT 9 SPANWISE ANGLE (PITCH ANGLE) CONTOURS (CONTOUR UNITS DEGREES)  
NATURAL INLET BOUNDARY LAYER  
X-AXIS TANGENTIAL CO-ORDINATE FROM TRAILING EDGE DATUM (MM)  
Y-AXIS SPANWISE CO-ORDINATE FROM PERSPEX ENDWALL (MM)

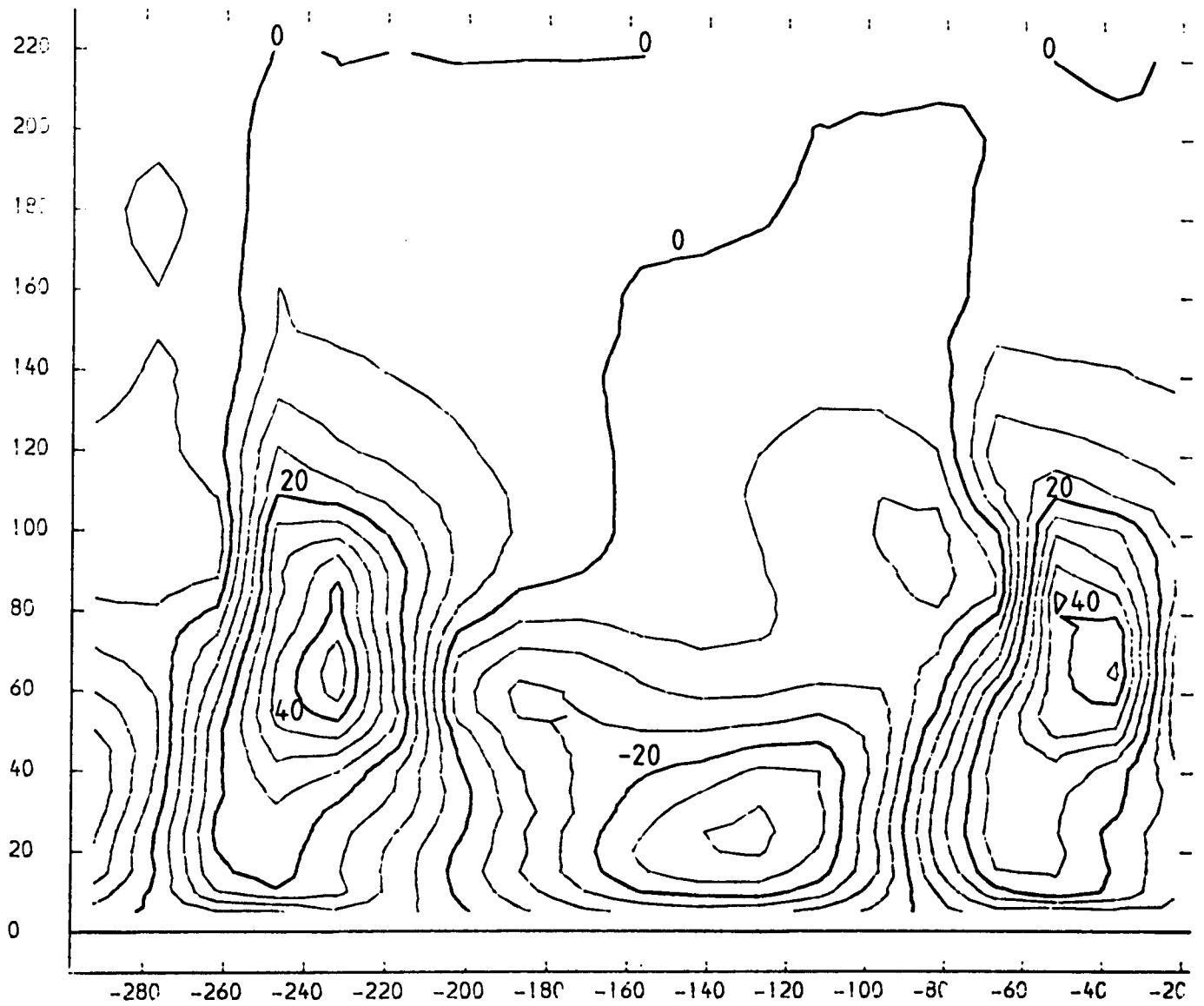


FIGURE 4.63

SLOT 9 YAW ANGLE CONTOURS (CONTOUR UNITS DEGREES)

NATURAL INLET BOUNDARY LAYER

X-AXIS TANGENTIAL CO-ORDINATE FROM TRAILING EDGE DATUM (MM)

Y-AXIS SPANWISE CO-ORDINATE FROM PERSPEX ENDWALL (MM)

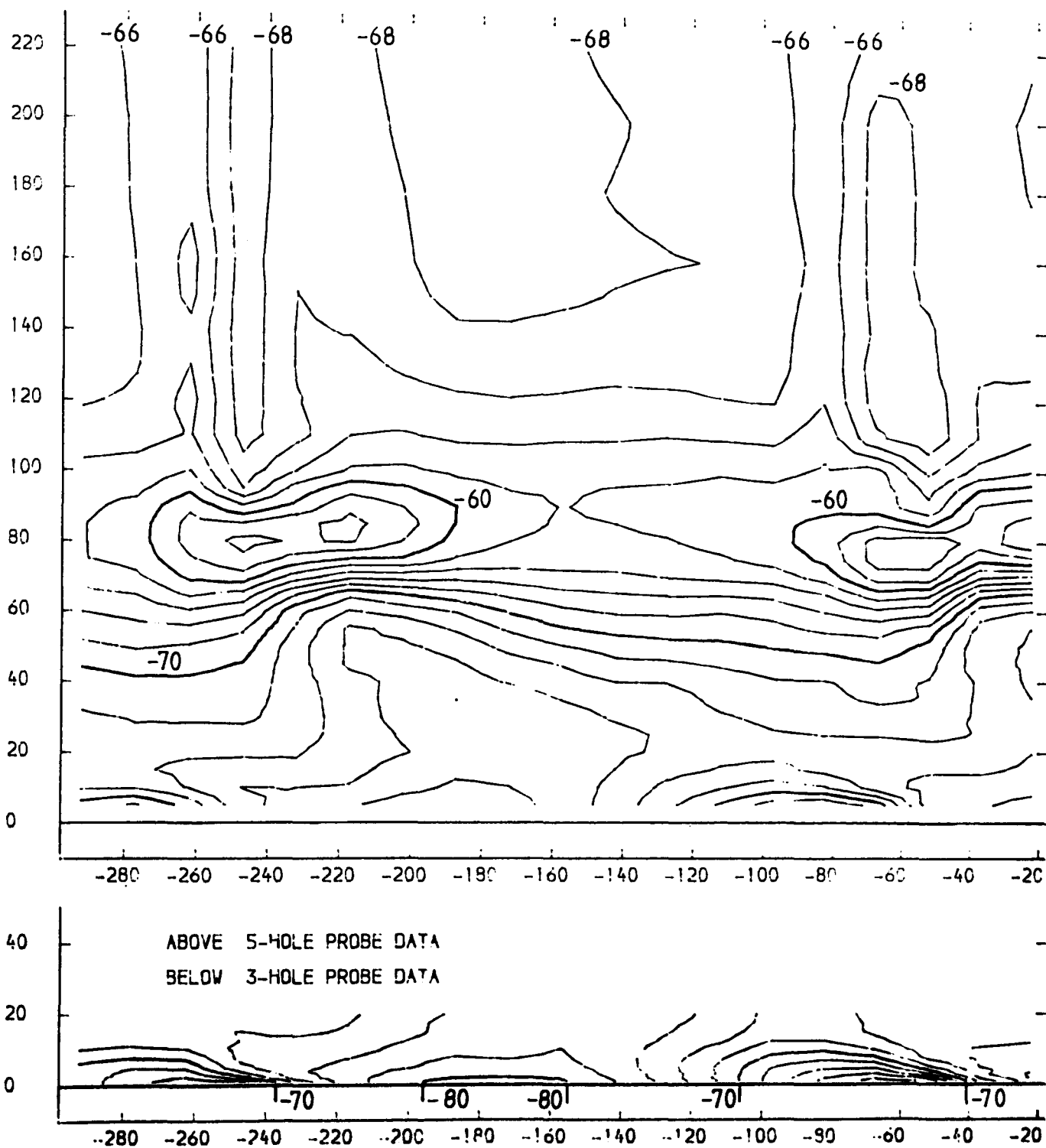


FIGURE 4.64



SLOT 9 STATIC PRESSURE COEFFICIENT (  $(P1-PLOCAL)/(P01-P1)$  ) CONTOURS  
 NATURAL INLET BOUNDARY LAYER  
 X-AXIS TANGENTIAL X-ORDINATE FROM TRAILING EDGE DATUM (MM)  
 Y-AXIS SPANWISE CO-ORDINATE FROM PERSPEX ENDWALL (MM)

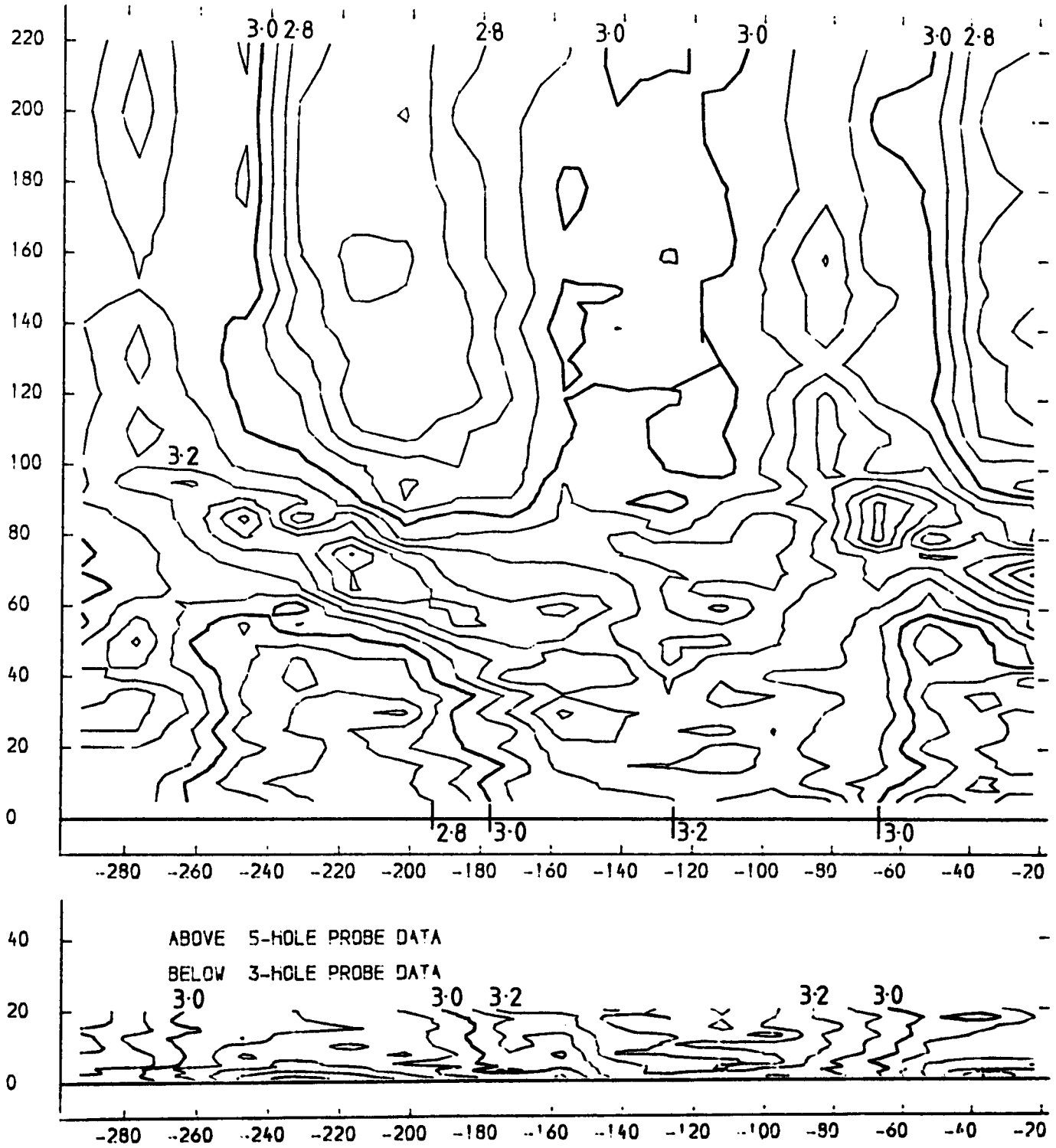


FIGURE 4.65

SLOT 10 EXPERIMENTAL DATA POINTS

NATURAL INLET BOUNDARY LAYER

X-AXIS TANGENTIAL CO-ORDINATE FROM TRAILING EDGE DATUM (MM)

Y-AXIS SPANWISE CO-ORDINATE FROM PERSPEX ENDWALL (MM)

+ PROBE DATA X MANUALLY INTERPOLATED DATA \* EXTRAPOLATED DATA

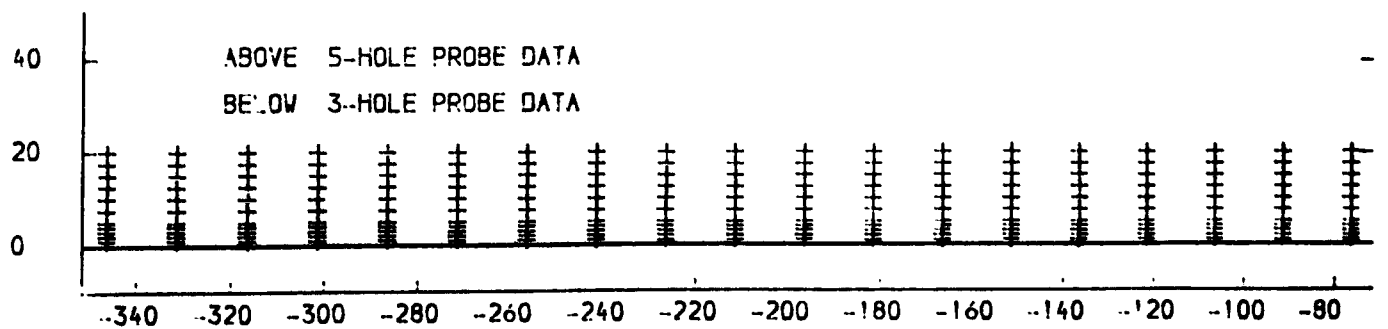
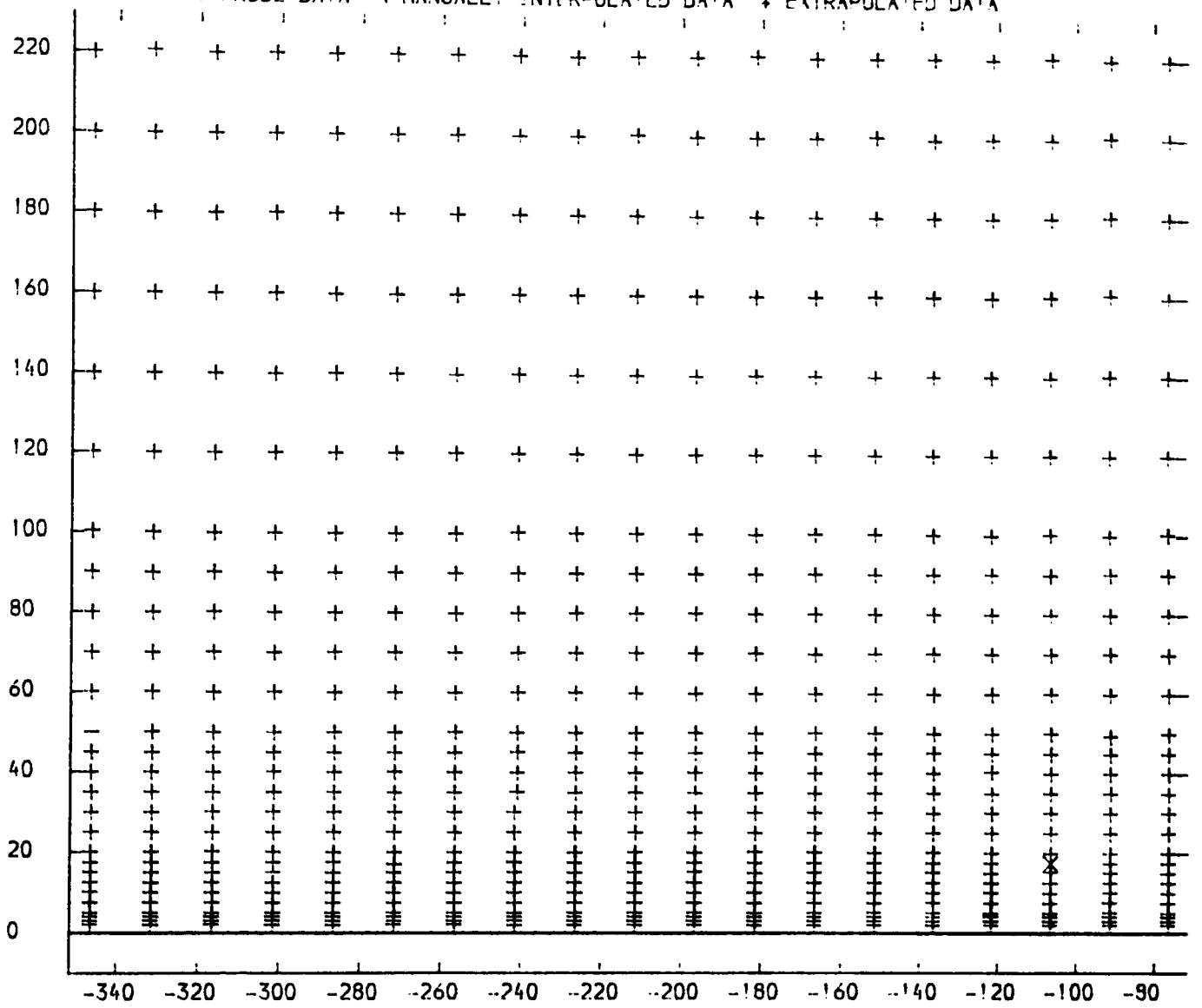


FIGURE 4.66

SLOT 10 TOTAL PRESSURE LOSS COEFFICIENT  $(P_{01} - P_{0LOCAL}) / (P_{01} - P_{11})$  CONTOURS  
 NATURAL INLET BOUNDARY LAYER  
 X-AXIS TANGENTIAL CO-ORDINATE FROM TRAILING EDGE DATUM (MM)  
 Y-AXIS SPANWISE CO-ORDINATE FROM PERSPEX ENDWALL (MM)

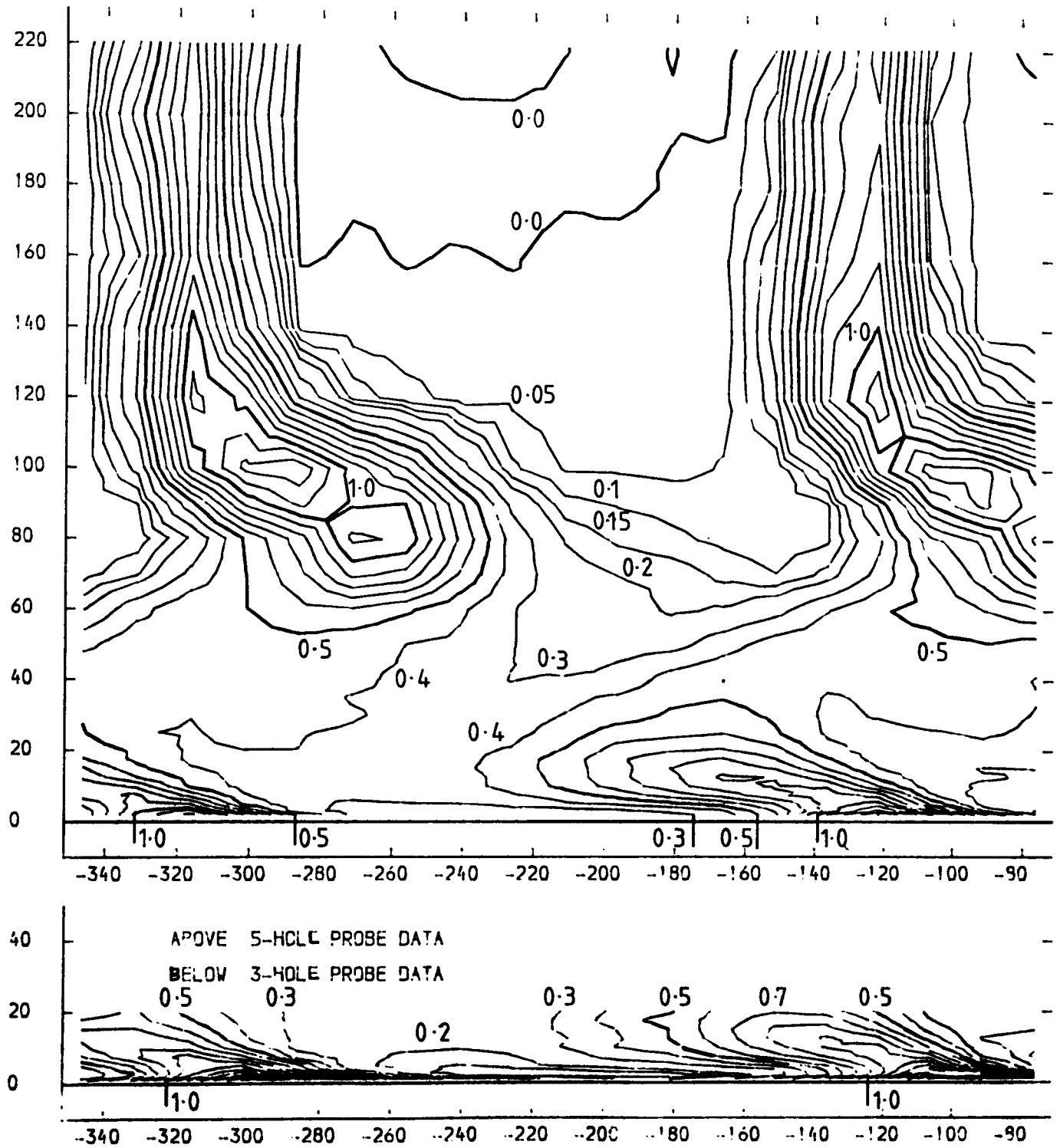


FIGURE 4.67

SLOT 10 MIDSPAN TANGENTIAL TRAVERSE RESULTS

NATURAL INLET BOUNDARY LAYER

X-AXIS TANGENTIAL CO-ORDINATE FROM TRAILING EDGE DATUM (MM)

UPPER Y-AXIS YAW ANGLE (DEGREES)

LOWER Y-AXIS TOTAL PRESSURE LOSS COEFFICIENT (  $(P_{01}-P_{0LOCAL}) / (P_{01}-P_1)$  )

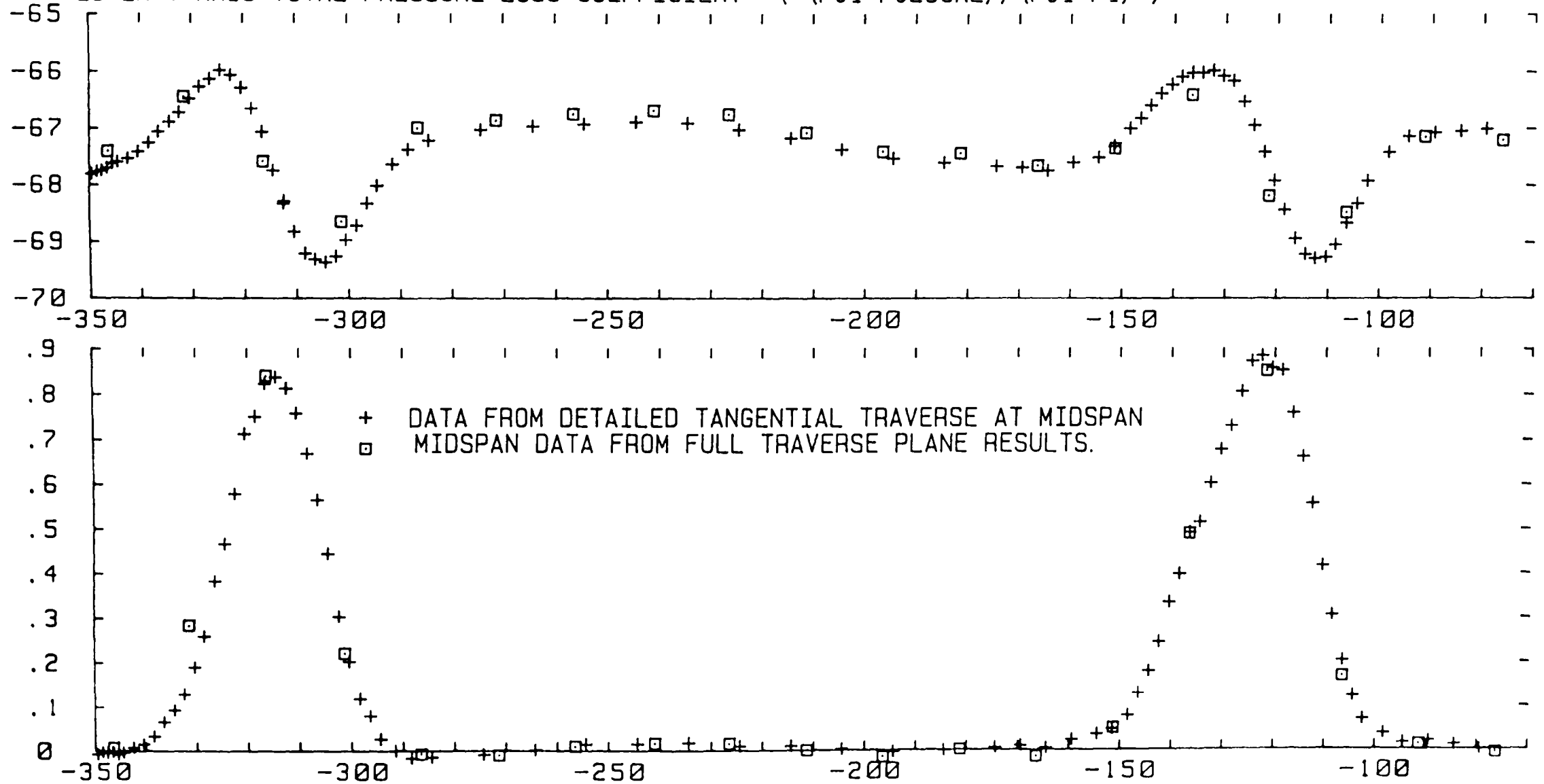


FIGURE 4.68

SLOT 10 TOTAL VELOCITY MAGNITUDE CONTOURS (CONTOUR UNITS METPES/SEC)  
 NATURAL INLET BOUNDARY LAYER  
 X-AXIS TANGENTIAL CO-ORDINATE FROM TRAILING EDGE DATUM (MM)  
 Y-AXIS SPANWISE CO-ORDINATE FROM PERSPEX ENDWALL (MM)

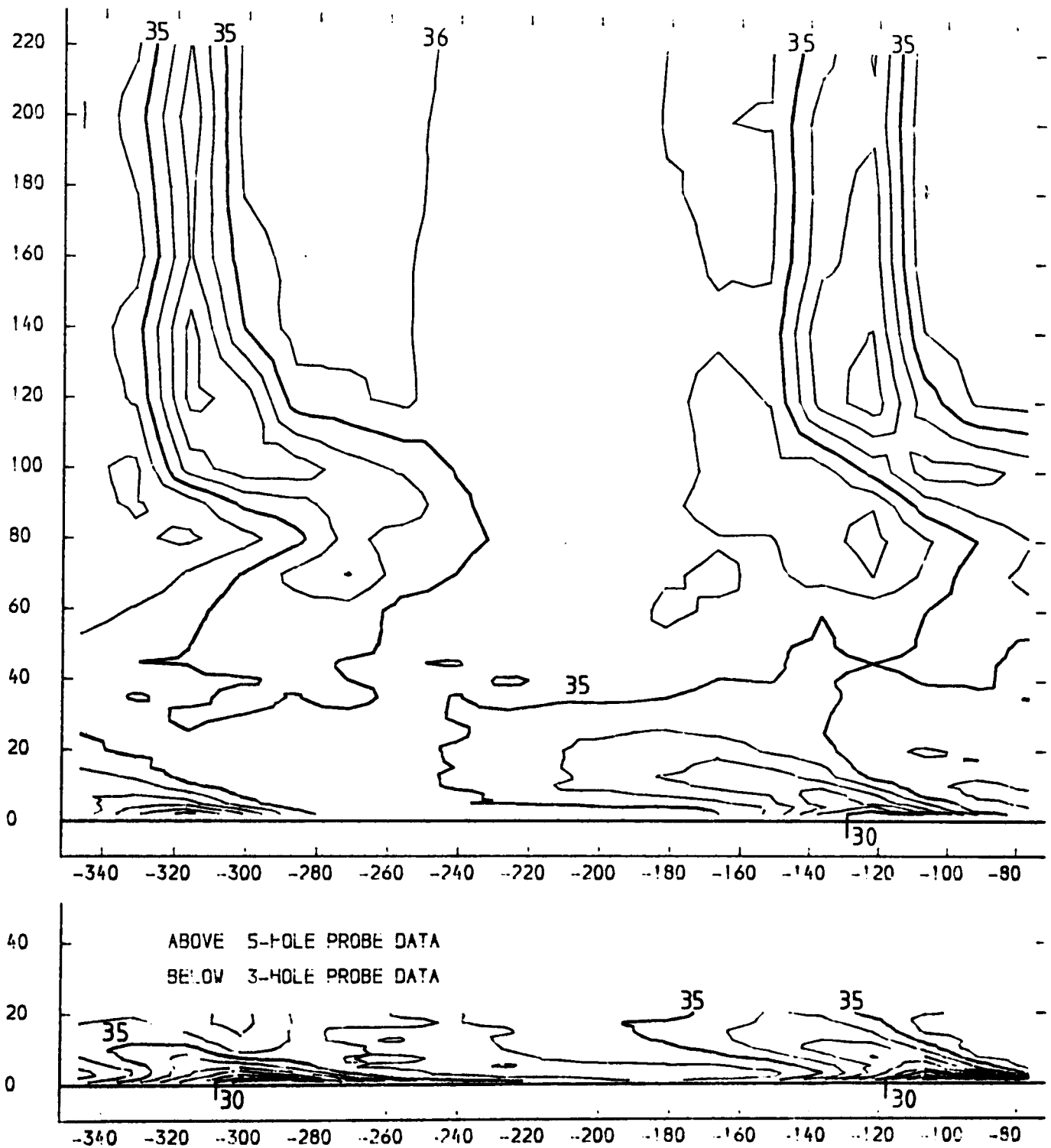
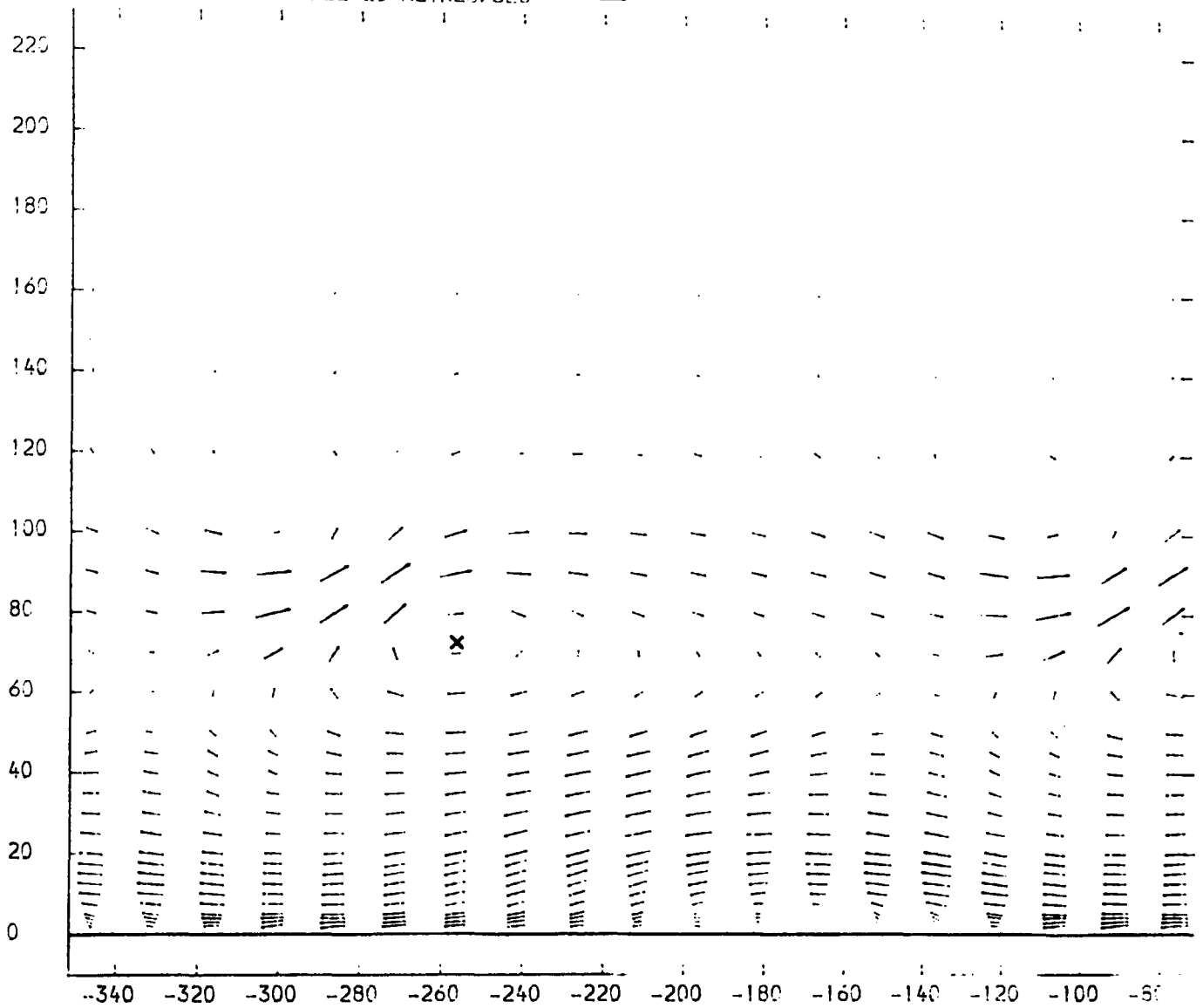


FIGURE 4.69

SLOT 10 VECTOR PLOT OF SECONDARY VELOCITIES  $(V_T(\text{SEC}) = V_T(\text{LOC}) - V_T(\text{M. S.}) + V_A(\text{LOC}) / V_A(\text{M. S.}))$   
 NATURAL INLET BOUNDARY LAYER  
 X-AXIS TANGENTIAL CO-ORDINATE FROM TRAILING EDGE DATUM (MM)  
 Y-AXIS SPANWISE CO-ORDINATE FROM PERFEX ENDWALL (MM)  
 VECTOR SCALE 20 METRES/SEC



x PASSAGE VORTEX CENTRE

FIGURE 4.70

SLOT 10 SPANWISE ANGLE (PITCH ANGLE) CONTOURS (CONTOUR UNITS DEGREE)  
NATURAL INLET BOUNDARY LAYER  
X-AXIS TANGENTIAL CO-ORDINATE FROM TRAILING EDGE DATUM (MM)  
Y-AXIS SPANWISE CO-ORDINATE FROM PERSPEX ENDWALL (MM)

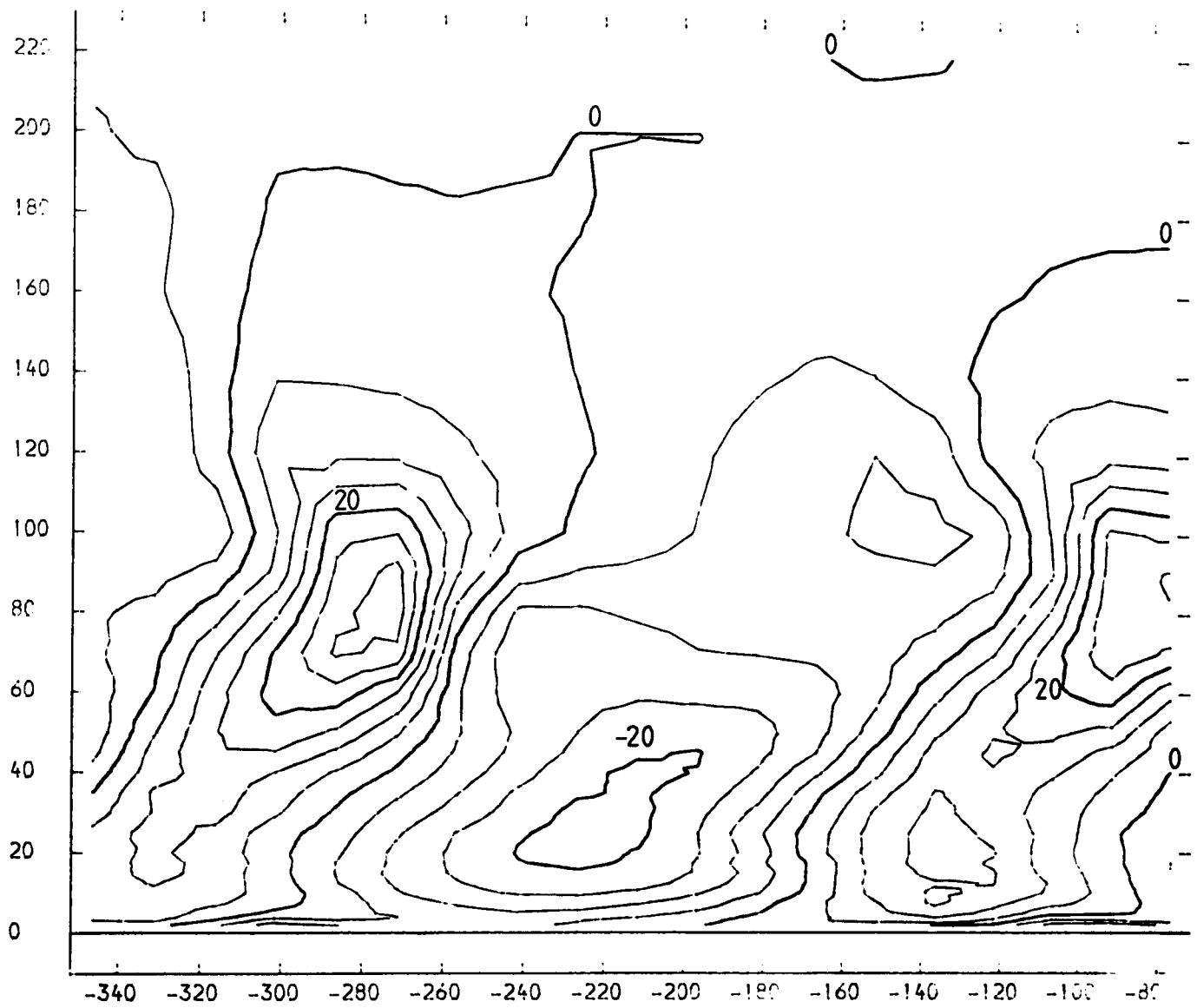


FIGURE 4.71

SLOT 10 YAW ANGLE CONTOURS (CONTOUR UNITS DEGREES)  
 NATURAL INLET BOUNDARY LAYER  
 X-AXIS TANGENTIAL CO-ORDINATE FROM TRAILING EDGE DATUM (MM)  
 Y-AXIS SPANWISE CO-ORDINATE FROM PERSPEX ENDWALL (MM)

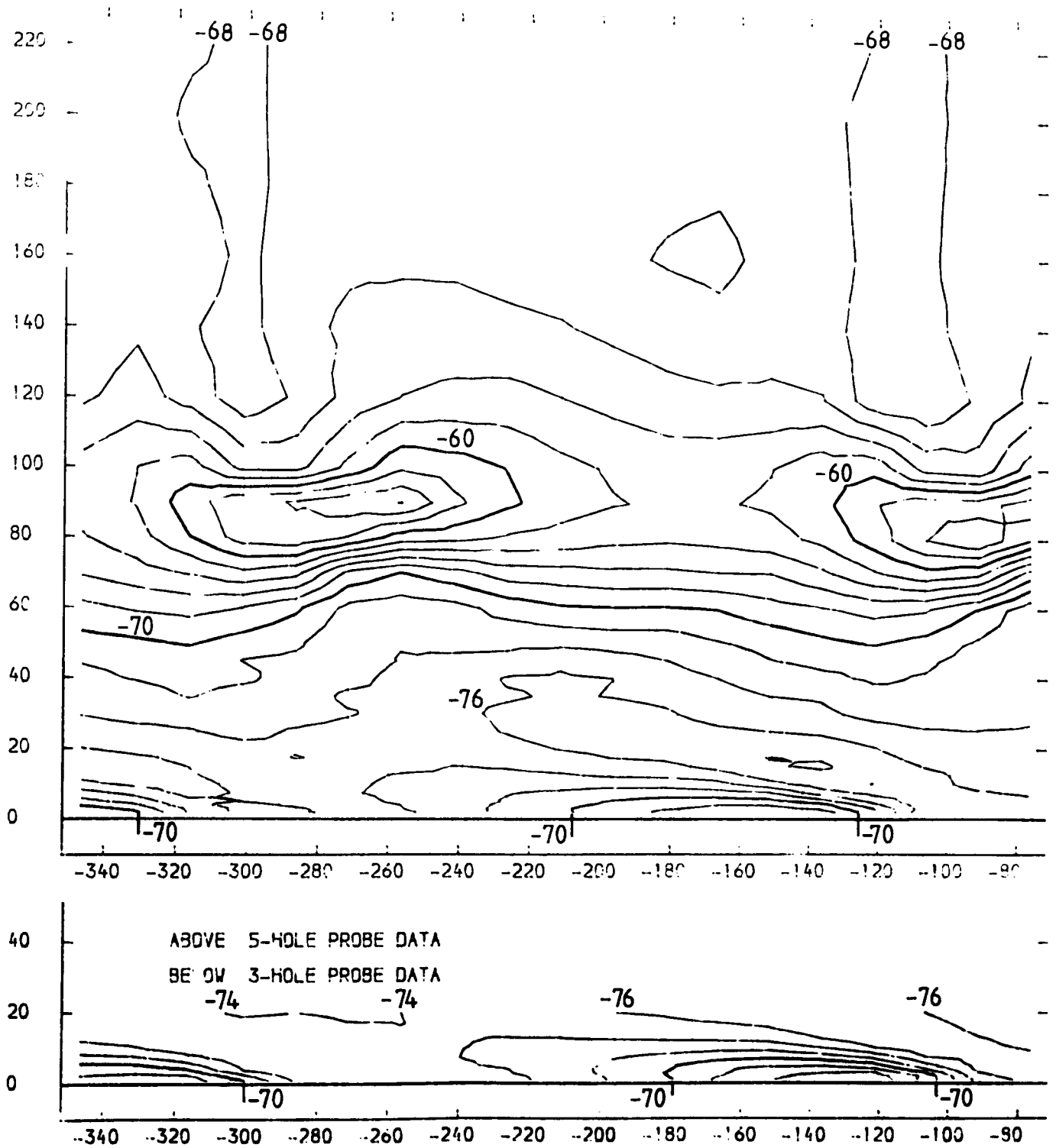


FIGURE 4.72



SLOT 10 STATIC PRESSURE COEFFICIENT (  $(P1-PLOCAL)/(P01-P1)$  ) CONTOURS  
 NATURAL INLET BOUNDARY LAYER  
 X-AXIS TANGENTIAL CO-ORDINATE FROM TRAILING EDGE DATUM (MM)  
 Y-AXIS SPANWISE CO-ORDINATE FROM PERSPEX ENDWALL (MM)

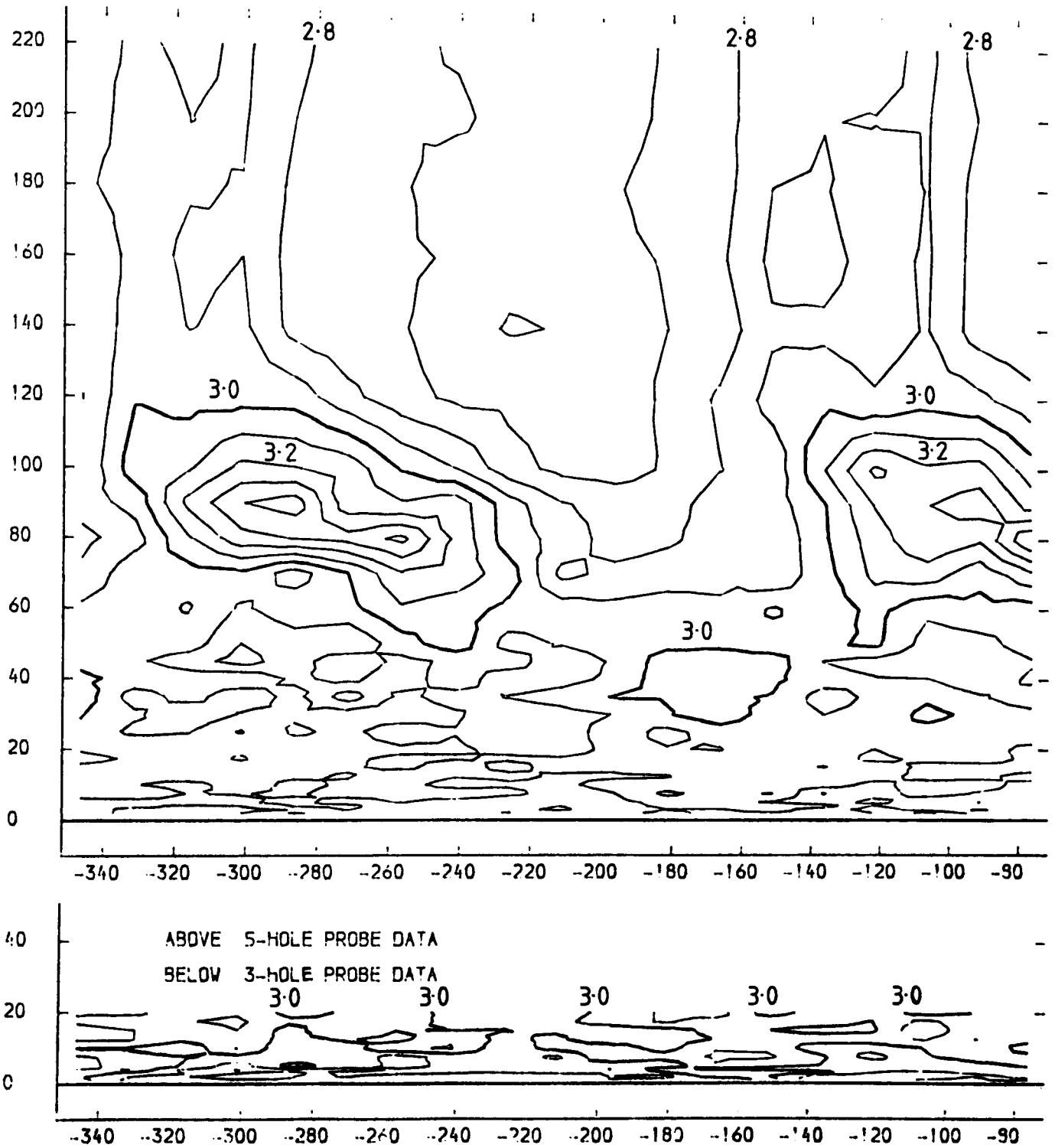
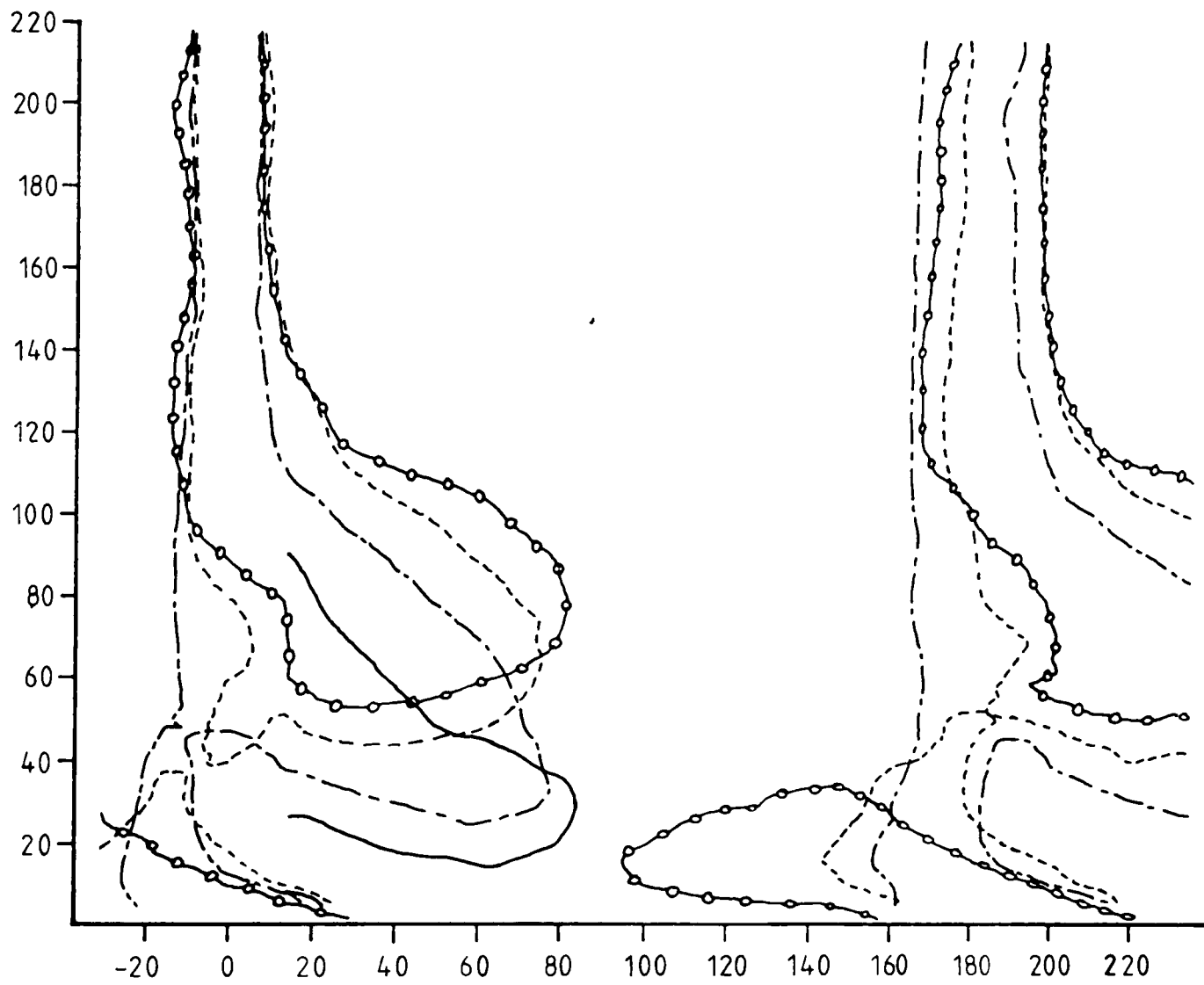
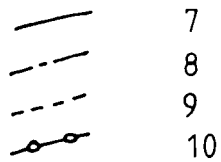


FIGURE 4.73

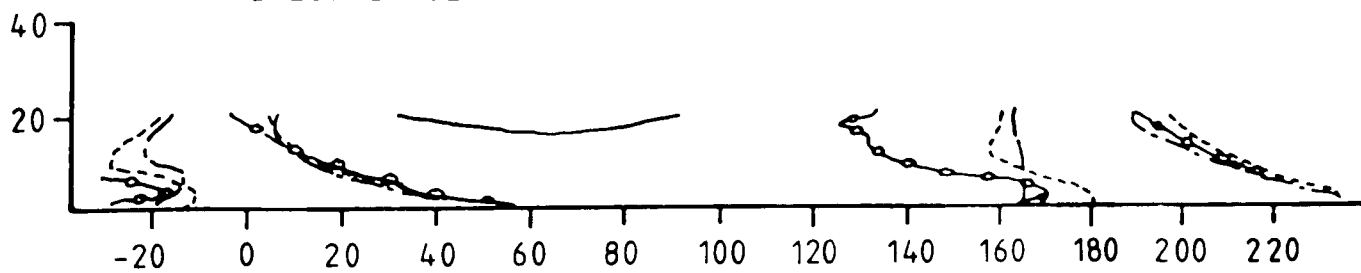
# LOSS CORE DEVELOPMENT DOWNSTREAM OF THE BLADE PASSAGE

X-AXIS TANGENTIAL CO-ORDINATE FROM BLADE SUCTION SURFACE OR  
TANGENTIAL CO-ORDINATE FROM WAKE CENTRE-LINE (MM)  
Y-AXIS SPANWISE CO-ORDINATE FROM PERSPEX ENDWALL (MM)

TRAVERSE  
SLOT NUMBER



ABOVE 5-HOLE PROBE DATA  
BELOW 3-HOLE PROBE DATA

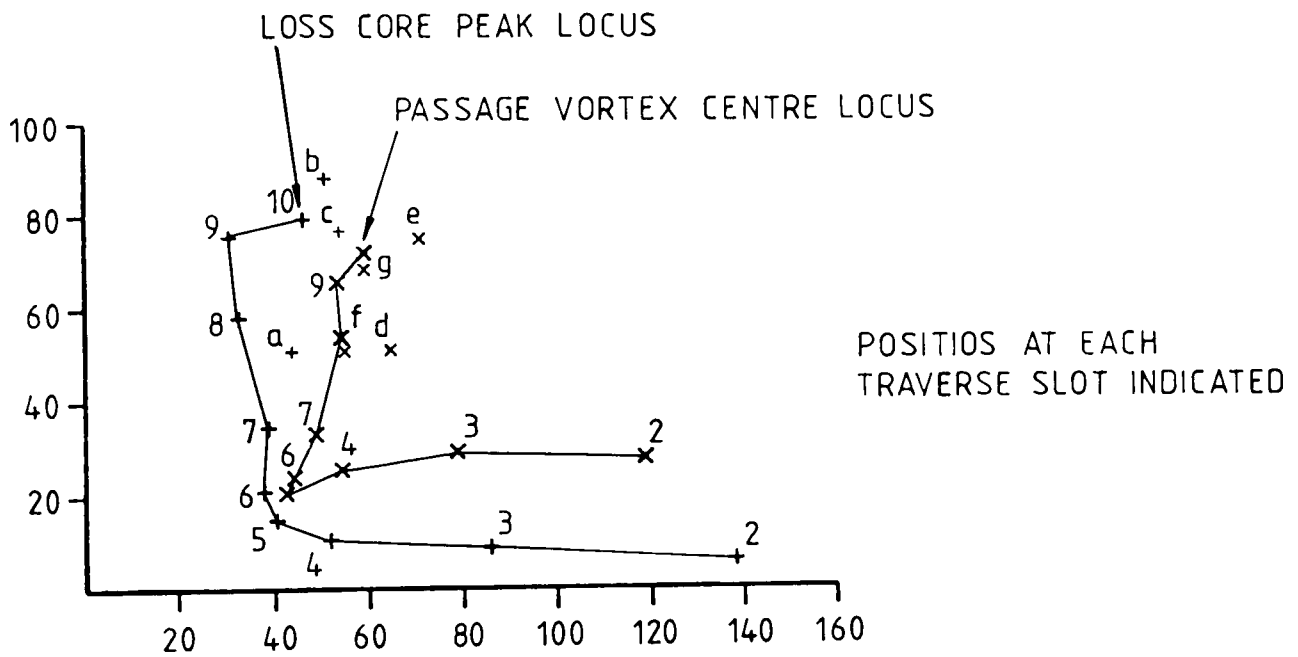


# LOCI OF PASSAGE VORTEX CENTRE AND LOSS CORE PEAK

X-AXIS TANGENTIAL CO-ORDINATE FROM BLADE SUCTION SURFACE OR TANGENTIAL CO-ORDINATE FROM WAKE CENTRE-LINE (MM)  
 Y-AXIS SPANWISE CO-ORDINATE FROM PERSPEX ENDWALL (MM)

## ADDITIONAL POINTS KEY

POINT	SLOT NO.	BOUNDARY LAYER AT CASCADE INLET	
a	8	THICKENED	LOSS CORE POSITION
b	10		
a	8	THINNED	
c	10		
d	8	THICKENED	PASSAGE VORTEX CENTRE
e	10		
f	8	THINNED	
g	10		



PASSAGE VORTEX CENTRE SITUATED AT INTERSECTION OF ZERO SPANWISE AND ZERO CROSS FLOW ANGLE CONTOURS ON EACH PROBE TRAVERSE PLANE

PITCHWISE MASS MEANED DATA UPSTREAM OF THE CASCADE  
 NATURAL INLET BOUNDARY LAYER

X-AXES SPANWISE CO-ORDINATE FROM PERSPEX ENDWALL (MM)

UPPER Y-AXIS YAW ANGLE (DEGREES)

LOWER Y-AXIS TOTAL PRESSURE LOSS COEFFICIENT ( (P01-POLOCAL) / (P01-P1) )

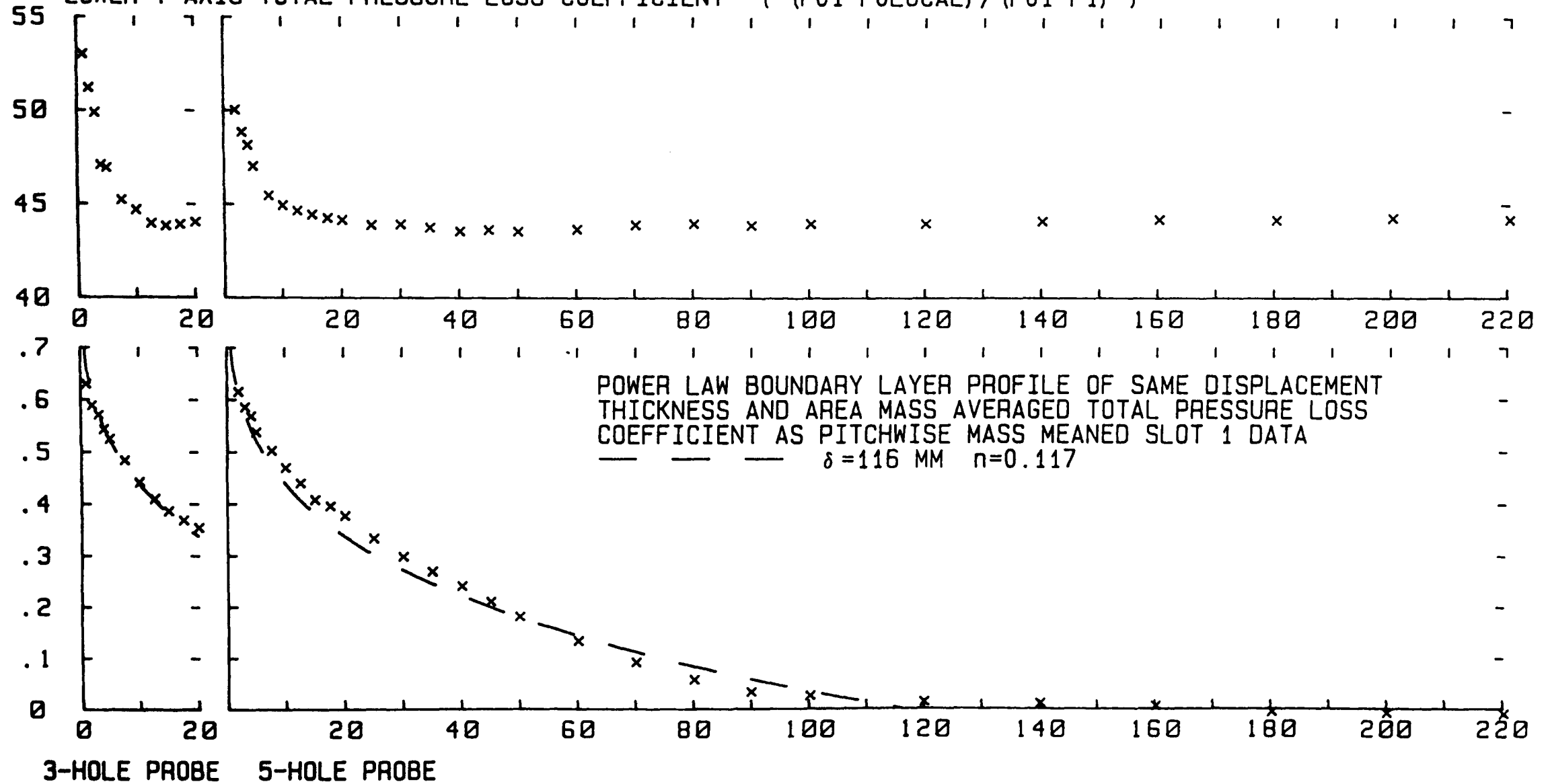


FIGURE 4.76

PITCHWISE MASS MEANED OVERTURNING ANGLE WITHIN THE BLADE PASSAGE  
 NATURAL INLET BOUNDARY LAYER

X-AXIS SPANWISE CO-ORDINATE FROM PERSPEX ENDWALL (MM)  
 Y-AXIS OVERTURNING ANGLE (DEGREES)

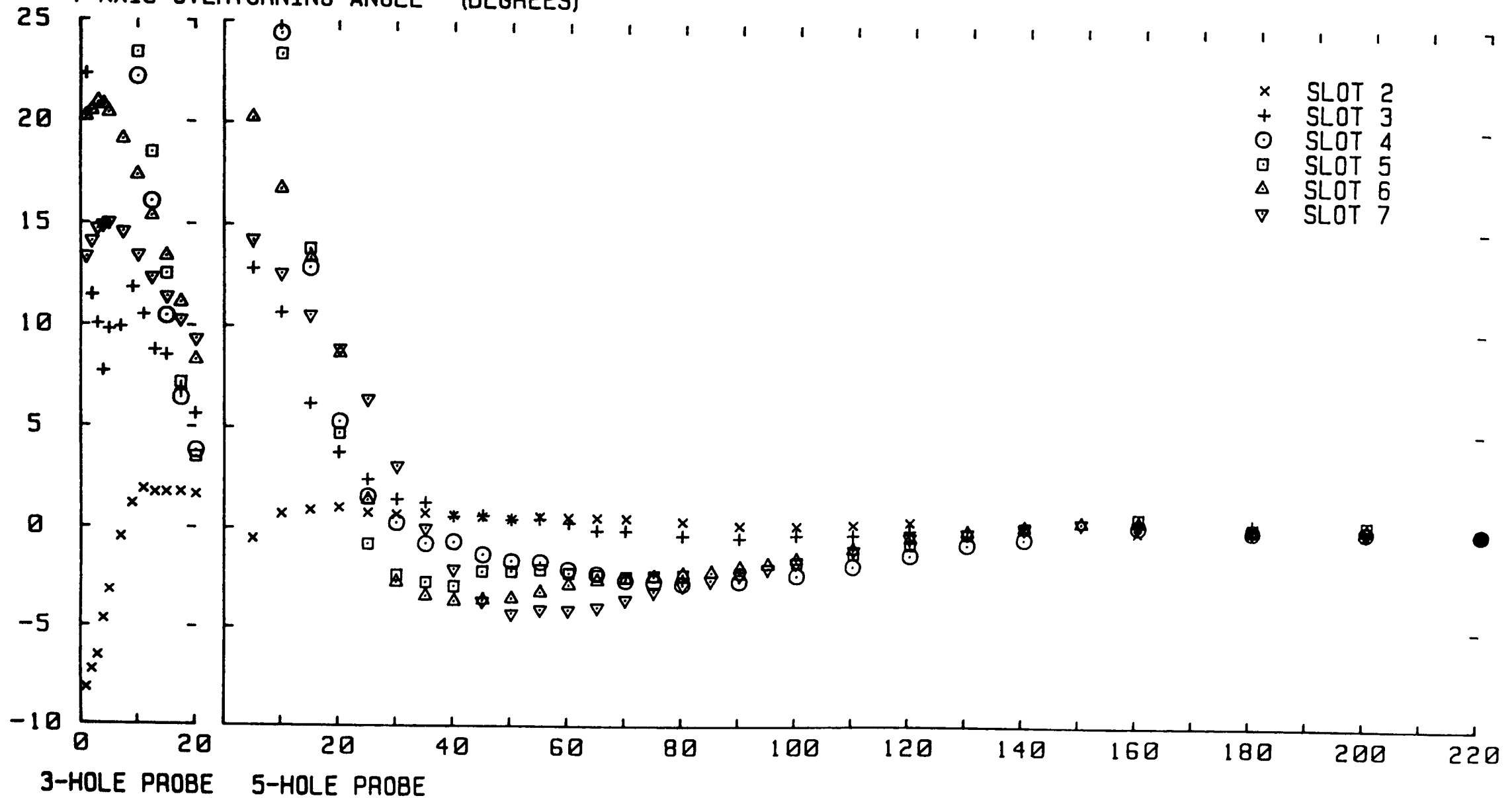


FIGURE 4.77

PITCHWISE MASS MEANED TOTAL PRESSURE LOSS COEFFICIENT WITHIN THE BLADE PASSAGE  
 NATURAL INLET BOUNDARY LAYER

X-AXIS SPANWISE CO-ORDINATE FROM PERSPEX ENDWALL (MM)  
 Y-AXIS TOTAL PRESSURE LOSS COEFFICIENT  $(P_{01} - P_{0LOCAL}) / (P_{01} - P_1)$

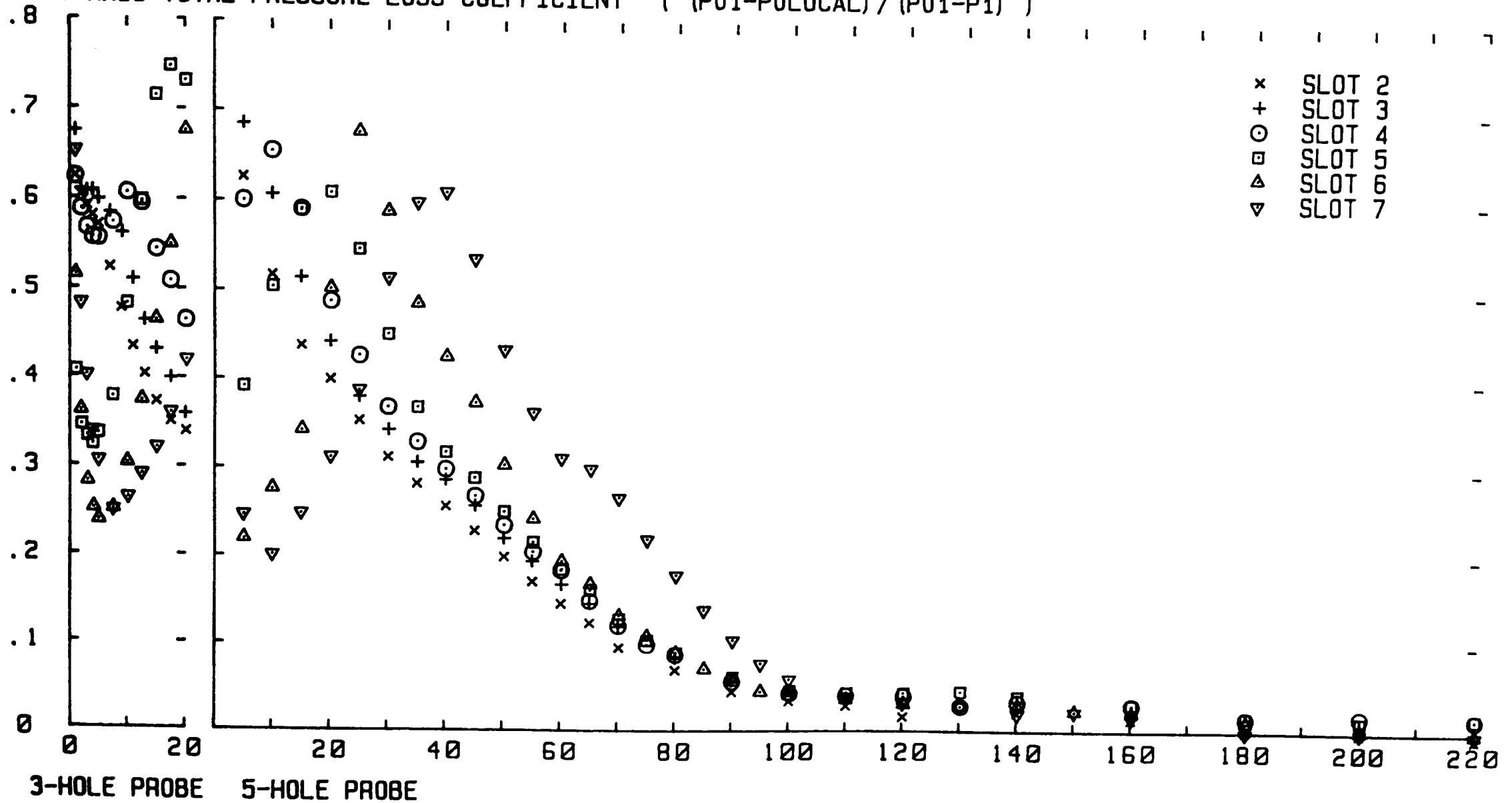


FIGURE 4.78

PITCHWISE MASS MEANED OVERTURNING ANGLE DOWNSTREAM OF THE CASCADE  
 NATURAL INLET BOUNDARY LAYER

X-AXIS SPANWISE CO-ORDINATE FROM PERSPEX ENDWALL (MM)  
 Y-AXIS OVERTURNING ANGLE (DEGREES)

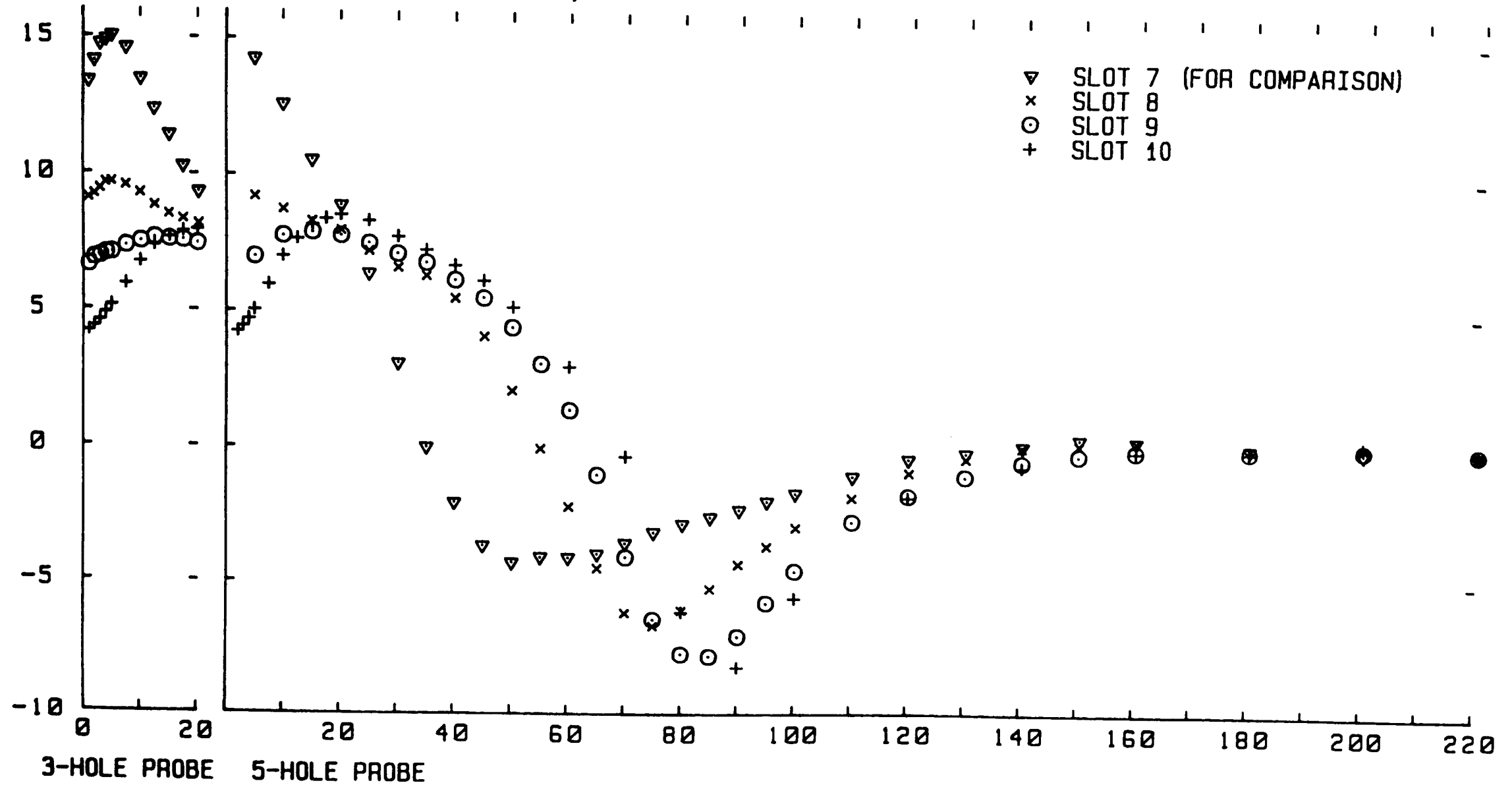


FIGURE 4.79

PITCHWISE MASS MEANED TOTAL PRESSURE LOSS COEFFICIENT DOWNSTREAM OF THE CASCADE  
 NATURAL INLET BOUNDARY LAYER

X-AXIS SPANWISE CO-ORDINATE FROM PERSPEX ENDWALL (MM)  
 Y-AXIS TOTAL PRESSURE LOSS COEFFICIENT  $(P_{01} - P_{0LOCAL}) / (P_{01} - P_1)$

- ▽ SLOT 7 (FOR COMPARISON)
- x SLOT 8
- SLOT 9
- + SLOT 10

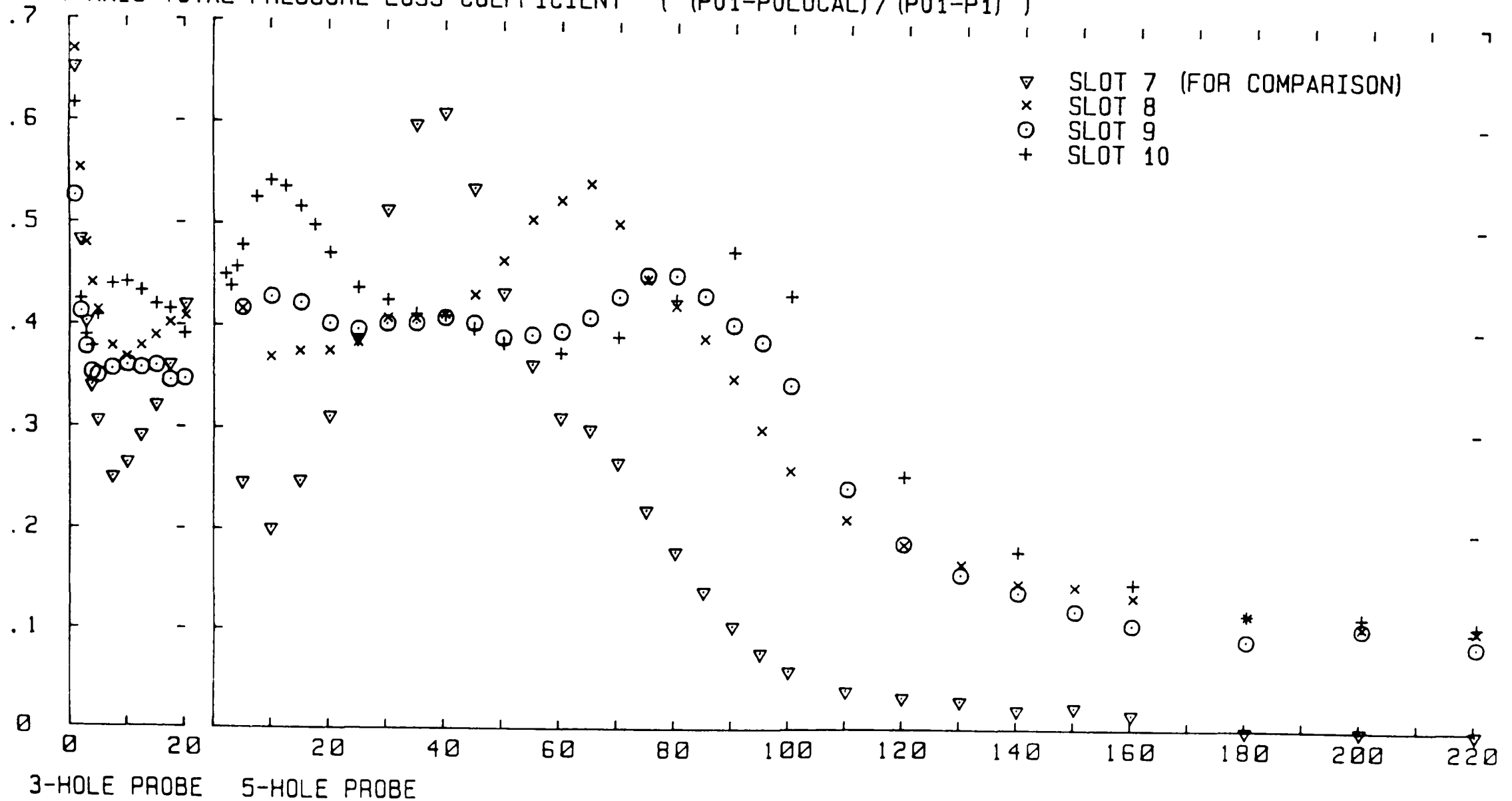


FIGURE 4.80



# DEVELOPMENT OF AREA MASS AVERAGED TOTAL PRESSURE LOSS COEFFICIENT

X-AXIS PERCENTAGE OF AXIAL CHORD FROM BLADE TRAILING EDGE  
Y-AXIS AREA MASS AVERAGED TOTAL PRESSURE LOSS COEFFICIENT

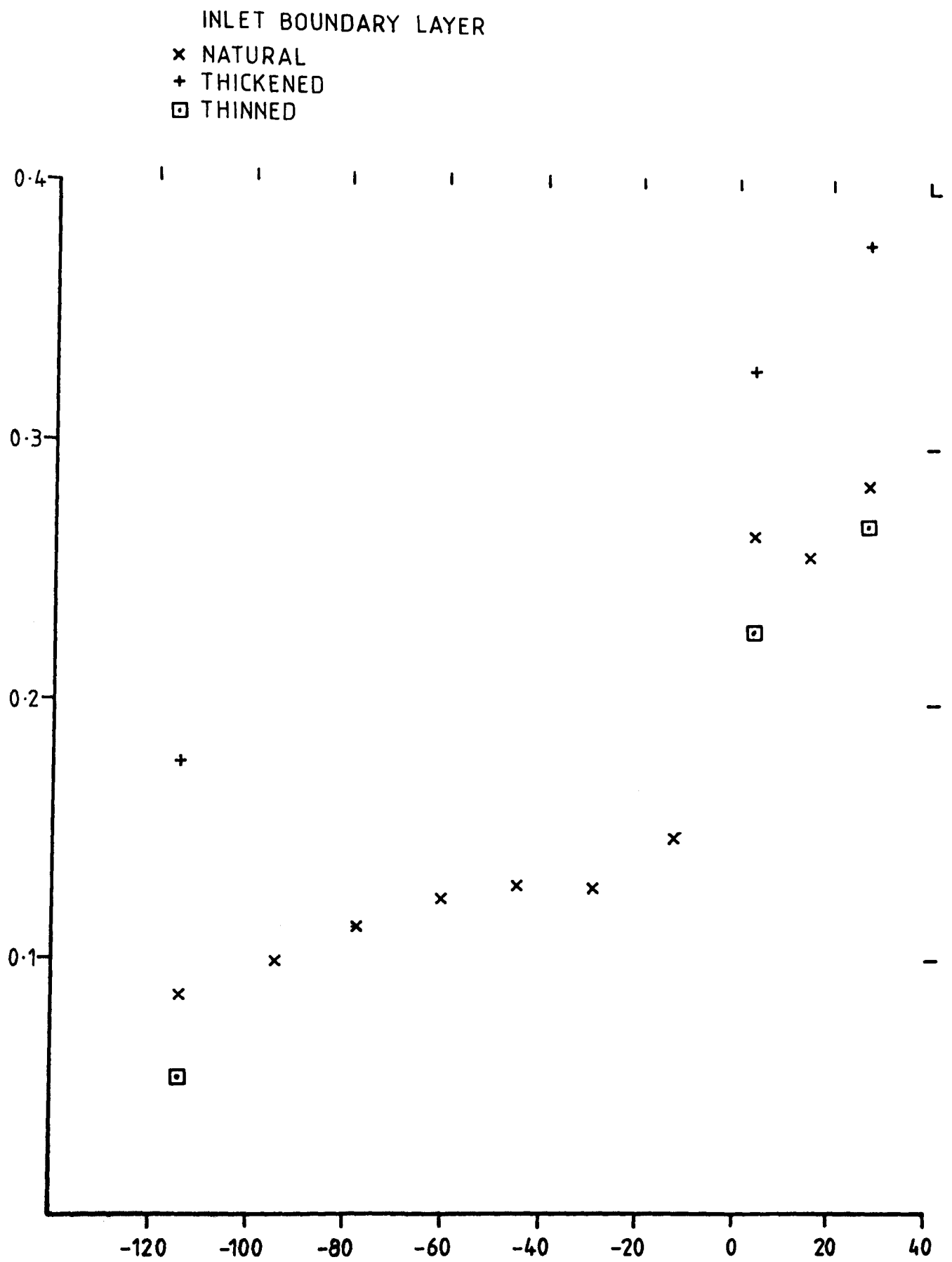


FIGURE 4.81

# DEVELOPMENT OF SECONDARY LOSSES

X-AXIS PERCENTAGE OF AXIAL CHORD FROM BLADE TRAILING EDGE  
 Y-AXIS SECONDARY TOTAL PRESSURE LOSS COEFFICIENT

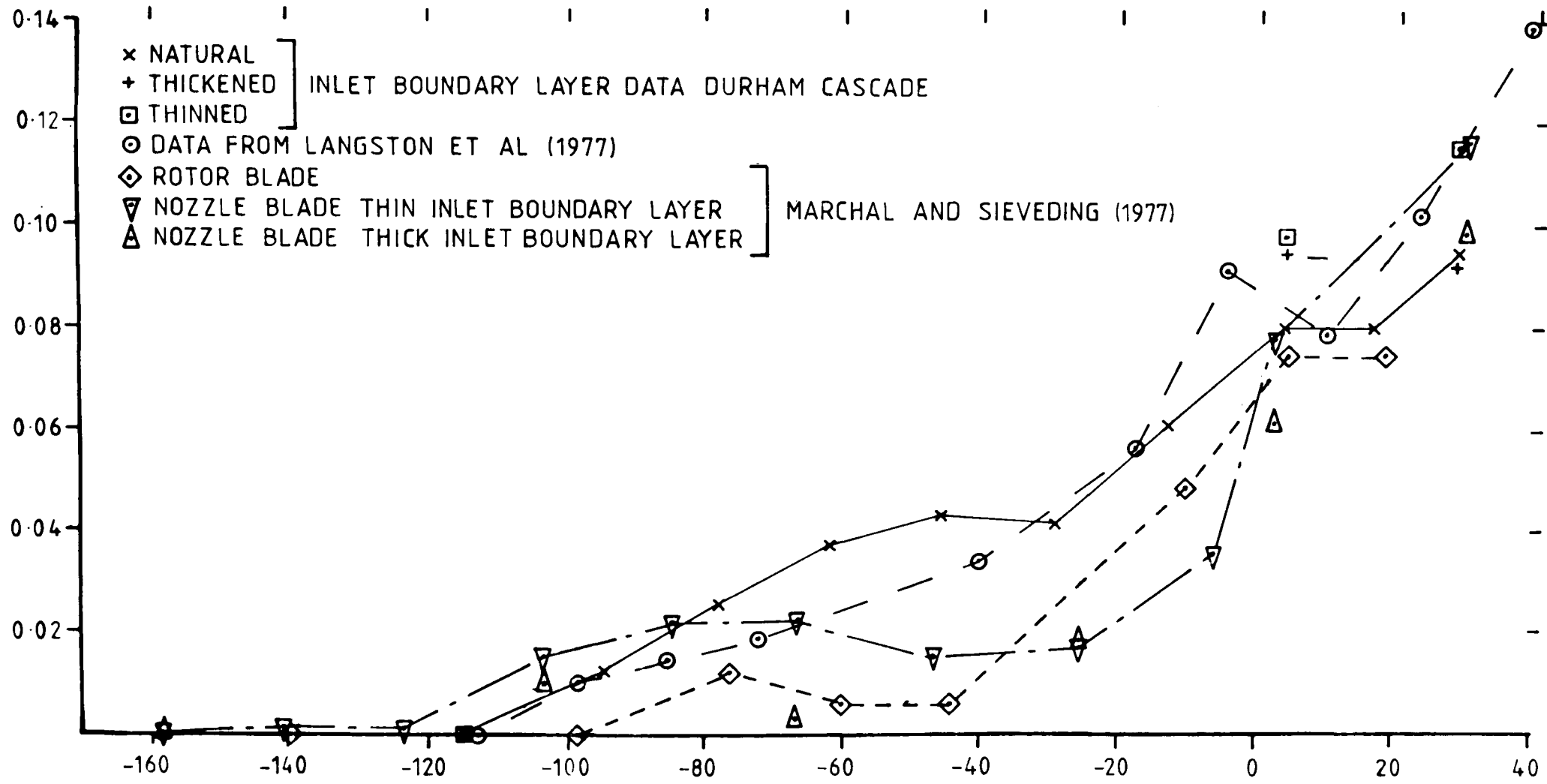


FIGURE 4.162

# NORMALIZED CASCADE MASS FLOW RATE

X-AXIS PERCENTAGE OF AXIAL CHORD FROM BLADE TRAILING EDGE  
 Y-AXIS CASCADE MASS FLOW RATE NORMALIZED USING INLET MASS FLOW  
 (DURHAM DATA NORMALISED USING NATURAL INLET BOUNDARY  
 LAYER DATA)

DURHAM INLET BOUNDARY LAYER

- x NATURAL
  - + THICKENED
  - THINNED
  - ◇ NATURAL
  - DATA FROM LANGSTON ET AL (1977)
- ] PRESSURE PROBE DATA
- ] HOT WIRE PROBE DATA

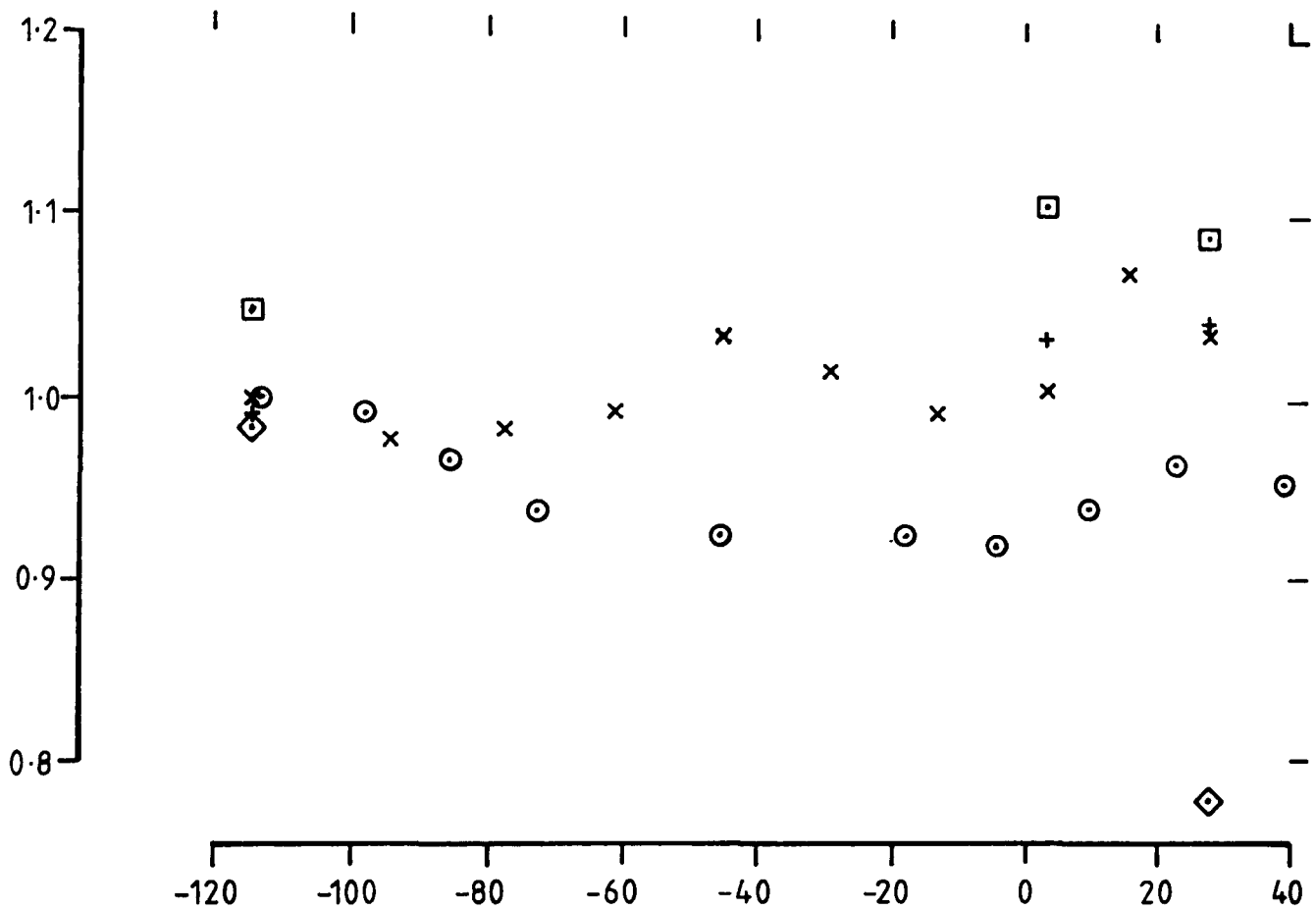


FIGURE 4.83

PLOT ON PLANE 20.1 MM FROM PERSPEX ENDWALL (5-HOLE PROBE DATA)

EXPERIMENTAL DATA POINTS

X-AXIS TANGENTIAL CO-ORDINATE FROM TRAILING EDGE DATUM (MM)

Y-AXIS AXIAL CO-ORDINATE FROM TRAILING EDGE DATUM (MM)

+ PROBE DATA    x MANUALLY INTERPOLATED DATA    \* EXTRAPOLATED DATA

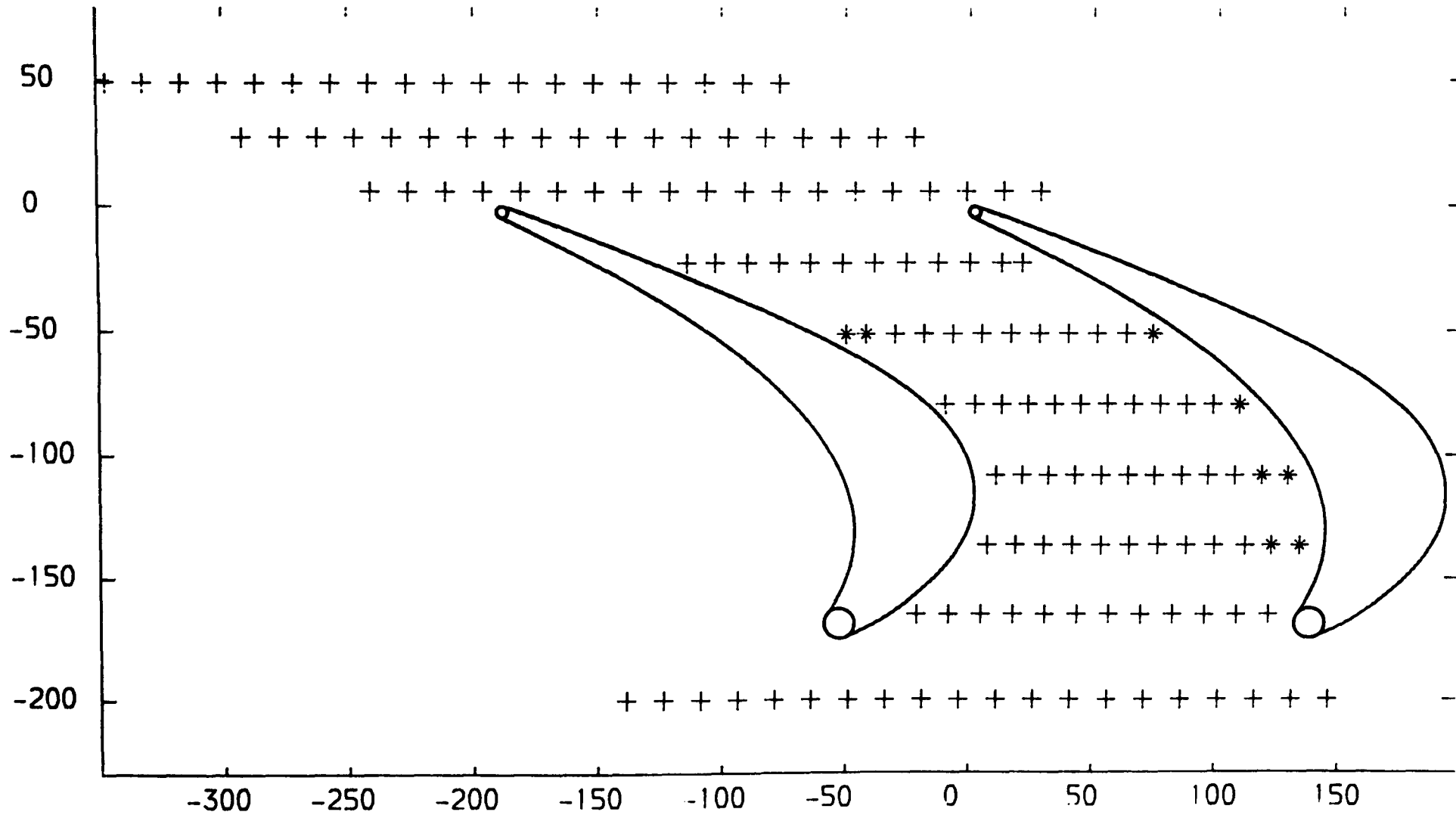


FIGURE 4.84

PLOT ON PLANE 1.0 MM FROM PERSPEX ENDWALL (3-HOLE PROBE DATA)  
TOTAL PRESSURE LOSS COEFFICIENT (  $(P_0 - P_{0LOCAL}) / (P_0 - P_1)$  ) CONTOURS  
X-AXIS TANGENTIAL CO-ORDINATE FROM TRAILING EDGE DATUM (MM)  
Y-AXIS AXIAL CO-ORDINATE FROM TRAILING EDGE DATUM (MM)

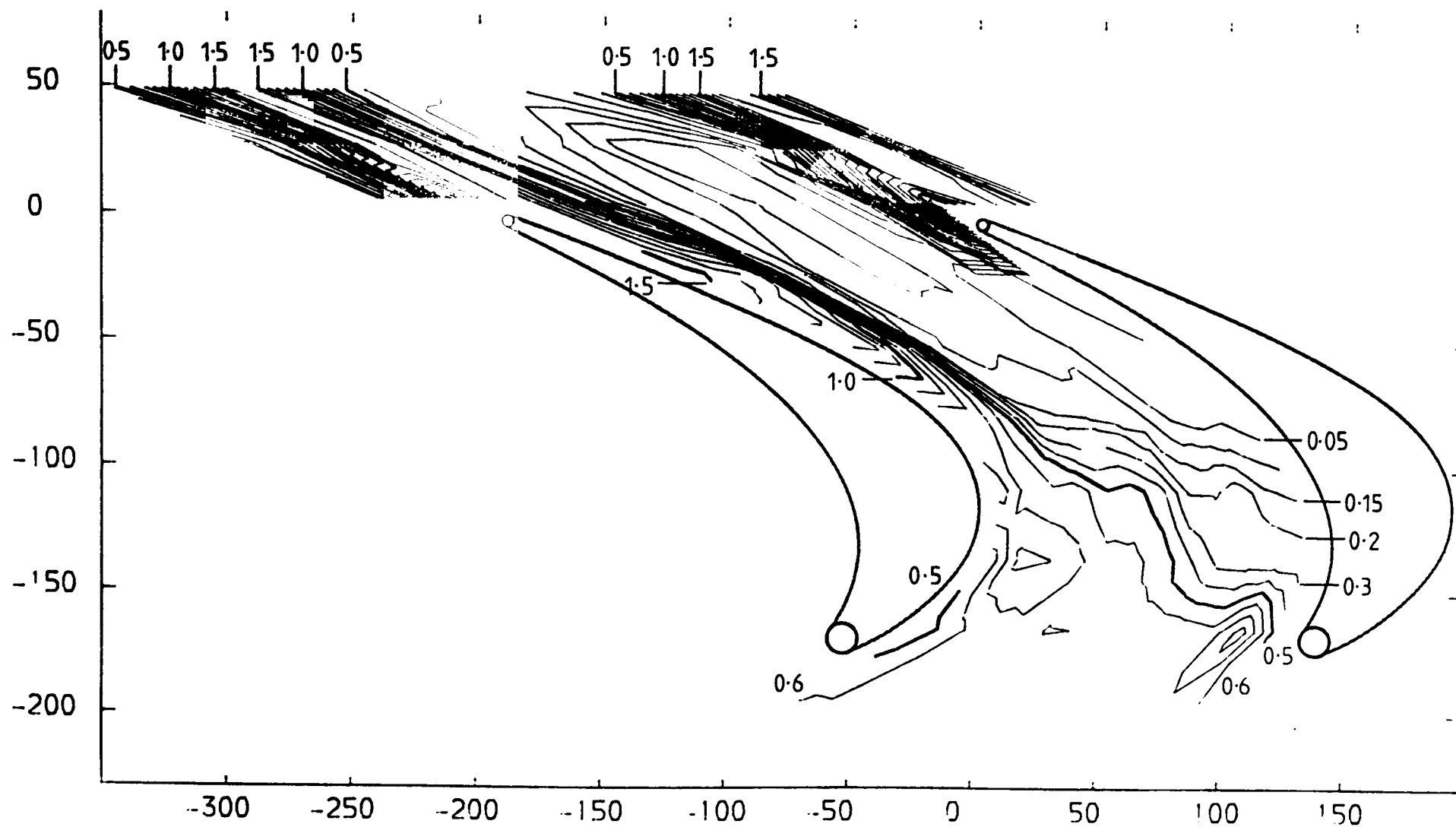


FIGURE 4.85

PLOT ON PLANE 5.0 MM FROM PERSPEX ENDWALL (5-HOLE PROBE DATA)  
TOTAL PRESSURE LOSS COEFFICIENT (  $(P_{01}-P_{0LOCAL}) / (P_{01}-P_1)$  ) CONTOURS  
X-AXIS TANGENTIAL CO-ORDINATE FROM TRAILING EDGE DATUM (MM)  
Y-AXIS AXIAL CO-ORDINATE FROM TRAILING EDGE DATUM (MM)

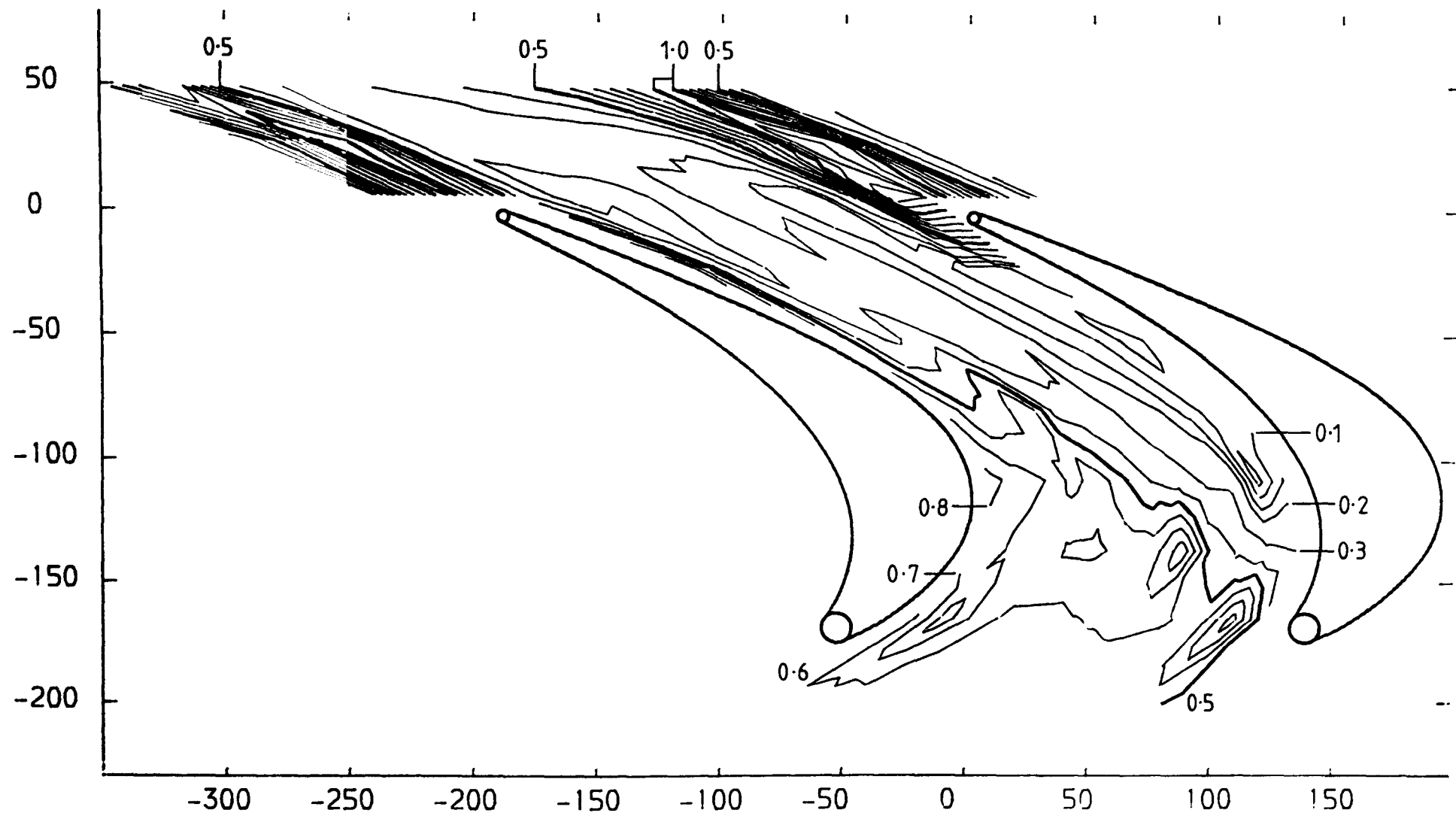


FIGURE 4.86

PLOT ON PLANE 5.0 MM FROM PERSPEX ENDWALL (3-HOLE PROBE DATA)  
 TOTAL PRESSURE LOSS COEFFICIENT (  $(P_0 - P_{0LOCAL}) / (P_{01} - P_1)$  ) CONTOURS  
 X-AXIS TANGENTIAL CO-ORDINATE FROM TRAILING EDGE DATUM (MM)  
 Y-AXIS AXIAL CO-ORDINATE FROM TRAILING EDGE DATUM (MM)

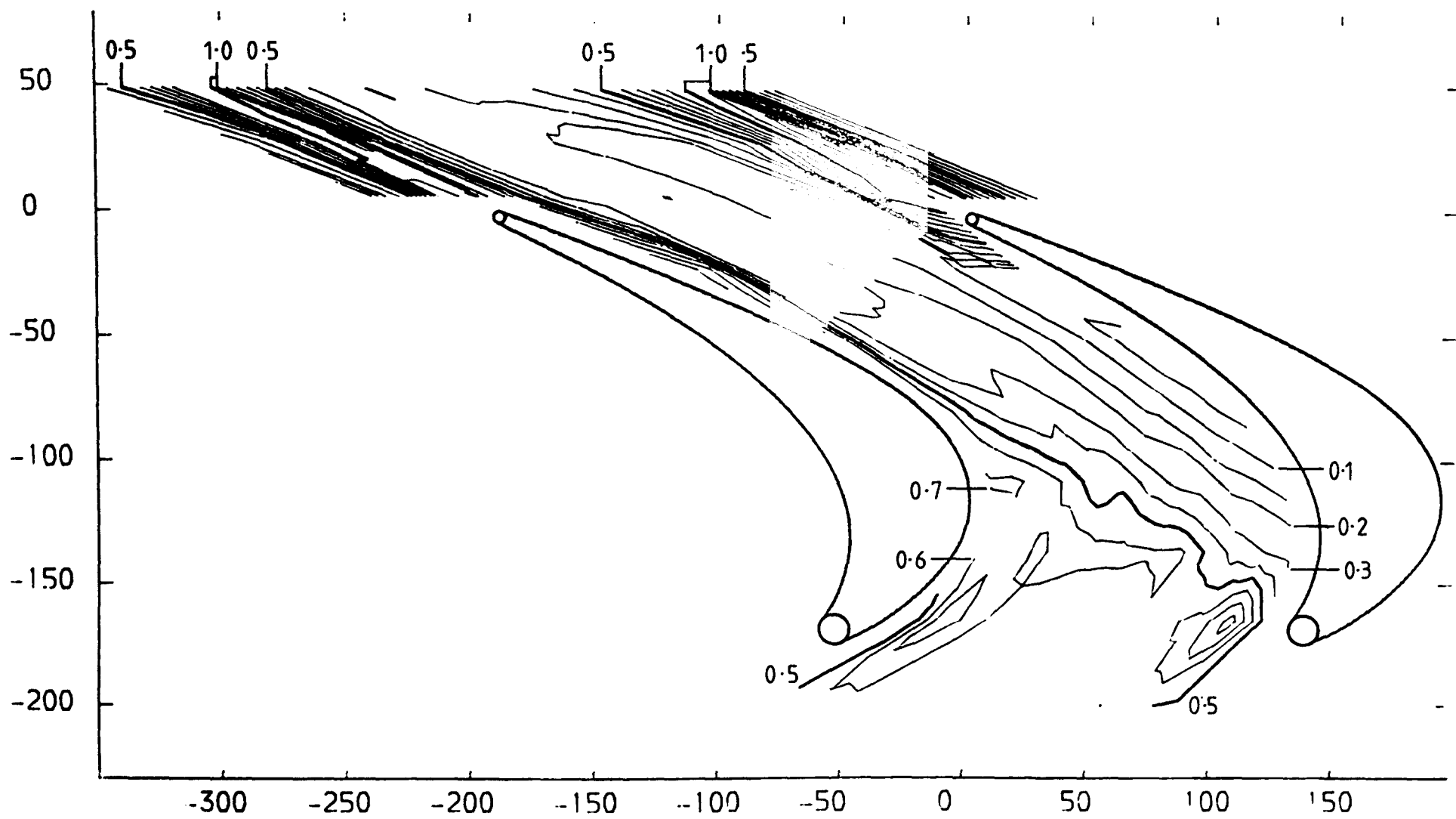


FIGURE 4.87

PLOT ON PLANE 20.1 MM FROM PERSPEX ENDWALL (5-HOLE PROBE DATA)  
TOTAL PRESSURE LOSS COEFFICIENT (  $(P_{01}-P_{0LOCAL}) / (P_{01}-P_1)$  ) CONTOURS  
X-AXIS TANGENTIAL CO-ORDINATE FROM TRAILING EDGE DATUM (MM)  
Y-AXIS AXIAL CO-ORDINATE FROM TRAILING EDGE DATUM (MM)

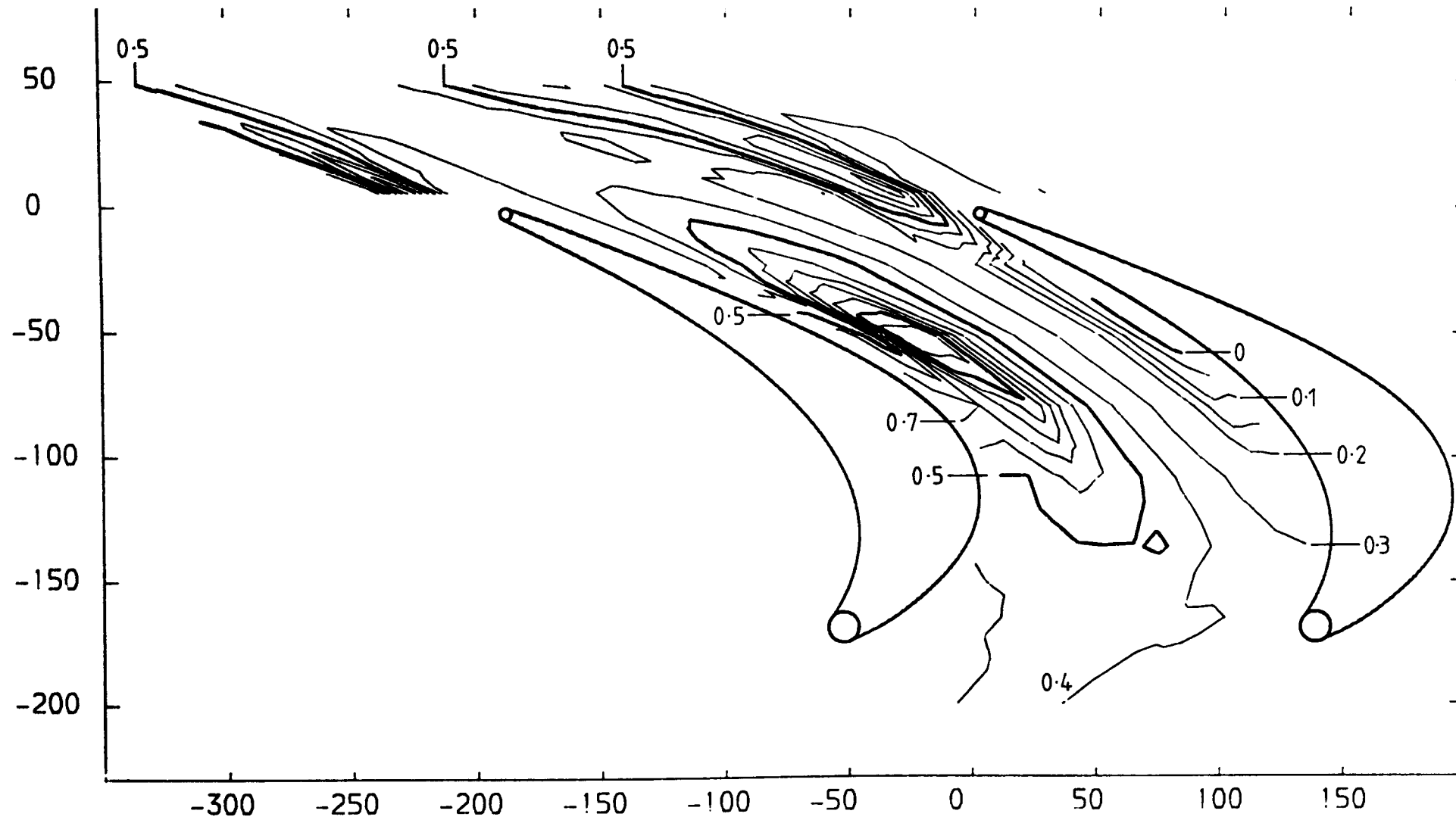


FIGURE 4.88



PLOT ON PLANE 20.1 MM FROM PERSPEX ENDWALL (3-HOLE PROBE DATA)  
TOTAL PRESSURE LOSS COEFFICIENT (  $(P_{01} - P_{0LOCAL}) / (P_{01} - P_1)$  ) CONTOURS  
X-AXIS TANGENTIAL CO-ORDINATE FROM TRAILING EDGE DATUM (MM)  
Y-AXIS AXIAL CO-ORDINATE FROM TRAILING EDGE DATUM (MM)

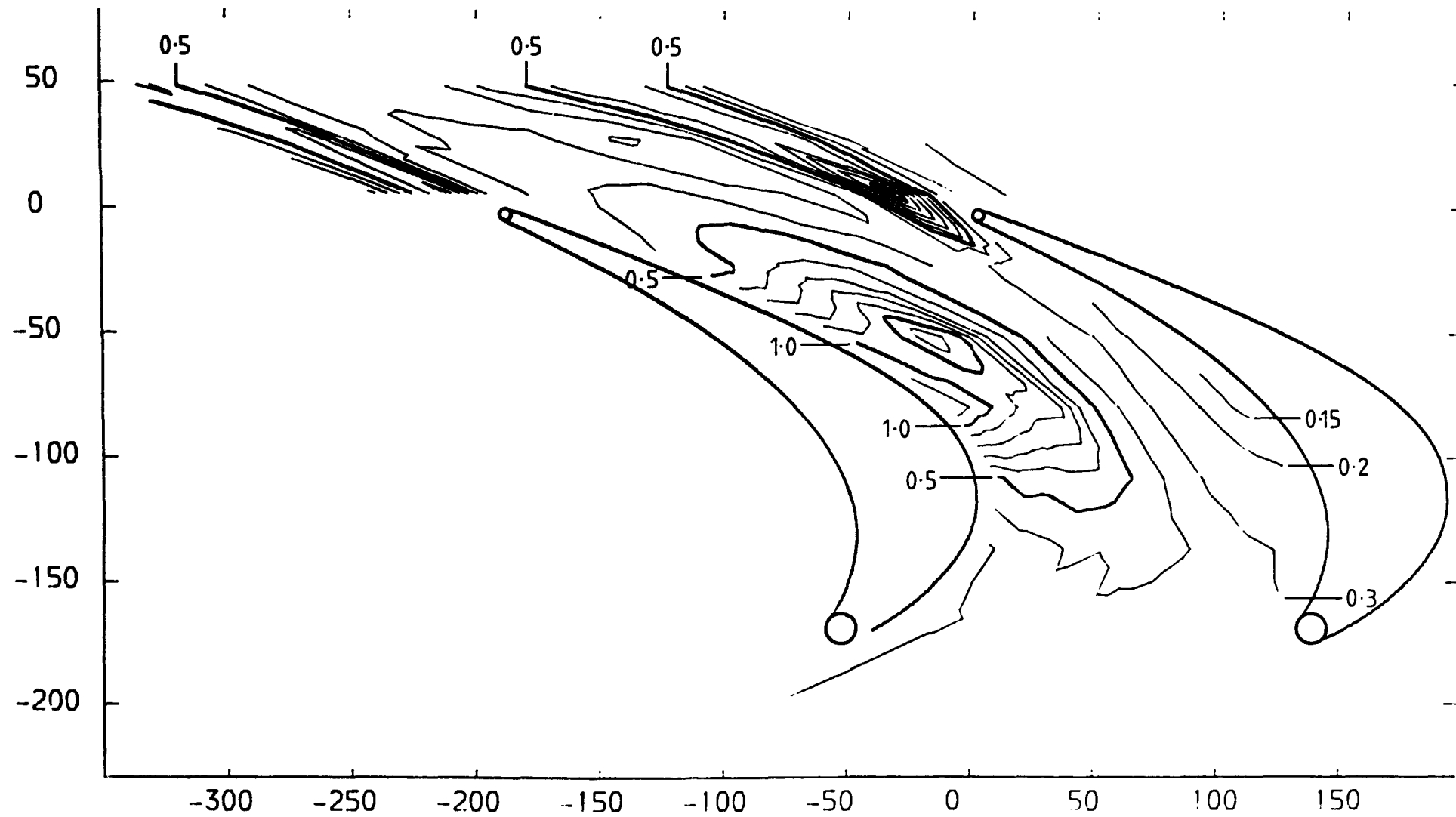


FIGURE 4.89

PLOT ON PLANE 40.0 MM FROM PERSPEX ENDWALL (5-HOLE PROBE DATA)  
TOTAL PRESSURE LOSS COEFFICIENT (  $(P_{01}-P_{0LOCAL}) / (P_{01}-P_1)$  ) CONTOURS  
X-AXIS TANGENTIAL CO-ORDINATE FROM TRAILING EDGE DATUM (MM)  
Y-AXIS AXIAL CO-ORDINATE FROM TRAILING EDGE DATUM (MM)

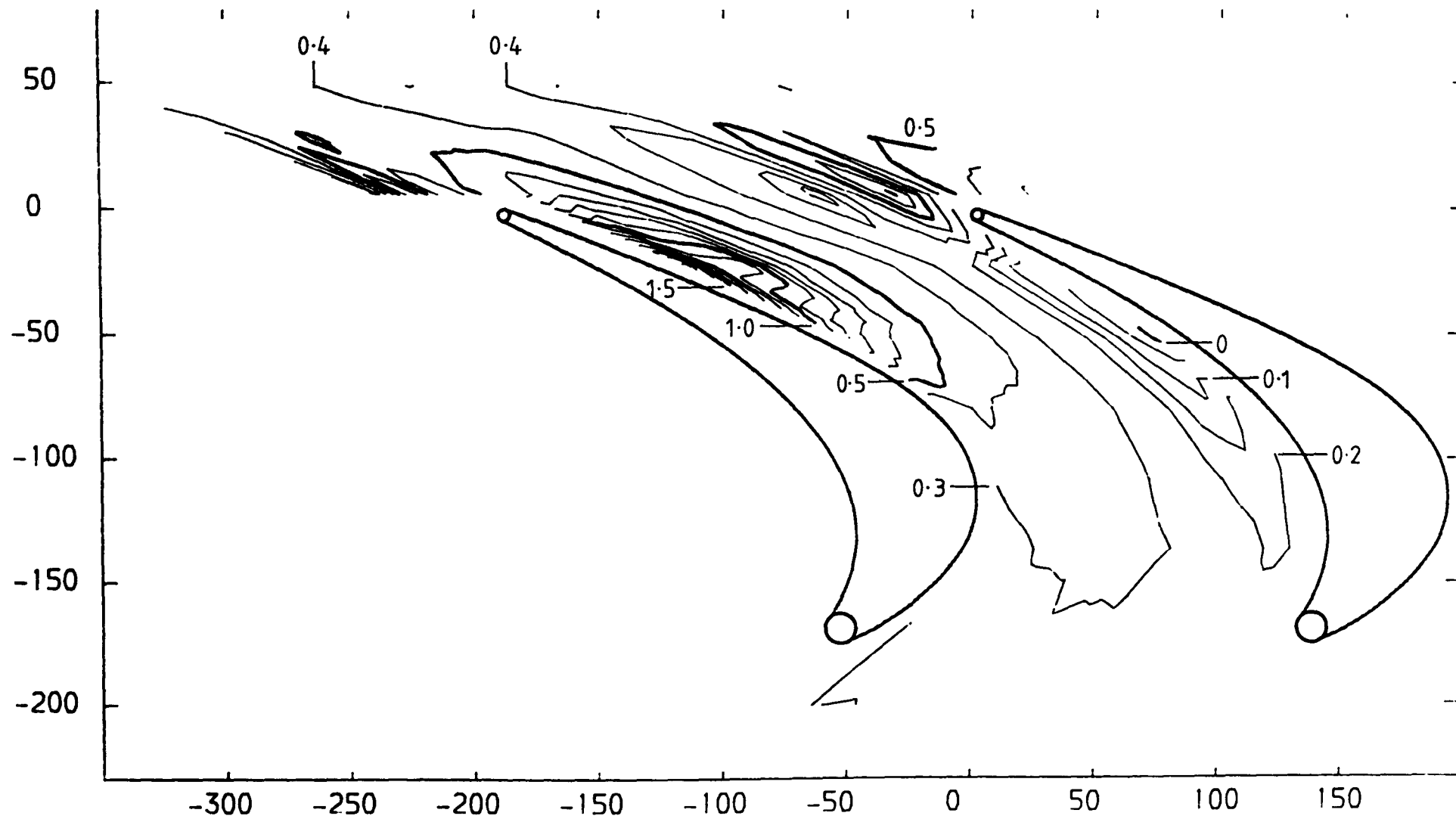


FIGURE 4.90

PLOT ON PLANE 60.0 MM FROM PERSPEX ENDWALL (5-HOLE PROBE DATA)  
TOTAL PRESSURE LOSS COEFFICIENT (  $(P_{01}-P_{0LOCAL}) / (P_{01}-P_1)$  ) CONTOURS  
X-AXIS TANGENTIAL CO-ORDINATE FROM TRAILING EDGE DATUM (MM)  
Y-AXIS AXIAL CO-ORDINATE FROM TRAILING EDGE DATUM (MM)

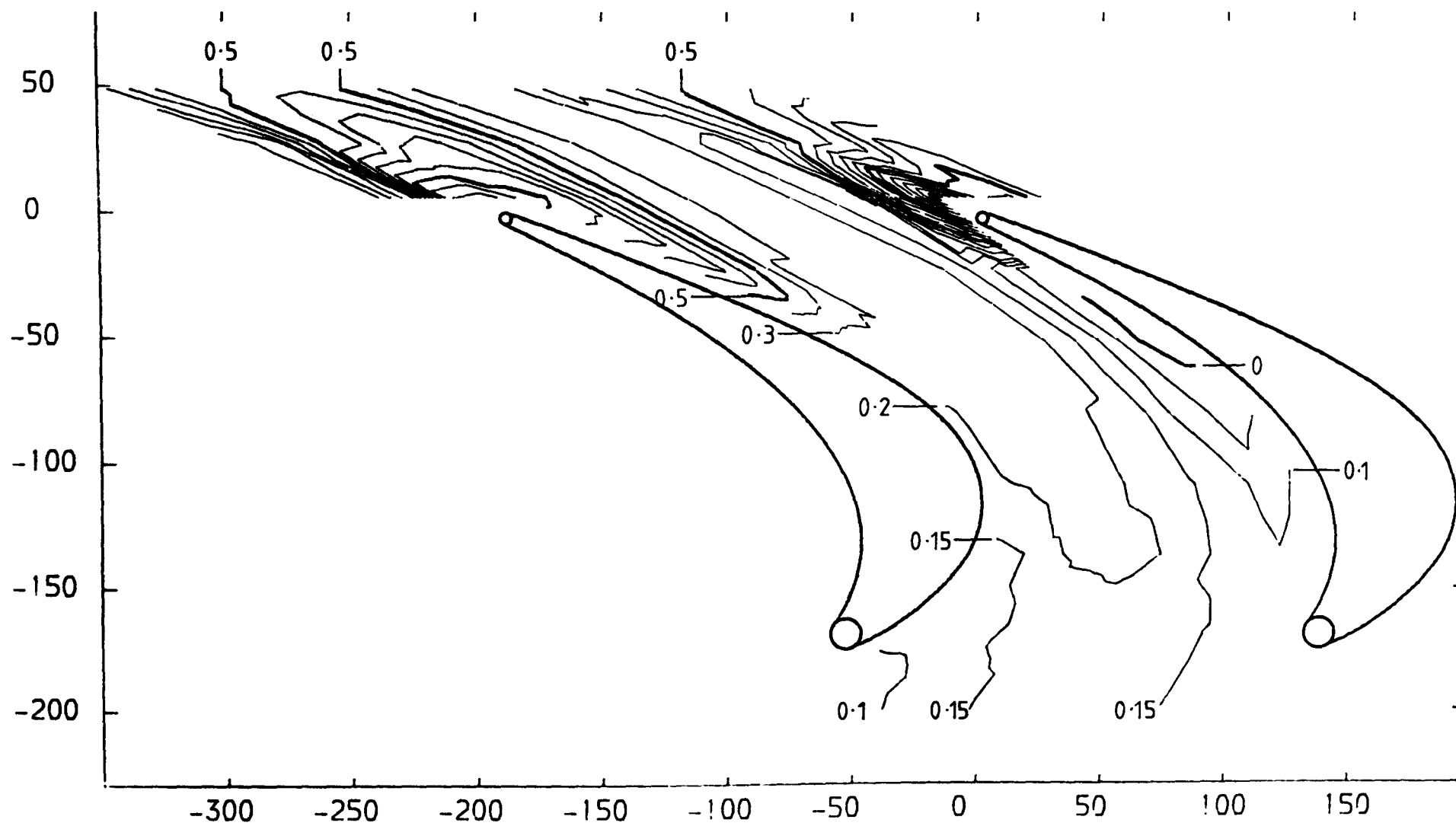


FIGURE 4.91

PLOT ON PLANE 80.0 MM FROM PERSPEX ENDWALL (5-HOLE PROBE DATA)  
TOTAL PRESSURE LOSS COEFFICIENT (  $(P_{01}-P_{0LOCAL}) / (P_{01}-P_1)$  ) CONTOURS  
X-AXIS TANGENTIAL CO-ORDINATE FROM TRAILING EDGE DATUM (MM)  
Y-AXIS AXIAL CO-ORDINATE FROM TRAILING EDGE DATUM (MM)

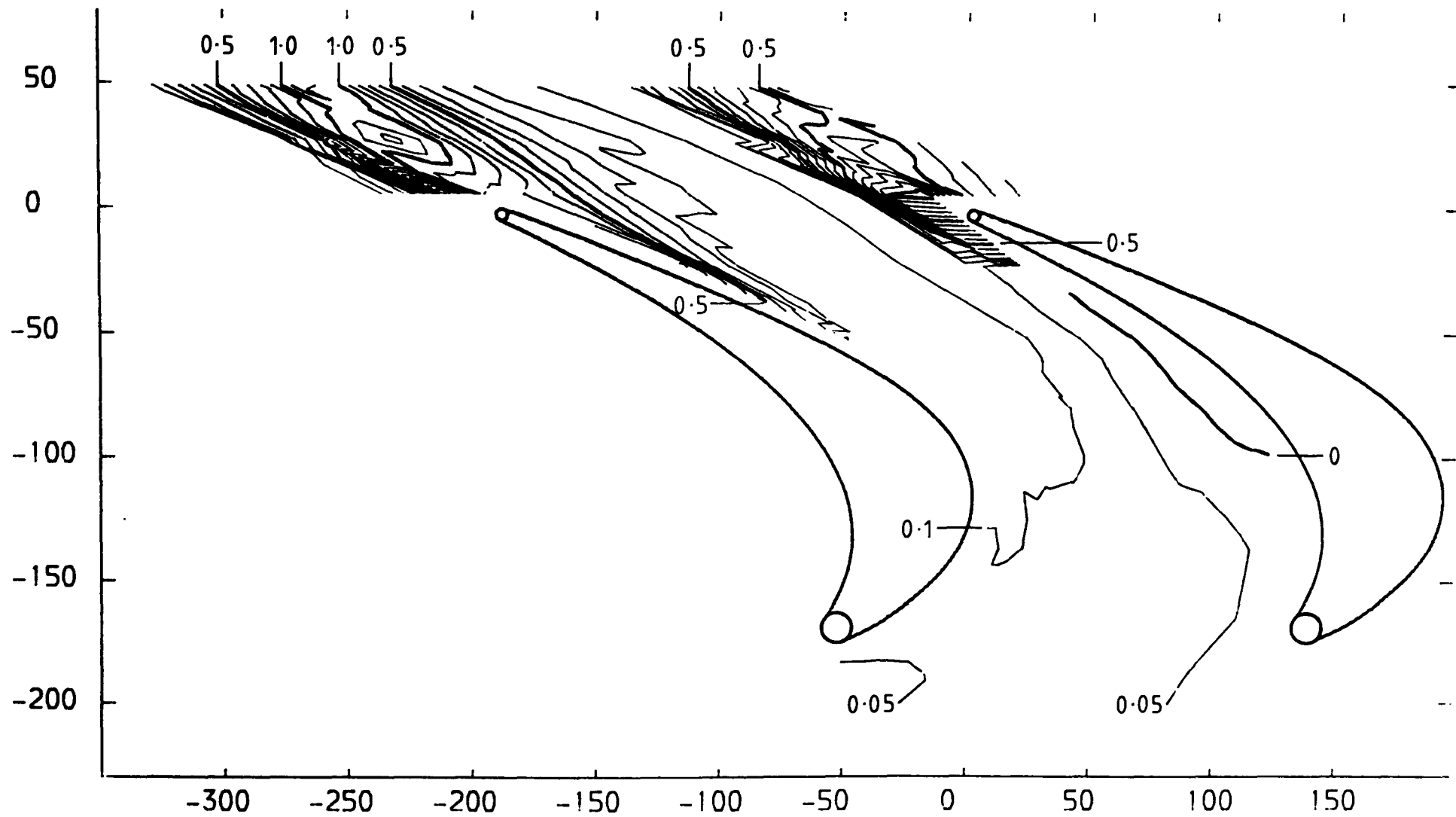


FIGURE 4.92

PLOT ON PLANE 100.1 MM FROM PERSPEX ENDWALL (5-HOLE PROBE DATA)  
TOTAL PRESSURE LOSS COEFFICIENT (  $(P_{01}-P_{0LOCAL}) / (P_{01}-P_1)$  ) CONTOURS  
X-AXIS TANGENTIAL CO-ORDINATE FROM TRAILING EDGE DATUM (MM)  
Y-AXIS AXIAL CO-ORDINATE FROM TRAILING EDGE DATUM (MM)

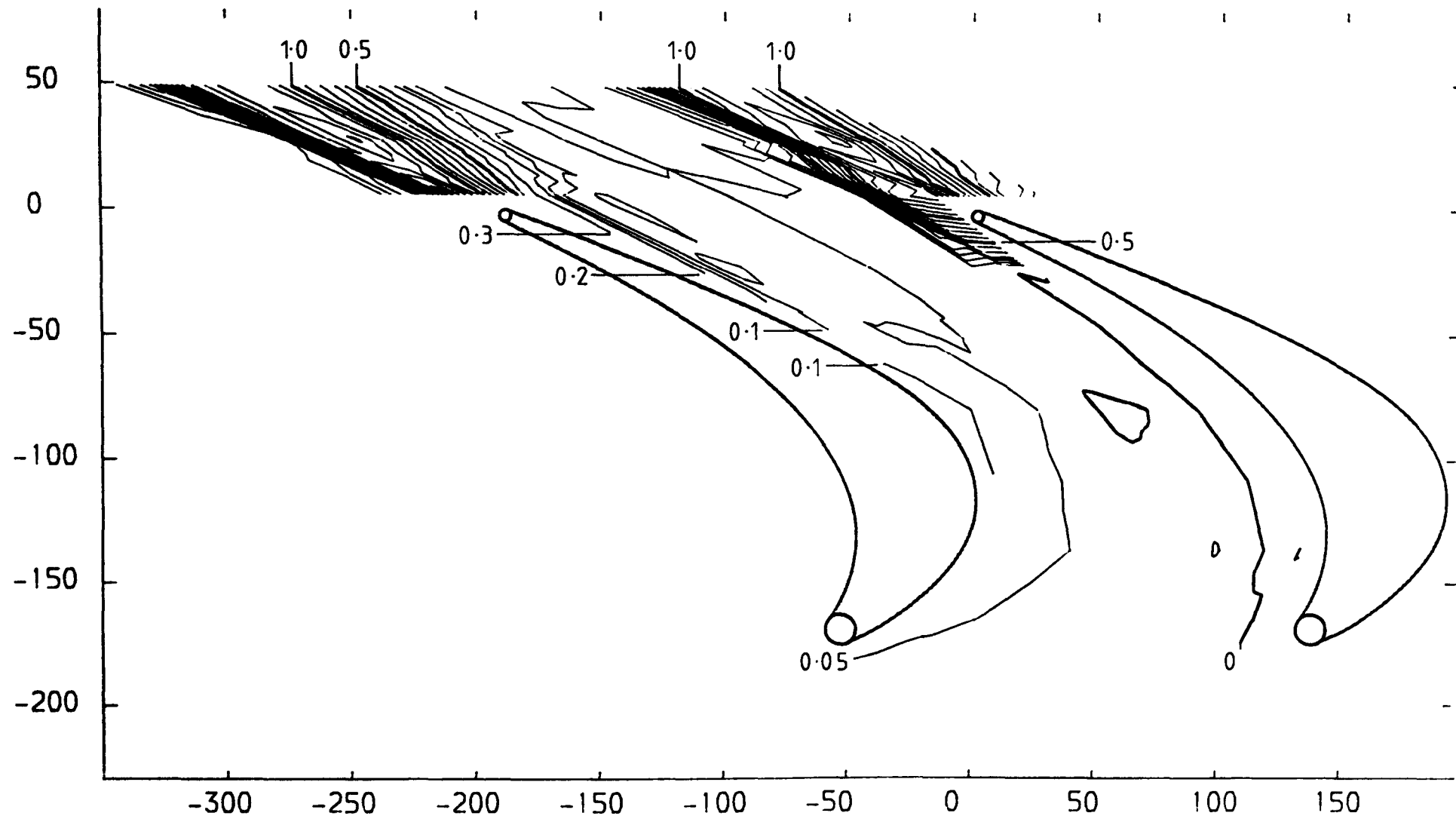


FIGURE 4.93

PLOT ON PLANE 140.1 MM FROM PERSPEX ENDWALL (5-HOLE PROBE DATA)  
TOTAL PRESSURE LOSS COEFFICIENT (  $(P_{01}-P_{0LOCAL}) / (P_{01}-P_1)$  ) CONTOURS  
X-AXIS TANGENTIAL CO-ORDINATE FROM TRAILING EDGE DATUM (MM)  
Y-AXIS AXIAL CO-ORDINATE FROM TRAILING EDGE DATUM (MM)

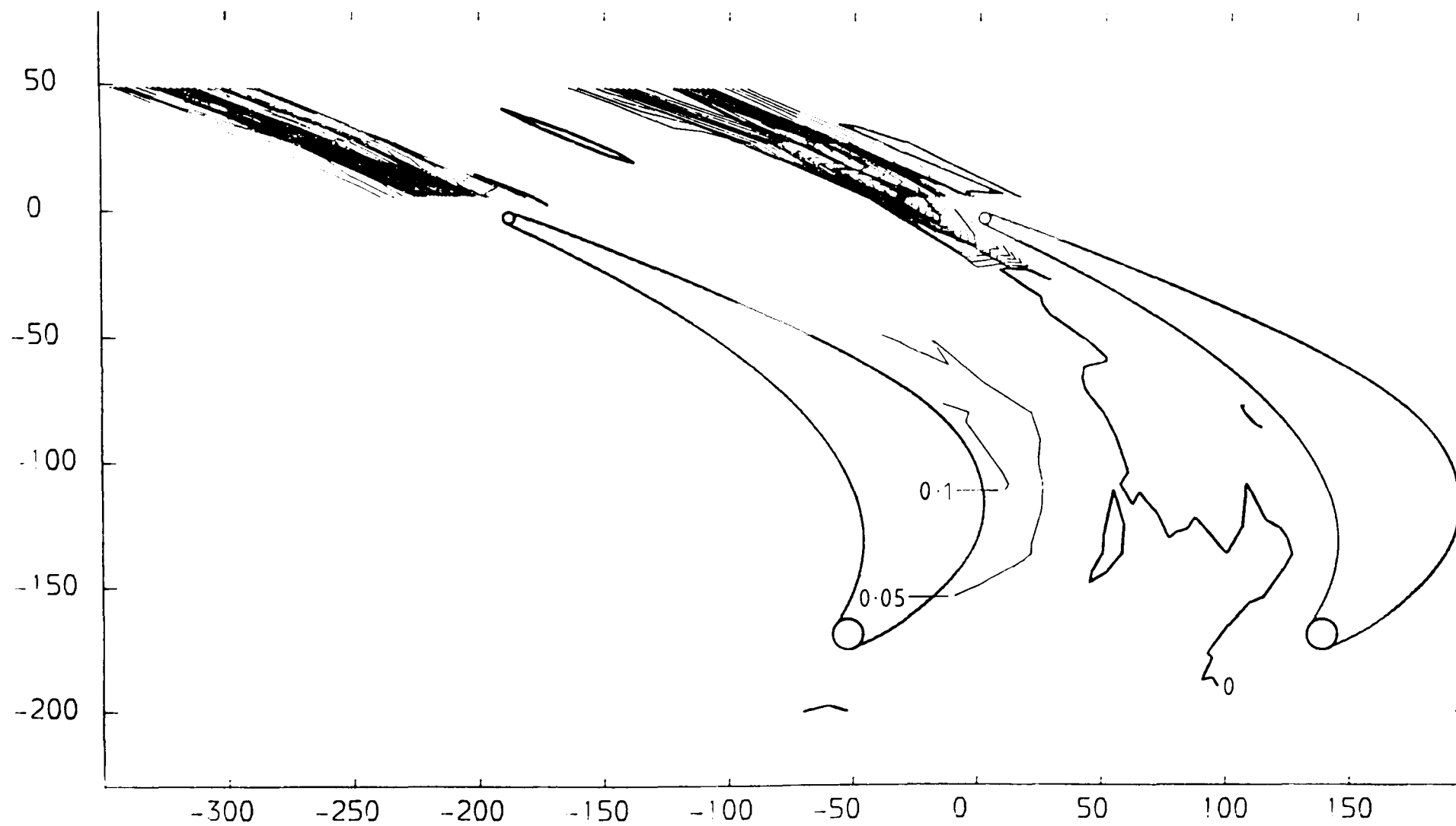


FIGURE 4.94

PLOT ON PLANE 220.1 MM FROM PERSPEX ENDWALL (5-HOLE PROBE DATA)  
TOTAL PRESSURE LOSS COEFFICIENT (  $(P_{01}-P_{0LOCAL}) / (P_{01}-P_1)$  ) CONTOURS  
X-AXIS TANGENTIAL CO-ORDINATE FROM TRAILING EDGE DATUM (MM)  
Y-AXIS AXIAL CO-ORDINATE FROM TRAILING EDGE DATUM (MM)

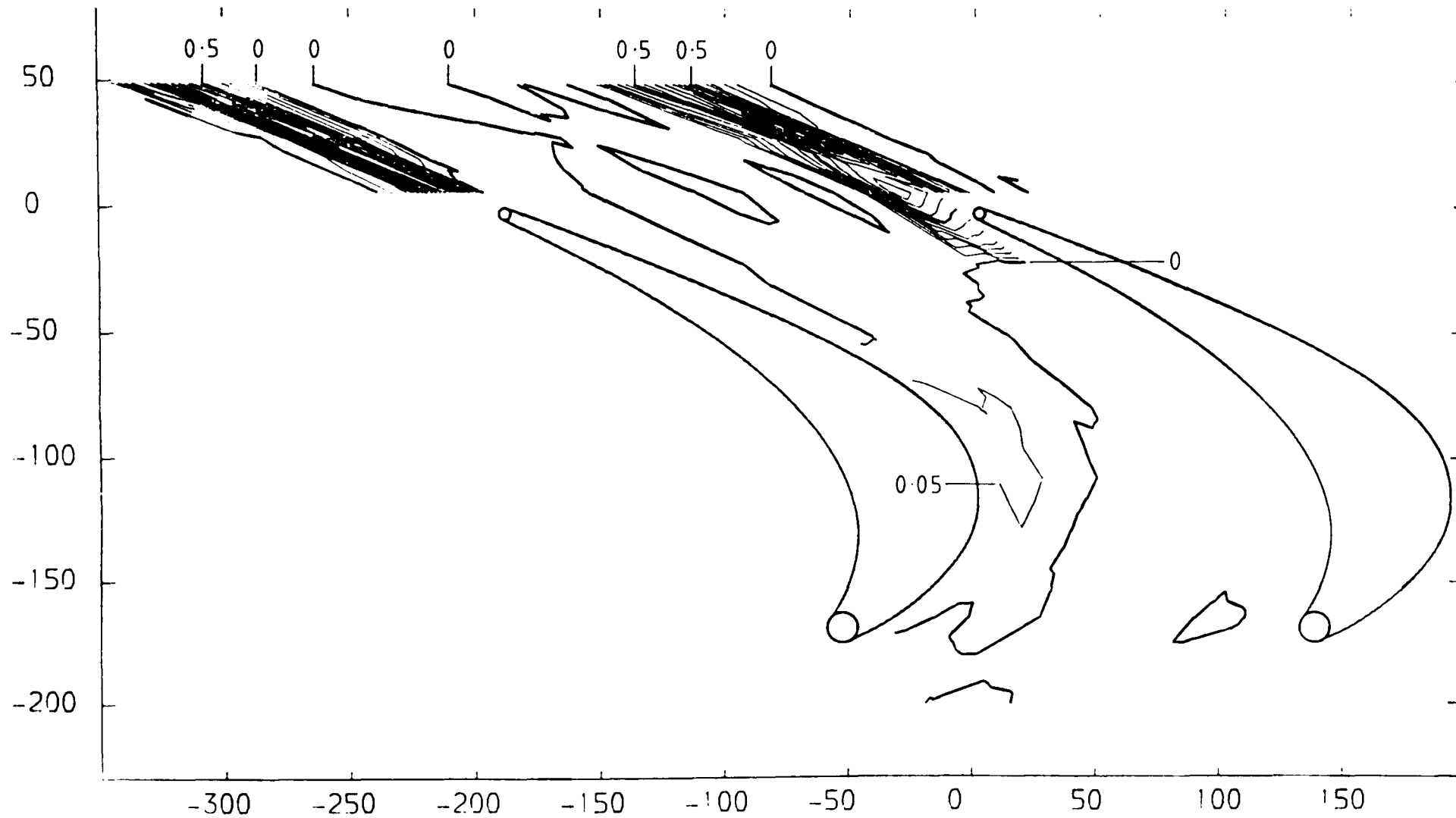


FIGURE 4.95

PLOT ON PLANE 1.0 MM FROM PERSPEX ENDWALL (3-HOLE PROBE DATA)  
TOTAL VELOCITY MAGNITUDE CONTOURS (CONTOUR UNITS METRES/SEC)  
X-AXIS TANGENTIAL CO-ORDINATE FROM TRAILING EDGE DATUM (MM)  
Y-AXIS AXIAL CO-ORDINATE FROM TRAILING EDGE DATUM (MM)

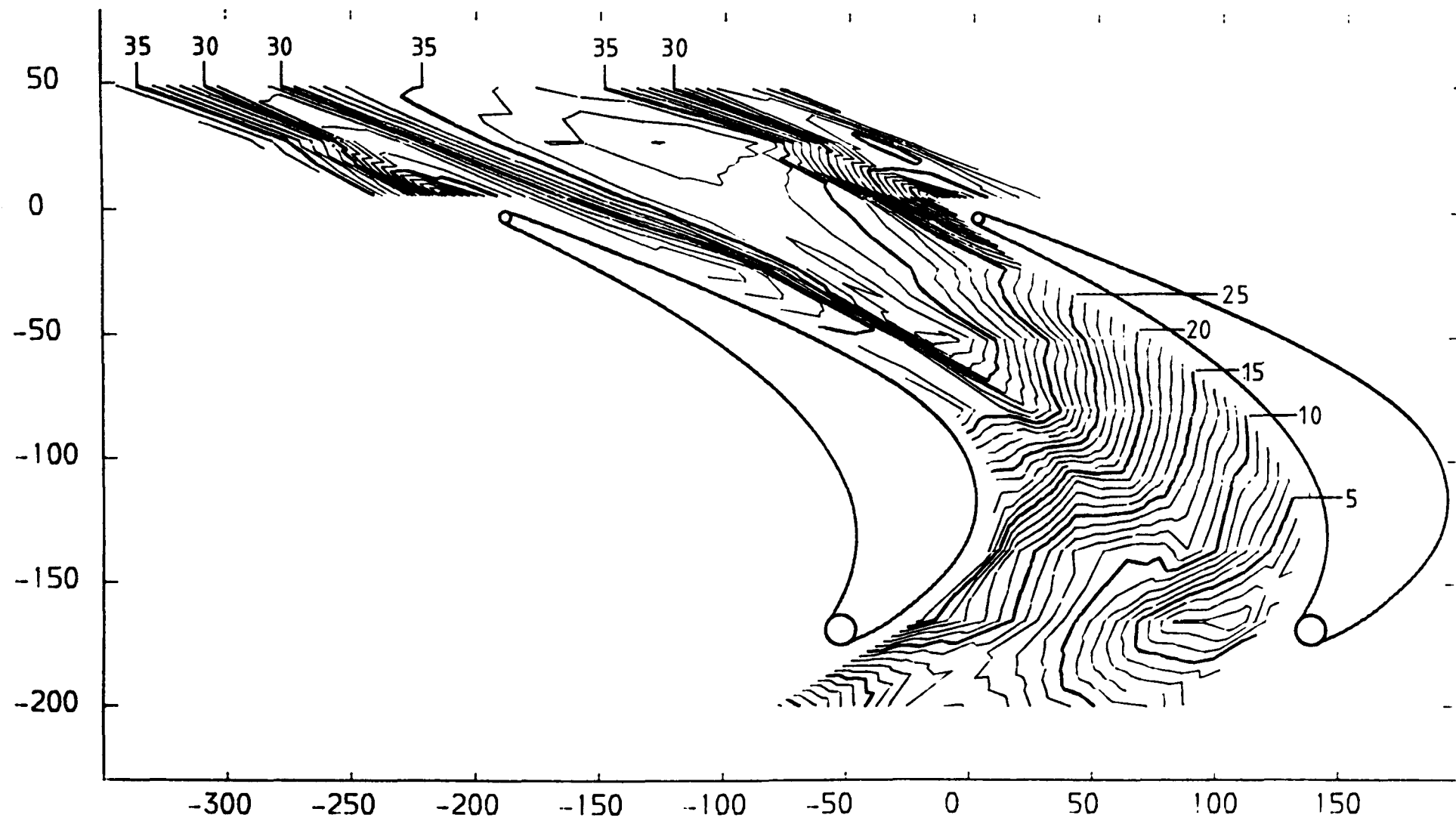


FIGURE 4.96



PLOT ON PLANE 20.1 MM FROM PERSPEX ENDWALL (5-HOLE PROBE DATA)  
TOTAL VELOCITY MAGNITUDE CONTOURS (CONTOUR UNITS METRES/SEC)  
X-AXIS TANGENTIAL CO-ORDINATE FROM TRAILING EDGE DATUM (MM)  
Y-AXIS AXIAL CO-ORDINATE FROM TRAILING EDGE DATUM (MM)

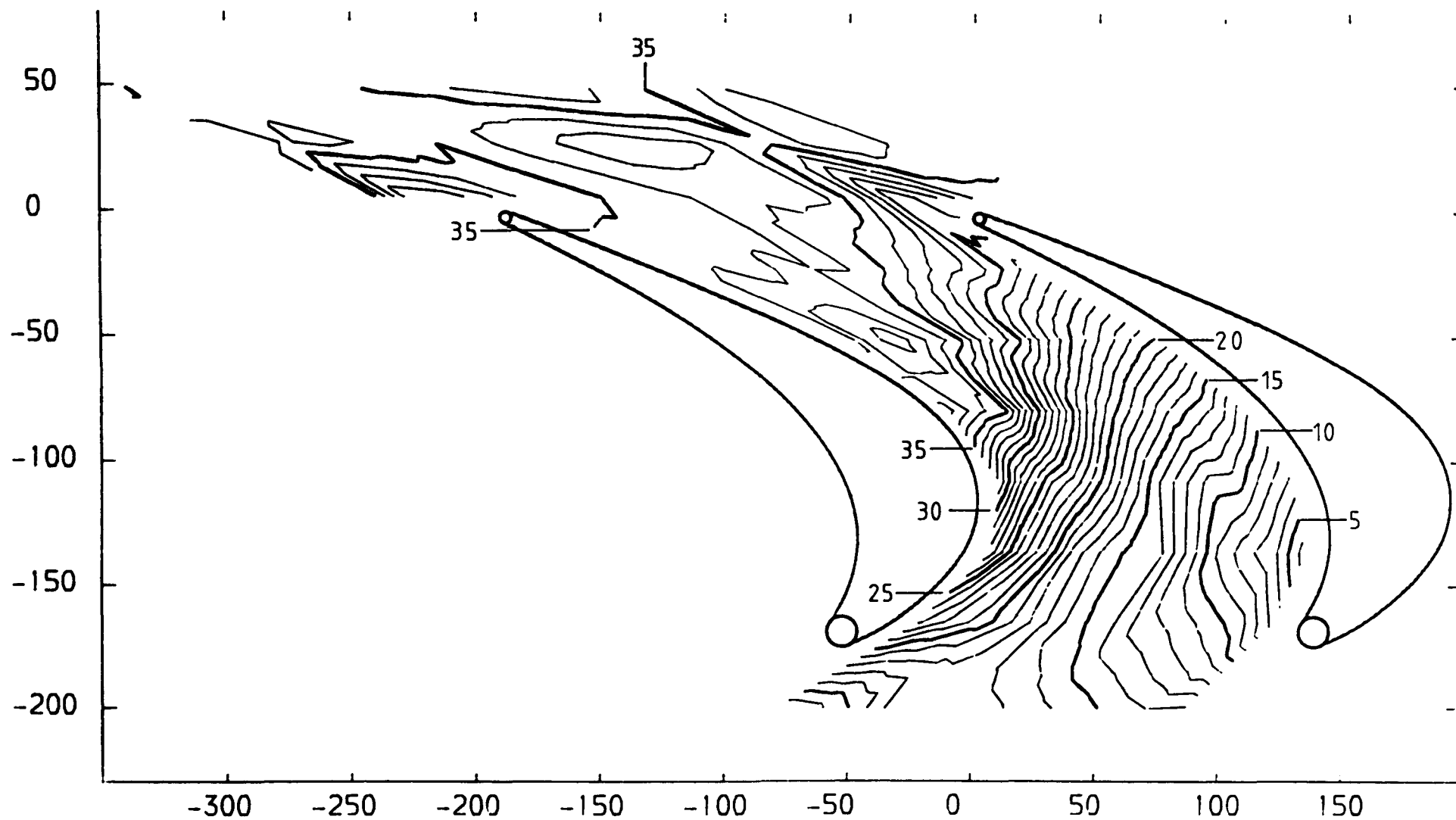


FIGURE 4.97

PLOT ON PLANE 20.1 MM FROM PERSPEX ENDWALL (3-HOLE PROBE DATA)  
TOTAL VELOCITY MAGNITUDE CONTOURS (CONTOUR UNITS METRES/SEC)  
X-AXIS TANGENTIAL CO-ORDINATE FROM TRAILING EDGE DATUM (MM)  
Y-AXIS AXIAL CO-ORDINATE FROM TRAILING EDGE DATUM (MM)

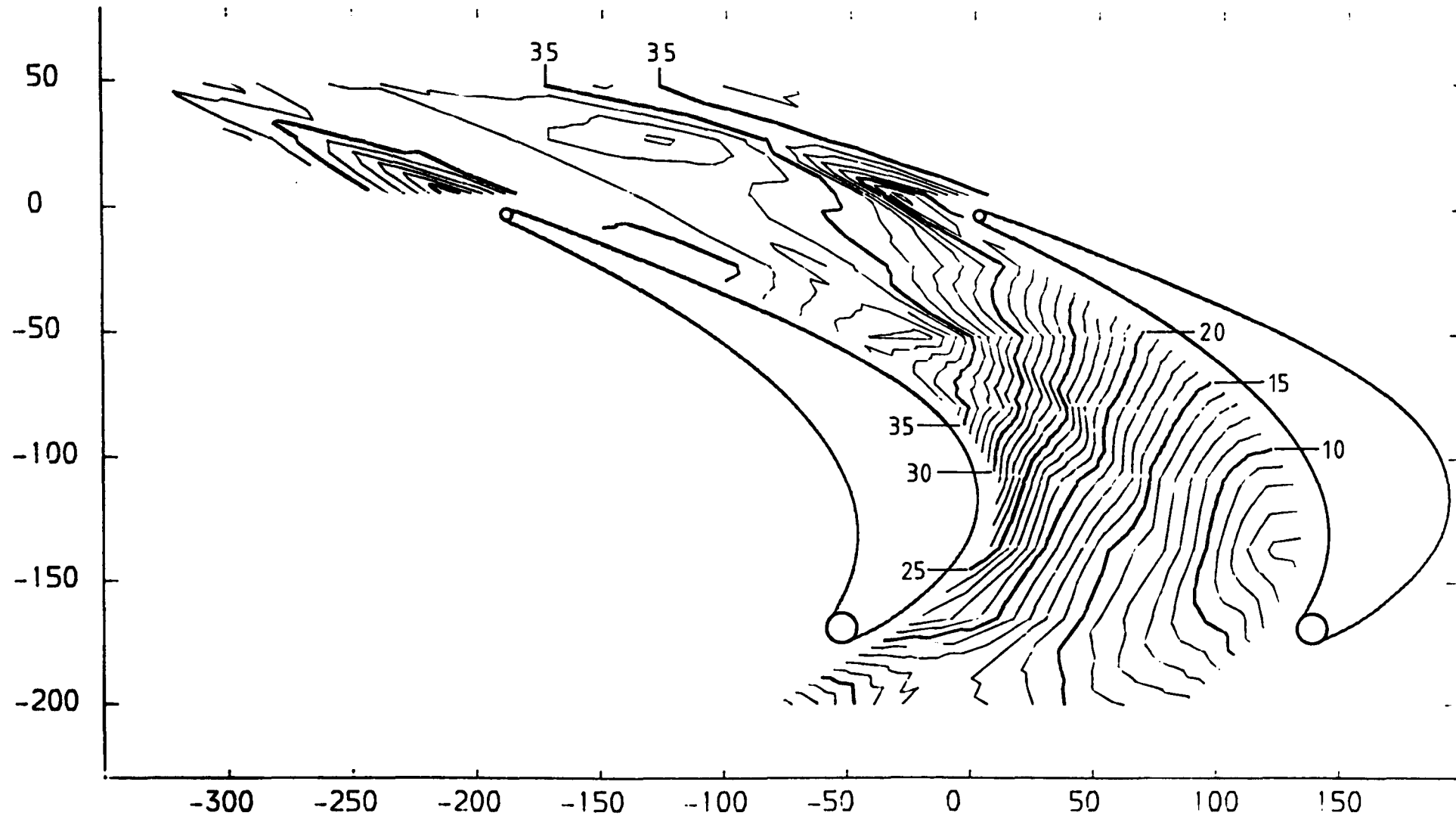


FIGURE 4.98

PLOT ON PLANE 50.1 MM FROM PERSPEX ENDWALL (5-HOLE PROBE DATA)  
TOTAL VELOCITY MAGNITUDE CONTOURS (CONTOUR UNITS METRES/SEC)  
X-AXIS TANGENTIAL CO-ORDINATE FROM TRAILING EDGE DATUM (MM)  
Y-AXIS AXIAL CO-ORDINATE FROM TRAILING EDGE DATUM (MM)

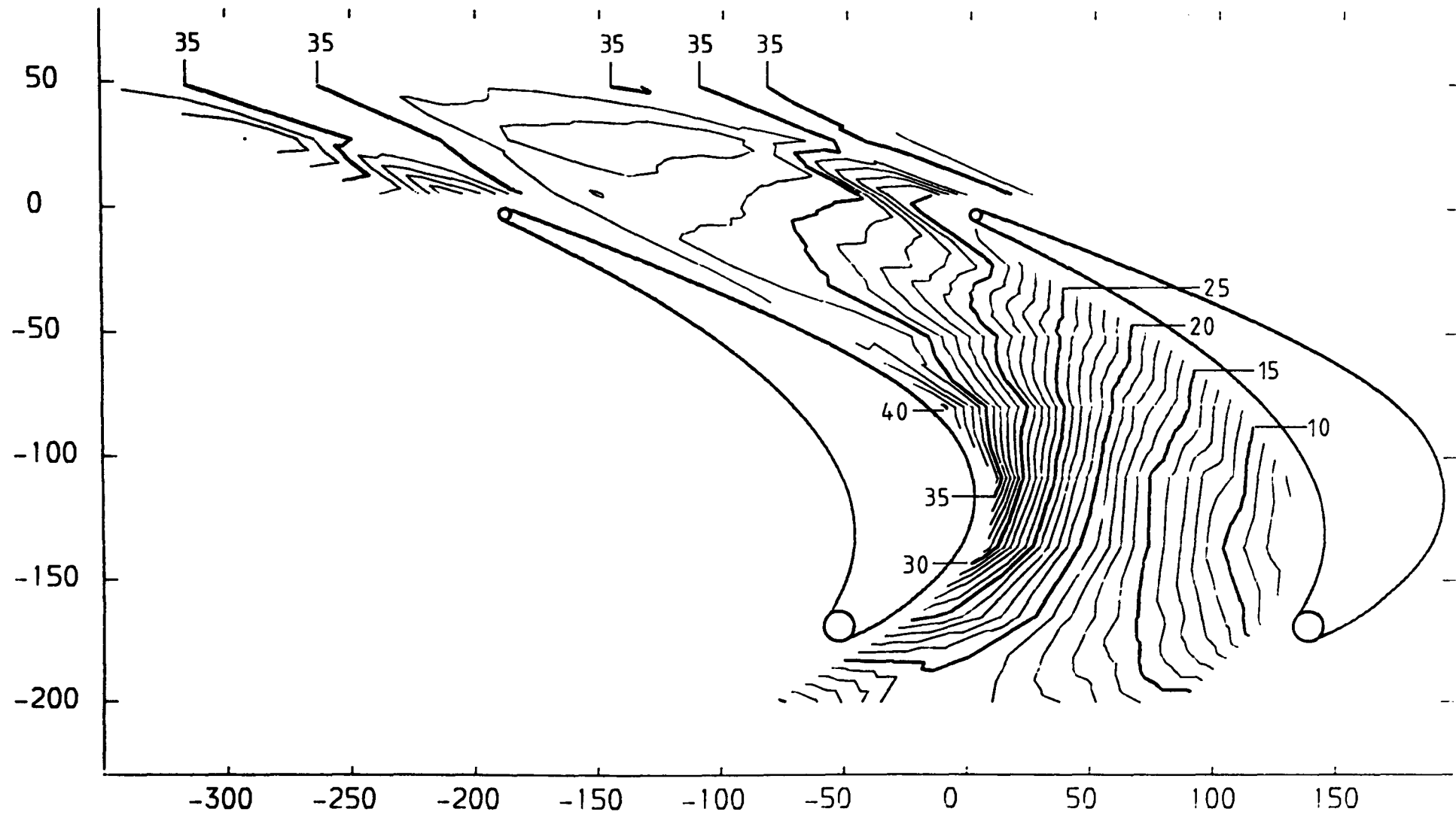


FIGURE 4.99

PLOT ON PLANE 220.1 MM FROM PERSPEX ENDWALL (5-HOLE PROBE DATA)  
TOTAL VELOCITY MAGNITUDE CONTOURS (CONTOUR UNITS METRES/SEC)  
X-AXIS TANGENTIAL CO-ORDINATE FROM TRAILING EDGE DATUM (MM)  
Y-AXIS AXIAL CO-ORDINATE FROM TRAILING EDGE DATUM (MM)

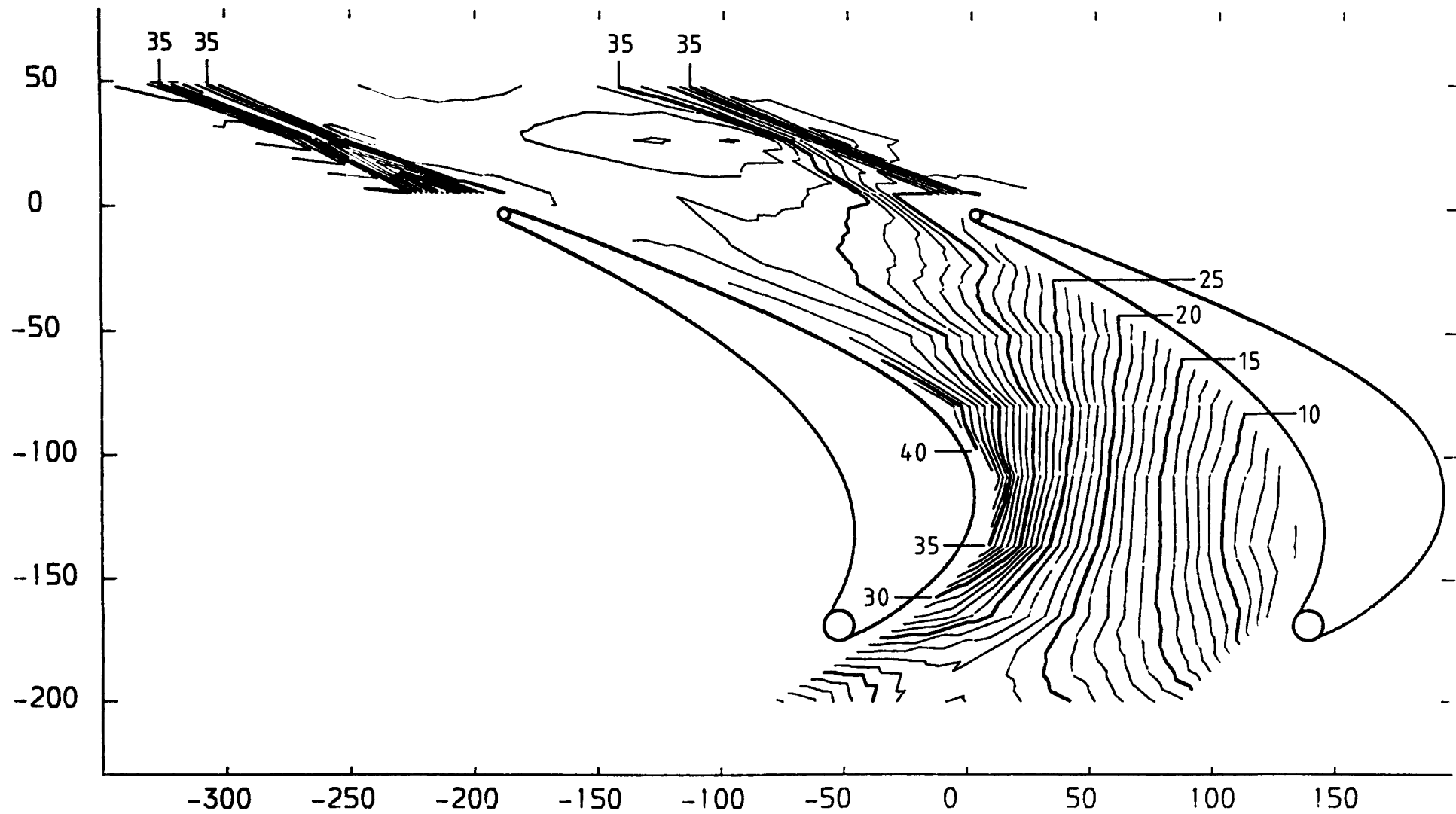


FIGURE 4.100

TWO DIMENSIONAL VELOCITY DISTRIBUTION  
PREDICTED VALUES (CONTOUR UNITS METRES/SEC)

X-AXIS AXIAL CO-ORDINATE FROM TRAILING EDGE DATUM (MM)  
Y-AXIS SPANWISE CO-ORDINATE FROM PERSPEX ENDWALL (MM)

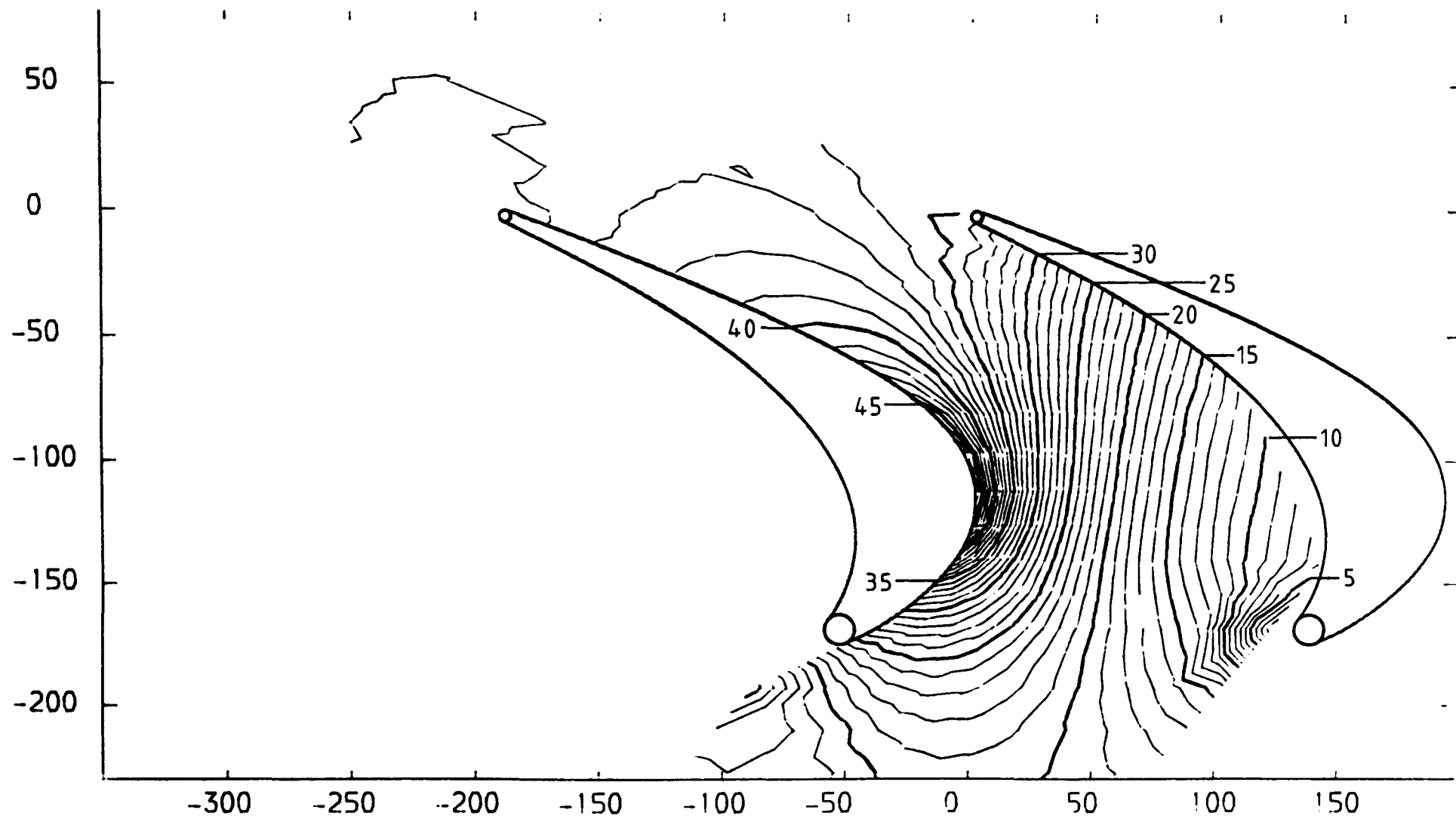


FIGURE 4.101

PLOT ON PLANE 1.0 MM FROM PERSPEX ENDWALL (3-HOLE PROBE DATA)

VECTOR PLOT OF AXIAL AND TANGENTIAL VELOCITIES

X-AXIS TANGENTIAL CO-ORDINATE FROM TRAILING EDGE DATUM (MM)

Y-AXIS AXIAL CO-ORDINATE FROM TRAILING EDGE DATUM (MM)

VECTOR SCALE 40 METRES/SEC  $\longrightarrow$

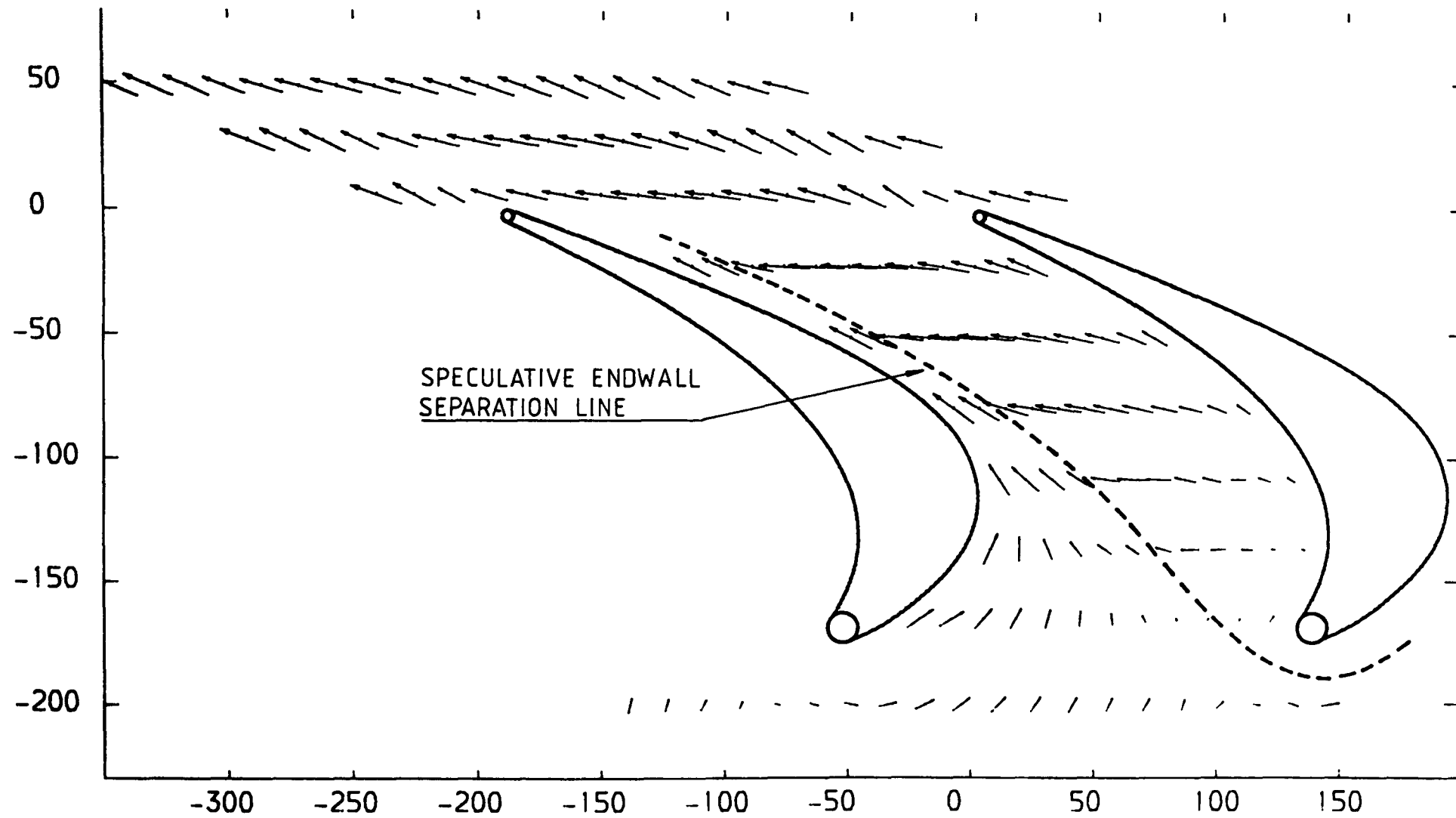


FIGURE 4.102

PLOT ON PLANE 2.0 MM FROM PERSPEX ENDWALL (3-HOLE PROBE DATA)  
VECTOR PLOT OF AXIAL AND TANGENTIAL VELOCITIES  
X-AXIS TANGENTIAL CO-ORDINATE FROM TRAILING EDGE DATUM (MM)  
Y-AXIS AXIAL CO-ORDINATE FROM TRAILING EDGE DATUM (MM)  
VECTOR SCALE 40 METRES/SEC →

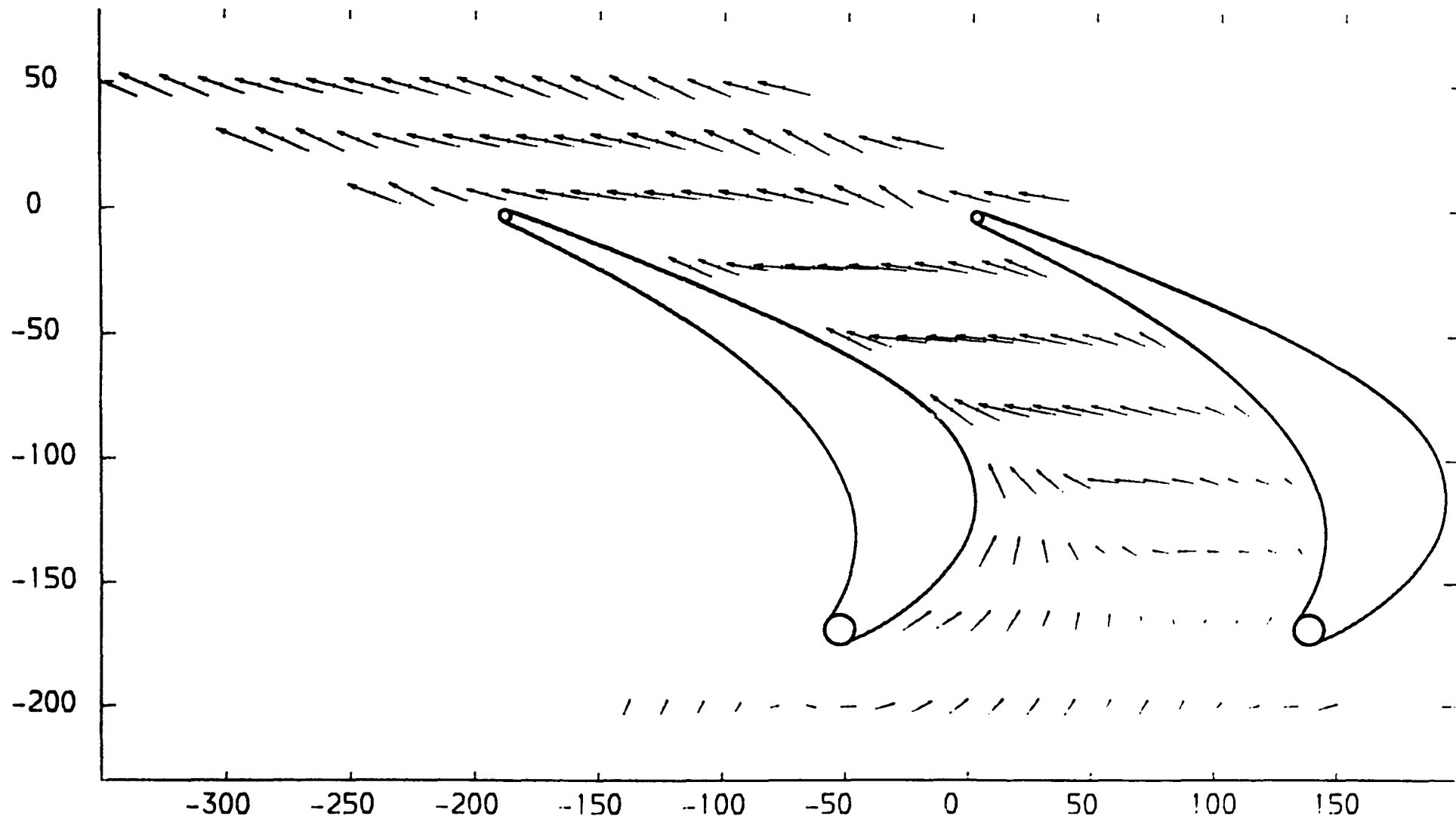


FIGURE 4.103

PLOT ON PLANE 3.0 MM FROM PERSPEX ENDWALL (3-HOLE PROBE DATA)  
VECTOR PLOT OF AXIAL AND TANGENTIAL VELOCITIES  
X-AXIS TANGENTIAL CO-ORDINATE FROM TRAILING EDGE DATUM (MM)  
Y-AXIS AXIAL CO-ORDINATE FROM TRAILING EDGE DATUM (MM)  
VECTOR SCALE 40 METRES/SEC  $\longrightarrow$

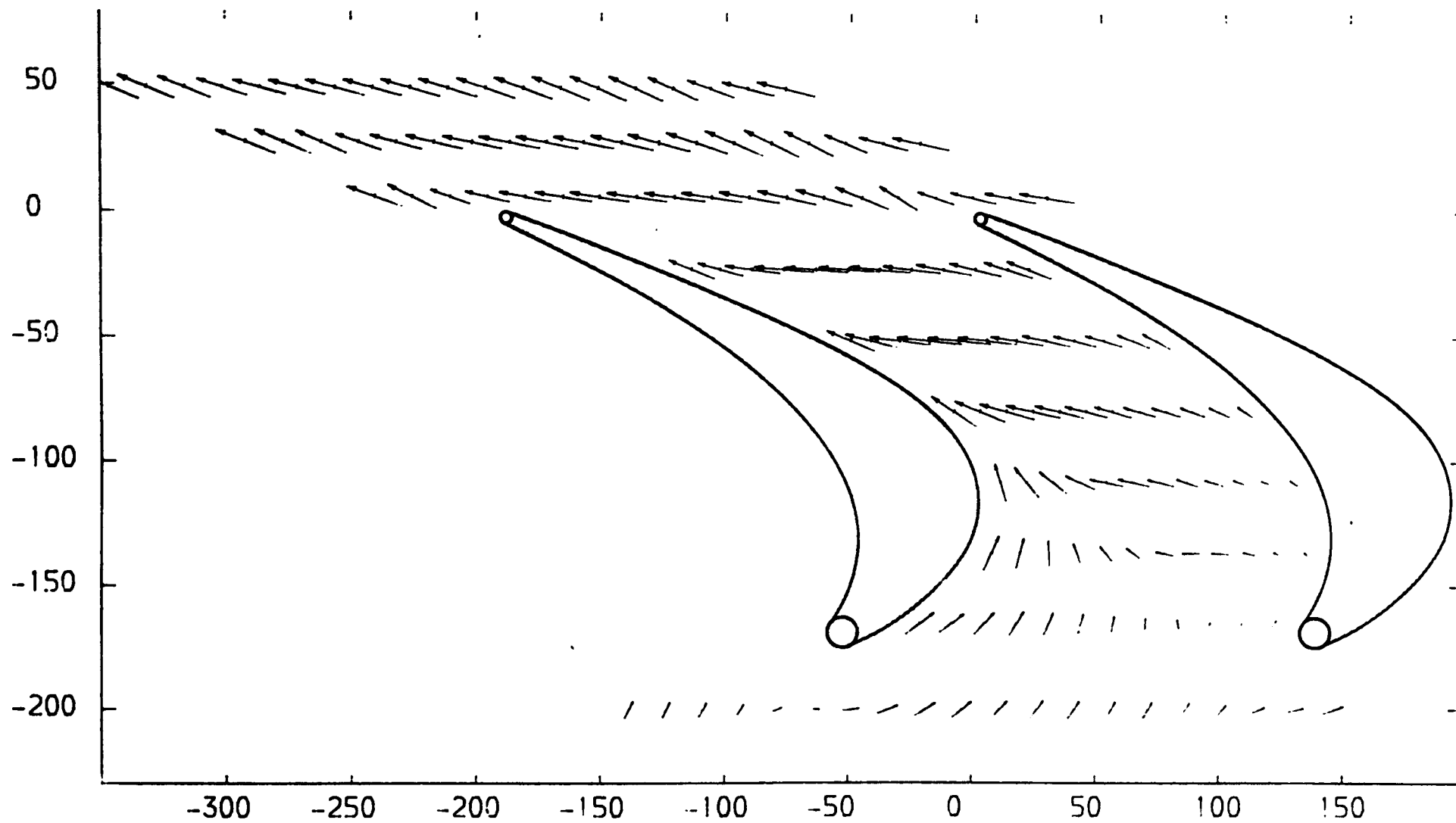


FIGURE 4.104



PLOT ON PLANE 4.0 MM FROM PERSPEX ENDWALL (3-HOLE PROBE DATA)  
VECTOR PLOT OF AXIAL AND TANGENTIAL VELOCITIES  
X-AXIS TANGENTIAL CO-ORDINATE FROM TRAILING EDGE DATUM (MM)  
Y-AXIS AXIAL CO-ORDINATE FROM TRAILING EDGE DATUM (MM)  
VECTOR SCALE 40 METRES/SEC  $\longrightarrow$

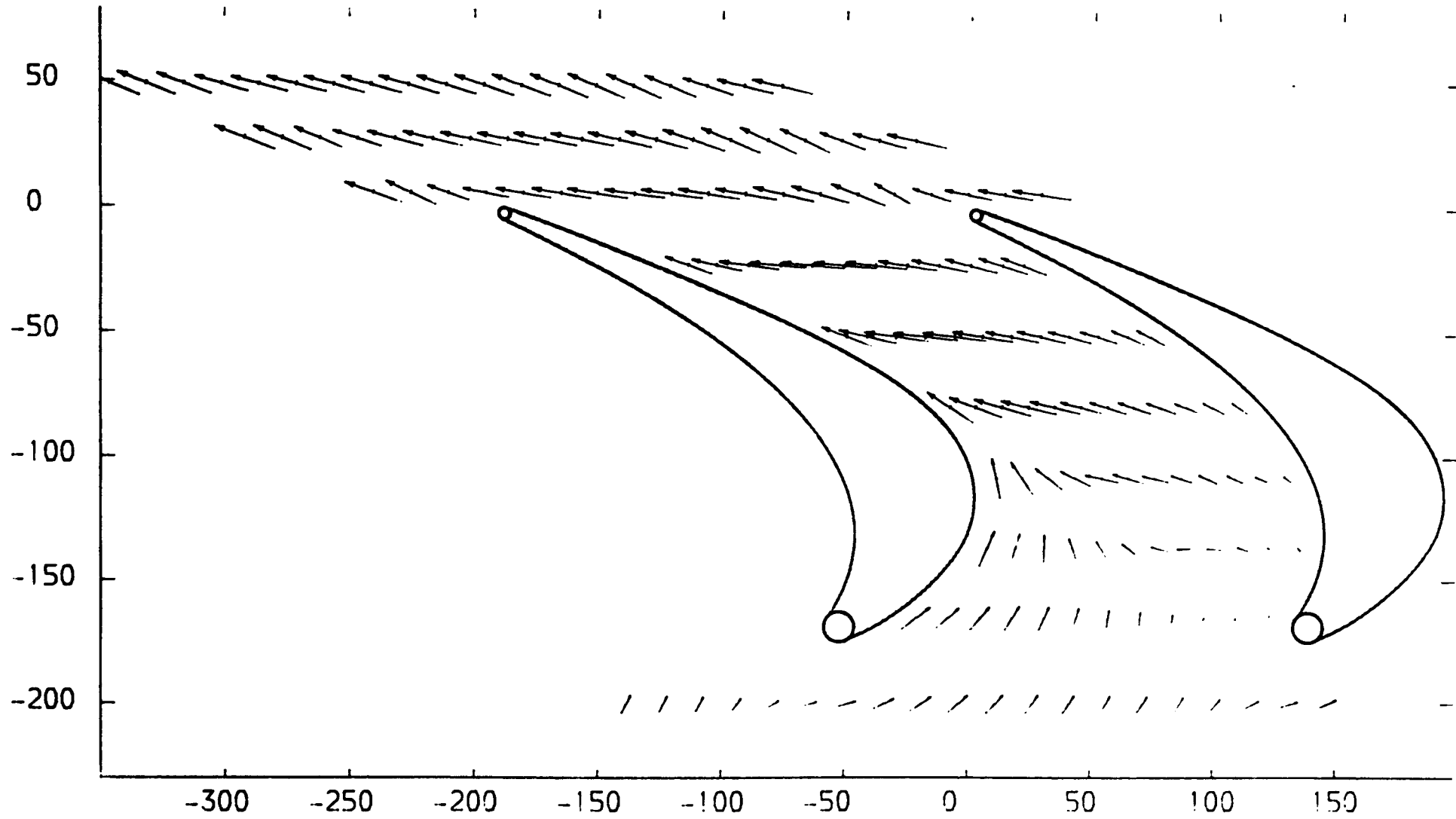


FIGURE 4.105

PLOT ON PLANE 5.0 MM FROM PERSPEX ENDWALL (3-HOLE PROBE DATA)  
VECTOR PLOT OF AXIAL AND TANGENTIAL VELOCITIES  
X-AXIS TANGENTIAL CO-ORDINATE FROM TRAILING EDGE DATUM (MM)  
Y-AXIS AXIAL CO-ORDINATE FROM TRAILING EDGE DATUM (MM)  
VECTOR SCALE 40 METRES/SEC  $\longrightarrow$

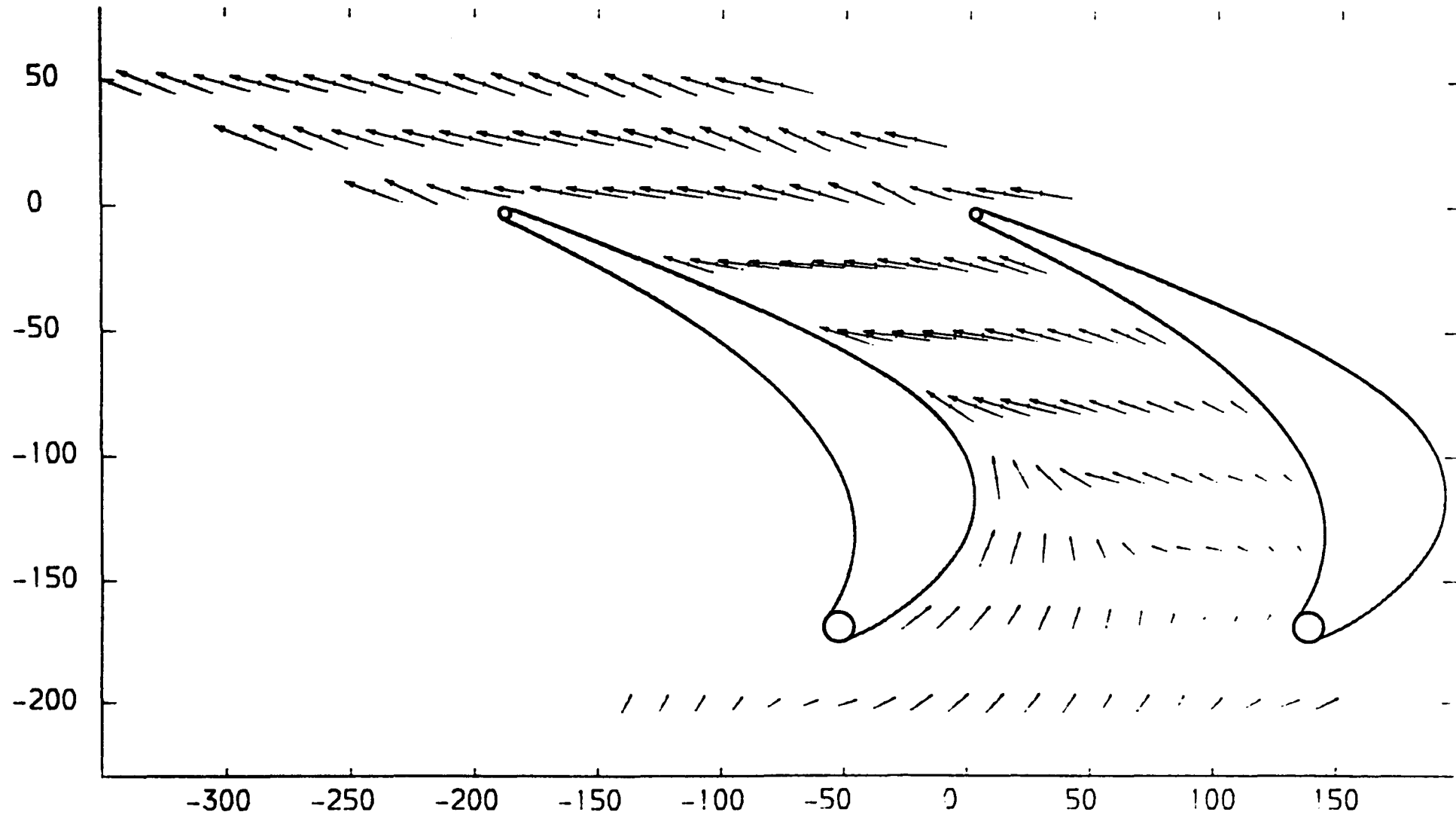


FIGURE 4.106

PLOT ON PLANE 7.4 MM FROM PERSPEX ENDWALL (3-HOLE PROBE DATA)  
VECTOR PLOT OF AXIAL AND TANGENTIAL VELOCITIES  
X-AXIS TANGENTIAL CO-ORDINATE FROM TRAILING EDGE DATUM (MM)  
Y-AXIS AXIAL CO-ORDINATE FROM TRAILING EDGE DATUM (MM)  
VECTOR SCALE 40 METRES/SEC  $\longrightarrow$

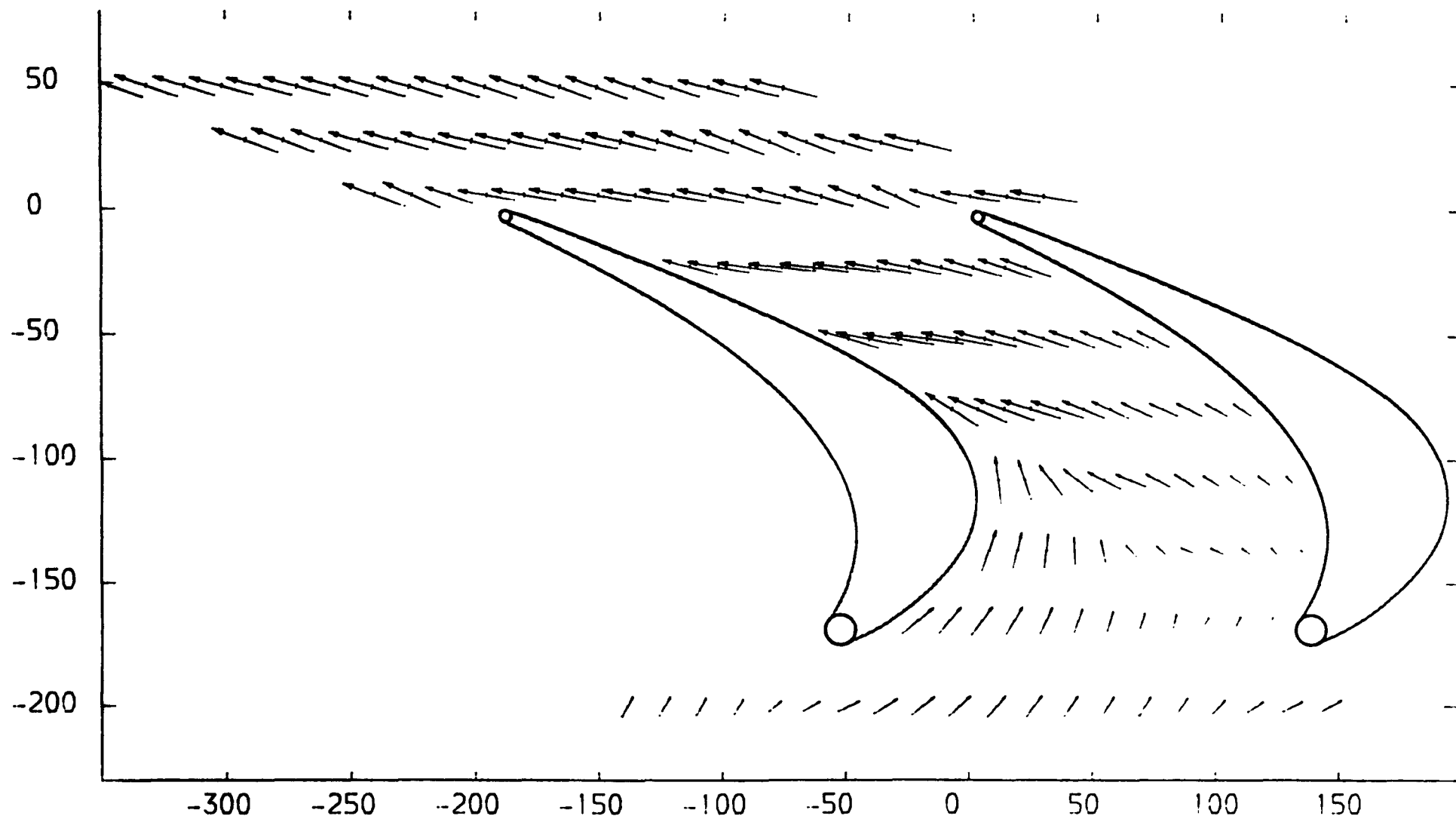


FIGURE 4.107

PLOT ON PLANE 15.0 MM FROM PERSPEX ENDWALL (5-HOLE PROBE DATA)  
VECTOR PLOT OF AXIAL AND TANGENTIAL VELOCITIES  
X-AXIS TANGENTIAL CO-ORDINATE FROM TRAILING EDGE DATUM (MM)  
Y-AXIS AXIAL CO-ORDINATE FROM TRAILING EDGE DATUM (MM)  
VECTOR SCALE 40 METRES/SEC →

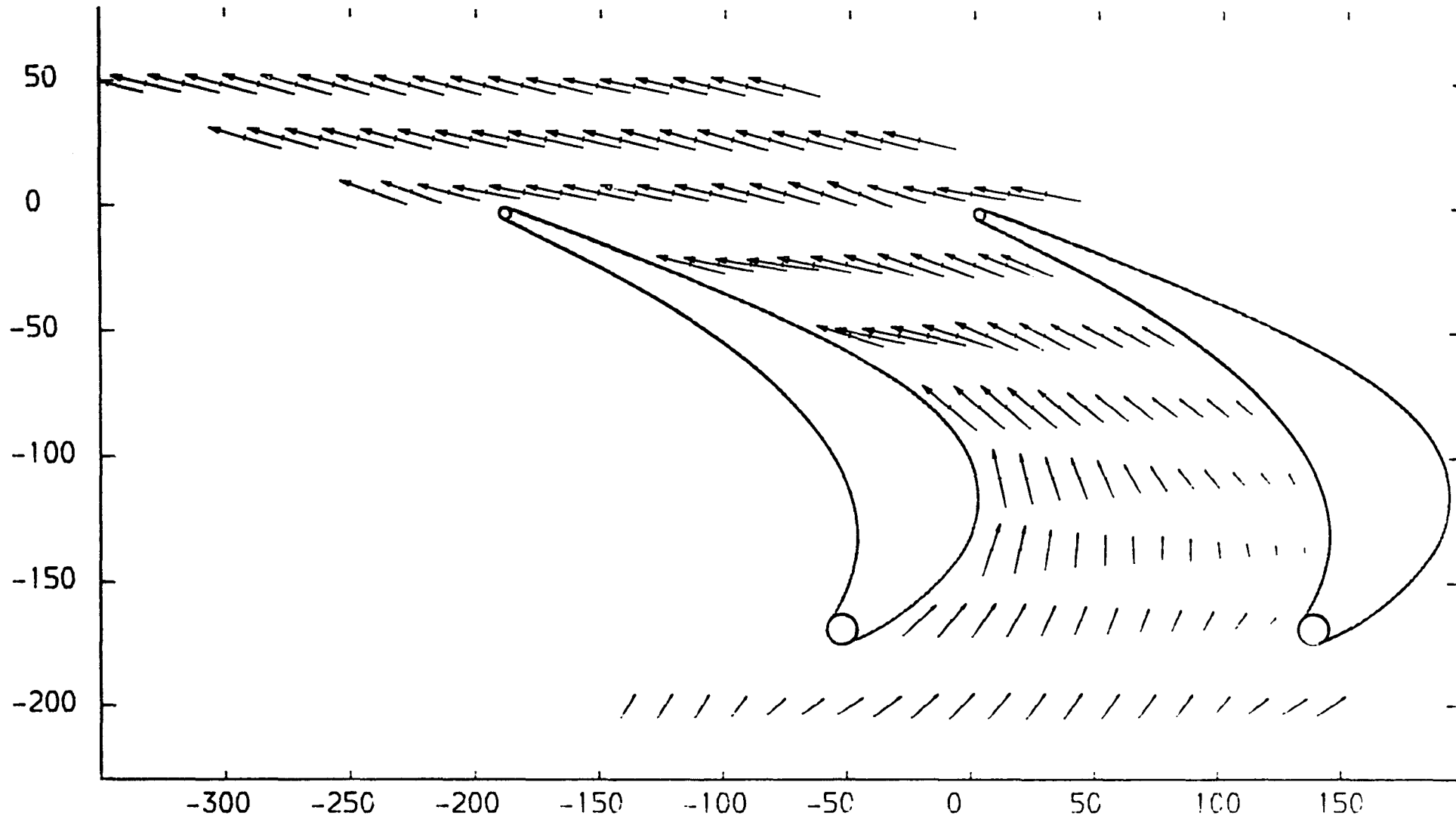


FIGURE 4.108

PLOT ON PLANE 40.0 MM FROM PERSPEX ENDWALL (5-HOLE PROBE DATA)  
VECTOR PLOT OF AXIAL AND TANGENTIAL VELOCITIES  
X-AXIS TANGENTIAL CO-ORDINATE FROM TRAILING EDGE DATUM (MM)  
Y-AXIS AXIAL CO-ORDINATE FROM TRAILING EDGE DATUM (MM)  
VECTOR SCALE 40 METRES/SEC  $\longrightarrow$

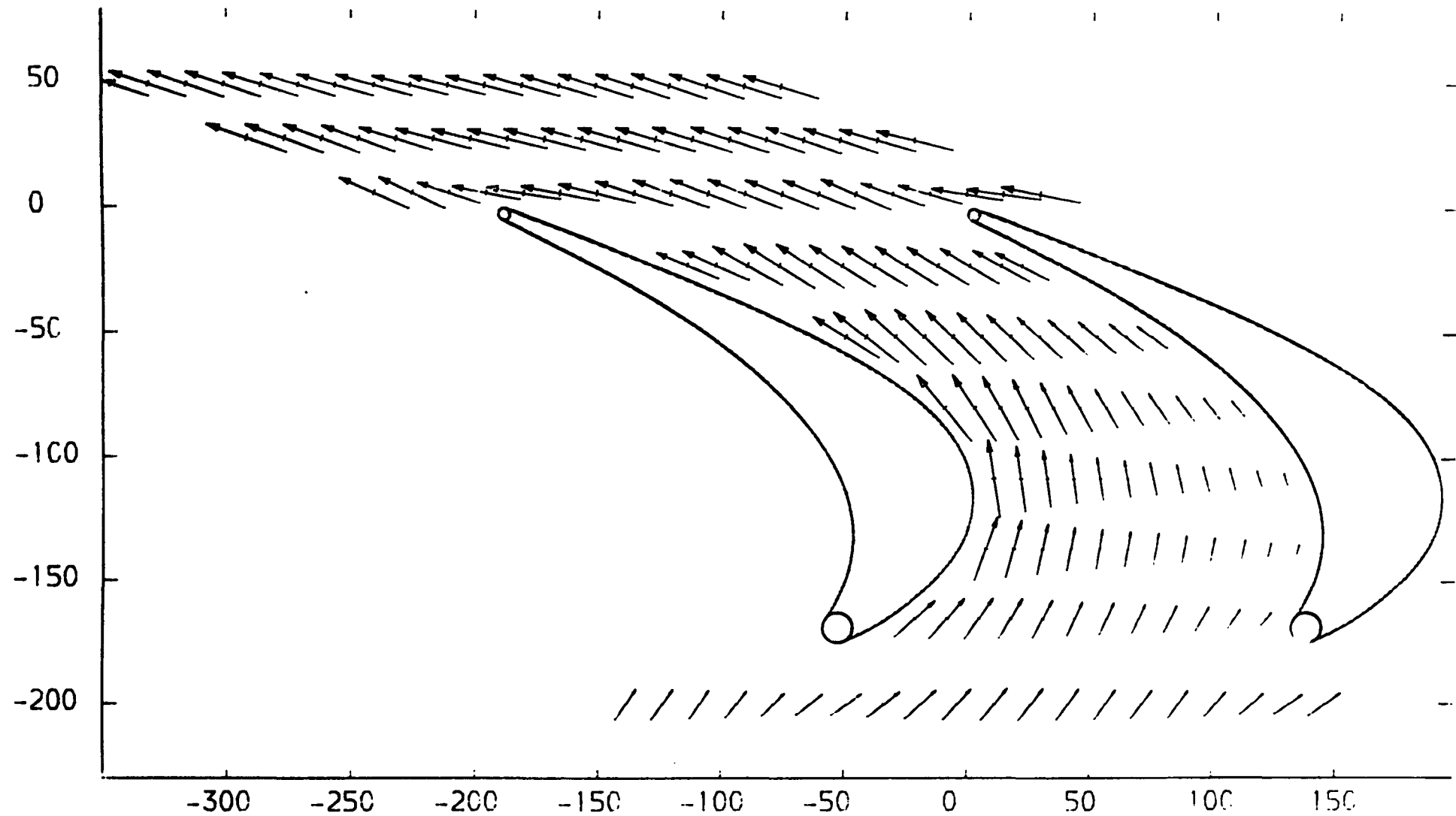


FIGURE 4.109

PLOT ON PLANE 60.0 MM FROM PERSPEX ENDWALL (5-HOLE PROBE DATA)  
VECTOR PLOT OF AXIAL AND TANGENTIAL VELOCITIES  
X-AXIS TANGENTIAL CO-ORDINATE FROM TRAILING EDGE DATUM (MM)  
Y-AXIS AXIAL CO-ORDINATE FROM TRAILING EDGE DATUM (MM)  
VECTOR SCALE 40 METRES/SEC  $\longrightarrow$

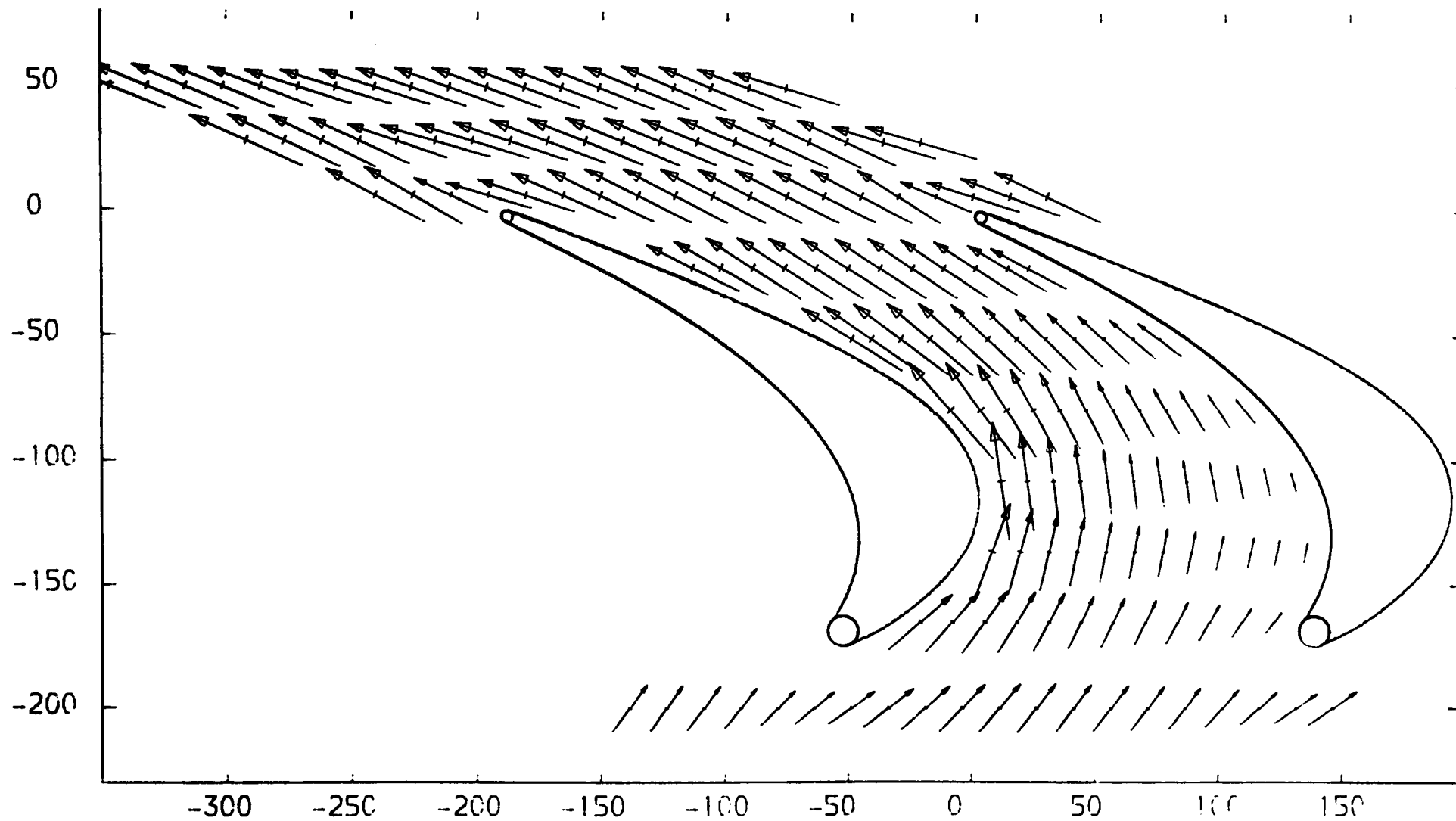


FIGURE 4.110

PLOT ON PLANE 100.1 MM FROM PERSPEX ENDWALL (5-HOLE PROBE DATA)  
VECTOR PLOT OF AXIAL AND TANGENTIAL VELOCITIES  
X-AXIS TANGENTIAL CO-ORDINATE FROM TRAILING EDGE DATUM (MM)  
Y-AXIS AXIAL CO-ORDINATE FROM TRAILING EDGE DATUM (MM)  
VECTOR SCALE 40 METRES/SEC  $\longrightarrow$

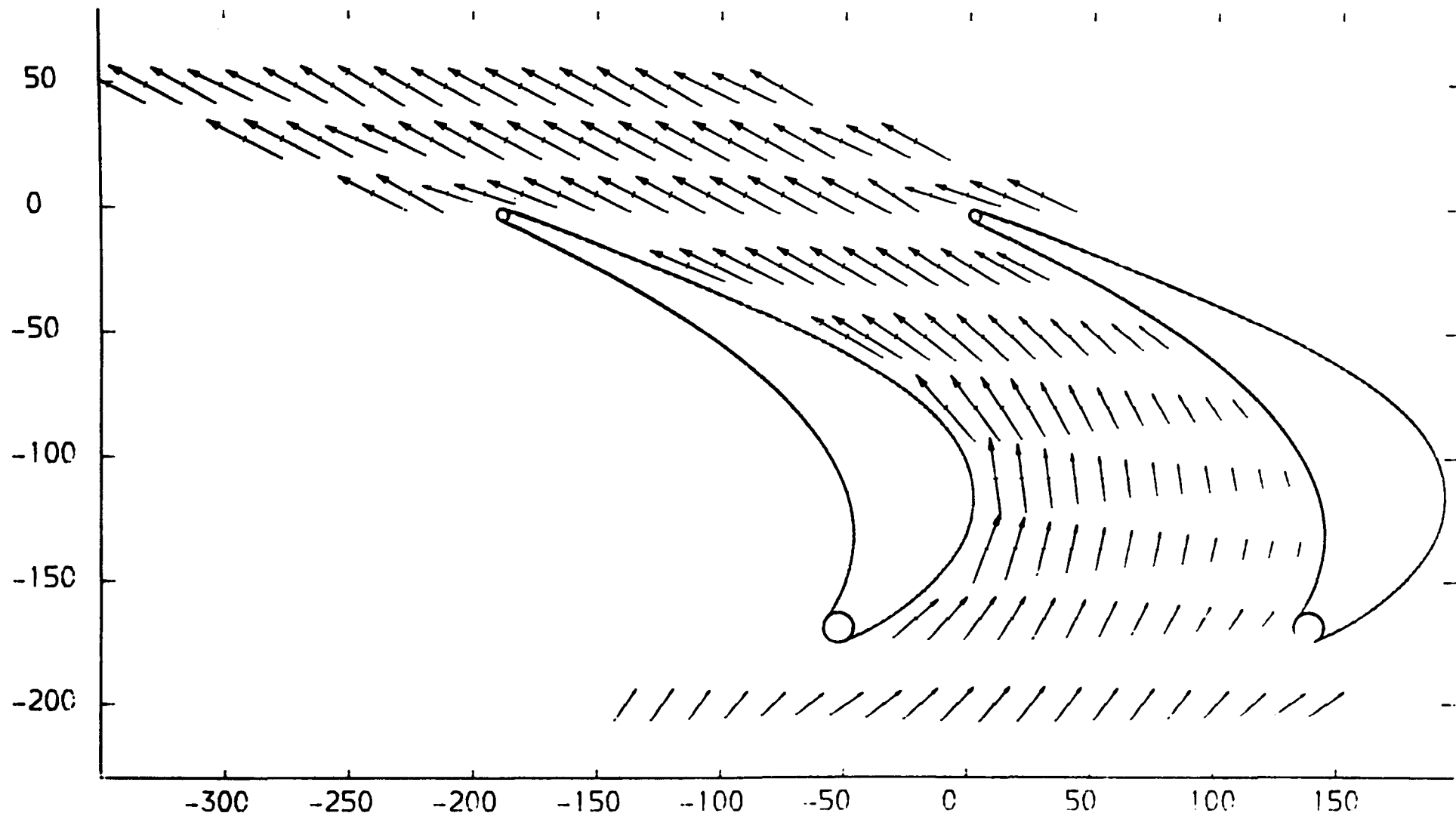


FIGURE 4.111

PLOT ON PLANE 220.1 MM FROM PERSPEX ENDWALL (5-HOLE PROBE DATA)

VECTOR PLOT OF AXIAL AND TANGENTIAL VELOCITIES

X-AXIS TANGENTIAL CO-ORDINATE FROM TRAILING EDGE DATUM (MM)

Y-AXIS AXIAL CO-ORDINATE FROM TRAILING EDGE DATUM (MM)

VECTOR SCALE 40 METRES/SEC  $\longrightarrow$

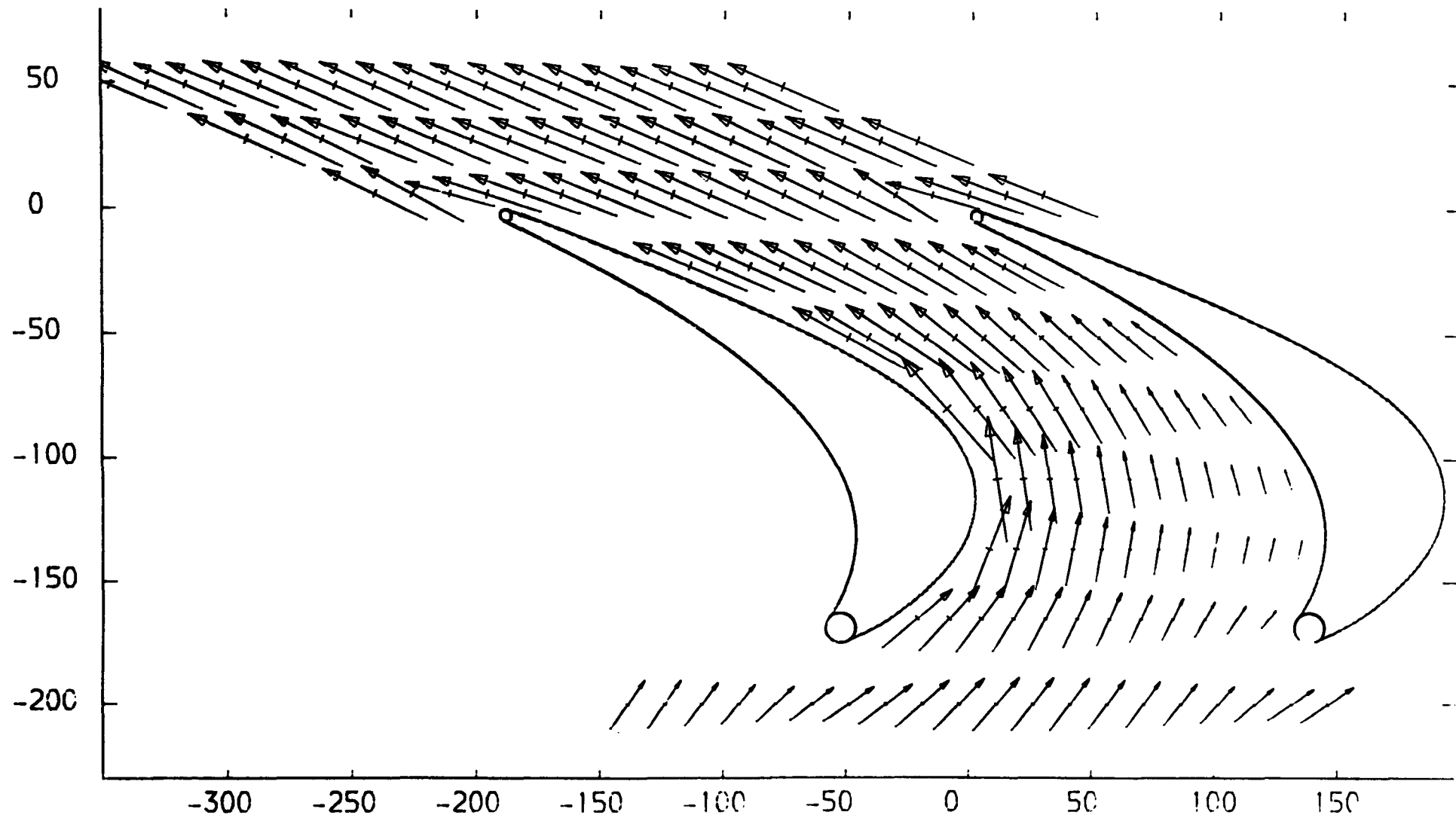


FIGURE 4.112



PLOT ON PLANE 20.1 MM FROM PERSPEX ENDWALL (5-HOLE PROBE DATA)  
SPANWISE ANGLE (PITCH ANGLE) CONTOURS (CONTOUR UNITS DEGREES)  
X-AXIS TANGENTIAL CO-ORDINATE FROM TRAILING EDGE DATUM (MM)  
Y-AXIS AXIAL CO-ORDINATE FROM TRAILING EDGE DATUM (MM)

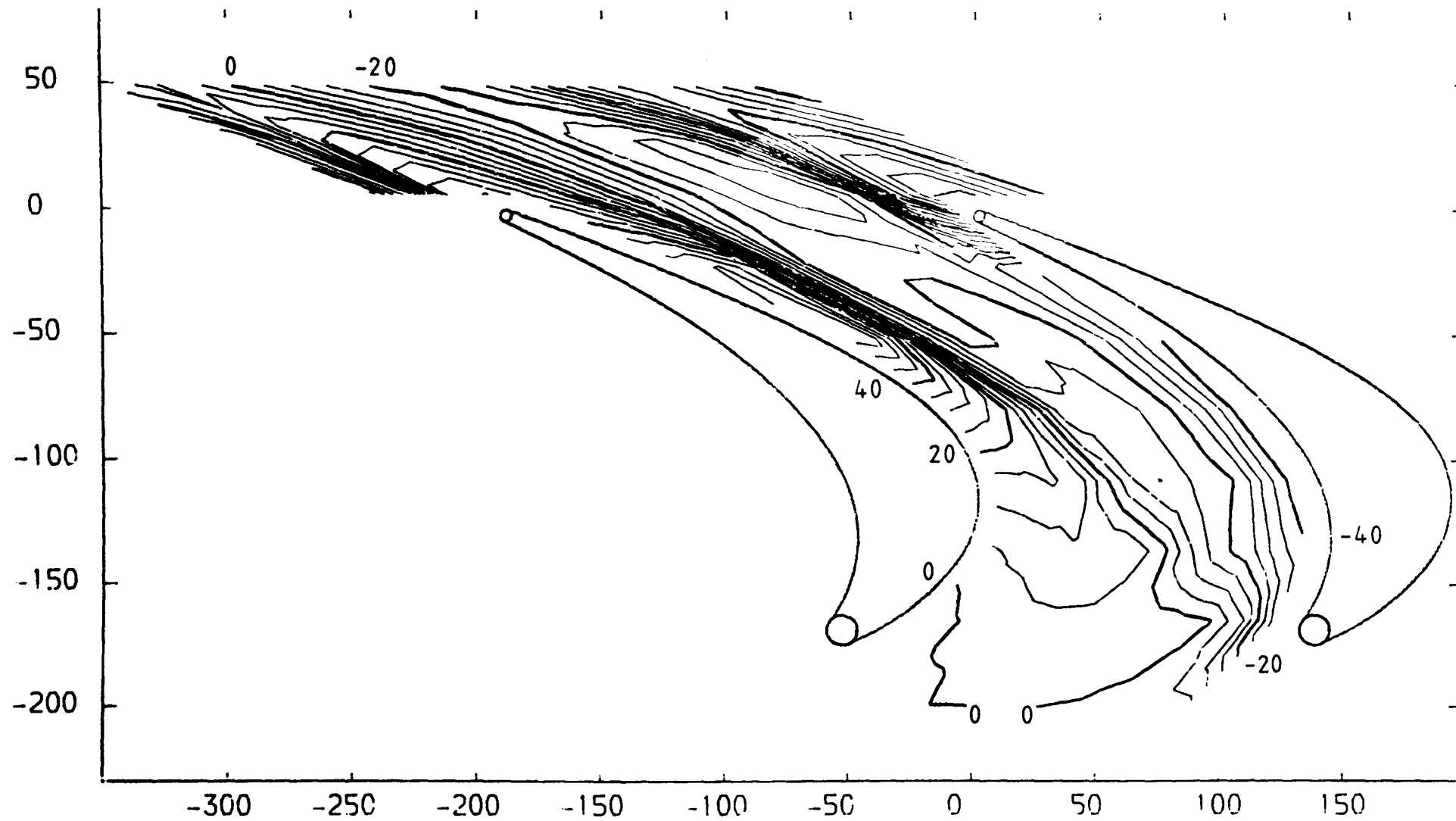


FIGURE 4.113

PLCT ON PLANE 20.1 MM FROM PERSPEX ENDWALL (5-HOLE PROBE DATA)  
YAW ANGLE CONTOURS (CONTOUR UNITS DEGREES)  
X-AXIS TANGENTIAL CO-ORDINATE FROM TRAILING EDGE DATUM (MM)  
Y-AXIS AXIAL CO-ORDINATE FROM TRAILING EDGE DATUM (MM)

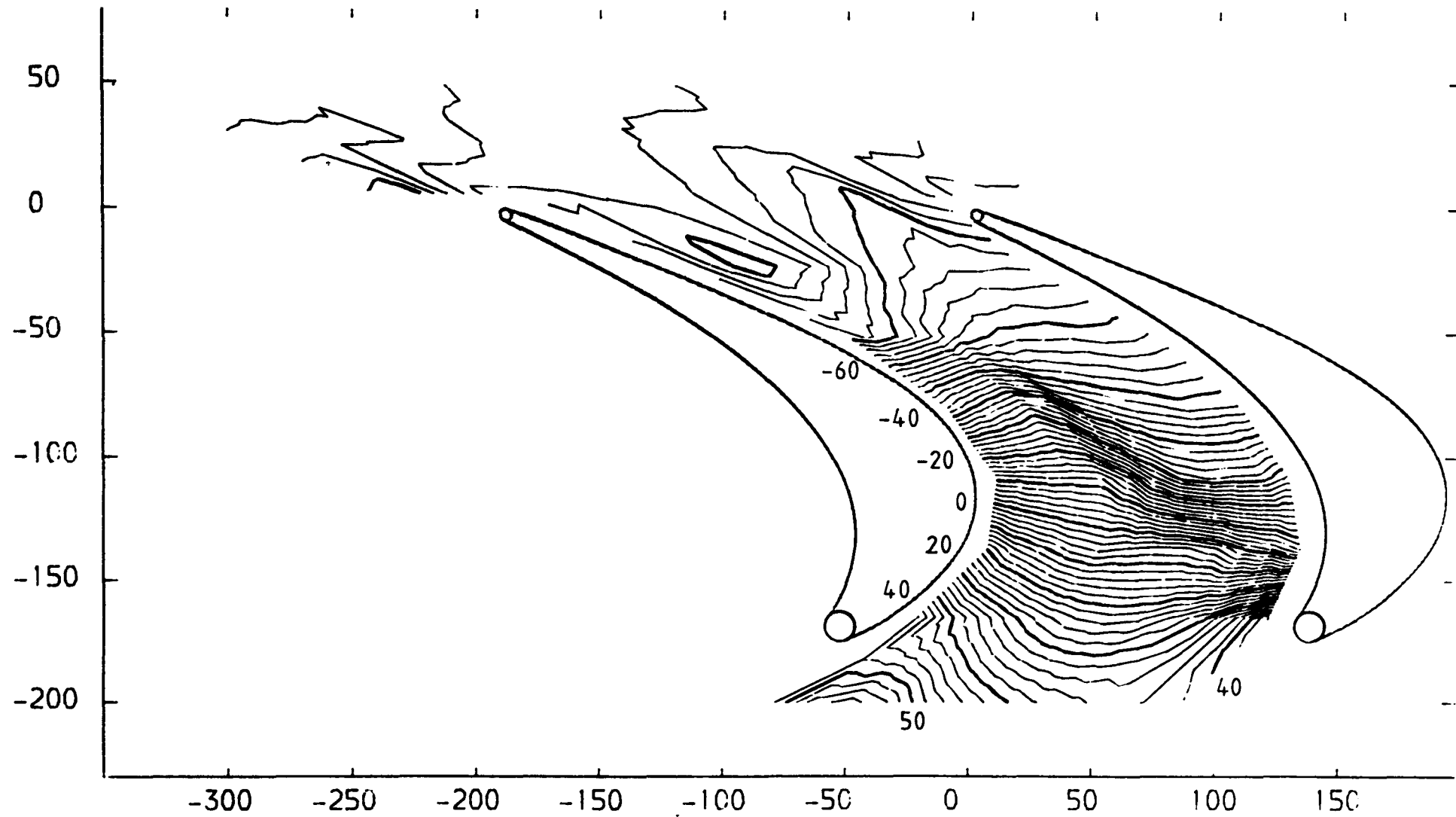


FIGURE 4.114

PLOT ON PLANE 220.1 MM FROM PERSPEX ENDWALL (5-HOLE PROBE DATA)  
SPANWISE ANGLE (PITCH ANGLE) CONTOURS (CONTOUR UNITS DEGREES)  
X-AXIS TANGENTIAL CO-ORDINATE FROM TRAILING EDGE DATUM (MM)  
Y-AXIS AXIAL CO-ORDINATE FROM TRAILING EDGE DATUM (MM)

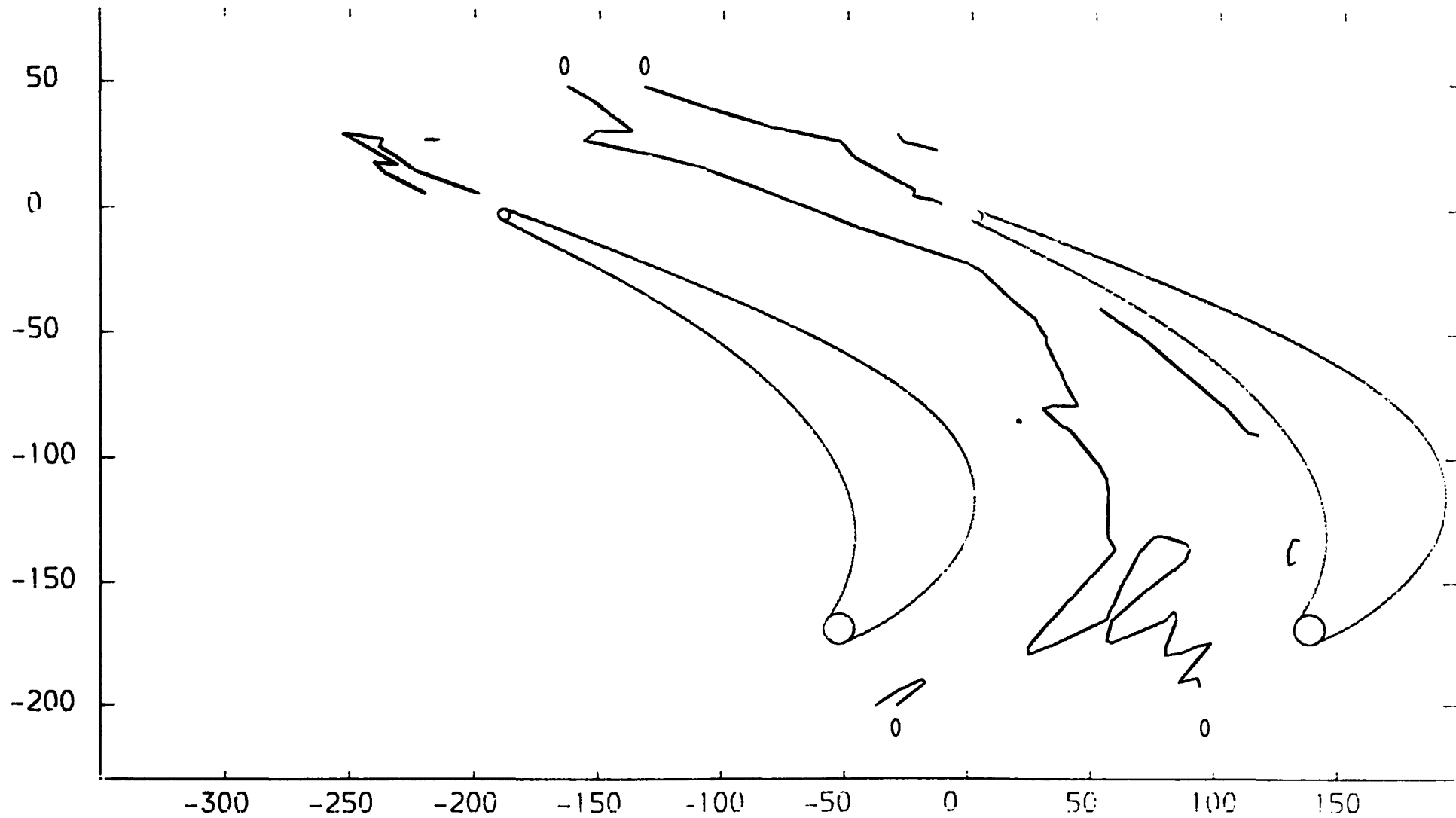


FIGURE 4.115

PLOT ON PLANE 220.1 MM FROM PERSPEX ENDWALL (5-HOLE PROBE DATA)  
YAW ANGLE CONTOURS (CONTOUR UNITS DEGREES)  
X-AXIS TANGENTIAL CO-ORDINATE FROM TRAILING EDGE DATUM (MM)  
Y-AXIS AXIAL CO-ORDINATE FROM TRAILING EDGE DATUM (MM)

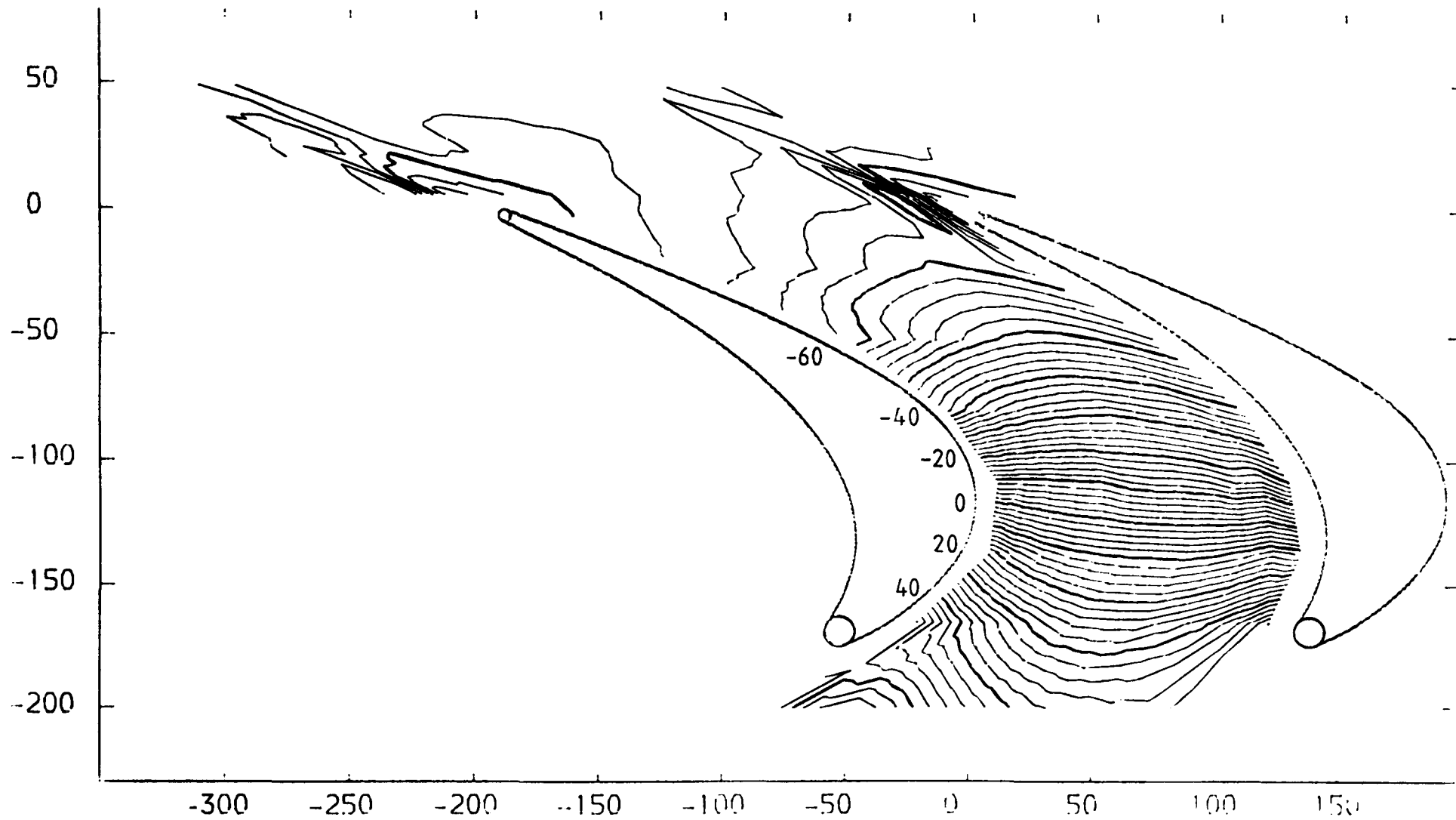


FIGURE 4.116

PLOT ON PLANE 1.0 MM FROM PERSPEX ENDWALL (3-HOLE PROBE DATA)  
STATIC PRESSURE COEFFICIENT (  $(P1-P_{LOCAL}) / (P01-P1)$  ) CONTOURS  
X-AXIS TANGENTIAL CO-ORDINATE FROM TRAILING EDGE DATUM (MM)  
Y-AXIS AXIAL CO-ORDINATE FROM TRAILING EDGE DATUM (MM)

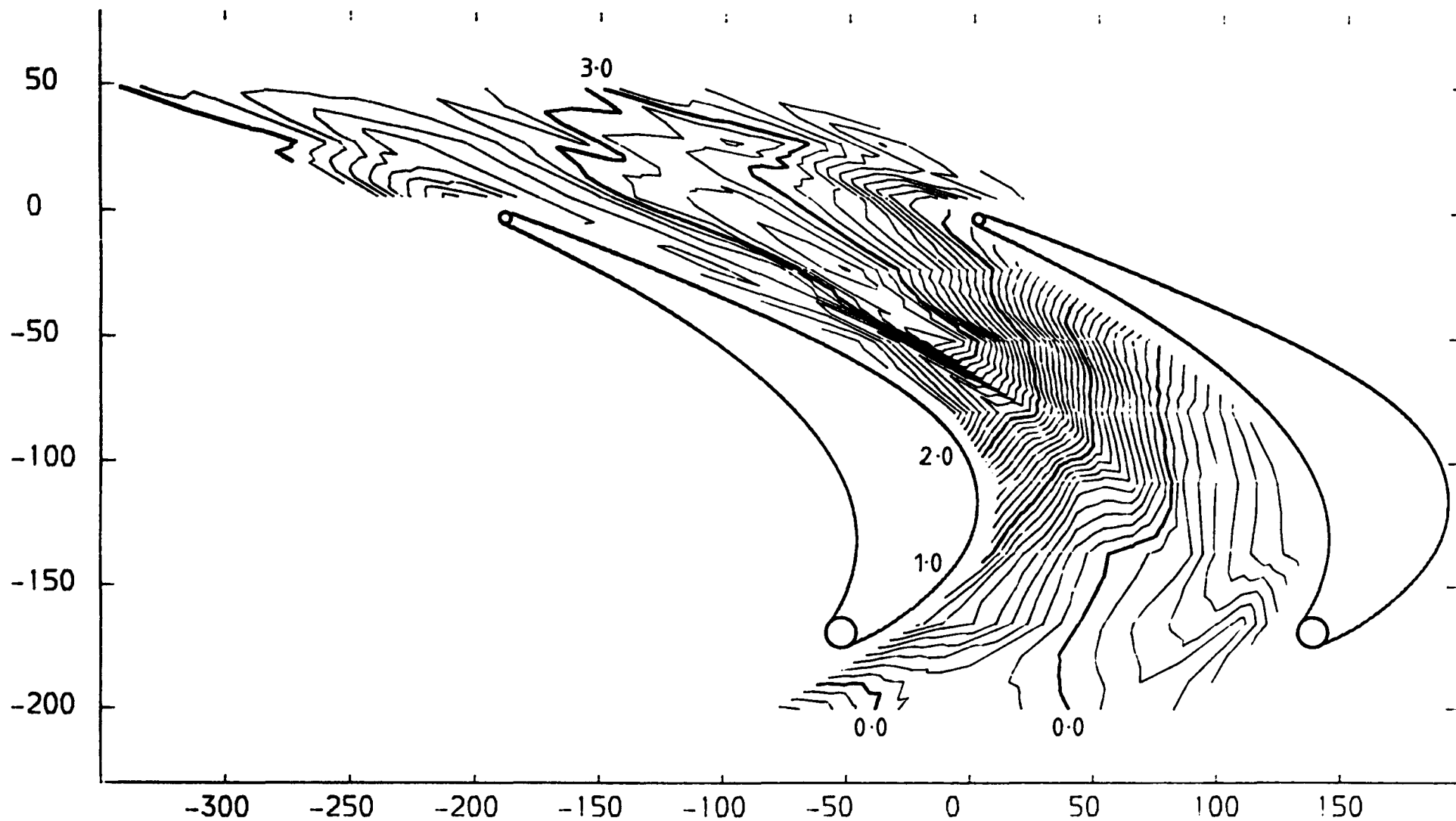


FIGURE 4.117

PLOT ON PLANE 20.1 MM FROM PERSPEX ENDWALL (5-HOLE PROBE DATA)  
STATIC PRESSURE COEFFICIENT (  $(P_1 - P_{LOCAL}) / (P_{01} - P_1)$  ) CONTOURS  
X-AXIS TANGENTIAL CO-ORDINATE FROM TRAILING EDGE DATUM (MM)  
Y-AXIS AXIAL CO-ORDINATE FROM TRAILING EDGE DATUM (MM)

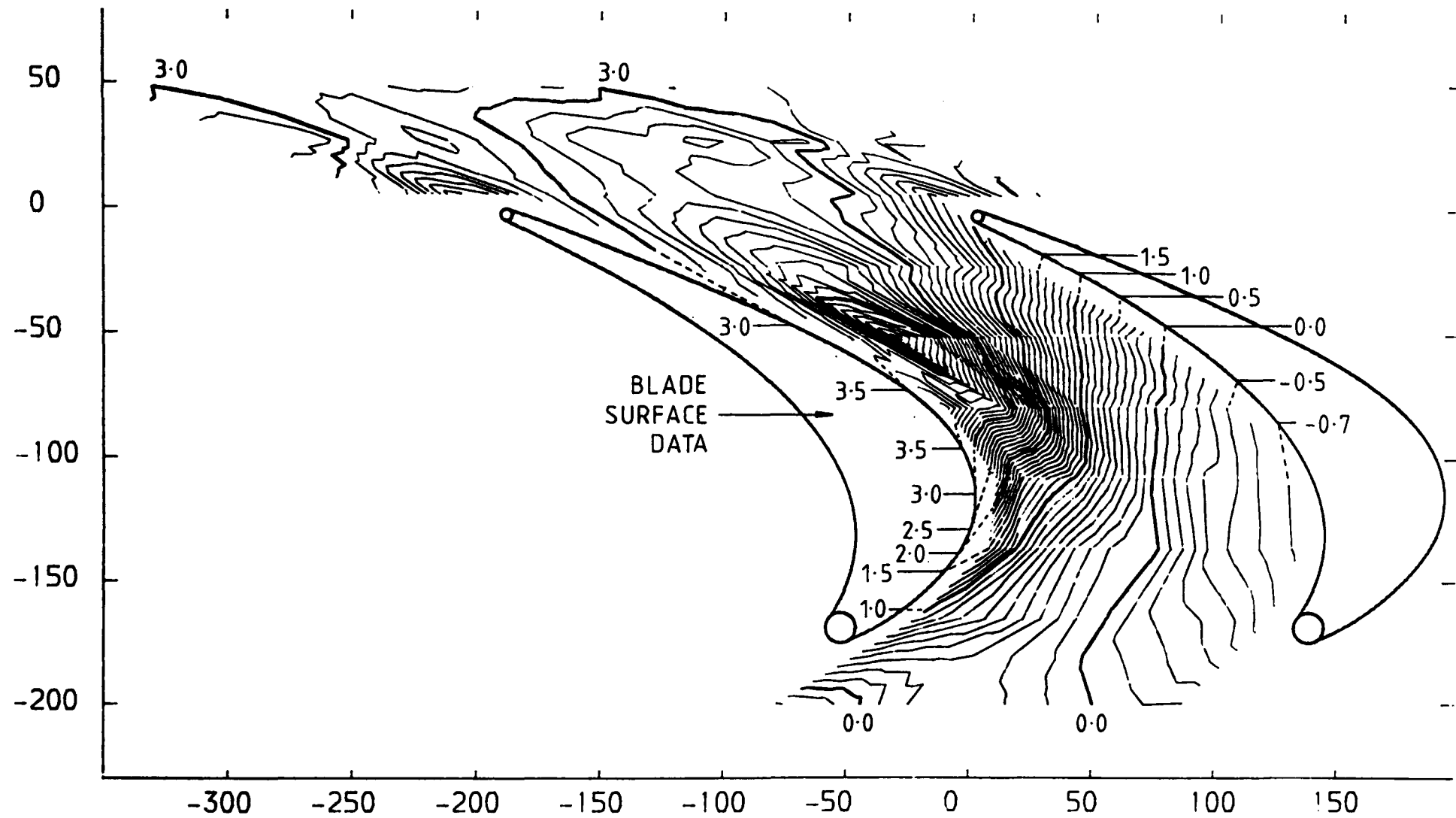


FIGURE 4.118

PLOT ON PLANE 20.1 MM FROM PERSPEX ENDWALL (3-HOLE PROBE DATA)  
STATIC PRESSURE COEFFICIENT (  $(P_1 - P_{LOCAL}) / (P_{01} - P_1)$  ) CONTOURS  
X-AXIS TANGENTIAL CO-ORDINATE FROM TRAILING EDGE DATUM (MM)  
Y-AXIS AXIAL CO-ORDINATE FROM TRAILING EDGE DATUM (MM)

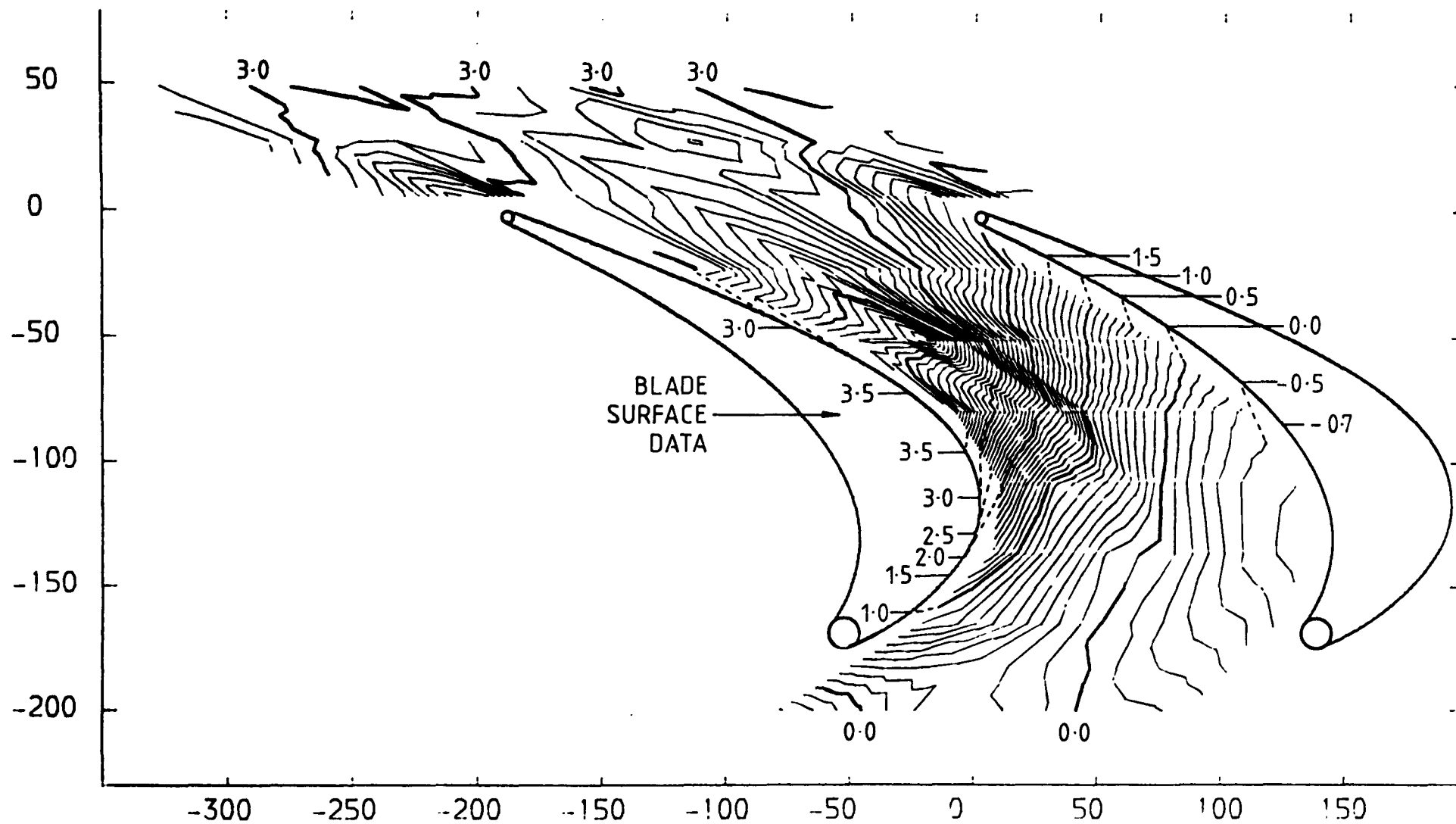


FIGURE 4.119

PLOT ON PLANE 30.0 MM FROM PERSPEX ENDWALL (5-HOLE PROBE DATA)  
STATIC PRESSURE COEFFICIENT (  $(P_1 - P_{LOCAL}) / (P_0 - P_1)$  ) CONTOURS  
X-AXIS TANGENTIAL CO-ORDINATE FROM TRAILING EDGE DATUM (MM)  
Y-AXIS AXIAL CO-ORDINATE FROM TRAILING EDGE DATUM (MM)

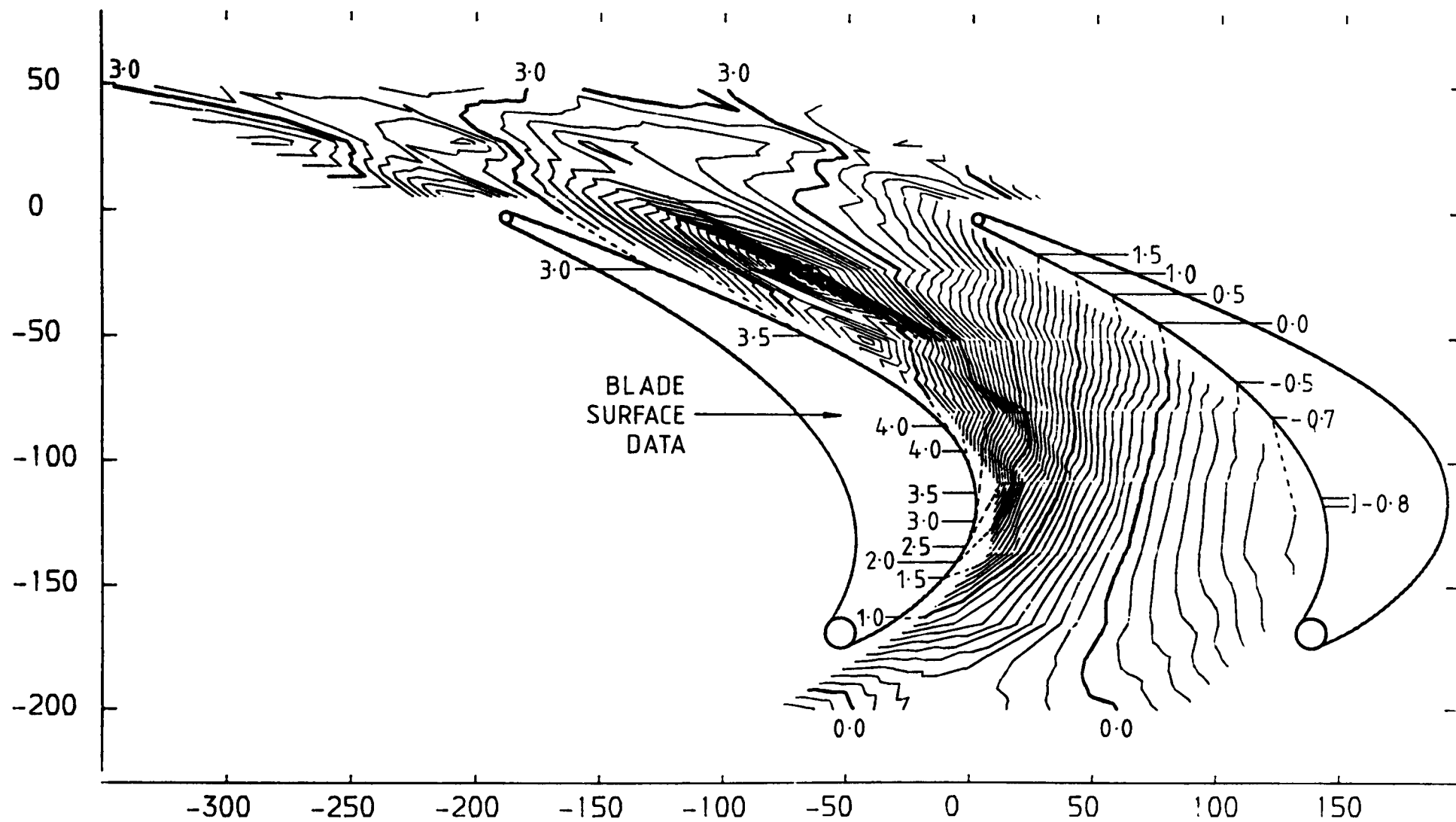


FIGURE 4.120



PLOT ON PLANE 60.0 MM FROM PERSPEX ENDWALL (5-HOLE PROBE DATA)  
STATIC PRESSURE COEFFICIENT (  $(P_1 - P_{LOCAL}) / (P_{01} - P_1)$  ) CONTOURS  
X-AXIS TANGENTIAL CO-ORDINATE FROM TRAILING EDGE DATUM (MM)  
Y-AXIS AXIAL CO-ORDINATE FROM TRAILING EDGE DATUM (MM)

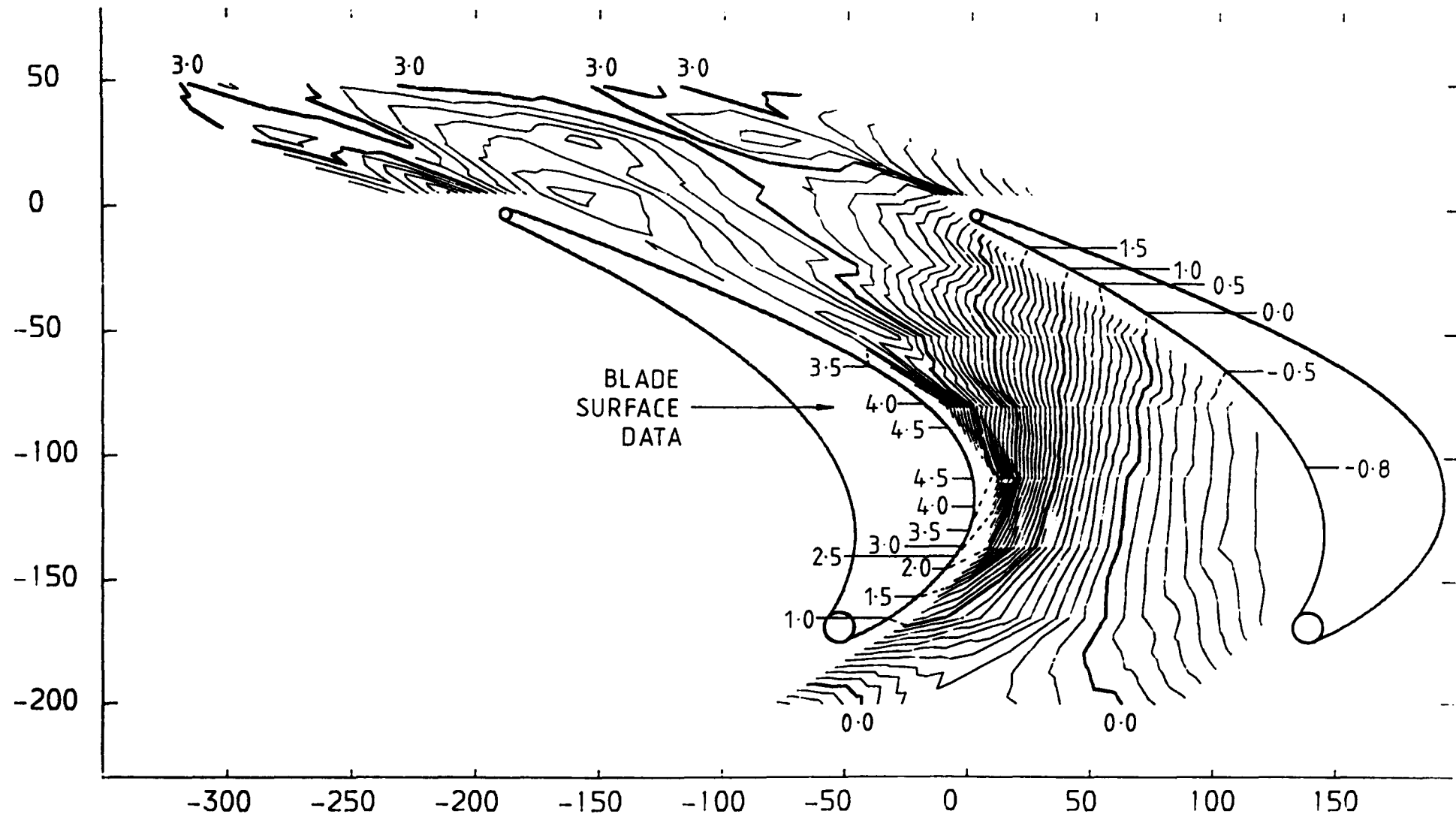


FIGURE 4.121

PLOT ON PLANE 220.1 MM FROM PERSPEX ENDWALL (5-HOLE PROBE DATA)  
STATIC PRESSURE COEFFICIENT (  $(P_1 - P_{LOCAL}) / (P_{01} - P_1)$  ) CONTOURS  
X-AXIS TANGENTIAL CO-ORDINATE FROM TRAILING EDGE DATUM (MM)  
Y-AXIS AXIAL CO-ORDINATE FROM TRAILING EDGE DATUM (MM)

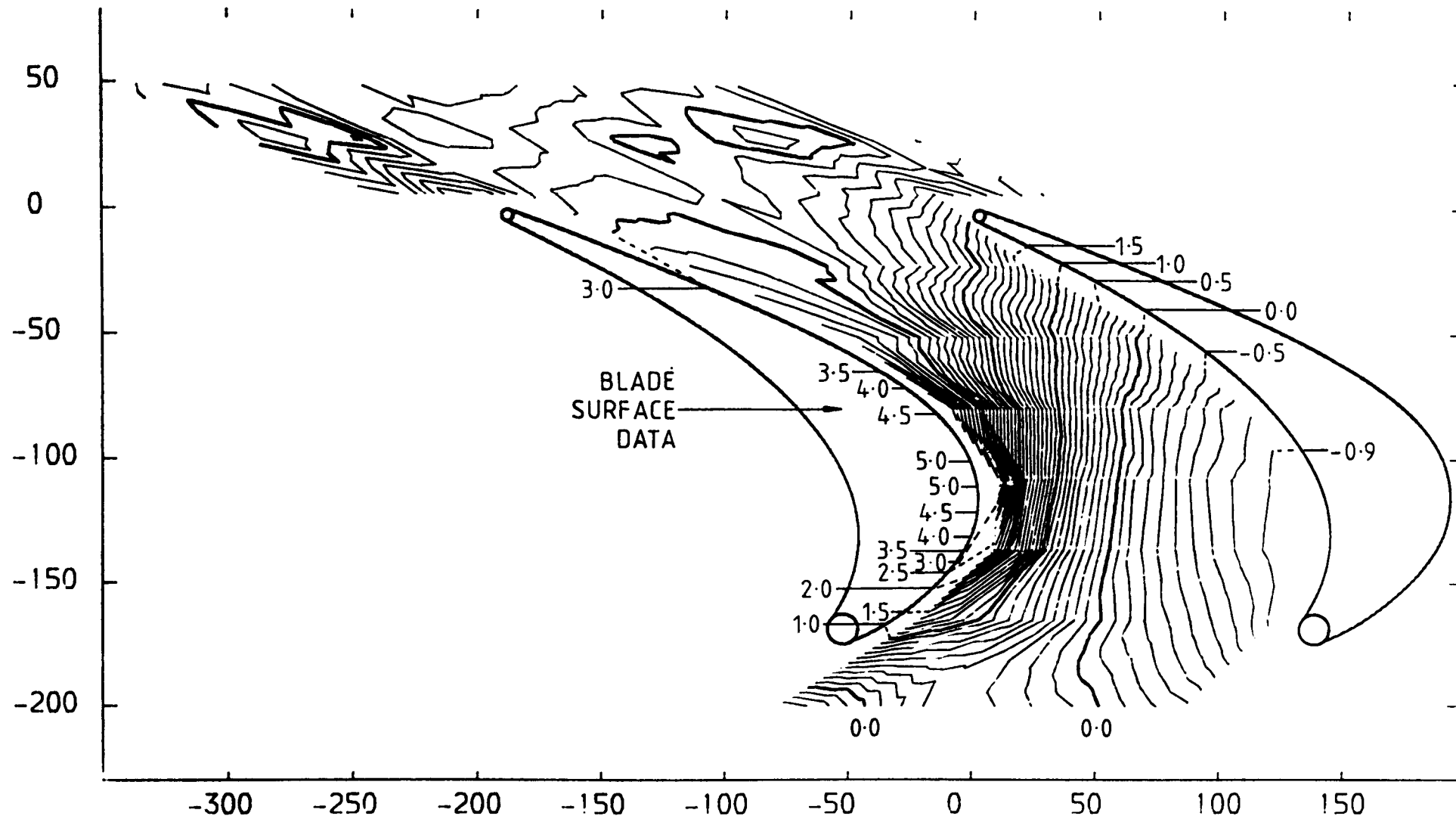


FIGURE 4.122

TWO DIMENSIONAL STATIC PRESSURE COEFFICIENT DISTRIBUTION  
PREDICTED VALUES (  $(P1-PLOCAL)/(P01-P1)$  ) CONTOURS

X-AXIS AXIAL CO-ORDINATE FROM TRAILING EDGE DATUM (MM)  
Y-AXIS SPANWISE CO-ORDINATE FROM PERSPEX ENDWALL (MM)

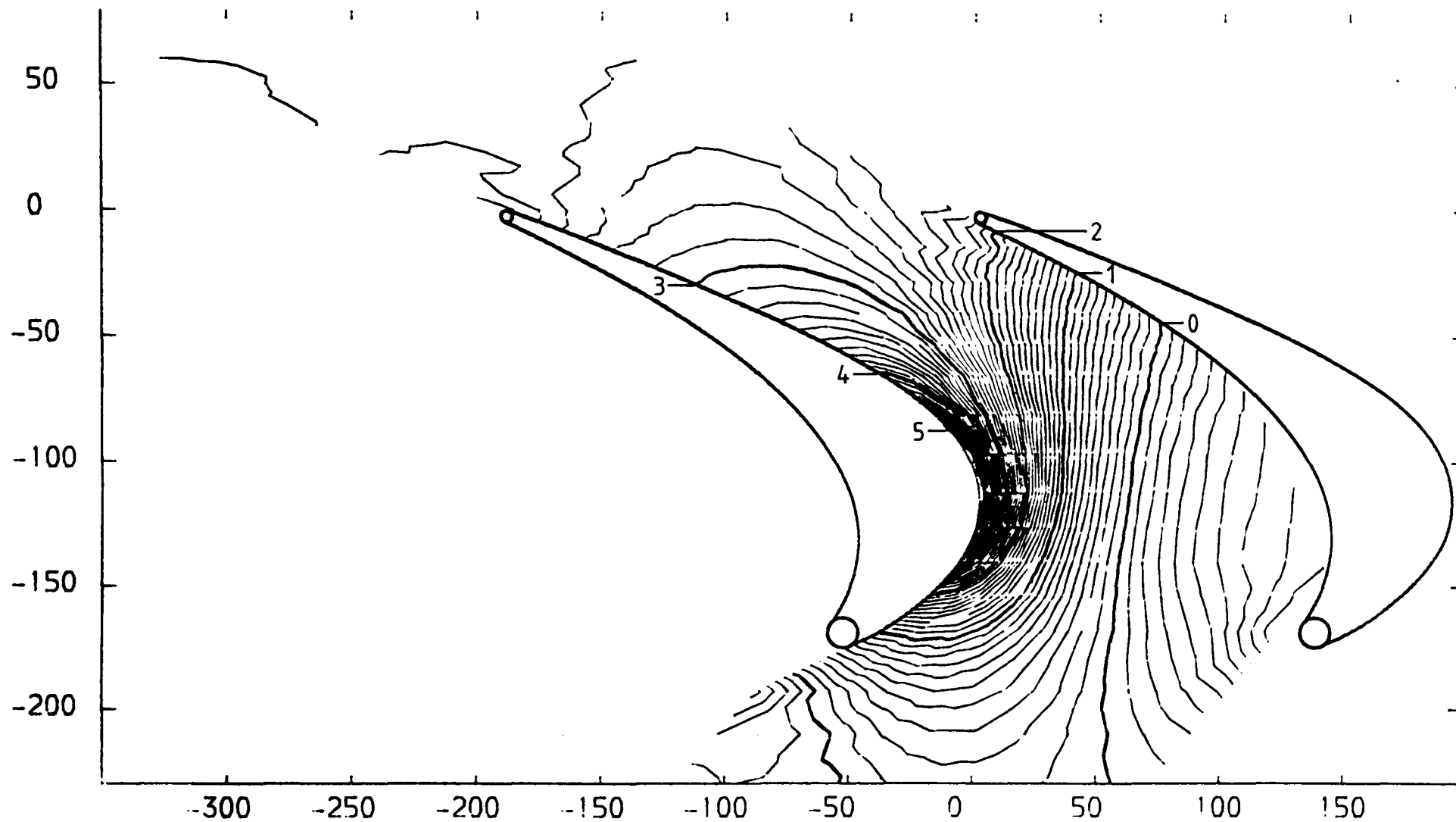


FIGURE 4.123

PLOT APPROXIMATELY 93.3 % OF BLADE PITCH LESS THICKNESS FROM SUCTION SURFACE  
AVERAGED TANGENTIAL EXPERIMENTAL POINTS

X-AXIS TANGENTIAL CO-ORDINATE FROM TRAILING EDGE DATUM (MM)

Y-AXIS AXIAL CO-ORDINATE FROM TRAILING EDGE DATUM (MM)

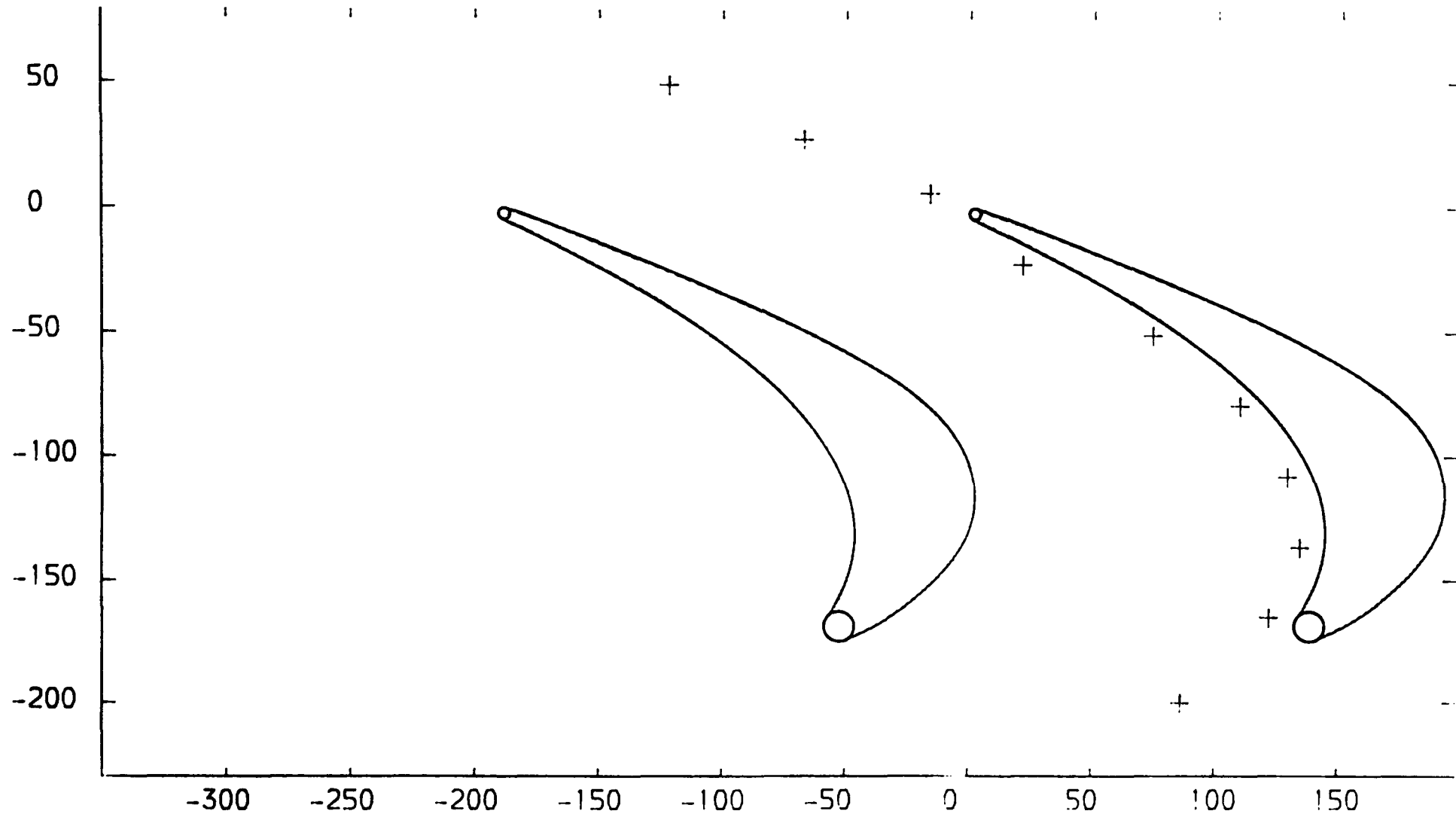


FIGURE 4.124

PLOT APPROXIMATELY 6.7 % OF BLADE PITCH LESS THICKNESS FROM SUCTION SURFACE  
AVERAGED TANGENTIAL EXPERIMENTAL POINTS  
X-AXIS TANGENTIAL CO-ORDINATE FROM TRAILING EDGE DATUM (MM)  
Y-AXIS AXIAL CO-ORDINATE FROM TRAILING EDGE DATUM (MM)

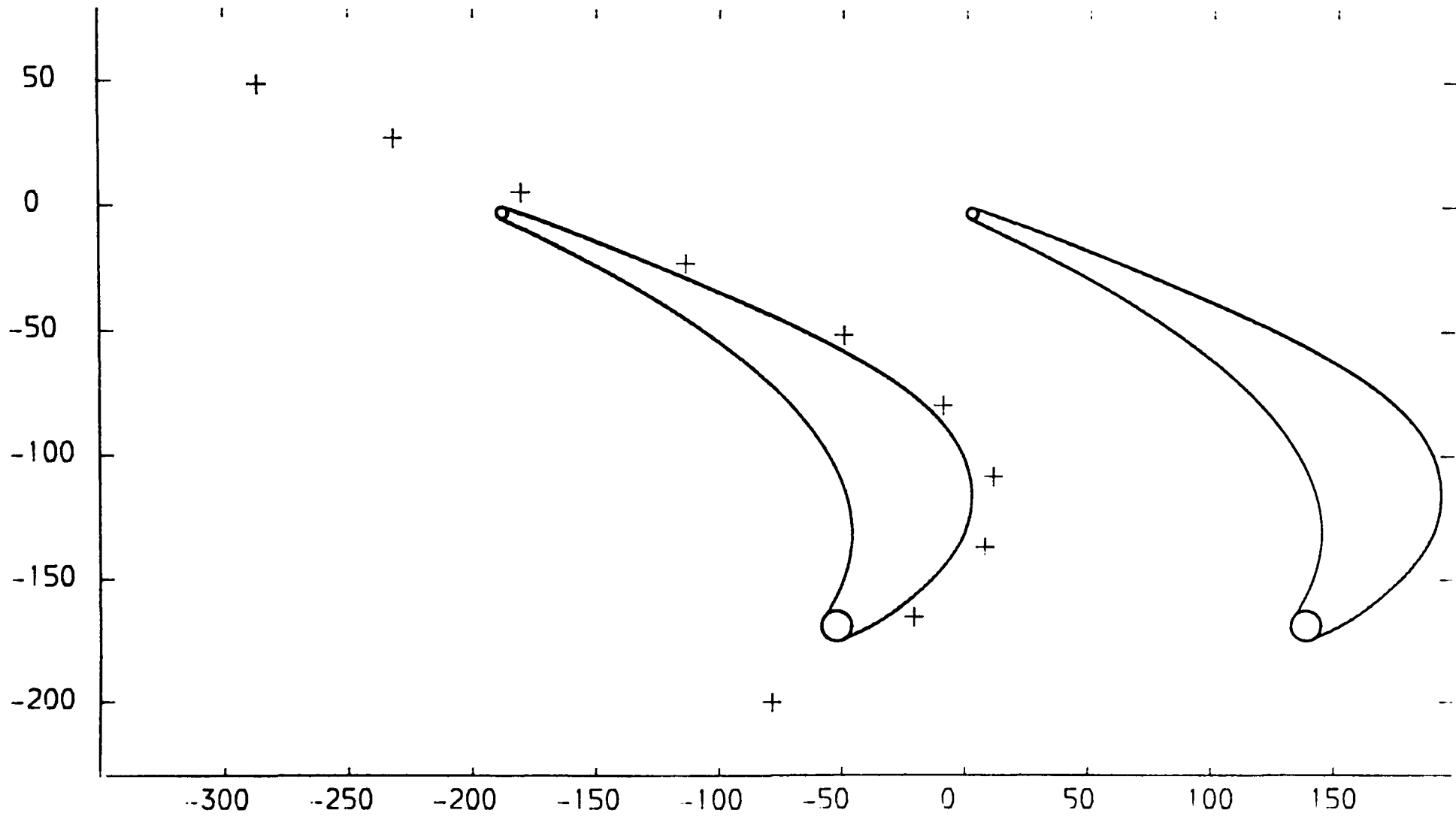


FIGURE 4.125

PLOT APPROXIMATELY 93.3 % OF BLADE PITCH LESS THICKNESS FROM SUCTION SURFACE  
 EXPERIMENTAL DATA POINTS

X-AXIS AXIAL CO-ORDINATE FROM TRAILING EDGE DATUM (MM)  
 Y-AXIS SPANWISE CO-ORDINATE FROM PERSPEX ENDWALL (MM)  
 + PROBE DATA    x MANUALLY INTERPOLATED DATA    \* EXTRAPOLATED DATA

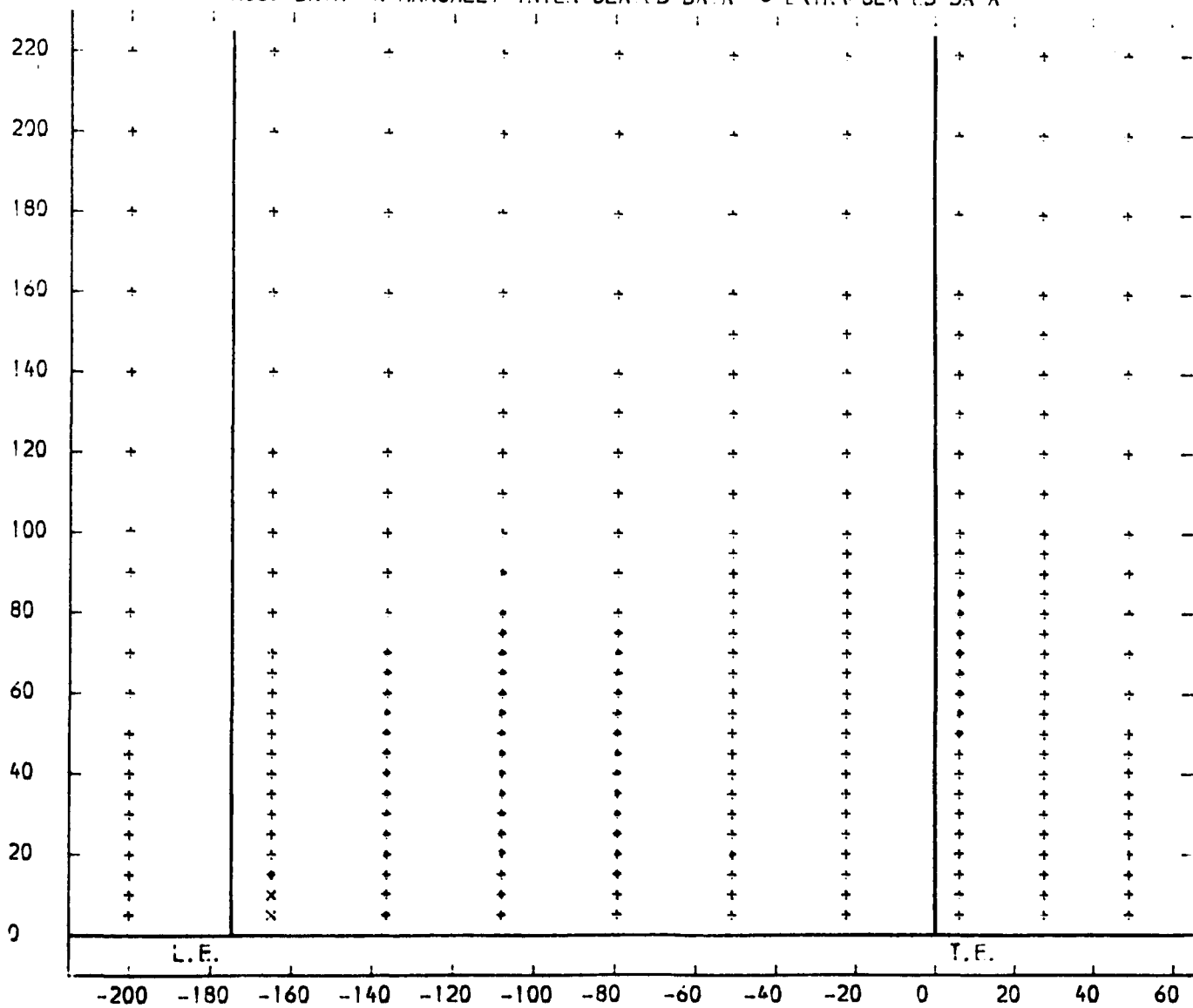


FIGURE 4.126

PLOT APPROXIMATELY 6.7 % OF BLADE PITCH LESS THICKNESS FROM SUCTION SURFACE  
 EXPERIMENTAL DATA POINTS

X-AXIS AXIAL CO-ORDINATE FROM TRAILING EDGE DATUM (MM)  
 Y-AXIS SPANWISE CO-ORDINATE FROM PERSPEX ENDWALL (MM)  
 + PROBE DATA x MANUALLY INTERPOLATED DATA \* EXTRAPOLATED DATA

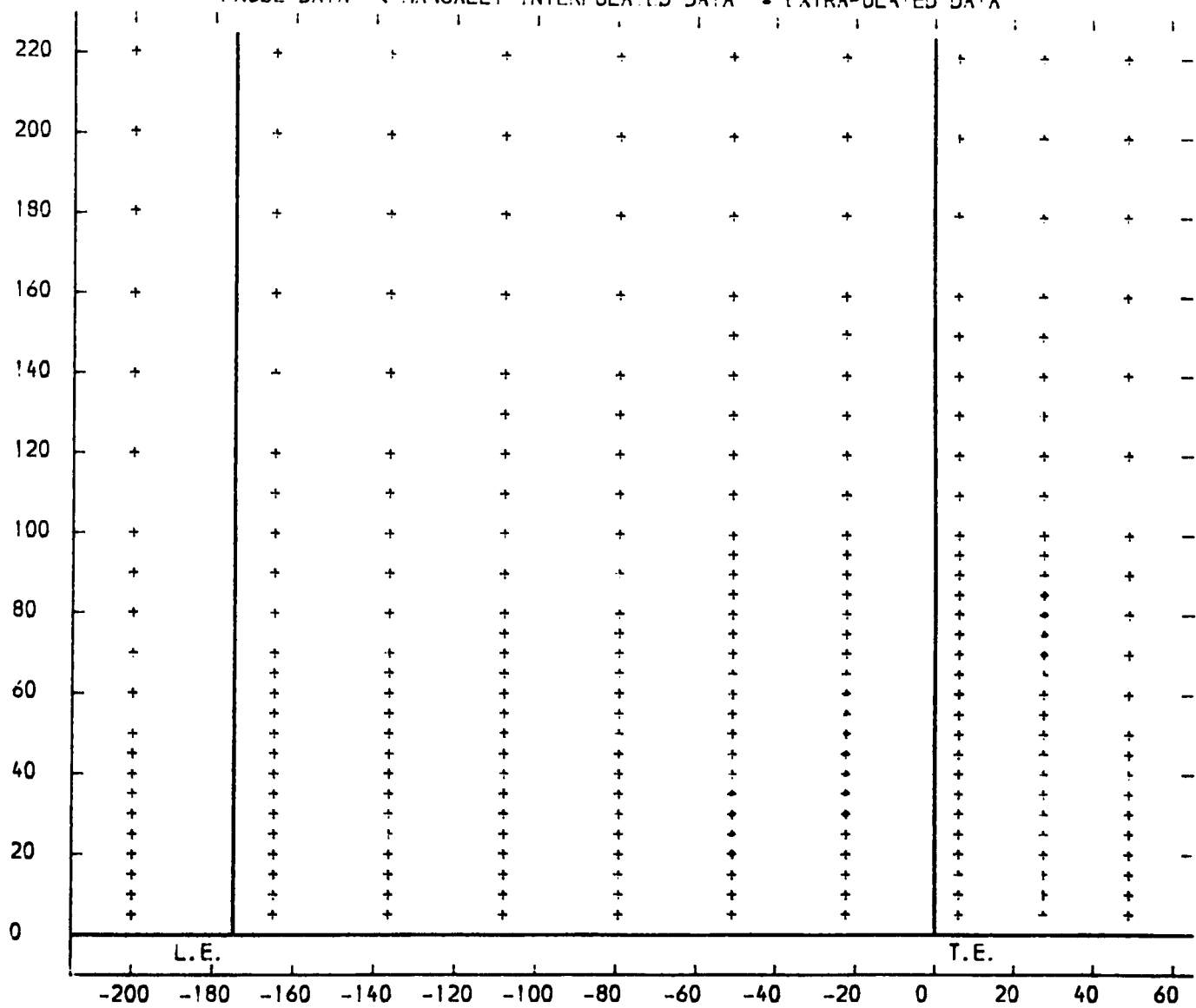


FIGURE 4.127

PLOT APPROXIMATELY 93.3 % OF BLADE PITCH LESS THICKNESS FROM SUCTION SURFACE  
 TOTAL PRESSURE LOSS COEFFICIENT (  $(P_{01}-P_{0LOCAL}) / (P_{01}-P_1)$  ) CONTOURS

X-AXIS AXIAL CO-ORDINATE FROM TRAILING EDGE DATUM (MM)  
 Y-AXIS SPANWISE CO-ORDINATE FROM PERSPEX ENDWALL (MM)

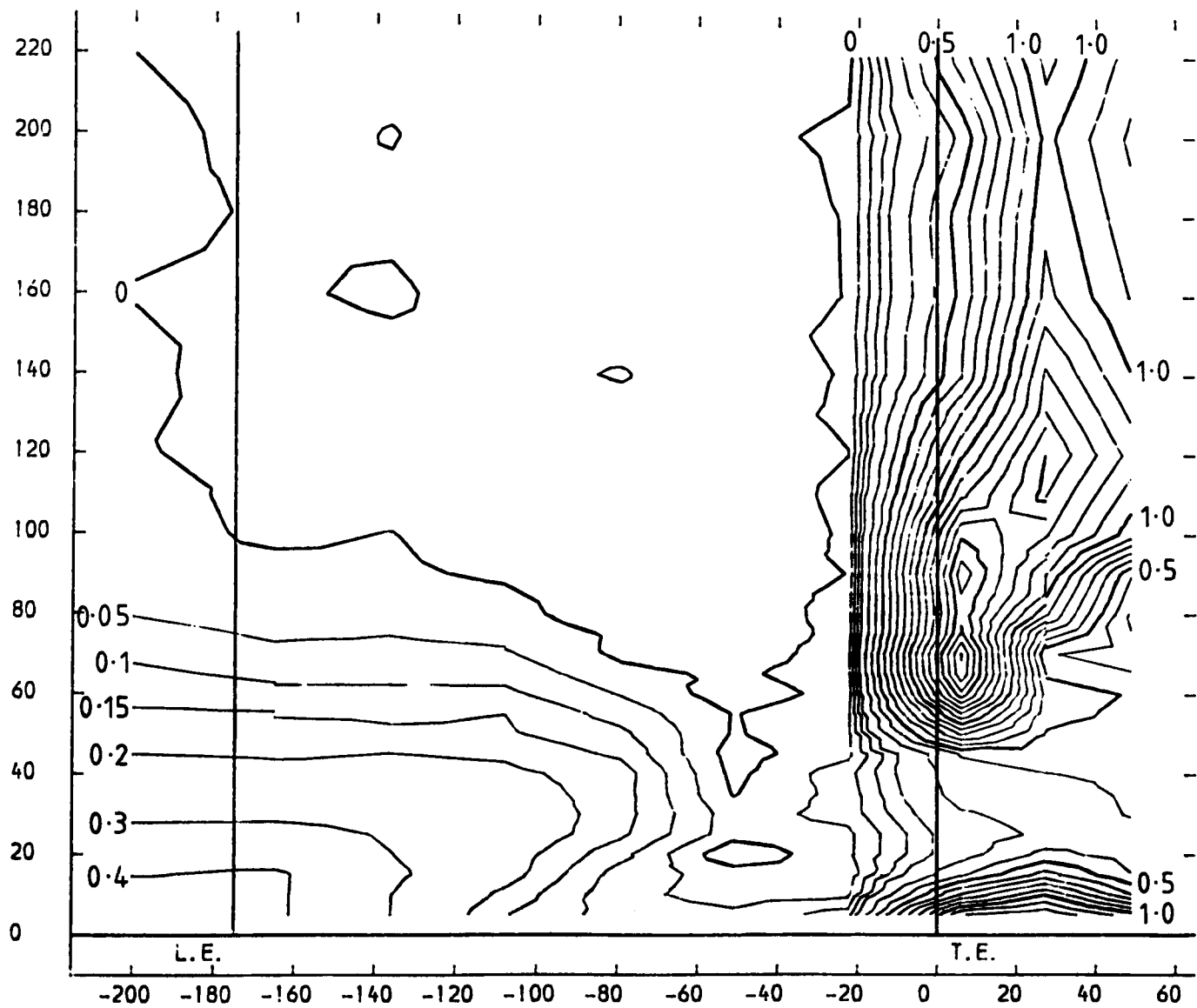


FIGURE 4.128



PLOT APPROXIMATELY 85.4 % OF BLADE PITCH LESS THICKNESS FROM SUCTION SURFACE  
TOTAL PRESSURE LOSS COEFFICIENT (  $(P_{01}-P_{0LOCAL}) / (P_{01}-P_1)$  ) CONTOURS

X-AXIS AXIAL CO-ORDINATE FROM TRAILING EDGE DATUM (MM)  
Y-AXIS SPANWISE CO-ORDINATE FROM PERSPEX ENDWALL (MM)

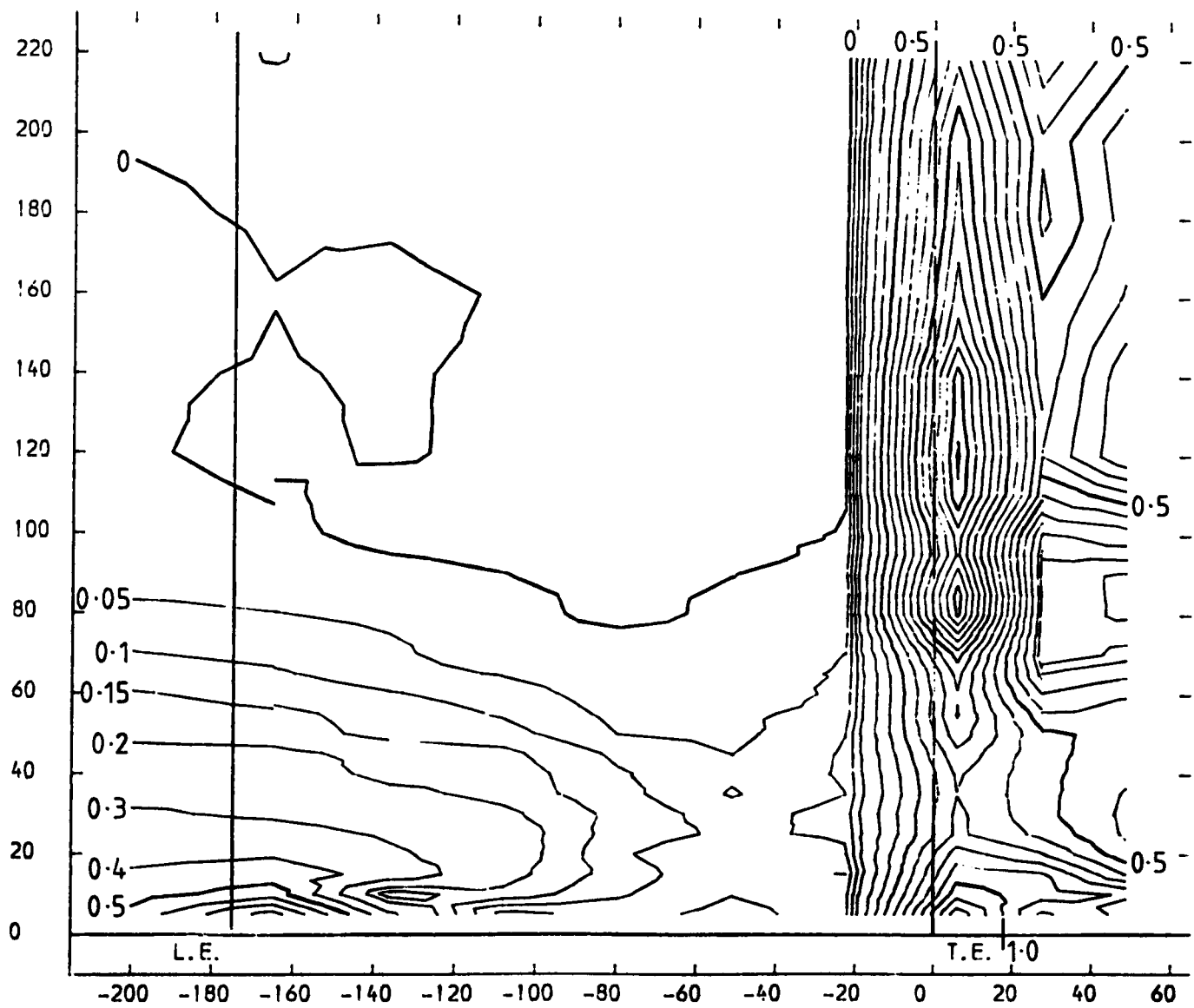


FIGURE 4.129

PLOT APPROXIMATELY 77.5 % OF BLADE PITCH LESS THICKNESS FROM SUCTION SURFACE  
TOTAL PRESSURE LOSS COEFFICIENT (  $(P_0! - P_{0LOCAL}) / (P_0! - P_1)$  ) CONTOURS

X-AXIS AXIAL CO-ORDINATE FROM TRAILING EDGE DATUM (MM)

Y-AXIS SPANWISE CO-ORDINATE FROM PERSPEX ENDWALL (MM)

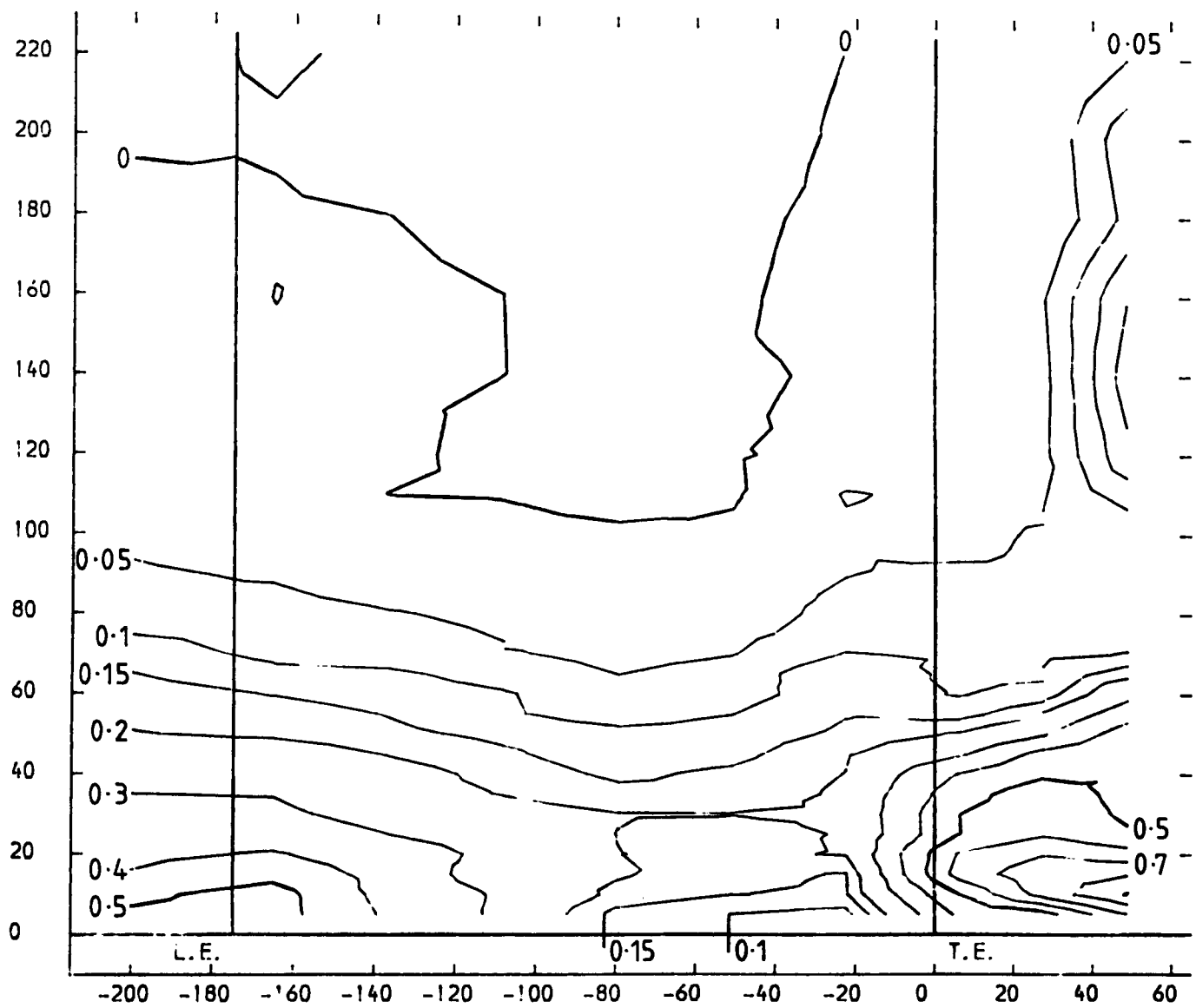


FIGURE 4.130

PLOT APPROXIMATELY 69.7% OF BLADE PITCH LESS THICKNESS FROM SUCTION SURFACE  
TOTAL PRESSURE LOSS COEFFICIENT  $(P_{01} - P_{0LOCAL}) / (P_{01} - P_{11})$  CONTOURS

X-AXIS AXIAL CO-ORDINATE FROM TRAILING EDGE DATUM (MM)  
Y-AXIS SPANWISE CO-ORDINATE FROM PERSPEX ENDWALL (MM)

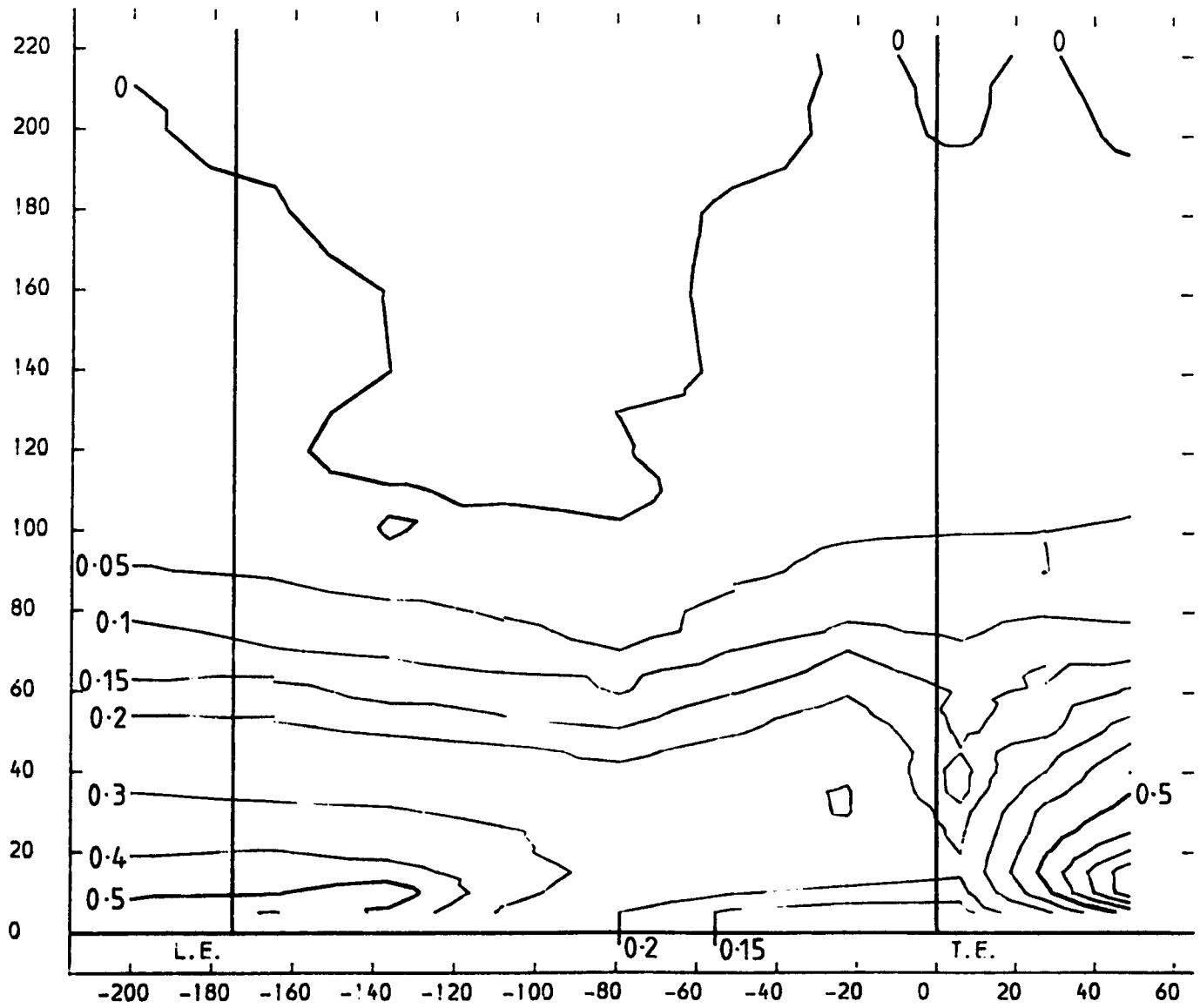


FIGURE 4.131

PLOT APPROXIMATELY 61.9 % OF BLADE PITCH LESS THICKNESS FROM SUCTION SURFACE  
TOTAL PRESSURE LOSS COEFFICIENT (  $(P_0 - P_{0LOCAL}) / (P_0 - P_1)$  ) CONTOURS

X-AXIS AXIAL CO-ORDINATE FROM TRAILING EDGE DATUM (MM)  
Y-AXIS SPANWISE CO-ORDINATE FROM PERSPEX ENDWALL (MM)

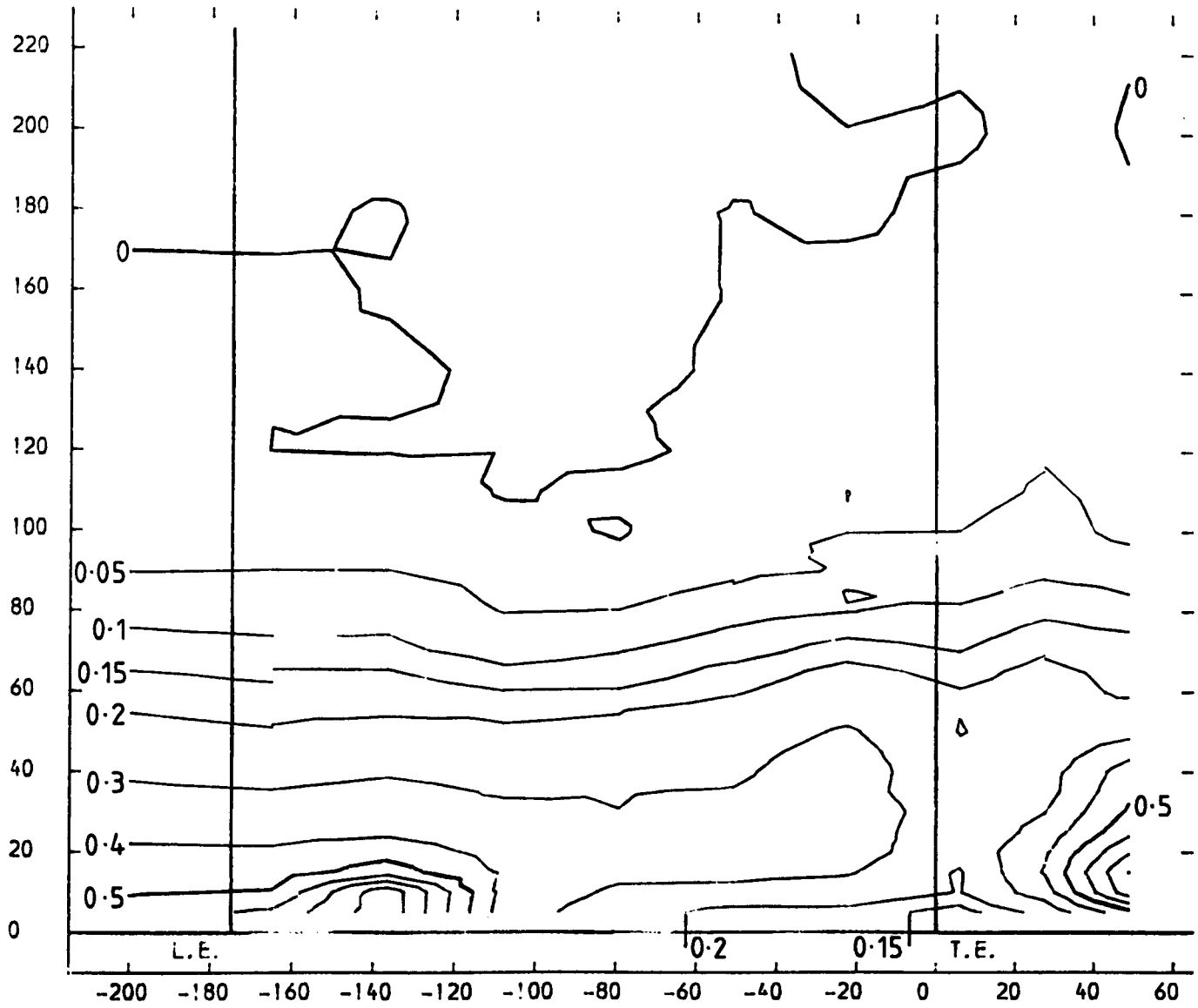


FIGURE 4.132

PLOT APPROXIMATELY 53.9 % OF BLADE PITCH LESS THICKNESS FROM SUCTION SURFACE  
TOTAL PRESSURE LOSS COEFFICIENT (  $(P_0! - P_{0LOCAL}) / (P_0! - P_1)$  ) CONTOURS

X-AXIS AXIAL CO-ORDINATE FROM TRAILING EDGE DATUM (MM)

Y-AXIS SPANWISE CO-ORDINATE FROM PERSPEX ENDWALL (MM)

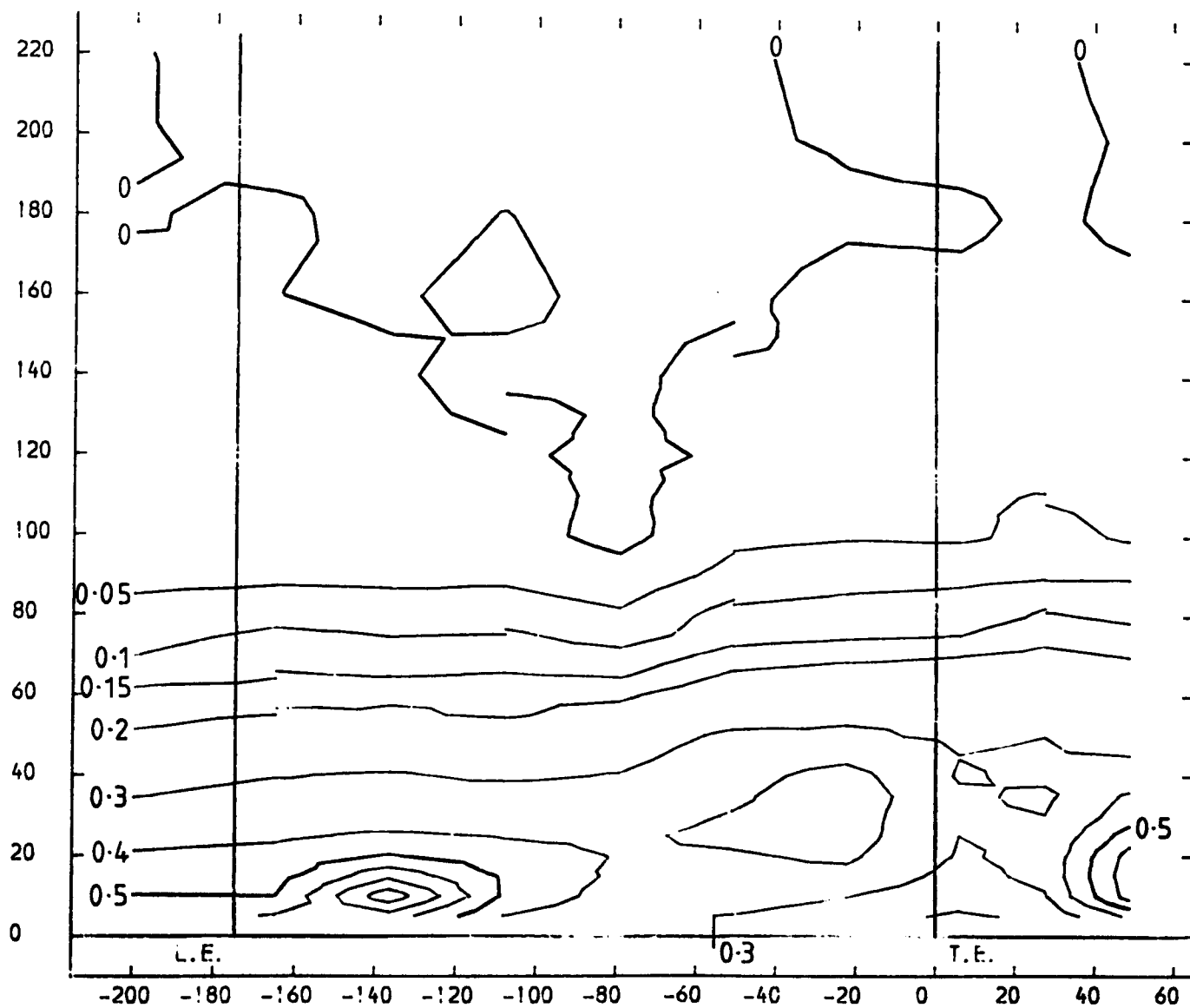


FIGURE 4.133

PLOT APPROXIMATELY 46.1 % OF BLADE PITCH LESS THICKNESS FROM SUCTION SURFACE  
 TOTAL PRESSURE LOSS COEFFICIENT (  $(P_0! - P_{0LOCAL}) / (P_0! - P_1)$  ) CONTOURS  
 X-AXIS AXIAL CO-ORDINATE FROM TRAILING EDGE DATUM (MM)  
 Y-AXIS SPANWISE CO-ORDINATE FROM PERSPEX ENDWALL (MM)

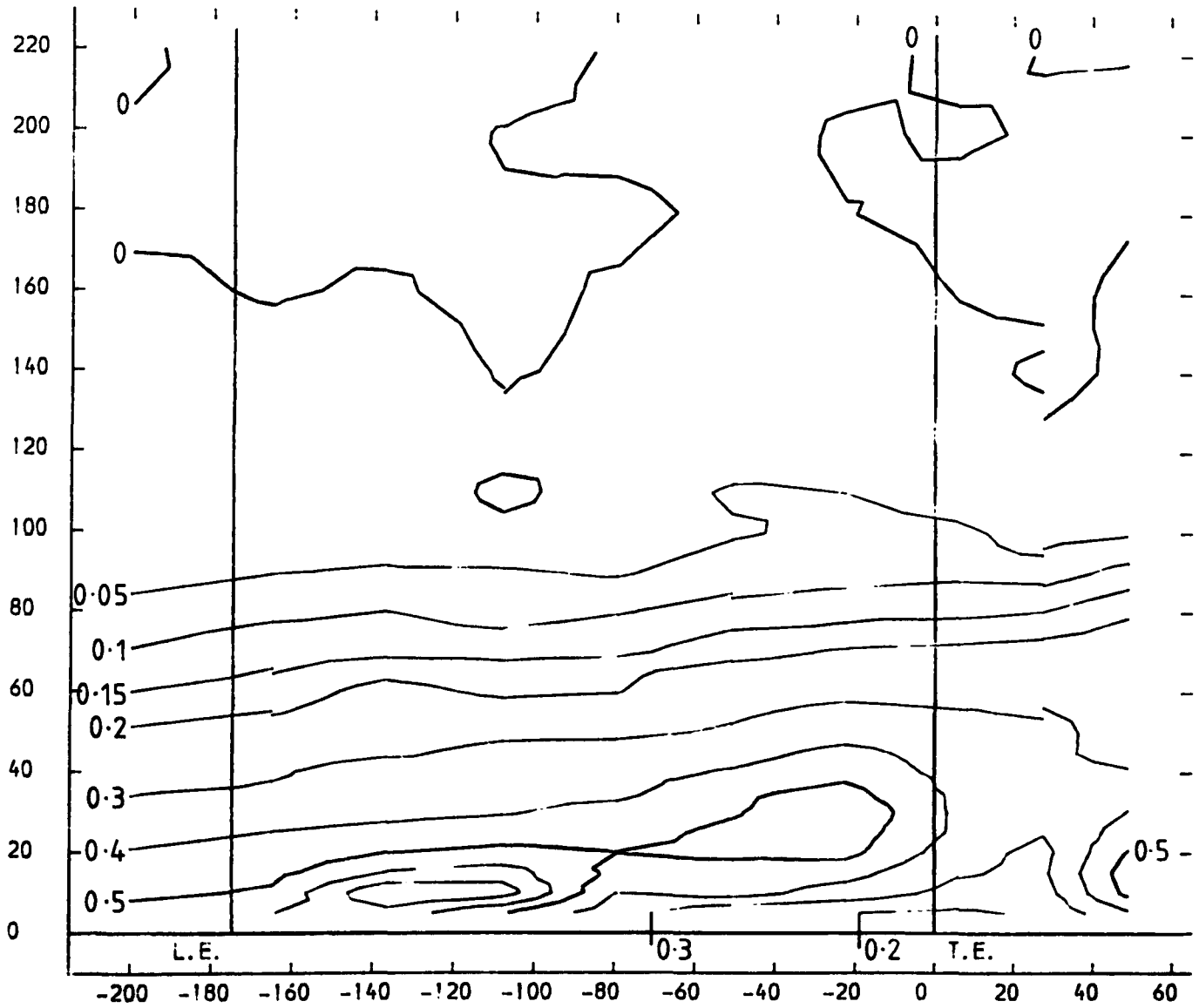


FIGURE 4.134

PLOT APPROXIMATELY 38.2 % OF BLADE PITCH LESS THICKNESS FROM SUCTION SURFACE  
TOTAL PRESSURE LOSS COEFFICIENT (  $(P_{01}-P_{0LOCAL}) / (P_{01}-P_1)$  ) CONTOURS

X-AXIS AXIAL CO-ORDINATE FROM TRAILING EDGE DATUM (MM)

Y-AXIS SPANWISE CO-ORDINATE FROM PERSPEX ENDWALL (MM)

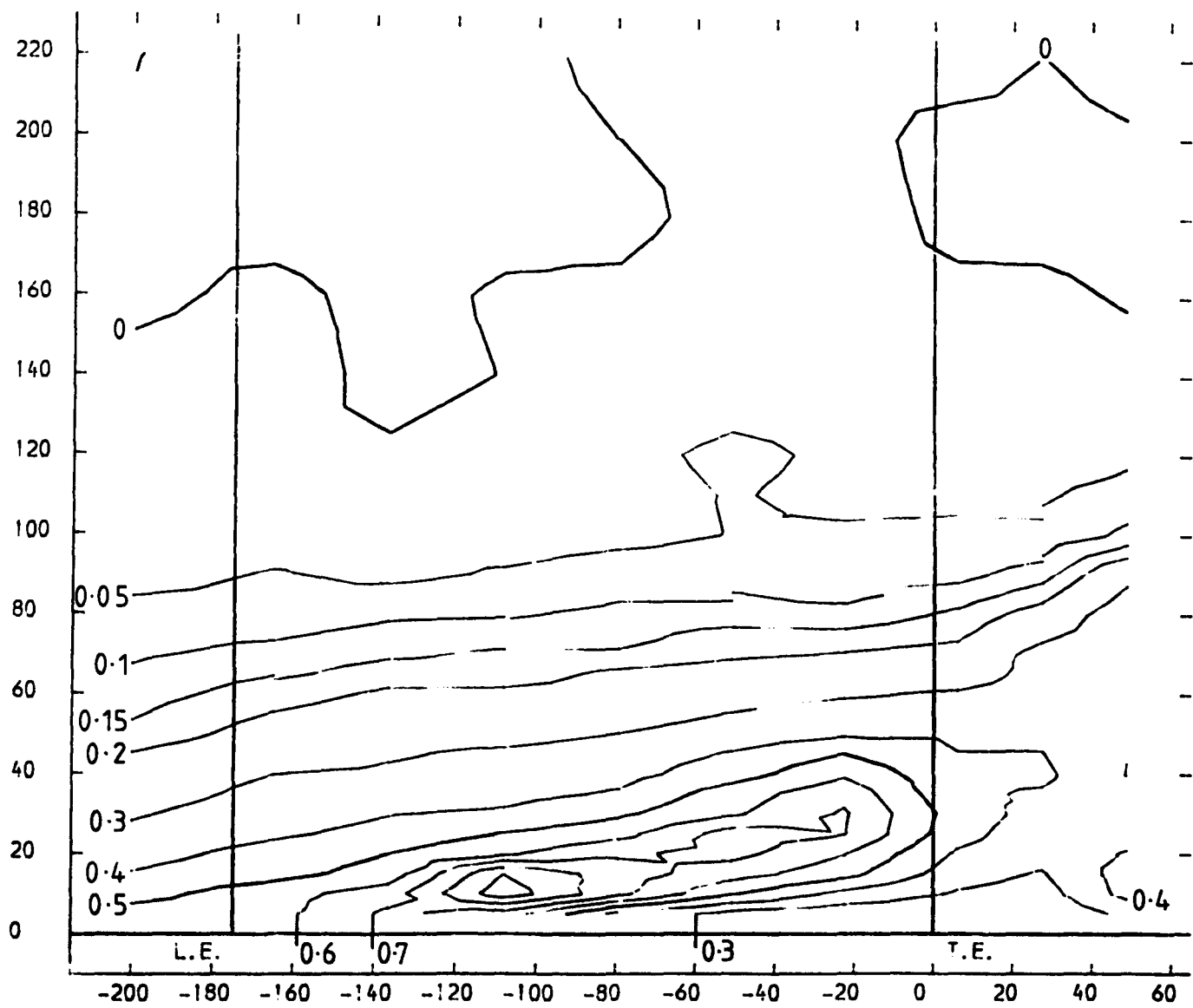


FIGURE 4.135

PLOT APPROXIMATELY 30.3 % OF BLADE PITCH LESS THICKNESS FROM SUCTION SURFACE  
TOTAL PRESSURE LOSS COEFFICIENT (  $(P_{01}-P_{0LOCAL}) / (P_{01}-P_1)$  ) CONTOURS

X-AXIS AXIAL CO-ORDINATE FROM TRAILING EDGE DATUM (MM)  
Y-AXIS SPANWISE CO-ORDINATE FROM PERSPEX ENDWALL (MM)

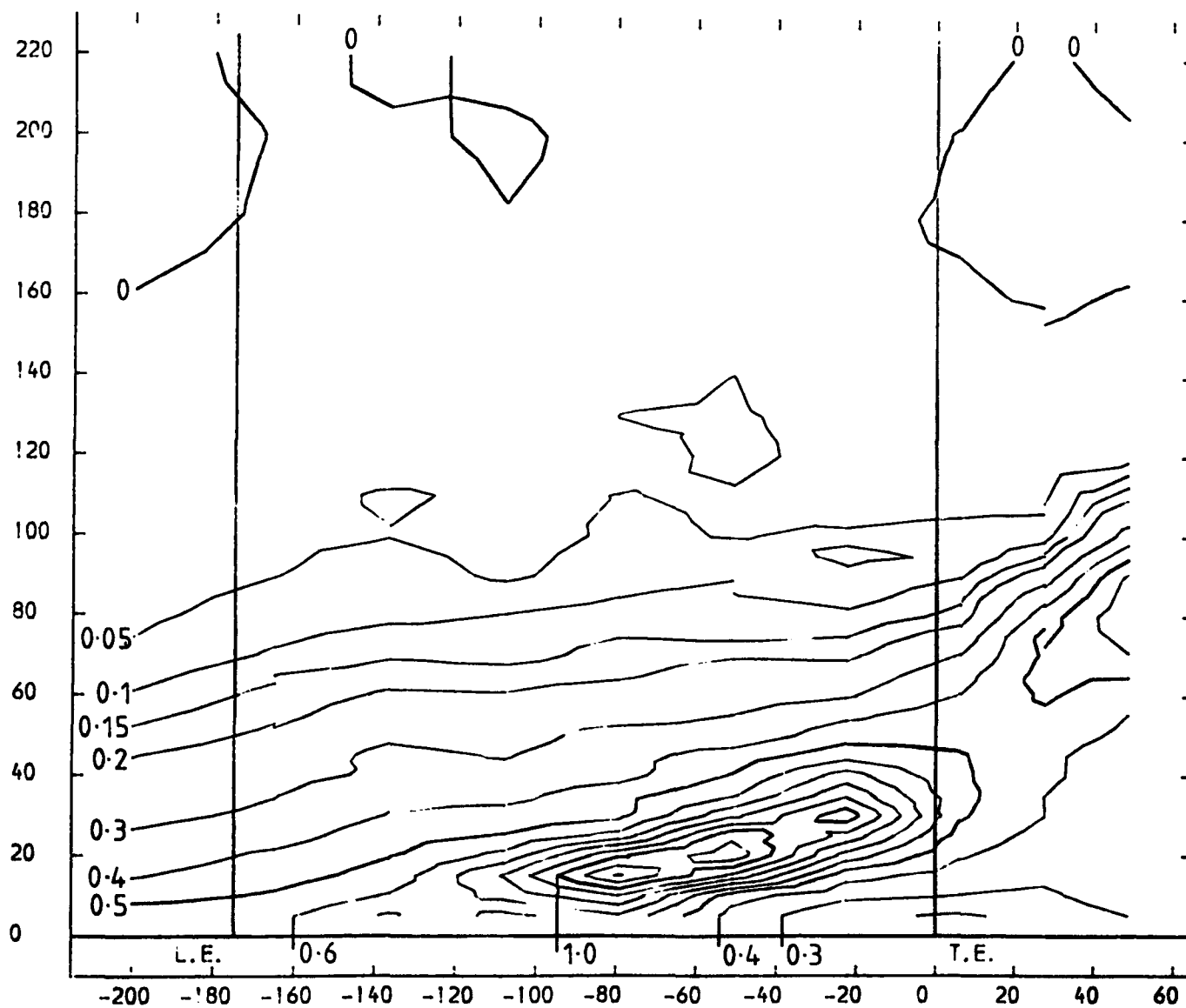


FIGURE 4.136



PLOT APPROXIMATELY 22.5 % OF BLADE PITCH LESS THICKNESS FROM SUCTION SURFACE  
TOTAL PRESSURE LOSS COEFFICIENT (  $(P_0! - P_{0LOCAL}) / (P_0! - P_1)$  ) CONTOURS

X-AXIS AXIAL CO-ORDINATE FROM TRAILING EDGE DATUM (MM)  
Y-AXIS SPANWISE CO-ORDINATE FROM PERSPEX ENDWALL (MM)

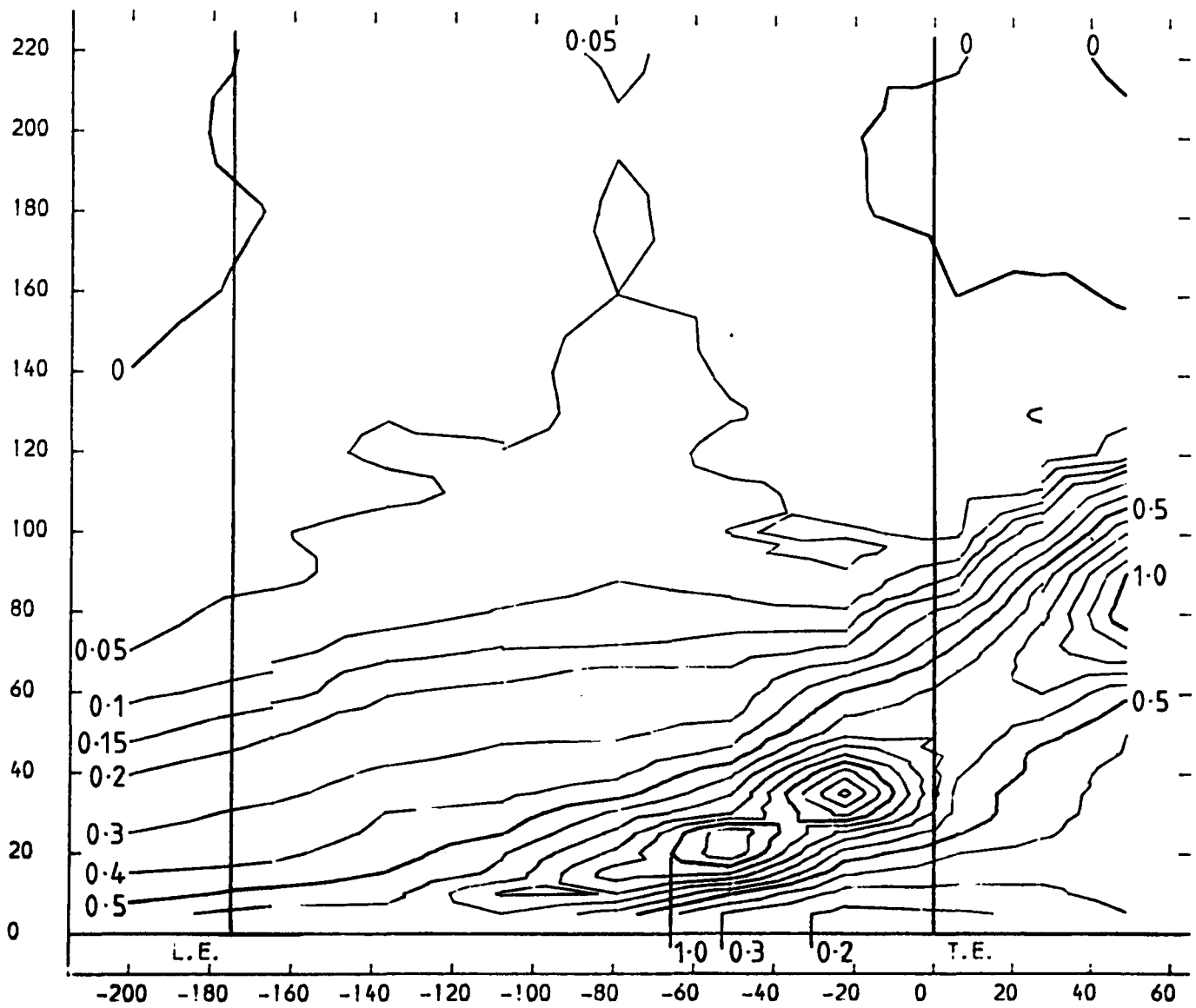


FIGURE 4.137

PLOT APPROXIMATELY 14.6 % OF BLADE PITCH LESS THICKNESS FROM SUCTION SURFACE  
TOTAL PRESSURE LOSS COEFFICIENT (  $(P_0! - P_{LOCAL}) / (P_0! - P_1)$  ) CONTOURS

X-AXIS AXIAL CO-ORDINATE FROM TRAILING EDGE DATUM (MM)  
Y-AXIS SPANWISE CO-ORDINATE FROM PERSPEX ENDWALL (MM)

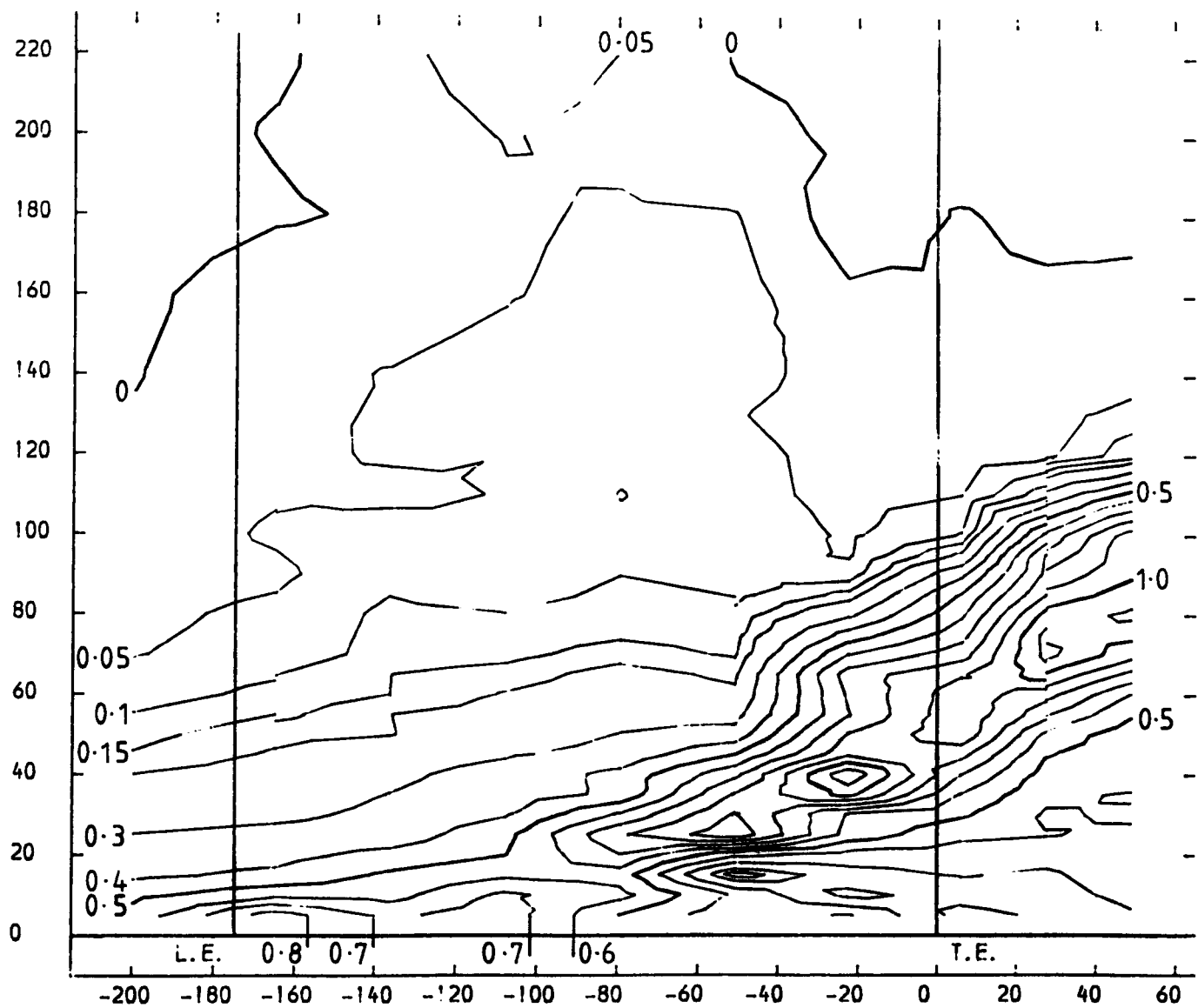


FIGURE 4.138

PLOT APPROXIMATELY 6.7 % OF BLADE PITCH LESS THICKNESS FROM SUCTION SURFACE  
 TOTAL PRESSURE LOSS COEFFICIENT (  $(P_01 - P_{0LOCAL}) / (P_01 - P_1)$  ) CONTOURS  
 X-AXIS AXIAL CO-ORDINATE FROM TRAILING EDGE DATUM (MM)  
 Y-AXIS SPANWISE CO-ORDINATE FROM PERSPEX ENDWALL (MM)

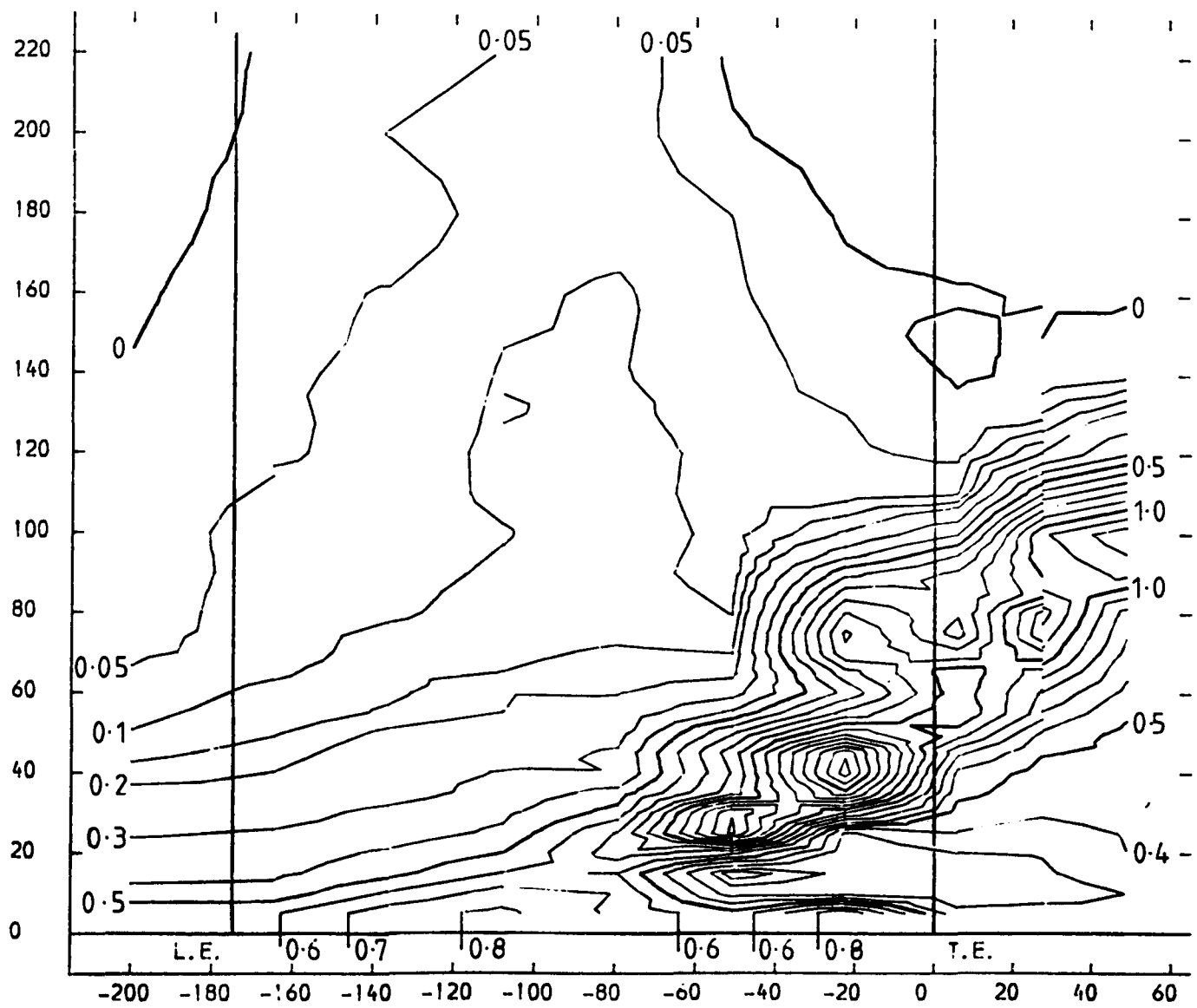


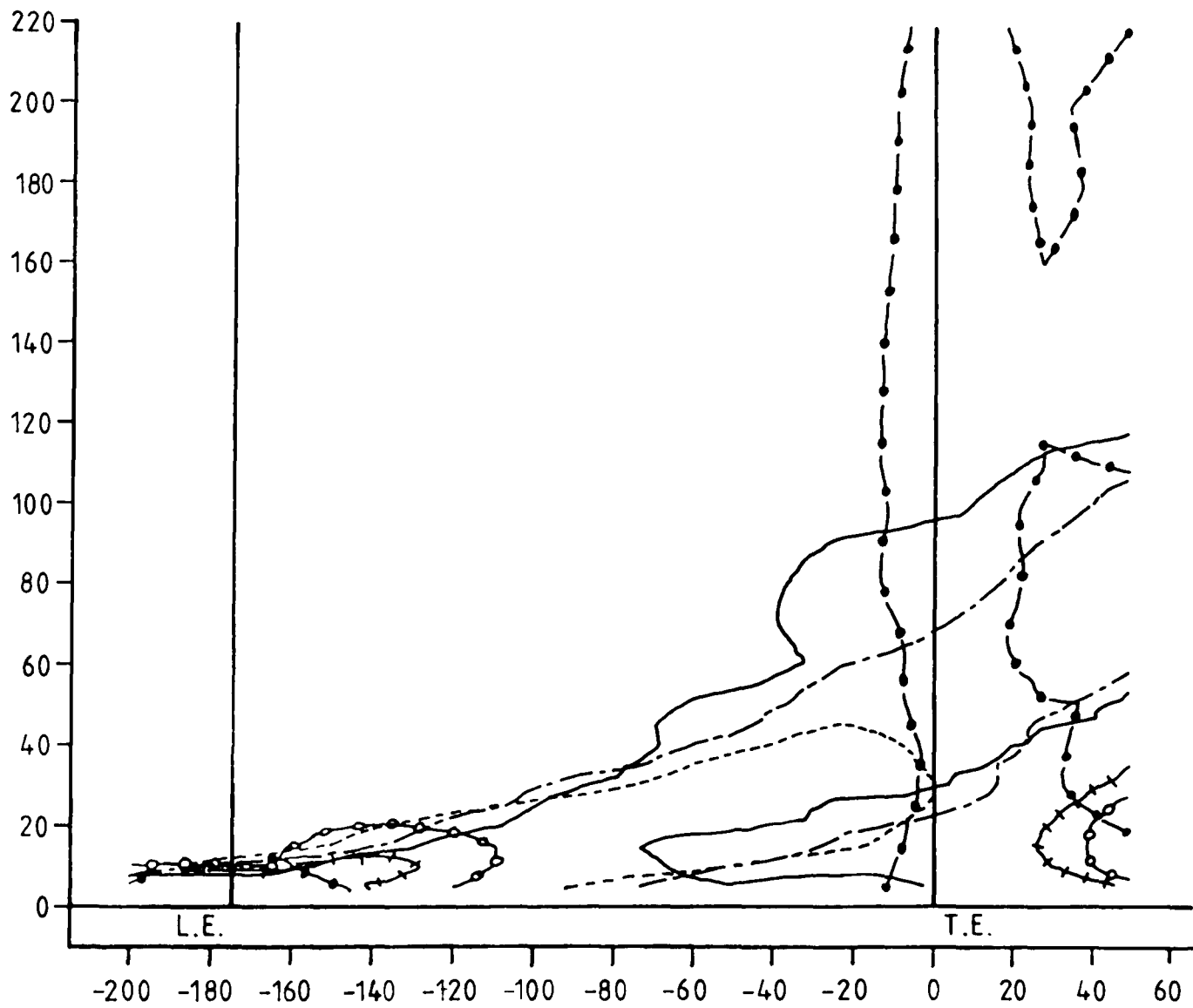
FIGURE 4.139

# SPANWISE MIGRATION OF THE LOSS CORE

X-AXIS AXIAL CO-ORDINATE FROM TRAILING EDGE DATUM (MM)  
Y-AXIS SPANWISE CO-ORDINATE FROM PERSPEX ENDWALL (MM)

PERCENTAGE OF BLADE PITCH LESS  
THICKNESS FROM SUCTION SURFACE

- 85.4
- x-x- 69.7
- 53.9
- - - 38.2
- · - 22.5
- 6.7



PLOT APPROXIMATELY 93.3 % OF BLADE PITCH LESS THICKNESS FROM SUCTION SURFACE  
TOTAL VELOCITY MAGNITUDE CONTOURS (CONTOUR UNITS METRES/SEC)

X-AXIS AXIAL CO-ORDINATE FROM TRAILING EDGE DATUM (MM)  
Y-AXIS SPANWISE CO-ORDINATE FROM PERSPEX ENDWALL (MM)

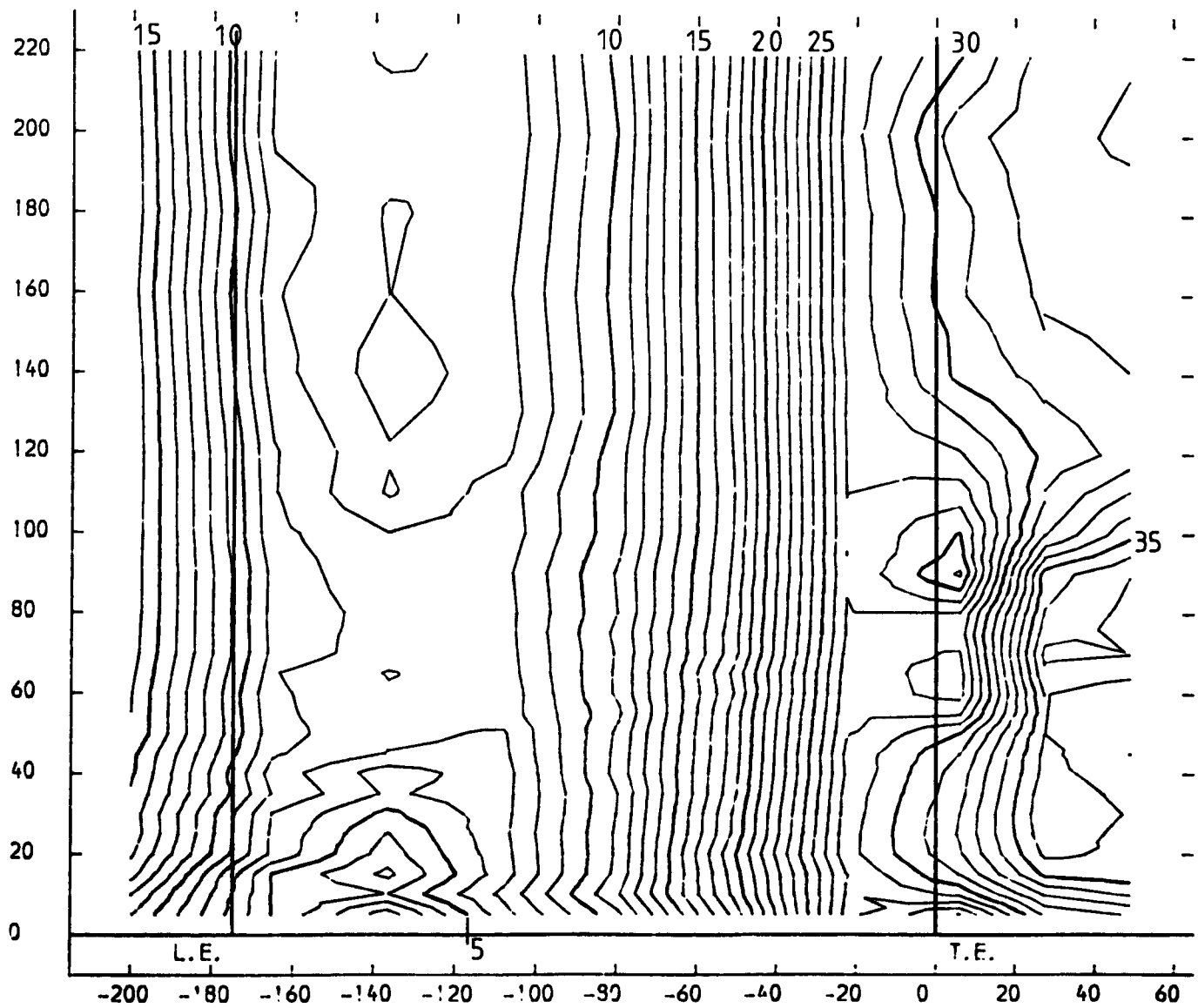


FIGURE 4.141

PLOT APPROXIMATELY 6.7% OF BLADE PITCH LESS THICKNESS FROM SUCTION SURFACE  
TOTAL VELOCITY MAGNITUDE CONTOURS (CONTOUR UNITS METRES/SEC)

X-AXIS AXIAL CO-ORDINATE FROM TRAILING EDGE DATUM (MM)  
Y-AXIS SPANWISE CO-ORDINATE FROM PERSPEX ENDWALL (MM)

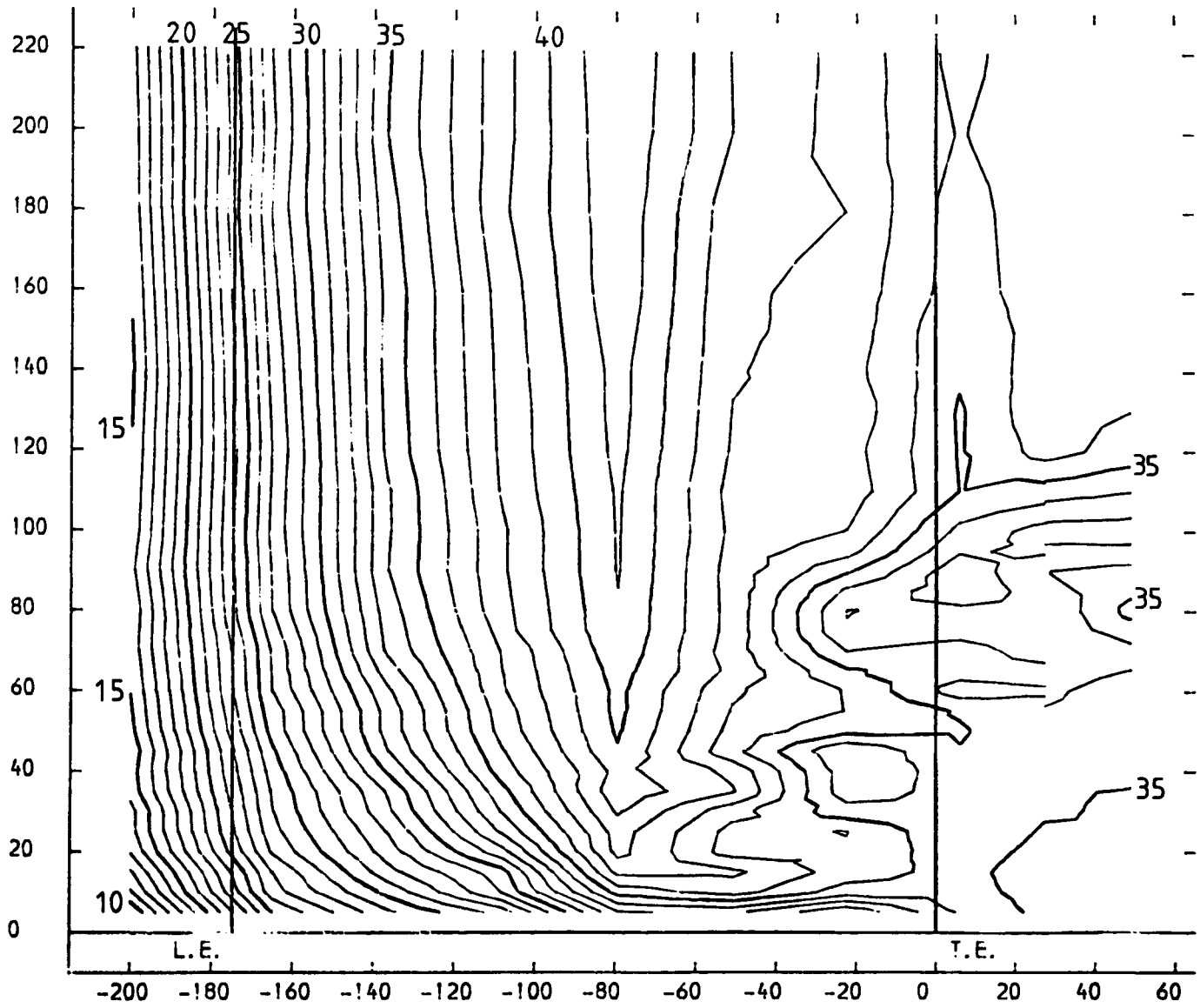


FIGURE 4.142

PLOT APPROXIMATELY 93.3 % OF BLADE PITCH LESS THICKNESS FROM SUCTION SURFACE  
VECTOR PLOT OF AXIAL AND SPANWISE (RADIAL) VELOCITIES

X-AXIS AXIAL CO-ORDINATE FROM TRAILING EDGE DATUM (MM)

Y-AXIS SPANWISE CO-ORDINATE FROM PERSPEX ENDWALL (MM)

VECTOR SCALE 40 METRES/SEC →

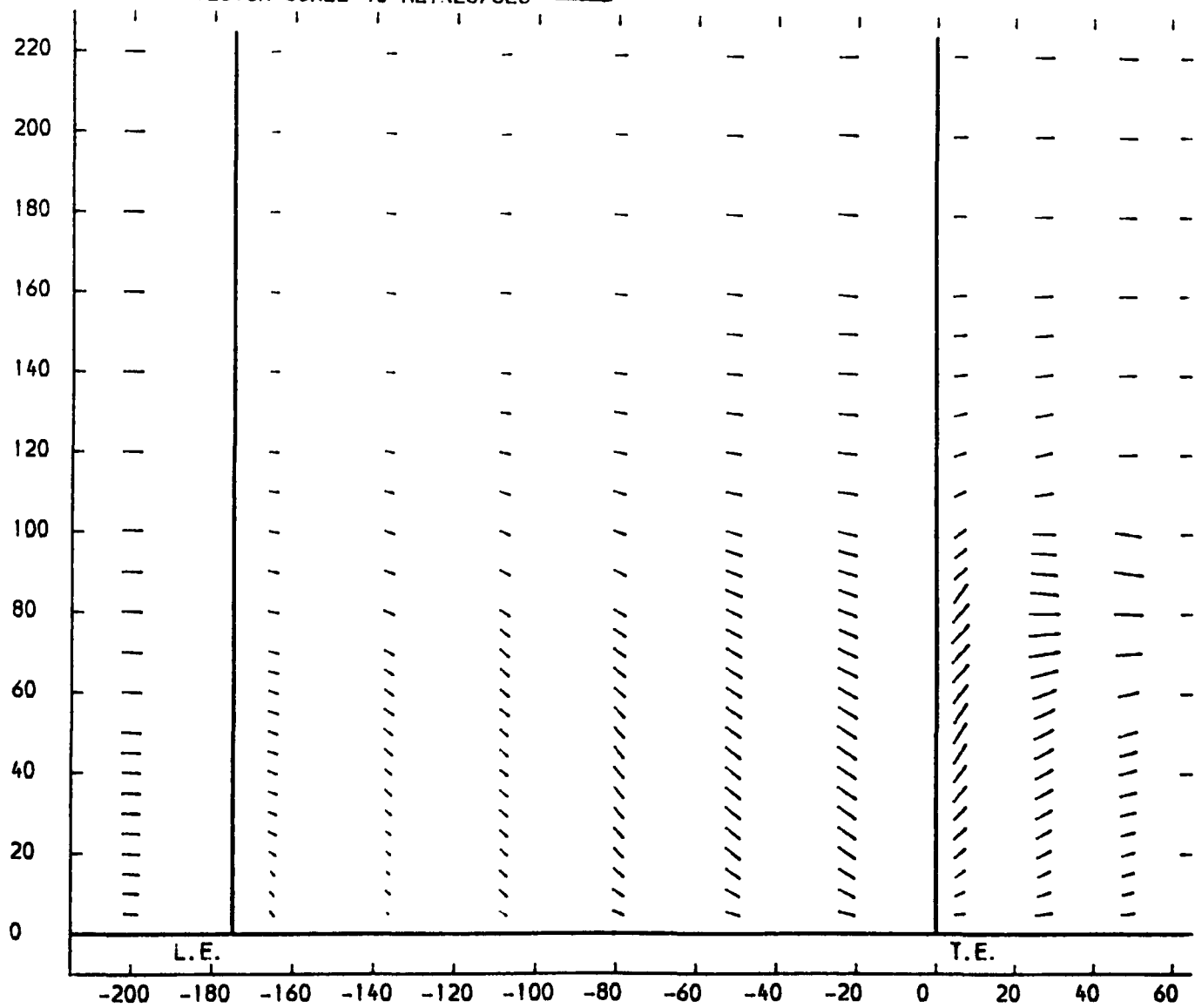


FIGURE 4.143

PLOT APPROXIMATELY 85.4 % OF BLADE PITCH LESS THICKNESS FROM SUCTION SURFACE  
VECTOR PLOT OF AXIAL AND SPANWISE (RADIAL) VELOCITIES

X-AXIS AXIAL CO-ORDINATE FROM TRAILING EDGE DATUM (MM)

Y-AXIS SPANWISE CO-ORDINATE FROM PERSPEX ENDWALL (MM)

VECTOR SCALE 40 METRES/SEC →

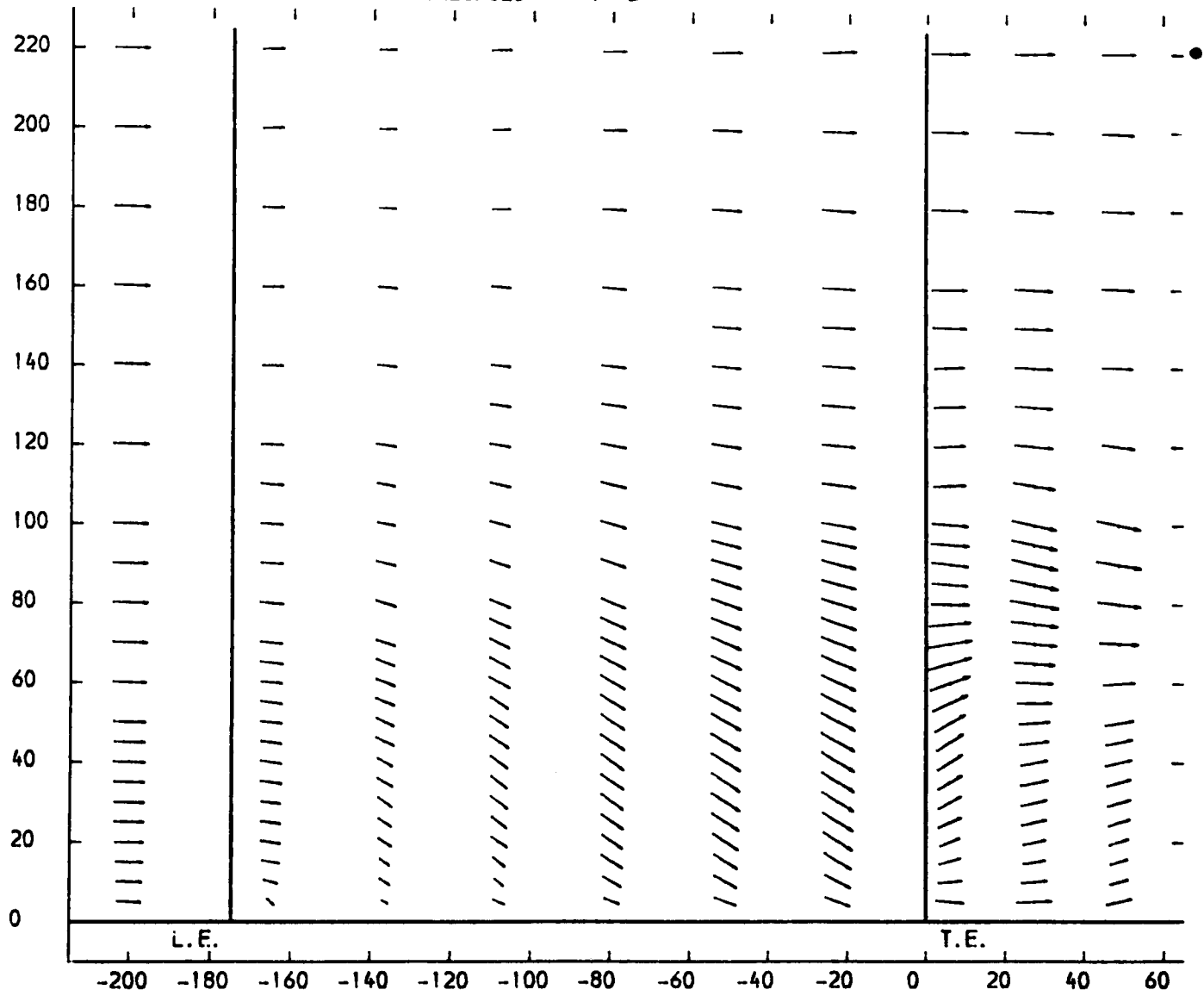


FIGURE 4.144



PLOT APPROXIMATELY 77.5 % OF BLADE PITCH LESS THICKNESS FROM SUCTION SURFACE  
VECTOR PLOT OF AXIAL AND SPANWISE (RADIAL) VELOCITIES

X-AXIS AXIAL CO-ORDINATE FROM TRAILING EDGE DATUM (MM)

Y-AXIS SPANWISE CO-ORDINATE FROM PERSPEX ENDWALL (MM)

VECTOR SCALE 40 METRES/SEC  $\longrightarrow$

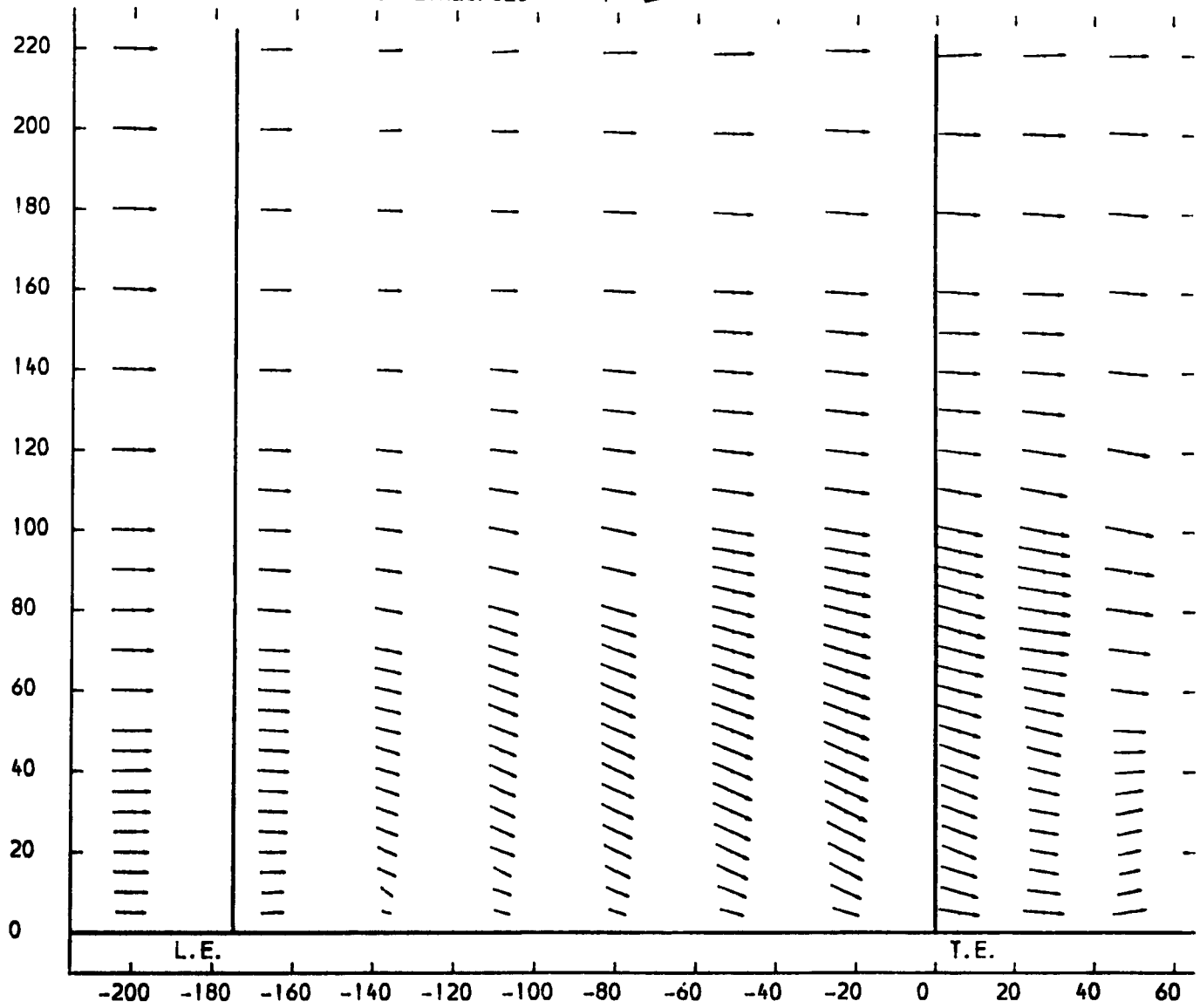


FIGURE 4.145

PLOT APPROXIMATELY 69.7 % OF BLADE PITCH LESS THICKNESS FROM SUCTION SURFACE  
VECTOR PLOT OF AXIAL AND SPANWISE (RADIAL) VELOCITIES

X-AXIS AXIAL CO-ORDINATE FROM TRAILING EDGE DATUM (MM)

Y-AXIS SPANWISE CO-ORDINATE FROM PERSPEX ENDWALL (MM)

VECTOR SCALE 40 METRES/SEC →

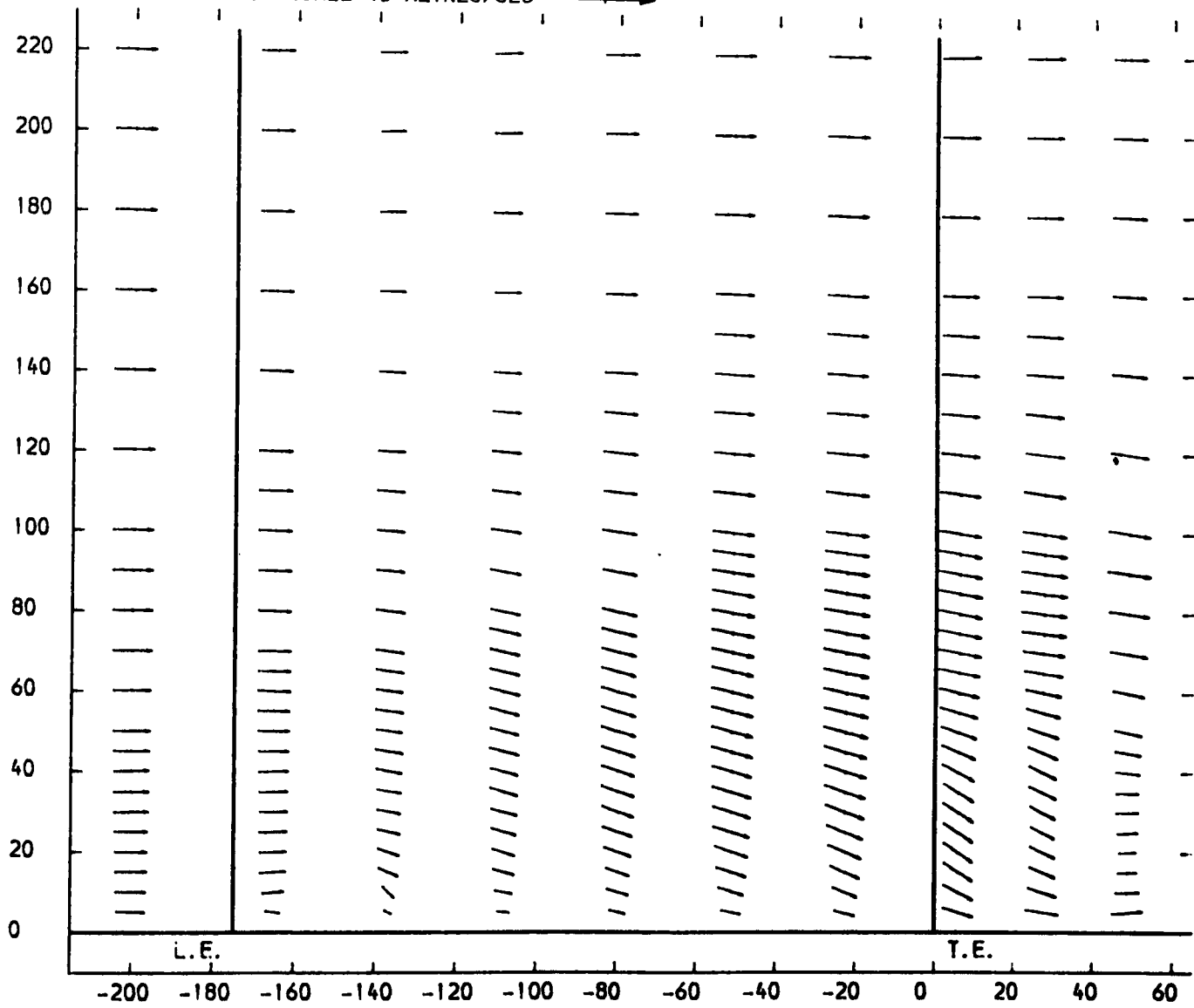


FIGURE 4.146

PLOT APPROXIMATELY 61.8 % OF BLADE PITCH LESS THICKNESS FROM SUCTION SURFACE  
VECTOR PLOT OF AXIAL AND SPANWISE (RADIAL) VELOCITIES

X-AXIS AXIAL CO-ORDINATE FROM TRAILING EDGE DATUM (MM)  
Y-AXIS SPANWISE CO-ORDINATE FROM PERSPEX ENDWALL (MM)  
VECTOR SCALE 40 METRES/SEC →

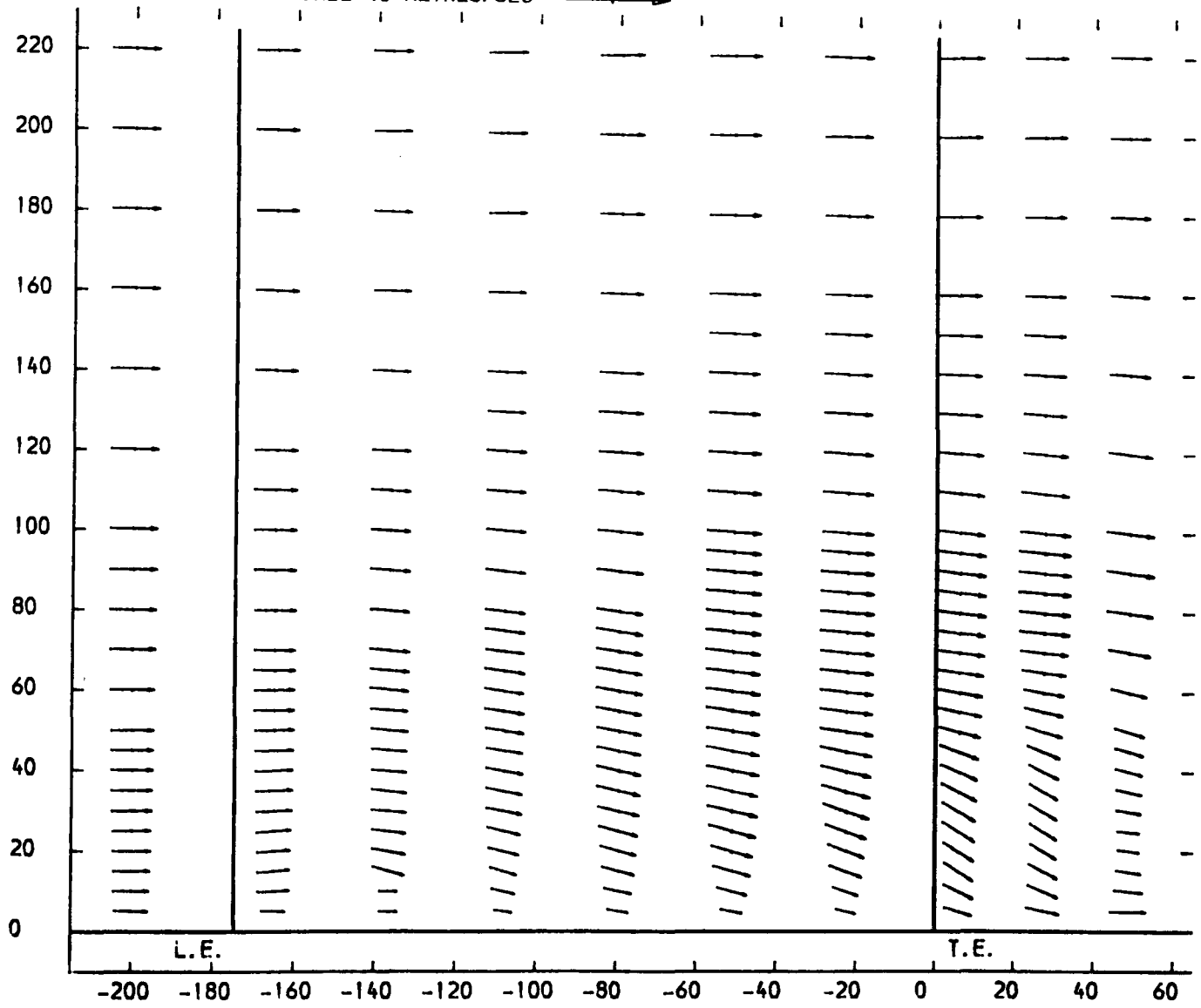


FIGURE 4.147

PLOT APPROXIMATELY 53.9 % OF BLADE PITCH LESS THICKNESS FROM SUCTION SURFACE  
VECTOR PLOT OF AXIAL AND SPANWISE (RADIAL) VELOCITIES

X-AXIS AXIAL CO-ORDINATE FROM TRAILING EDGE DATUM (MM)  
Y-AXIS SPANWISE CO-ORDINATE FROM PERSPEX ENDWALL (MM)  
VECTOR SCALE 40 METRES/SEC →

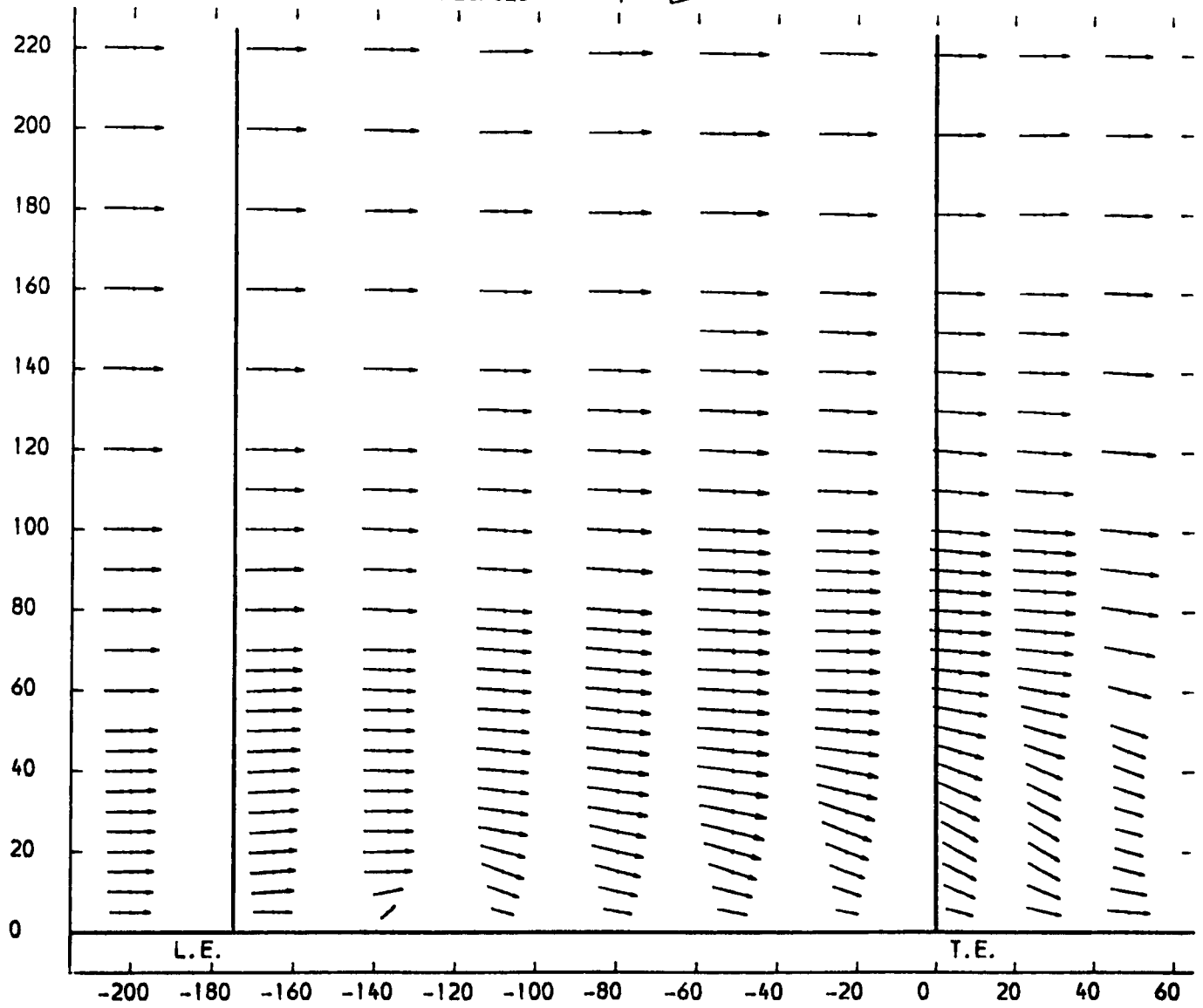


FIGURE 4.148

PLOT APPROXIMATELY 46.1% OF BLADE PITCH LESS THICKNESS FROM SUCTION SURFACE  
VECTOR PLOT OF AXIAL AND SPANWISE (RADIAL) VELOCITIES

X-AXIS AXIAL CO-ORDINATE FROM TRAILING EDGE DATUM (MM)

Y-AXIS SPANWISE CO-ORDINATE FROM PERSPEX ENDWALL (MM)

VECTOR SCALE 40 METRES/SEC  $\longrightarrow$

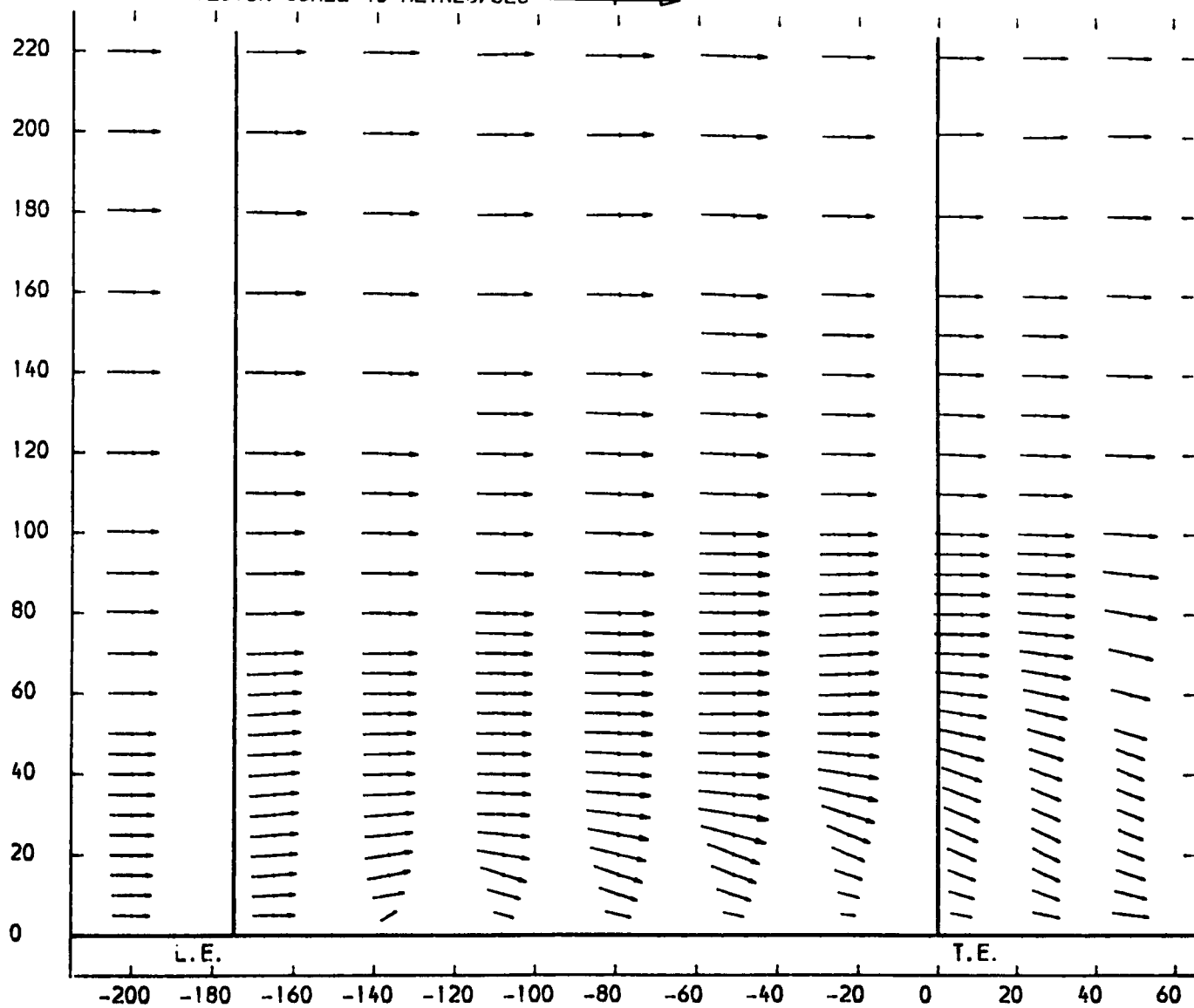
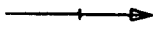


FIGURE 4.149

PLOT APPROXIMATELY 38.2 % OF BLADE PITCH LESS THICKNESS FROM SUCTION SURFACE  
VECTOR PLOT OF AXIAL AND SPANWISE (RADIAL) VELOCITIES

X-AXIS AXIAL CO-ORDINATE FROM TRAILING EDGE DATUM (MM)

Y-AXIS SPANWISE CO-ORDINATE FROM PERSPEX ENDWALL (MM)

VECTOR SCALE 40 METRES/SEC 

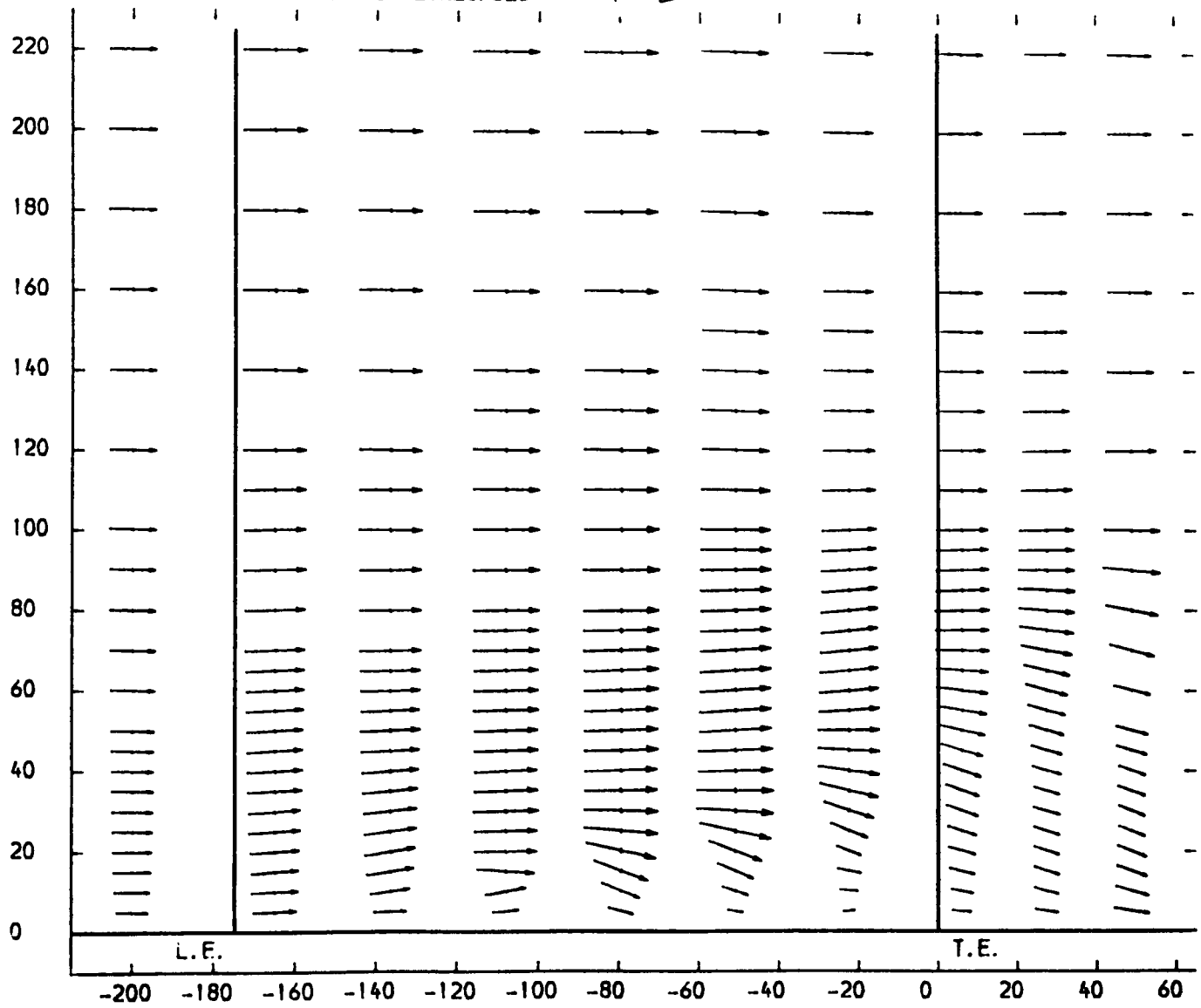


FIGURE 4.150

PLOT APPROXIMATELY 30.3 % OF BLADE PITCH LESS THICKNESS FROM SUCTION SURFACE  
VECTOR PLOT OF AXIAL AND SPANWISE (RADIAL) VELOCITIES

X-AXIS AXIAL CO-ORDINATE FROM TRAILING EDGE DATUM (MM)  
Y-AXIS SPANWISE CO-ORDINATE FROM PERSPEX ENDWALL (MM)  
VECTOR SCALE 40 METRES/SEC

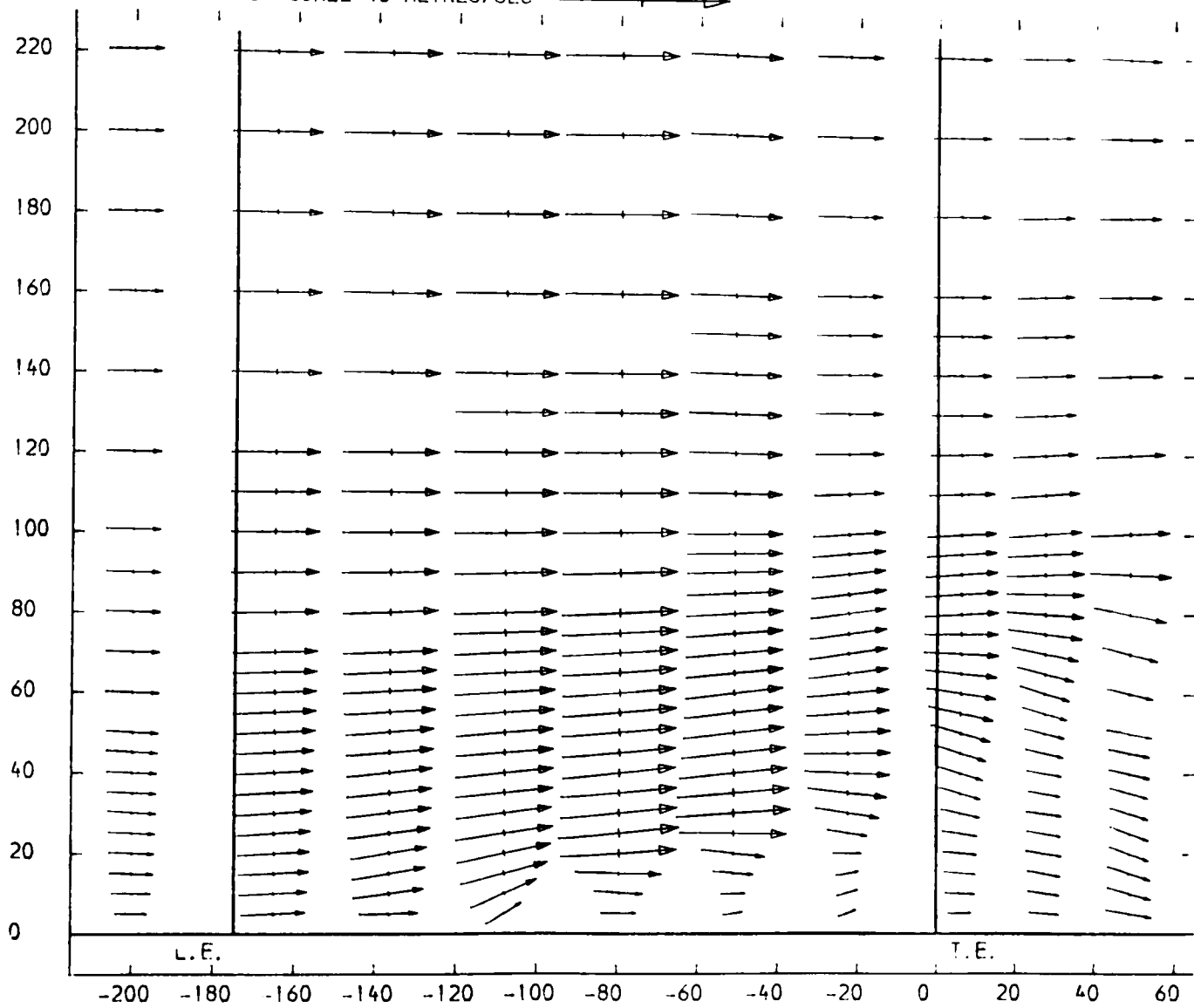


FIGURE 4.151

PLOT APPROXIMATELY 22.5 % OF BLADE PITCH LESS THICKNESS FROM SUCTION SURFACE  
VECTOR PLOT OF AXIAL AND SPANWISE (RADIAL) VELOCITIES

X-AXIS AXIAL CO-ORDINATE FROM TRAILING EDGE DATUM (MM)

Y-AXIS SPANWISE CO-ORDINATE FROM PERSPEX ENDWALL (MM)

VECTOR SCALE 40 METRES/SEC  $\longrightarrow$

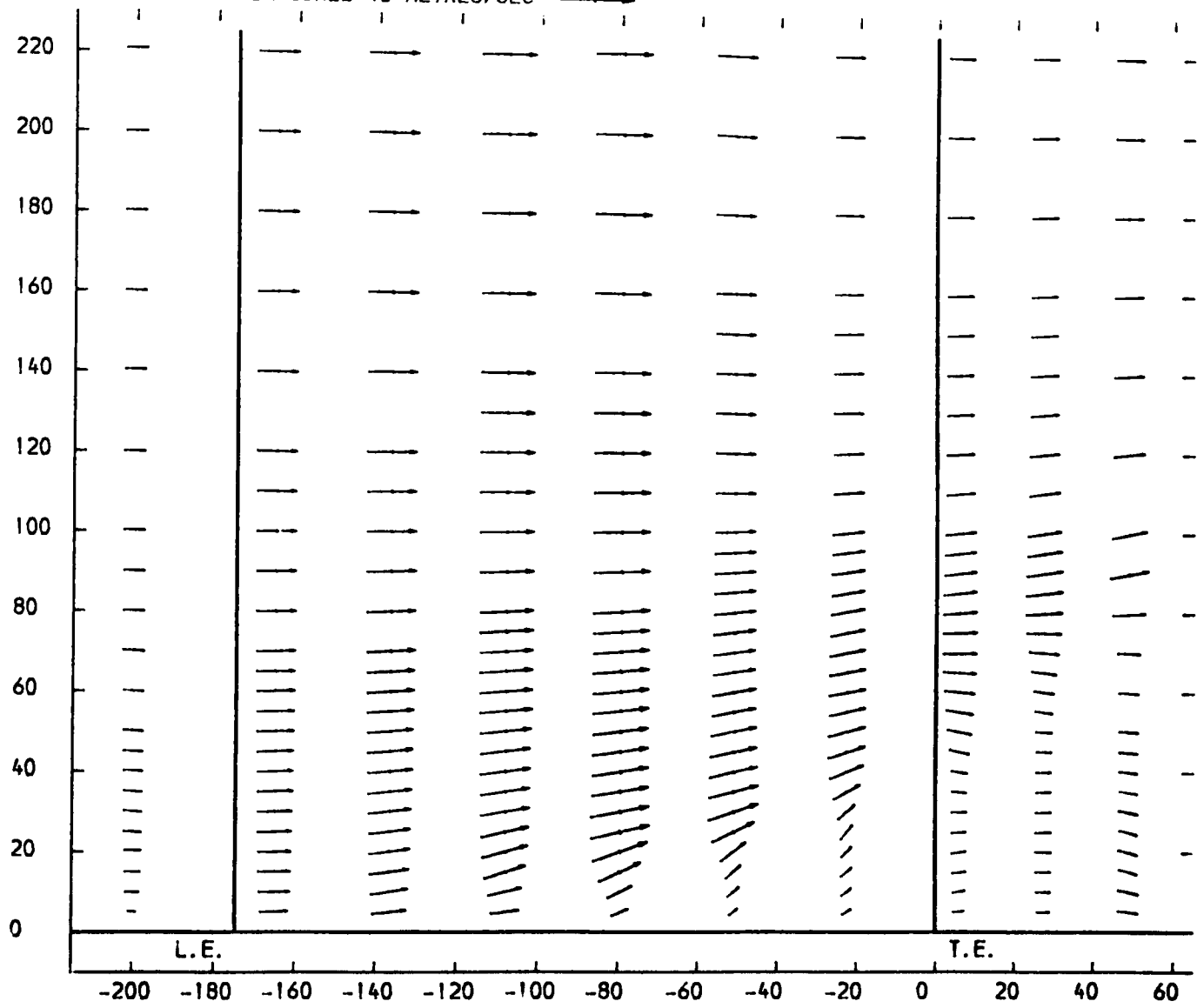



FIGURE 4.152



PLOT APPROXIMATELY 14.6 % OF BLADE PITCH LESS THICKNESS FROM SUCTION SURFACE  
VECTOR PLOT OF AXIAL AND SPANWISE (RADIAL) VELOCITIES

X-AXIS AXIAL CO-ORDINATE FROM TRAILING EDGE DATUM (MM)

Y-AXIS SPANWISE CO-ORDINATE FROM PERSPEX ENDWALL (MM)

VECTOR SCALE 40 METRES/SEC 

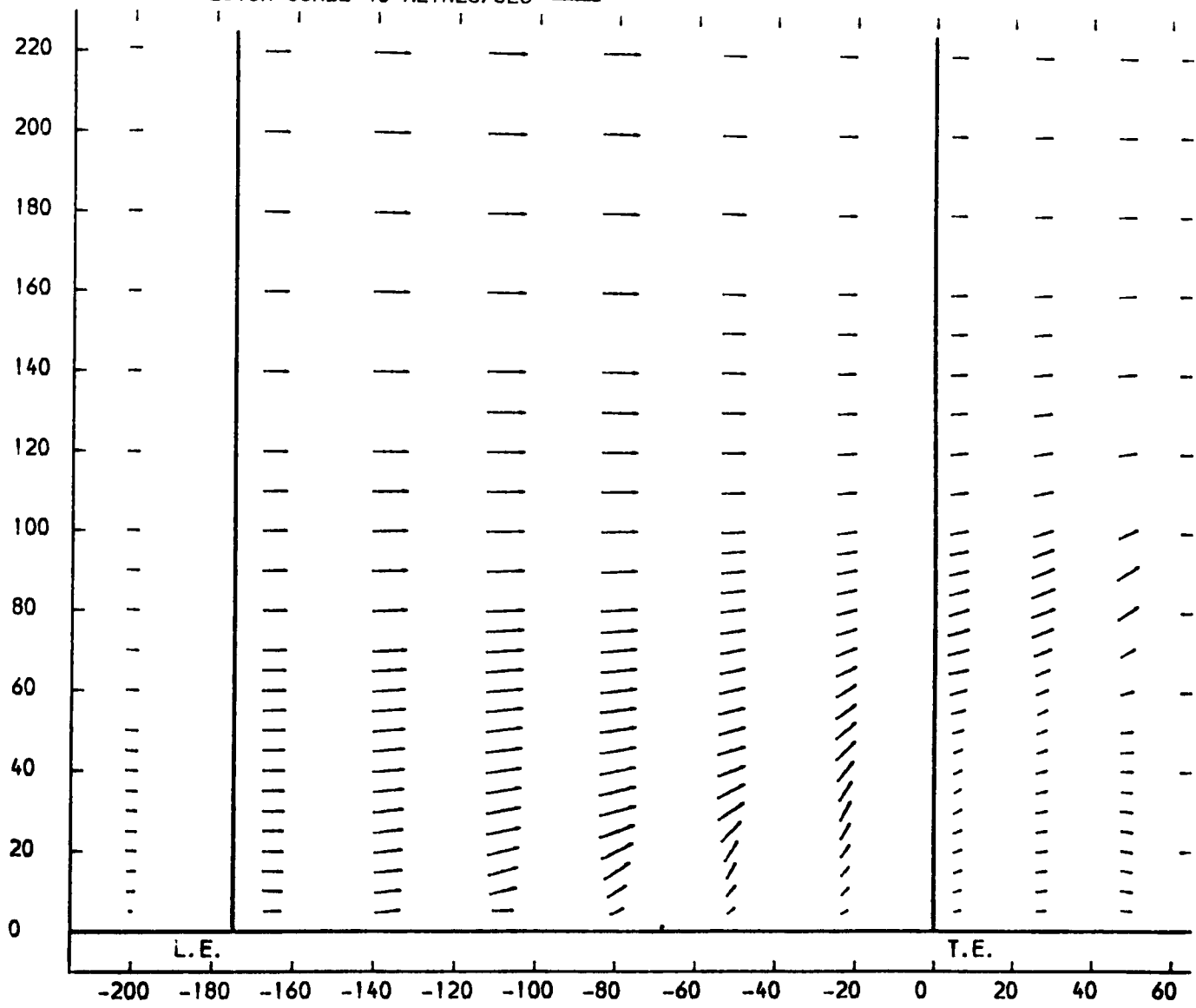


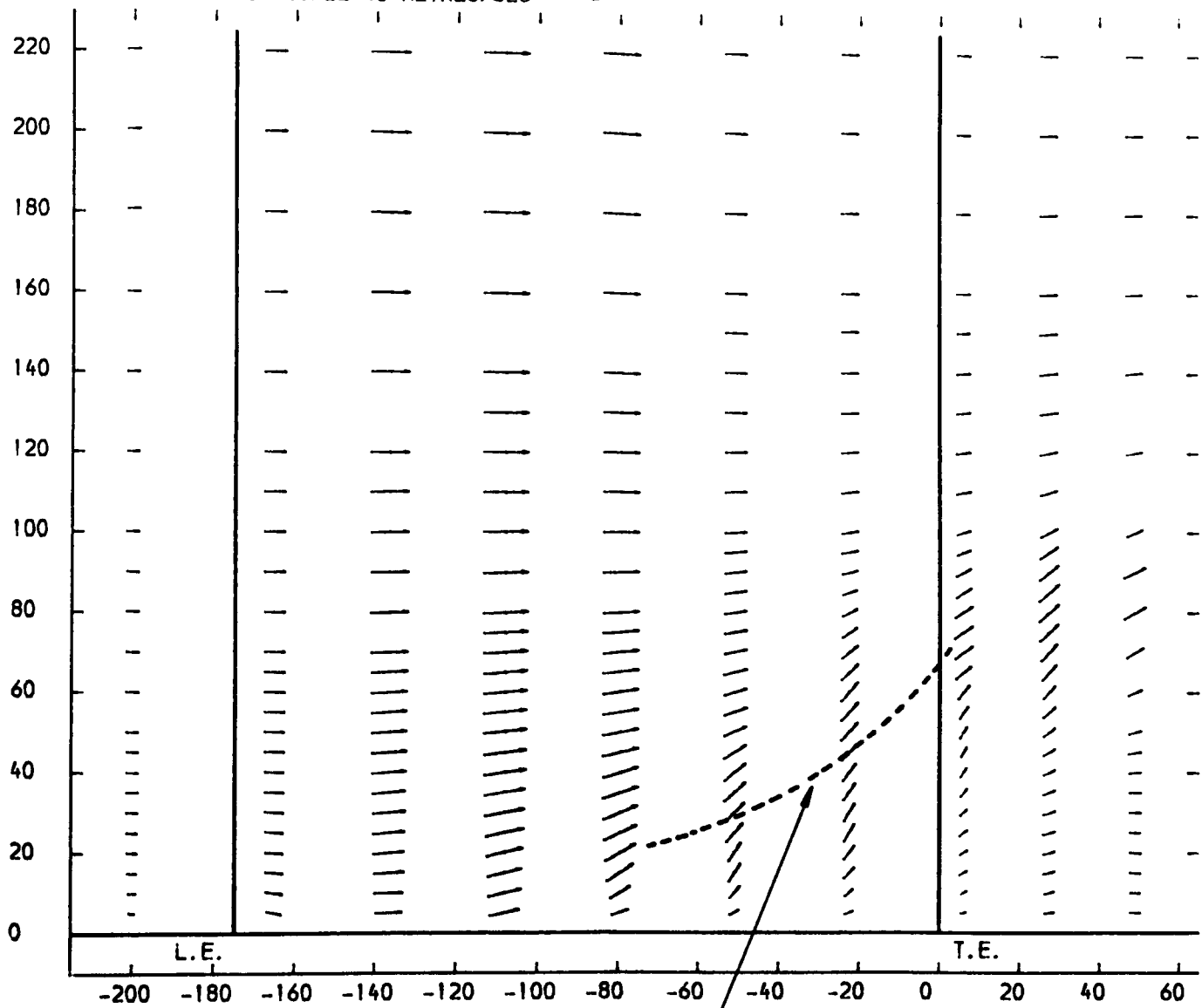
FIGURE 4.153

PLOT APPROXIMATELY 6.7 % OF BLADE PITCH LESS THICKNESS FROM SUCTION SURFACE  
VECTOR PLOT OF AXIAL AND SPANWISE (RADIAL) VELOCITIES

X-AXIS AXIAL CO-ORDINATE FROM TRAILING EDGE DATUM (MM)

Y-AXIS SPANWISE CO-ORDINATE FROM PERSPEX ENDWALL (MM)

VECTOR SCALE 40 METRES/SEC  $\rightarrow$



SPECULATIVE SUCTION SURFACE  
SEPARATION LINE

FIGURE 4.154

PLOT APPROXIMATELY 6.7 % OF BLADE PITCH LESS THICKNESS FROM SUCTION SURFACE  
YAW ANGLE CONTOURS (CONTOUR UNITS DEGREES)

X-AXIS AXIAL CO-ORDINATE FROM TRAILING EDGE DATUM (MM)  
Y-AXIS SPANWISE CO-ORDINATE FROM PERSPEX ENDWALL (MM)

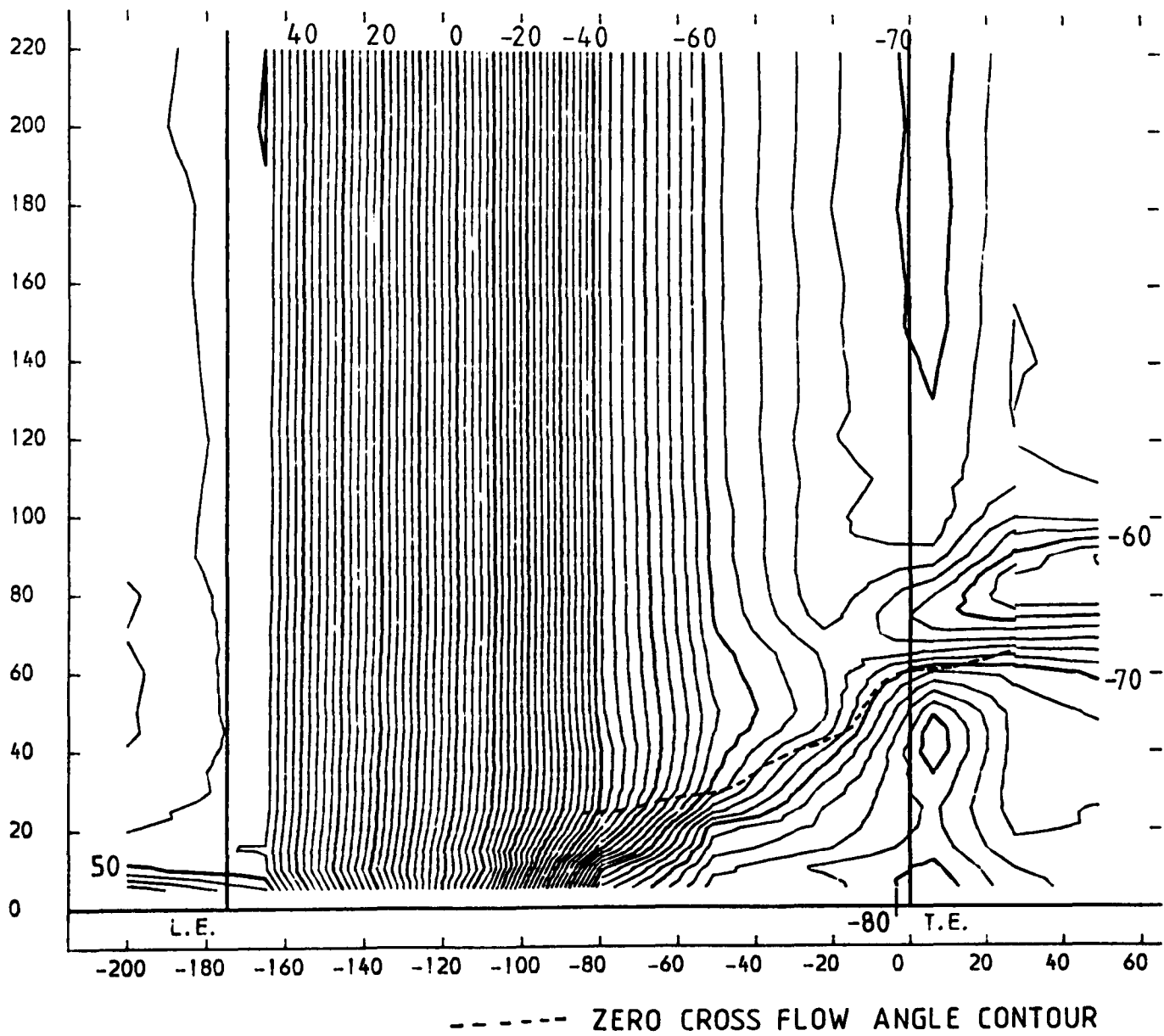


FIGURE 4.155

# ZERO CROSS FLOW ANGLE CONTOURS CLOSE TO THE BLADE SUCTION SURFACE

X-AXIS AXIAL CO-ORDINATE FROM TRAILING EDGE DATUM (MM)  
Y-AXIS SPANWISE CO-ORDINATE FROM PERSPEX ENDWALL (MM)

PERCENTAGE OF BLADE PITCH LESS THICKNESS FROM SUCTION SURFACE

- 30.3
- 22.5
- · - · 14.6
- 6.7

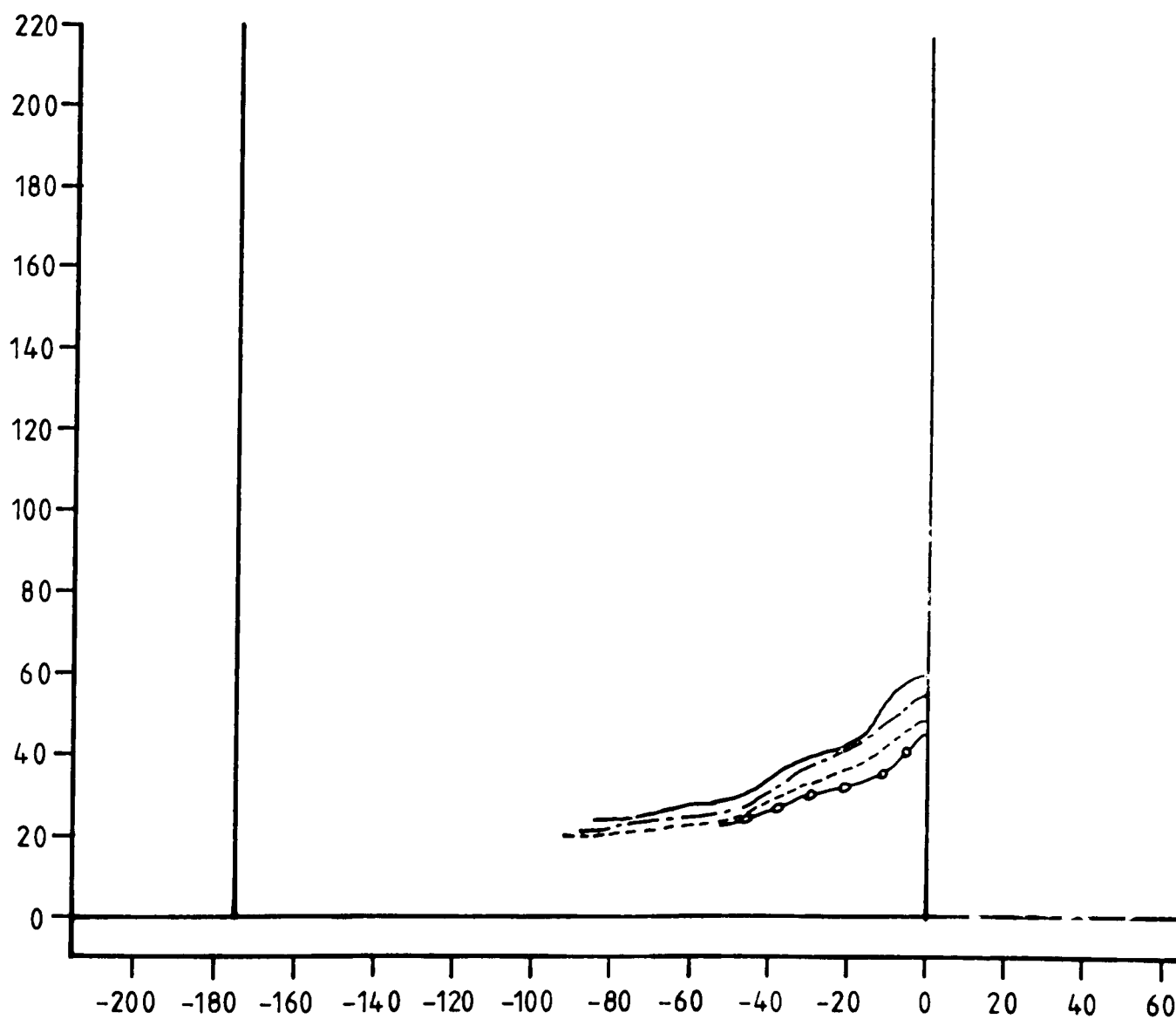


FIGURE 4.156

PLOT APPROXIMATELY 93.3 % OF BLADE PITCH LESS THICKNESS FROM SUCTION SURFACE  
STATIC PRESSURE COEFFICIENT (  $(P_1 - P_{LOCAL}) / (P_0 - P_1)$  ) CONTOURS

X-AXIS AXIAL CO-ORDINATE FROM TRAILING EDGE DATUM (MM)  
Y-AXIS SPANWISE CO-ORDINATE FROM PERSPEX ENDWALL (MM)

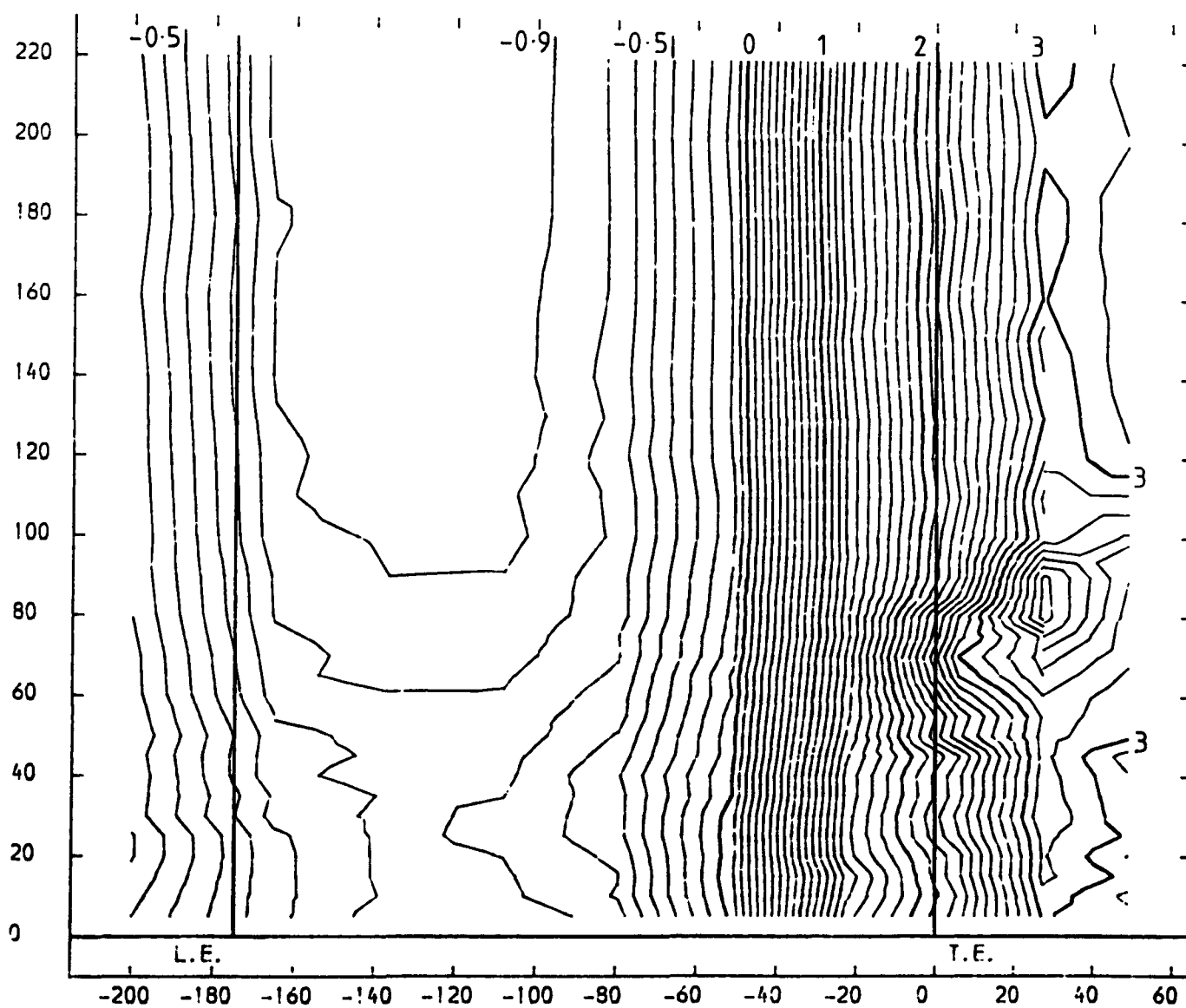


FIGURE 4.157

PLOT APPROXIMATELY 53.9 % OF BLADE PITCH LESS THICKNESS FROM SUCTION SURFACE  
STATIC PRESSURE COEFFICIENT (  $(P1-LOCAL)/(P01-P1)$  ) CONTOURS

X-AXIS AXIAL CO-ORDINATE FROM TRAILING EDGE DATUM (MM)  
Y-AXIS SPANWISE CO-ORDINATE FROM PERSPEX ENDWALL (MM)

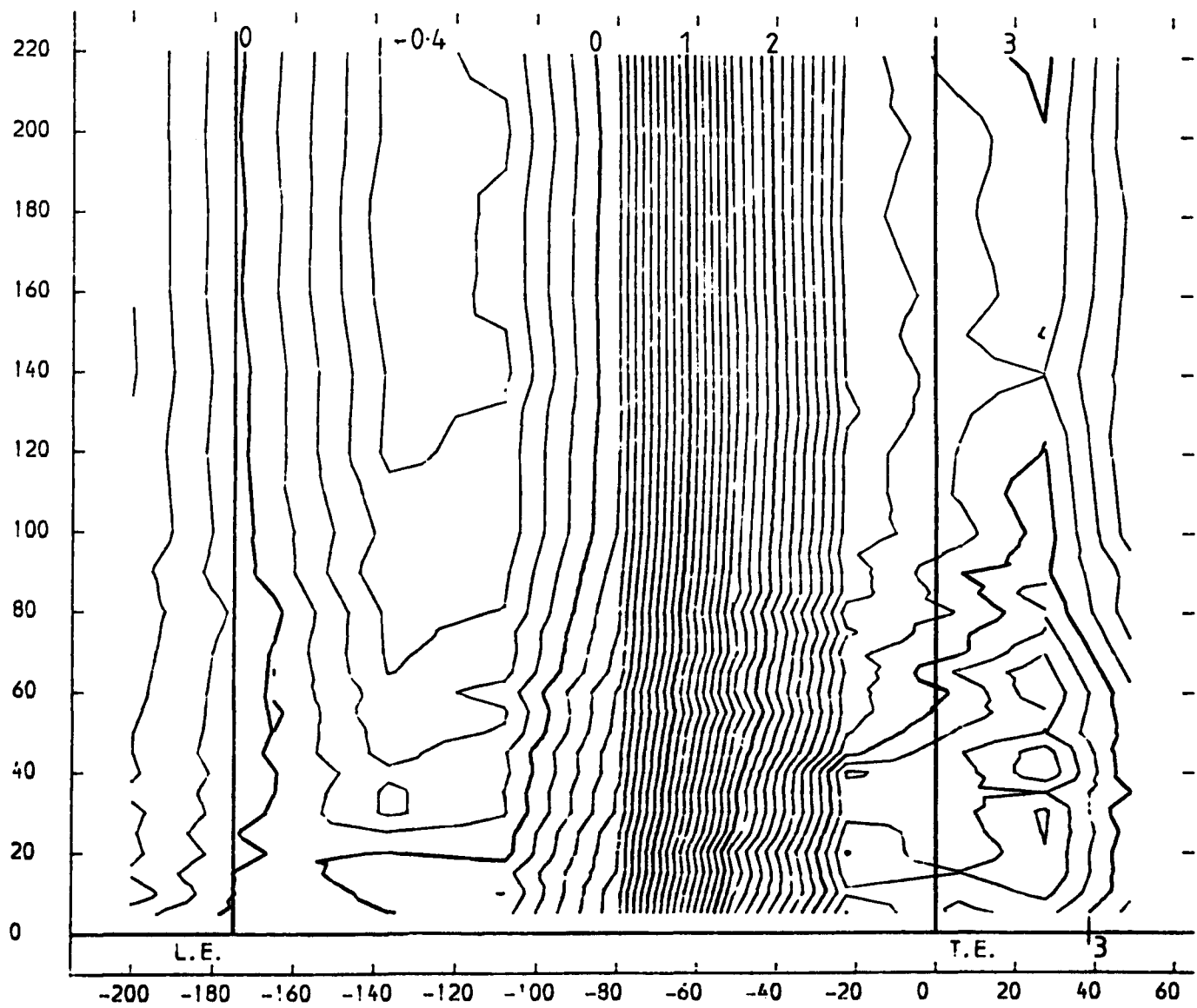


FIGURE 4.158

PLOT APPROXIMATELY 38.2 % OF BLADE PITCH LESS THICKNESS FROM SUCTION SURFACE  
STATIC PRESSURE COEFFICIENT (  $(P_1 - P_{LOCAL}) / (P_0 - P_1)$  ) CONTOURS

X-AXIS AXIAL CO-ORDINATE FROM TRAILING EDGE DATUM (MM)  
Y-AXIS SPANWISE CO-ORDINATE FROM PERSPEX ENDWALL (MM)

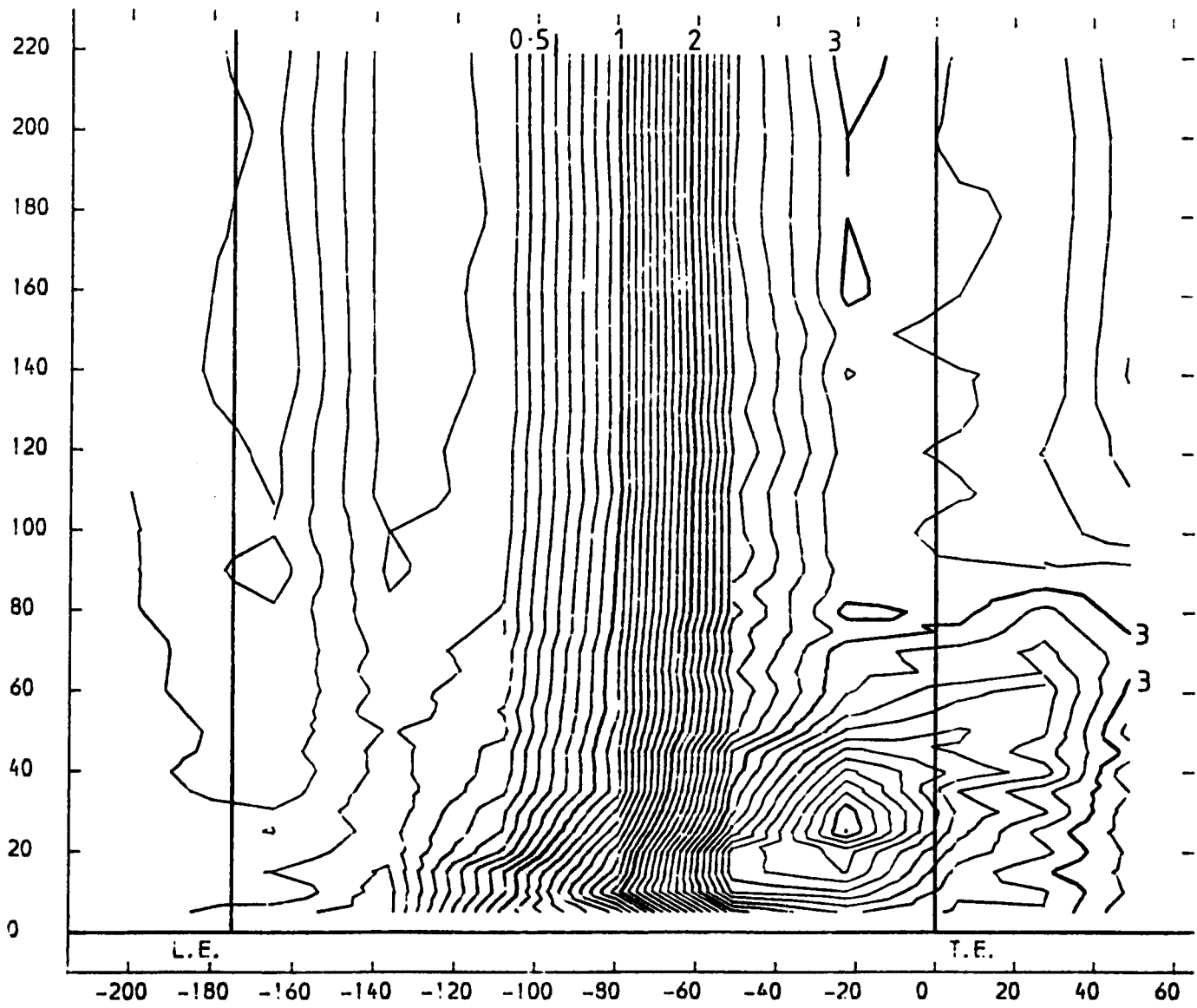


FIGURE 4.159

PLOT APPROXIMATELY 22.5 % OF BLADE PITCH LESS THICKNESS FROM SUCTION SURFACE  
STATIC PRESSURE COEFFICIENT (  $(P1-LOCAL)/(P01-P1)$  ) CONTOURS

X-AXIS AXIAL CO-ORDINATE FROM TRAILING EDGE DATUM (MM)  
Y-AXIS SPANWISE CO-ORDINATE FROM PERSPEX ENDWALL (MM)

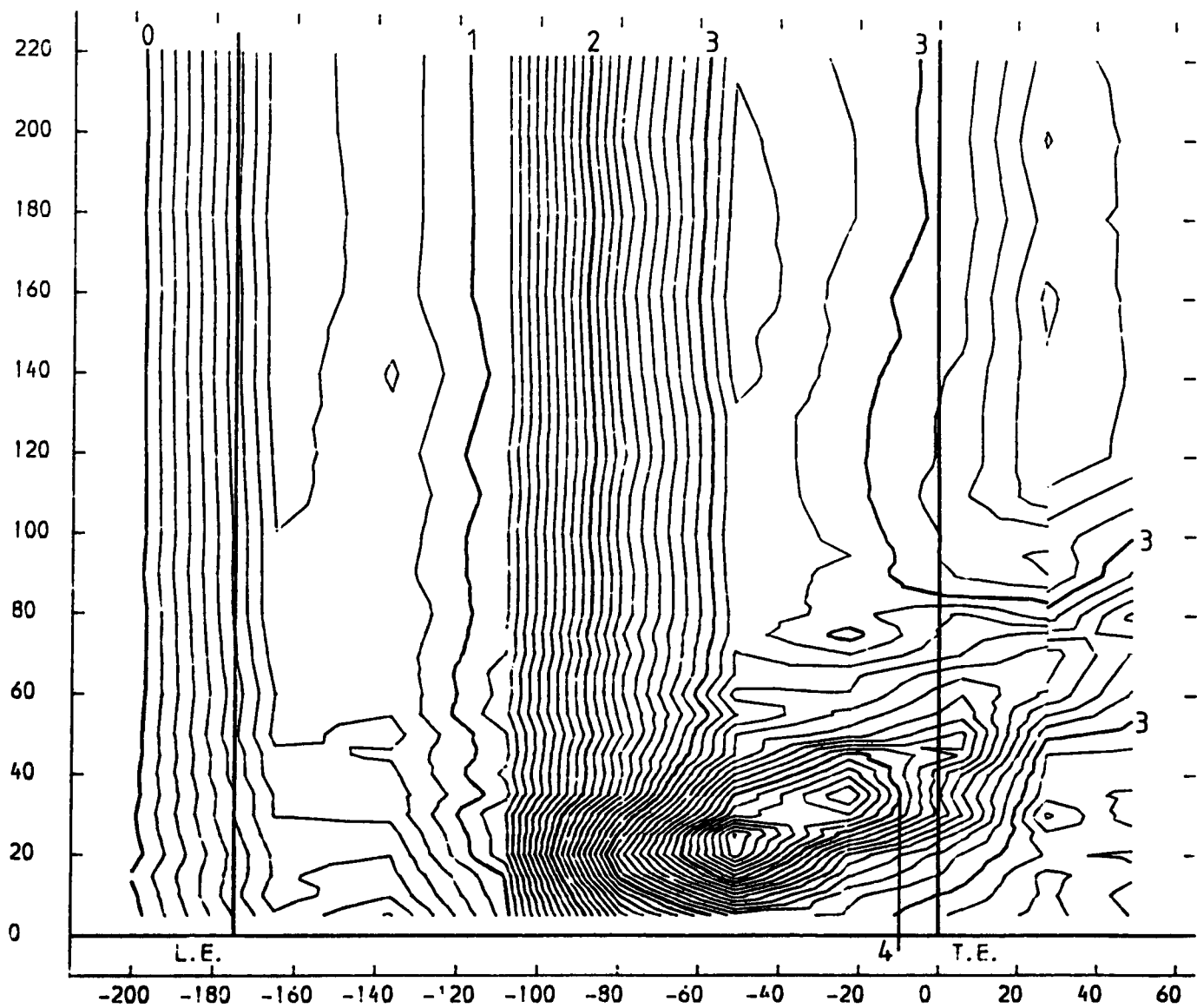


FIGURE 4.160



PLOT APPROXIMATELY 6.7 % OF BLADE PITCH LESS THICKNESS FROM SUCTION SURFACE  
STATIC PRESSURE COEFFICIENT (  $(P_1 - P_{LOCAL}) / (P_0 - P_1)$  ) CONTOURS

X-AXIS AXIAL CO-ORDINATE FROM TRAILING EDGE DATUM (MM)  
Y-AXIS SPANWISE CO-ORDINATE FROM PERSPEX ENDWALL (MM)

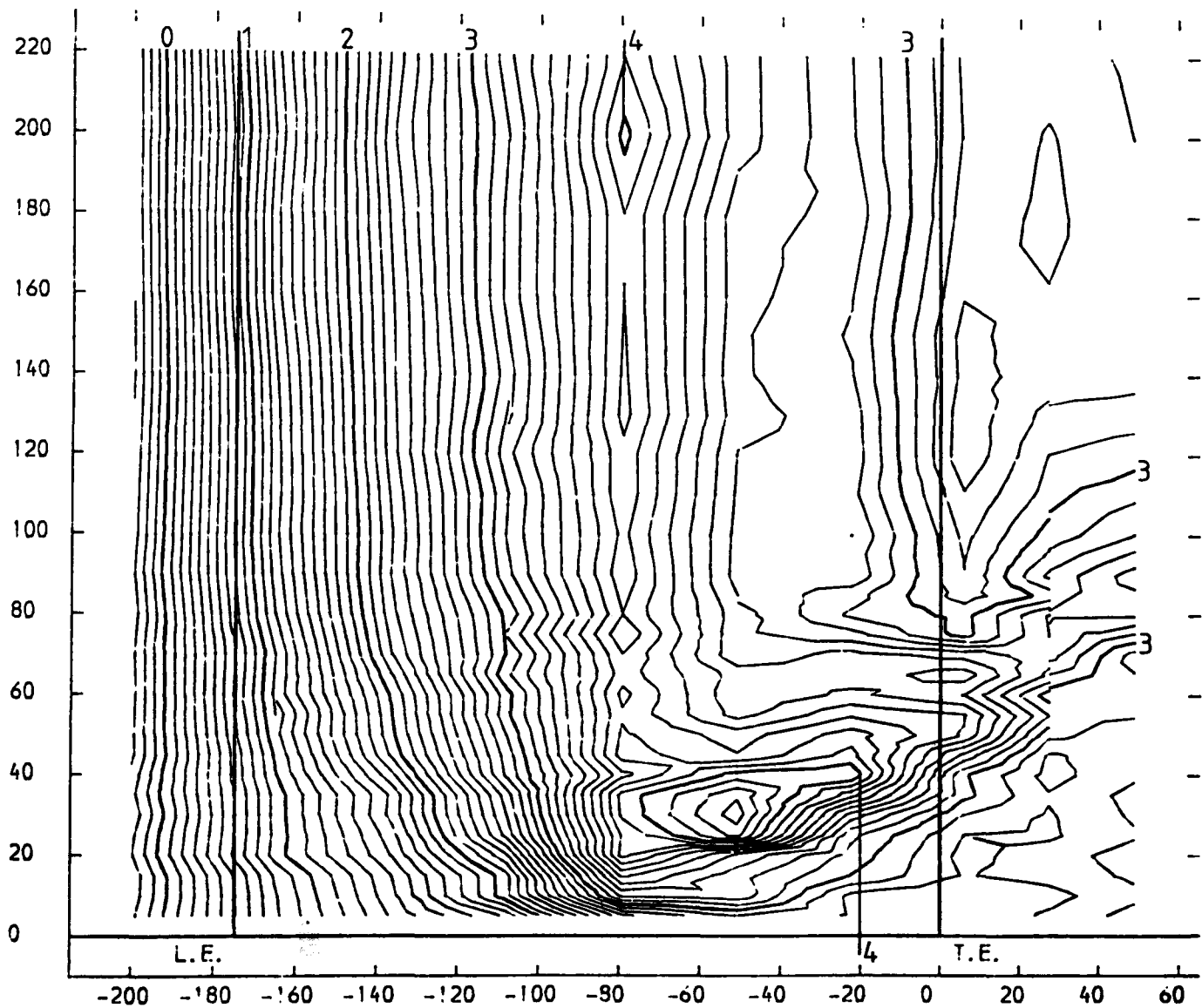


FIGURE 4.161

BLADE SURFACE STATIC PRESSURE COEFFICIENT DISTRIBUTION  
 (SHOWING DATA FROM ADJACENT PASSAGES)  
 NATURAL BOUNDARY LAYER DATA

X-AXIS AXIAL CO-ORDINATE FROM TRAILING EDGE DATUM (MM)

Y-AXIS STATIC PRESSURE COEFFICIENT (  $(P1 - P_{LOCAL}) / (P01 - P1)$  )

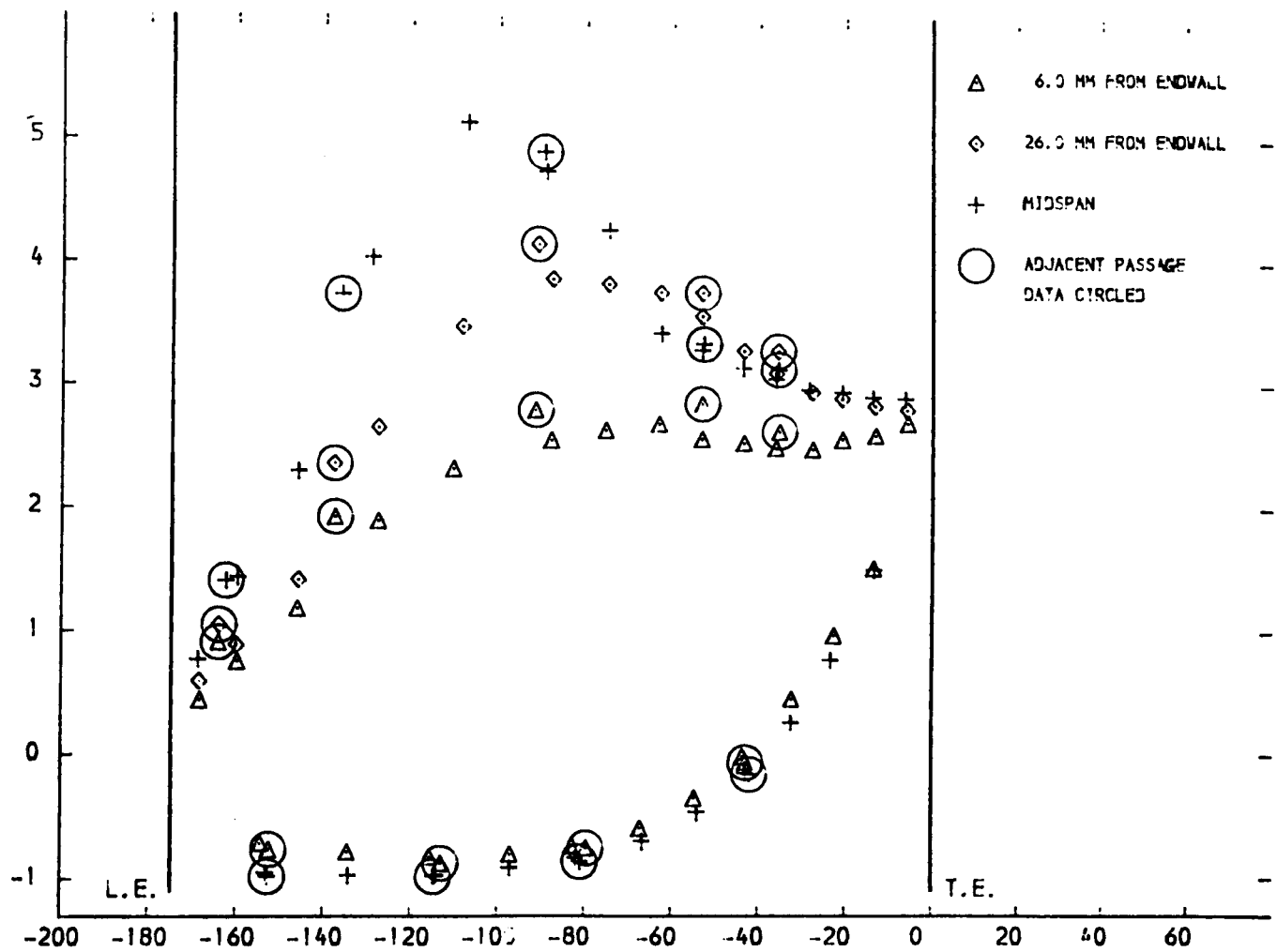


FIGURE 4.162

BLADE SURFACE STATIC PRESSURE COEFFICIENT DISTRIBUTION

NATURAL BOUNDARY LAYER DATA

X-AXIS AXIAL CO-ORDINATE FROM TRAILING EDGE DATUM (MM)

Y-AXIS STATIC PRESSURE COEFFICIENT (  $(P1-PL_{CAL}) / (P01-P1)$  )

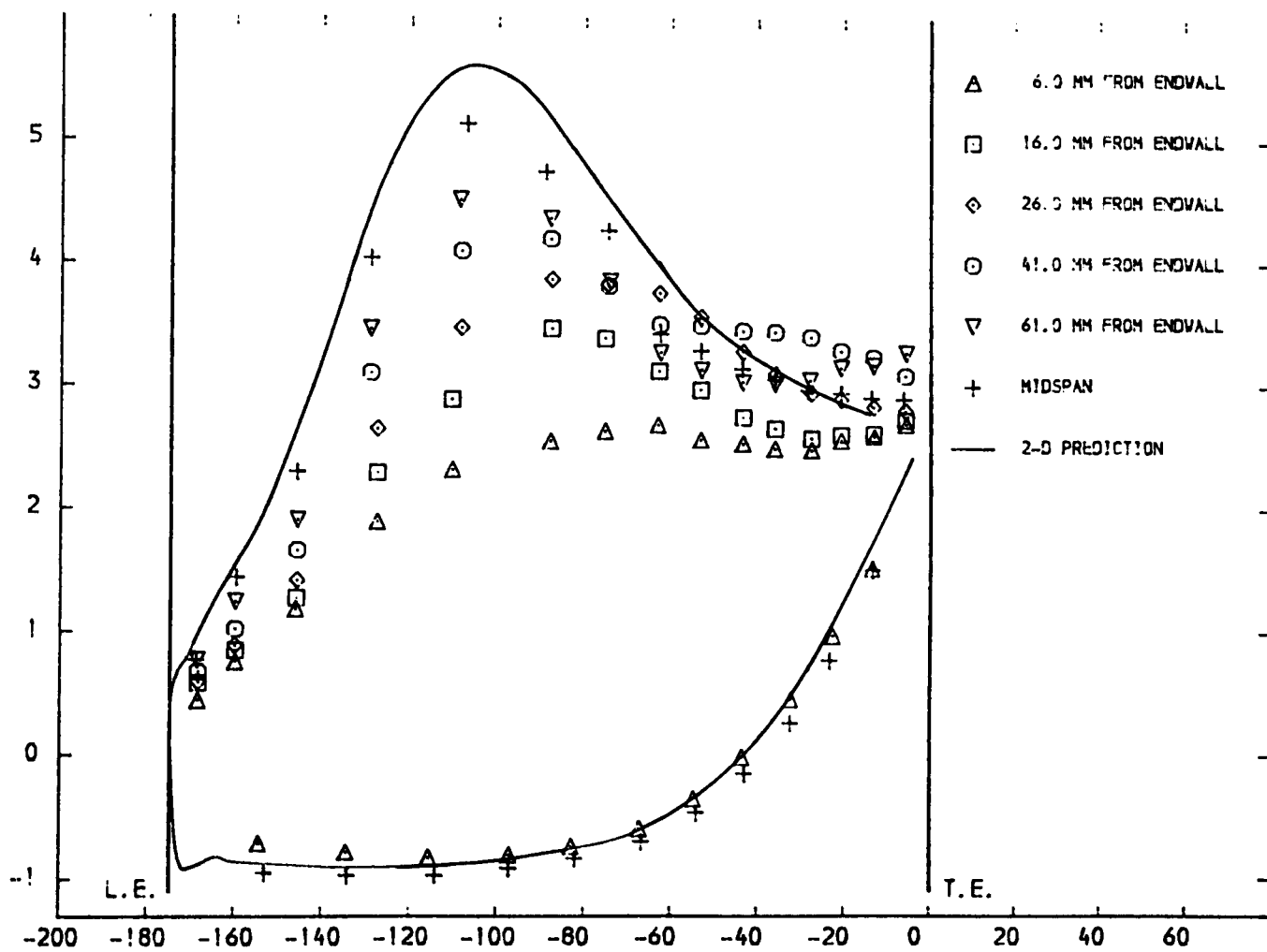


FIGURE 4.163

PLOT ON BLADE PRESSURE SURFACE

LOCATION OF BLADE SURFACE STATIC PRESSURE TAPPINGS

X-AXIS AXIAL CO-ORDINATE FROM TRAILING EDGE DATUM (MM)

Y-AXIS SPANWISE CO-ORDINATE FROM PERSPEX ENDWALL (MM)

+ SPANWISE DATA FROM PERSPEX WALL x SPANWISE DATA FROM SLOTTED WALL

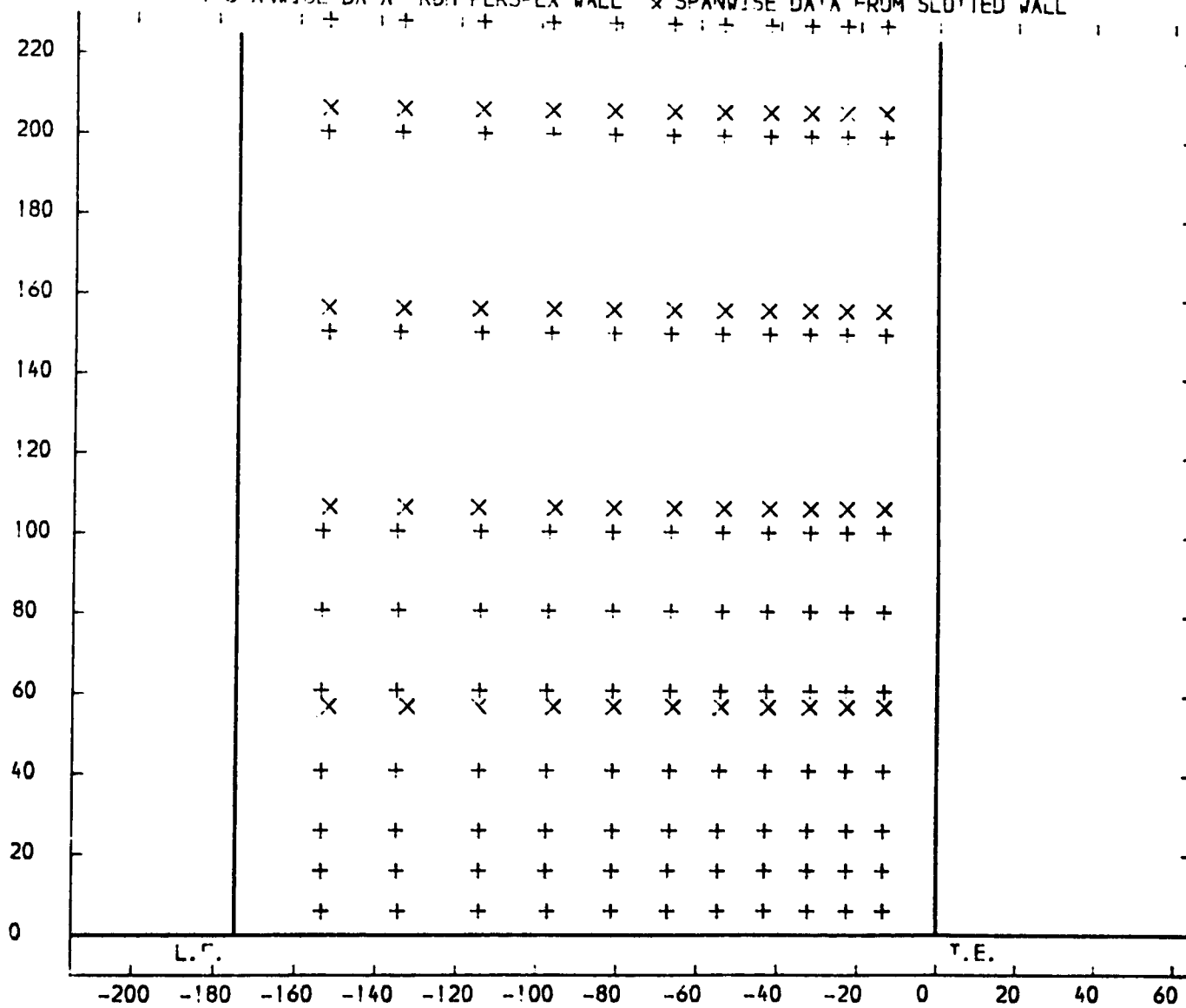


FIGURE 4.164

PLOT ON BLADE SUCTION SURFACE

LOCATION OF BLADE SURFACE STATIC PRESSURE TAPPINGS

X-AXIS AXIAL CO-ORDINATE FROM TRAILING EDGE DATUM (MM)

Y-AXIS SPANWISE CO-ORDINATE FROM PERSPEX ENDWALL (MM)

+ SPANWISE DATA FROM PERSPEX WALL x SPANWISE DATA FROM SLOTTED WALL

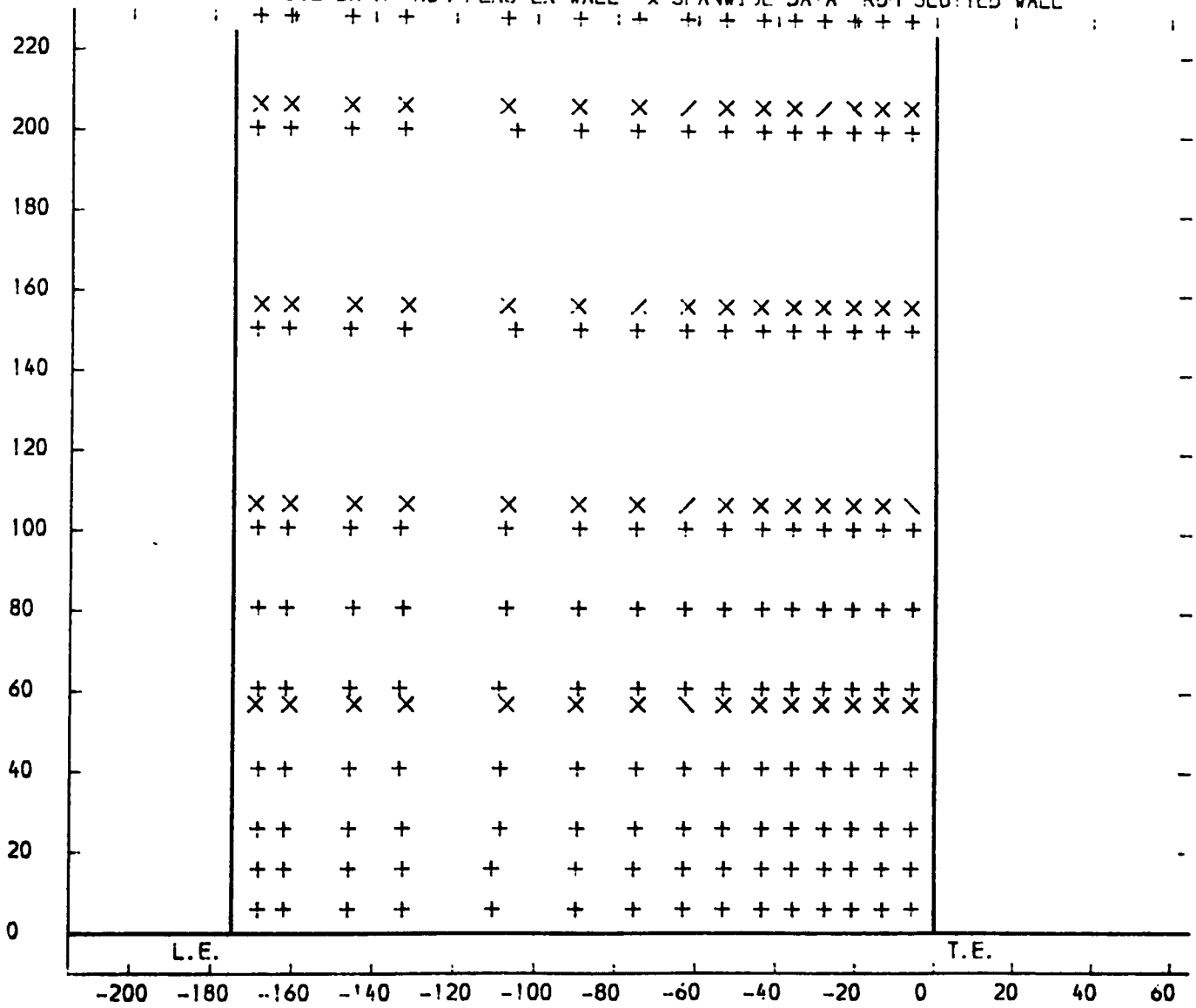


FIGURE 4.165

PLOT ON BLADE PRESSURE SURFACE NATURAL BOUNDARY LAYER DATA  
STATIC PRESSURE COEFFICIENT (  $(P_1 - P_{LOCAL}) / (P_0 - P_1)$  ) CONTOURS

X-AXIS AXIAL CO-ORDINATE FROM TRAILING EDGE DATUM (MM)  
Y-AXIS SPANWISE CO-ORDINATE FROM PERSPEX ENDWALL (MM)

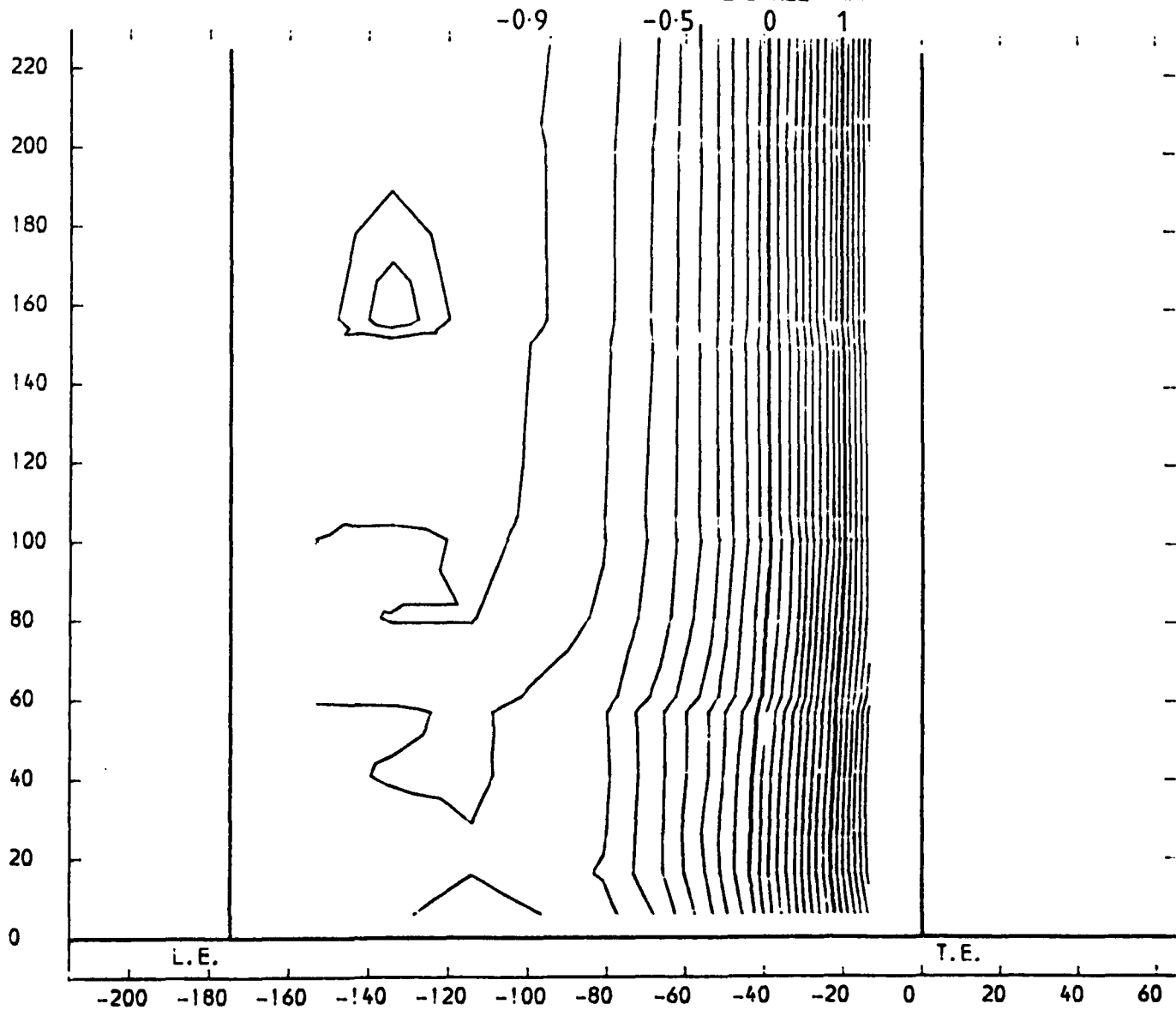


FIGURE 4.166

PLOT ON BLADE SUCTION SURFACE NATURAL BOUNDARY LAYER DATA  
 STATIC PRESSURE COEFFICIENT (  $(P_1 - P_{LOCAL}) / (P_{01} - P_1)$  ) CONTOURS  
 X-AXIS AXIAL CO-ORDINATE FROM TRAILING EDGE DATUM (MM)  
 Y-AXIS SPANWISE CO-ORDINATE FROM PERSPEX ENDWALL (MM)

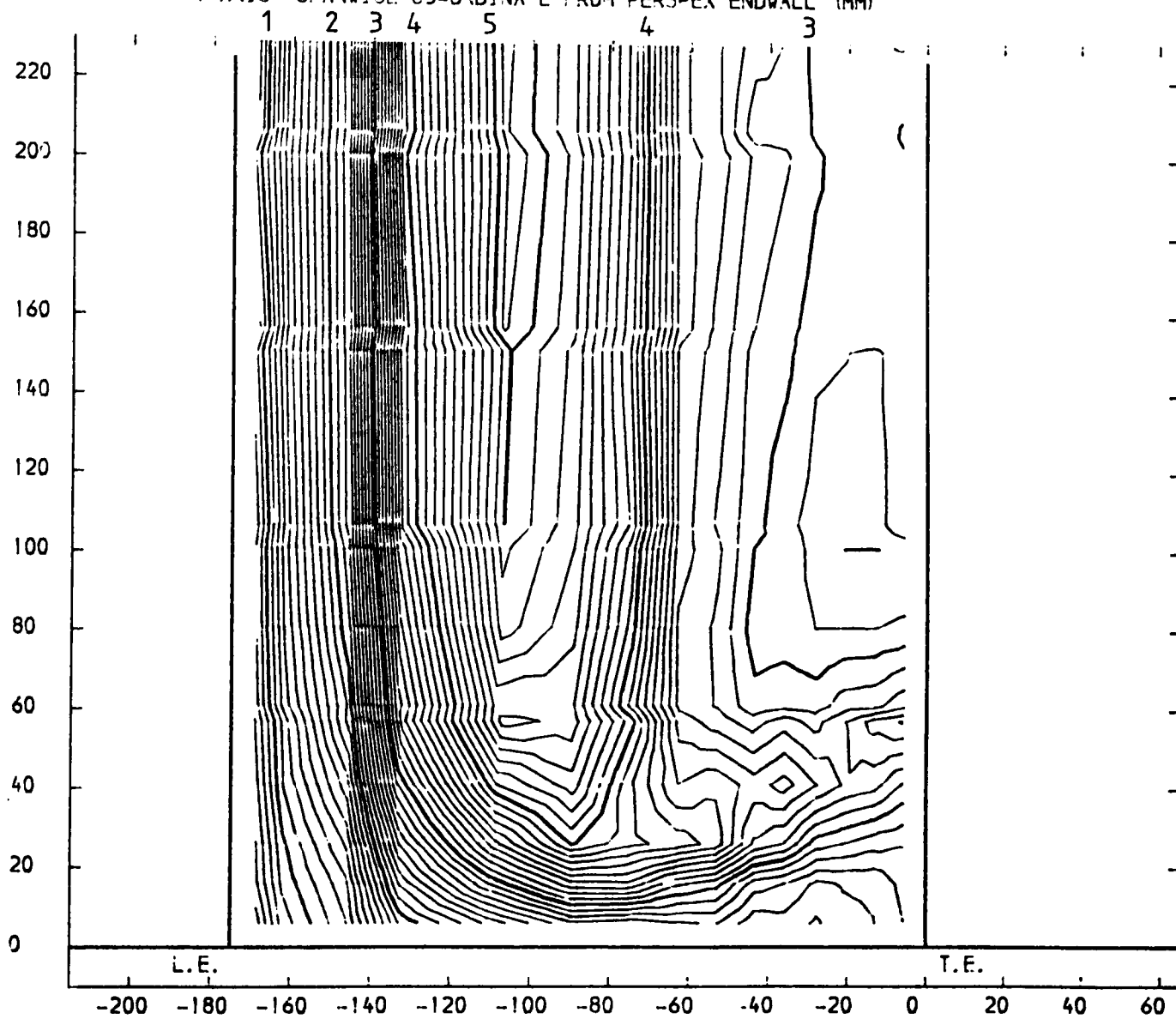
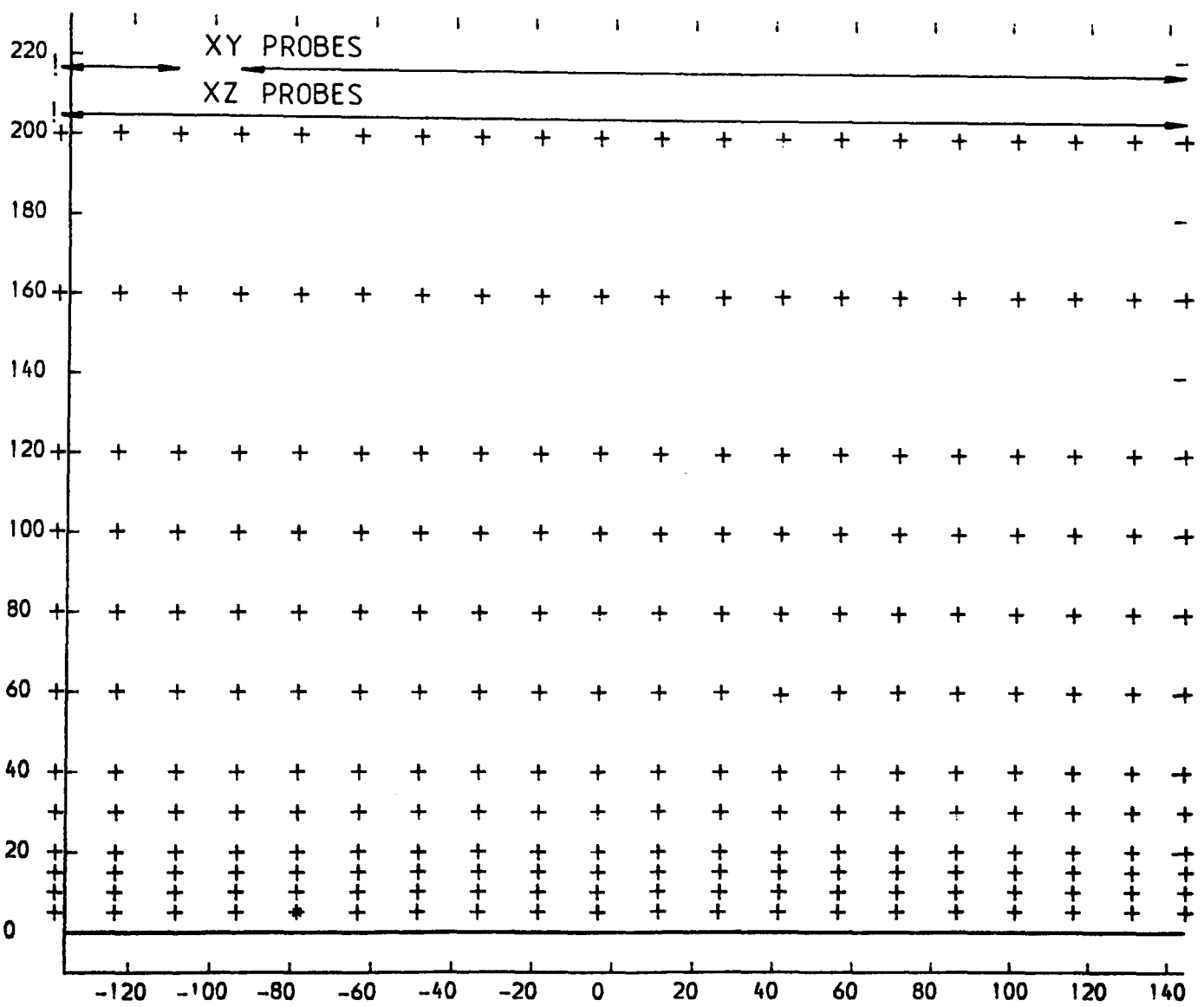


FIGURE 4.167

SLOT 1 HOT WIRE EXPERIMENTAL DATA POINTS

X-AXIS TANGENTIAL CO-ORDINATE FROM TRAILING EDGE DATUM (MM)  
 Y-AXIS SPANWISE CO-ORDINATE FROM PERSPEX ENDWALL (MM)  
 + DATA FROM REFINED ANALYSIS \* DATA FROM FIRST ORDER ANALYSIS



←→ TRAVERSING SESSIONS  
 ! PROBE TIP CHANGE

FIGURE 5.1



SLOT 1 TOTAL VELOCITY MAGNITUDE CONTOURS (CONTOUR UNITS METRES/SEC)

X-AXIS TANGENTIAL CO-ORDINATE FROM TRAILING EDGE DATUM (MM)

Y-AXIS SPANWISE CO-ORDINATE FROM PERSPEX ENDWALL (MM)

CONTOURS OBTAINED FROM HOT-WIRE MEAN VELOCITY DATA

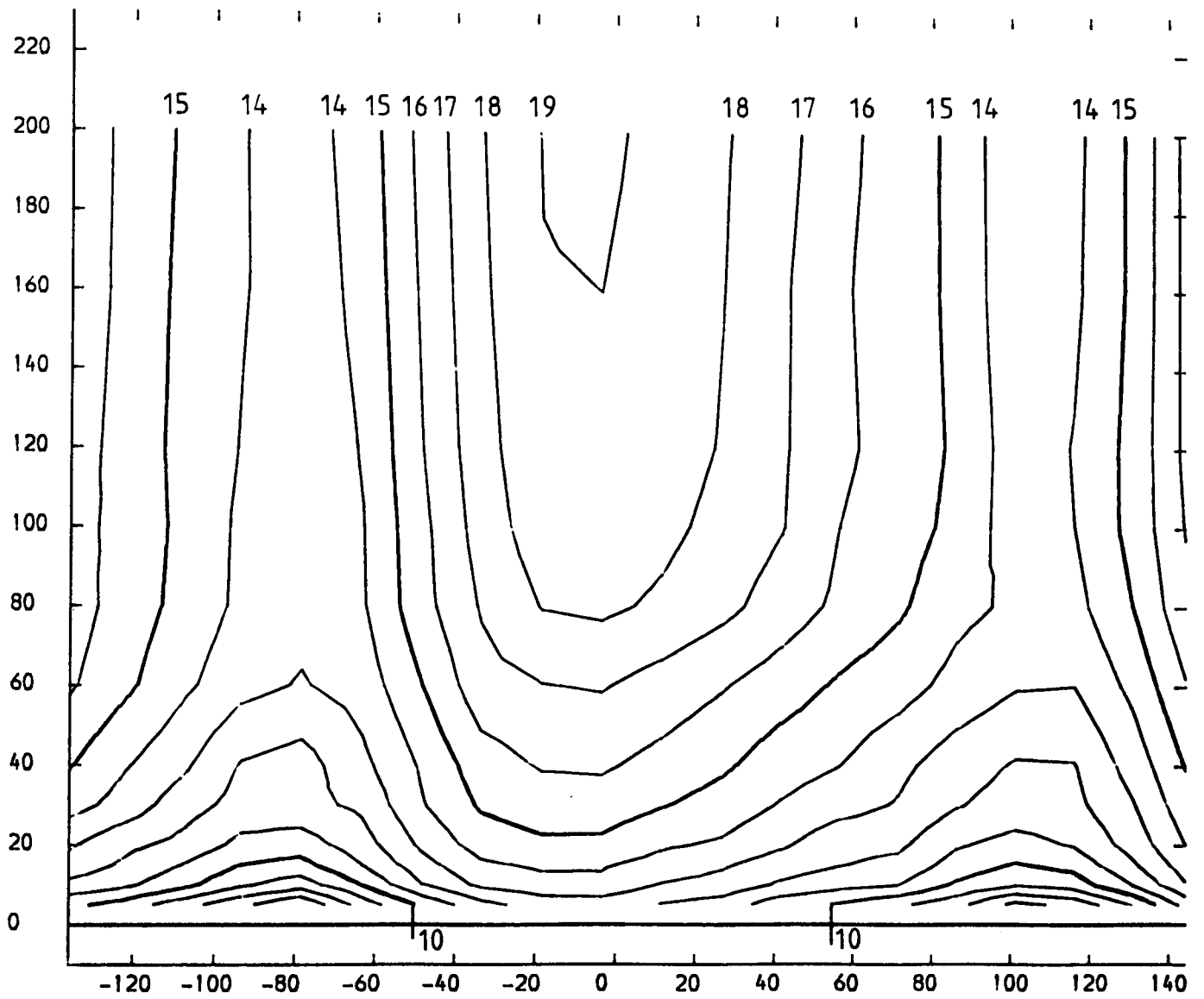


FIGURE 5.2

SLOT 1 YAW ANGLE CONTOURS (CONTOUR UNITS DEGREES)

X-AXIS TANGENTIAL CO-ORDINATE FROM TRAILING EDGE DATUM (MM)

Y-AXIS SPANWISE CO-ORDINATE FROM PERSPEX ENDWALL (MM)

CONTOURS OBTAINED FROM HOT-WIRE MEAN VELOCITY DATA

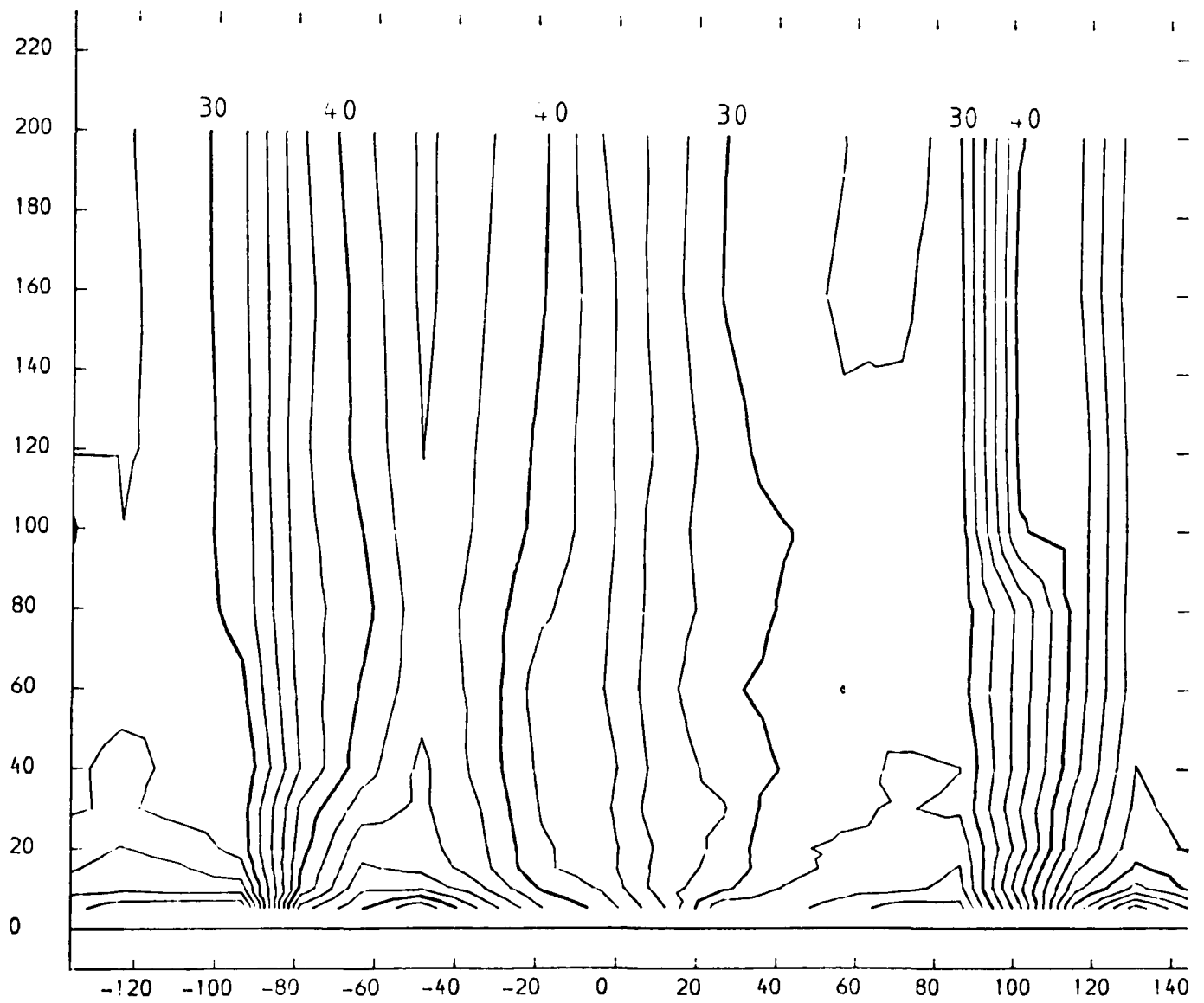


FIGURE 5.3

SLOT 1 PITCHWISE MASS MEANED HOT WIRE PROBE DATA  
 NATURAL INLET BOUNDARY LAYER

X-AXIS SPANWISE CO-ORDINATE FROM PERSPEX ENDWALL (MM)  
 Y-AXIS YAW ANGLE (DEGREES)

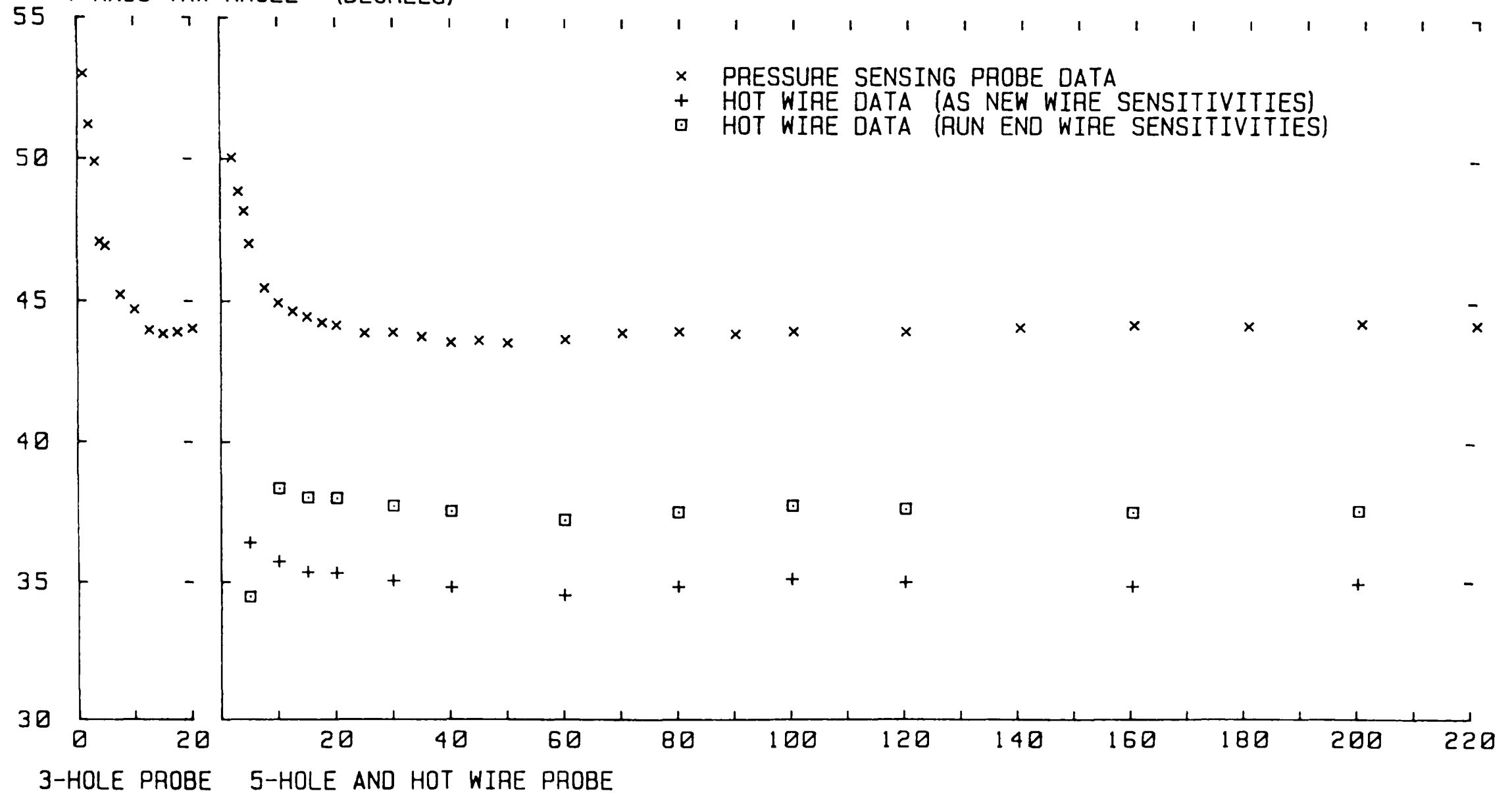


FIGURE 5.4

SLOT 1 STREAMWISE SPANWISE ANGLE CONTOURS (CONTOUR UNITS DEGREES)  
X-AXIS TANGENTIAL CO-ORDINATE FROM TRAILING EDGE DATUM (MM)  
Y-AXIS SPANWISE CO-ORDINATE FROM PERSPEX ENDWALL (MM)  
CONTOURS OBTAINED FROM HOT-WIRE MEAN VELOCITY DATA

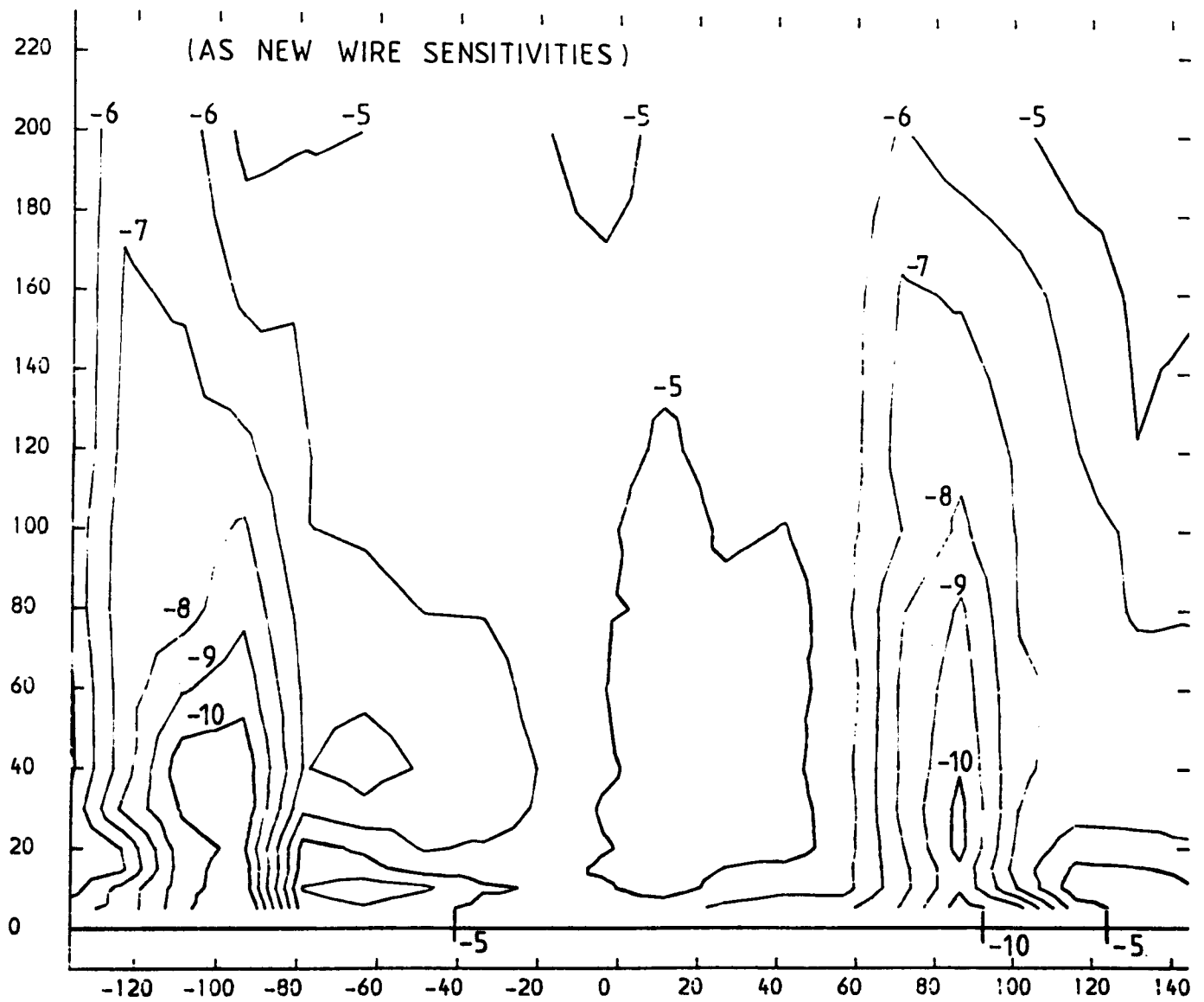


FIGURE 5.5

SLOT 1 STREAMWISE SPANWISE ANGLE CONTOURS (CONTOUR UNITS DEGREES)

X-AXIS TANGENTIAL CO-ORDINATE FROM TRAILING EDGE DATUM (MM)

Y-AXIS SPANWISE CO-ORDINATE FROM PERSPEX ENDWALL (MM)

CONTOURS OBTAINED FROM HOT-WIRE MEAN VELOCITY DATA

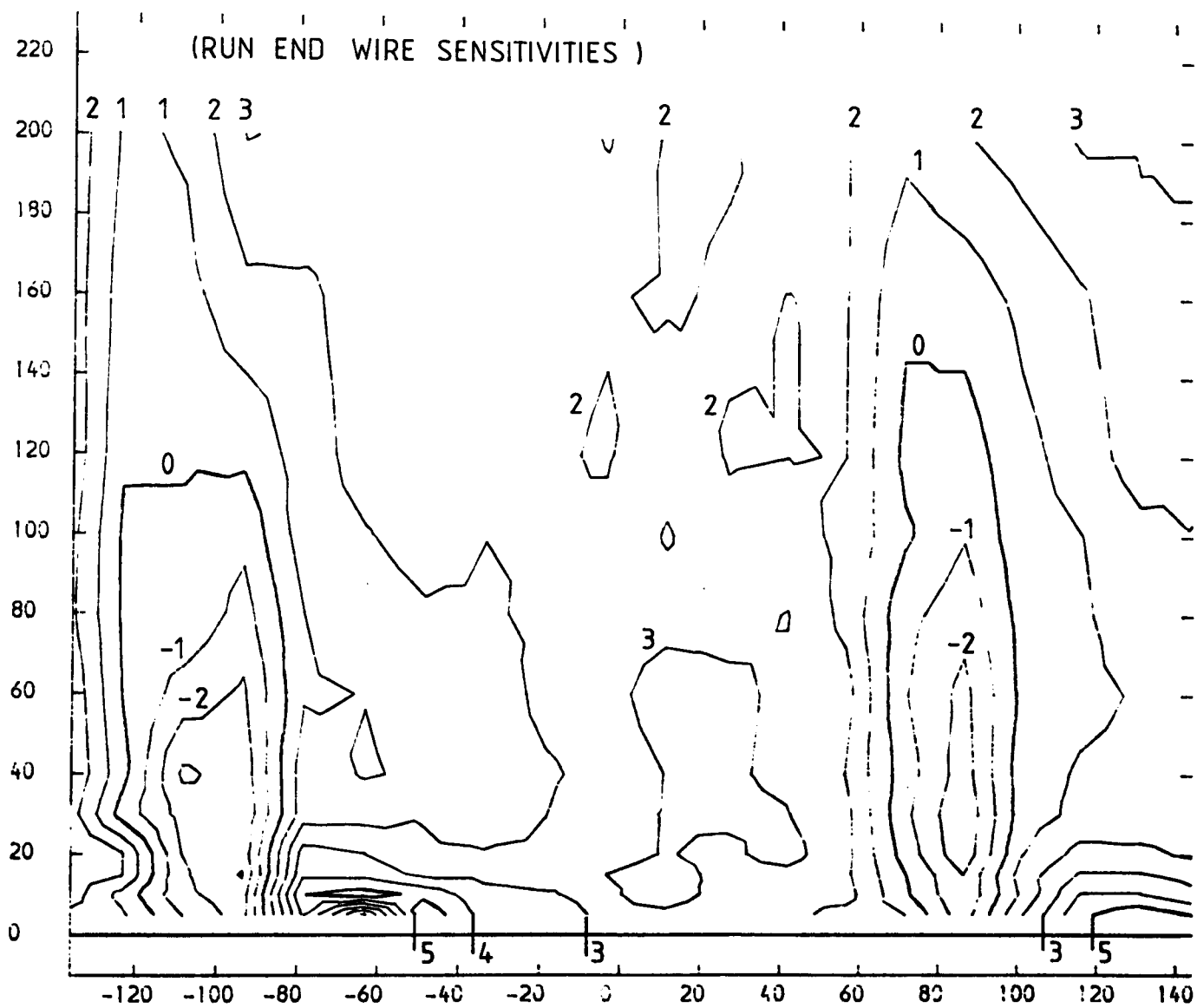


FIGURE 5.6

SLOT 1 NORMALIZED TURBULENT KINETIC ENERGY CONTOURS

X-AXIS TANGENTIAL CO-ORDINATE FROM TRAILING EDGE DATUM (MM)

Y-AXIS SPANWISE CO-ORDINATE FROM PERSPEX ENDWALL (MM)

CONTOURS NORMALIZED USING UPSTREAM REFERENCE DYNAMIC HEAD

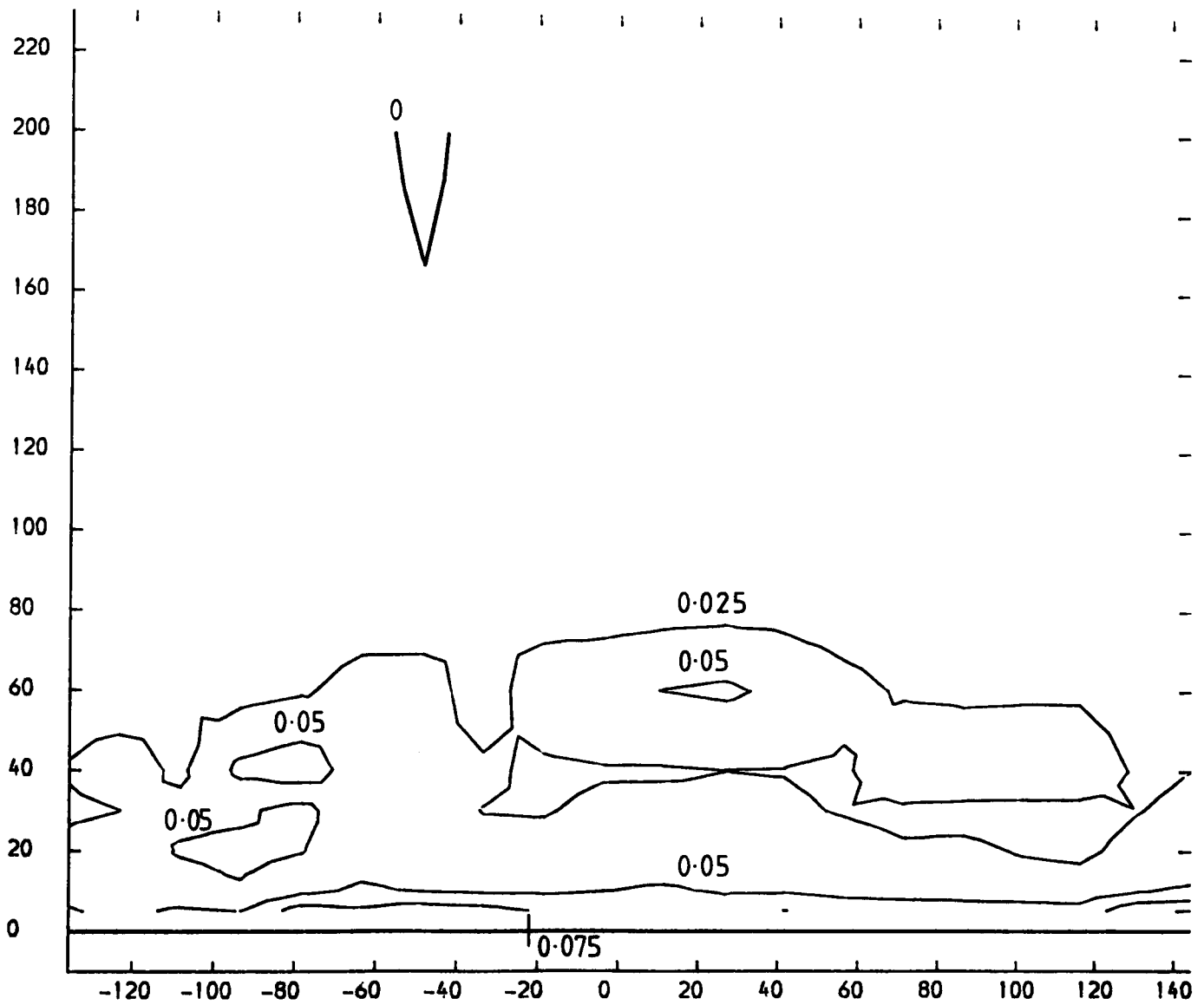


FIGURE 5.7

SLOT 1 TURBULENCE INTENSITY CONTOURS FOR U DASH

X-AXIS TANGENTIAL CO-ORDINATE FROM TRAILING EDGE DATUM (MM)  
Y-AXIS SPANWISE CO-ORDINATE FROM PERSPEX ENDWALL (MM)  
CONTOURS NORMALIZED USING UPSTREAM REFERENCE VELOCITY

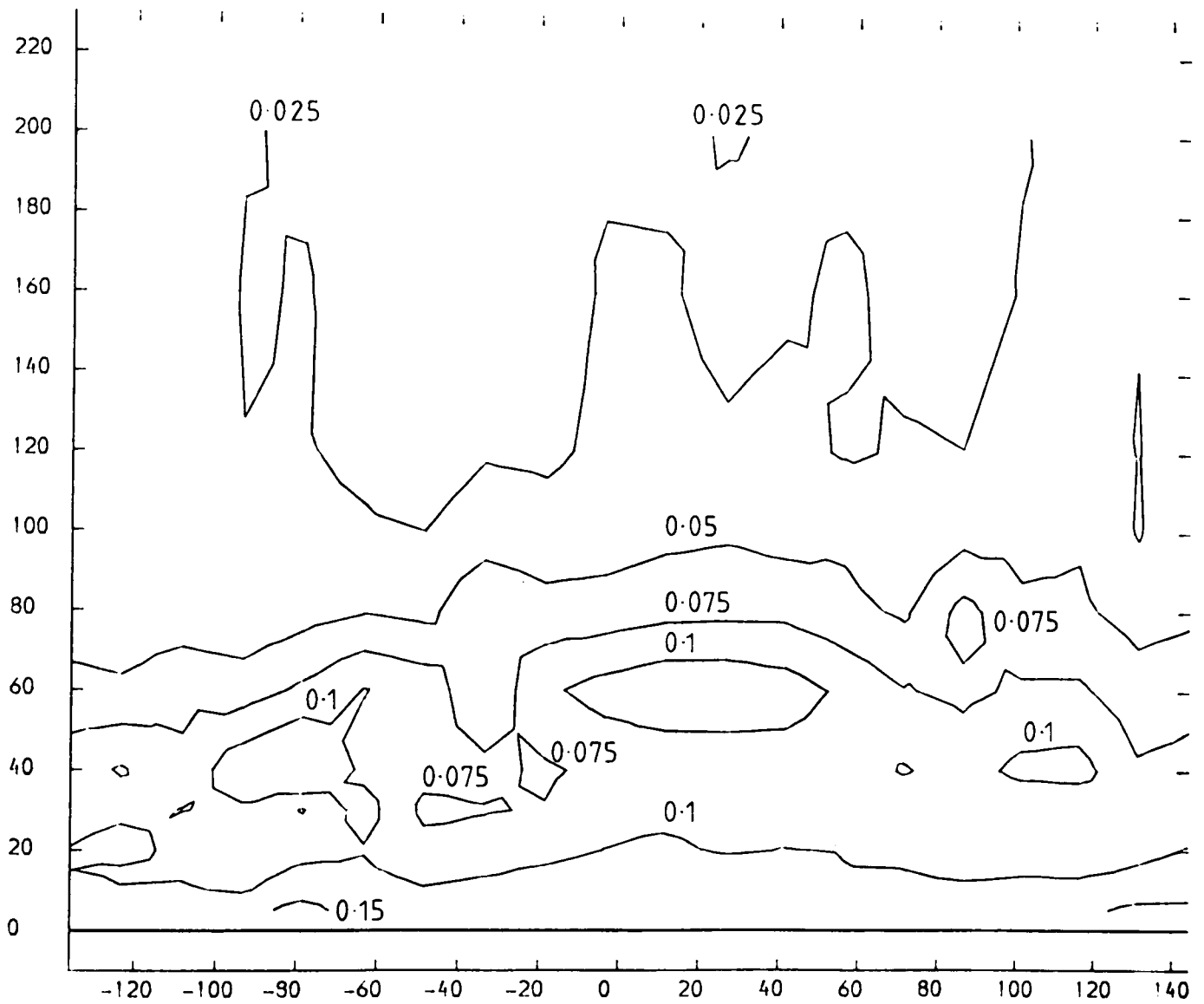


FIGURE 5.8

SLOT 1 TURBULENCE INTENSITY CONTOURS FOR V DASH

X-AXIS TANGENTIAL CO-ORDINATE FROM TRAILING EDGE DATUM (MM)

Y-AXIS SPANWISE CO-ORDINATE FROM PERSPEX ENDWALL (MM)

CONTOURS NORMALIZED USING UPSTREAM REFERENCE VELOCITY

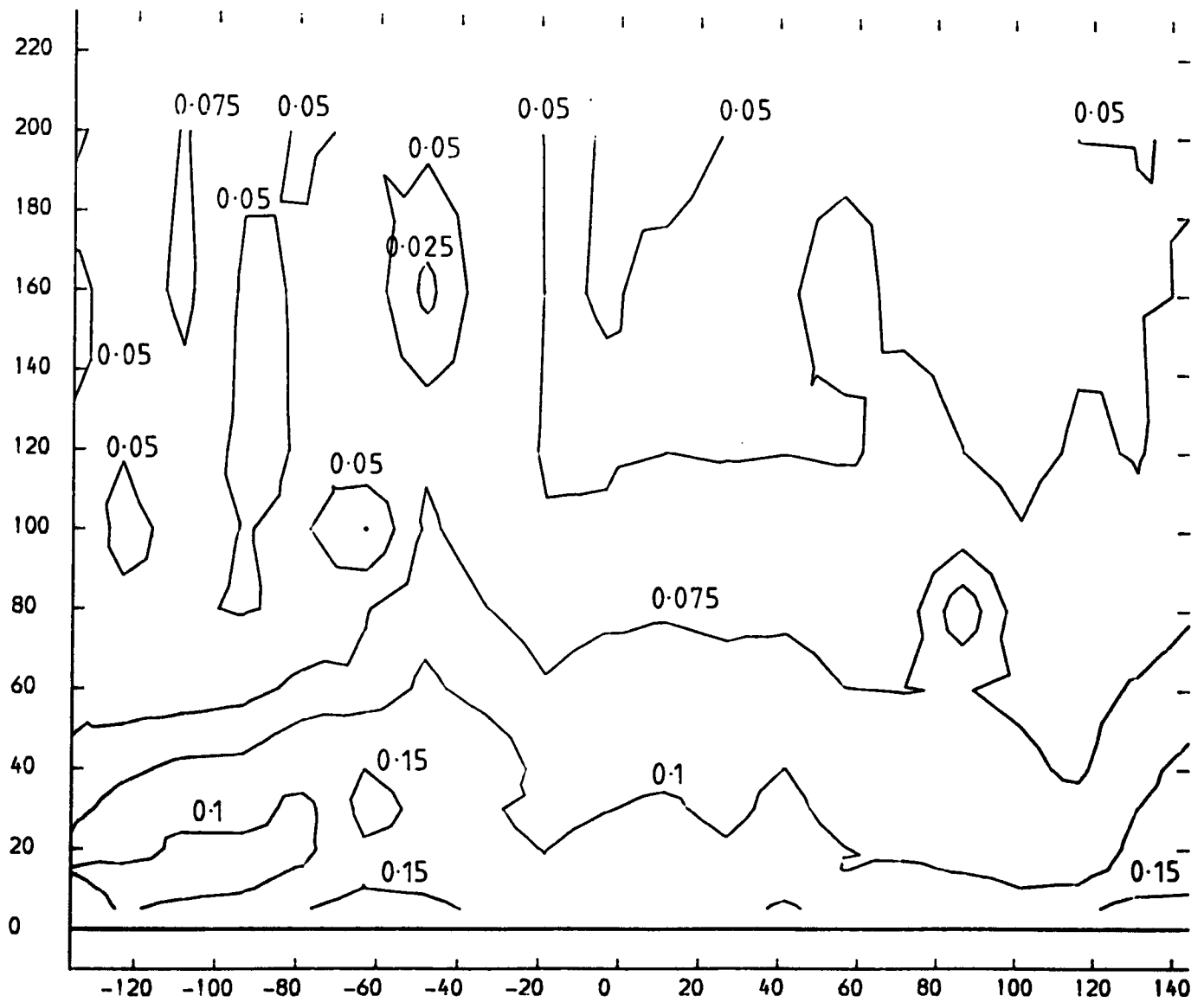


FIGURE 5.9



SLOT 1 TURBULENCE INTENSITY CONTOURS FOR W DASH

X-AXIS TANGENTIAL CO-ORDINATE FROM TRAILING EDGE DATUM (MM)

Y-AXIS SPANWISE CO-ORDINATE FROM PERSPEX ENDWALL (MM)

CONTOURS NORMALIZED USING UPSTREAM REFERENCE VELOCITY

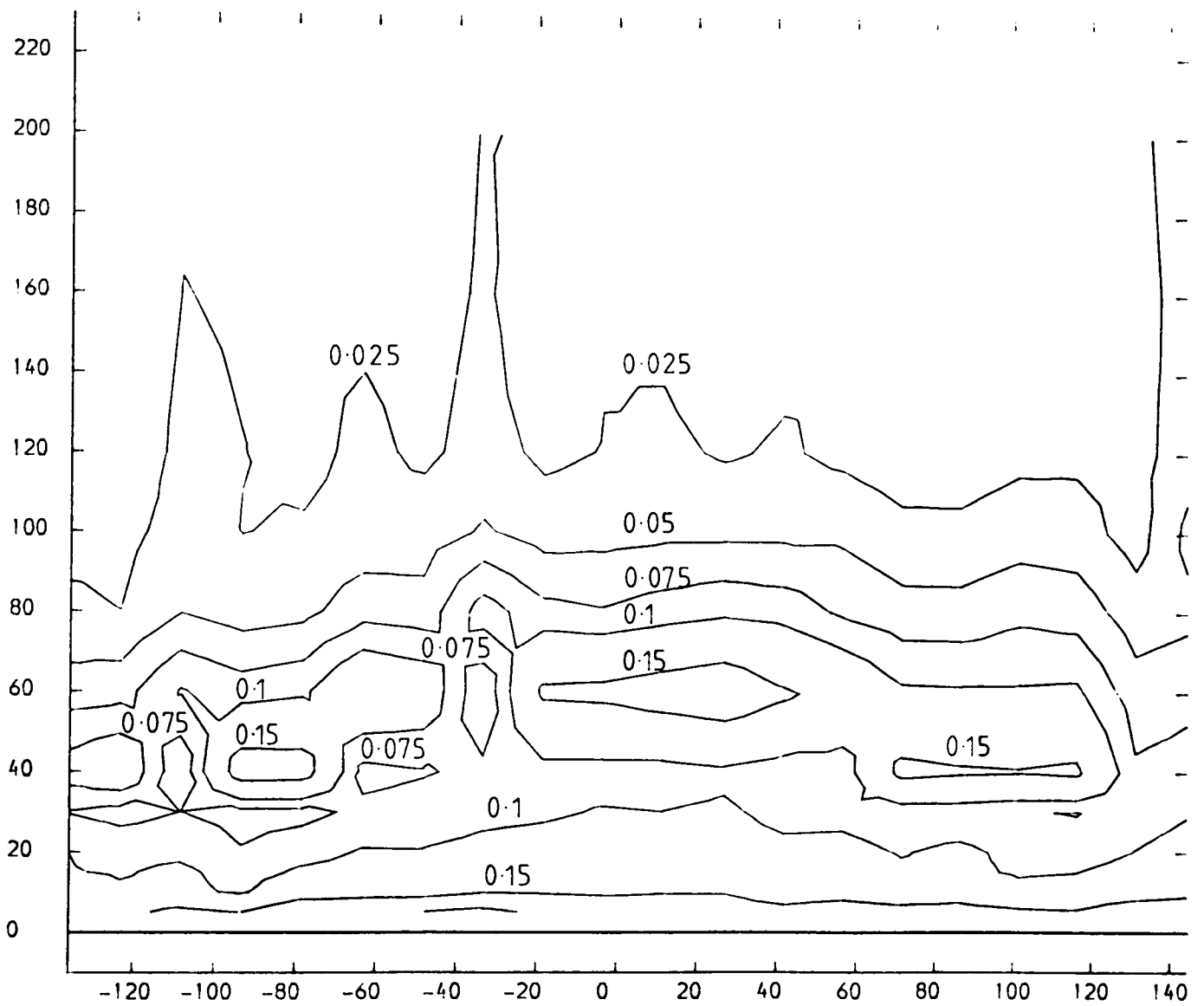


FIGURE 5.10

SLOT 1 PITCHWISE MASS MEANED RELATIVE TURBULENCE INTENSITIES (AS NEW WIRE SENSITIVITIES)  
 NATURAL INLET BOUNDARY LAYER

X-AXIS SPANWISE CO-ORDINATE FROM PERSPEX ENDWALL (MM)  
 Y-AXIS NORMALIZED TURBULENCE DATA

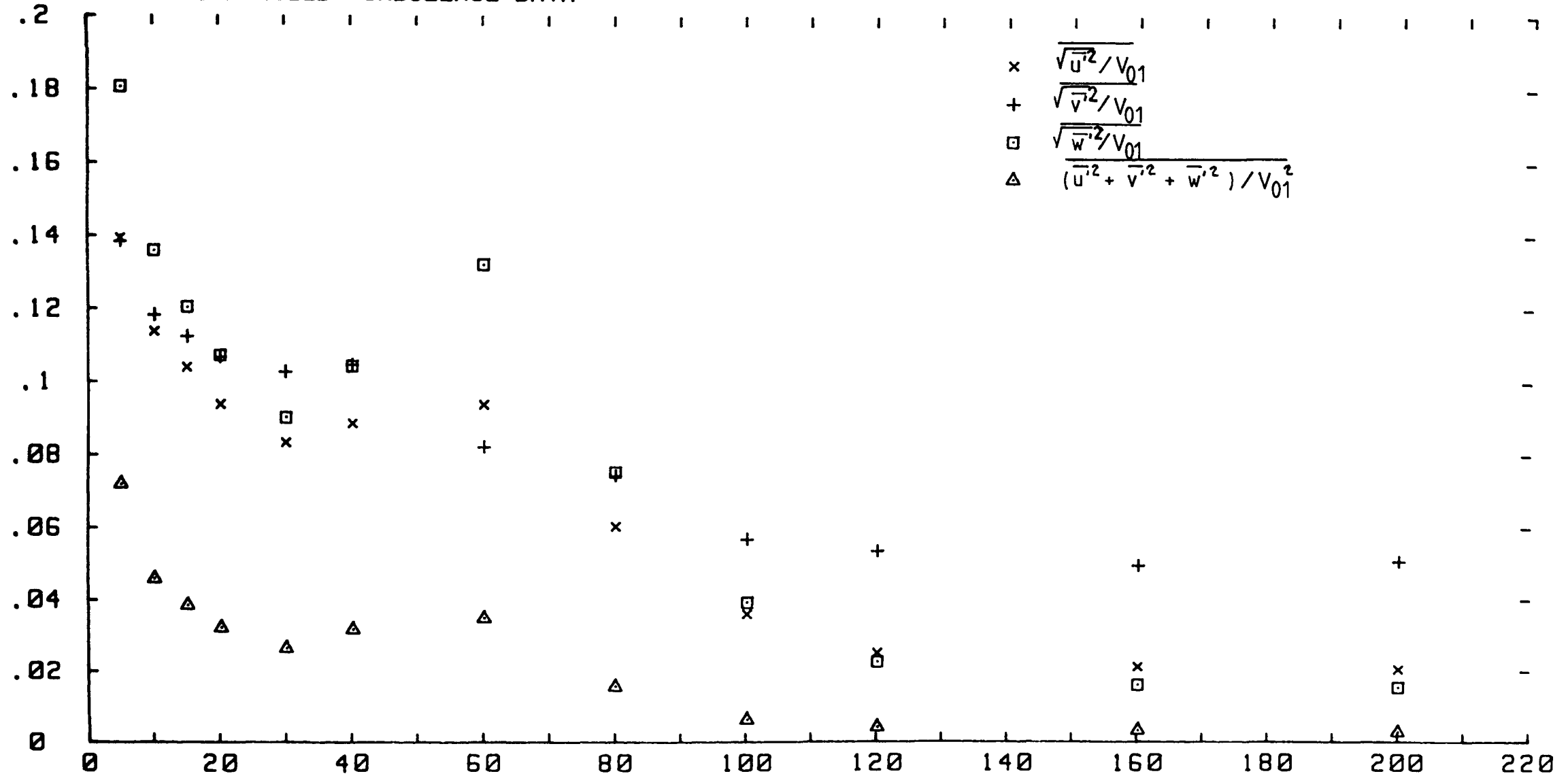


FIGURE 5.11

SLOT 1 PITCHWISE MASS MEANED RELATIVE TURBULENCE INTENSITIES (RUN END WIRE SENSITIVITIES)  
 NATURAL INLET BOUNDARY LAYER

X-AXIS SPANWISE CO-ORDINATE FROM PERSPEX ENDWALL (MM)  
 Y-AXIS NORMALIZED TURBULENCE DATA

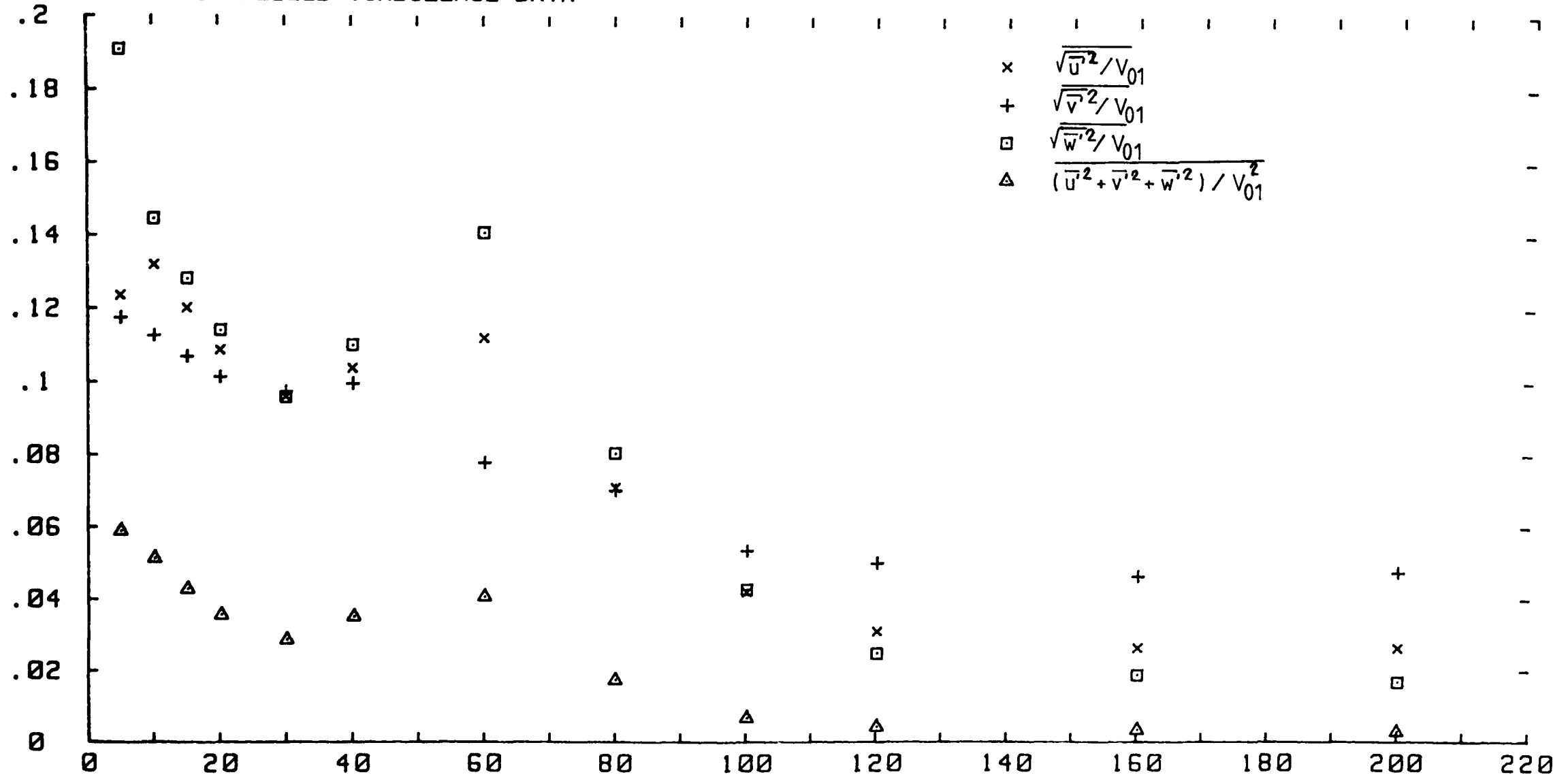


FIGURE 5.12

SLOT 1 NORMALIZED SHEAR STRESS CONTOURS (FROM UV CORRELATION)  
X-AXIS TANGENTIAL CO-ORDINATE FROM TRAILING EDGE DATUM (MM)  
Y-AXIS SPANWISE CO-ORDINATE FROM PERSPEX ENDWALL (MM)  
CONTOURS NORMALIZED USING UPSTREAM REFERENCE DYNAMIC HEAD

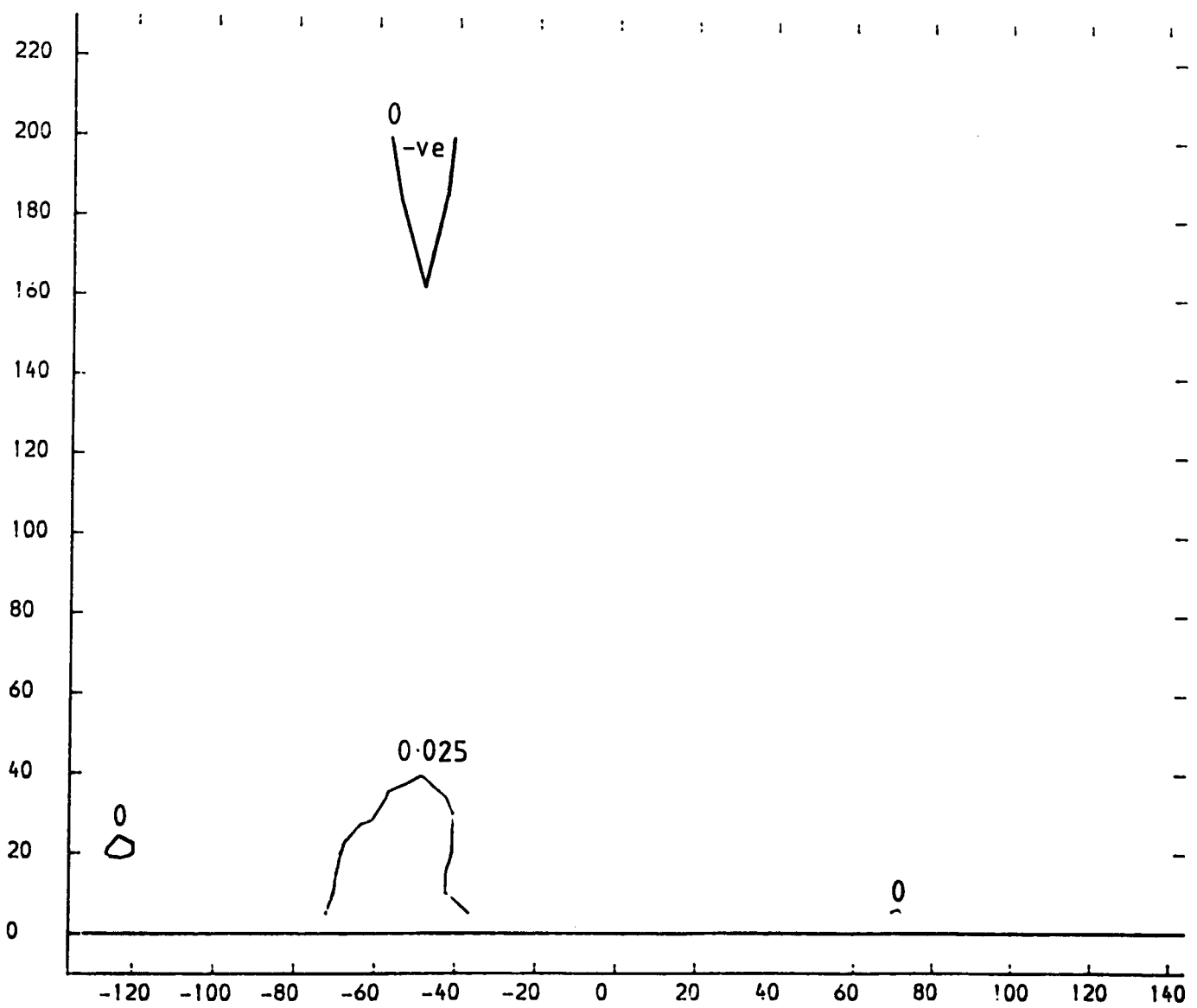


FIGURE 5.13

SLOT 1 NORMALIZED SHEAR STRESS CONTOURS (FROM UW CORRELATION)

X-AXIS TANGENTIAL CO-ORDINATE FROM TRAILING EDGE DATUM (MM)

Y-AXIS SPANWISE CO-ORDINATE FROM PERSPEX ENDWALL (MM)

CONTOURS NORMALIZED USING UPSTREAM REFERENCE DYNAMIC HEAD

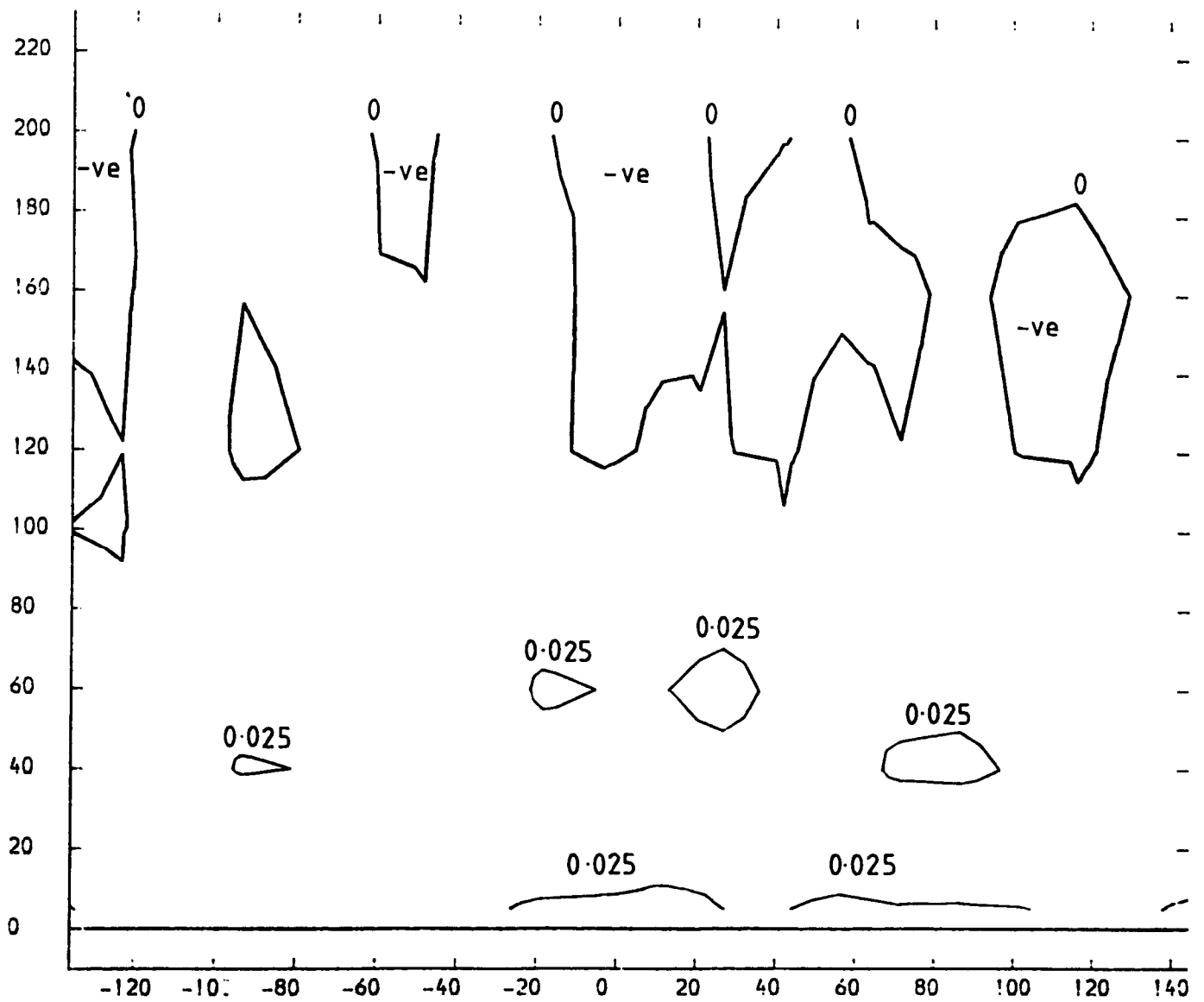
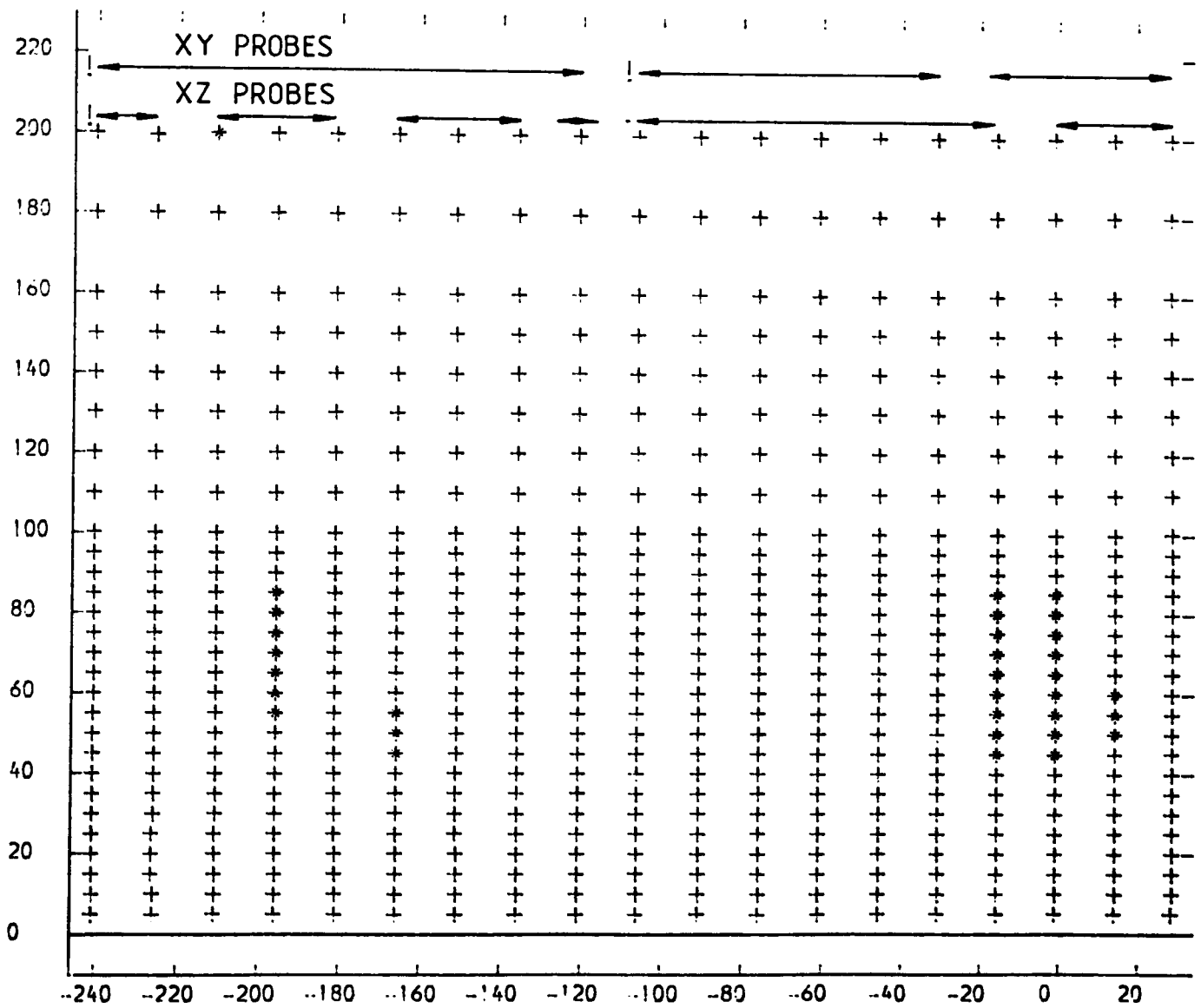


FIGURE 5.14

SLOT 8 HOT WIRE EXPERIMENTAL DATA POINTS

X-AXIS TANGENTIAL CO-ORDINATE FROM TRAILING EDGE DATUM (MM)  
 Y-AXIS SPANWISE CO-ORDINATE FROM PERSPEX ENDWALL (MM)  
 + DATA POINT \* IMAGINARY ROOT FOR ONE UBAR OTHER VALUED USED



←→ TRAVERSING SESSIONS  
 ! PROBE TIP CHANGE

FIGURE 5.15

SLOT 8 TOTAL VELOCITY MAGNITUDE CONTOURS (CONTOUR UNITS METRES/SEC)

X-AXIS TANGENTIAL CO-ORDINATE FROM TRAILING EDGE DATUM (MM)

Y-AXIS SPANWISE CO-ORDINATE FROM PERSPEX ENDWALL (MM)

CONTOURS OBTAINED FROM HOT-WIRE MEAN VELOCITY DATA

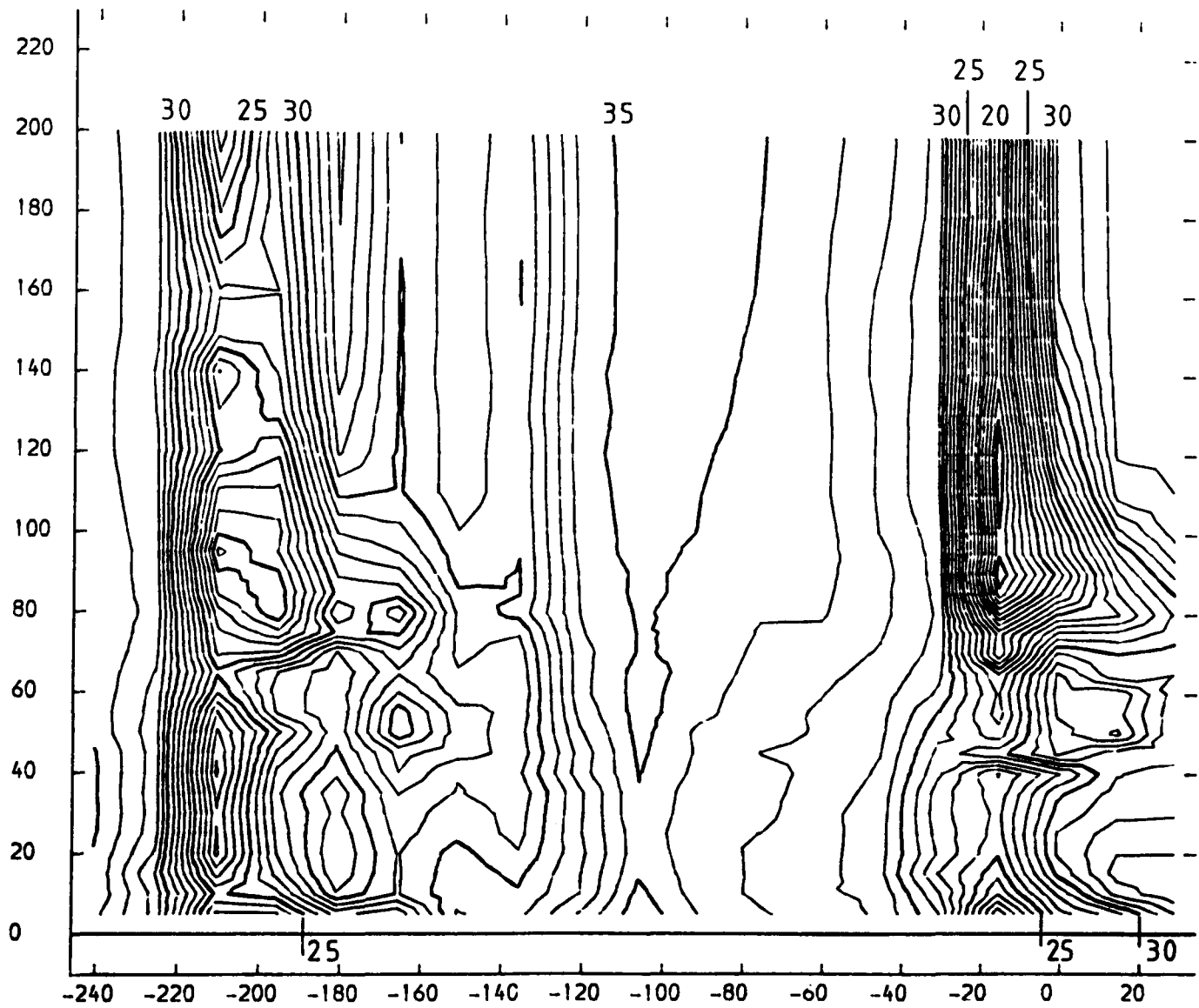


FIGURE 5.16

SLOT 8 YAW ANGLE CONTOURS (CONTOUR UNITS DEGREES)

X-AXIS TANGENTIAL CO-ORDINATE FROM TRAILING EDGE DATUM (MM)

Y-AXIS SPANWISE CO-ORDINATE FROM PERSPEX ENDWALL (MM)

CONTOURS OBTAINED FROM HOT-WIRE MEAN VELOCITY DATA

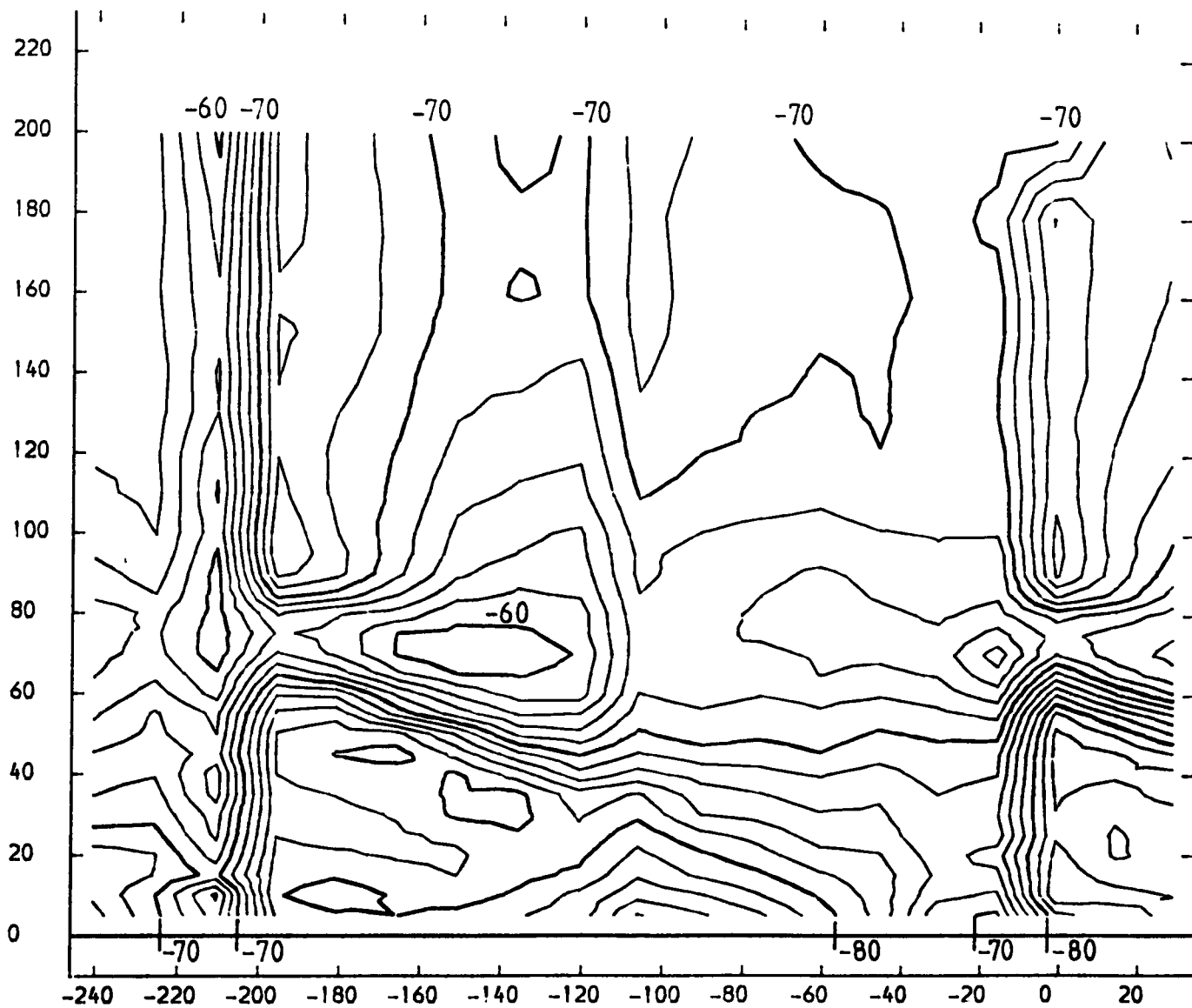


FIGURE 5.17



SLOT 8 PITCHWISE MASS MEANED HOT WIRE PROBE DATA  
 NATURAL INLET BOUNDARY LAYER

X-AXIS SPANWISE CO-ORDINATE FROM PERSPEX ENDWALL (MM)  
 Y-AXIS YAW ANGLE (DEGREES)

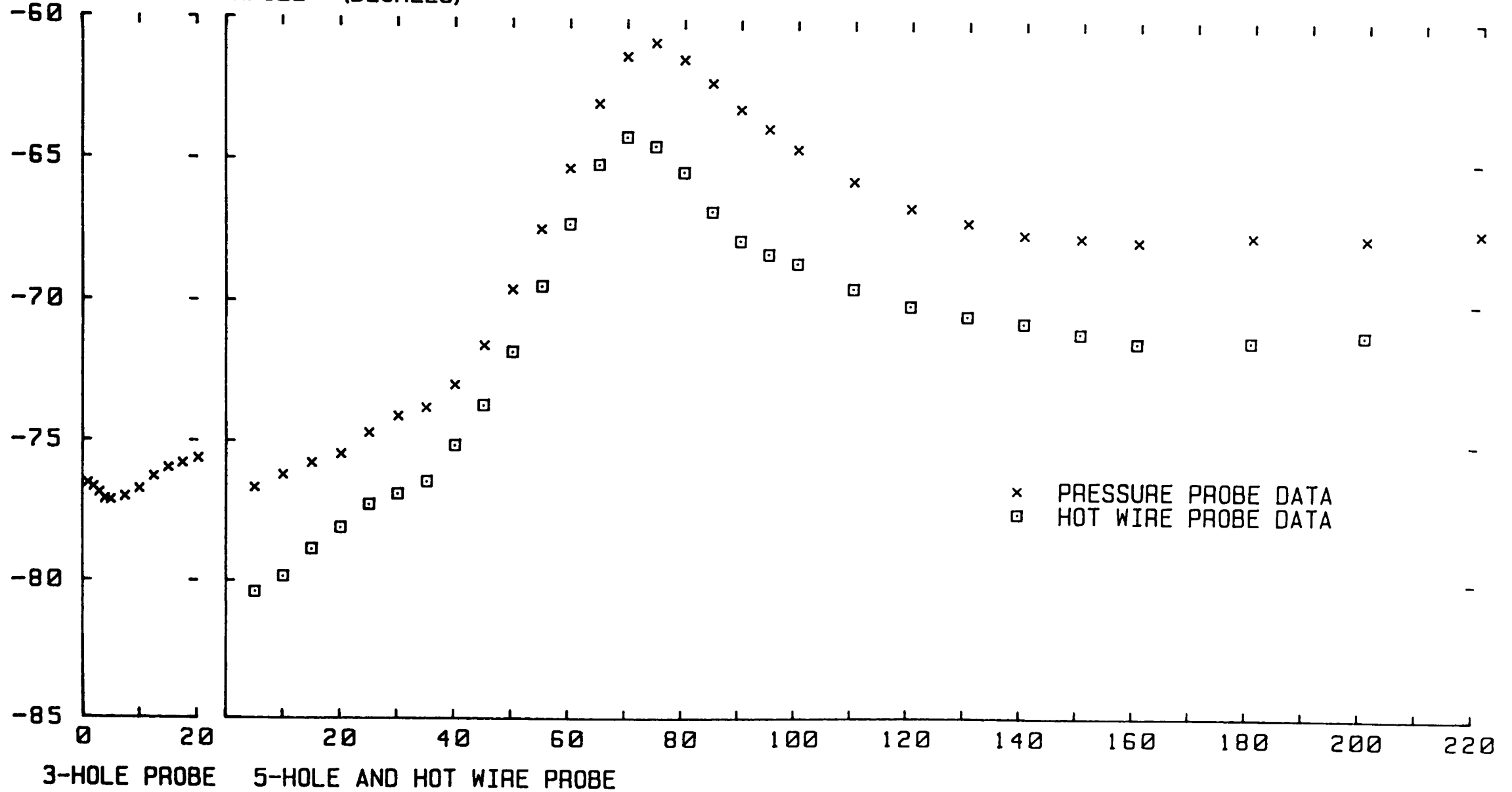


FIGURE 5.18

SLOT 8 SPANWISE ANGLE (PITCH ANGLE) CONTOURS (CONTOUR UNITS DEGREES)

X-AXIS TANGENTIAL CO-ORDINATE FROM TRAILING EDGE DATUM (MM)

Y-AXIS SPANWISE CO-ORDINATE FROM PERSPEX ENDWALL (MM)

CONTOURS OBTAINED FROM HOT-WIRE MEAN VELOCITY DATA

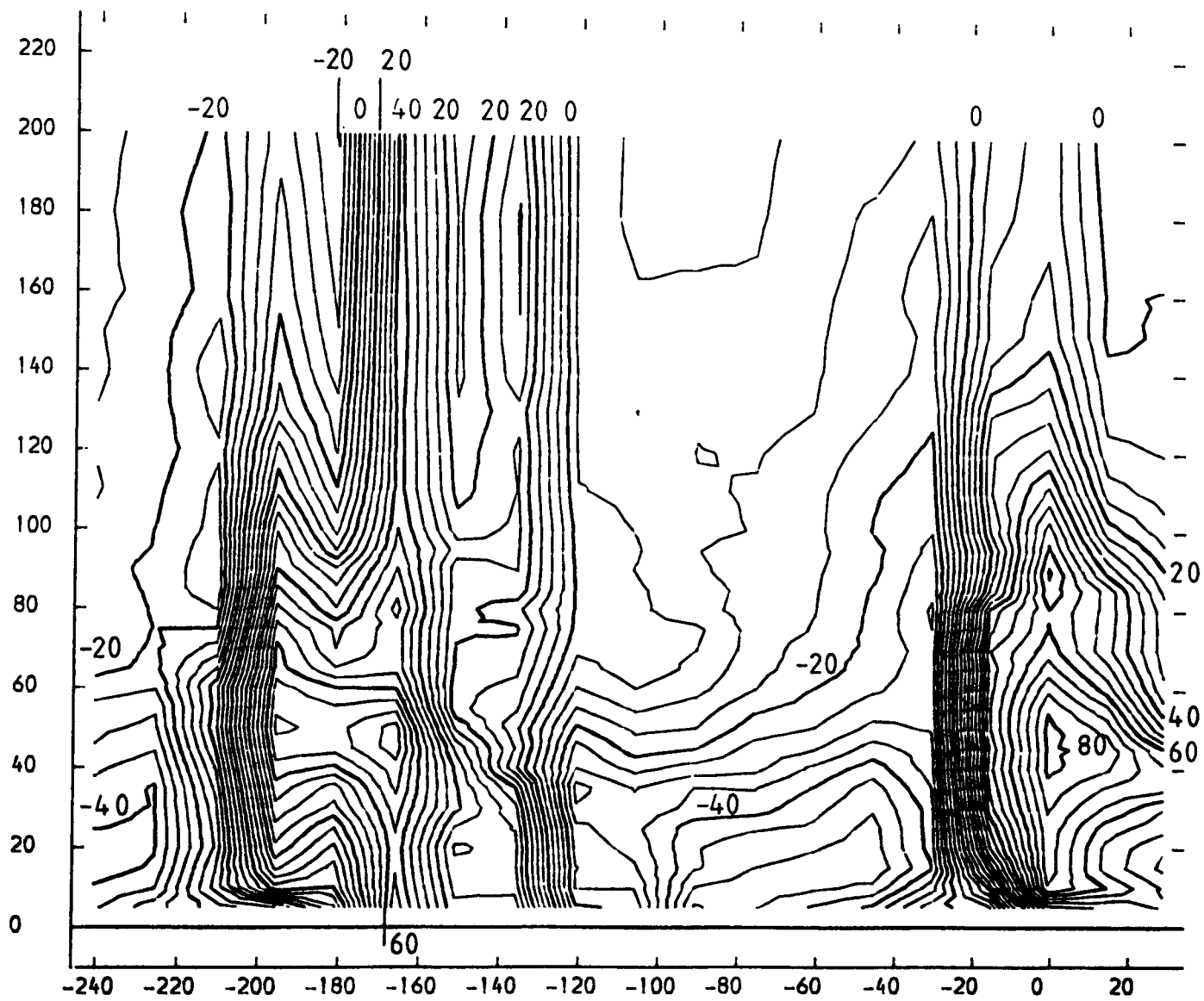


FIGURE 5.19

SLOT 8 NORMALIZED TURBULENT KINETIC ENERGY CONTOURS

X-AXIS TANGENTIAL CO-ORDINATE FROM TRAILING EDGE DATUM (MM)  
Y-AXIS SPANWISE CO-ORDINATE FROM PERSPEX ENDWALL (MM)  
CONTOURS NORMALIZED USING UPSTREAM REFERENCE DYNAMIC HEAD

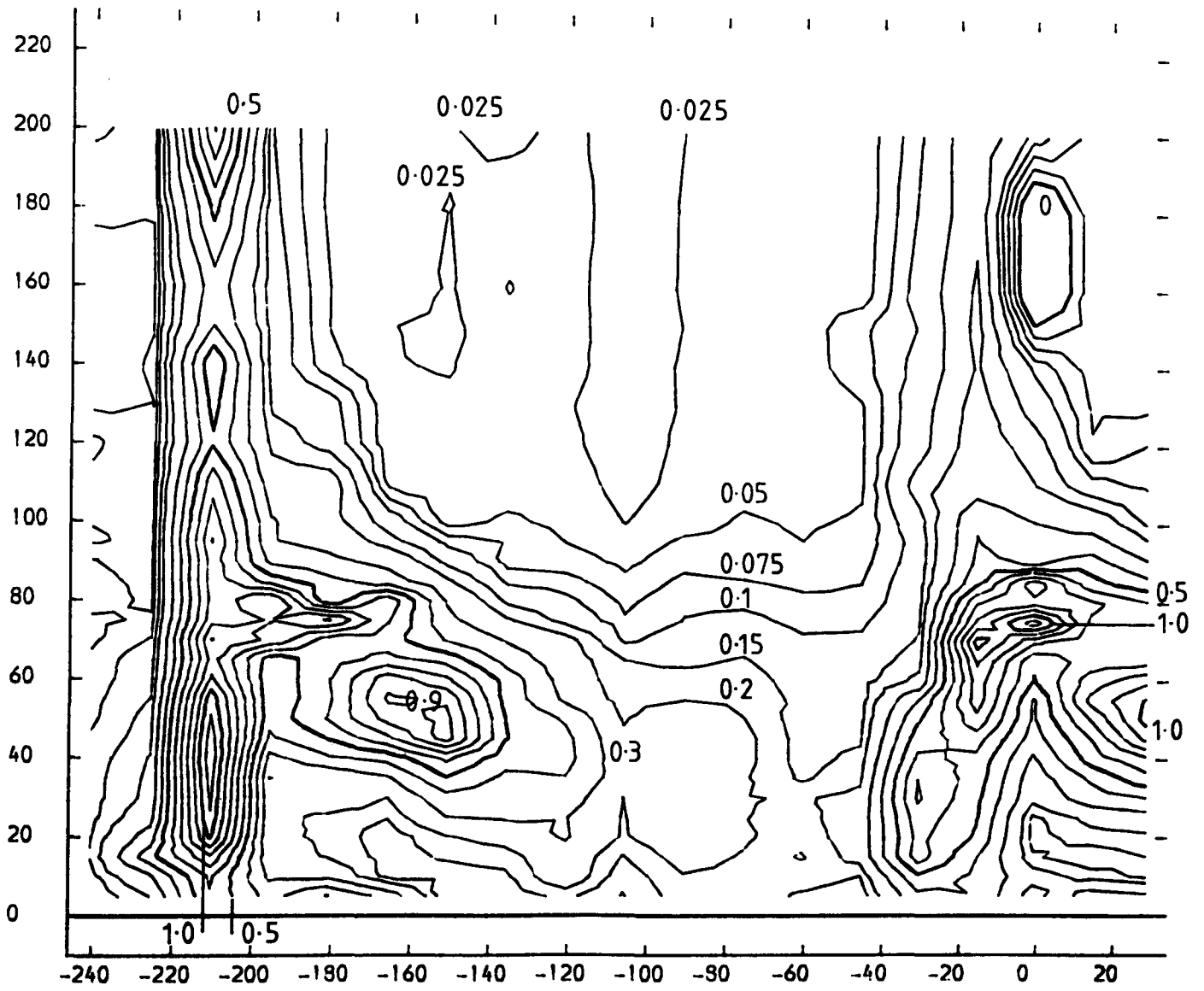


FIGURE 5.20

SLOT 8 TURBULENCE INTENSITY CONTOURS FOR U DASH

X-AXIS TANGENTIAL CO-ORDINATE FROM TRAILING EDGE DATUM (MM)  
Y-AXIS SPANWISE CO-ORDINATE FROM PERSPEX ENDWALL (MM)  
CONTOURS NORMALIZED USING UPSTREAM REFERENCE VELOCITY

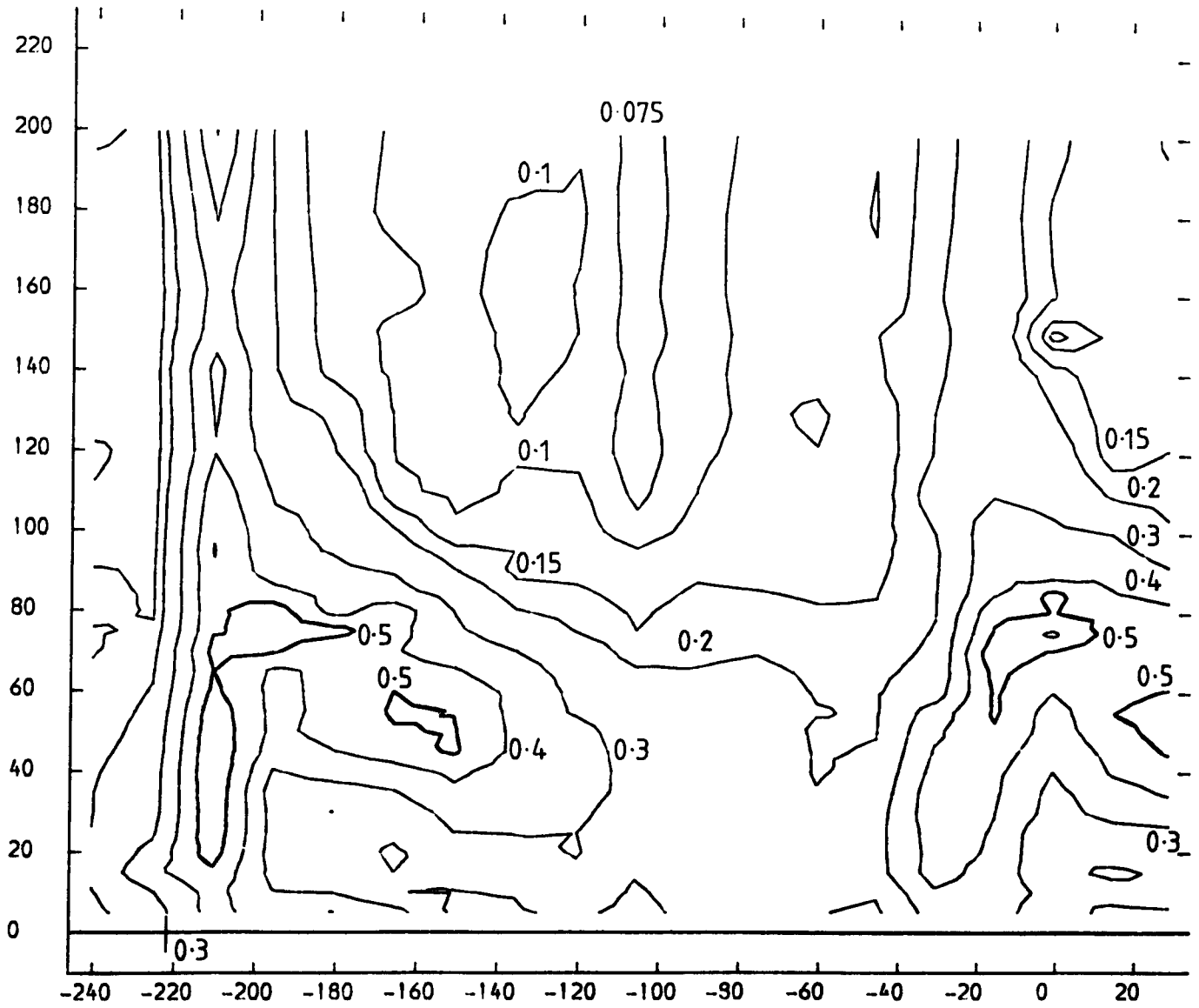


FIGURE 5.21

SLOT 8 TURBULENCE INTENSITY CONTOURS FOR V DASH

X-AXIS TANGENTIAL CO-ORDINATE FROM TRAILING EDGE DATUM (MM)

Y-AXIS SPANWISE CO-ORDINATE FROM PERSPEX ENDWALL (MM)

CONTOURS NORMALIZED USING UPSTREAM REFERENCE VELOCITY

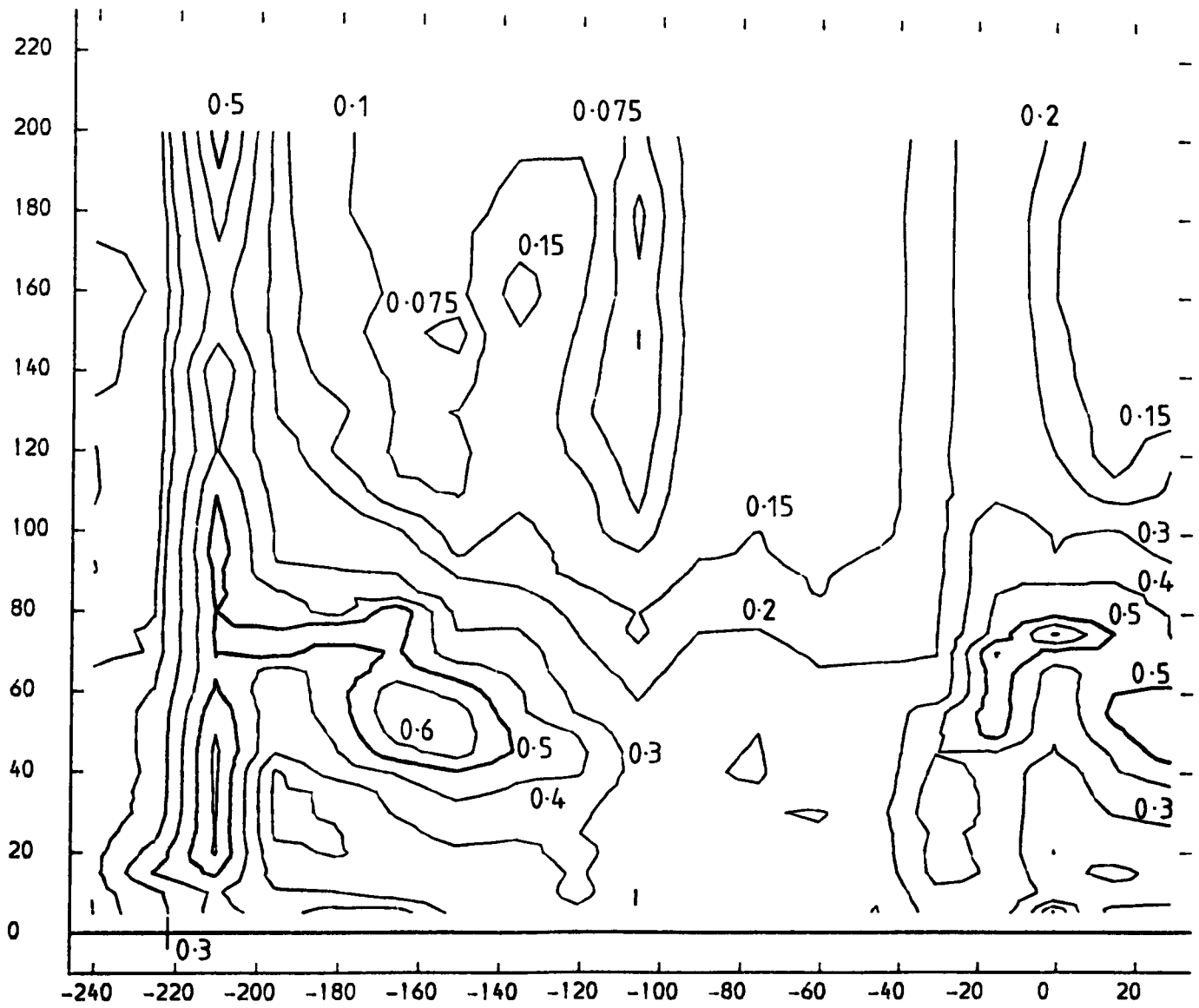


FIGURE 5.22

SLOT 8 TURBULENCE INTENSITY CONTOURS FOR W DASH

X-AXIS TANGENTIAL CO-ORDINATE FROM TRAILING EDGE DATUM (MM)  
Y-AXIS SPANWISE CO-ORDINATE FROM PERSPEX ENDWALL (MM)  
CONTOURS NORMALIZED USING UPSTREAM REFERENCE VELOCITY

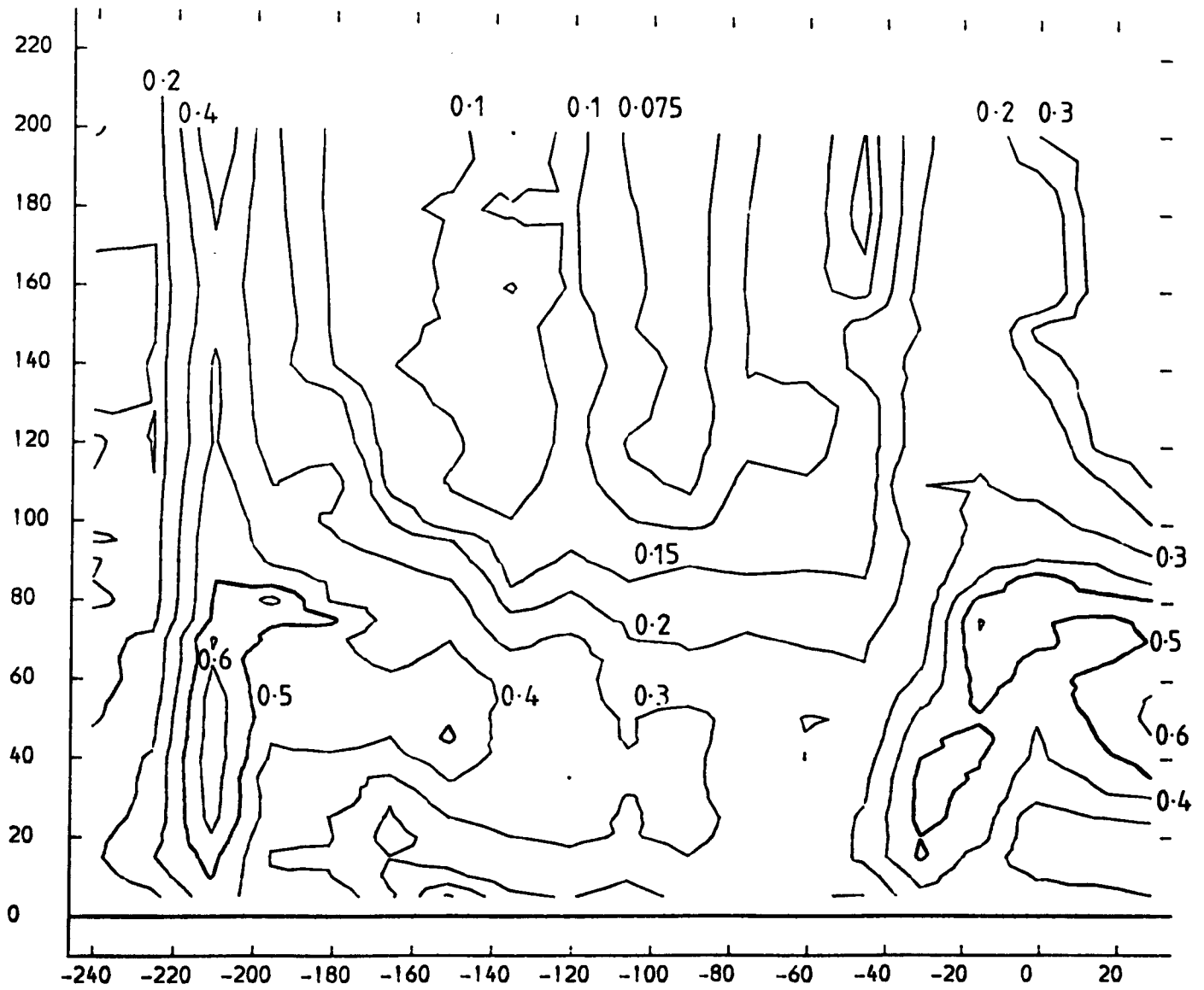


FIGURE 5.23

SLOT 8 PITCHWISE MASS MEANED RELATIVE TURBULENCE INTENSITIES  
 NATURAL INLET BOUNDARY LAYER

X-AXIS SPANWISE CO-ORDINATE FROM PERSPEX ENDWALL (MM)

Y-AXIS NORMALIZED TURBULENCE DATA

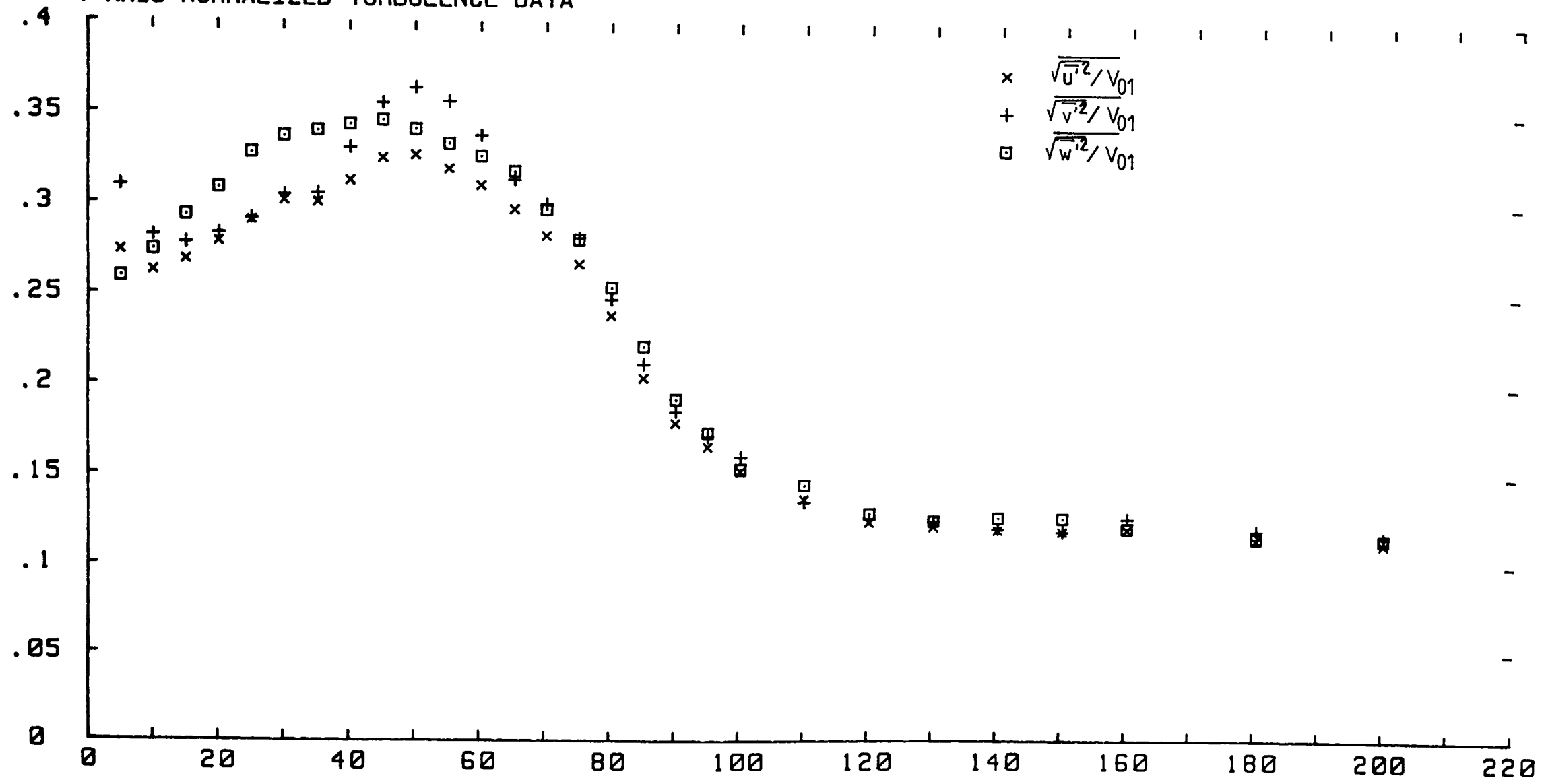


FIGURE 5.24

SLOT 8 PITCHWISE MASS MEANED RELATIVE TURBULENT KINETIC ENERGY AND TOTAL PRESSURE LOSS COEFFICIENT  
 NATURAL INLET BOUNDARY LAYER

X-AXIS SPANWISE CO-ORDINATE FROM PERSPEX ENDWALL (MM)

Y-AXIS RELATIVE TURBULENT KINETIC ENERGY AND TOTAL PRESSURE LOSS COEFFICIENT

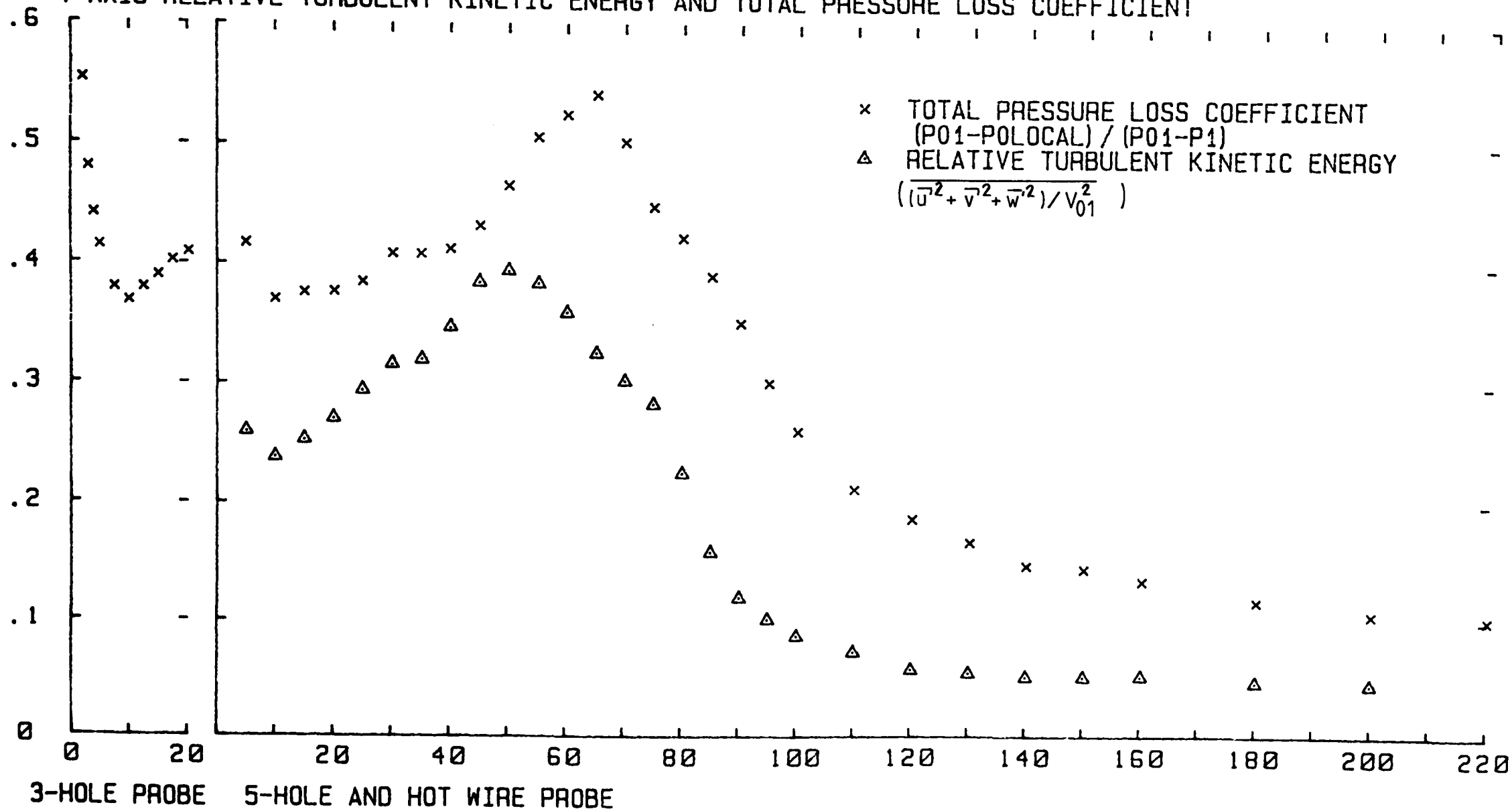


FIGURE 5.25



SLOT 8 NORMALIZED SHEAR STRESS CONTOURS (FROM UV CORRELATION)

X-AXIS TANGENTIAL CO-ORDINATE FROM TRAILING EDGE DATUM (MM)

Y-AXIS SPANWISE CO-ORDINATE FROM PERSPEX ENDWALL (MM)

CONTOURS NORMALIZED USING UPSTREAM REFERENCE DYNAMIC HEAD

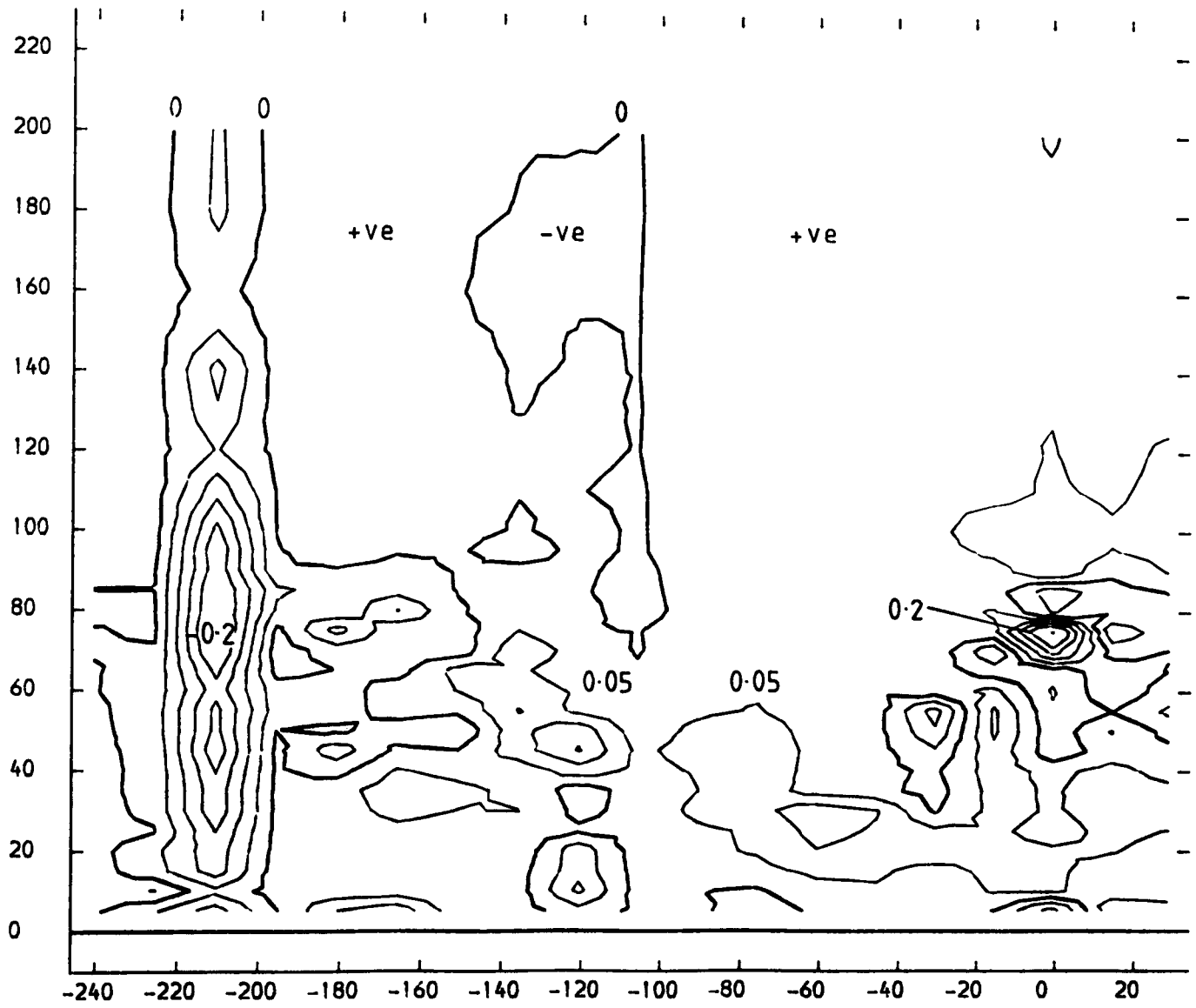


FIGURE 5.26

SLOT 8 NORMALIZED SHEAR STRESS CONTOURS (FROM UW CORRELATION)

X-AXIS TANGENTIAL CO-ORDINATE FROM TRAILING EDGE DATUM (MM)

Y-AXIS SPANWISE CO-ORDINATE FROM PERSPEX ENDWALL (MM)

CONTOURS NORMALIZED USING UPSTREAM REFERENCE DYNAMIC HEAD

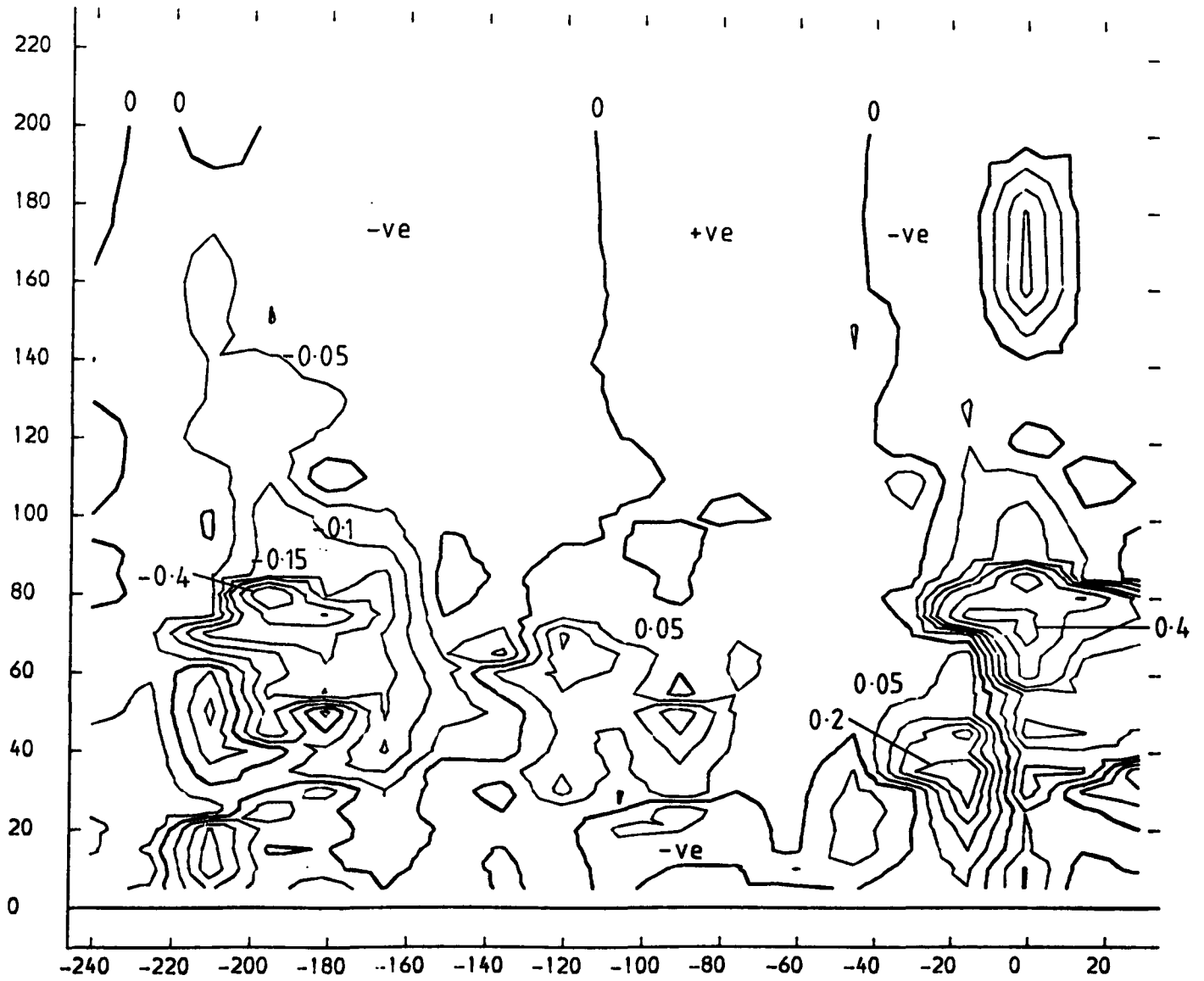


FIGURE 5.27

SLOT 1 EXPERIMENTAL DATA POINTS

THICKENED INLET BOUNDARY LAYER

X-AXIS TANGENTIAL CO-ORDINATE FROM TRAILING EDGE DATUM (MM)

Y-AXIS SPANWISE CO-ORDINATE FROM PERSPEX ENDWALL (MM)

+ PROBE DATA X MANUALLY INTERPOLATED DATA \* EXTRAPOLATED DATA

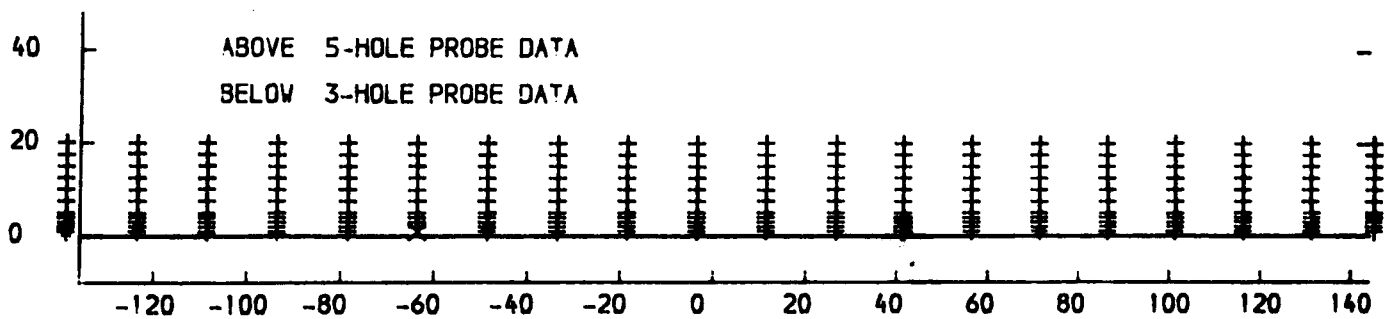
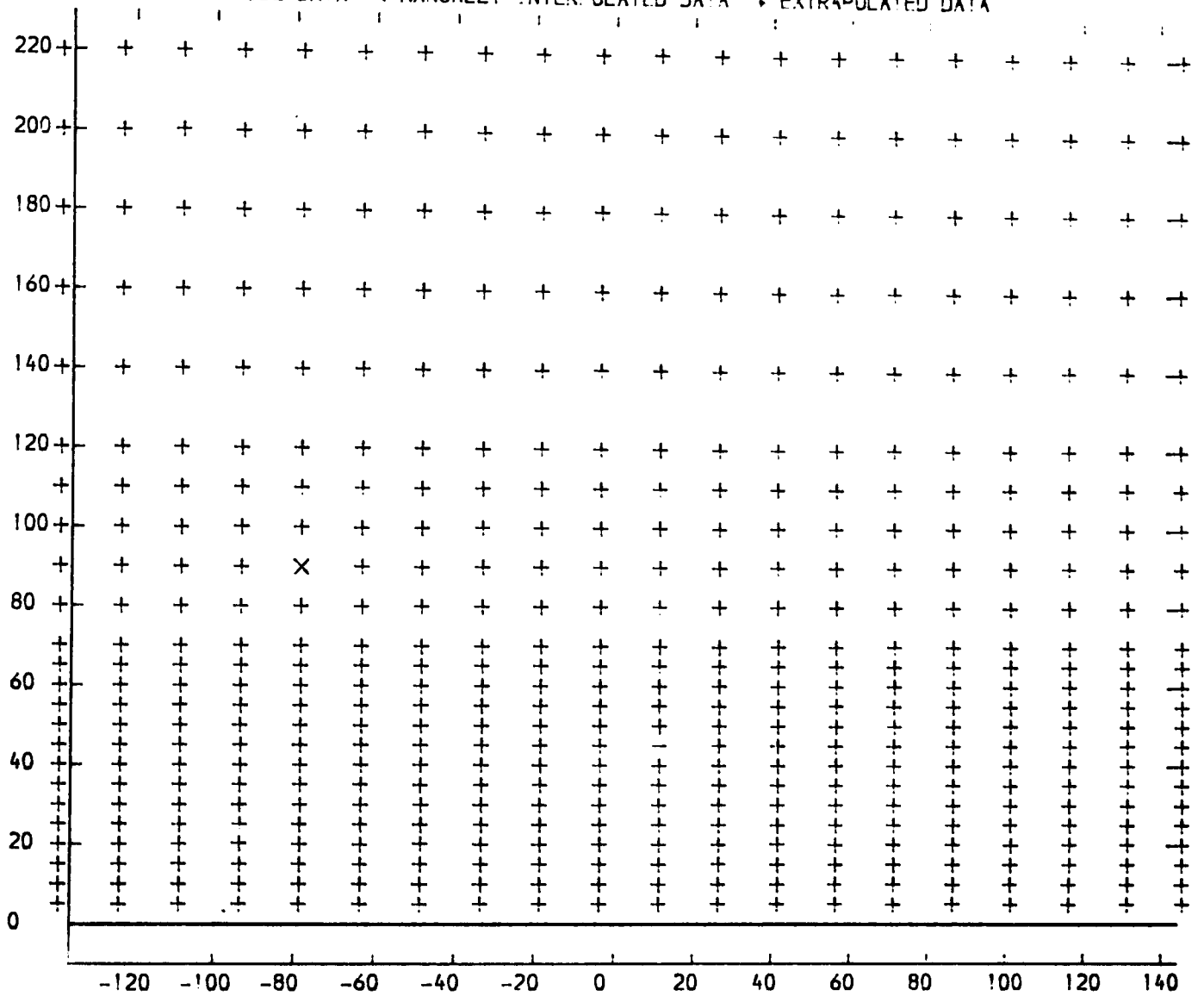


FIGURE 6.1

SLOT 1 TOTAL PRESSURE LOSS COEFFICIENT  $(P_{01}-P_{0LOCAL}) / (P_{01}-P_1)$  CONTOURS  
 THICKENED INLET BOUNDARY LAYER  
 X-AXIS TANGENTIAL CO-ORDINATE FROM TRAILING EDGE DATUM (MM)  
 Y-AXIS SPANWISE CO-ORDINATE FROM PERSPEX ENDWALL (MM)

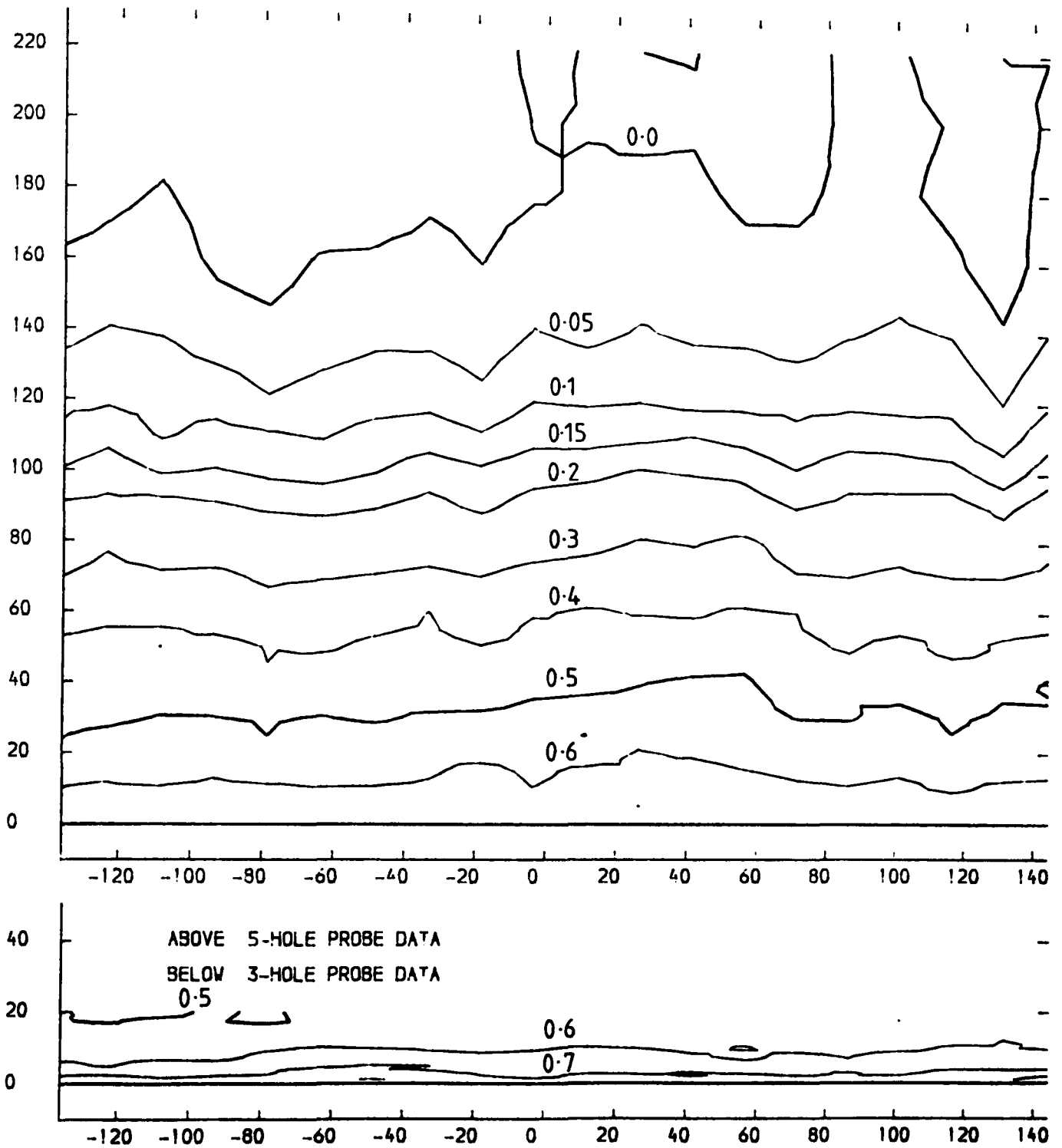


FIGURE 6.2

SLOT 1 TOTAL PRESSURE LOSS COEFFICIENT (  $(P01-P0LOCAL) / (P01-P1)$  ) CONTOURS  
 THINNED INLET BOUNDARY LAYER  
 X-AXIS TANGENTIAL CO ORDINATE FROM TRAILING EDGE DATUM (MM)  
 Y-AXIS SPANWISE CO-ORDINATE FROM PERSPEX ENDWALL (MM)

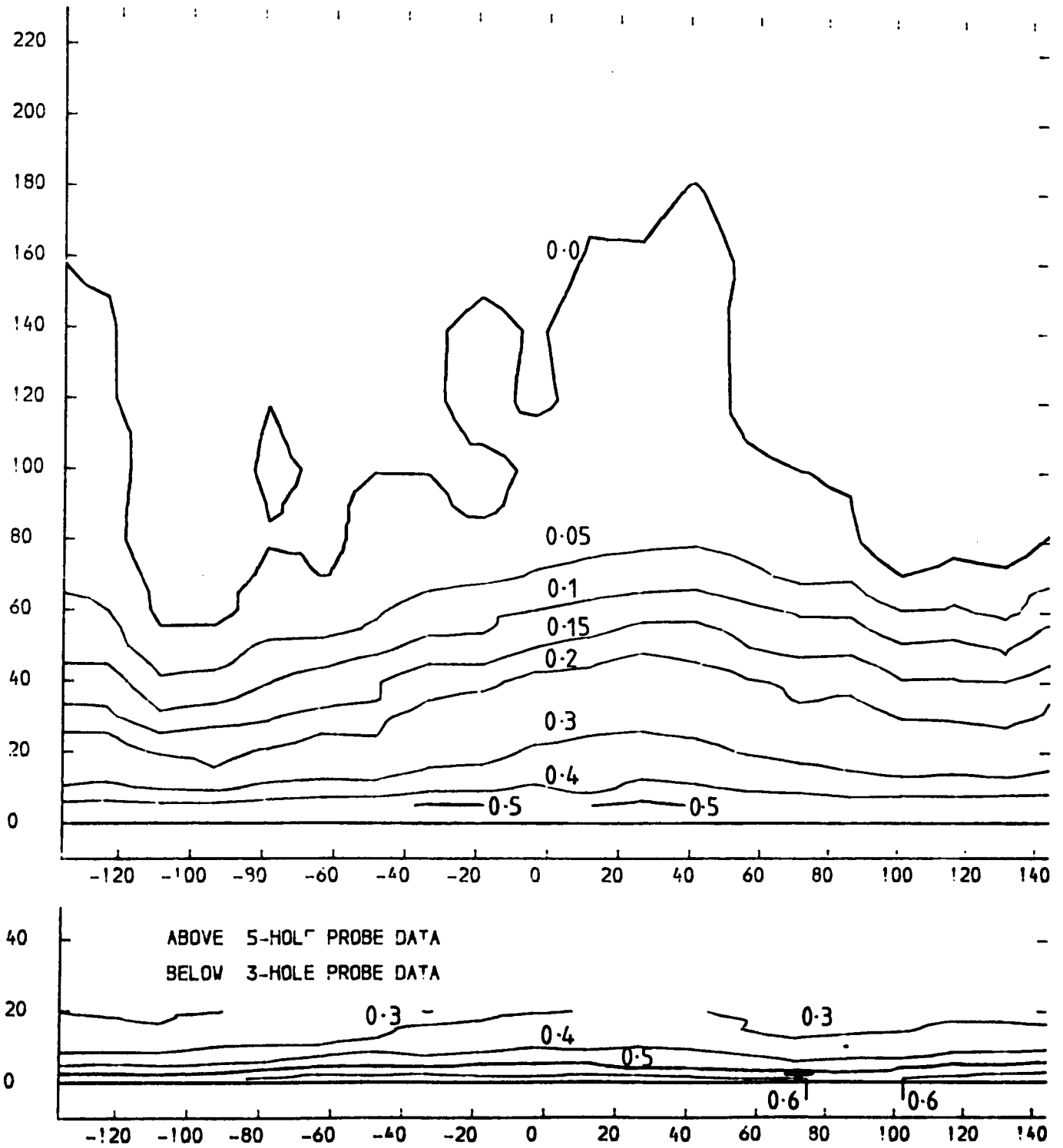
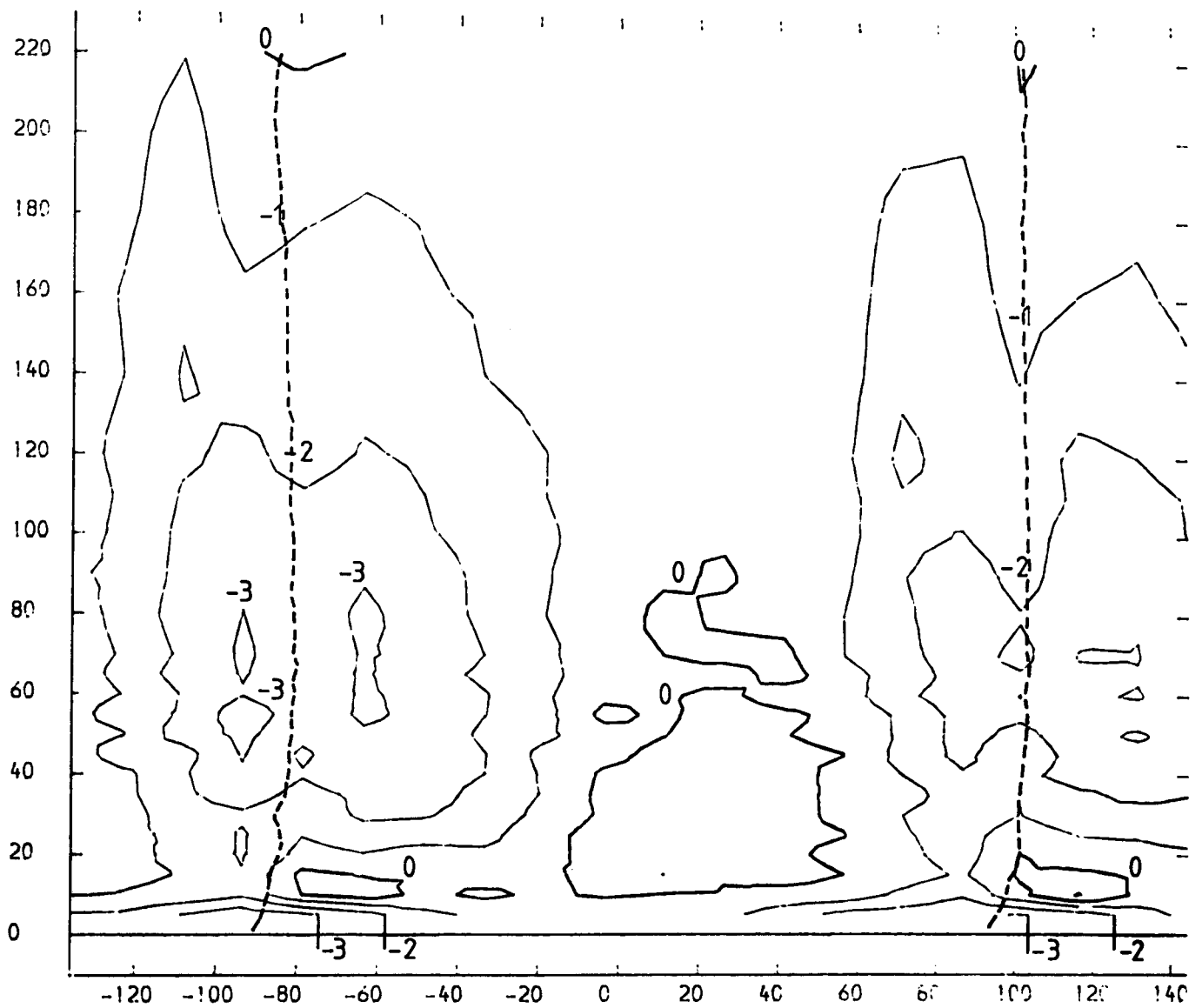


FIGURE 6.3

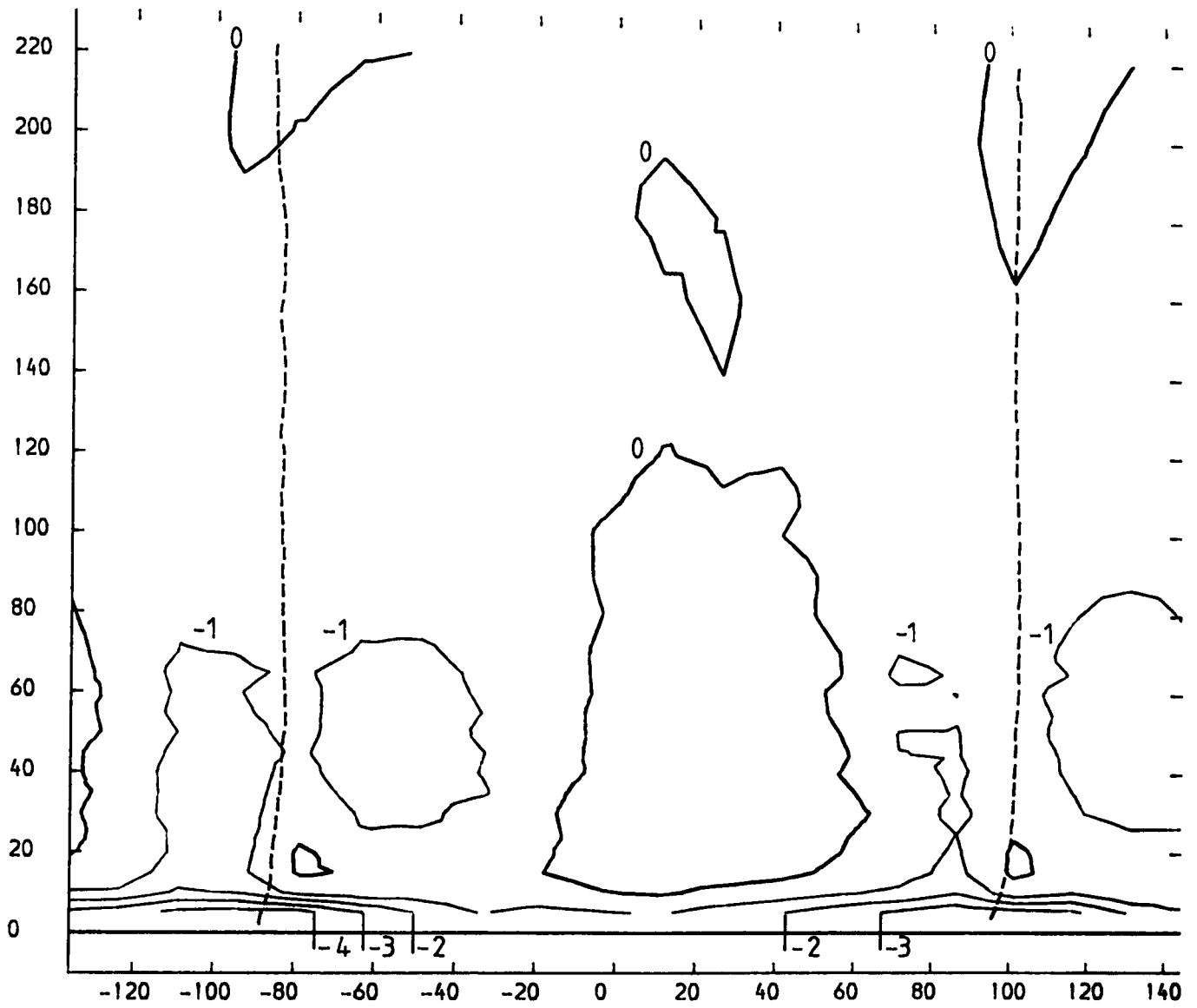
SLOT 1 STREAMWISE SPANWISE ANGLE CONTOURS (CONTOUR UNITS DEGREE)  
THICKENED INLET BOUNDARY LAYER  
X-AXIS TANGENTIAL CO-ORDINATE FROM TRAILING EDGE DATUM (MM)  
Y-AXIS SPANWISE CO-ORDINATE FROM PERSPEX ENDWALL (MM)



----- 44° YAW ANGLE CONTOUR

FIGURE 6.4

SLOT 1 STREAMWISE SPANWISE ANGLE CONTOURS (CONTOUR UNITS DEGREES)  
 THINNED INLET BOUNDARY LAYER  
 X-AXIS TANGENTIAL CO-ORDINATE FROM TRAILING EDGE DATUM (MM)  
 Y-AXIS SPANWISE CO-ORDINATE FROM PERSPEX ENDWALL (MM)



----- 44° YAW ANGLE CONTOUR

FIGURE 6.5

SLOT 1 TOTAL VELOCITY MAGNITUDE CONTOURS (CONTOUR UNITS METRES/SEC)  
 THICKENED INLET BOUNDARY LAYER  
 X-AXIS TANGENTIAL CO-ORDINATE FROM TRAILING EDGE DATUM (MM)  
 Y-AXIS SPANWISE CO-ORDINATE FROM PERSPEX ENDWALL (MM)

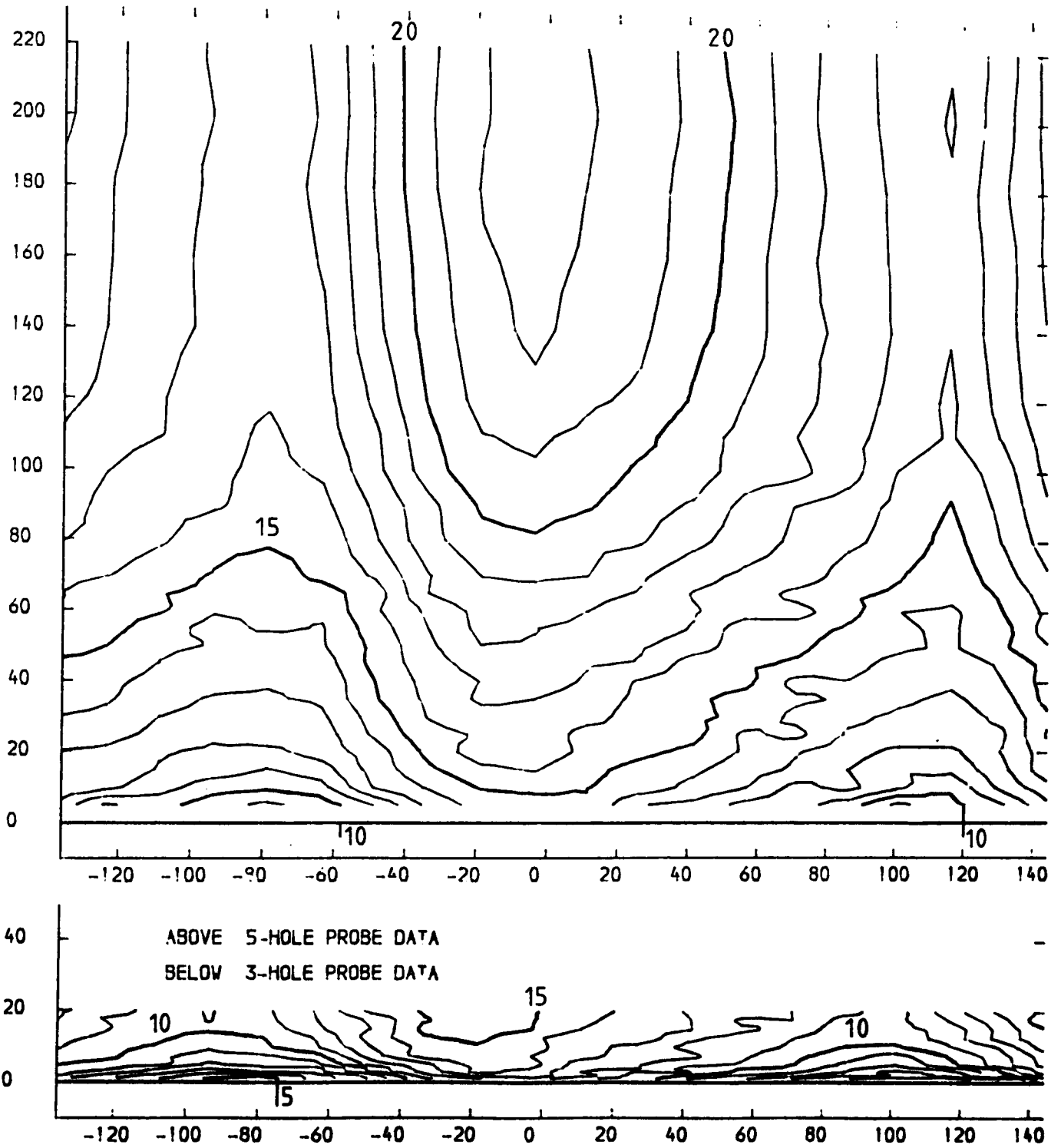


FIGURE 6.6



SLOT 1 TOTAL VELOCITY MAGNITUDE CONTOURS (CONTOUR UNITS METRES / SEC)  
 THINNED INLET BOUNDARY LAYER  
 X-AXIS TANGENTIAL CO-ORDINATE FROM TRAILING EDGE DATUM (MM)  
 Y-AXIS SPANWISE CO-ORDINATE FROM PERSPEX ENDWALL (MM)

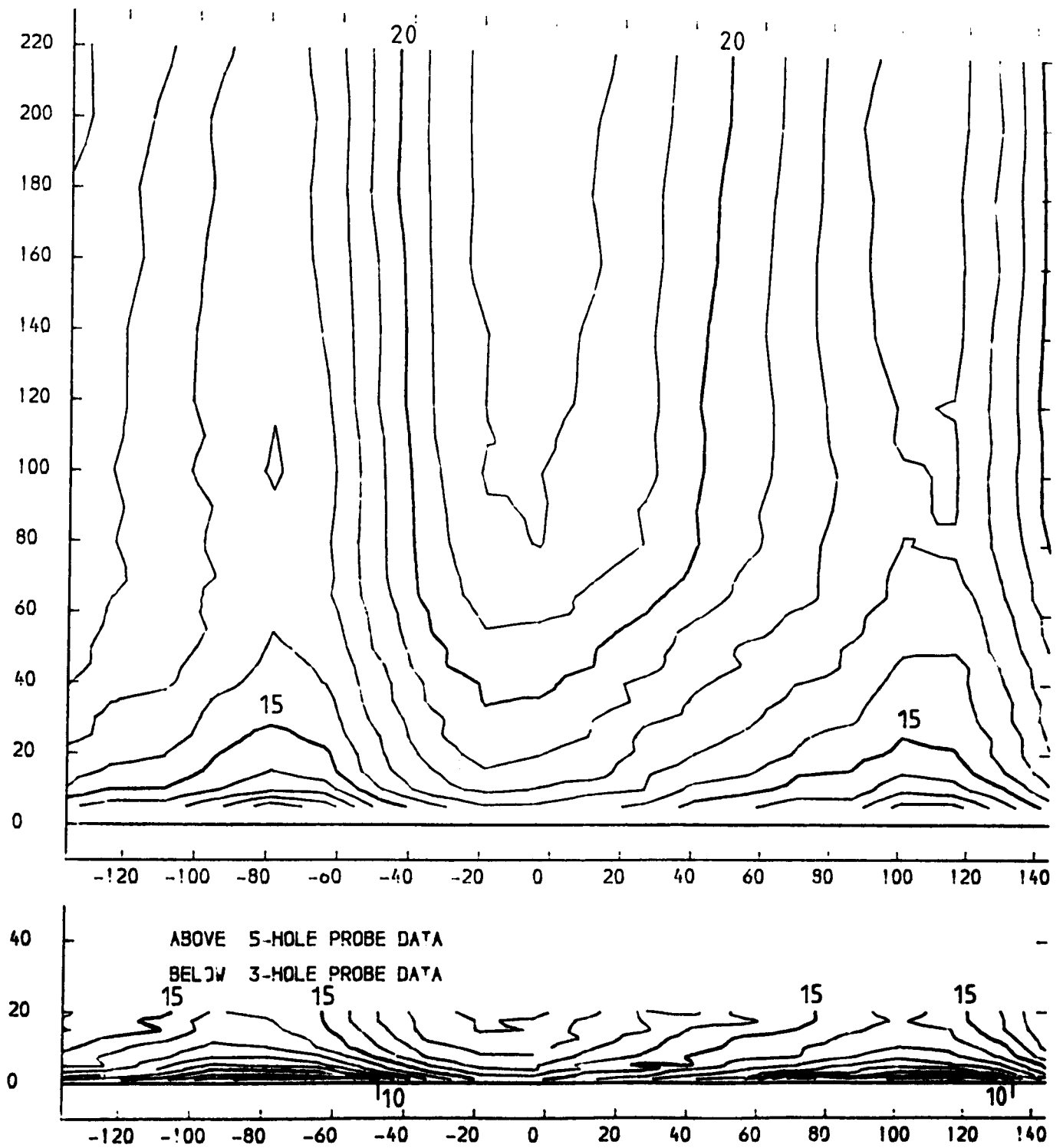


FIGURE 6.7

SLOT 8 TOTAL PRESSURE LOSS COEFFICIENT  $(P_{01}-P_{0LOCAL}) / (P_{01}-P_{11})$  CONTOURS  
 THICKENED INLET BOUNDARY LAYER  
 Y-AXIS TANGENTIAL CO-ORDINATE FROM TRAILING EDGE DATUM (MM)  
 Y-AXIS SPANWISE CO-ORDINATE FROM PERSPEX ENDWALL (MM)

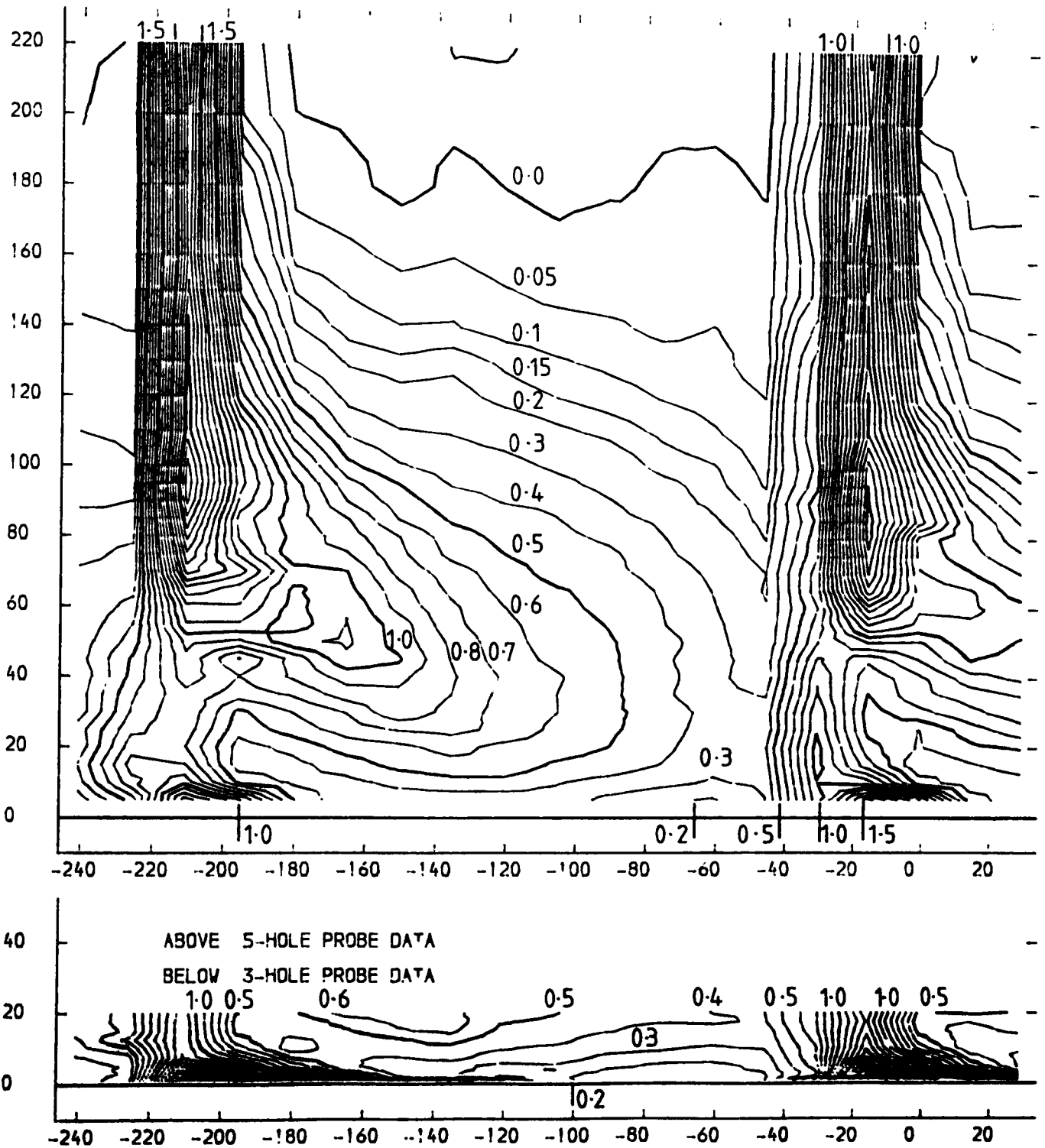


FIGURE 6.8

SLOT 9 TOTAL PRESSURE LOSS COEFFICIENT (  $(P01 - P0LOCAL) / (P01 - P1)$  ) CONTOURS  
 THINNED INLET BOUNDARY LAYER  
 X-AXIS TANGENTIAL CO-ORDINATE FROM TRAILING EDGE DATUM (MM)  
 Y-AXIS SPANWISE CO-ORDINATE FROM PERSPEX ENDWALL (MM)

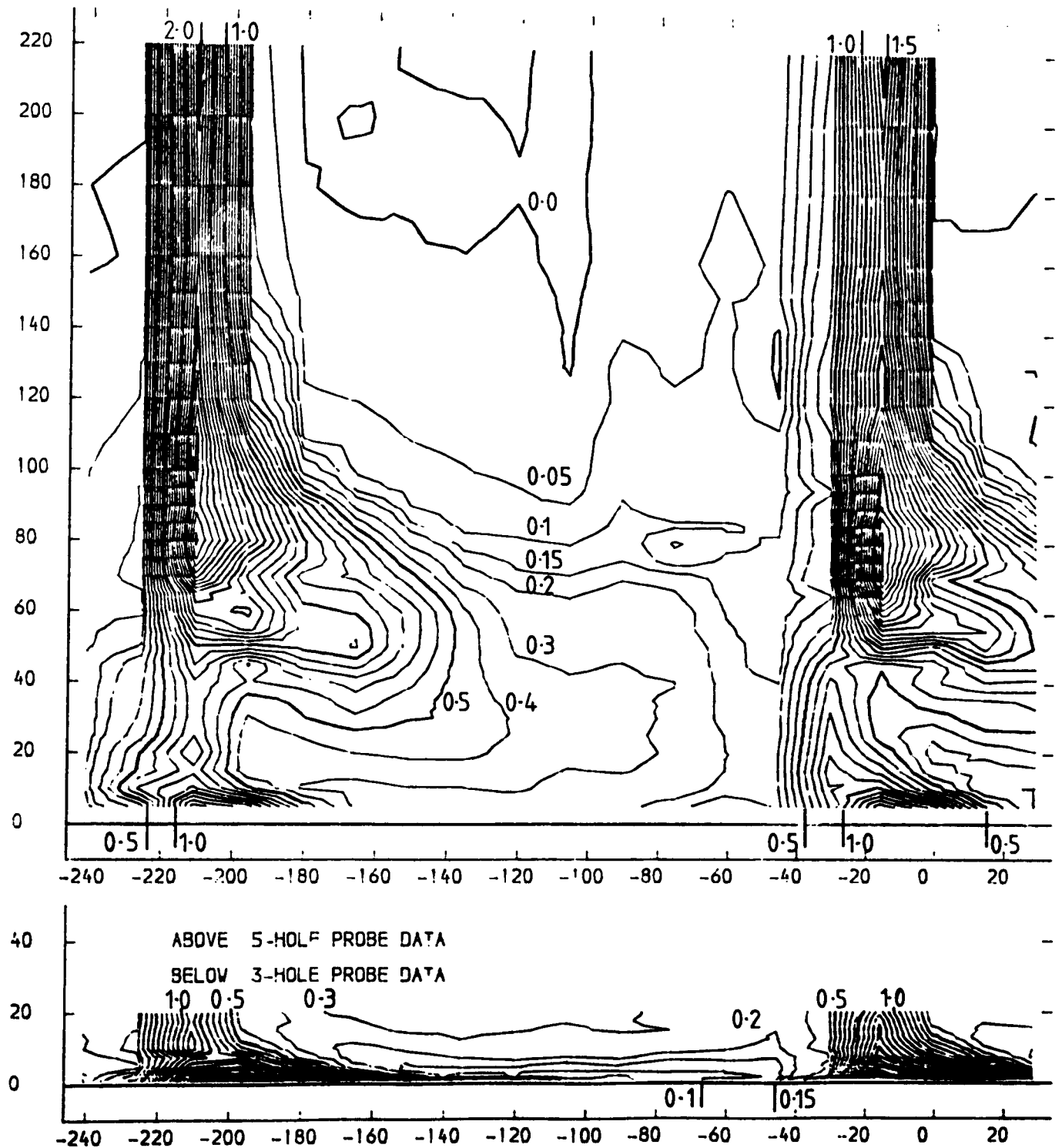


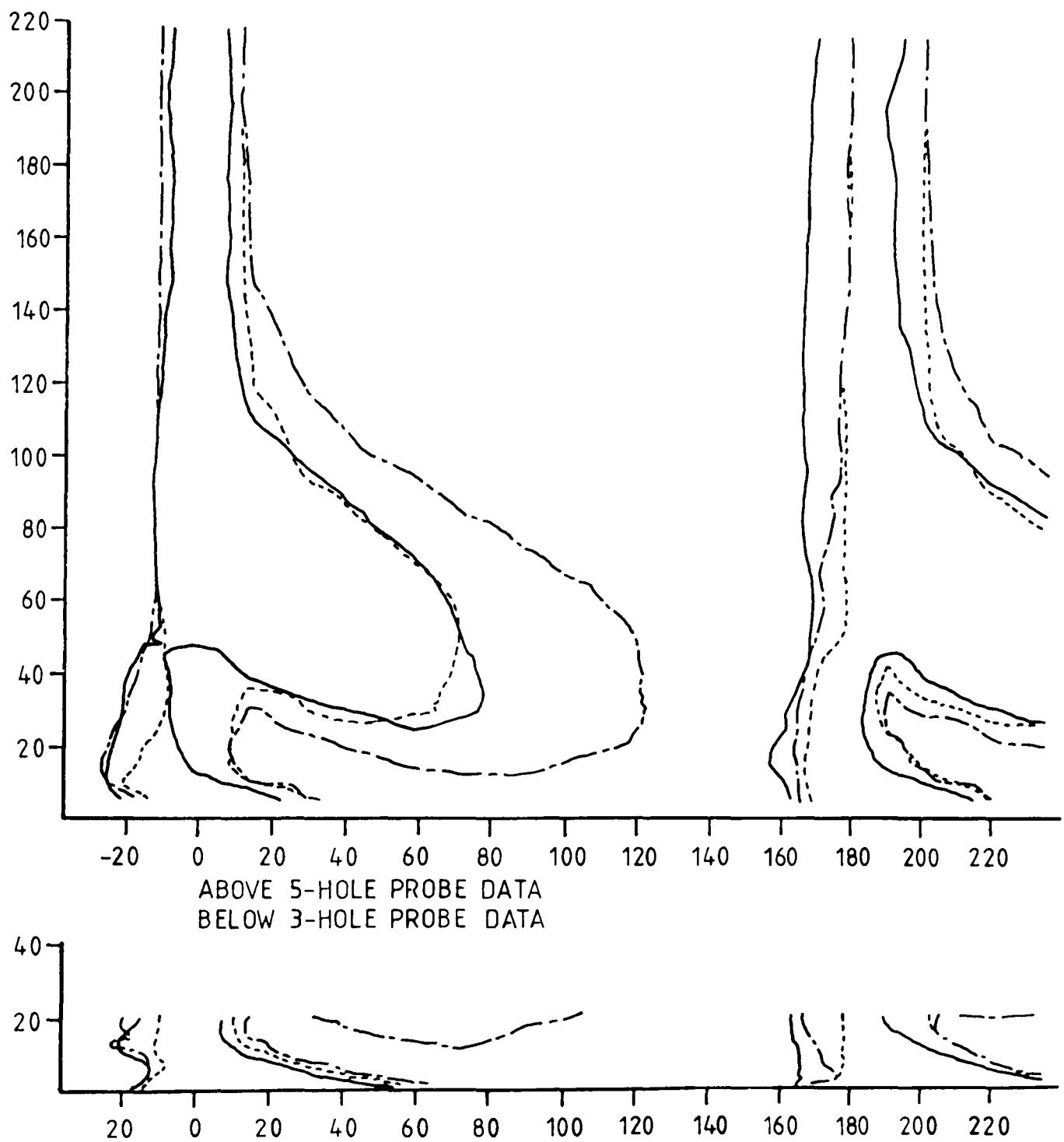
FIGURE 6.9

# SLOT 8 COMPARISON OF THE THREE INLET BOUNDARY LAYER LOSS CORES

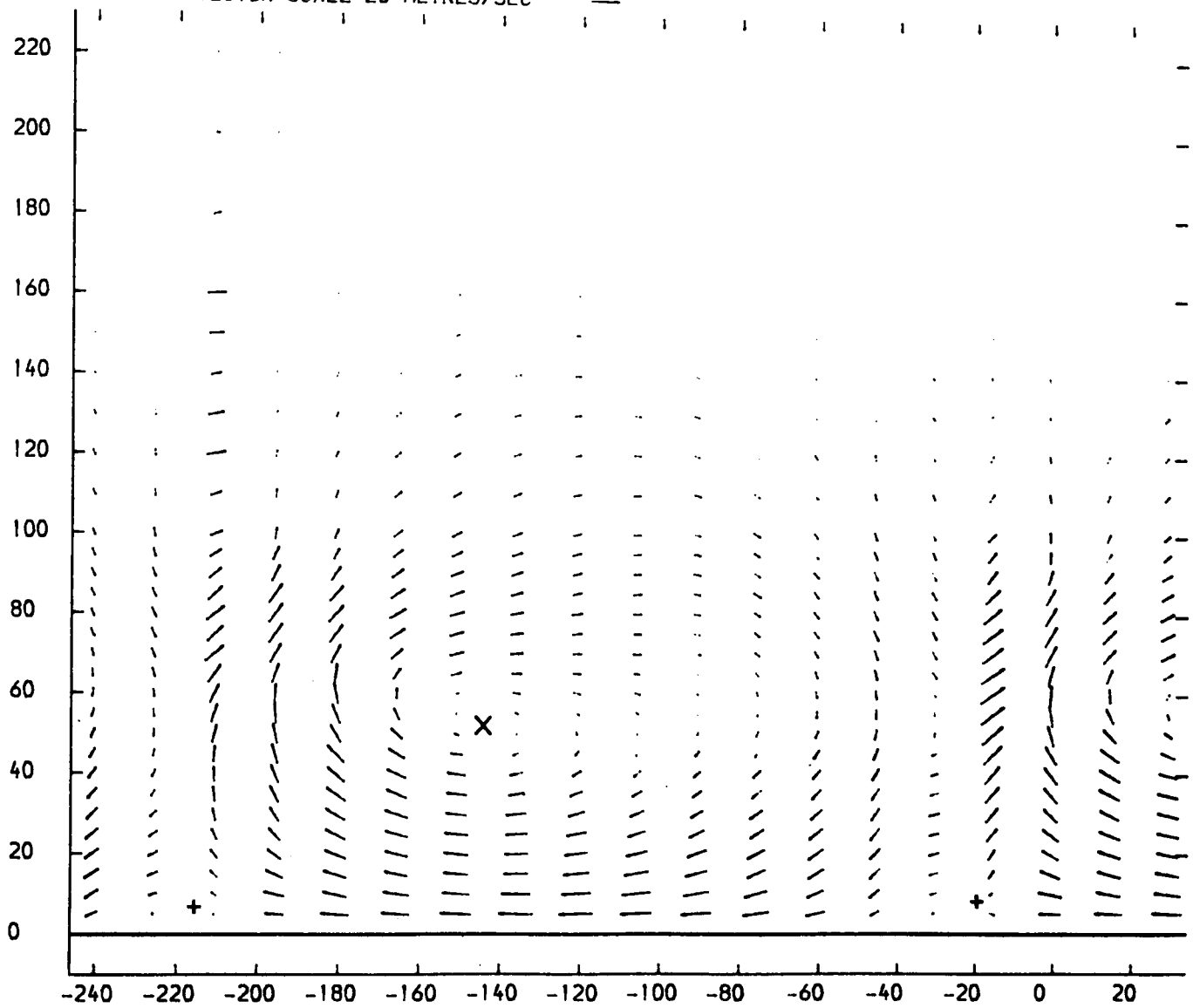
X-AXIS TANGENTIAL CO-ORDINATE FROM WAKE CENTRE-LINE (MM)  
 Y-AXIS SPANWISE CO-ORDINATE FROM PERSPEX ENDWALL (MM)

BOUNDARY LAYER  
 AT CASCADE INLET

- NATURAL
- - - THICKENED
- · - THINNED



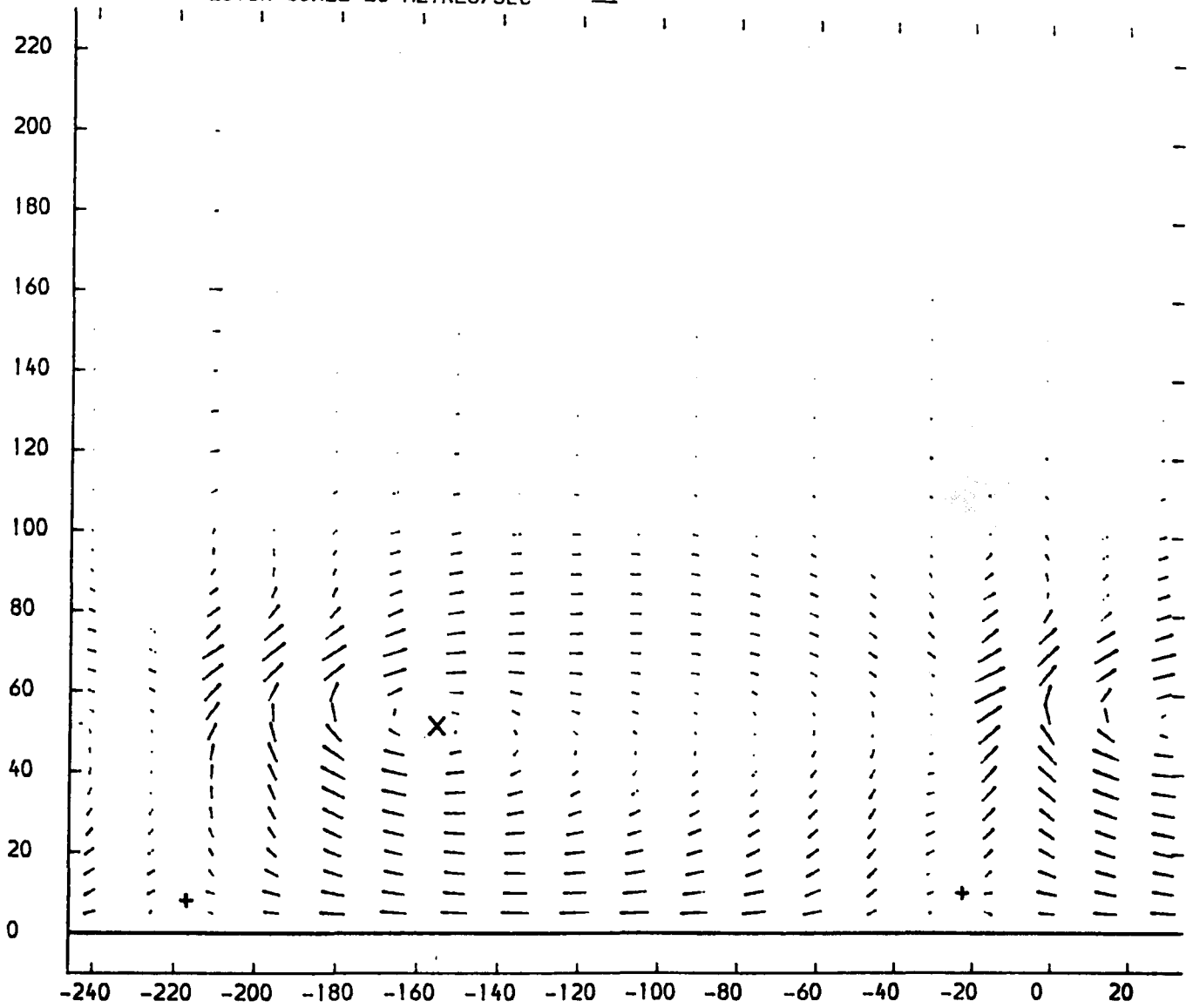
SLOT 8 VECTOR PLOT OF SECONDARY VELOCITIES  $(V_T(\text{SEC}) = V_T(\text{LOC}) - V_T(\text{M.S.}) \cdot V_A(\text{LOC}) / V_A(\text{M.S.}))$   
 THICKENED INLET BOUNDARY LAYER  
 X-AXIS TANGENTIAL CO-ORDINATE FROM TRAILING EDGE DATUM (MM)  
 Y-AXIS SPANWISE CO-ORDINATE FROM PERSPEX ENDWALL (MM)  
 VECTOR SCALE 20 METRES/SEC



X PASSAGE VORTEX CENTRE  
 + COUNTER VORTEX CENTRES

FIGURE 6.11

SLOT 8 VECTOR PLOT OF SECONDARY VELOCITIES ( $V_T(\text{SEC}) = V_T(\text{LOC}) - V_T(\text{M.S.}) + V_A(\text{LOC}) / V_A(\text{M.S.})$ )  
 THINNED INLET BOUNDARY LAYER  
 X-AXIS TANGENTIAL CO-ORDINATE FROM TRAILING EDGE DATUM (MM)  
 Y-AXIS SPANWISE CO-ORDINATE FROM PERSPEX ENDWALL (MM)  
 VECTOR SCALE 20 METRES/SEC



X PASSAGE VORTEX CENTRE  
 + COUNTER VORTEX CENTRES

FIGURE 6.12

SLOT 8 STATIC PRESSURE COEFFICIENT  $(P^* - P_{LOCAL}) / (P_{01} - P_1)$  CONTOURS  
 THICKENED INLET BOUNDARY LAYER  
 X-AXIS TANGENTIAL CO-ORDINATE FROM TRAILING EDGE DATUM (MM)  
 Y-AXIS SPANWISE CO-ORDINATE FROM PERSPEX ENDWALL (MM)

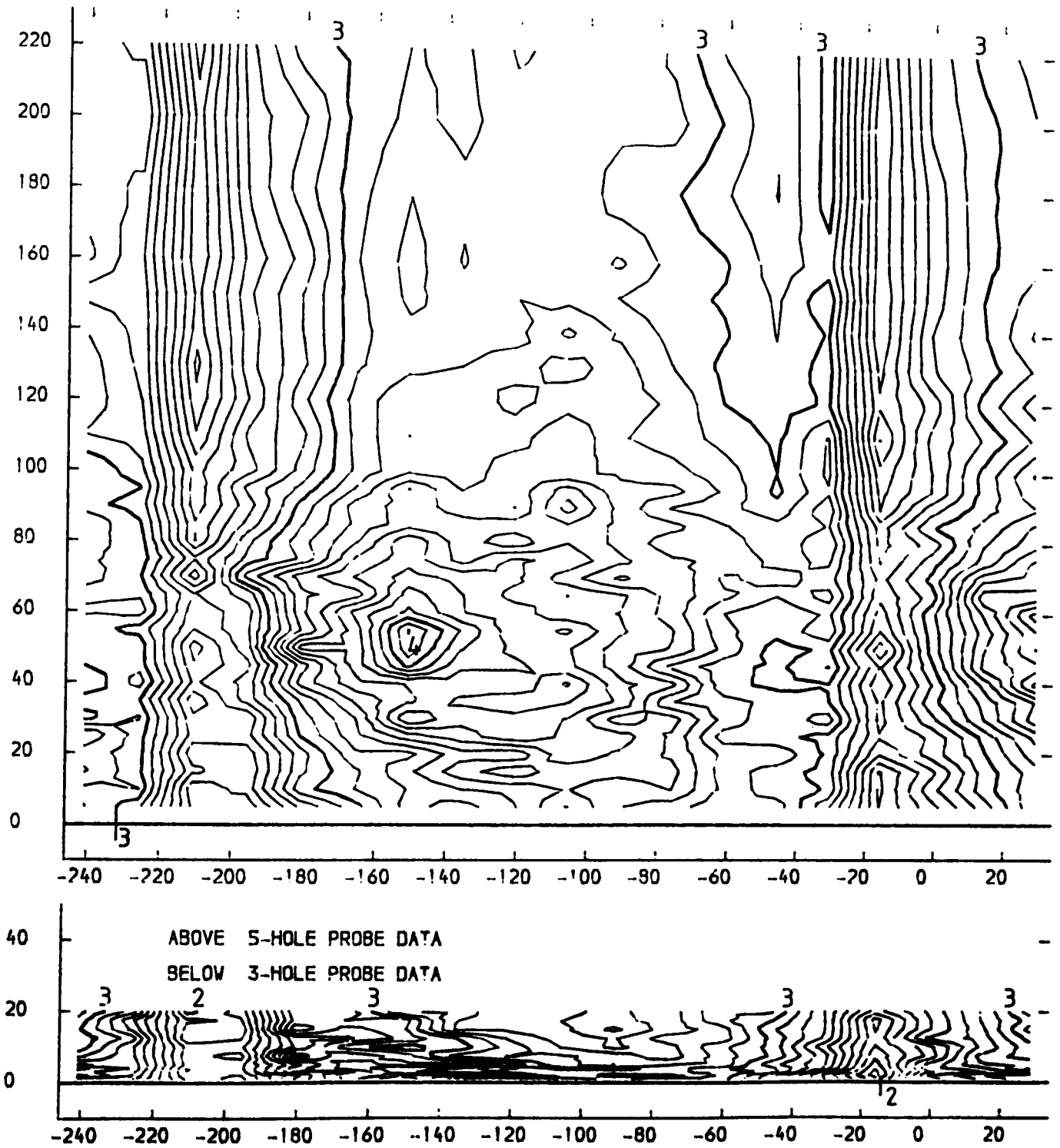


FIGURE 6.13

SLOT 8 STATIC PRESSURE COEFFICIENT (  $(P1-PLocal) / (P01-P1)$  ) CONTOURS  
 THINNED INLET BOUNDARY LAYER  
 X-AXIS TANGENTIAL O-ORDINATE FROM TRAILING EDGE DATUM (MM)  
 Y-AXIS SPANWISE CO-ORDINATE FROM PER PEX ENDOVALL (MM)

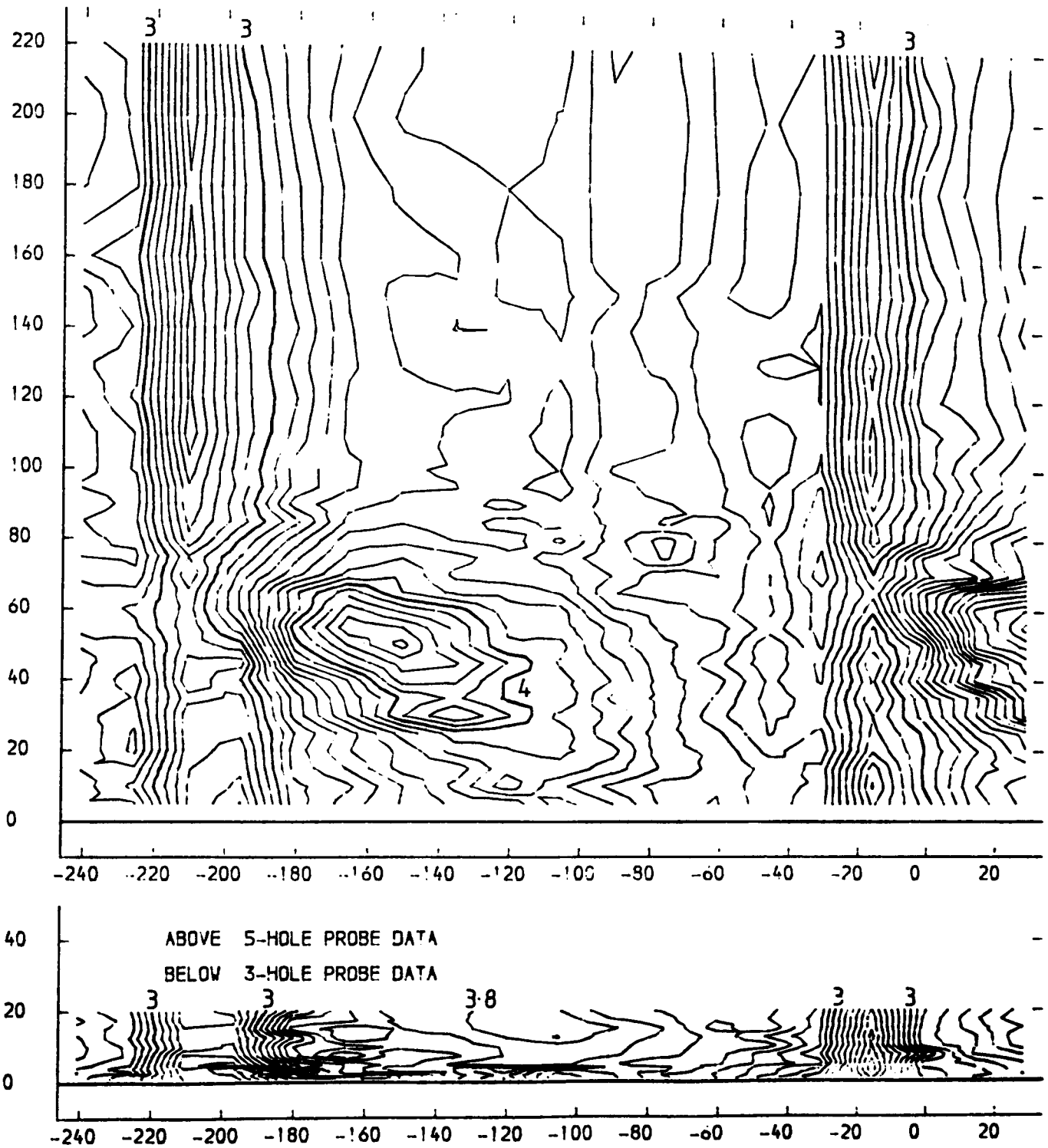


FIGURE 6.14



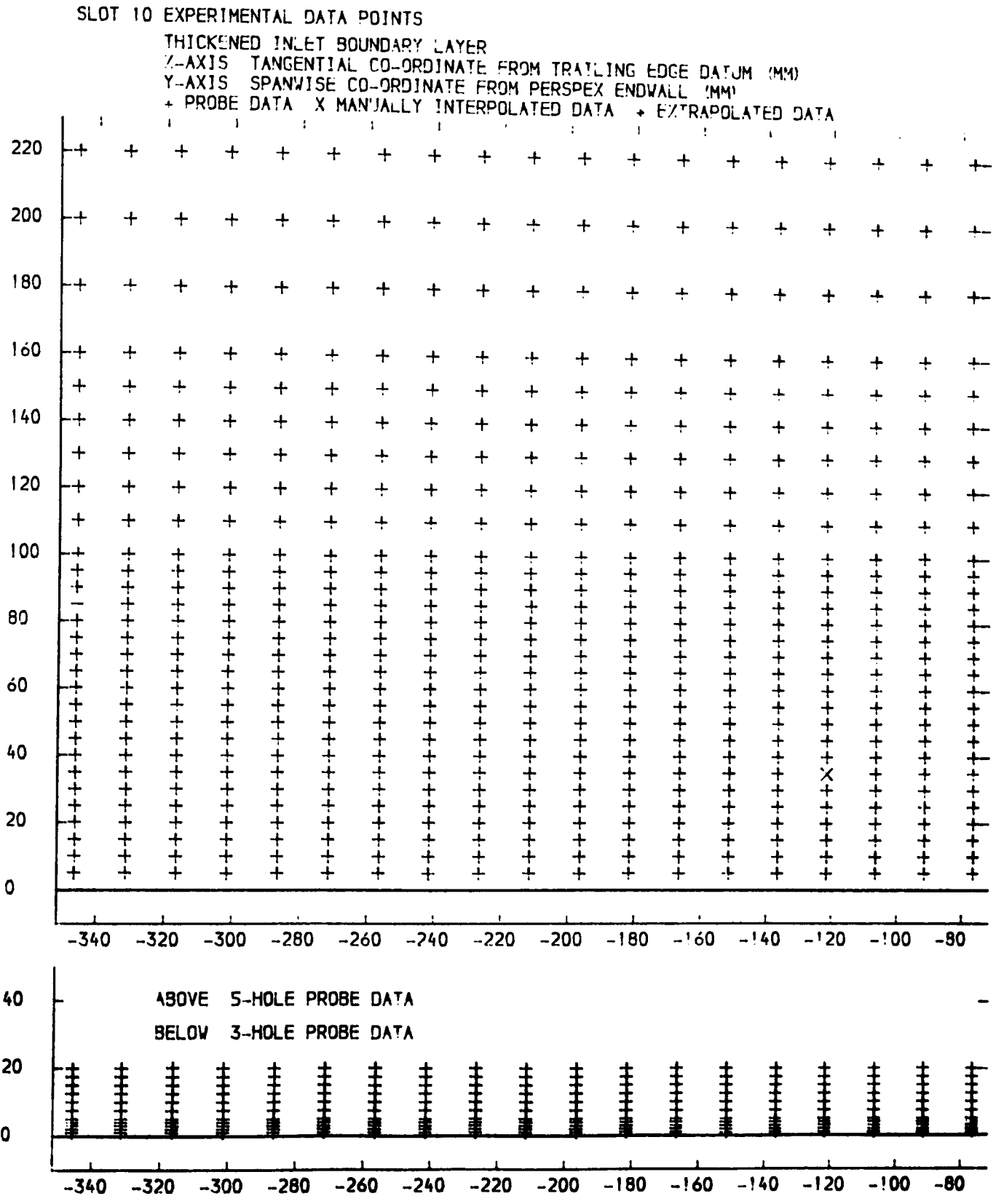


FIGURE 6.15

SLOT 10 TOTAL PRESSURE LOSS COEFFICIENT  $(P_{01} - P_{0LOCAL}) / (P_{01} - P_1)$  CONTOURS  
 THICKENED INLET BOUNDARY LAYER  
 X-AXIS TANGENTIAL CO ORDINATE FROM TRAILING EDGE DATUM (MM)  
 Y-AXIS SPANWISE CO-ORDINATE FROM PERSPEX ENDWALL (MM)

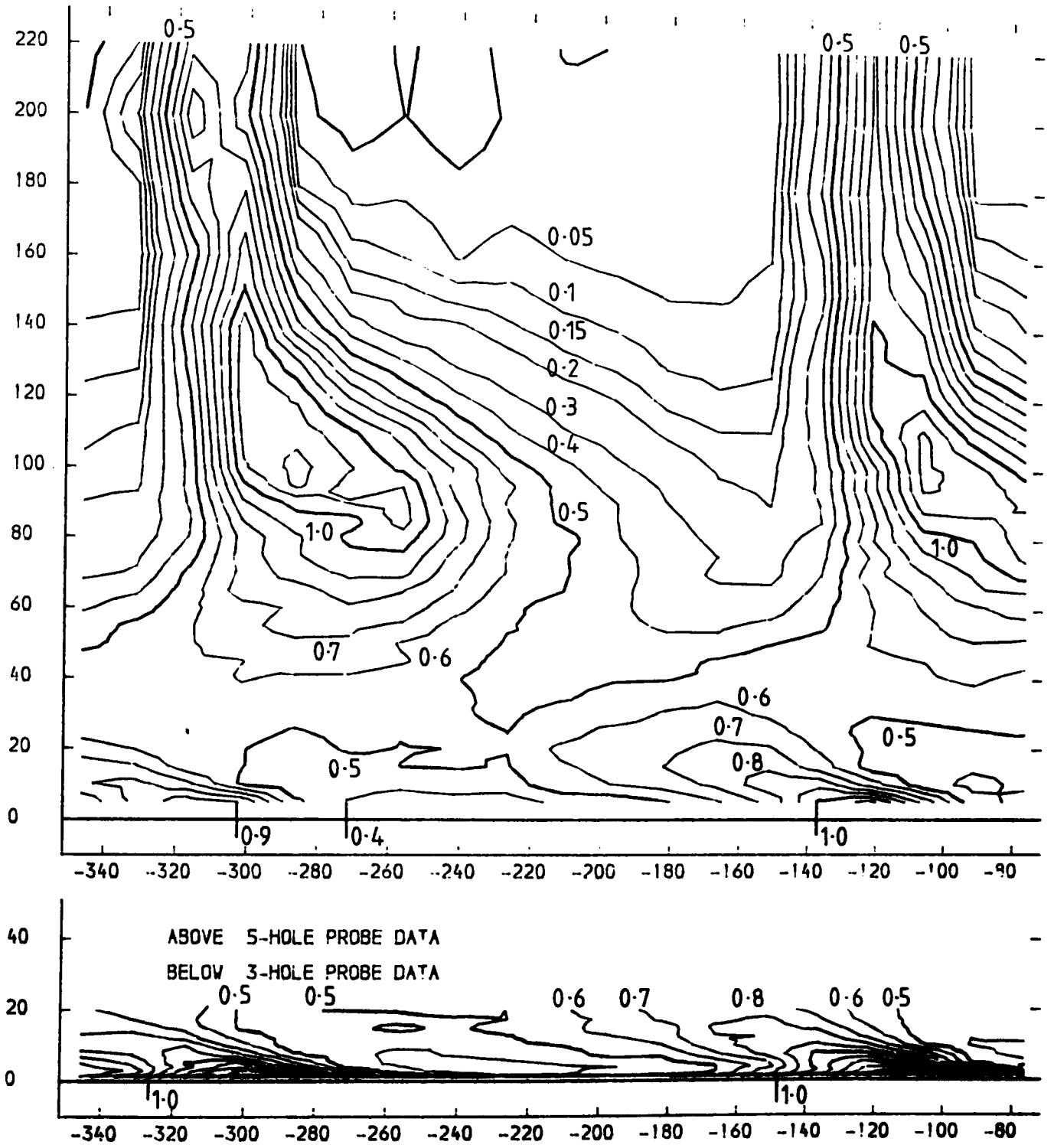


FIGURE 6.16

SLOT 10 TOTAL PRESSURE LOSS COEFFICIENT  $(P_{01}-P_{0LOCAL})/(P_{01}-P_{01})$  CONTOURS  
 THINNED INLET BOUNDARY LAYER  
 X-AXIS TANGENTIAL CO-ORDINATE FROM TRAILING EDGE DATUM (MM)  
 Y-AXIS SPANWISE CO-ORDINATE FROM PERSPECTIVE ENDWALL (MM)

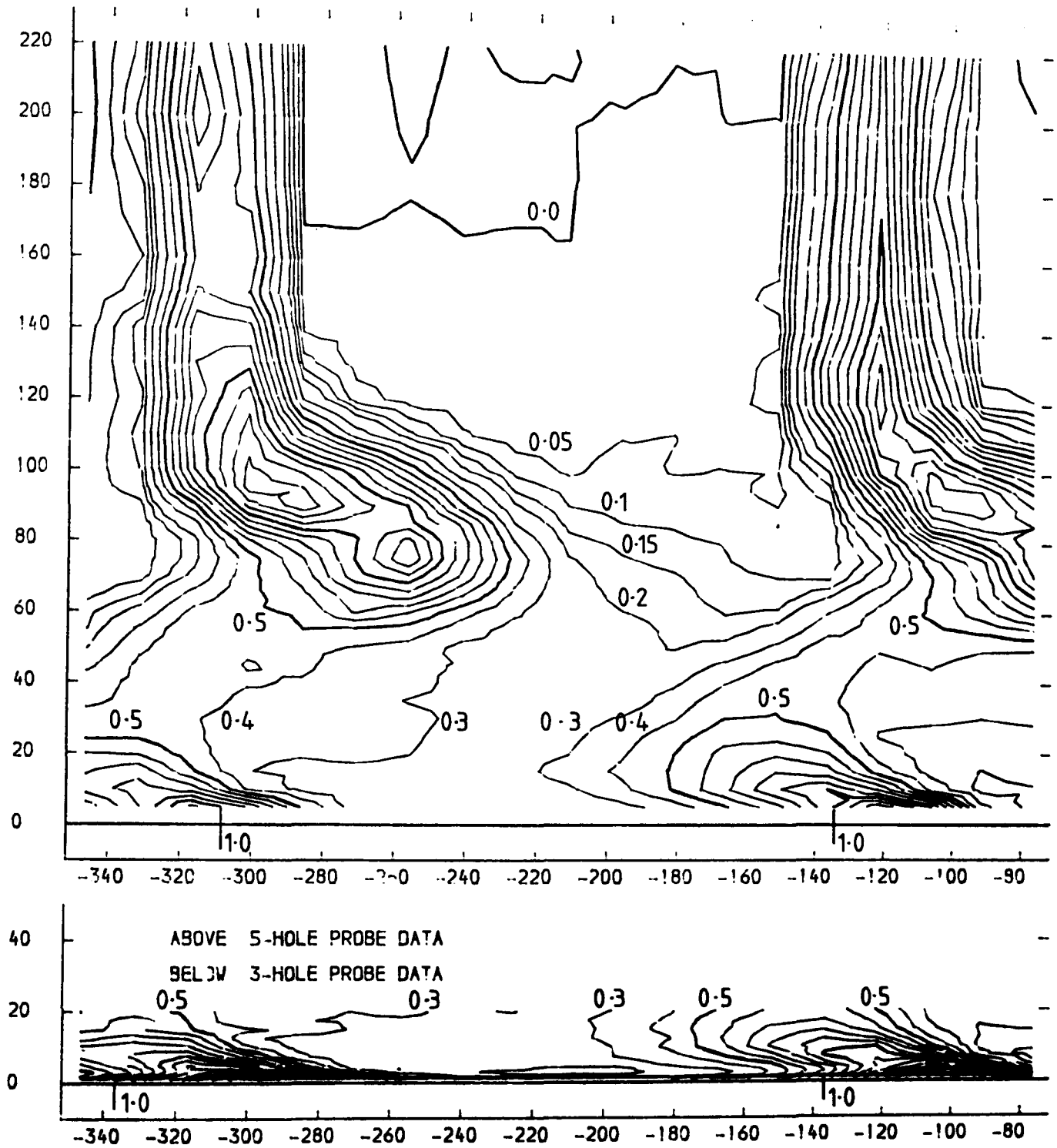


FIGURE 6.17

# SLOT 10 COMPARISON OF THE THREE INLET BOUNDARY LAYER LOSS CORES

X-AXIS TANGENTIAL CO-ORDINATE FROM WAKE CENTRE-LINE (MM)  
Y-AXIS SPANWISE CO-ORDINATE FROM PERSPEX ENDWALL (MM)

BOUNDARY LAYER  
AT CASCADE INLET

- NATURAL
- - THICKENED
- · - THINNED

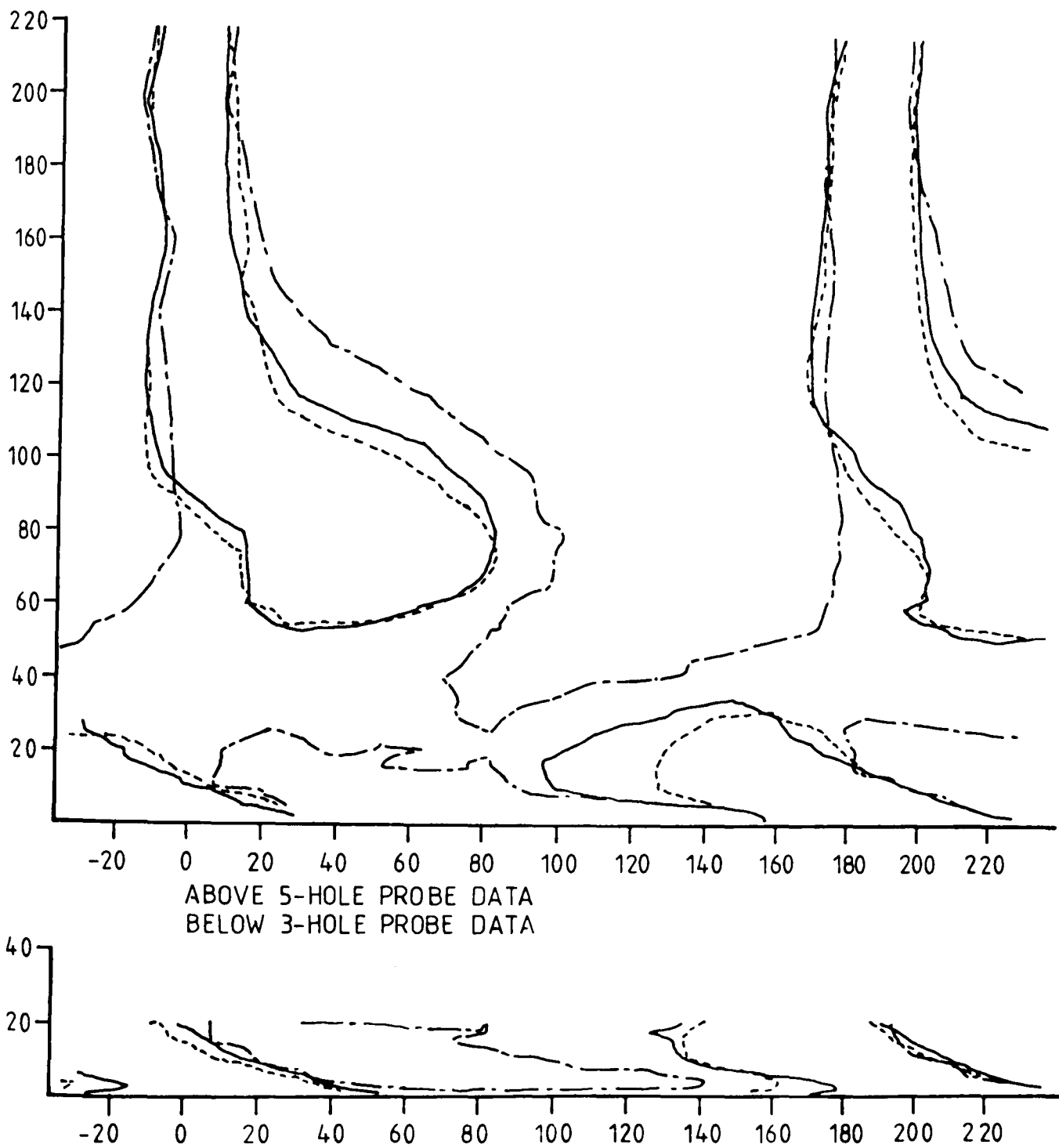
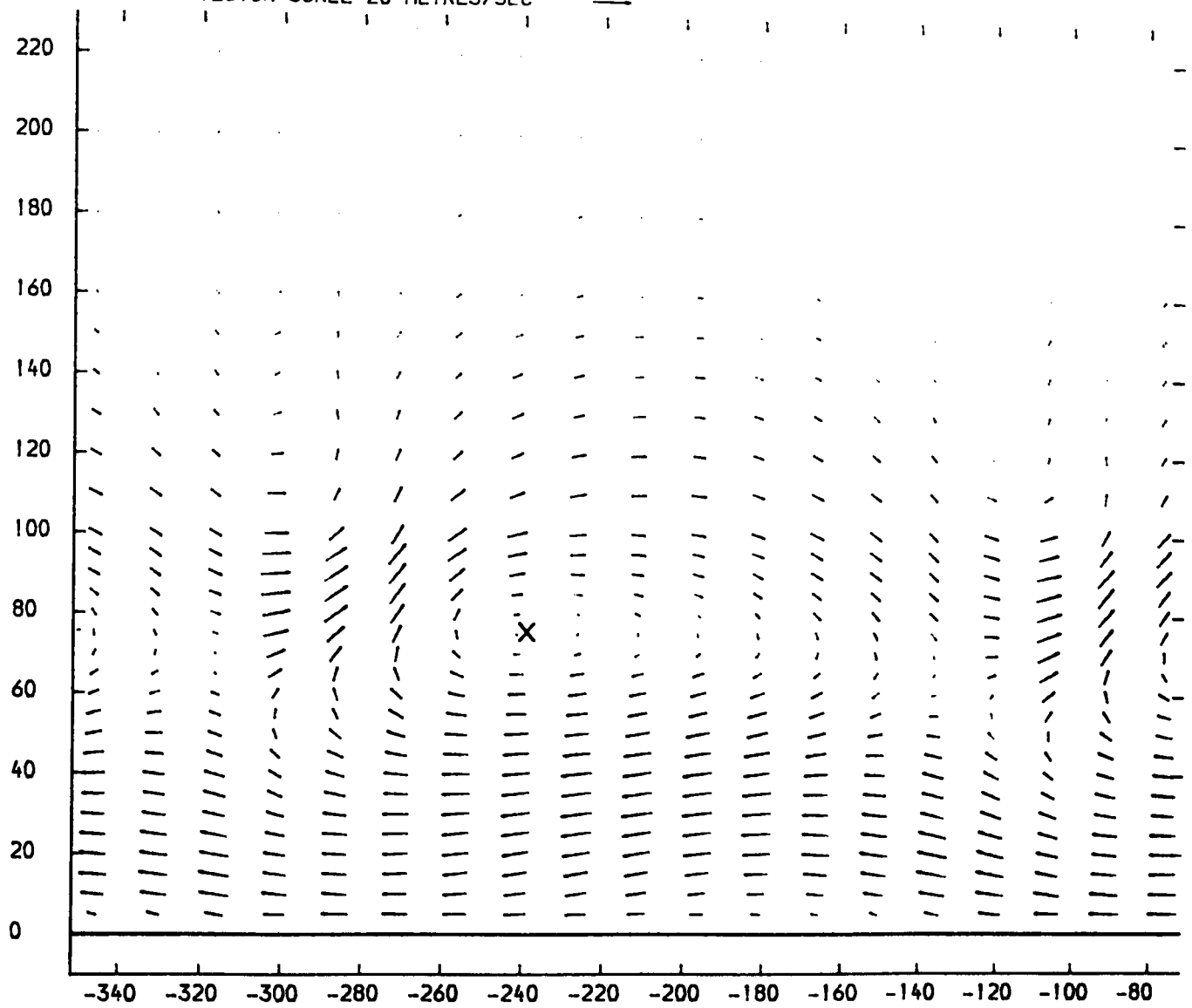


FIGURE 6.18

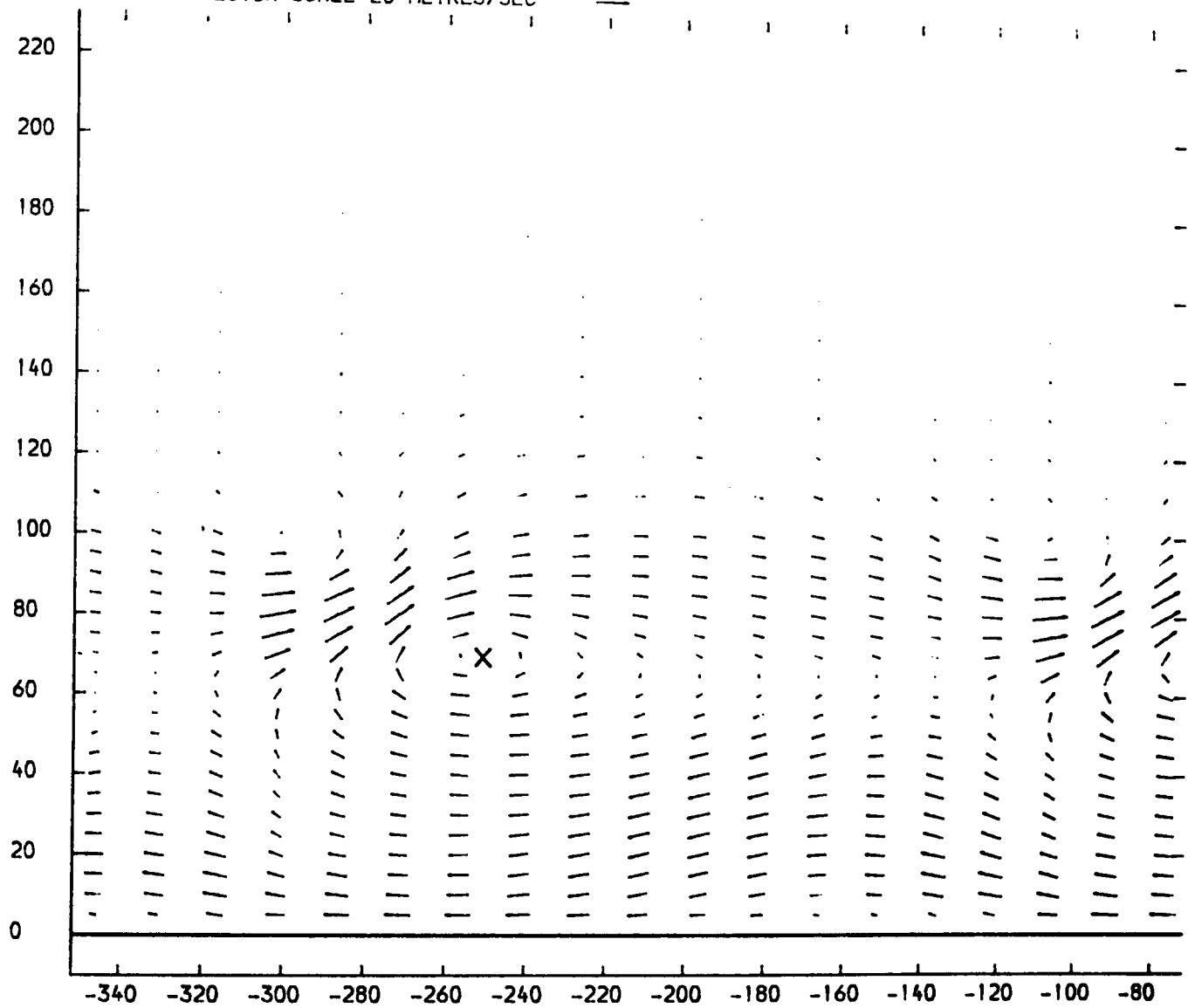
SLOT 10 VECTOR PLOT OF SECONDARY VELOCITIES  $(V_T(\text{SEC}) = V_T(\text{LOC}) - V_T(\text{M.S.}) + V_A(\text{LOC}) / V_A(\text{M.S.}))$   
THICKENED INLET BOUNDARY LAYER  
X-AXIS TANGENTIAL CO-ORDINATE FROM TRAILING EDGE DATUM (MM)  
Y-AXIS SPANWISE CO-ORDINATE FROM PERSPEX ENDWALL (MM)  
VECTOR SCALE 20 METRES/SEC



X PASSAGE VORTEX CENTRE

FIGURE 6.19

SLOT 10 VECTOR PLOT OF SECONDARY VELOCITIES  $(V_T(\text{SEC}) = V_T(\text{LOC}) - V_T(\text{M.S.}) + V_A(\text{LOC}) / V_A(\text{M.S.}))$   
 THINNED INLET BOUNDARY LAYER  
 X-AXIS TANGENTIAL CO-ORDINATE FROM TRAILING EDGE DATUM (MM)  
 Y-AXIS SPANWISE CO-ORDINATE FROM PERSPEX ENDWALL (MM)  
 VECTOR SCALE 20 METRES/SEC



X PASSAGE VORTEX CENTRE

FIGURE 6.20

SLOT 10 STATIC PRESSURE COEFFICIENT  $(P1-PLOCAL)/(P01-P1)$  CONTOURS  
 THICKENED INLET BOUNDARY LAYER  
 X-AXIS TANGENTIAL CO-ORDINATE FROM TRAILING EDGE DATUM (MM)  
 Y-AXIS SPANWISE CO-ORDINATE FROM PERSPEX ENDWALL (MM)

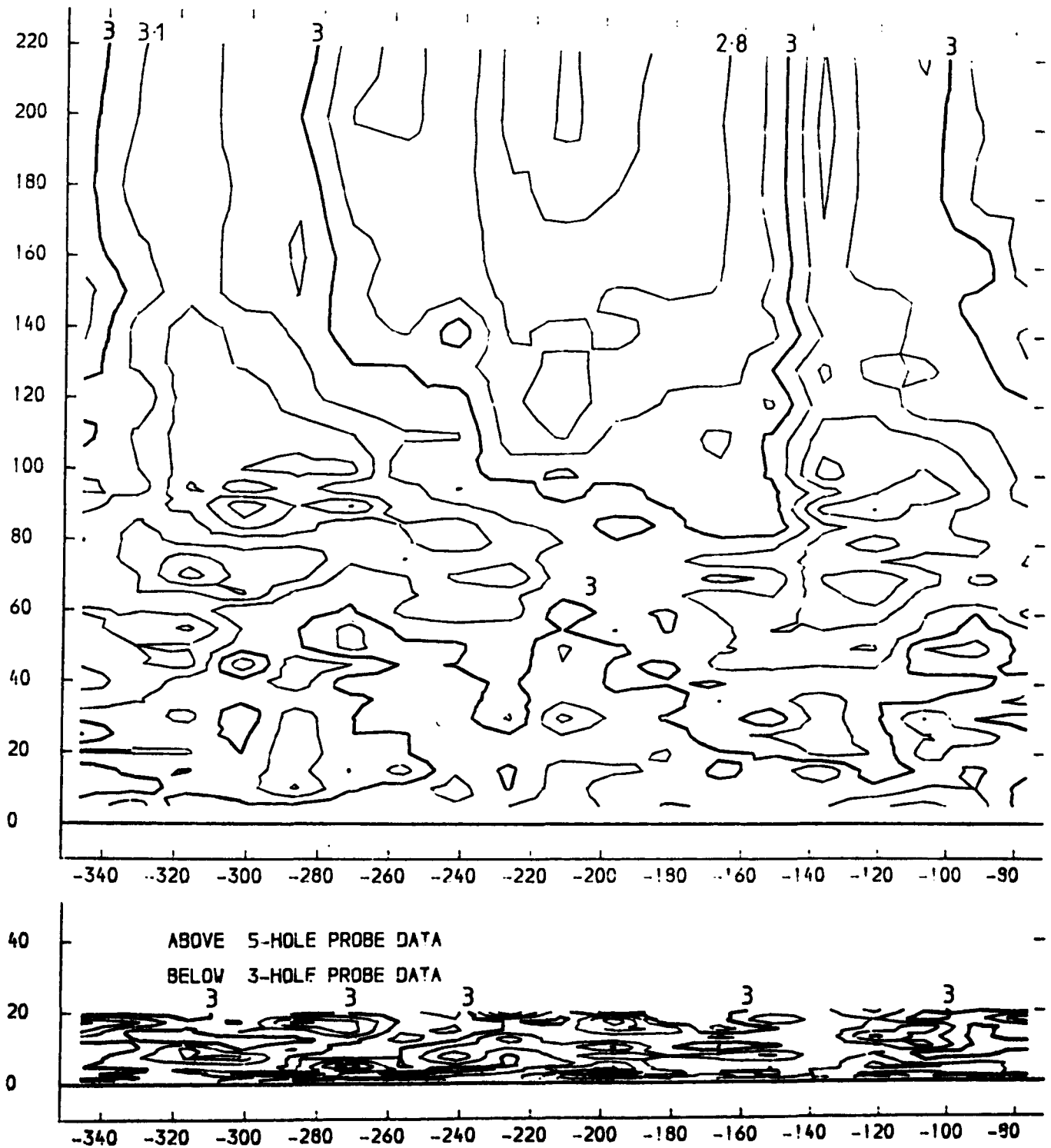


FIGURE 6.21

SLOT 10 STATIC PRESSURE COEFFICIENT (  $(P1-PLOCAL) / (P0-P1)$  ) CONTOURS  
 THINNED INLET BOUNDARY LAYER  
 X-AXIS TANGENTIAL CO-ORDINATE FROM TRAILING EDGE DATUM (MM)  
 Y-AXIS SPANWISE CO-ORDINATE FROM PERSPEX ENDWALL (MM)

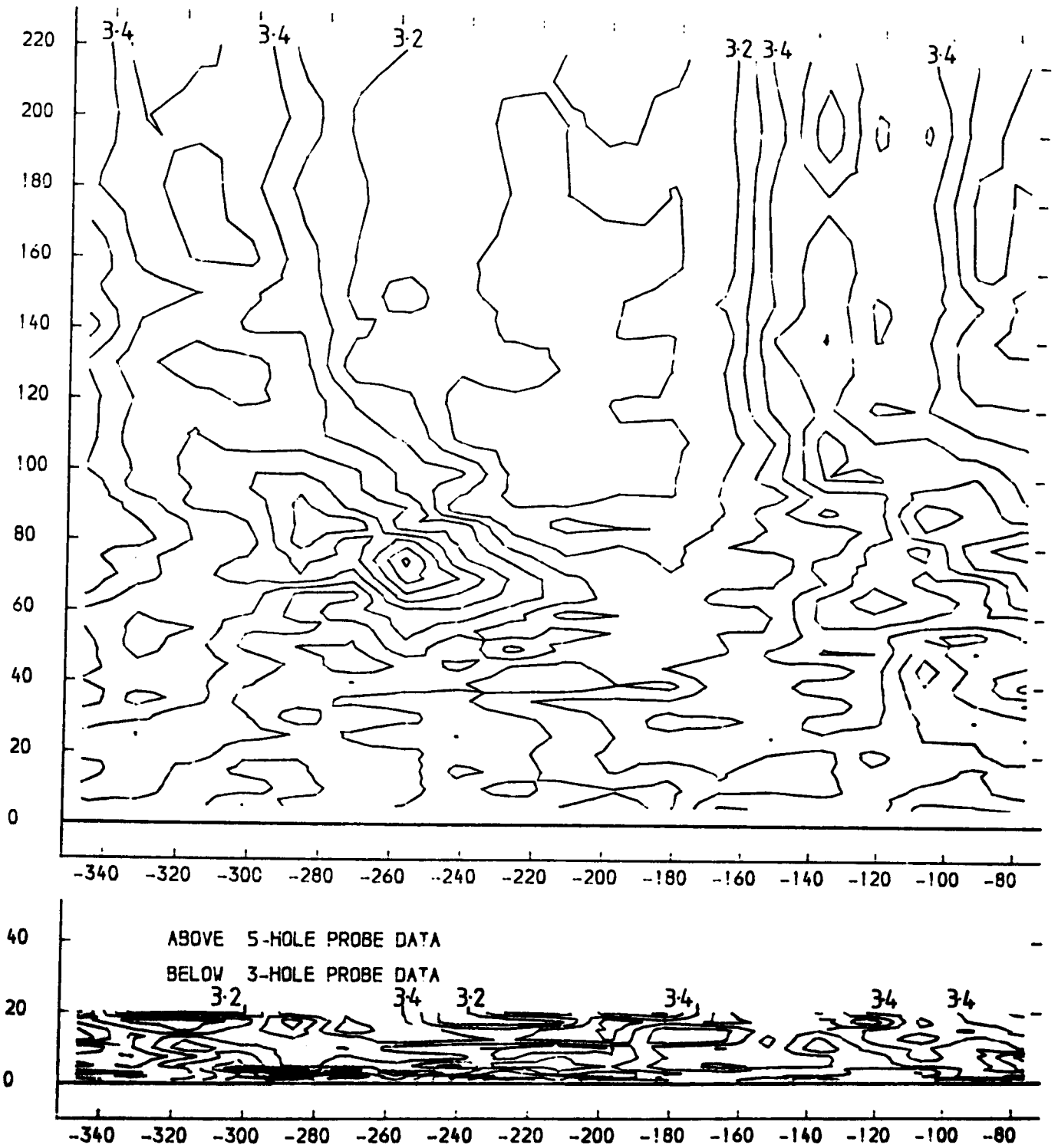


FIGURE 6.22



PITCHWISE MASS MEANED YAW ANGLE UPSTREAM OF THE CASCADE  
VARIABLE INLET BOUNDARY LAYER

X-AXIS SPANWISE CO-ORDINATE FROM PERSPEX ENDWALL (MM)  
Y-AXIS YAW ANGLE (DEGREES)

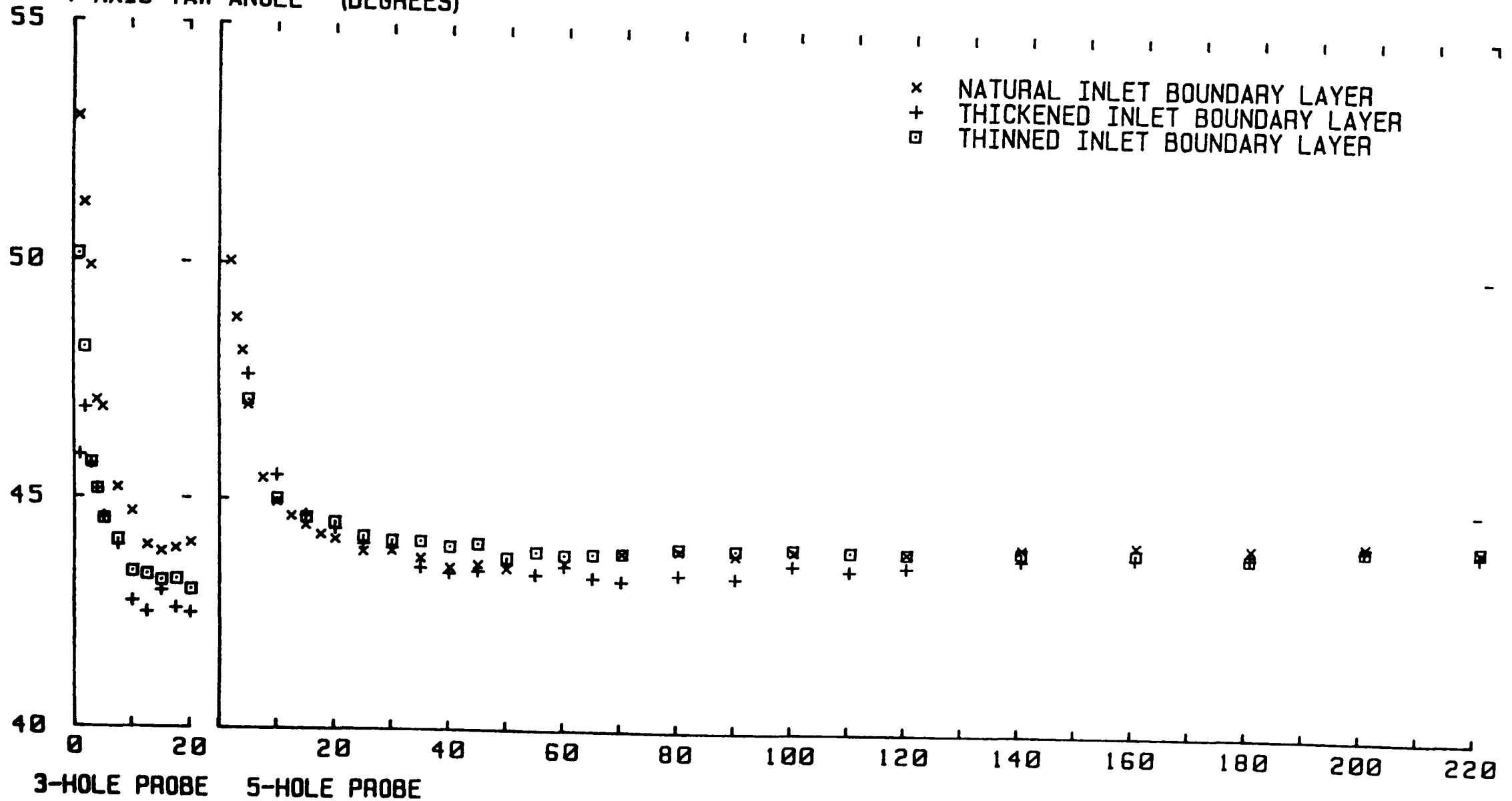


FIGURE 8.23

PITCHWISE MASS MEANED TOTAL PRESSURE LOSS COEFFICIENT UPSTREAM OF THE CASCADE  
 VARIABLE INLET BOUNDARY LAYER

X-AXIS SPANWISE CO-ORDINATE FROM PERSPEX ENDWALL (MM)  
 Y-AXIS TOTAL PRESSURE LOSS COEFFICIENT  $(P_{01} - P_{0LOCAL}) / (P_{01} - P_1)$

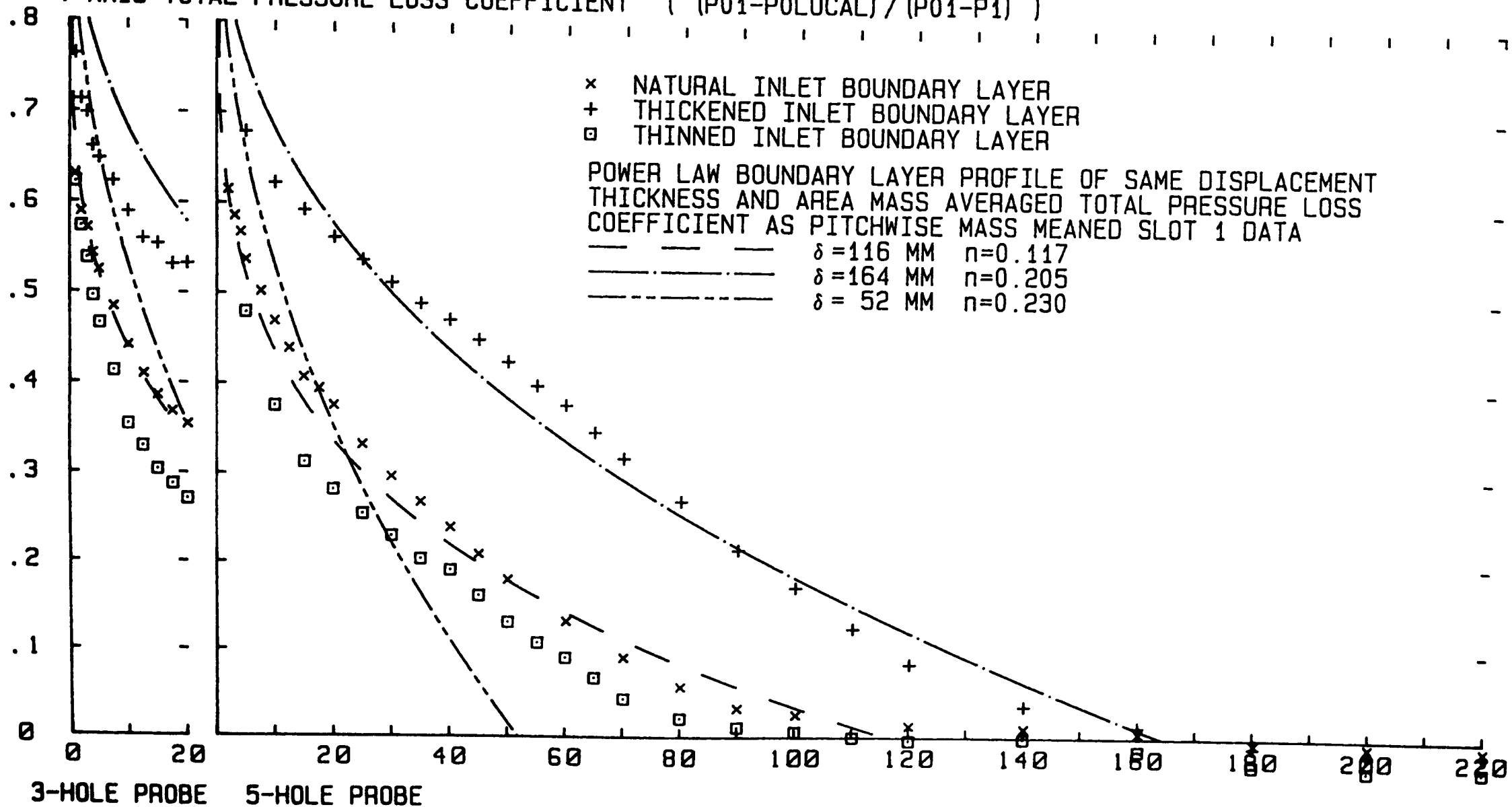


FIGURE 6.24

SLOT 8 PITCHWISE MASS MEANED YAW ANGLE  
 VARIABLE INLET BOUNDARY LAYER

X-AXIS SPANWISE CO-ORDINATE FROM PERSPEX ENDWALL (MM)  
 Y-AXIS YAW ANGLE (DEGREES)

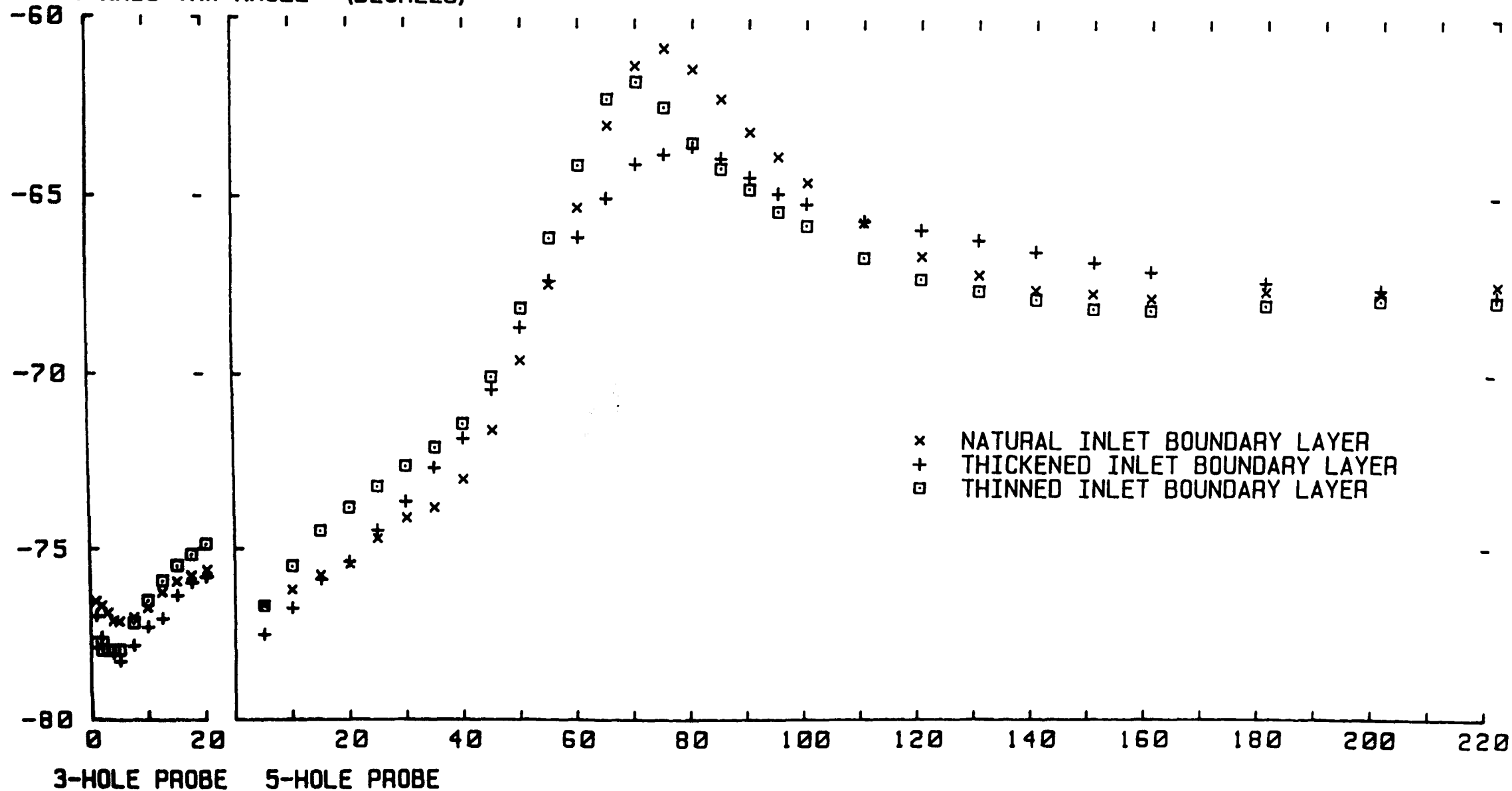


FIGURE 6.25

SLOT 10 PITCHWISE MASS MEANED YAW ANGLE  
 VARIABLE INLET BOUNDARY LAYER

X-AXIS SPANWISE CO-ORDINATE FROM PERSPEX ENDWALL (MM)  
 Y-AXIS YAW ANGLE (DEGREES)

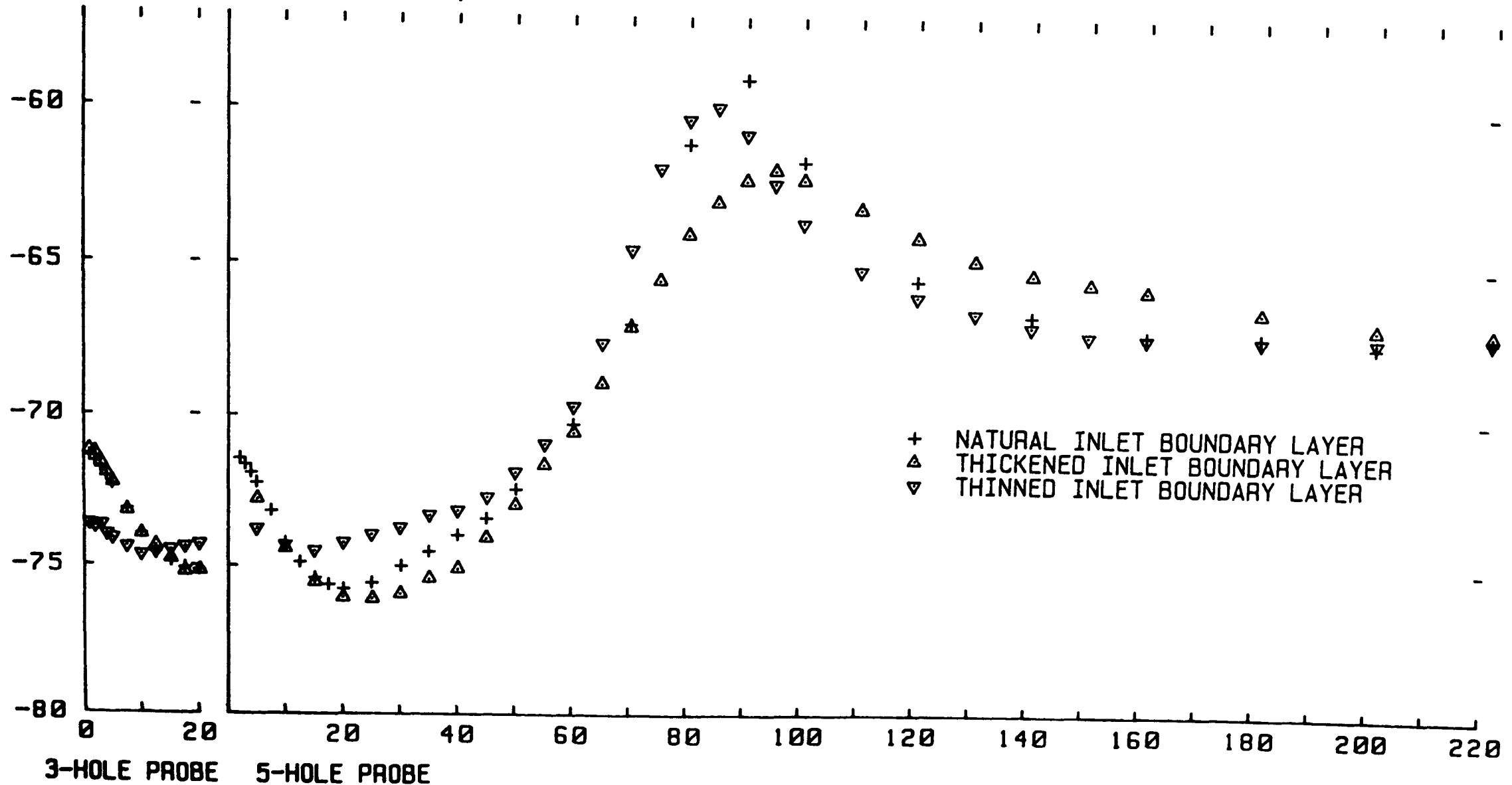


FIGURE 6.26

SLOT 8 PITCHWISE MASS MEANED TOTAL PRESSURE LOSS COEFFICIENT  
 VARIABLE INLET BOUNDARY LAYER

X-AXIS SPANWISE CO-ORDINATE FROM PERSPEX ENDWALL (MM)  
 Y-AXIS TOTAL PRESSURE LOSS COEFFICIENT (  $(P_{01}-P_{0LOCAL}) / (P_{01}-P_1)$  )

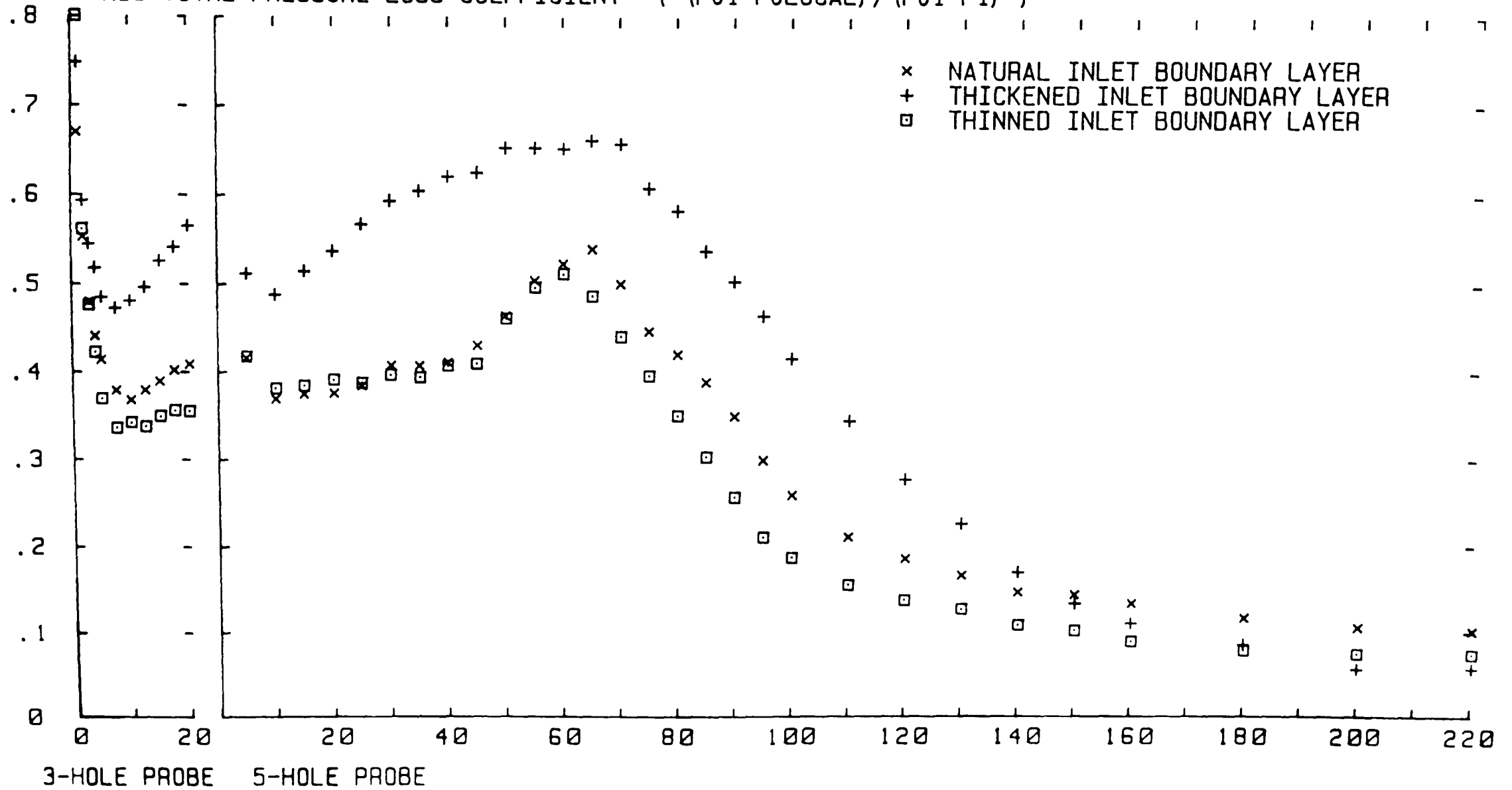


FIGURE 6.27

SLOT 10 PITCHWISE MASS MEANED TOTAL PRESSURE LOSS COEFFICIENT  
 VARIABLE INLET BOUNDARY LAYER

X-AXIS SPANWISE CO-ORDINATE FROM PERSPEX ENDWALL (MM)  
 Y-AXIS TOTAL PRESSURE LOSS COEFFICIENT (  $(P_{01}-P_{0LOCAL}) / (P_{01}-P_1)$  )

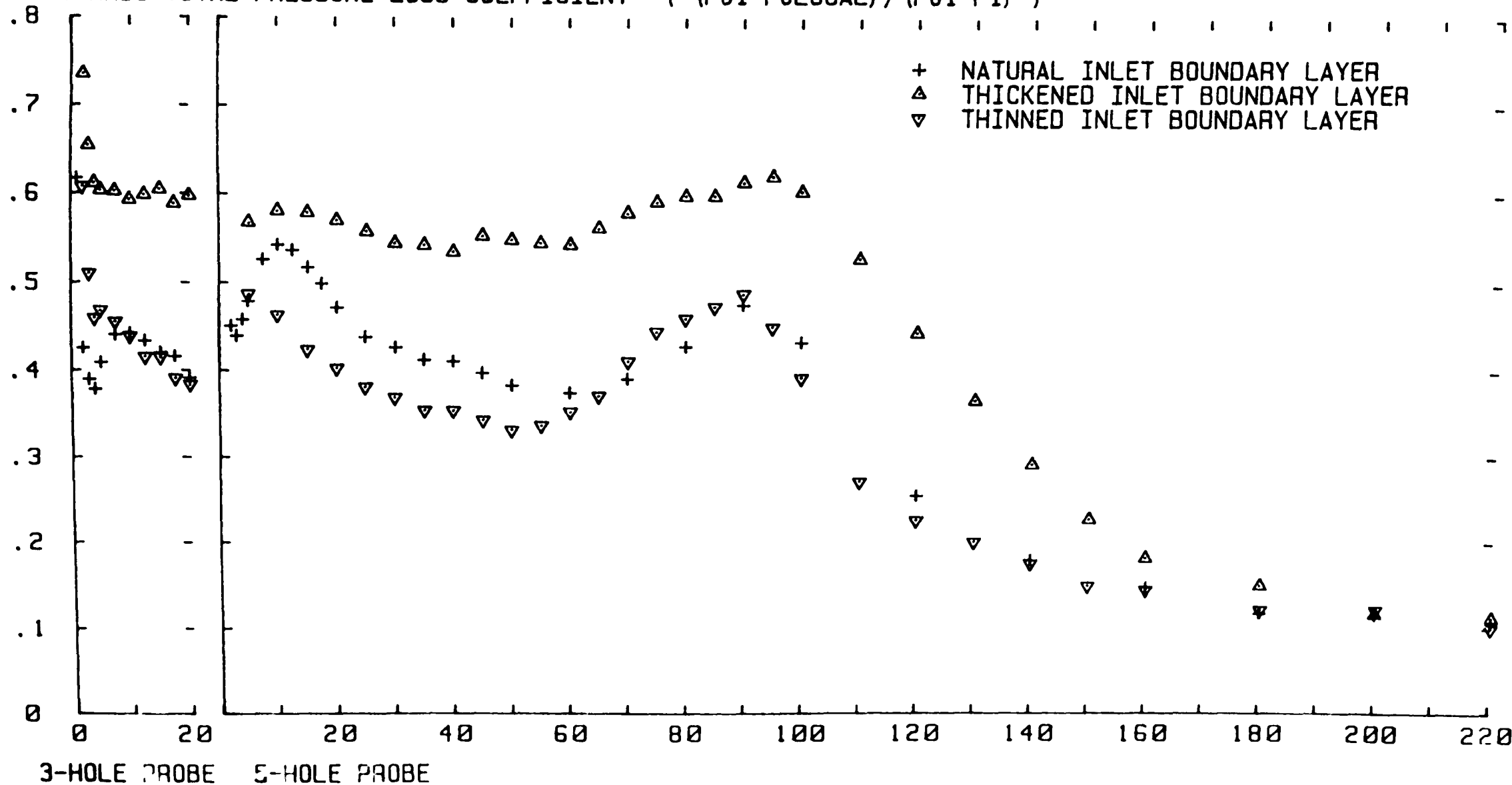


FIGURE 6.28

BLADE SURFACE STATIC PRESSURE COEFFICIENT DISTRIBUTION

THICKENED BOUNDARY LAYER DATA

X-AXIS AXIAL CO-ORDINATE FROM TRAILING EDGE DATUM (MM)

Y-AXIS STATIC PRESSURE COEFFICIENT (  $(P_1 - P_{LOCAL}) / (P_0 - P_1)$  )

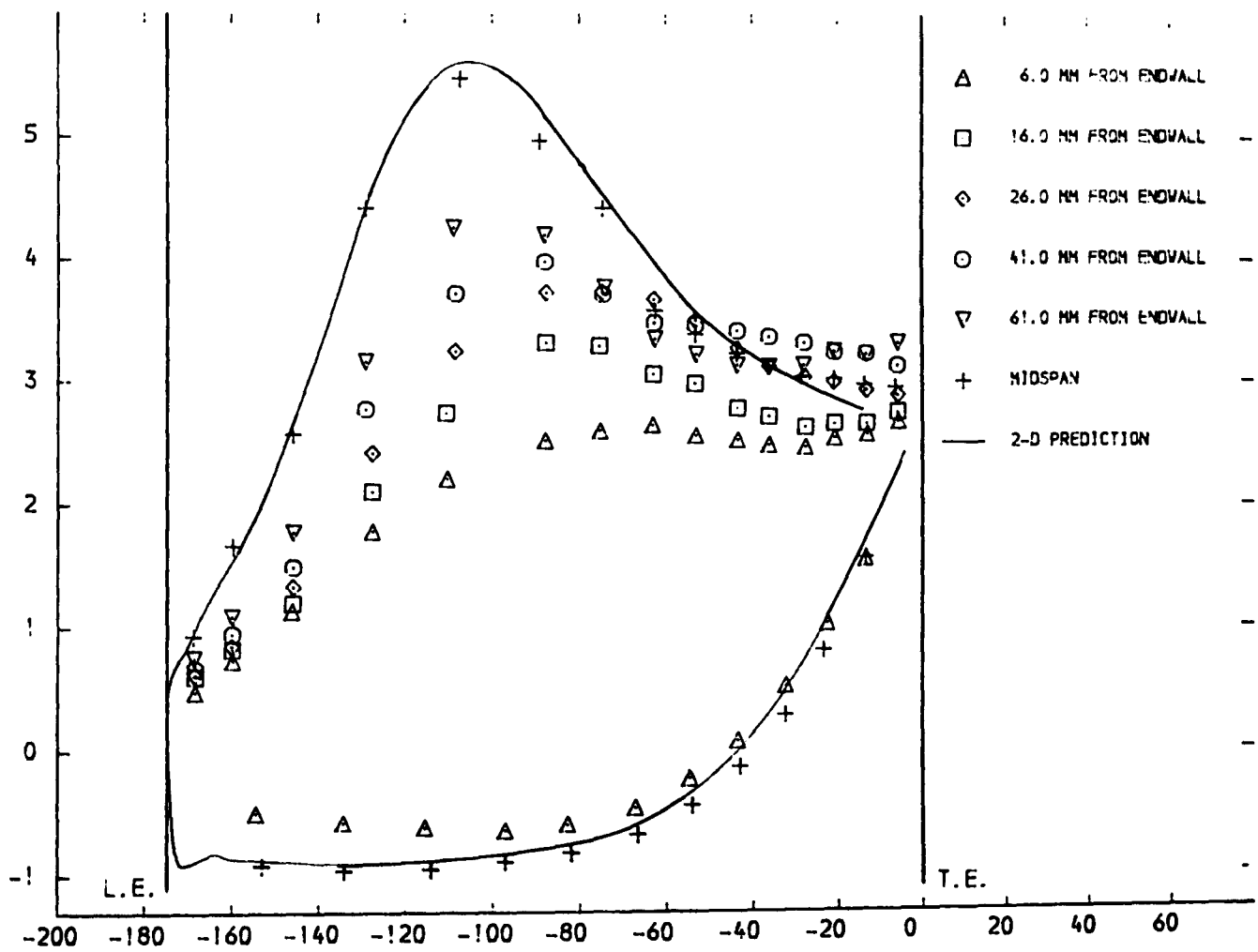


FIGURE 6.29

BLADE SURFACE STATIC PRESSURE COEFFICIENT DISTRIBUTION

THINNED BOUNDARY LAYER DATA

X-AXIS AXIAL CO-ORDINATE FROM TRAILING EDGE DATUM (MM)

Y-AXIS STATIC PRESSURE COEFFICIENT (  $(P1 - PLOCAL) / (P01 - P1)$  )

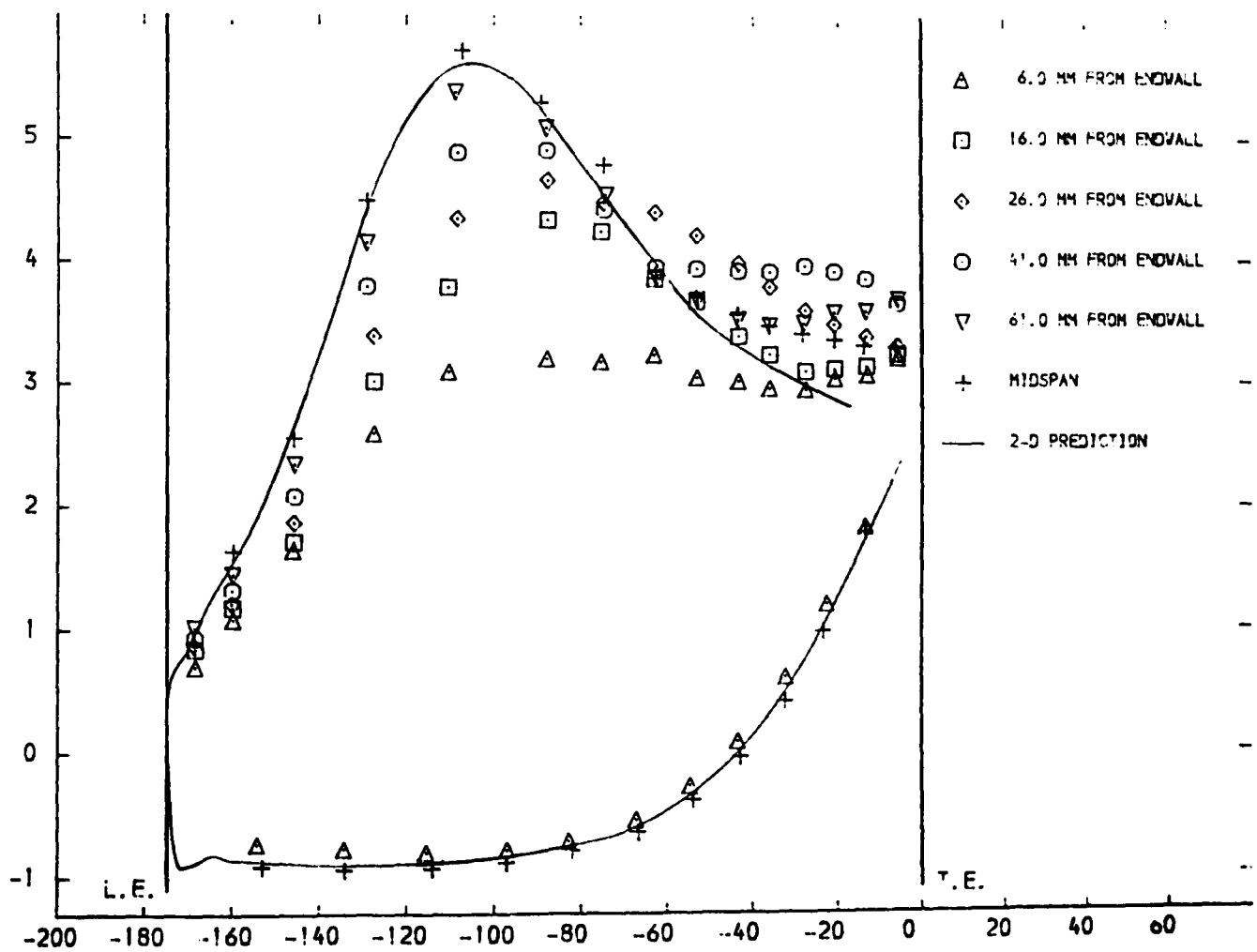


FIGURE 6.30



PLOT ON BLADE PRESSURE SURFACE THICKENED BOUNDARY LAYER DATA  
 STATIC PRESSURE COEFFICIENT (  $(P_1 - P_{LOCAL}) / (P_0 - P_1)$  ) CONTOURS  
 X-AXIS AXIAL CO-ORDINATE FROM TRAILING EDGE DATUM (MM)  
 Y-AXIS SPANWISE CO-ORDINATE FROM PERSPEX ENDWALL (MM)

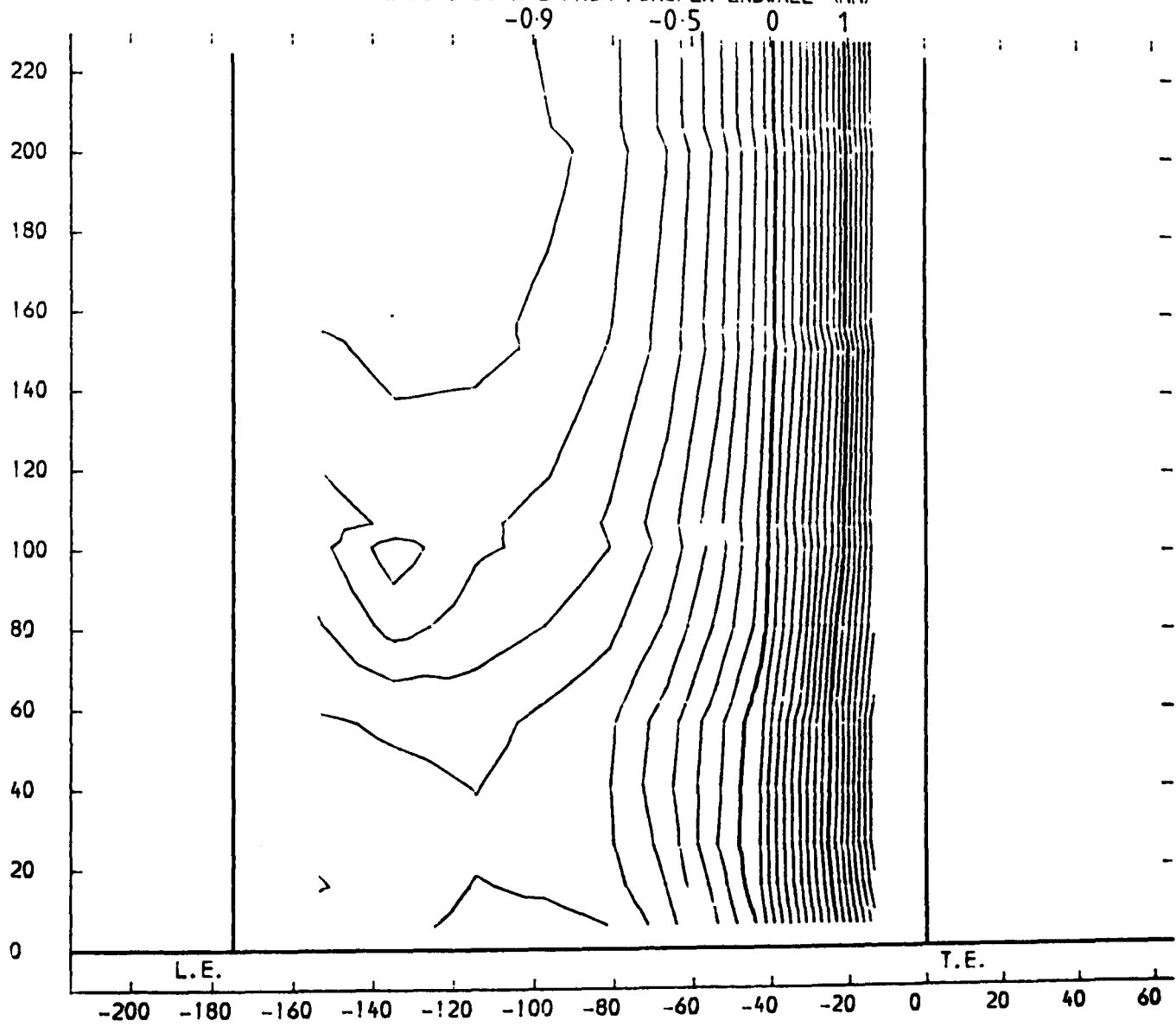


FIGURE 6.31

PLOT ON BLADE PRESSURE SURFACE THINNED BOUNDARY LAYER DATA  
 STATIC PRESSURE COEFFICIENT (  $(P_1 - P_{LOCAL}) / (P_01 - P_1)$  ) CONTOURS  
 X-AXIS AXIAL CO-ORDINATE FROM TRAILING EDGE DATUM (MM)  
 Y-AXIS SPANWISE CO-ORDINATE FROM PERSPEX ENDWALL (MM)

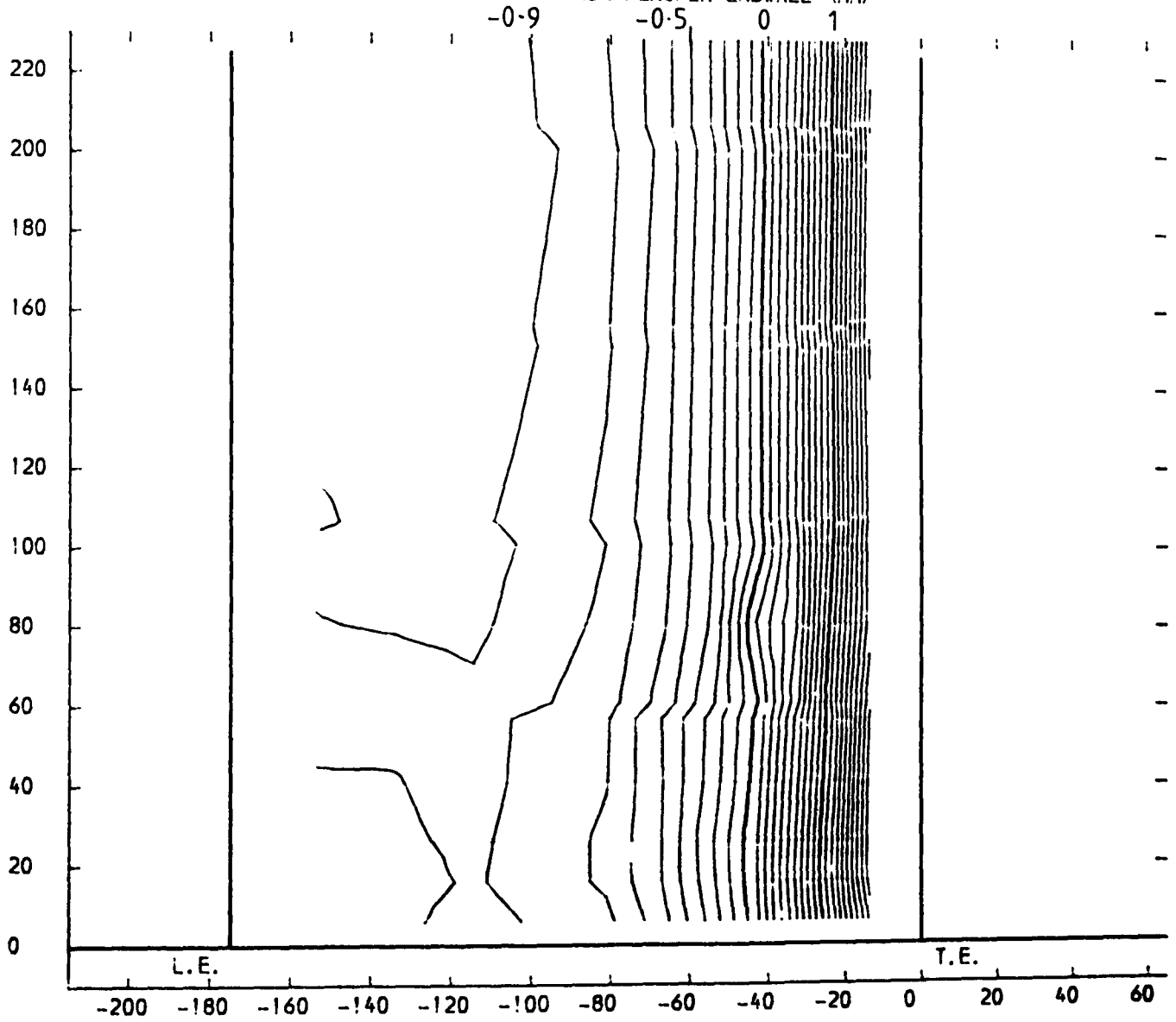


FIGURE 6.32

PLOT ON BLADE SUCTION SURFACE THICKENED BOUNDARY LAYER DATA  
 STATIC PRESSURE COEFFICIENT (  $(P_1 - P_{LOCAL}) / (P_0 - P_1)$  ) CONTOURS

X-AXIS AXIAL CO-ORDINATE FROM TRAILING EDGE DATUM (MM)

Y-AXIS SPANWISE CO-ORDINATE FROM PERSPEX ENDWALL (MM)

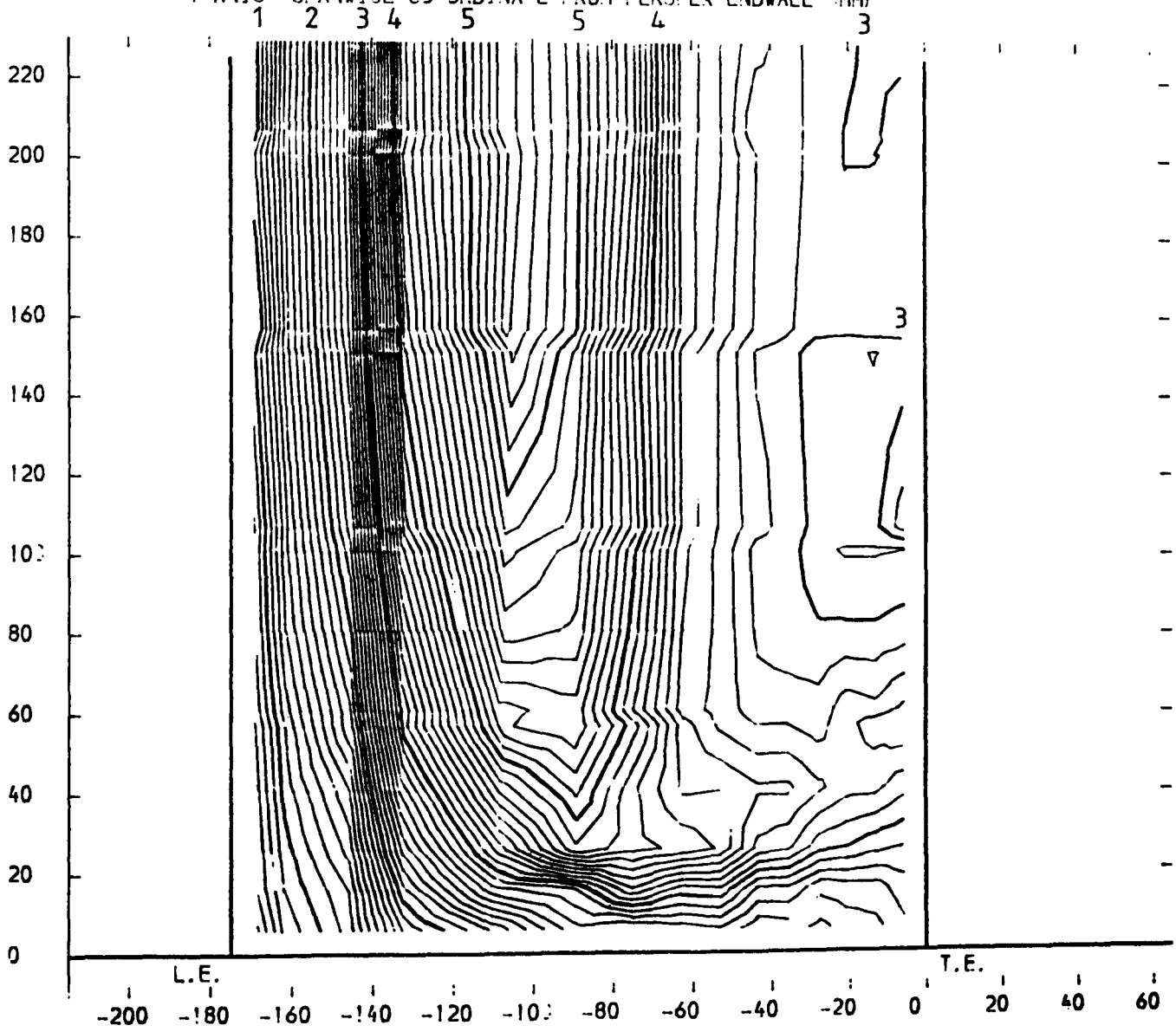


FIGURE 6.33

PLOT ON BLADE SUCTION SURFACE THINNED BOUNDARY LAYER DATA  
STATIC PRESSURE COEFFICIENT (  $(P_1 - P_{LOCAL}) / (P_0 - P_1)$  ) CONTOURS

X-AXIS AXIAL CO-ORDINATE FROM TRAILING EDGE DATUM (MM)  
Y-AXIS SPANWISE CO-ORDINATE FROM PERSPEX ENDWALL (MM)

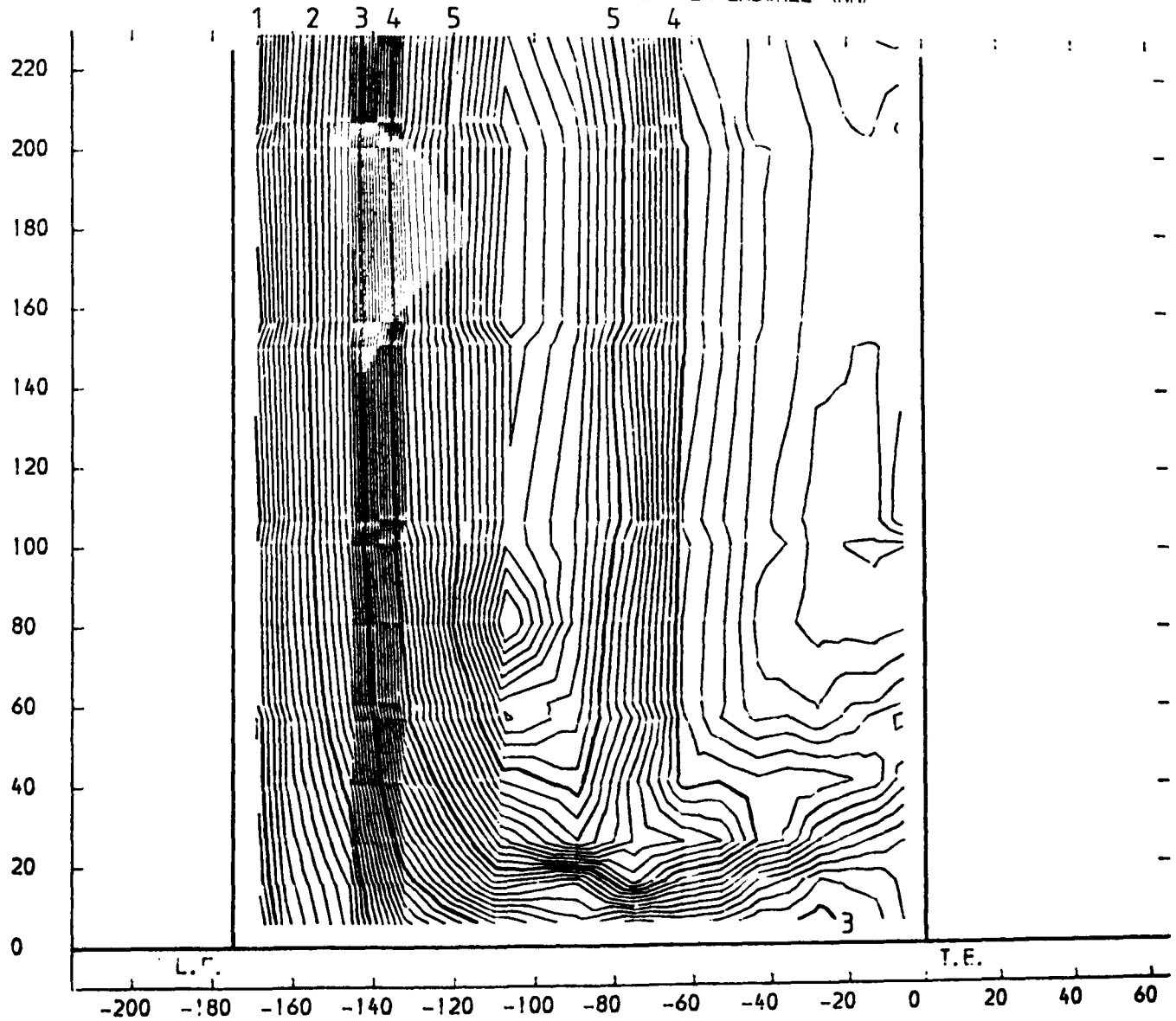
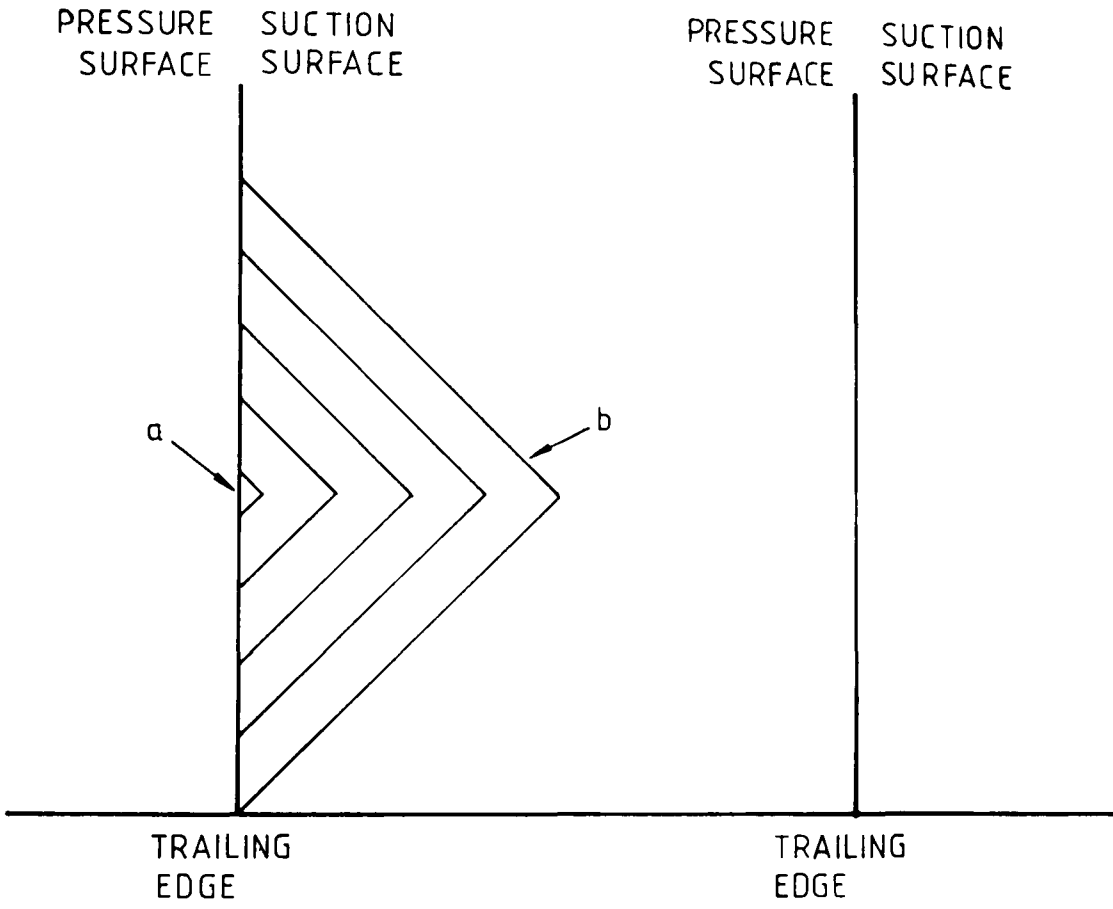


FIGURE 6.34

# THE TRIANGULAR LOSS CORE



- a POINT OF MINIMUM PRESSURE ( $P_{0LOC} = P_1$ )
- b OUTER TOTAL PRESSURE LOSS COEFFICIENT CONTOUR

FIGURE 7.1

DURHAM CASCADE EXIT ANGLE PREDICTION  
 NATURAL INLET BOUNDARY LAYER  
 X-AXIS SPANWISE CO-ORDINATE FROM PERSPEX ENDWALL (MM)  
 Y-AXIS YAW ANGLE (DEGREES)

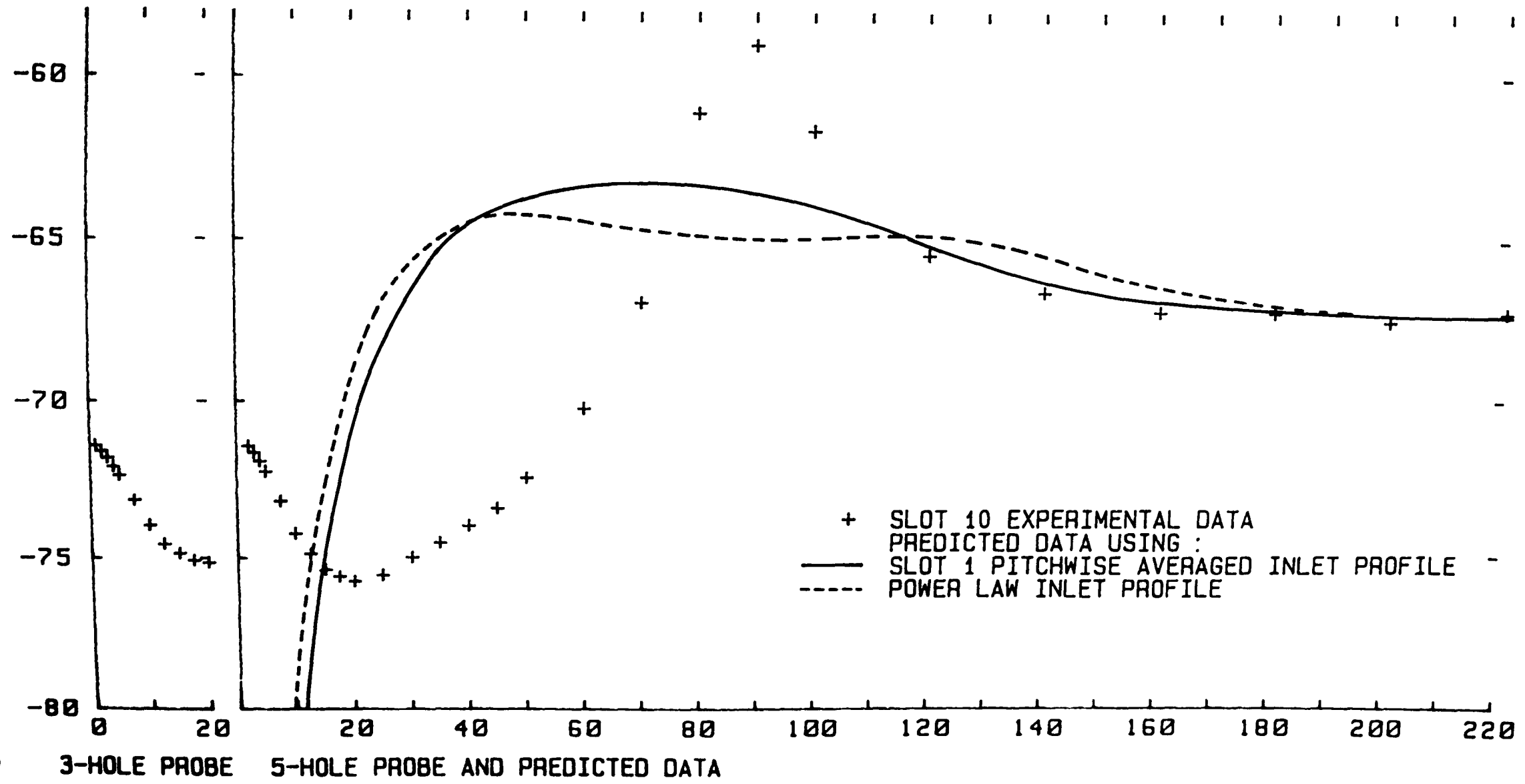


FIGURE 7.2

DURHAM CASCADE SECONDARY LOSS PREDICTION  
 NATURAL INLET BOUNDARY LAYER

X-AXIS SPANWISE CO-ORDINATE FROM PERSPEX ENDWALL (MM)  
 Y-AXIS SECONDARY LOSS COEFFICIENT (NORMALIZED USING INLET DYNAMIC HEAD)

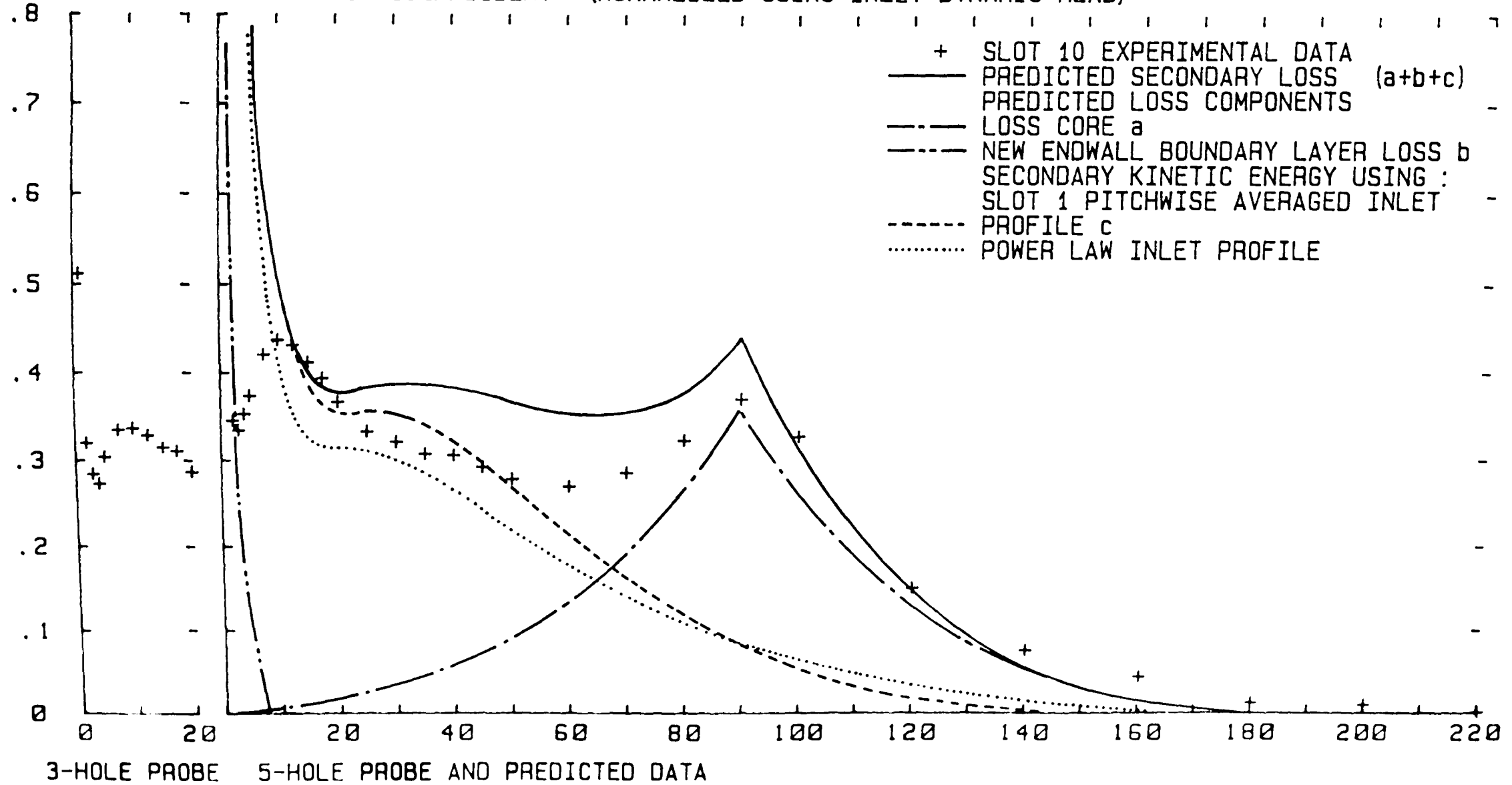


FIGURE 7.3

DURHAM CASCADE EXIT ANGLE PREDICTION  
 THICKENED INLET BOUNDARY LAYER

X-AXIS SPANWISE CO-ORDINATE FROM PERSPEX ENDWALL (MM)  
 Y-AXIS YAW ANGLE (DEGREES)

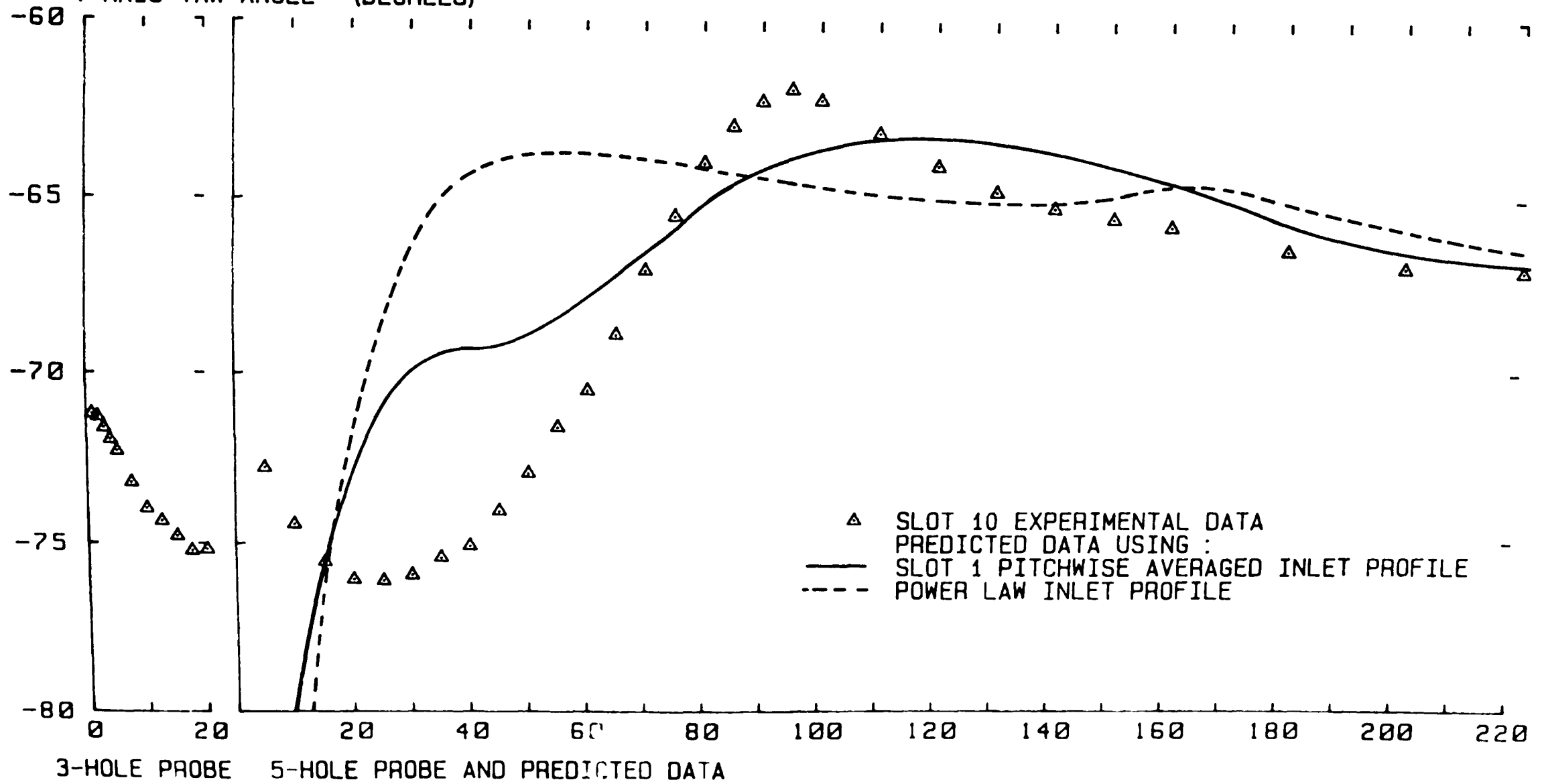


FIGURE 7.4



DURHAM CASCADE SECONDARY LOSS PREDICTION  
 THICKENED INLET BOUNDARY LAYER

X-AXIS SPANWISE CO-ORDINATE FROM PERSPEX ENDWALL (MM)  
 Y-AXIS SECONDARY LOSS COEFFICIENT (NORMALIZED USING INLET DYNAMIC HEAD)

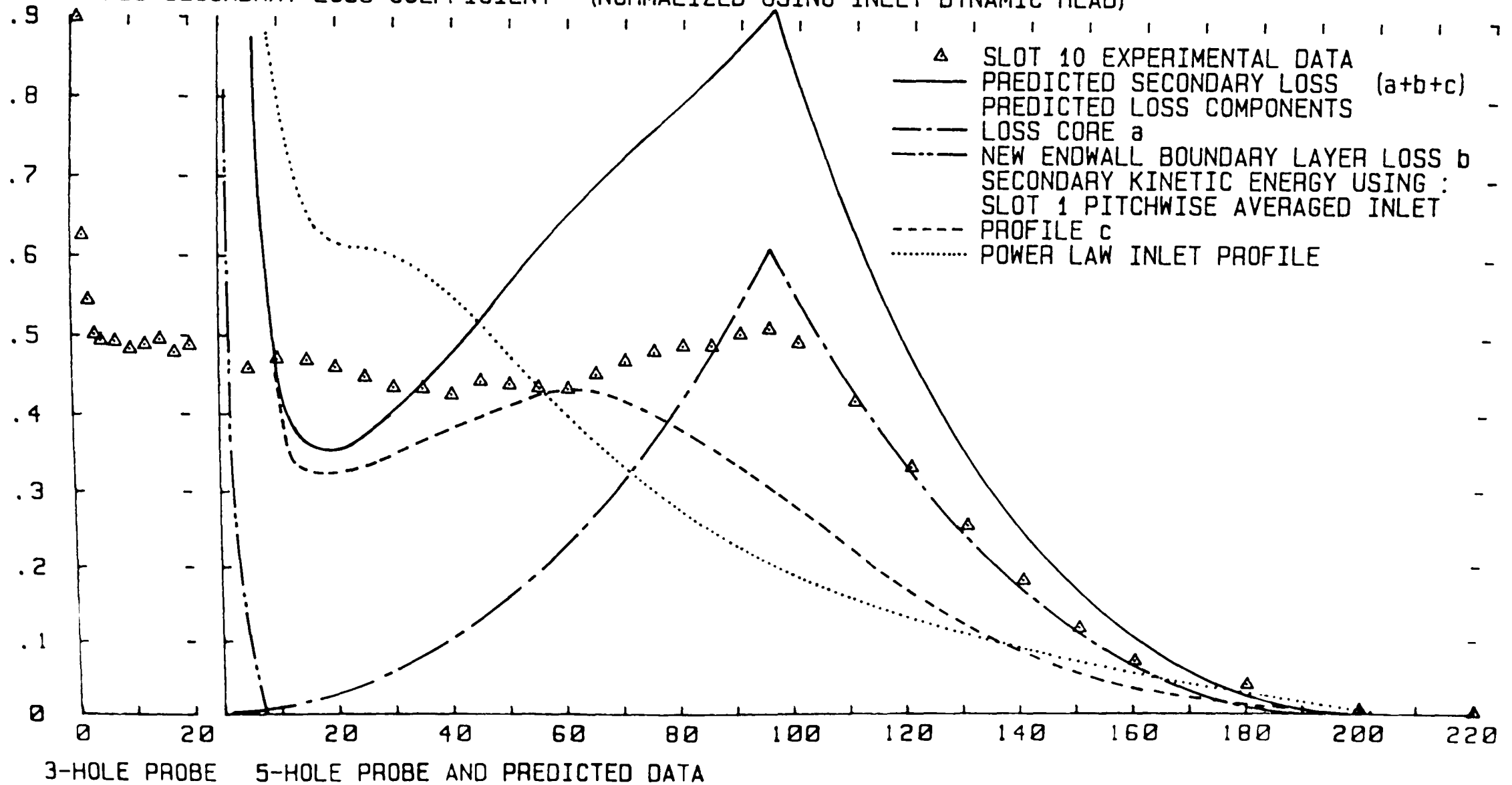
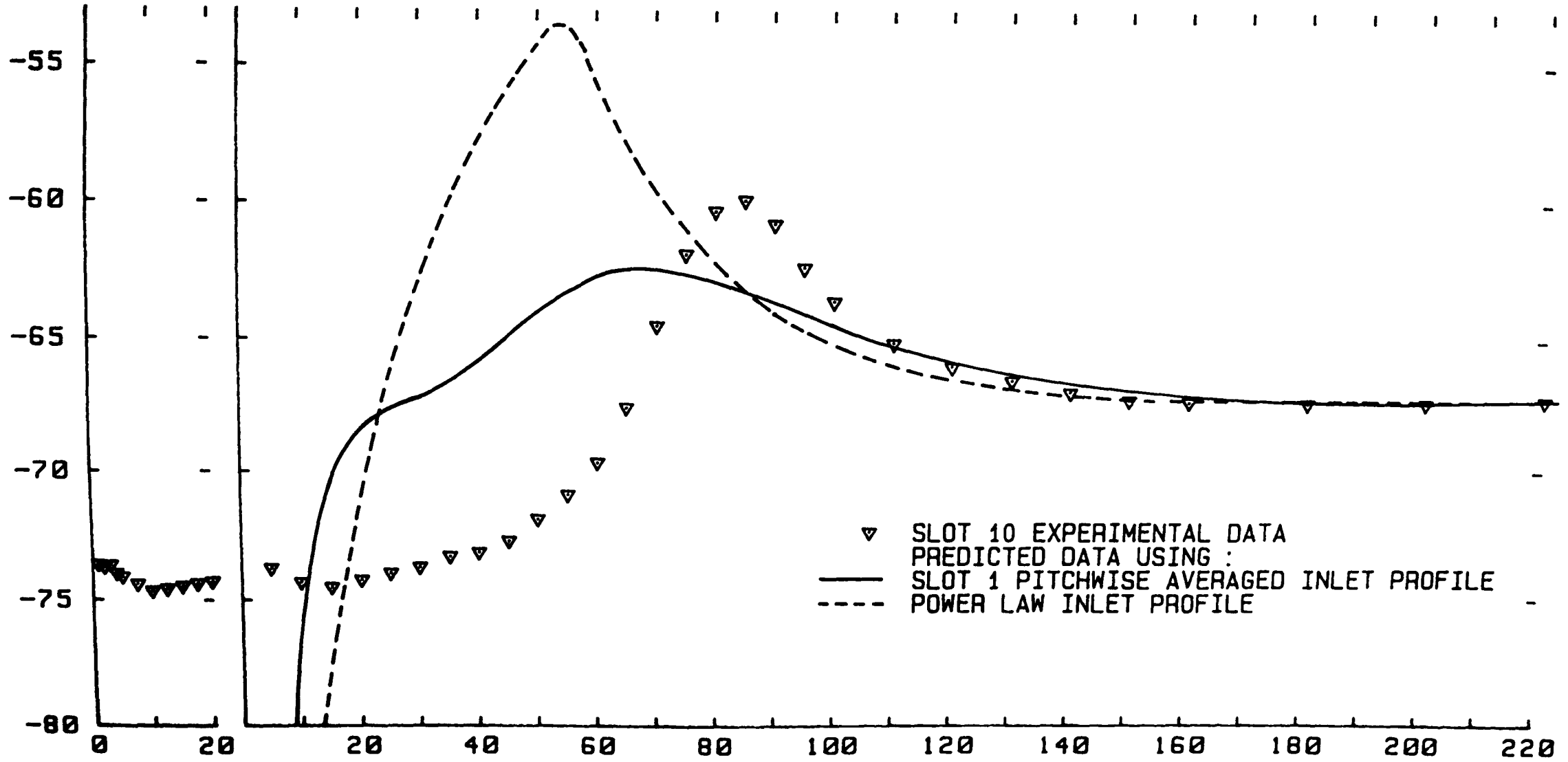


FIGURE 7.5

DURHAM CASCADE EXIT ANGLE PREDICTION  
 THINNED INLET BOUNDARY LAYER  
 X-AXIS SPANWISE CO-ORDINATE FROM PERSPEX ENDWALL (MM)  
 Y-AXIS YAW ANGLE (DEGREES)



▽ SLOT 10 EXPERIMENTAL DATA  
 — PREDICTED DATA USING :  
 — SLOT 1 PITCHWISE AVERAGED INLET PROFILE  
 - - - POWER LAW INLET PROFILE

FIGURE 7.6

3-HOLE PROBE 5-HOLE PROBE AND PREDICTED DATA

DURHAM CASCADE SECONDARY LOSS PREDICTION  
 THINNED INLET BOUNDARY LAYER

X-AXIS SPANWISE CO-ORDINATE FROM PERSPEX ENDWALL (MM)  
 Y-AXIS SECONDARY LOSS COEFFICIENT (NORMALIZED USING INLET DYNAMIC HEAD)

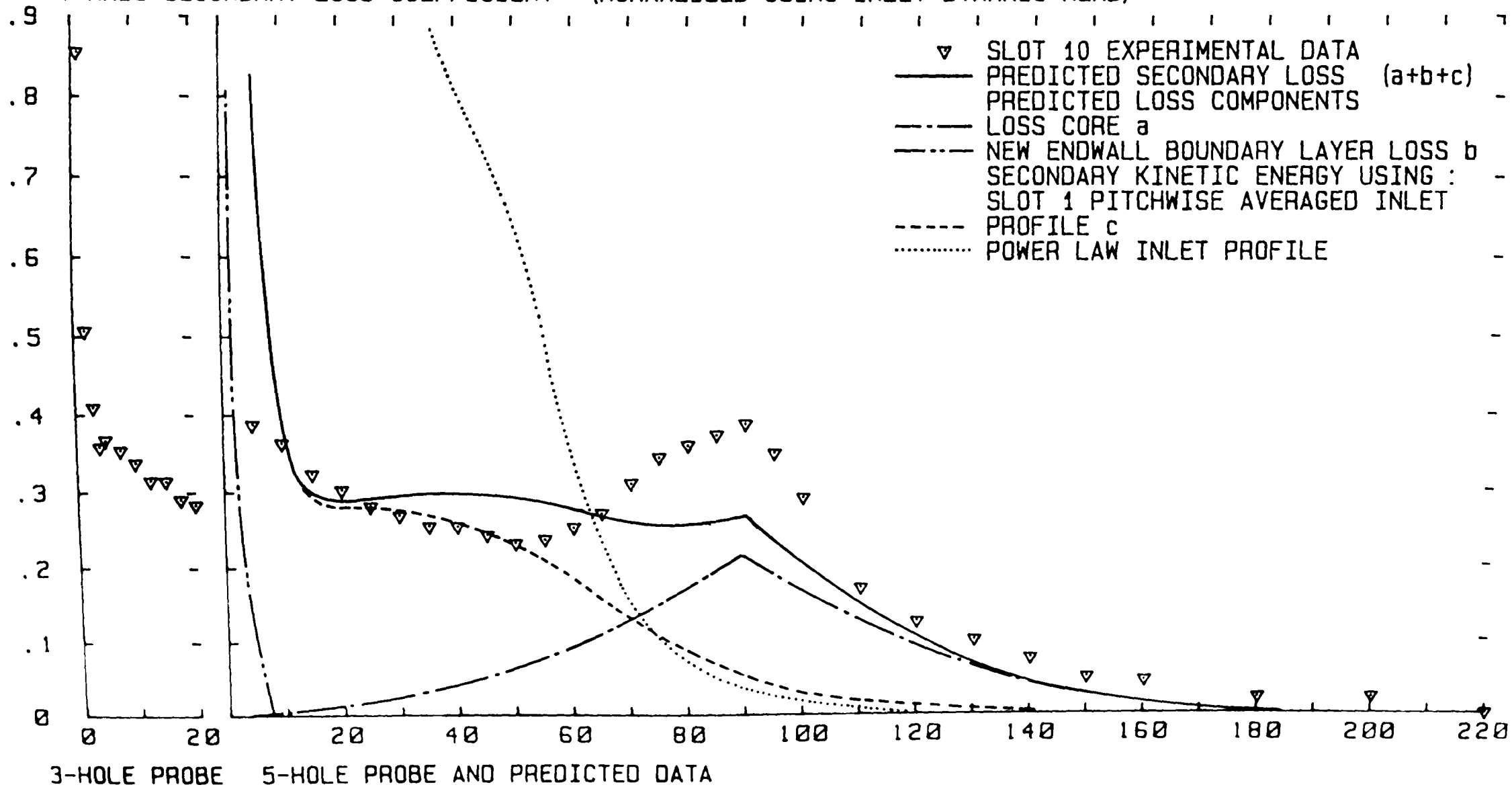


FIGURE 7.7

# CARRICK'S CASCADE SECONDARY LOSS PREDICTION ZERO INLET SKEW LOW REYNOLDS No.

X-AXIS PERCENTAGE OF BLADE SPAN FROM ENDWALL

Y-AXIS SECONDARY LOSS COEFFICIENT (NORMALIZED USING INLET DYNAMIC HEAD)

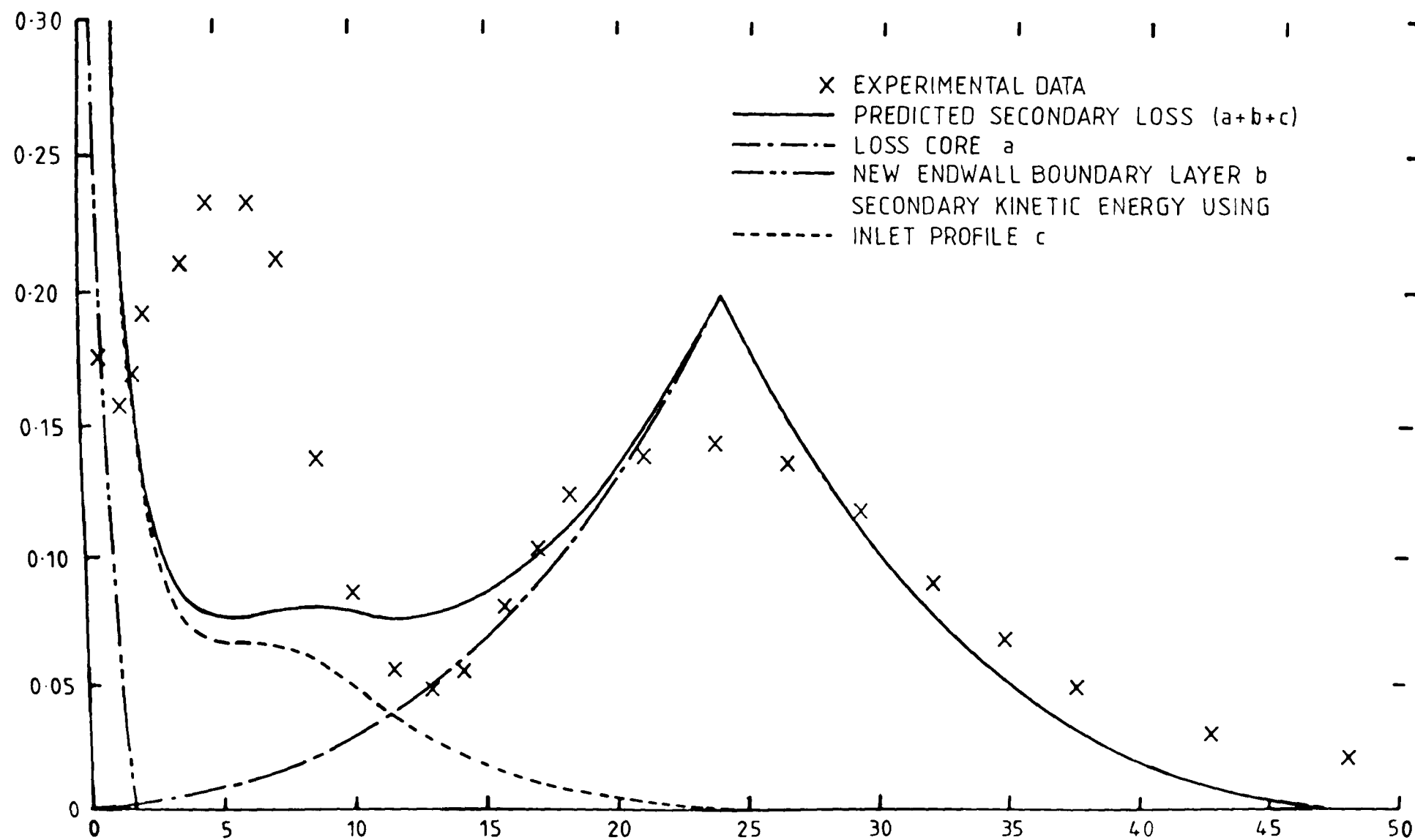


FIGURE 7.8

# CARRICK'S CASCADE SECONDARY LOSS PREDICTION HIGH INLET SKEW LOW REYNOLDS No.

X-AXIS PERCENTAGE OF BLADE SPAN FROM ENDWALL

Y-AXIS SECONDARY LOSS COEFFICIENT (NORMALIZED USING INLET DYNAMIC HEAD)

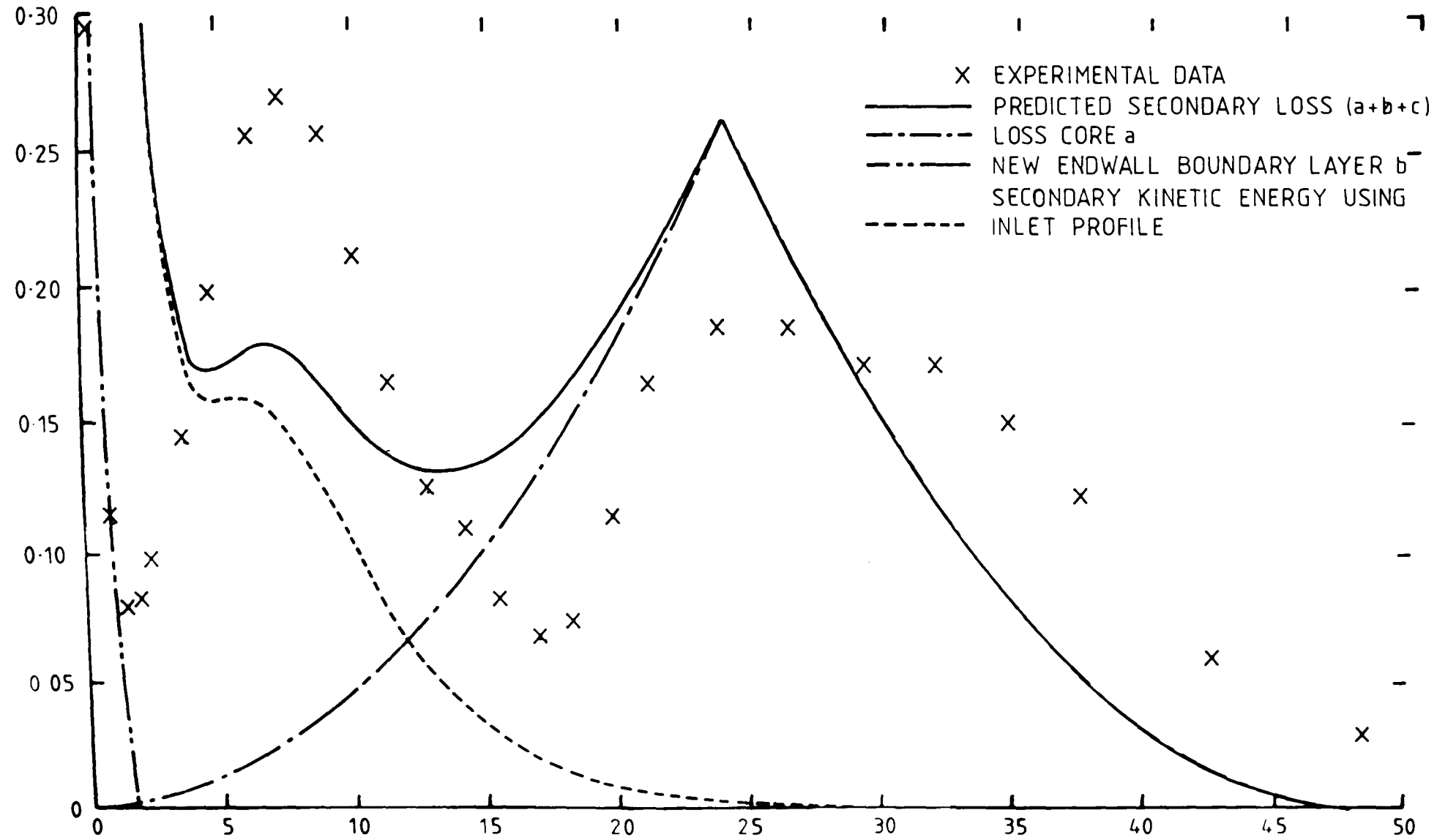


FIGURE 7.9

# SJOLANDER'S CASCADE SECONDARY LOSS PREDICTION

X-AXIS PERCENTAGE OF ANNULUS HEIGHT FROM HUB  
 Y-AXIS SECONDARY LOSS COEFFICIENT (NORMALIZED USING INLET DYNAMIC HEAD)

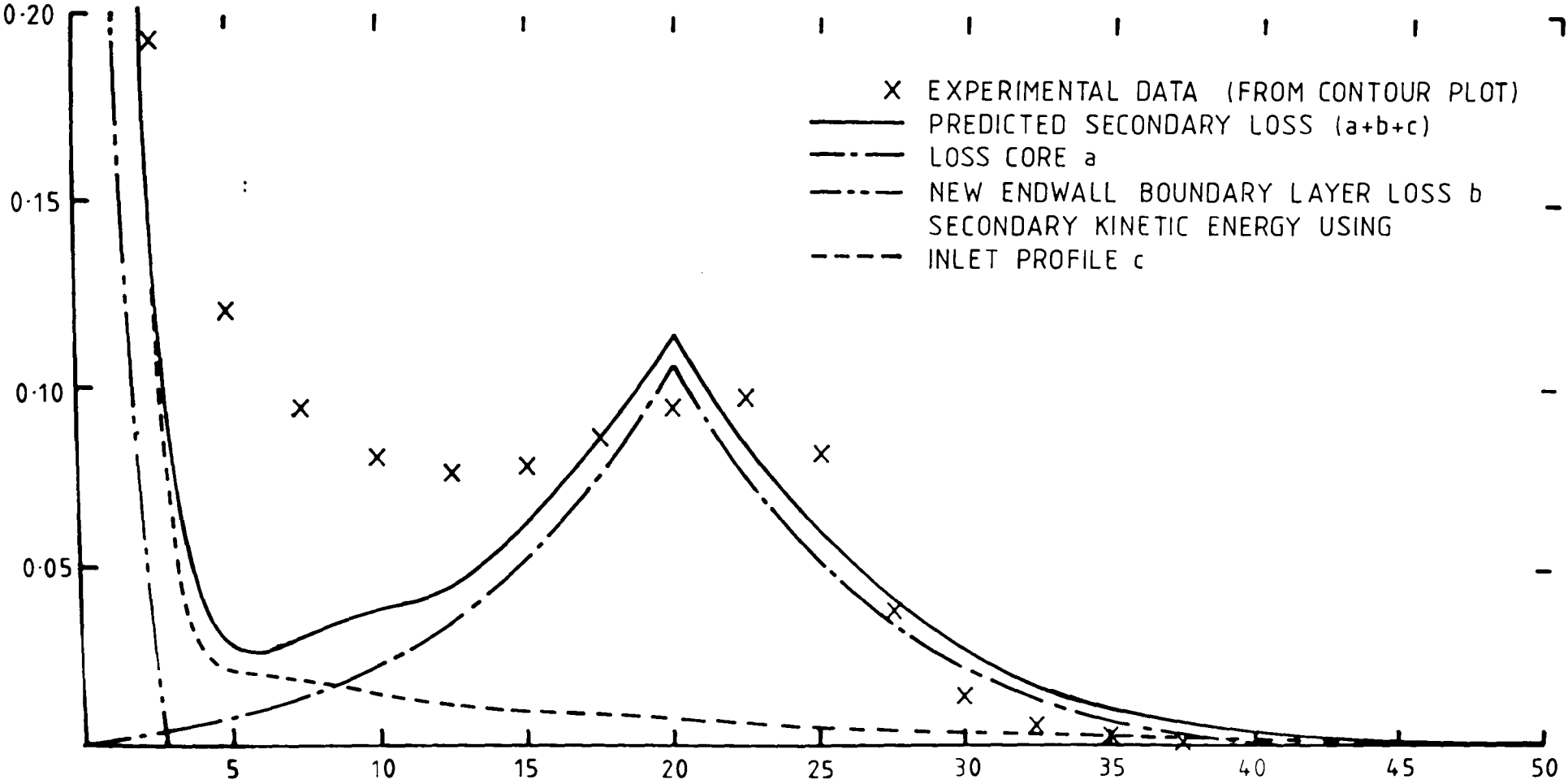


FIGURE 7.10

# TEST TURBINE NOZZLE GUIDE VANE EXIT ANGLE PREDICTION

X-AXIS PERCENTAGE OF ANNULUS HEIGHT FROM HUB  
Y-AXIS YAW ANGLE (DEGREES)

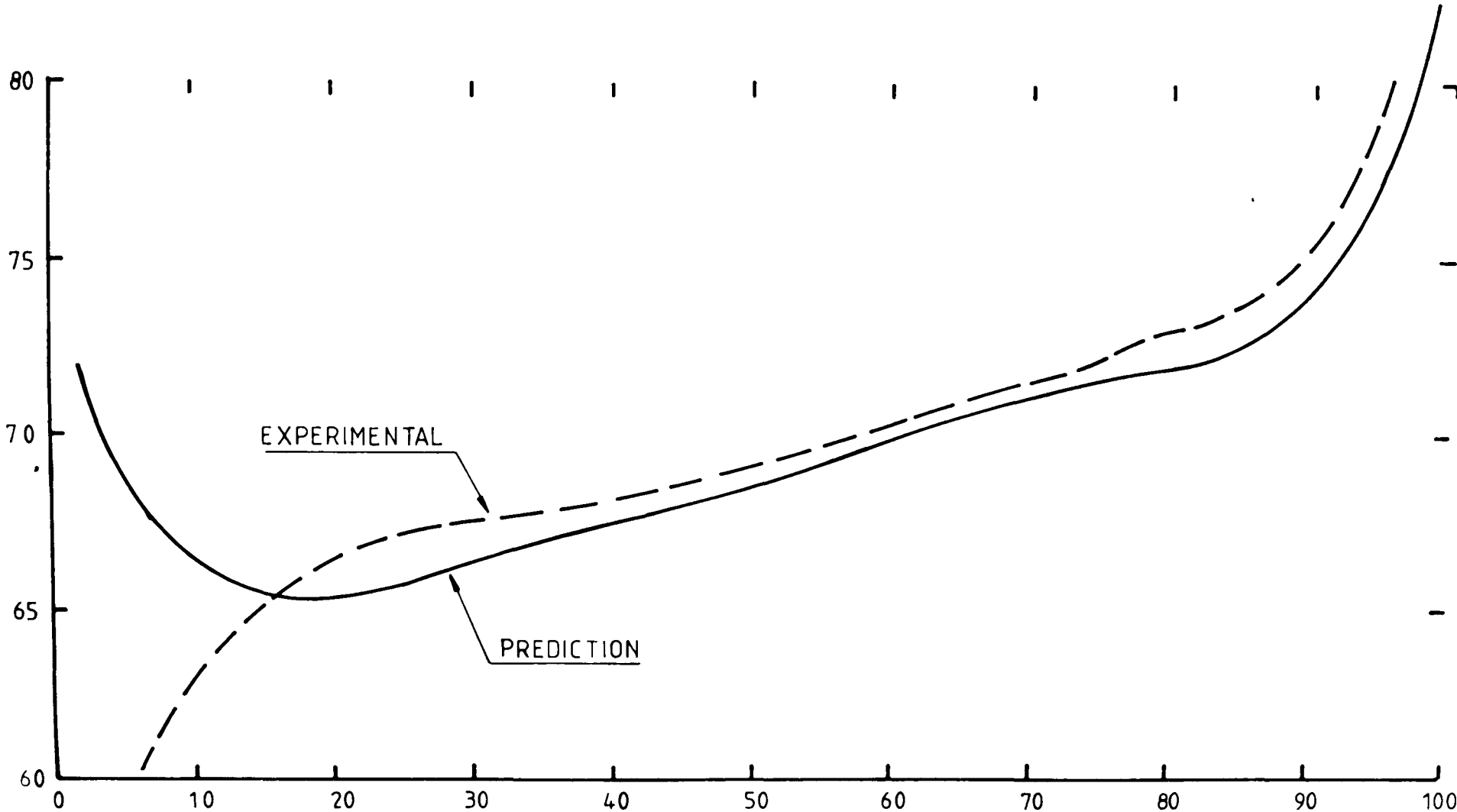


FIGURE 11

# TEST TURBINE NOZZLE GUIDE VANE SECONDARY LOSS PREDICTION

X-AXIS PERCENTAGE OF ANNULUS HEIGHT FROM HUB

Y-AXIS SECONDARY LOSS COEFFICIENT (NORMALIZED USING EXIT DYNAMIC HEAD)

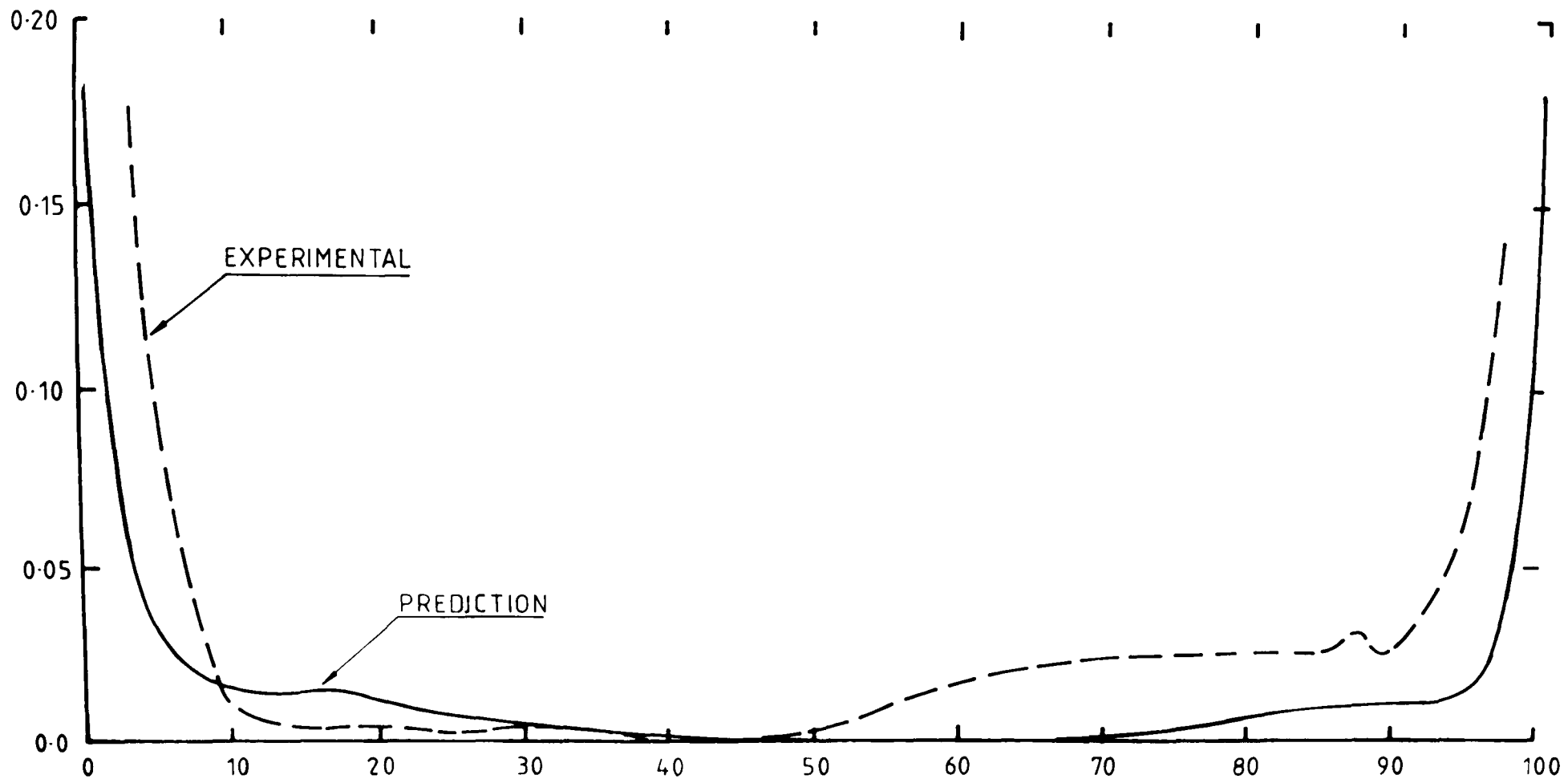
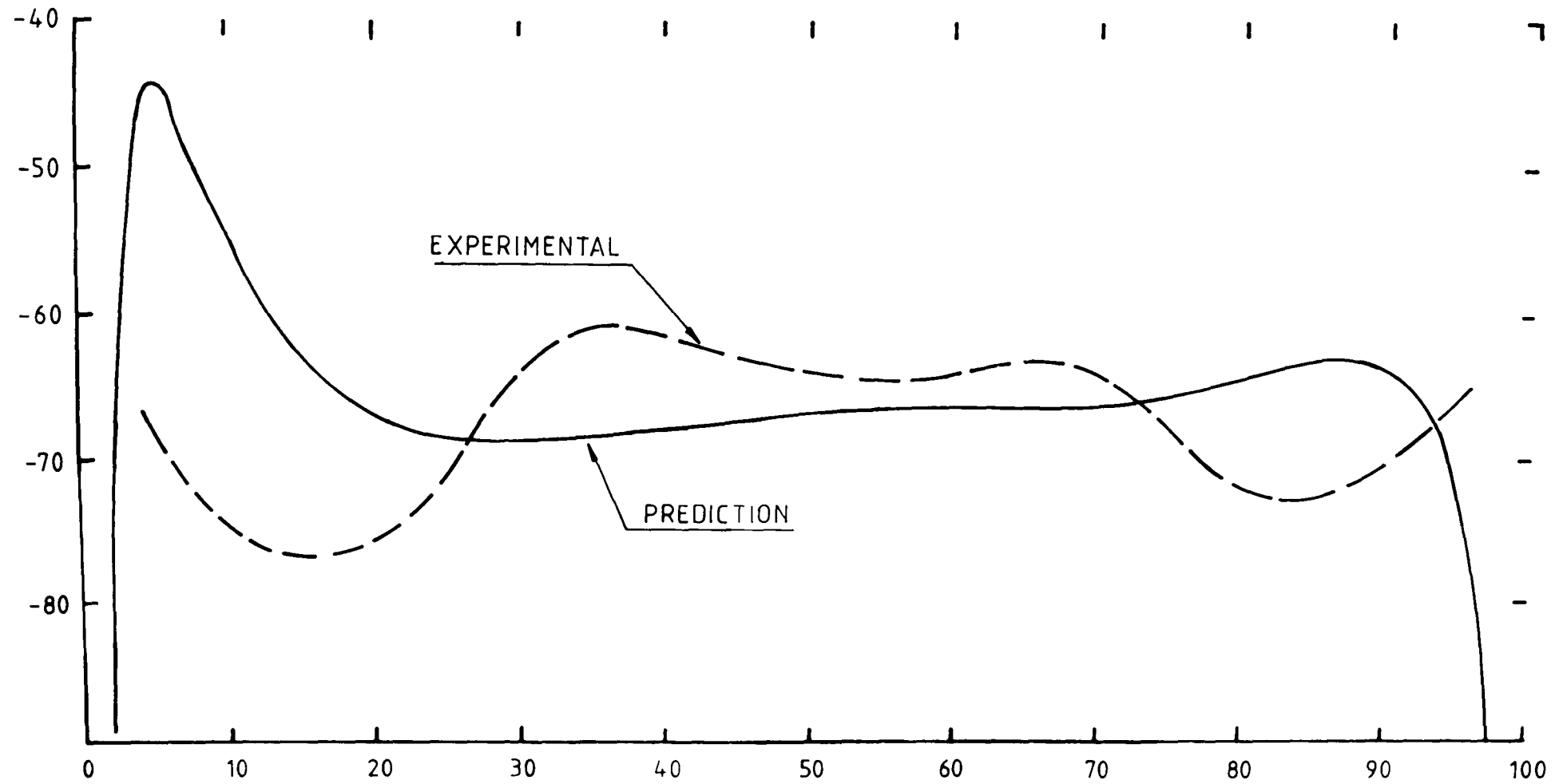


FIGURE 7.12



# TEST TURBINE ROTOR EXIT ANGLE PREDICTION

X-AXIS PERCENTAGE OF ANNULUS HEIGHT FROM HUB  
Y-AXIS YAW ANGLE (DEGREES ROTOR RELATIVE)



# TEST TURBINE ROTOR SECONDARY LOSS PREDICTION

X-AXIS PERCENTAGE OF ANNULUS HEIGHT FROM HUB

Y-AXIS SECONDARY LOSS COEFFICIENT IN STATIC FRAME OF REFERENCE (NORMALIZED USING ROTOR EXIT DYNAMIC HEAD)

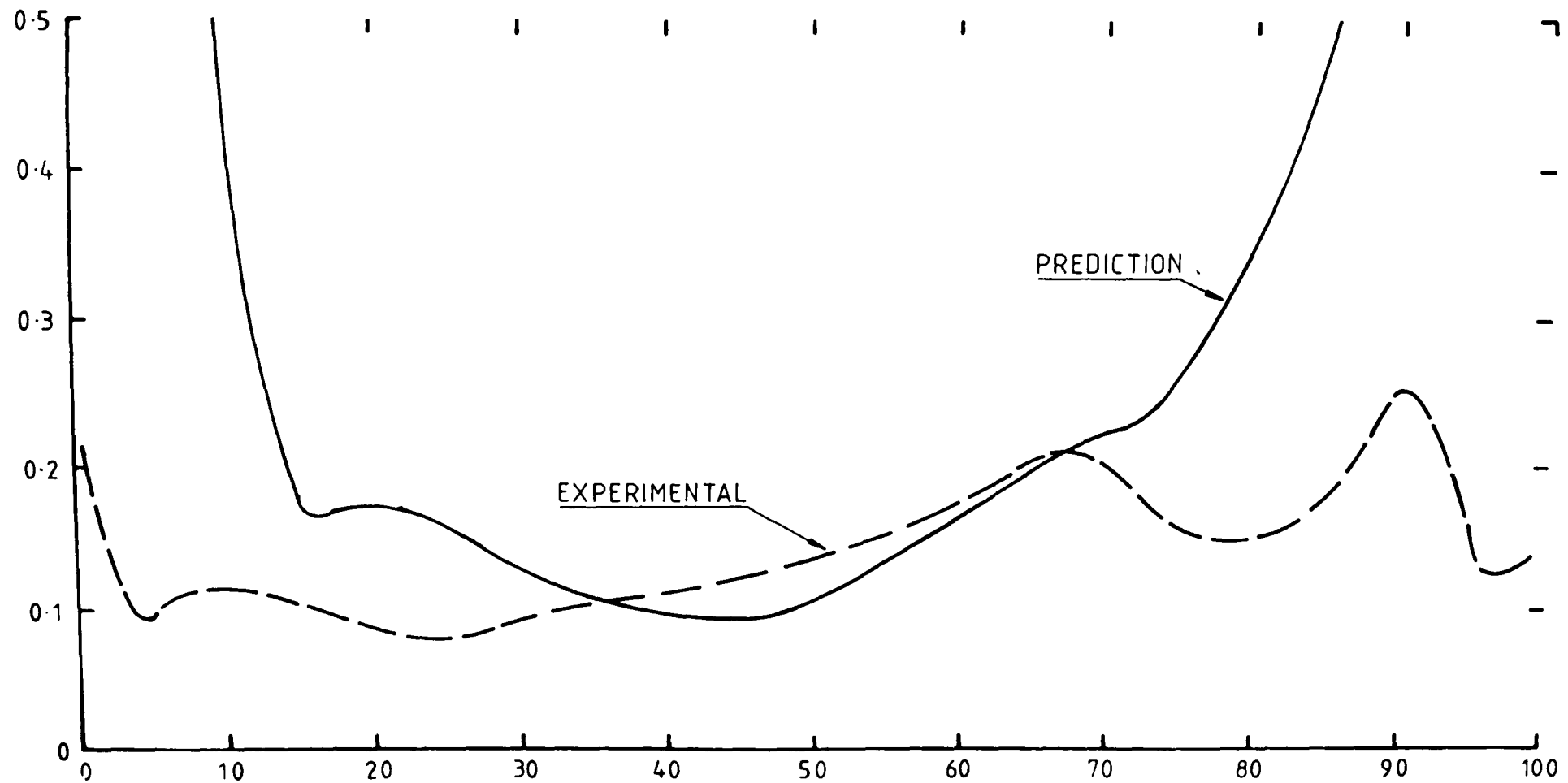


FIGURE 7.24

# HOT WIRE PROBE VELOCITY COMPONENTS

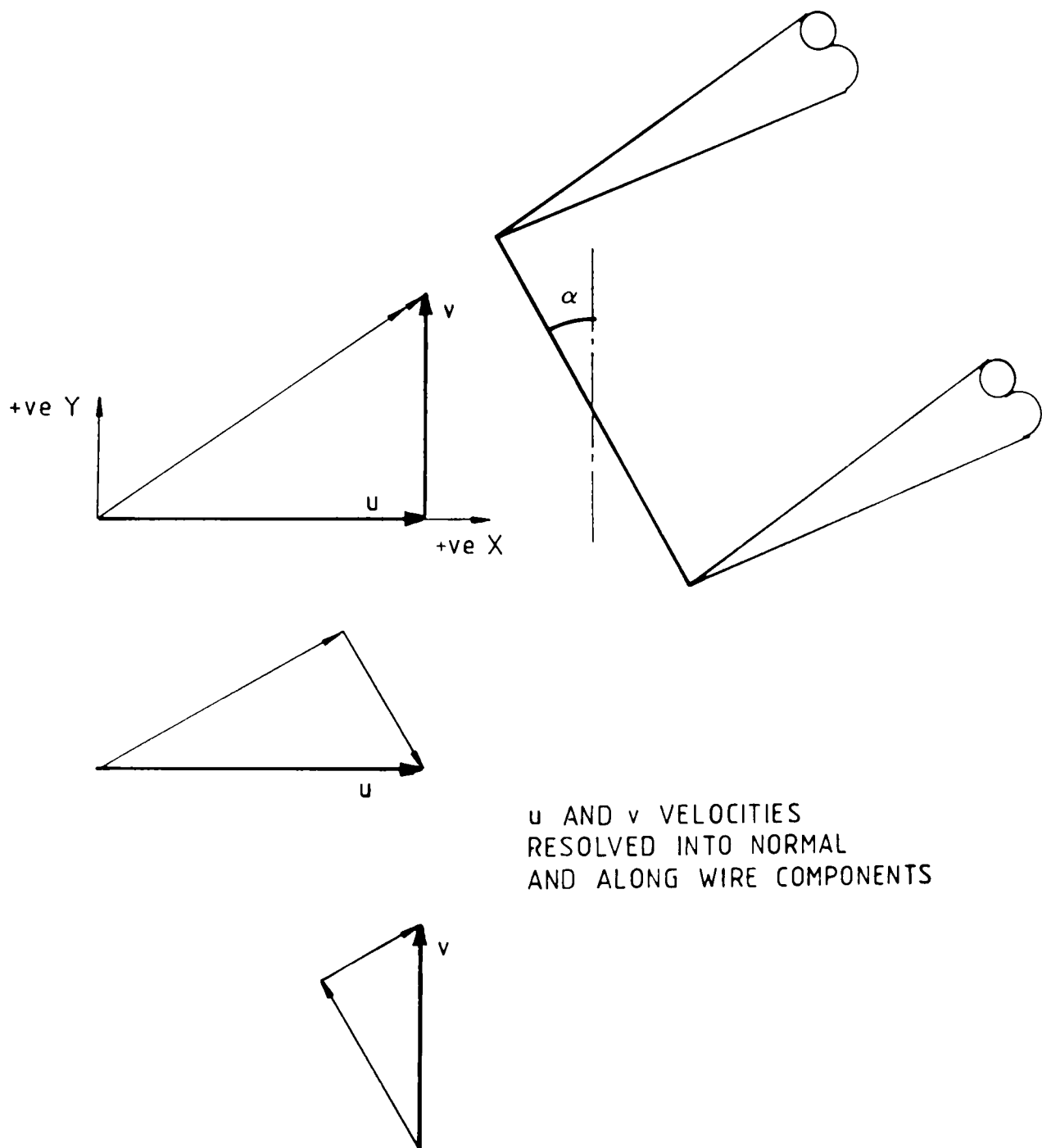


FIGURE AIII.1

# HOT WIRE PROBE CASCADE VELOCITY COMPONENTS

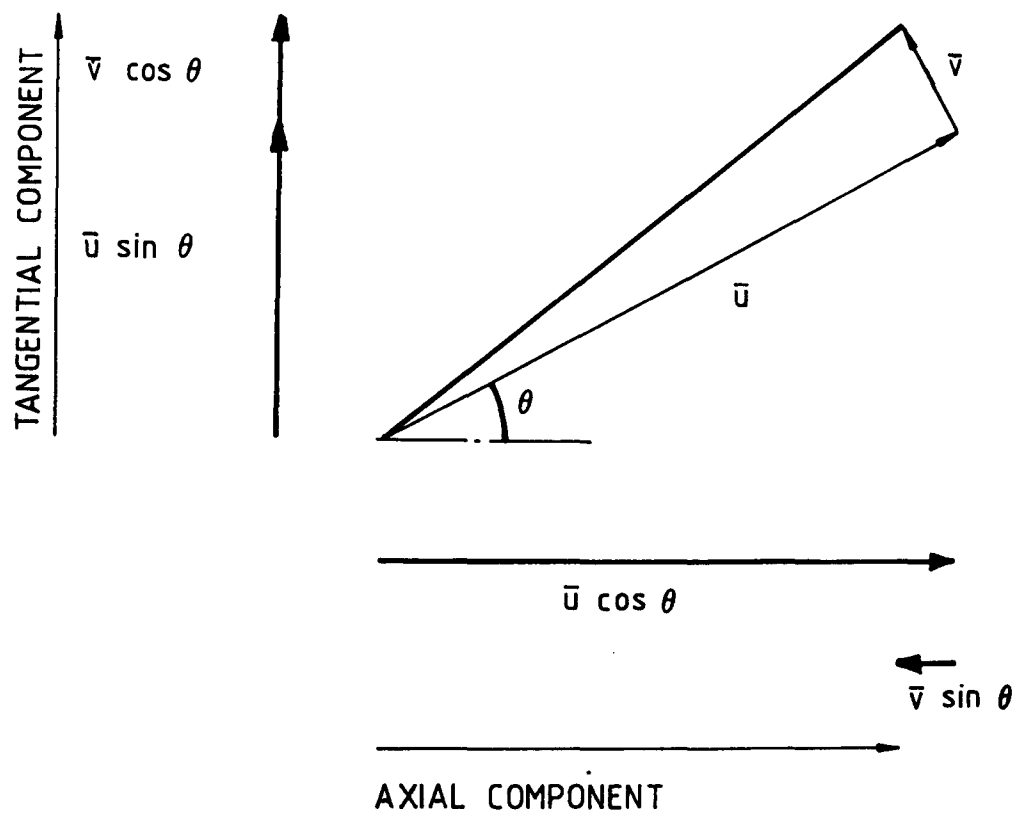


FIGURE AIII.2